Identification of Phenolic Compounds from Peanut Skin using HPLC-MS^n

By

Kyle A. Reed

Dissertation submitted to the Faculty of the Virginia Polytechnic Institute and State University in partial fulfillment of the requirements for the degree of

Doctor of Philosophy

In

Food Science and Technology

Committee:

Sean O'Keefe (Committee Chair)
Rebecca O'Malley (Committee Co-Chair)
Susan Duncan
Kumar Mallikarjunan
Joseph Marcy

December 7, 2009
Blacksburg, Virginia

Keywords: peanut skin, oligomeric proanthocyanidins, polyphenol, HPLC-MS^n

Identification of Phenolic Compounds from Peanut Skin using HPLC-MS^n

By

Kyle A. Reed

ABSTRACT

Consumers view natural antioxidants as a safe means to reduce spoilage in foods. In addition, these compounds have been reported to be responsible for human health benefits. Identification of these compounds in peanut skins may enhance consumer interest, improve sales, and increase the value of peanuts. This study evaluated analytical methods which have not been previously incorporated for the analysis of peanut skins. Toyopearl size-exclusion chromatography (SEC) was used for separating phenolic size-classes in raw methanolic extract from skins of Gregory peanuts. This allowed for an enhanced analysis of phenolic content and antioxidant activity based on compound classes, and provided a viable preparatory separation technique for further identification. Toyopearl SEC of raw methanolic peanut skin extract produced nine fractions based on molecular size. Analysis of total phenolics in these fractions indicated Gregory peanut skins contain high concentrations of phenolic compounds. Further studies revealed the fractions contained compounds which exhibited antioxidant activities that were significantly higher than that of butylated hydroxyanisole (BHA), a common synthetic antioxidant used in the food industry. This indicates peanut skin extracts are a viable antioxidant source, and that synthetic antioxidants can be replaced with those naturally-derived from peanut by-products. Structures contained in each fraction were identified using high performance liquid chromatography (HPLC) coupled with electrospray ionization (ESI) ion trap mass spectrometry (MS^n). Prior to this study, approximately 20 compounds have been identified in peanut skins. The combination of Toyopearl SEC with ESI-HPLC-MS^n allowed for the identification of 314 phenolic-based compounds, most of which are newly discovered compounds in peanut skins. Many compounds identified are known to have powerful antioxidant effects, and also have been reported to exhibit numerous beneficial chemical and biological activities, including the treatment of various human health-related conditions. It is evident that peanut skins may be a potential untapped source for the extraction of natural food antioxidants, nutracueticals, and even pharmaceuticals. Because peanut skins are largely a wasted resource to peanut processors, the novel polyphenols identified in this research could have a significant financial impact on the peanut industry.

Dedication

I would like to dedicate this dissertation to my grandfather, the late Sanford (Sandy) H. Stiles. Known to his family as “Pop Pop”, Sandy was an inspiration to both his community and family alike. He was an instrumental driving force in my life, and taught me the necessary values required to succeed both academically, and personally. For everyone who had the pleasure to know him, he made us realize that nothing in life comes easy, and that only through hard work and dedication will you succeed. He lived by the mantra to “Show ‘em what fer!”, which always gave me the hope of achieving my goals during these often tenacious years of graduate school. Pop Pop, although you are no longer here, you will always be with us, and in my heart forever.

Acknowledgements

I would like to thank all the faculty and staff in the Food Technology Department at Virginia Tech, who gave me this fantastic opportunity to not only hone my skills for my future career, but also to make this research project a reality. My sincere appreciation goes to my major advisor, Dr. Sean O'Keefe, for his true friendship, guidance, financial support, and vast sea of never-ending knowledge. A heartfelt thanks goes to my co-advisor, Dr. Rebecca O'Malley, who graciously took me under her wing for this project. In addition to her friendship, she gave me the necessary knowledge, tools, and support required to achieve my goals. Another sincere appreciation goes to my committee members, Dr. Joseph Marcy, Dr. Susan Duncan, and Dr. Kumar Mallikarjunan. Your friendship, guidance, and support were integral to the success of this research, and also made graduate school at VT an enjoyable and memorable experience. A special thanks also goes to Dr. Jodie Johnson, who devoted much of his time and energy toward helping me with this project.

Reaching this point has been a long and arduous journey, full of life's unexpected twists and turns. Traversing this road has been made simpler by my having people in my life who inspired me to never give up. I'd like to thank all of them who believed in me; I am grateful to all my friends for their support and encouragement. Also, a special thanks to Denise Gardner, not only for her help and support, but also for being such a huge inspiration in both my academic and my personal life. Most of all, I would like to thank my family for being my rock and my foundation. To my mother and father, Laurie and Paul Dietrich, and my brother, Kent Reed, a special thank you for their love and encouragement. I couldn't have done it without you!

TABLE OF CONTENTS

LIST OF TABLES AND FIGURES

CHAPTER I

CHAPTER II

CHAPTER III

INTRODUCTION

Oxidation is a major factor that limits the quality of food products. In the past, many consumers have opposed the use of synthetic antioxidants as a means of reducing spoilage in their foods. Many food companies have taken steps toward removing synthetic antioxidants from their products due to consumer demands. However, consumers view natural antioxidants as a safe means to reduce oxidation and spoilage in food products. The development of these antioxidants from natural sources has become a continuing challenge to the food industry.

Arachis hypogaea, also known as the peanut or groundnut, is very important as an oilseed and food crop in many tropical/subtropical countries. In the past, peanut skins have been viewed as a low value byproduct of peanut processing and roasting. Recent studies have shown that these byproducts contain compounds including isoflavones, isorhamnetin, epicatechin, catechin, resveratrol, and quercetin. Previous research has revealed that these compounds exhibit high oxyradical quenching abilities. In addition, these natural antioxidants also have been reported to be responsible for health benefits in humans consuming wines and other plant materials. The discovery of the relationship between red wine phenolic antioxidants and reduced risk of cancer and heart disease has caused a renewed interest in the consumption of grapes and wines. The identification of similar compounds in peanut skins may result in similar consumer interest, improved sales, and increased value of peanuts. It is evident that peanut skins may be a potential untapped source for the extraction of natural food antioxidants, nutracueticals, and even pharmaceuticals.

The objective of this research is to identify compounds in peanut skin extracts which can be utilized as a natural antioxidant source for foods, with the potential use as nutraceuticals and/or pharmaceuticals. Enhancing the value of peanuts by increasing uses of their low-value byproducts could have several effects. The first advantage is additional value from extracts. Second, there could be renewed consumer interest in peanuts if valuable bioactive compounds are identified. Because peanut skins are largely a wasted resource to peanut processors, identifying novel polyphenols could have a significant financial impact on the value of peanuts.

The information available on the composition of polyphenols in peanut skins is incomplete. Some information has been previously reported on polyphenols present in peanut skins; however, few compounds have been identified due to the detection methods utilized in those studies. However, preliminary studies of the current research revealed that high quantities of unique compounds actually exist in peanut skin extracts. This study aimed to reveal these compounds by first using a preparatory Size Exclusion Chromatography (SEC) technique. Individual fractions were analyzed for total phenolic content using the Folin-Ciocalteau method, and antioxidant activity using the DPPH oxyradical scavenging method. Compounds in each fraction were identified using an ESI-HPLC-MS^n Ion Trap (MS/MS/MS) technique. This combination of methods has never been performed in the analysis of peanut skin extracts, and resulted in the discovery of novel phenolic and flavonoid-based compounds. The ultimate goal of utilizing HPLC-ESI-MS^n is not only to identify structures which have known antioxidant activity, but also determine if compounds are present which exhibit specific biological activities from a pharmaceutical and/or nutraceutical standpoint.

CHAPTER I: REVIEW OF THE LITERATURE

Peanut Industry

Arachis hypogaea, also known as the peanut or groundnut, is an important oilseed and food crop in many tropical/subtropical countries. The major peanut producing regions include India, China, Africa, and the United States (U.S.). Although the U.S. only produces roughly 10% of the world's peanut crops, it does however produce higher average yields per acre (~3,000lbs/acre) than the rest of the world (~1,000lbs/acre) due to more advanced technology production practices (Acquaah et al., 2005). Domestically, peanuts are an important agricultural crop in many Southern states. Total U.S. production in 2008 was 5.15 billion pounds, with Alabama, Florida, Georgia, North Caroline, South Carolina, and Texas having the highest production (USDA, 2009). In 2008, Georgia produced nearly three times more peanuts than Texas (2.33 billion vs 860 million lbs.), the next highest producing state. Other important top-ten producers included Oklahoma, Virginia, New Mexico and Mississippi.

In 2002, the Farm Bill caused drastic changes regarding the manner in which the federal government managed peanut production, moving from a quota system to a federal loan program. The years following this act saw a consistent drop in peanut production in the state of Virginia, from 235 thousand tons to 96 thousand tons. Comparatively, the total U.S. production fluctuated during this time, but remained somewhat stable (Boriss and Kreith, 2006). Increasing the value of peanuts for farmers and processors is difficult with low priced imports steadily eroding market share for American peanut farmers. For this reason, peanut farmers are constantly searching for new ways to create additional revenue streams from unutilized and underutilized peanut parts. (Fletcher et al., 2000).

Peanut Varieties

The four main market types of peanuts grown in the U.S. include Virginia, Runner, Spanish and Valencia. Spanish peanuts are largely grown in Texas and Oklahoma, while Valencia types are mainly produced in New Mexico and Texas. In the past 30 years, Runner peanuts have become the dominant type due to the enormous success of the Florunner variety. This variety was released by the University of Florida breeding program in 1969, and has seen excellent production characteristics under a variety of environmental conditions. However, other varieties have been released in recent years which out-perform Florunner, primarily Virginia-type peanut varieties. Virginia type peanuts are mostly grown in South-Eastern Virginia and North-Eastern North Carolina. The Gregory variety has become an increasingly popular Virginia type peanut, due to its extremely large pod size and low susceptibility to tomato spotted-wilt virus (which is a common problem with other peanut varieties) (Virginia Peanut Production Guide, 2009).

By-Products of the Peanut Industry

Some common uses of peanut kernels include: whole peanut products (such as roasted peanuts, peanut butter, peanut cake and meal), fermented peanut products, extracted products (such as peanut oil, peanut protein isolates, and peanut flour), and as inclusions or ingredients in candies and cookies. However, obtaining the kernels results in several by-products as a result of harvesting and production. After harvesting, peanut plants are either baled (for use as animal feed) or left in the field (Golden et al., 2001). Other than shell material (or hulls), one of the most notable by-products is peanut skins.

Peanut skins are a low value by-product of peanut blanching, which is the process of removing peanut skins (from peanuts) before roasting. Peanut skins also can be obtained as a by-product of the roasting process. A typical peanut mill may produce 17 tons of peanut skins per week. (Lee, 1996).

Peanut skins currently have almost no value, and sell for as little as $0.01 per pound. In most cases, they are utilized as a low-cost animal feed. It has been shown that peanut skins can be used in poultry and ruminant diets at levels around 5-10% (of the total diet) without negative consequences on growth rates. However, higher levels of feeding may result in lower growth performance, since tannins interfere with protein utilization (Atuahene et al., 1989; Hill, 2002).

Crude skins obtained from milling contain small amounts of peanuts and peanut oil, although some blanchers have the ability to separate these components to produce highly pure skins. Peanut skins often are pelletized after blanching, which reduces their bulk density for easier handling/distribution (and also lowers the risk of fire). Several studies have shown that unutilized and underutilized parts of the peanut and peanut plant have significant concentrations of phenolic compounds that exhibit antioxidant and biological effects (Lou et al., 1999, 2001, 2004; Nepote et al., 2000; Wang et al., 2007; Yu et al., 2005, 2006). Therefore, the discovery of possible uses for these underutilized parts (such as natural antioxidants and/or nutraceuticals) could effectively turn these by-products into value-added commodities for peanut farmers.

Peanut Composition and Health

In recent years, peanuts have received significant attention regarding their possible role as a functional food. Peanuts were previously considered somewhat unhealthy, due to their high fat content of 50% w/w or more (Francisco and Resurreccion, 2008). However, in the last decade peanuts have been continually evaluated regarding their positive role in heart-healthy diets (Kris – Etherton et al., 1999). The benefits of consuming peanuts and peanut products have been shown to be associated with their nutritional profile, including essential fatty acids, and recent discoveries of bioactive components (Griel et al., 2004). The bioactive compounds, which have been presumed to induce beneficial health effects, include proteins, micronutrients, dietary fiber, plant sterols, and various phytochemicals (Kris – Etherton et al., 2002). Many of these compounds elicit their beneficial biological attributes by exhibiting antioxidant effects (Chun et al., 2005), inhibiting bacterial and viral activity (Moure et al., 2001), reducing cholesterol metabolism (Kris – Etherton et al., 2001), activating detoxification enzyme release in the liver (Percival, 1997), and reducing platelet aggregation (Pignatelli et al., 2000). Research continues to emerge revealing data showing the significant contribution that peanuts have on human health (Higgs, 2003).

Peanuts are considered one of the most concentrated foods on earth because of their high protein and oil content. Among high protein foods, peanuts have one of the highest caloric values. A whole peanut contains about 75-80% kernel, and 20-25% shell. A peanut seed consists of roughly 50% oil, 25% protein, 15% carbohydrate, 6% moisture, 2% fiber, and 2% ash. The oil in peanuts contain around 82% unsaturated fatty acids and is mainly comprised of oleic and linoleic acid. The high proportion of unsaturated fatty

acids gives peanut oil a high iodine value (measure of unsaturation) and low storage stability (Adsule et al., 1989).

Protein content in peanuts varies from 25-35% and is classified as albumin, arachin, glutelin, and conarachin. The main proteins are arachin and conarachin, which make up over 85% of the total protein content. The amino acid composition of peanut protein contains high levels of acidic amino acids and low amounts of sulfur-containing amino acids. Limiting amino acids include methionine, lysine, threonine, and very low amounts of tryptophan. Amino acids such as glutamic acid, aspartic acid, phenylalanine, and histidine react with sugars to contribute to the flavor quality of roasted peanuts (Adsule et al., 1989).

Florunner has been the most commonly grown peanut cultivar in the U.S. for many years. Florunner peanuts contain roughly 53% oleic acid and 27% linoleic acid. However, newer cultivars with better oil stability and quality have been released in the past few years. The University of Florida developed a high-oleic peanut (HOP) variety that contains approximately 80% oleic acid and 3% linoleic acid (Gorbet and Knauft, 1997). Altering the fatty acid composition allows for a product that has improved resistance to oxidation, therefore increasing overall flavor stability. According to Gorbet and Knauft (1997), the new peanut lines also have improved yields, grades, less pod spotting, and less damage from tomato spotted wilt virus.

The unique fatty acid composition of peanut oil allows peanuts to have a high nutritional value. The high oleic acid content, especially in HOP lines, is desirable because it has a hypocholesterolemic effect. Mono and polyunsaturated fatty acids have

been shown to lower blood serum cholesterol levels and low density lipoproteins, therefore reducing the risk of coronary heart disease (Shephard and Rudolph, 1991).

Peanut oil contains less than 1% unsaponifiable sterols, squalene, tocopherols, and other antioxidants and hydrocarbons. The antioxidants consist mainly of α- and β-tocopherols, 18.6 and 13.8 mg/100g, respectively (Adsule et al., 1989). The phospholipids in the oil consist of phosphatidyl-ethanolamines, serines, and cholines. In addition to oil, carbohydrates are also an important functional component of peanuts. Peanuts contain around 10-20% carbohydrates. In peanut flour, the majority of the carbohydrates are sucrose and starch. The carbohydrates are the precursors to many of the flavor characteristics found in roasted peanuts. Although many peanut lines have no significant variation in reducing sugar content, they do, however, reveal differences in total sugar content (Adsule et al., 1989).

Peanuts are a good source of vitamins and minerals. The main minerals contained in peanuts include phosphorus, calcium, magnesium, and potassium. Variations in minerals such as iron, copper, manganese, and zinc can be found among different lines. Although peanuts contain only small amounts of vitamins A, C, and D, they are a good source of B vitamins. Peanut kernels contain high amounts of niacin, thiamin, riboflavin, panthothenic acid, pyridoxine, biotin, inositol, and folic acid (Adsule et al., 1989).

In recent years, peanut kernels have been shown to contain significant levels of phytochemicals, specifically resveratrol (Sanders and McMichael, 2000). Resveratrol (3,5,4'-trihydroxy-stilbene) has been shown to exhibit several beneficial biological activities, including the reduced risk of cardiovascular disease (Goldberg and Soleas, 1999) and cancer (Jang et al., 1997). Resveratrol is a stilbene compound, which is

produced by the peanut plant as a defense mechanism against exogenous stimuli, such as fungi and UV light (Ingham, 1976). In addition to peanuts, this compound has been reported in numerous types of plants including grapes (Jeandel et al., 1991), and has also been shown to be one of the possible compounds responsible for the human health benefits that are associated with the consumption of red wines (Siemann and Creasy, 1992). Numerous researchers have taken a great interest in the compound resveratrol because of its alleged role in the French Paradox (Frankel et al., 1993; Kopp, 1998), which states that the French have relatively low incidences of cardiovascular disease while having high intakes of saturated fats (and other risk factors). A study by Wu et al. (2001) supported this theory by confirming the cardioprotective attributes of resveratrol. Interestingly, the presence of resveratrol was discovered in peanuts long before it gained attention for its important biological properties (Ingham,1976). Resveratrol has been detected in commercial peanut products at a concentration range of 0.06 ppm in roasted peanuts to 5.1 ppm in peanut butter (Sobolev and Cole, 1999), which is similar to the 0.6 – 8.0 ppm levels found in red wine (Sanders et al., 2000).

In addition to peanut kernels, recent studies have shown that by-products of the peanut industry, including unutilized and underutilized portions such as peanut roots, leaves, and hulls, contain compounds that have potential health benefits. Peanut roots have been shown to contain resveratrol and other bioflavonoids which exhibit antioxidant and nutraceutical characteristics (Dean et al., 2008). Of significant importance is the concentration of resveratrol in peanut roots, which was reported to be much higher than that found in red wines (Chen et al., 2002; Liu et al., 2003). Variations in resveratrol levels were reported by Chen et al. (2002), which showed extremely high levels (up to

1330 ppm) during one growing season, but much lower levels the next season (27 – 37 ppm). Resveratrol is a phytoalexin which is produced (by a plant) as a defense mechanism, therefore, year to year variations may be a factor related to changes in disease incidence (or other plant stressors) that initiates synthesis of these types of compounds. Another study reported resveratrol concentrations of over 114 ppm in peanut roots (Liu et al., 2003), which is significantly higher than the levels found in red wines.

In addition to resveratrol, another study (Dean et al., 2008) reported the existence of flavones and isoflavones in peanut roots. This study also reported extremely high levels of phenolic compounds in peanut leaves, which exhibited powerful antioxidant activities. Other studies that investigated extracts from peanut hulls revealed powerful antioxidant activities due to the presence of phenolic compounds such as luteolin (Duh et al., 1992; Yen and Duh, 1995), which also has been shown to exhibit anti-cancer activities (Chowdhury et al., 2002).

One of the most interesting by-products of the peanut industry, from a phenolic and bioflavanoid standpoint, is peanut skins. Peanut skins have been used in traditional Chinese medicine for centuries for the treatment of disorders related to atherosclerosis, ulcers, mucous secretion inhibition, inflammation, liver/kidney problems, and hypertension (Haslam, 1996, 1998; Shahidi and Naczk, 1996). Peanut skins were thought to be toxic to humans in the early 1940's; however, a study by Dr. Jack Masquelier at the University of Bordeaux in France, showed that peanut skins were in fact non-toxic. The study also revealed that peanut skin extracts had the ability to protect and strengthen blood vessels (Louis et al., 1999). Recent studies have revealed the presence of

important phenolic-based compounds in peanut skins, such as isoflavones, isorhamnetin, quercetin, catechin, epicatechin, resveratrol, and proanthocyanidins (Lou et al., 1999, 2001; Yu et al., 2005). These compounds have been shown to exhibit powerful free-radical scavenging effects (Lou et al., 2001; Shahidi et al., 1997), and also have been reported to be responsible for the health benefits associated with wine and other plant products (Goldberg et al., 1998; Kampa et al., 2000; Kim et al., 2000; Kinsella et al., 1993). Phenolic compounds such as catechin and resveratrol have been shown to lower LDL oxidation *in vivo* (Andrikopolous et al., 2003; Das et al., 1999; Frankel et al., 1993; O'Byrne et al., 2002). Other researchers have reported that resveratrol has a wide range of other beneficial biological effects, such as vasodilation via endothelium dependant relaxation (EDR) (Fitzpatrick et al., 1993, 2000), reduction of platelet aggregation (Pace-Asciak et al., 1995), and cancer prevention (Jang et al., 1997). It has been shown that peanut kernels contain up to 1.8 ppm of resveratrol; however, the reported levels detected in peanut skins were five times the concentration found in kernels alone (Sanders et al., 2000). These numbers equal or exceed the levels (0.6 – 8.0 ppm) found in red wines.

In addition to resveratrol, the phenolic flavonoid quercetin also has been shown to exhibit anti-cancer activities (Huang and Ferraro, 1992). DiSanto et al. (2003) reported that membrane receptors involved in the coagulation cascade (known as tissue factor), are down-regulated by both resveratrol and quercetin. Other compounds discovered in peanut skins that have potential human health benefits include A-type proanthocyanidins (Lou et al., 1999). Das et al. (1999) indicated that extracts of red wines, which included resveratrol and proanthocyanidins, are equally efficient in reducing damage related to myocardial ischemic reperfusion. This research revealed the significant function in

which these antioxidants play in protecting the heart during certain types of ischemic events.

Although the health benefits of flavonoid-based compounds is clear, their bioavailability is somewhat ambiguous. Manach et al. (2005) indicated that of the roughly 4,000 flavonoids that exist, the bioavailability of these compounds varies greatly. In addition, some of the most common dietary flavonoids do not have the most efficient bioavailability profile. Of the most abundant flavonoids, isoflavones have the highest bioavailability, followed by catechin, flavanones, and quercetin-based glycosides. The lowest bioavailability profile among the flavonoids is exhibited by proanthocyanidins, galloylated catechins, and anthocyanins (Manach et al., 2005).

Phenolic Compounds in Peanuts and Other Plants

Peanuts fall into the plant family known as *Fabacea*. These species are classified as dicotyledonous plants that produce legume or loments fruit (such as peanuts, peas, and beans), and have root nodules containing bacteria that fix nitrogen (Hopkins and Huner, 2004). As in the case of all plant species, this family uses the process of photosynthesis to produce energy gathered from the sun. This harnessed energy results in the formation of sugars via the photosynthetic pathway, which are then utilized in further plant functions and metabolism. One of the most important nutrients in plant metabolism is nitrogen, which is also one of the most abundant in plants. Obtaining nitrogen is a crucial requirement in plant metabolism for the creation of plant metabolites, proteins, and acids (Vance, 2002). Legumes form root nodules, which contain a symbiotic bacteria known as *Rhizobia*. These bacteria produce the enzyme nitrogenase, which reduces nitrogen gas

to ammonia (which can then be used for metabolic processes). Legumes are capable of nitrogen fixation via symbiotic interaction between the roots and *Rhizobia* bacteria. These bacteria form in the root nodules due to compounds released by the plant called chemoattracts, which include phenolic flavonoids, isoflavonoids, carboxylic acids, aromatic acids, and amino acids. Not only do these compounds aid in the growth of *Rhizobia* bacteria, but they also provide a nutrient source and function in plant defense (Daroka and Phillips, 2002). According to Vance (2002), nodulation in legume plants is initiated by flavonoids and isoflavonoids such as luteolin, hesperitin, daidzein, and apigenin. In addition, isoflavonoids are important inhibiters of certain diseases, and act as phytoalexin antiobiotics during microbial infections. The accumulation of these isoflavonoids also inhibits the growth of attacking organisms (Burns et al., 2002; Chung et al., 2003).

Plant materials contain numerous classes of phenolic and polyphenolic compounds. As part of their structure, plants produce a complex set of secondary metabolites which incorporate phenolic rings with hydroxyl (and sometimes methoxy) substitutions. From a biological standpoint, minor structural differences can have drastic effects on chemical and biological activities. These chemical and biological attributes depend on factors such as structural class, degree of hydroxylation, degree of methoxylation, the presence of substitutions such as glycosidic (sugar) side-groups, and conjugations among A and B rings (Francisco and Resurreccion, 2008).

A significant amount of research has been conducted on phenolic compounds over the last decade, and over 6,000 different flavonoids are currently known (Harborne and Williams, 2000). In addition, about 400 flavone aglycones, 450 flavonol aglycones,

350 flavanone aglycones, 300 isoflavone aglycones, 19 anthocyanidins, and 250 chalcone aglycones have been reported (Iwashina, 2000). Results from these studies have literally created a new food trend, in which foods are now considered "healthy" if they contain certain concentrations of flavonoid compounds (Escarpa and Gonzalez, 2001). This increase in interest regarding phenolic-based compounds was sparked by the phenomenon known as the French Paradox, which attributed phenolic antioxidants in red wine to low rates of coronary heart disease in France (Frankel et al., 1993).

Phenolic compounds are an extremely diverse class of secondary plant metabolites, which are found in most types of plant species. These compounds include phenolic acids, flavonoids, chalcones, coumarins, and tannins (Anderson and Markham, 2006). The presence of polyphenolic structures are a result of the shikimic acid and acetate pathways (Fennema, 1996). Different types of phenolic acids include hydroxycinnamic and hydroxybenzoic acids, which encompass the majority of phenolic acids found in the plant kingdom (Wrolstad et al., 2005). Flavonoids are considered the most abundant of phenolic compounds found in plants. They constitute a relatively large family of aromatic molecules that are derived from shikimic acid and phenylalanine (Figure 1). Flavonoids are classified according to their structures, and include the flavones, isoflavones, flavonols, isoflavonols, flavanones, isoflavanones, flavanols, isoflavanols, flavanes, dihydroflavonols, flavandiols (leucoanthocyanins), anthocyanins, proanthocyanins and procyanidins (condensed tannins) (Havsteen, 2002). Flavonoids such as flavones (apigenin, luteolin), flavonols (quercetin, myricetin, kaempferol, and isorhamnetin), flavanones (eriodictyol, hesperitin, and naringenin), isoflavones (genistein, daidzein), and flavan-3-ols (or flavanols, such as catechin and epicatechin) are

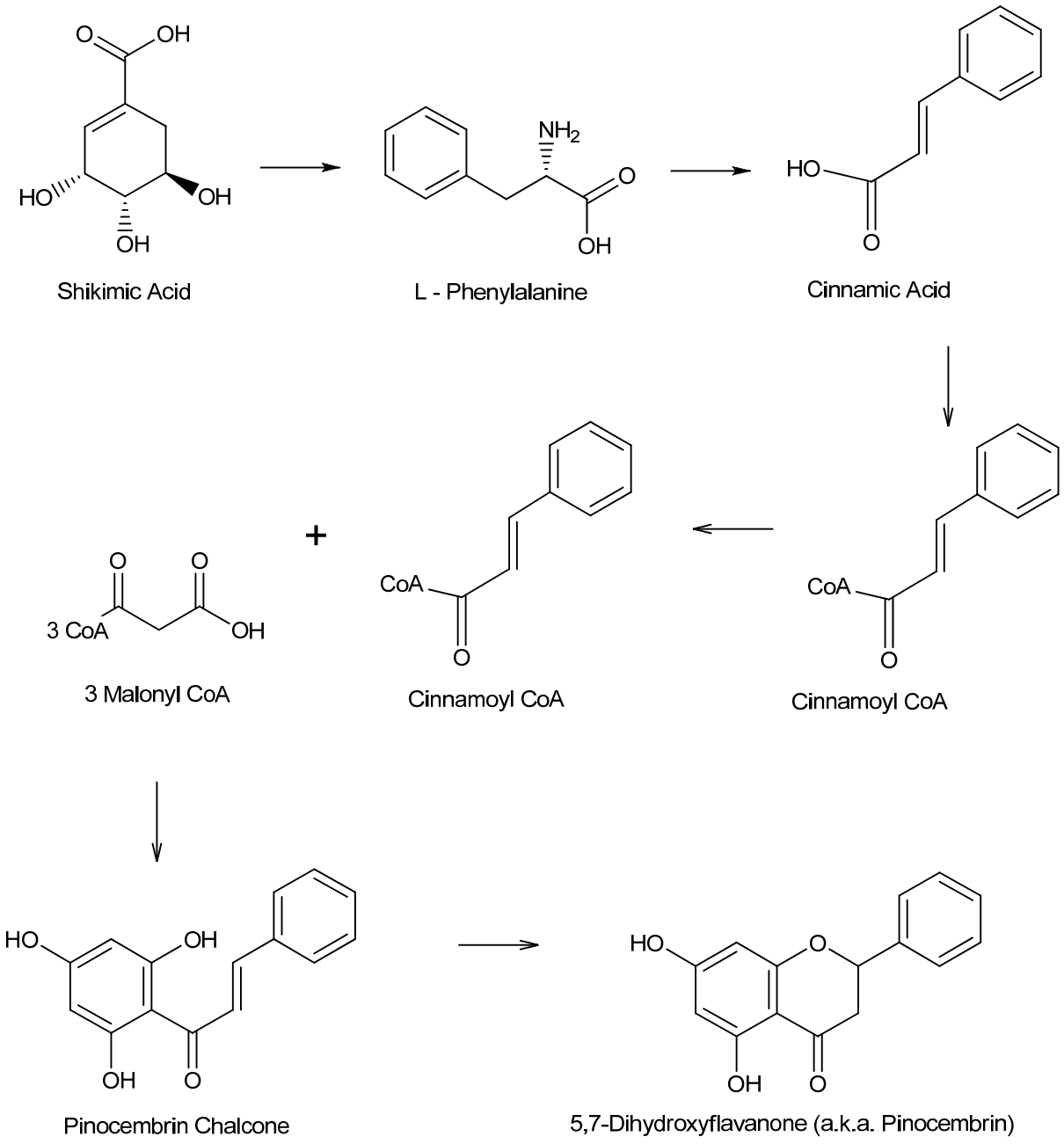

Figure 1: Shikimic Acid Pathway: Example of the Shikimic Acid Pathway for 5,7-dihydroxyflavanone (a.k.a. Pinocembrin).

common and widely distributed in plants. Based on the flavonoid nucleus structure below (Figure 2), flavanols are missing the 2,3-double bond and 4-one structure (Rice-Evans et al., 1997). Flavones and flavonols exhibit similar C-ring structures, with both having double bonds at the 2,3 position (although, flavones lack a hydroxyl group at the 3-position) (Hollman and Arts, 2000). Most of these compounds exhibit low molecular weights; however, polymeric tannins can have molecular weights up to 30KDa. Higher molecular weight tannins have been a topic of research for years, due to their binding of dietary proteins and enzymes, which lowers their digestibility. Tannins are hydrolysable, and can be split into gallic or ellagic acids (and other condensation products), and then re-condensed. The monomer units that form condensed tannins include flavan-3-ols (catechin, epicatechin). These structures can be hydroxylated at the 4 position on the flavonoid C-ring to form leucoanthocyanins (flavan-3,4-diols) (Bravo, 1998). The polymers (or oligomers) of flavan-3-ols also are known as proanthocyanidins, and are the second most abundant of all naturally occurring phenolics. The size of a given proanthocyanidin molecule is governed by the degree of polymerization (Francisco and Resurreccion, 2008). Monomer units are typically linked via C4-C8 bonds, although C4-C6 bonds also are found. The oligomeric procyanidins (OPC's) formed by these types of bonds are called B-type procyanidins, due to the B-type linkages between the monomer units. In contrast, condensed tannins also can be linked via A-type linkages, which are formed when additional C2-C7 ether bonds result in a double-linkage of the flavan-3-ol monomer units (Rasmussen et al., 2005). Proanthocyanidins consist of only catechin and epicatechin monomer units, and are generally called procyanidins (Francisco and Resurreccion, 2008). A study by Karchesy and Hemingway (1986) reported that peanut

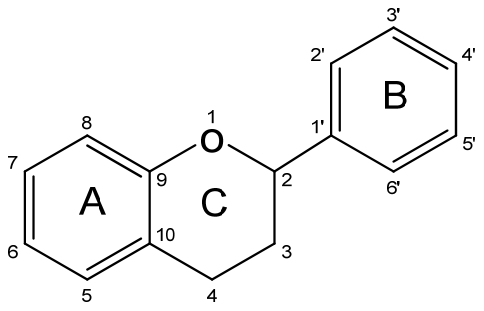

Flavonoid Nucleus

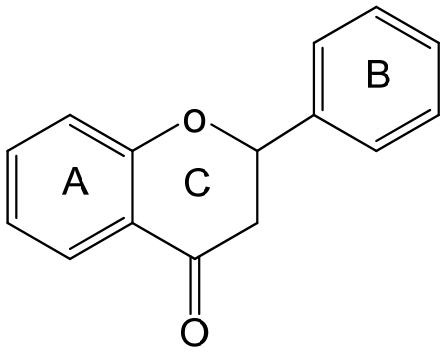

Flavanone

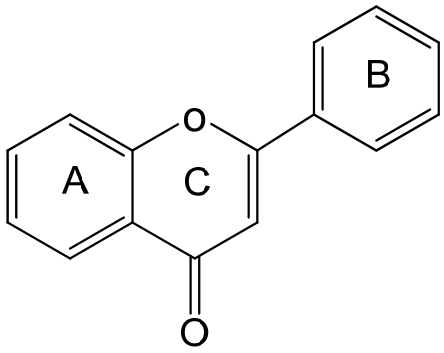

Flavone

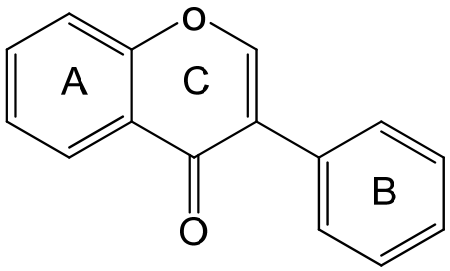

Isoflavone

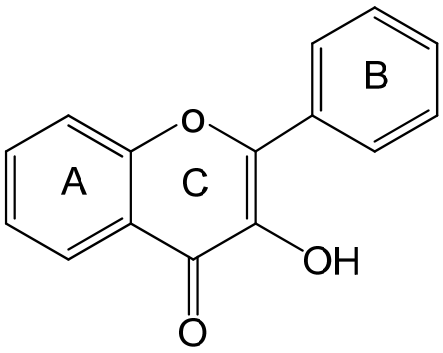

Flavonol

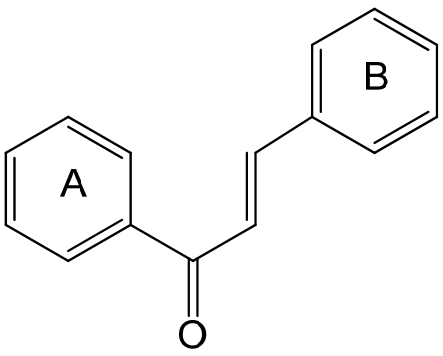

Chalcone

Figure 2: Flavonoid Classes: Showing flavonoid nucleas, and base-structures for the main flavonoid classes (including flavanone, flavones, isoflavone, flavonol, and chalcone).

skins contain approximately 17% procyanidins by weight, of which 50% were lower molecular weight oligomers. Studies by Lou et al. (1999, 2001) revealed six A-type proanthocyanidins (including types A-1 and A-2) and three newly discovered epicatechin oligomers in peanut skins. Further studies by Lou et al. (2004) indicated the presence of several B-type proanthocyanidins in peanut skins, including B-2, B-3, and B-4. Yu et al. (2006) reported the presence of both A-type and B-type procyanidin dimers, trimers, and tetramers in peanut skins.

The formation of flavonoids is part of the shikimic acid pathway, and results from a series of condensation reactions among cinnamic acids (between B-ring and carbon atoms 2, 3 and 4 of the C-ring) and malonyl residues (A-ring), forming a C6—C3—C6 base structure (Figure 1). The bridge (of three carbons) between the phenyl rings is often cyclized to form a third ring, which becomes the flavonoid C-ring (Cuyckens and Claeys, 2004). Depending on the cyclization reaction, and the degree of unsaturation and oxidation of the three-carbon segment, the resulting flavonoid can be classified into several groups (Cuyckens and Claeys, 2004).

The foundation for the numerous configurations exhibited by all flavonoids is the basic flavonoid nucleus structure (Figure 1). Some of the fundamental structures which make up the skeletons for various flavonoid classes also can be found in Figure 1. Individual compounds in each class are distinguished by the pattern of substitution(s) on the flavonoid A and B rings (Pietta, 2000; Stalikas, 2007). Groups of flavonoids are classified by hydroxylation of the basic nucleus structure, and many of these phenolic compounds exist as glycosides (i.e., sugar-linked). Using the numbering system denoted in Figure 1, glycosylation often occurs on the number 3 carbon on the flavonoid C-ring.

However, glycosylation also can occur at other positions on the flavonoid ring, including the number 5 and 7 positions (Cuyckens and Claeys, 2004). Common glycosidic units include glucose, galactose, arabinose, and rhamnose.

Oxidation and Antioxidants

The process in which electrons are removed from atoms or pairs of atoms is known as oxidation. The molecule then becomes oxidized via the loss of an electron. At the same time, another molecule may become reduced from receiving an electron (via oxidation-reduction reactions). The end result is of specific importance because of the formation of free radicals (Lee et al., 2003; Wong and Pavlath, 1992). Free radicals that are oxygen-centered are known as reactive oxygen species. Chemical reactions involving reactive oxygen species are of particular concern because they are thought to cause adverse biological effects such as cancer, heart disease, accelerated aging, and damage to cell membranes (Nijveldt et al., 2001; Steinberg, 1993). In addition to human health, free radical chain reactions via the autoxidation of lipids are an issue in the food industry. Lipid oxidation can result in decreased shelf-life and the development of off-flavors in food products. Other undesirable side-effects include the reduction of quality and nutritional value. The rate of oxidation in lipids can be affected by several factors, including fatty acid composition, temperature, oxygen levels, relative humidity, surface area, radiant energy, and the presence of antioxidant compounds (Fennema, 1996; Dziezak, 1986). In addition to lipid oxidation, proteins also can undergo chemical oxidation, resulting in changes in chemical and physical properties due to protein cross-linking. Other mechanisms involve enzymatic oxidation, such as the oxygenation of

unsaturated fatty acids by lipoxygenase, polyphenol oxidase catalyzed browning reactions, and glucose to lactose converstion by glucose oxidase (Buford, 1988).

Traditional synthetic antioxidants, as well as natural antioxidants, work to inhibit oxidative processes in foods (Buford, 1988). Oxidative reactions can be chemical or enzymatic (Dziezak, 1986). One of the best examples of the oxidation mechanism involves the chemical oxidation of lipids. Lipid oxidation can occur either by photosynthesized oxidation or via autoxidation. The autoxidation process is a free-radical chain reaction involving three steps: initiation, propagation, and termination (Fennema, 1996). During initiation, loosely held hydrogen atoms are lost from the fatty acid, typically from carbons adjacent to double bonds on the carbon chain. Fatty acids with multiple double bonds undergo higher levels of oxidation based on the degree of saturation, since more allylic and doubly allylic sites are available for free radical formation. The removal of this hydrogen results in a fat free radical, which can react with oxygen to form peroxyl free radicals. Peroxyl free radicals can continue the oxidation chain reaction by acting as strong initiators (or catalysts), since they can remove additional hydrogen atoms from other fat molecules, and thereby triggering the prorogation step (McCord, 1994). During propogation, peroxyl free radicals strip hydrogen atoms from other lipids to form (relatively) stable hydroperoxides, resulting in an additional newly formed unstable fatty radical. This unstable fatty radical can continue the chain reaction by reacting with oxygen to create another newly formed reactive peroxyl free radical. The final step in the autoxidation process (termination) involves hydroperoxides breaking-down to form additional short-chain organic compounds, such as aldehydes, ketones, acids, and alcohols (all of which are the

contributors to off-flavors and off-odors associated with fat and oil rancidity) (Fennema, 1996). Autoxidation ends by the reaction between two unstable radicals, or when fatty free radicals react with a stable antioxidant radical. Antioxidants use two mechanisms to alter the free radical chain reaction. First, they can terminate oxidation during the initiation step by donating hydrogen atoms to fat free radicals, thereby reforming the fat molecule. Until the antioxidant compounds are used-up, this phenomenon can delay further oxidative reactions (Dziezak, 1986). Antioxidants also can function to break the chain-reaction by donating hydrogens to peroxyl free radicals, forming antioxidant free-radicals and hydroxperoxides (which are more stable than fat free-radicals). Antioxidant free radicals also are more stable than fat free radicals, because of the electron spin-resonance structure in the aromatic (phenolic) ring. (Buford, 1988; Dziezak, 1986; Fennema, 1996; McCord, 1994).

Many of the phytochemicals found in plants, such as tocopherols, carotenoids, acids (such as ascorbic acid), and phenolic-based compounds, exhibit some level of antioxidant activity. The level of antioxidant activity typically depends on the chemical compound itself, as well as the model system being used for study. The mode of the antioxidant activity can occur in several different ways. First, polyvalent phenolics may exert antioxidant activity by chelating effects, through the binding and deactivating of metal ions which have pro-oxidant activity. Many of these phenolic compounds can play a role as primary antioxidants by breaking the free radical chain reaction, or by scavenging or binding with active oxygen radicals such as superoxide anion (Reische et al., 2002).

The use of antioxidants can help prevent the formation of undesirable/unstable structures in foods which can lead to cellular damage. Multiple studies have been conducted on naturally-derived antioxidants to investigate the potential health impact of antioxidants contained in common foods. Many of these studies are based on the possible negative effects exhibited by synthetic antioxidants and preservatives utilized in the food supply (Peschel et al., 2006). Many researchers have begun to investigate the possible dangers associated with ingesting synthetic antioxidants, such as butylated hydroxytoluene (BHT), butylated hydroxyanixole (BHA), tertiary butylated hydroxyl-quinone (TBHQ), ethylenediaminetetraacetic acid (EDTA), and propyl gallate (PG). This has generated extreme interest in naturally-derived antioxidant compounds. The incorporation of natural antioxidants (as opposed to synthetically-derived) could have significant impacts on human health (Nepote et al., 2004). The use of natural antioxidants in herbs and spices (such as sage and rosemary) has been used for years in the meat industry; however, their applications are limited based on the significant herb flavor conveyed in the product (Chang et al., 1977).

Even though phenolic-based compounds are considered non-nutritive, they do however have significant health effects related to antioxidant activity. In recent years, a considerable amount of research has been conducted on phenolic compounds in relation to their antioxidant activity and ability to scavenge free-radicals (Buford, 1988; Escarpa and Gonzalez, 2001). In addition to their antioxidant defense mechanisms among biological processes, these phenolic-based compounds exhibit antioxidant properties which offer significant stability to food systems (Dziezak, 1986; Macheix and Fleuriet, 1998). Polyphenols in plants can perform the function of reducing agents, thereby acting

as hydrogen donators and quenchers of singlet oxygen. Phenolic compounds often found in nature that are capable of such reactions include p-hydroxybenzoic acid (or p-coumaric acid), chlorogenic acid, caffeic acid, ferulic acid, resveratrol, catechin, and epicatechin. Onions contain large quantities of quercetin, which is the main flavonol in the human diet (Yang et al., 2001). Flavonoids including catechin, epicatechin, kaempferol, quercetin (and their flavonoid-glycoside derivatives) have been previously found in teas and wine (Nijveldt et al., 2001), all of which exhibit powerful oxyradical quenching properties. Flavonoid antioxidant compounds also are found in many types of nuts, including walnuts (which have been shown to have the highest flavonoid content), pecans, pistachios, cashews and almonds (Yang et al., 2009). Reports by Shahidi and Naczk (1996) indicate that the polyphenolic content of peanut kernels is low, however, the content in the skins is much higher (Nepote et al., 2000). In addition, data have revealed that the antioxidant potential of compounds detected in peanuts can contribute to human health (Higgs, 2003).

Numerous studies on phenolic compounds extracted from by-products of the peanut industry have indicated they exhibit powerful antioxidant activity. A study on peanut hulls confirmed the presence of 5,7-dihydroxychromone, eriodictoyl, and luteolin (Daigle et al., 1985). In addition to the aforementioned compounds, another study identified three additional flavonoids (Lin et al., 1999). They also used a copper catalyzed LDL oxidation model system to mimic LDL oxidation in vivo. The results indicated that eriodictyol and luteolin had the greatest antioxidant activity. Other studies have investigated the antioxidant potential of peanut skin extracts. Pratt and Miller (1984) reported antioxidant activity in Spanish peanuts, although, with the skins left on

the kernels. They indicated the antioxidant activity was due to the flavonoid compound known as dihydroquercetin. Another study reported catechin, epicatechin, and oligomeric procyanidins (OPC's) in the form of dimeric flavonoids (Karchesy and Hemmingway, 1986). Later studies indicated these compounds (including proanthocyanidin A-1 and A-2) exhibited substantial inhibitory activity against hyaluronidase (Lou et al., 1999). The presence of ethyl protocatechuate also was identified in peanut skins, and was reported to have antioxidant activity in a linoleic acid model system (Huang et al., 2003). Crude methanol and ethanol extracts from the peanut skins of Florunner peanuts were reported to have high radical scavenging activity (Nepote et al., 2000). This study utilized a sunflower model system, which indicated that methanol and ethanol peanut skin extracts had lower antioxidant activity (at 500ppm) than BHT exhibited at 200ppm. This contradicts other studies that compared the antioxidant activity of peanut skin extracts to that of synthetic antioxidants (such as BHA, BHT, TBHQ, etc.). This is in part due to the incorporated mechanism of the sunflower oil anhydrous model system. Most antioxidant activity techniques measure the ability to scavenge free radicals, which is often considered a more efficient way of interpreting a compounds ability to act as an antioxidant. However, when measuring the antioxidant activity in food model systems, specific antioxidant compounds often can perform well, while others are inadequate. For this reason, oil model systems cannot easily predict a compound's antioxidant potential, since some compounds may be poor oxyradical scavengers in oil-based systems, but more powerful in other food models (or pure radical scavenging models).

As previously discussed, the activity in which each flavonoid plays in human health is determined by its chemical configuration. This also holds true regarding a flavonoids ability to act as an antioxidant. Antioxidant activity is generally governed by the positions and types (and number) of substitutions of the flavonoid nucleus. Antioxidant and chelating activity is directly related to the number of hydroxyl groups on the flavonoid structure. Plant phenolics exhibit what is known as primary antioxidant activity. These types of structures form stable products from free radicals by donating hydrogen or electrons, thereby terminating the free radical chain reaction. (Dziezak, 1986).

The potential industry development of naturally-derived antioxidants from plant sources not only could enhance the nutritional value of foods, but also aid in preservation. These raw extracts from fruits, vegetables, nuts, and other plant sources, have progressively become an important topic in the food industry because of their possible role as antioxidants from natural sources (Sang et al., 2002). Many consumers have become more aware of the possible dangers associated with synthetic-based ingredients, specifically antioxidants and preservatives. The growing trend toward whole foods, organics, and ingredients from natural sources has been largely due to increased education into practices utilized by the food industry. This move toward more healthy foods also impacts research into natural sources in which to extract compounds with possible antioxidant activity. Many of the potential sources for these naturally-derived antioxidants come from by-products of the food industry, such as peels, seeds, and hulls (Lee et al., 2003). In order to retain the ability to germinate (and for long-term protection and preservation), seeds from plants typically contain powerful antioxidants around the

kernels or germs. Other than peanuts, an example of seed-coats (or skins) that contain flavonoids and flavonoid-glycosides with antioxidant activity are those found in almonds (Frison and Sporns, 2002; Milbury et al., 2006; Wijeratne et al., 2006). In addition, leaves and barks are typically exposed to sunlight and oxygen, and often contain antioxidants to protect against UV light and oxidation. Diverse by-products of the agricultural industries are produced in immense volumes, and signify an enormous underutilized resource (Francisco and Resurreccion, 2008). This could have a huge impact on both the economy and environment, by reducing disposal of typical waste-products through the creation of renewable uses from by-products such as natural antioxidants, functional foods and nutraceuticals. Other economic implications would be a function of added revenue through the creation of value-added commodities for specific agricultural industries. However, many challenges exist including those associated with extracting and isolating these compounds from the raw agricultural product. Other factors include the cost of such procedures, the possibility of environmental waste, and the simultaneous extraction of other unwanted compounds.

Extraction Methods

The utilization of an extraction method is critical for the removal of phenolic-based compounds from plant sources. The process of extraction is a common laboratory procedure to carry out the isolation and/or purification of compounds from a source. Typical methods include liquid-liquid, solid-liquid, and acid-base extractions (Moure et al., 2001; Shi et al., 2005; Silva et al., 1998). Many different forms of these methods have been incorporated for isolating active compounds from plants with varied levels of

success. Methods are selected based on the original sample form, the desired resulting form, and the further analytical methods used after extraction. Extraction methods are also custom-tailored to allow certain physical and chemical properties of the extracted components to remain intact. The majority of extraction methods for plant-related compounds utilize a form of solid-liquid extraction, in which a solid material comes in direct contact with a liquid solvent (Houghton and Raman, 1998). Organic solvents (such as ethanol) are commonly used, which solubilize compounds of similar polarity by diffusing into solid plant material. Solvents often are chosen based on the class of compounds being extracted. Polar organic solvents include water, methanol, and acetone, and are used to extract polar structures. Nonpolar solvents such as hexane and dichloromethane are typically utilized for the extraction of nonpolar compounds. (Moure et al., 2001; Shi et al., 2005; Silva et al., 1998)

Several prior studies have been conducted that investigated the yield of peanut skin extracts using various solvents. Huang et al. (2003) indicated that polar solvents offered better extraction yields than less polar solvents. Yu et al. (2005) showed that methanol and ethanol were more efficient than water for extracting phenolic-based compounds. The use of methanol as an extraction solvent yielded roughly 200mg extract per gram peanut skin. Additional studies that incorporated ethanol as an extraction solvent offered approximately 50% (or more) reduction in extraction efficiency. Wang et al. (2007) showed 0.107 ± 0.003g extract per gram peanut skin. Other reports indicated that the utilization of ethanol resulted in extracts of 0.051g (Huang et al., 2003) and 0.099g (Nepote et al., 2005) per gram peanut skin. In addition, several groups have examined the optimum solvents for extracting antioxidants from peanut hulls. Duh et al.

(1992) revealed that methanol resulted in more than 50% higher yields of antioxidant extracts from peanut hulls when compared to ethanol (other solvents gave even lower yields). The difference in extraction yield (between methanol and ethanol) also was revealed in this study. Conversely, Li et al. (1995) reported that extracts using ethanol had the most potent antioxidant activity. The compounds that exhibited antioxidant activity extracted from peanut hulls then was investigated by Lin et al. (1999). They reported the strongest antioxidant effects in a model system of copper catalyzed low density lipoprotein (LDL) using the main extracted components, luteolin and eriodictoyl (structural difference is double bond at C3 in flavonoid structure). Although peanut hulls contain compounds with significant biological activity, their potential as a suitable raw material for the extraction of bioactive compounds is relatively low (versus peanut skins) based on their low bulk-density.

In the case of peanut by-products, several other factors can have an effect on the extraction levels of phenolic-based compounds. Yu et al. (2005) indicated that blanched peeling greatly reduced the concentration of total phenols in methanolic peanut skin extracts versus direct peeling or roast peeling (11.6 mg/g versus 90.1 mg/g and 96.7 mg/g respectively). The lower total phenolic content in that study was assumed to be due to the leaching of phenolics out of the skin (into the water) during the blanching process. A similar result was obtained in a prior study on the total phenols contained in peanut hulls. Yen and Duh (1995) showed significant differences in the total extracted phenolic concentration (including the total luteolin content) in various peanut hulls obtained from different cultivars. This shows that in addition to peanut hulls, other forms of peanut by-

products (such as peanut skins) can contain varying levels of extracted phenolics based on differences in cultivars.

One of the most notable methods for the extraction of phenolic antioxidants from peanut skins was reported by Ballard et al. (2009). The extraction technique developed for this study incorporated a novel response surface methodology to estimate the optimum extraction conditions for several solvents, including methanol, ethanol, and water. The study determined the optimum solvent concentration, temperature, and time required for maximum extraction of phenolic antioxidants (such as resveratrol) from peanut skins. The data obtained from this study could increase the potential for peanut skins to become a viable extraction medium for naturally derived antioxidants, and also provide efficient methods for extracting bioactive compounds from this plant source.

Antioxidant Activity Methods

Several different methods exist that are capable of measuring the antioxidant activity of plant phenolics and extracts. These techniques work in several different manners, which typically concentrate on one reaction mechanism. These actions include the ability to scavenge oxygen and hydroxyl radicals, chelate metal ions, reduce lipid peroxyl radicals, or inhibit lipid oxidation. One method, known as the Oxygen Radical Absorbance Capacity (ORAC), is used to verify the ability of an antioxidant compound to scavenge free radicals generated by a given system. Another method that utilizes this mechanism is the Trolox Equivalent Antioxidant Capacity (TEAC). Other mechanisms include the ability of an antioxidant to inhibit lipid peroxidation products, such as malonaldehyde by way of Thiobarbituric Acid Reactive Substances (TBARS) (Nielsen et

al., 1993). Additional methods simply measure the capacity of an antioxidant to scavenge free radicals, such as in the case of the DPPH assay (2,2-diphenyl-1-picrylhydrazyl) (Re et al., 1999). DPPH is often used for its simplicity in analyzing antioxidant capacity (Huang et al., 2005). The reaction involves the ability of a sample to donate electrons (or hydrogen) in order to quench DPPH radicals. The overall mechanism imitates the ability of an antioxidant to inhibit free radical chain reactions via hydrogen atom transfer. As free radicals become quenched (by the presence of an antioxidant compound), the DPPH solution changes from a puruple to yellow color. The reduction in absorbance at 520nm is a direct indication of quenching capacity (Brand-Williams et al., 1995; Koleva et al., 2002). This method was used to successfully compare the antioxidant capacity of crude peanut skin extracts to that of BHA (a common synthetic preservative). The study by Wang et al., (2007) revealed a significant increase in the scavenging activity of peanut skin extract over BHA, and indicated that significantly lower levels of extract were required (versus BHA) to scavenge 50% of the radicals in the reaction mixture (known as the EC_{50} Value). Another study by Yu et al. (2006) utilized the DPPH method to show significant differences in antioxidant activity between direct peeled, blanched, and roasted peanut skin extracts.

Total Phenols Method

The assay known as the total phenolic method was developed by Singleton and Rossi (1965), which is a colorimetric technique utilizing a chemical reduction of the Folin-Ciocalteau reagent. The procedure involves the addition of the Folin-Ciocalteau reagent for a period of two hours in a dark environment. Metal oxides contained within

the Folin-Ciocalteau reagent are reduced by phenols, which then absorb light at 765nm. The light intensity at this given spectrum is directly proportional to the phenolic concentration. A standard curve must be developed for each procedure, and is accomplished by plotting the concentration of a phenolic standard (such as gallic acid or catechin) versus the absorption intensity (Stevanato et al., 2004). The resulting concentration of phenolics is calculated as equivalents of a sample using the given standard curve, such as gallic acid equivalents (GAE) or catechin equivalents (CE). The most commonly used reference compound is gallic acid, based on the fact that it is highly pure, inexpensive, and often found in small amounts in plant materials (Wrolstad et al., 2005). In addition, gallic acid is highly stable, and the standard solution will only lose approximately 5% potency over a two week period (Waterhouse, 2006).

Analytical Methods for Separation and Identification

Many analytical difficulties exist in the identification of polyphenols in foods. According to Bravo (1998), information contained in literature regarding the composition and content of polyphenols in plants are not only incomplete, but also can be contradictory and difficult to compare. For this reason, a more standardized way of analyzing these compounds is needed. Few attempts have been made to create a systematic screening method for the identification of all types of flavonoids, glycosylated flavonoids, and other phenolic compounds from plant materials (Lin and Harnly, 2007).

The isolation and identification of phenolic-based plant extracts typically incorporates some form of chromatography. The term chromatography refers to a process in which chemical mixtures are separated into different components based on

variations among solutes (Anderson and Markham, 2006). The separation of individual components within a mixture of various substances is the main goal of utilizing this analytical technique. Compounds in a mixture are separated based on factors such as their affinity for a specific medium (or stationary phase), molecular weight, or solubility in a solvent. One commonly used method of identification is retention separation, in which retention is the measure of distance a substance moves (via mobile phase) in a chromatographic system between the time the sample is administered and when it is detected after traveling through a stationary phase (Nielsen, 1993). The point in which a compound is detected is known as its retention time. Compound retention may differ between systems based on environmental factors (such as temperature), and the utilized instruments (and their specific settings). Other variables include samples differences, and variations in mobile and stationary phases. For this reason, experiments using standard compounds must be conducted under identical experimental conditions in order to compare and validate results (Fennema, 1996; Nielsen, 1993).

Prior to analysis, many researchers utilize some form of preparatory technique before incorporating analytical methods. In addition to extraction methods, preparatory techniques should remove possible contaminants from the sample, which can reduce interference and thereby increase selectivity of the analytical method. Another aim of using preparatory methods includes converting the analyte into more suitable forms for detection and separation (Smith, 2003). In addition to typical sample preparation methods, such as filtration and liquid-liquid extraction, newer techniques are now incorporated to achieve specific results (Tura and Robards, 2002). For example, solid-phase extraction (SPE) is a fast and economical way of fractioning flavonoid-glycosides

and phenolic compounds prior to high performance liquid chromatography (HPLC) analysis (Chen et al., 2001). Another method which has seen increasing use in recent years for the separation of phenolic-based compounds into fractions (prior to HPLC analysis) is size-exclusion chromatography (SEC). Size-exclusion chromatography separates compounds based on size (or molecular weight). Utilization of this method (prior to analytical testing) results in better separation of compounds when using further HPLC analysis, and prevents the masking of compounds when using mass spectrometry techniques. Studies by Fitzpatrick et al. (2000) successfully utilized SEC (Toyopearl HW-40) to prepare grape-seed extracts for HPLC-MS^n analysis. In addition, Lou et al. (1999) used Toyopearl HW-40 SEC to separate phenolic compounds in peanut skin extracts, allowing for the further separation and identification of A-type proanthocyanidins.

The analysis of phenolics and polyphenolic flavonoids often include the incorporation of some form of gas liquid chromatography (GLC) or HPLC (Musingo et al., 2001). In general, gas chromatography (GC) techniques offer better sensitivity of that of HPLC for the analysis of food components. However, analysis of phenolic-based compounds using GC is impractical, since this method primarily analyzes volatile compounds of lower molecular weight. Therefore, HPLC techniques using various detection methods are commonly used. HPLC is a type of liquid chromatography that separates compounds dissolved in solvent solutions. An HPLC system consists of a mobile phase reservoir, a pump (typically a dual-reciprocating pump), an injector port, a column which contains a chromatographic stationary phase for separation of compounds, and a detector. Mobile phase compositions are typically altered during analysis in the

form of gradient elution, which changes the solvation power or polarity to allow for better separation of analytes (Anderson and Markham, 2006). This allows for the simultaneous detection of different types of phenolic-based compounds in a single run, such as hydrophobic flavonoid aglycones and hydrophilic glycosides. Solvents and modifiers are chosen based on the type of stationary phase, analyte, and detection method.

The use of HPLC has been the dominant method for the separation and characterization of phenolic-based compounds in the last several decades (Stalikas, 2007). For analytical HPLC analysis (qualitative and/or quantitative) of phenolic-based compounds such as flavonoids, the stationary phase, solvent system, and gradient program must first be optimized for maximum resolution/separation (Anderson and Markham, 2006). When properly configured, HPLC allows concurrent separation and analysis of phenolic-based compounds, along with their derivatives and degradation products. In addition, HPLC allows for the detection of analytes in low-concentration, even in the presence of interfering and coeluting structures.

One of the key advantages of HPLC for the analysis of phenolics is the diverse amount of columns (i.e., stationary phases) and detection methods. Separation typically takes place on various forms of extremely non-polar octadecylsilyl bonded (ODS) C_{18} reverse-phase columns. No single HPLC method exists that can properly elute all flavonoid-based compounds without difficulties related to co-elution or interference. In most cases, flavonoid-glycosides elute before aglycones on C_{18} columns. Flavonoids with higher numbers of hydroxyl groups will elute before less substituted derivatives (Crozier et al., 1997). Flavone C-glycosides generally elute at shorter retention times that

their O-glycosidic counterparts. Flavanones elute before flavones, due to the level of unsaturation between carbons 2 and 3 on the flavonoid C-ring. The use of acetonitrile-water or methanol-water mixtures (along with acid modifiers) is common for mobile-phase solvent systems. These solvents are compatible with ultraviolet-visible light (UV-vis) detectors, which typically operate at one of the optimum absorption bands utilized for the identification of flavonoid compounds. Band I operates at a maximum absorption range of 300 to 550nm (due to the substitution pattern and conjugation of the C-ring), while Band II has a maximum absorption range of 240 to 285nm (due to the flavonoid A-ring) (Stalikas, 2007; Wrolstad et al., 2005). To solve this problem, the use of photodiode arrays are commonly used in the detection of phenolic-based compounds, since they allow for the simultaneous detection at multiple wavelengths. However, the most commonly used wavelength for routine detection is 280nm, which represents a compromise between the two band ranges (Anderson and Markham, 2006).

In addition to HPLC-UV techniques, one of the most common methods available for the analysis of phenolic-based compounds is high performance liquid chromatography mass spectrometry (HPLC-MS). This technique combines the sample separation characteristics of HPLC with the ability to analyze the mass of analytes contained within a sample mixture. The use of a mass spectrometer enables the identification of structures which have been separated by an HPLC technique. This analytical technique allows for the measurement of compounds in the form of mass-to-charge ratios of analyte ions. The instrument generates a plot of intensity versus mass-to-charge ratio, and results are reported as a mass spectrum. A compound's mass spectrum is based on the distribution of fragment ions generated from the dissociation of a given analyte (Harborne and

Williams, 2000). The detection, interpretation, and identification of compounds is based on the theory that different structures often have unique molecular weights, and in most cases, dissimilar dissociation patterns. Understanding the dissociation pathways of different types of compounds allows researchers to properly interpret the various fragment ions in a mass spectrum, allowing for the identification of a given structure. In the case of flavonoid-based compounds, the dissociation scheme that occurs in a mass spectrometer is known as the Retro-Diels Alder (RDA) ring opening mechanism. An example of the fragmentation pattern as a result of the RDA mechanism can be seen below for catechin (Figures 3 and 4). Since all flavonoids follow this dissociation scheme, understanding this pathway allows for the possible MS interpretation of various flavonoid classes. Oligomeric flavonoids (such as procyanidins) have three characteristic fragmentation pathways, including Retro-Diels Alder, quinone methide (QM), and heterocyclic ring fission (HRF) cleavage (Gu et al., 2003).

Various types of mass spectrometric techniques can be applied to the analysis of phenolic-based compounds. One of the most powerful techniques for this type of analysis is multi-stage methods such as tandem mass spectrometry (MS/MS) or MS^n, combined with collision-induced dissociation (CID) (Appledorn et al., 2009). These methods allow for more detailed structural information when analyzing flavonoid-based compounds, such as: a) the type of substituent attached to the flavonoid base-unit (including carbohydrates such as mono- and polysaccharides), b) the aglycone base-unit, c) the stereochemistry of terminal monosaccharide units, d) interglycosidic linkages, e) locations of substituents on the aglycone, and f) the type of inter-flavonoid linkages (IFL) or inter-flavonoid bonds (IFB) (Cuyckens and Claeys, 2004). Although certain structural

characteristics can be deduced using LC-MS, the use of MS/MS allows for further structural identification when compared to single-step MS techniques. In many cases, even the use MS^n (MS/MS/MS) cannot determine full stereochemistry, which is typically left to techniques such as nuclear magnetic resonance (NMR). However, the use of MS/MS can be used to determine the prevalence of prior identified compounds, therefore minimizing the effort lost in their isolation. The use of multi-stage MS techniques also allows for the identification of labile compounds in solution, such as flavonoid acyl groups (Constant and Beecher, 1995).

The incorporated ionization source (entering the MS) and type of mass spectrometer can have a drastic effect on the identification of phenolic-based compounds. Rauha et al. (2001) reported that the use of electrospray ionization (ESI) in negative mode offers the highest sensitivity for the analysis of flavonoid compounds. However, even though positive ion CID spectra is the most frequently used method for the structural analysis of flavonoids, the use of negative ion CID spectra is considered to be more difficult to interpret (Cuyckens and Claeys, 2004). The combination of ESI with an ion trap analyzer is considered a powerful tool for the analysis of flavonoids, because it offers benefits of both ESI and MS^n (MS/MS/MS). Ion trap analyzers have the ability to store ions, isolate specific mass-to-charge (m/z), induce dissociation of desired ions, and then eject ions for mass analysis. The quadropolar field incorporated in the trap allows for the simultaneous capture of a wide range of m/z values. This is of particular interest, because it allows for the identification of multiple compounds that exhibit different molecular weights. Another advantage of ESI-MS^n (Ion Trap) for flavonoid-based compounds include the fact that it is considered a soft ionization process, allowing

molecular ions to undergo little fragmentation before it reaches the trap. This allows for the efficient identification of flavonoid-glycosides, due to their labile nature. First-order mass spectra only provide limited structural information except for molecular mass. However, the use of ESI-MS^n incorporates MS/MS analysis with CID to effectively fragment individual sugar compounds off the flavonoid aglycone. Further dissociation of the aglycone not only allows for the idenfication of both the mono- or polysaccharide moieties, but also the flavonoid monomer itself (Anderson and Markham, 2006).

Patentability

Several patents exist regarding phenolic-based compounds from plant extracts, and their uses in relation to specific chemical and biological activities. Several of these patents involve peanut skins, including the utilization of extracts to create a novel adjuvant and/or immunomodulator that can aid in the preparation of immunogenic compositions and vaccines. The invention also provides a method of stimulating acquisition of protective immunity by administering peanut skin extracts prior to vaccination (Mcdougald and Fuller, 2007). Another invention relates to food products, including confectionaries and pet foods, which incorporate polyphenols from nut skins (such as peanuts and/or almonds) or cocoa for the purpose of inducing vasodilation (Chevaux et al., 2008). Numerous patents exist regarding the chemical and biological activity of cocoa extracts. For example, one invention involves the use of polyphenolic compounds from cocoa (including monomers and oligomeric procyanidins) for bacterial inhibition, a dietary supplement, and a possible pharmaceutical (Romanczyk, Jr. et al., 2003). Another invention combines cocoa procyanidins with acetylsalicylic acid to form

an anti-platelet therapy (Schmitz, 2003), while another uses cocoa procyanidins alone to reduce postprandial oxidative stress and related pathologies (Schmitz and Romanczyk, Jr., 2001). A final example incorporates flavonoids (including flavones and flavanones) for the protection of ascorbic acid and ascorbyl compounds from oxidation (Schonrock and Kruse, 2004). The existence of these patents reveal that opportunities still exist regarding the patentability of future discoveries related to phenolic-based compounds from plant extracts, and their functions regarding possible chemical, biological, nutraceutical, and pharmaceutical activities.

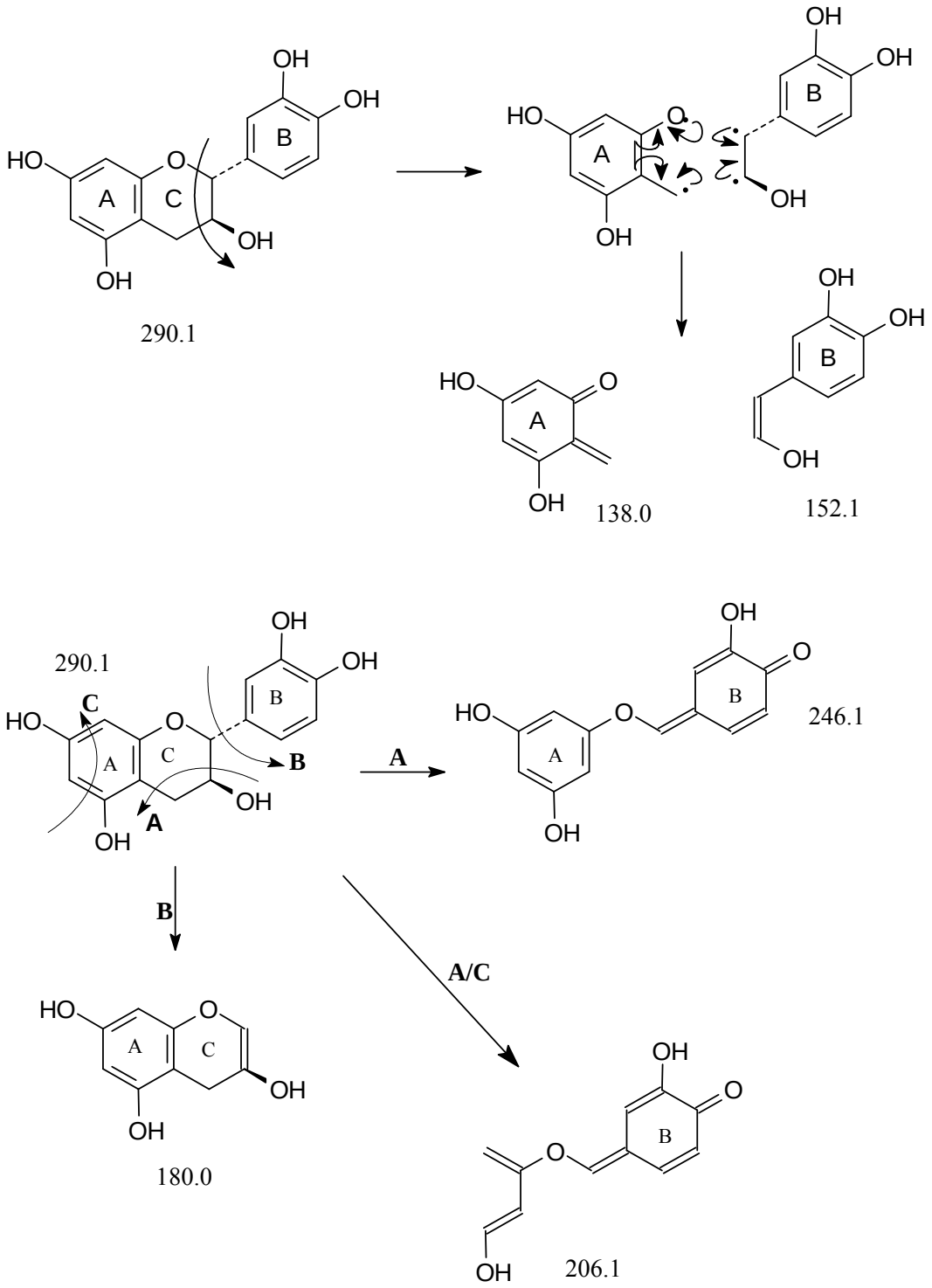

Figure 3: Retro Diels-Alder (RDA) Mechanism: Ring opening mechanism for catechin using negative mode ionization (Fiztpatrick, Fleming, O'Malley et al., 2000. Used with permisstion).

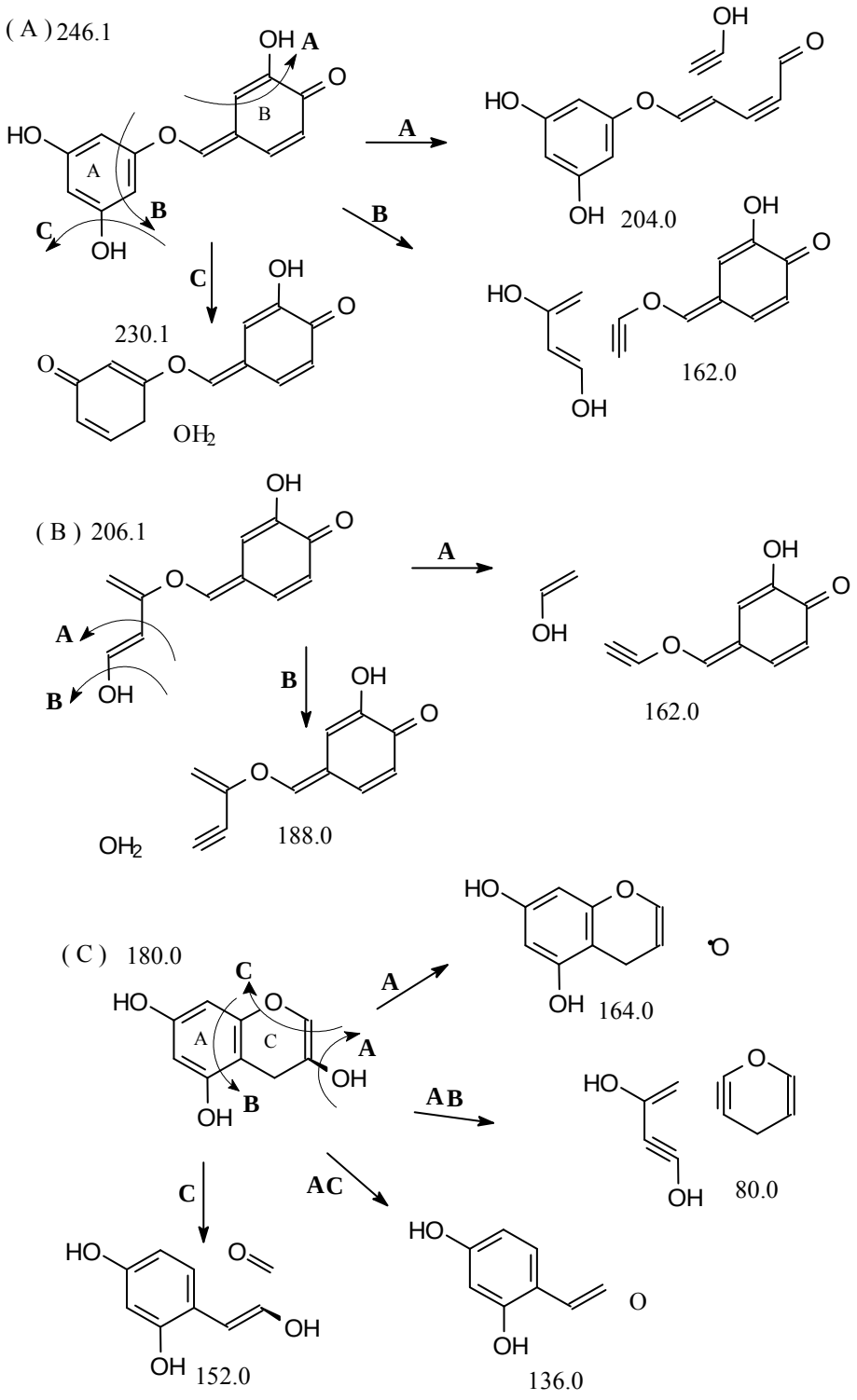

Figure 4: Retro Diels-Alder (RDA) Mechanism: Ring opening mechanism for catechin using negative mode ionization (Fiztpatrick, Fleming, O'Malley et al., 2000. Used with permisstion).

References

Acquaah, G. (2005). *Principles of Crop Production: Theory, Techniques, and Technology*. New Jersey: Pearson Education, Inc.

Adsule R. N., Kadam S. S., and Salunkhe D. K. (1989). *CRC Handbook of World Food Legumes: Nutritional Chemistry, Processing Technology, and Utilization. Vol II*. Boca Raton: CRC Press, Inc.

Anderson, O. M. and Markham, K. R. (2006). *Flavonoids: Chemistry, Biochemistry, and Applications*. Boca Raton, FL: CRC Press.

Andrikopoulos, N. K., Kaliora, A. C.; Assimopoulou, A. N. and Papageorgiou, V. P. (2003). Inhibitory activity of minor polyphenolic and nonpolyphenolic constituents of olive oil against in vitro low density lipoprotein oxidation. *J. Med. Food, 5*, 1-7.

Appledoorn, M. M., Sanders, M., Vincken, J.-P., Cheynier, V., Guernevé, C. L., Hollman, P. C. H., and Gruppen, H. (2009). Efficient isolation of procyanidin A-type dimers from peanut skins and B-type dimers from grape seeds. *Food Chem., 117*, 713-720.

Atuahene, C. C., Donkoh, A., and Mensah-Afoakwa, K. (1989). Value of peanut skins as a dietary ingredient for broiler chickens. *Br. Poultry Sci., 30*, 289-293.

Ballard, T. S., Mallikarjunan, P., Zhou, K., O'Keefe, S. F. (2009). Optimizing the extraction of phenolic antioxidants from peanut skins using response surface methodology. *J. Agric. Food Chem., 57*, 3064-3072.

Boriss, H. and Kreith, M. (Februrary 2006). *Commodity profile: peanut*. Agricultural Marketing Resource Center. Agricultural Issues Center, University of California: http://aic.ucdavis.edu/profiles/Peanuts-2006.pdf.

Brand-Williams, W., Cuveleir, M., and Berset, C. (1995). Use of a free radical method to evaluate antioxidant activity. *Lebensm. Wiss. Technol. 28*, 25-31.

Bravo, L. (1998). Polyphenols: Chemistry, dietary sources, metabolism and nutritional significance. *Nutr. Rev., 56*, 317-333.

Buford, R. (1988). Extending shelf life by using traditional phenolic antioxidants. *Cereal Foods World, 33*(2), 207-209.

Burns, J., Yokota, T., Ashihara, H., Lean, M. E. J., and Crozier, A. (2002). Plant foods and herbal sources of resveratrol. *J. Agric. Food Chem., 50*, 3337-3340.

Chang, S., Ostric-Matijasevic, B., Hsieh, O. A. L., and Huang, C. (1977). Natural antioxidants from rosemary and sage. *J. Food Sci., 42*, 1102-1106.

Chen, H., Zuo, Y., and Deng, Y. (2001). Separation and determination of flavonoids and other phenolic compounds in cranberry juice by high-performance liquid chromatography, *J. Chromatogr. A, 913*(1-2), 387-395.

Chen, R. S., Wu, P. L., Chiou, R. Y. Y. (2002). Peanut roots as a source of resveratrol. *J. Agric. Food Chem., 50*, 1665-1667.

Chevaux, K. A., Schmitz, H. H., and Romanczyk, L. J. (2008). Nut skin products. US patent 20080063690: http://www.freepatentsonline.com/y2008/0063690.html

Chowdhury, A. R., Sharma, S., Mandal, S., Goswami, A., Mukhopadhyay, S., and Majumder, H. K. (2002). Luteolin, an emerging anti-cancer flavonoid, poisons eukaryotic DNA topoisomerase I. *Biochem. J., 366*, 653-661.

Chun, O. K., Kim, D. O., Smith, N., Schroeder, D., Han, J. T., and Lee, C. Y. (2005). Daily consumption of phenolics and total antioxidant capacity from fruit and vegetables in the American diets. *J. Sci. Food Agric., 85*, 1715-1724.

Chung, I-M., Park, M. R., Chun, J. C., and Yun, S. J. (2003). Resveratrol accumulation and resveratrol synthase gene expression in response to abiotic stress and hormones in peanut plants. *Plant Sci., 164*, 103-109.

Constant, H. L. and Beecher, C. W. W. (1995). A method for the dereplication of natural product extracts using electrospray HPLC/MS. *Nat. Prod. Lett., 6*, 193-196.

Crozier, A., Jensen, E., Lean, M. E., J., and McDonald, M. S. (1997). Quantitative analysis of flavonoids by reversed-phase high performance liquid chromatography. *J. Chromatogr. A, 761*(1-2), 315-321.

Cuyckens, F. and Claeys, M. (2004). Mass spectrometry in the structural analysis of flavanoids. *J. Mass Spectrom., 39*, 1-15.

Daigle, D. J., Ory, R. L., and Branch, W. D. (1985). The presence of 5,7-hihydroxyisoflavone in peanuts by high performance liquid chromatography analysis. *Peanut Sci., 12*, 60-62.

Dakora, F. and Phillips, D. (2002). Root exudates as mediators of mineral acquisition in low nutrient environments. *Plants Soil, 245*, 35-45.

Das, D. K., Sato, M., Ray, P. S., Maulik, G., Engelman, R. M., Bertelli, A. A., Bertelli, A. (1999). Cardioprotection of red wine: role of polyphenolic antioxidants. *Drugs Exp. Clin. Res., 25*, 115-20.

Dean, L. L., Davis, J. P., Shofran, B. G., and Sanders, T. H. (2008). Phenolic profiles and antioxidant activity of extracts from peanut plant parts. *The Open Natural Prod, 1*, 1-6.

DiSanto, A., Mezzetti, A., Napoleone, E., Di Tommaso, R., Donati, M. B., De Gaetano, G., and Lorenzet, R. (2003). Resveratrol and quercetin down-regulate tissue factor expression by human stimulated vascular cells. *Thrombosis Hemostasis, 1*, 1089-1095.

Duh, P. D., Yeh, D. B., and Yen, G. C. (1992). Extraction and identification of an antioxidative component from peanut hulls. *J. Agric. Food Chem., 69*, 814-818.

Dziezak, J. D. (1986). Antioxidants: The ultimate answer to oxidation. *Food Technol, 40*(9), 94-101.

Edenharder, R., Keller, G., Platt, K. L., and Unger, K. K. (2001). Isolation and characterization of structurally novel antimutagenic flavonoids from spinach (*Spinacia oleracea*). *J. Agric. Food Chem., 49*, 2767-2773.

Escarpa, A. and Gonzalez, M. (2001). An overview of analytical chemistry of phenolic compounds in foods. *Crit. Rev. Anal. Chem., 31*(2), 57-137.

Fennema, O. (1996). *Food Chemistry*. New York: Marcel Dekker.

Fitzpatrick, D. F., Fleming, R. C., Bing, B., Maggi, D. A., and O'Malley, R. M. (2000). Isolation and characterization of endothelium-dependent vasorelaxing compounds from grape seeds. *J. Agric. Food Chem., 48*, 6384-6390.

Fitzpatrick, D. F., Hirshfield, S. L., and Coffey, R. G. (1993). Endothelium-dependent vasorelaxing activity of wine and other grape products. *Am. J. Physiol., 265*(pt 2), H774-778.

Fletcher, S. M. (2000). Peanuts. In D. Colyer, P. L. Kennedy, W. A. Amponsah, S. M. Fletcher, and C. M. Jolly (Eds.), *Competition in agriculture: the United States in the world market*. New York: The Haworth Press, Inc.

Francisco, M. L. D. L. and Resurreccion, A. V. A. 2008. Functional components in peanuts. *Crit. Rev. Food Sci. Nutr., 48*(8), 715-746.

Frankel, E. N., Waterhouse, A. L., and Kinsella, J. E. (1993). Inhibition of human LDL oxidation by resveratrol. *Lancet, 341*, 1103-1104.

Frison, S., and Sporns, P. (2002). Variation in the flavonol glycoside composition of almond seedcoats as determined by MALDI-TOF mass spectrometry. *J. Agric. Food Chem., 50*, 6818-6822.

Golden, P. (Sept. 2001). Perennial profit. In *Farm Progress,* (pp. 12-13).

Goldberg, D. M., Karumanchiri, A., Tsang, E., and Soleas, G. J. (1998). Catechin and epicatechin concentrations in red wines: Regional and cultivar related differences. *Am. J. Enol. Vitic., 49*(1), 23-34.

Goldberg, D. M. and Soleas, G. J. (1999). Analysis of antioxidant wine polyphenols by high-performance liquid chromatography. *Methods Enzymol., 299*, 122-137.

Gorbet, D. W. and Knauft, D. A. (1997). SunOleic97R peanut. Improved oil chemistry runner type. Florida Agricultural Experimental Station, Institute of Food and Agricultural Sciences, University of Florida: http://edis.ifas.ufl.edu/

Griel, A. E., Eissenstat, B., Juturu, V., Hsieh, G., and Kris-Etherton, P. M. (2004). Improved diet quality with peanut consumption. *J. Am. Coll. Nutr., 23*, 660-668.

Gu, L., Kelm, M. A., Hammerston, J. F., Beecher, G., Holden, J., Haytowitz, D., and Prior, R. L. (2003). Screening of foods containing proanthocyanidins and their structural characterization using LC-MS/MS and thiolytic degradation. *J. Agric. Food Chem, 51*, 7513-7521.

Harborne, J. and Williams, C. (2000). Advances in flavonoid research since 1992. *Phytochemistry, 55*(6), 481-503.

Haslam, E. (1996). Natural polyphenols (vegetable tannins) as drugs: Possible modes of action. *J. Nat. Prod., 59*, 205-215.

Haslam, E. (1998). *Plant Polyphenols, Vegetable Tannins Revisited*. Cambridge, England: Cambridge University Press.

Havsteen, B. H. (2002). The biochemistry and medical significance of the flavonoids. *Pharmacol. Ther., 96*, 67-202.

Higgs, J. (2003). The beneficial role of peanuts in the diet – Part 2. *Nutr Food Sci, 33*, 56-64.

Hill, G. M. (2002). Peanut by-products fed to cattle. *Vet. Clin. North Am. Food Anim. Pract., 18*, 295-315.

Hollman, P. C. H. and Arts, I. C. W. (2000). Flavonols, flavones and flavanols – nature, occurrence and dietary burden. *J. Sci. Food Agric., 80*, 1081-1093.

Hopkins, W. and Huner, N. (2004). *Introduction to Plant Physiology*. Hoboken, NJ: Wiley & Sons, Inc.

Houghton, P. and Raman, A. (1998). *Laboratory Handbook for the Fractionation of Natural Extracts*. New York: Chapman and Hall.

Huang, D., Ou, B., Pryor, R. (2005). The chemistry behind antioxidant capacity assays. *J. Agric. Food Chem., 53*, 1841-1850.

Huang, M-T., and Ferraro, T. (1992). Phenolic compounds and cancer prevention. Chapter 2 in "Phenolic Compounds in Foods and their Effects on Health II. In M-T. Huang. C-T. Ho, and C.Y. Lee (Eds.), *ACS symposium series 507*. Washington, DC: American Chemical Society.

Huang, S. C., Yen, G-C., Chang, L-W., Yen, W-J., and Duh, P-D. (2003). Identification of an antioxidant, ethyl protocatechuate, in peanut seed testa. *J. Agric. Food Chem., 51*, 2380-2383.

Ingham, J. L. (1976). 3,5,4'-trihydroxystilbene as a phytoalexin from groundnut (Arachis hypogeae). *Phytochemistry, 15*, 1791-1793.

Iwashina T. (2000). The structure and distribution of the flavonoids in plants. *J. Plant Res., 113,* 287.

Jang, M., Cai, L., Udeani, G.O., Slowing, K. V., Thomas, C. F., Beecher, C. W., Fong, H. H., Farnsworth, N. R., Kinghorn, A. D., Mehta, R. G., Moon, R. C., and Pezzuto, J. M. (1997). Cancer chemopreventative activity of resveratrol, a natural product derived from grapes. *Science, 275*, 218-220.

Jeandel, P., Bessis, R., and Gautheron, B. (1991). The production of resveratrol (3,5,4'-trihydroxystilbene) by grape berries in different developmental stages. *Am. J. Enol. Vitic., 42*, 41-46.

Kampa, M., Hatzogolu, A., Notas, G., Damianaki, A., Bakogeorgou, E., Gemetzi, C., Kouroumalis, E., Martin, P. M., and Castanas, E. (2000). Wine antioxidant polyphenols inhibit the proliferation of human prostrate cancer lines. *Nutr Cancer, 37*(2), 223-233.

Karchesy, J. J. and Hemingway, R. W. (1986). Condensed tannins: (4β→8;2β →O→7)-linked procyanidins in *Arachis hypogoea* L. *J. Agric. Food Chem., 34*, 966-970.

Kim, S., Lee, M. J., Hong, J., Li, C., Smith, T. J., Yang, G. Y., Seril, D. N., and Yang, C. S. (2000). Plasma and tissue levels of catechins in rats and mice during chronic consumption of green tea polyphenols. *Nutr Cancer, 37*(1), 41-48.

Kim, S. Y., Jeong, S. M., Park, W. P., Nam, K. C., Ahn, D. U., and Lee, S. C. (2006). Effect of heating conditions of grape seeds on the antioxidant activity of grape seed extracts. *Food Chem., 97*, 472-479.

Kinsella, J. E., Frankel, E., German, B., and Kanner, J. (1993). Possible mechanisms for the protective role of antioxidants in wine and plant foods. *Food Technol, 47*, 85-89.

Koleva, I. I., van Beek, T. A., Linssen, J. P. H., de Groot, A., and Evstatieva, L. N. (2002). Screening of plant extracts for antioxidant activity: A comparative study on three testing methods. *Phytochem. Anal., 13*, 8-17.

Kopp, P. (1998). Resveratrol , a phytoestrogen found in red wine. A possible explanation for the conundrum of the 'French paradox'? *European Endocrinol, 138*, 619-620.

Kris-Etherton, P. M., Hecker, K. D., Bonanome, A., Coval, S. M., Binkoski, A. E., Hilpert, K. F., Friel, A. E., and Etherton, T. D. (2002). Bioactive compounds in foods: Their role in the prevention of cardiovascular disease and cancers. *Am. J. Med., 113*(9B), 71S-88S.

Kris-Etherton, P. M., Yu-Poth, S., Sabate, J. Ratcliffe, H. E., Zhao, G. and Etherton, T. D. (1999). Nuts and their bioactive constituents: Effects on serum lipids and other factors that affect disease risk. *Am. J. Clin. Nutr., 70*(suppl), 504S-511S.

Kris-Etherton, P. M., Zhao, G., Kinkoski, A. E., Coval, S. M., and Etherton, T. D. (2001). The effect of nuts on coronary heart disease risk. *Nutr. Rev., 59*(4), 103-111.

Lee, J. (1996). USDA scientists find treasure in peanut skins. *Agricultural Research Service News, December 12, 1996*: http://www.ars.usda.gov/is/pr/1996/skins1296.htm.

Lee, K., Kim, Y., Lee, H., and Lee, C. (2003). Cocoa has more phenolic phytochemicals and higher antioxidant capacity than teas and red wine. *J. Agric. Food Chem., 51*(25), 7292 -7294.

Louis, R. (1999). Masquelier's OPC aids heart and immune system. *Well Being Journal, 8*, 1-3.

Li, B., Qingzan, Z., and Chen, C. (1995). Study on extraction of natural antioxidative components from peanut hulls. *Xian dai hua gong (Modern Chemical Industry), 10*, 31-33.

Lin, L.-Z. and Harnly, J. M. (2007). A screening method for the identification of glycosylated flavonoids and other phenolic compounds using a standard analytical approach for all plant materials. *J. Agric. Food Chem., 55*, 1084-1096.

Lin, Y. L., Shiao, M. S., Kuo, Y. H., and Tsai, W. J. (1999). Antioxidative principles from peanut hulls. *Chinese Pharmaceut (Taipei), 51*, 397-401.

Liu, C., Wen, Y., Chiou, J., Wang, K., Chiou, R. (2003). Comparative characterization of peanuts grown by aquatic floating cultivation and field cultivation for seed and resveratrol production. *J. Agric. Food Chem., 51*, 1582–1585.

Lou, H., Yamazaki, Y., Saski, T., Uchida, M., Tanaka, H. and Oka, S. (1999). A-type proanthocyanidins from peanut skins. *Phytochemistry, 51*, 297-308.

Lou, H., Yuan, H., Ma, B., Ren, D., Ji, M., and Oka, S. (2004). Polyphenols from peanut skins and their free radical-scavenging effects. *Phytochemistry, 65*, 2391-2399.

Lou, H., Yuan, H., Yamazaki, Y., Sasaki, T., and Oka, S. (2001). Alkaloids and flavanoids from peanut skins. *Planta Med., 67*, 345-349.

Macheix, J. and Fleuriet, A. (1998). *Flavonoids in Health and Disease*. New York: Marcel Dekker, Inc.

Manach, C., Williamson, G., Morand, C., Scalbert, A., and Remesy, C. (2005). Bioavailability and bioefficiency of polyphenols in humans. I. Review of 97 bioavailability studies. *Am. J. Clin. Nutr., 81*(suppl), 230S-242S.

McCord, J. M. (1994). Free radicals and prooxidants in health and nutrition. *Food Technol, 48*(5), 106-109.

Mcdougald, L. R. and Fuller, A. L. (2007). Novel peanut skin extract as a vaccine adjuvant. European patent EP20050733210: http://www.freepatentsonline.com/EP1742656.html.

Milbury, P. E., Chen, C.-Y., Dolnikowski, G. G., and Blumberg, J. B. (2006). Determination of flavonoids and phenolics and their distribution in almonds. *J. Agric. Food Chem., 54*, 5027-5033.

Moure, A., Cruz, J. M., Franco, D., Dominguez, J. M. Sineiro, J., Dominguez, H., Nunez, M. J., and Parajo, J. C. (2001). Natural antioxidants from residual sources. *Food Chem., 72*, 145-171.

Musingo, M. N., Sims, C. A., Bates, R. P., O'Keefe, S.F. and Lamikanra, O. (2001). Changes in ellagic acid and other phenols in muscadine grape (*Vitus rotundifolia*) juices and wines during storage. *Am. J. Enol.Vitic., 52*(2),109-114.

Nepote, V., Grosso, N. R., and Guzman, C. A. (2000). Antioxidant activity of methanolic extracts from peanut skins. *Molecules, 5,* 487-488.

Nepote, V., Grosso, N. R., and Guzman, C. A. (2002). Extraction of antioxidant compounds from peanut skins. *Grasas y Aceites, 53*, 391-395.

Nepote, V., Grosso, N. R., and Guzman, C. A. (2005). Optimization of extraction of phenolic antioxidants from peanut skins. *J. Sci. Food Agric., 85*(1), 33-38.

Nepote, V., Mestrallet, M. G., and Grosso, N. R. (2004). Natural antioxidant effect from peanut skins in honey-roasted peanuts. *J. Food Sci., 69*(7), S295-S300.

Nielsen, S. S. (1993). *Introduction to the Chemical Analysis of Foods.* London, England: Jones and Bartlett Publishers.

Nijveldt, R., Nood, E., Hoorn, D., Boelens, P., Norren, K., and Leeuwen, P. (2001). Flavonoids: Review of probable mechanisms of action and potential applications. *Amer. J. Clin. Nutr., 74*, 418-424.

Novus Research. (2009). Phenolic compounds in plants. *Research on Phytochemicals*: http://www.organicashitaba.com/pc.html.

O'Byrne, D. J., Devaraj, S., Gundy, S. M. and Jialal, I. (2002). Comparison of the antioxidant effects of concord grape juice flavonoids and α-tocopherol on markers of oxidative stress in healthy adults. *Am. J. Clin. Nutr., 76,* 1367-1374.

Pace-Asciak, C. R., Hahn, S., Diamandis, E. P., Soleas, G., and Goldberg, D. M. (1995). The red wine phenolics trans-resveratrol and quercetin block human platelet aggregation and eicosanoid synthesis: Implications for protection against coronary heart disease. *Clin. Chim Acta, 235*, 207-209.

Percival, M. (1997). Phytonutrients and detoxification. *Clinical Nutrition Insights, 5*(2), 1-4.

Peschel, W., Sanchez-Rabaneda, F., Diekmann, W., Plescher, A., Gartzia, I., Jimenez, D., Lamuela-Raventos, R., Buxaderas, S., and Codina, C. (2006). An industrial approach in the search of natural antioxidants from vegetable and fruit wastes. *Food Chem, 97*, 137-150.

Pietta, P. (2000). Flavonoids as antioxidants. *J. Nat. Prod., 62*, 1035-1041.

Pignatelli, P., Pulcinelli, F. M., Celestini, A., Lenti, L. Chiselli, A., Gazzaniga, P. P. And Violi, F. (2000). The flavonoids quercetin and catechin synergistically inhibit platelet function by antagonizing the intracellular production of hydrogen peroxide. *Am. J. Clin. Nutr., 72*, 1150-1155.

Pratt, D. E. and Miller, E. E. (1984). A flavonoid antioxidant in Spanish peanuts (*Arachis hypogoea*). *J. Agric. Food Chem., 61*, 1064-1067.

Rasmussen, S. E., Frederiksen, H., Krogholm, K. S., and Poulsen, L. (2005). Dietary proanthocyanidins: Occurrence, dietary intake, bioavailability, and protection against cardiovascular disease. *Mol. Nutr. Food Res., 49*, 159-174.

Rauha, J. P., Vuorela, H., and Kostiainen, R. (2001). Effect of eluent on the ionization efficiency of flavonoids by ion spray, atmospheric pressure chemical ionization, and atmospheric pressure photoionization mass spectrometry. *J. Mass Spectrom., 36*, 1269-1280.

Re, R., Pellegrini, N., Protegente, A., Pannala, A., Yang, M., and Rice-Evans, C. (1999). Antioxidant activity applying and improved ABTS radical cation decolorization assay. *Free Rad. Biol. Med., 26*, 1231-1236.

Reische, D. W., Lillard, D. A., and Eitenmiller, R. R. (2002). Antioxidants. In C. C. Akoh and D. B. Min (Eds.) *Food Lipids, Ch 15.* (pp. 489-516). New York: Marcel Dekker.

Rice-Evans, C. A., Miller, N. J., and Paganga, G. (1997). Antioxidant properties of phenolic compounds. *Trends Plant Sci, 2*(4), 152-159.

Romanczyk, Jr., L. J., Hammerstone, Jr., J. F., Buck, M. M., Post, L. S., Cipolla, G. G., McClelland, C. A., Mundt, J. A., Schmitz, H. H. (2003). Cocoa extract compounds and methods for making and using the same. US patent 6297273: http://www.freepatentsonline.com/6670390.html.

Sanders, T.H., McMichael, Jr., R.W., and Hexdrix, K.W. (2000). Occurrence of resveratrol in edible peanuts. *J. Agric. Food Chem., 48*, 1243-1246.

Sang, S., Lapsley, K., Jeong, W. S., Lachance, P. A., Ho, C. T., and Rosen, R. T. (2002). Antioxidative phenolic compounds isolated from almond skins (*Prunus amygdalus Batsch*). *J. Agric. Food Chem., 50*, 2459-2463.

Schmitz, H. H. (2003). Use of cocoa procyanidins combined with acelylsalicyclic acid as an anti-platelet therapy. US patent 6524630: http://www.freepatentsonline.com/6524630.html.

Schmitz, H. H. and Romanczyk, Jr., L. J. (2001). Method for reducing postprandial oxidative stress using cocoa procyanidins. US patent 6207702: http://www.freepatentsonline.com/6207702.html.

Schonrock, U. and Kruse, I. (2004). Use of flavones, flavanones and flavonoids for protecting ascorbic acid and/or ascorbyl compounds from oxidation. US patent 20040109882: http://www.freepatentsonline.com/EP0945128.html

Shahidi, F. and Naczk, M. (1996). *Food Phenolics, Sources, Chemistry, Effects, Applications*. Lancaster, PA: Technomic Publishing Co.

Shahidi, F., Wanasundara, U. N., He, Y., and Shukla, V. K. S. (1997). Marine lipids and their stabilization with green tea and catechins. In *Flavor and Lipid Chemistry of Seafoods*, (pp. 186-197). Washington DC: American Chemical Society.

Shephard, A. J., and Rudolf, T. S. (1991). Analysis of peanut products for total lipids, fatty acids and proximates. *Peanut Sci., 18*, 51-55.

Shi, J. Nawaz, H., Pohorly, J., Mittal, G., Kakuda, Y., and Jiang, Y. (2005). Extraction of polyphenolics from plant material for function foods – Engineering and technology. *Food Rev. Inter., 21*, 139-166.

Siemann, E. H. and Creasy, L. L. (1992). Concentration of the phytoalexin resveratrol in wine. *Am. J. Enol. Vitic., 43*, 49-52.

Silva, G. L., Lee, I. K., and Kinghorn, A. D. (1998). Special problems with the extraction of plants. In R. J. P. Cannell (Ed.), *Natural Products Isolation: Methods in Biotechnology 4*, (pp. 343-347). Totowa, NJ: Humana Press.

Singelton, V. L. and Rossi, J. A. (1965). Colormetry of total phenolics with phosphotunstic acid reagents. *Am. J. Enol. Vitic., 16*, 144-158.

Smith, R. M. (2003). Before the injection-modern methods of sample preparation for separation techniques. *J. Chromatogr. A, 1000*(1-2), 3-27.

Sobolev, V. S., and Cole, R. J. (1999). trans-Resveratrol content in commercial peanuts and peanut products. *J. Agric. Food Chem., 47*, 1435-1439.

Stalikas, C. D. (2007). Review: Extraction, separation and detection methods for phenolic acids and flavonoids. *J. Sep. Sci., 30*, 3268-3295.

Steinberg, D. (1993). Antioxidant vitamins and coronary heart disease. *New England J. Med., 328*(20), 1487-1489.

Stevanato, R., Fabris, S., and Momo, F. (2004). New enzymatic method for the determination of total phenolic content in tea and wine. *J. Agric. Food Chem., 52*, 6287-6293.

Tura, D., and Robards, K. (2002). Sample handling strategies for the determination of biophenols in food and plants. *J. Chromatogr. A, 975*, 71-93.

USDA, FAS. (June 2009). Production Estimates and Crop Assessment Division. *Peanut area, yield, and production*: http://www.usda.gov/nass/PUBS/TODAYRPT/crop0909.txt.

Vance, C. (2002). Root-cacteria interactions: Symbiotic N_2 fixation. In Y. Waisel, A. Eshel, and U. Kafkafi, *Plant Roots, the Hidden Half*, (pp. 839-866). New York: Marcel Dekker, Inc.

Virginia Peanut Production Guide. (2009). Virginia Peanut Growers Association and Virginia Cooperative Extension, Virginia Tech: http://pubs.ext.vt.edu/2810/2810-1017/2810-1017.html.

Wang, J., Yuan, X., Jin, Z., Tian, Y., and Song, H. (2007). Free radical and reactive oxygen species scavenging activities of peanut skins extract. *Food Chem., 104*, 242-250.

Waterhouse, A. (2006). Folin-Ciocalteau micro method for total phenol in wine: http://waterhouse.ucdavis.edu/phenol/folinmicro.htm.

Wijeratne, S. S. K., Abou-Zaid, M. M., and Shahidi, F. (2006). Antioxidant polyphenols in almond and its coproducts. *J. Agric. Food Chem., 54*, 312-318.

Wrolstad, R., Acree, T., Decker, E., Penner, Reid, D., Schwartz, S., Shoemaker, C., Smith, D., and Sporns, P. (2005). *Handbook of Food Analytical Chemistry*. Hoboken, NY: John Wiley & Sons.

Wong, D. W. S. and Pavlath, A. E. (1992). Oxidation. In Y. H. Hui (Ed.), *Encyclopedia of Food Science and Technology*, (pp. 1965-1970). New York: Wiley and Sons, Inc.

Wu, J. M.,Wang, Z. R., Hsieh, T. C., Bruder, J. L., Zou, J.G., and Huang, Y. Z. (2001). Mechanism of cardioprotection by resveratrol, a phenolic antioxidant present in red wine (Review). *Int. J. Mol. Med., 8*, 3-17.

Yang, C. S., Landau, J. M., Huang, M. T., and Newmark, H. L. (2001). Inhibition of carcinogenesis by dietary polyphenolic compounds. *Ann. Rev. Nutr., 21*, 381-406.

Yang, J., Liu, R. H., and Halim, L. (2009). Antioxidant and antiproliferative activities of common edible nut seeds. *Lebensmittel – Wissenschaft and Technologie, 42*(1), 1-8.

Yen, G. C., and Duh, P. D. (1995). Antioxidative activity of methanolic extracts of peanut hulls from various cultivars. *JAOCS, 72*(9), 1065-1067.

Yu, J., Ahmedna, M., and Goktepe, I. (2005). Effects of processing methods and extraction solvents on concentration and antioxidant activity of peanut skin phenolics. *Food Chem., 90*, 199-206.

Yu, J., Ahmedna, M., Goktepe, I., and Dai, J. (2006). Peanut skin procyanidins:Composition and antioxidant activities as affected by processing. *J. Food Comp. Anal., 19*, 364-371.

CHAPTER II: TOTAL PHENOL CONTENT AND ANTIOXIDANT ACTIVITY OF FRACTIONS OBTAINED FROM SIZE-EXCLUSION CHROMATOGRAPHY (SEC) OF RAW METHANOLIC PEANUT SKIN EXTRACT

ABSTRACT

The total phenol and antioxidant profile of methanolic extracts from the skins of Gregory peanuts were analyzed. The use of methanol as an extraction solvent yielded roughly 200mg extract per gram peanut skin. Toyopearl SEC of the raw methanolic peanut skin extract resulted in the separation of nine fractions based on different size classes. Analysis of total phenolics in these fractions using the Folin-Ciocalteau (FC) method revealed no significant differences among the various fractions ($P<0.05$). The average total phenol content for all fractions was 143.8 mg gallic acid equivalents per gram peanut skin (GAE/g). The DPPH radical scavenging method revealed compounds in each fraction with antioxidant activities significantly higher than that of BHA. No significant differences were found in the radical scavenging activity among the various fractions, which agrees with the similar concentrations of total phenols found in these samples. The levels of scavenging activities among all fractions correlated to the levels of phenolics found using the FC Total Phenols method. Significant differences ($P<0.05$) also were noted in the rate of increase of scavenging activity from the 0 to 100 μg/ml concentration range for each fraction. The percent scavenging activity of all fractions leveled-off at approximately a 200 μg/mL concentration of extract. No significant differences were noted in the efficient concentration values (EC_{50}) among the different peanut skin fractions, but all were significantly higher than that of BHA, and required lower concentrations to achieve a 50% quenching of all radicals. The average estimated EC_{50} value among all fractions was 28.6 μg/mL. The BHA treatment achieved an estimated EC_{50} value of 50.4 μg/mL, indicating that peanut skin fractions exhibited a 43% average increase in antioxidant activity over that of BHA. This indicates that the structures contained in each of these fractions can be utilized as a viable antioxidant source, and have the ability to replace synthetic antioxidants (such as BHA) with those that are naturally-derived from peanut skins.

INTRODUCTION

Prior studies have indicated that peanut skin extracts exhibit powerful oxyradical quenching activity, which is due to the high concentration of total phenolic compounds (Lou et al., 2004; Yu et al., 2005). However, only a handful of phenolic-based compounds (such as phenolic acids, flavonoid monomers, proanthocyanidins, oligomeric procyanidins, etc.) have been identified in peanut skin extracts (Lou et al., 1999, 2001, 2004; Nepote et al., 2004; Yu et al. 2005). In addition, few studies have been conducted to determine which structures are responsible for the antioxidant activity associated with peanut skin extracts. Preliminary experiments using HPLC with ultraviolet (UV) detection on raw peanut skin extracts revealed this plant source contains large numbers of compounds, most of which exhibited co-elution based on the sheer number of structures (Figure A.1). This would make identification of these compounds difficult, since qualitative analysis using HPLC-MS would only allow the recognition of the most intense peaks, causing less-intense compounds to be masked by more prominent components which elute nearby. This discovery indicated that in order to properly identify these compounds, the need for preparatory separations would be required to decrease co-elution during further HPLC-MS^n analysis.

The use of a preparatory method such as size exclusion chromatography (SEC) would allow for the separation of phenolic classes based on their size, resulting in maximum resolution/separation during HPLC analysis. This method was successfully performed in a past study on flavonoid-based compounds in grape seed extracts (Fitzpatrick et al., 2000), which incorporated a SEC column using Toyopearl HW-40S media. The integration of SEC in that study enabled the collection of phenolic classes in

the form of fractions. For this particular research, the incorporation of such a method offers several other benefits. First, each of these fractions can be analyzed for their total phenolic content, giving insight into the total concentration of different size-classes of phenolic-based compounds in peanut skins. Second, the various fractions then can be tested for antioxidant activity, which provides an indication of which phenolic classes are contributing to the oxyradical scavenging effects exhibited by peanut skin extracts. Finally, the separation of these classes (using a preparatory method such as SEC) prepares fractions that can be further characterized for the proper identification of the full phenolic profile contained within peanut skins. The utilization of this method for the analysis of peanut skins has never been performed prior to this study. Further identification of the phenolic-based compounds in each fraction (using HPLC-MS^n) then will give an indication as to which compounds are responsible for a given total phenol content and antioxidant activity (as determined for each fraction). The purpose of this study is not only to prepare raw extracts for maximum detection of individual compounds during later HPLC studies, but also to give general conclusions regarding the concentrations of various classes of phenolic compounds and their associated oxyradical scavenging capabilities.

MATERIALS AND METHODS

Experimental Design

The basic experimental design for this study is illustrated in the figure below (Figure 1). This diagram indicates the overall path of experiments conducted on peanut skins (Gregory peanut line) during the course of this research. The materials and

methods for each experimental study is outlined below (except for (-)ESI-HPLC-MS^n, which can be found in Chapter 3).

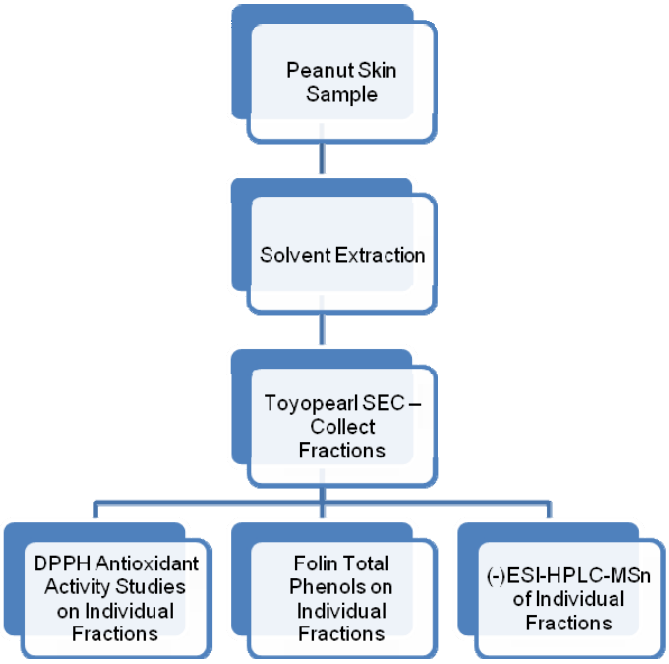

Figure 1: Experimental Design: Illustrating the basic experimental design for this sudy.

Extraction of Antioxidant Components from Peanut Skins

Blanched peanut skins (Gregory line) were acquired from Walter Mozingo of the Tidewater Agricultural Research & Extension Center in Suffolk, VA (peanut skins were obtained using a lab-scale blancher). Methanol was chosen as the extraction solvent based on high % yields of extracted antioxidant components indicated in a prior study (Duh et al., 1992). A total of 10g of peanut skins were ground into a fine powder, and extracted using a 10:1 (v/w) ratio of methanol (100mL) to peanut skin (10g), stirring constantly for 24 hours. Extracts then were filtered using Whatman #1 filter paper, and the extraction was repeated a second time. Filtrates were centrifuged for 30 minutes to remove particulates. The combined filtrates then were evaporated to dryness using a rotary evaporator, and weighed to determine yield of soluble components for later

analysis of Folin-Ciocalteau (FC) Total Phenols and DPPH Oxygen Scavenging Capacity. Rotary-evaporation was performed using almost no heat, so as not to cause damage/polymerization reactions to the phenolic compounds. The peanut skin extract was then re-dissolved in 10mL methanol for Toyopearl SEC.

Size-Exclusion Chromatography using Toyopearl HW-40S

A glass column measuring 55 x 2.5cm was packed with Toyopearl HW-40S Size-Exclusion Chromatography (SEC) media. The mobile phase used was Fisher Scientific HPLC-grade methanol, and the apparatus was fed using a Fisher Scientific Variable Flow Mini-Pump (0.45mL/min flow rate). The SEC column was connected to a LKB Bromma 2238 UVicord SII Detector (280nm), which then fed into a LKB Bromma 2112 Redirac Fraction Collector (tube change rate = 1 tube/min, 4.5mL/tube). An LKB Bromma 2210 2-Channel Recorder was used to record UV intensity, time, and tube numbers. All connections between sample-containing devices incorporated PTFE tubing. Peanut skin extract (10mL) was loaded onto the column, and allowed to run until UV intensity reached its original baseline of methanol alone (22 hours, 10 minutes). Tubes corresponding to each detected fraction then were combined and rotary evaporated to dryness, with volumes and weights recorded for calculation of FC Total Phenols and DPPH Oxygen Scavenging Capacity. Individual fractions then were re-dissolved in 10mL HPLC-grade methanol for further analysis of Total Phenols, DPPH oxygen scavenging capacity, and (-)ESI-HPLC-MS^n.

Total Phenolics (TP) using Folin-Ciocalteau (FC) Method

Concentrations of TP's in each peanut skin fraction (A through H) were determined using the Folin-Ciocalteau Total Phenol method as described by Singleton and Rossi (1965). According to Engelhardt (2001), FC is the most efficient method for the analysis of total phenolics and high molecular weight tannins. It is a colorimetric technique which utilizes the Folin-Ciocalteau reagent (Sigma Chemical Corp.) to react with phenolic-based compounds, and accurately determine their concentration at 765nm. Gallic acid was used as the standard, and results determined as mg/mL of gallic acid equivalents (GAE). Findings were converted to mg GAE per gram peanut skin, to give real-world correlation to the amount of phenolics in Gregory line peanut skins.

DPPH Radical Scavenging (Antioxidant) Activity

The antioxidant (scavenging) activity of peanut skin fractions was measured using the DPPH (1,1-diphenyl-2-picrylhydrazyl radical) free radical scavenging assay, and was carried out as described by Blois (1958). Methanol fractions (A through H) of peanut skins at various concentrations (0, 10, 20, 50, 100, 200, and 500 μg/mL) were added to a solution of 1.5 x 10^{-4}M DPPH (Sigma, USA) in methanol. The mixture was shaken vigorously and allowed to react for 5 minutes. In this assay, the ability of antioxidant compounds to scavenge DPPH radicals is defined as the discoloration of the DPPH solution (relative decrease in absorption) after 5 minutes at 520nm. The radical scavenging activity was obtained from the following equation: Radical Scavenging Activity (%) = $\{(Abs_{control} - Abs_{sample})/Abs_{control}\}$ x 100. The antioxidant activity is expressed as EC_{50} (efficient concentration value), which is defined as the concentration

(in μg/mL) of each extract fraction required to inhibit the formation of DPPH radical by 50%. DPPH radical scavenging activity was conducted for each peanut skin fraction at various concentrations, and compared to an antioxidant/preservative commonly used in food systems known as butylated hydroxyanisole (BHA).

Statistical Analysis

All experiments on individual peanut skin fractions (A through H) obtained from Toyopearl SEC were performed in triplicate. Experimental results were expressed as means ± standard deviations (SD). The values for EC_{50} were estimated by nonlinear regression analysis using Statistica 8.0 (StatSoft, Tulsa, OK). Other data was analyzed using ANOVA ($P<0.05$) with means separated by Duncan's Multiple Range Test.

RESULTS AND DISCUSSION

In this study, 10g of peanut skins were extracted using 100% HPLC-grade methanol, yielding 2.001g of dried extract. Several prior studies have been conducted which investigated the yield of peanut skin extracts using various solvents. Huang et al. (2003) indicated that polar solvents offered better extraction yields than less polar solvents. Yu et al. (2005) reported that methanol and ethanol were more efficient than water for extracting phenolic-based compounds. Duh et al. (1992) revealed that methanol resulted in more than 50% higher yields of antioxidant extracts from peanut hulls when compared to ethanol (other solvents gave even lower yields). The efficient extraction yield of utilitizing methanol as an extraction solvent was also revealed in this study. The use of methanol as an extraction solvent yielded roughly 200mg extract per gram peanut skin. Other studies which incorporated ethanol as an extraction solvent offered

approximately 50% (or more) reduction in extraction efficiency. Wang et al. (2007) reported 0.107 ± 0.003g extract per gram peanut skin. Other studies that utilized ethanol resulted in extracts of 0.051g (Huang et al., 2003) and 0.099g (Nepote et al. 2005) per gram peanut skin. The results in this study support the findings by Duh et al (1992), providing solid evidence that utilizing methanol as an extraction solvent can provide optimum yields of peanut skin extract.

Peanut skin extract obtained from the methanolic extraction process was run through a SEC column containing Toyopearl HW-40S. The sample run lasted a total of 22:10 (min), and was discontinued upon the return of a methanol-only baseline. Major peaks/valleys indicated in the UV (280nm) chromatogram output were used to generate individual fractions based on the size of different compound classes contained within the peanut skin raw extract. The overall number of peaks (among the duration of the Toyopearl sample run), along with their shapes, heights, and intensities, was similar to that reported by Fitzpatrick et al. (2000) for the separation of grape seed extracts. A total of nine fractions were obtained (Figure 2), which included fractions A, B, C, D, E, F, G-Red, G, and H. Tubes obtained from the fraction collector were combined to form the sample for each given fraction. Colors associated with each combined fraction were initially clear (Fraction A), and changed from yellow (Fraction B and C), to orange (D and E), to brownish-red (F through H). The major peaks and valleys which made up Fraction G included numerous tubes which had an extreme bright-red color. These tubes corresponded to the first peak (in the series of peaks) that made up Fraction G. In order to further investigate the compound(s) responsible for this extreme change in visible

spectrum, these tubes were collected separately from the rest of Fraction G, and then combined to form Fraction G-Red.

Folin-Ciocalteu Total Phenols method was used to determine the concentration of phenolic-based compounds in each peanut skin fraction (A through H) obtained from Toyopearl SEC. The data shown in Figure 3 reveal that peanut skins contain high levels of total phenolics (mg GAE/g peanut skin). Surprisingly, each fraction contained relatively the same amount of total phenolics, and no significant differences were seen when comparing the concentrations among the various fractions. This could indicate that there is an even distribution in concentration among different phenolic classes (based on size) in peanut skins. Yu et al. (2005) indicated that blanched peeling greatly reduced the concentration of total phenols in methanolic peanut skin extracts versus direct peeling or roast peeling (11.6 mg/g versus 90.1 mg/g and 96.7 mg/g respectively). The lower total phenolic content in that study was assumed to be due to the leaching of phenolics out of the skin (into the water) during the blanching process. However, even though the skins in this current research were obtained through a blanching process, the data still indicated much higher concentrations of phenolics in the peanut skin fractions of the Gregory line (even when compared to the direct peeled or roast peeled treatments in the prior 2005 study). This could possibly be due to several factors, including the blanching process incorporated for that given study. Another possible explanation is differences in the phenolic profile in the peanut skins of the Gregory line versus other peanut lines/cultivars (such as Runner varieties). This could indicate that the Gregory line has much higher concentrations of total phenols when compared to other varieties. A similar result was obtained in a prior study on the total phenols contained in peanut hulls. Yen and Duh

(1995) reported significant differences in the total phenolic concentration (including the total luteolin content) in various peanut hulls obtained from different cultivars. This shows that in addition to peanut hulls, other forms of peanut by-products (such as peanut skins) can contain varying levels of phenolics based on differences in cultivars.

The antioxidant activities of peanut skin fractions (A though H) obtained from Toyopearl SEC were examined using the DPPH free radical scavenging activity method. Due to their ability to donate hydrogen (or electrons) to produce stable radical intermediates, the phenolic-based structures found in many plants are viewed as powerful antioxidant compounds (Scalbert et al., 2005). The stable nitrogen-centered free radical found in 1,1-diphenyl-2-picrylhydrazyl (DPPH) enables it to be utilized for the relatively quick analysis of oxyradical quenching capabilities found in naturally-derived antioxidant compounds. The technique works via the associated absorbance reduction (at 520nm) observed when a proton-donating substance is added to a methanolic DPPH solution. The result of this combination is a diamagnetic molecule, formed from the acceptance of an electron or hydrogen radical (Soares et al., 1997). This method was chosen based on these prior successes using the DPPH method to analyze the antioxidant capacity of various types of plant extracts. In this study, the DPPH radical scavenging results for each peanut skin fraction were compared to the scavenging activity of a synthetic antioxidant commonly used in the food industry, known as butylated hydroxyanisole (BHA). The DPPH radical scavenging activity (%) for each fraction (including that of BHA) can be seen in Figure 4. The various peanut skin fractions showed extremely high antioxidant activity, and were all significantly higher than that of BHA (at a $P<0.05$ significance level). No significant differences were found in the radical scavenging

activity among the various fractions, which agrees with the similar concentrations of total phenols found in these samples. In fact, the levels of scavenging activities among the different peanut skin fractions (Figure 4) appeared to have similar patterns to the levels of phenolics found using the FC Total Phenols method (Figure 3). Significant differences ($P<0.05$) also were noted in the rate of increase of scavenging activity from the 0 to 100 μg/ml concentration range for each fraction when compared to BHA. This was in agreement with a previous study by Wang et al (2007). For each fraction, the percent scavenging activity leveled-off at a concentration of approximately 200 μg/mL. The estimated EC_{50} values indicate the concentration of antioxidant required to scavenge 50% of all radicals in the DPPH reaction mixture, of which no significant differences were noted among the different peanut skin fractions (A through H). However, the EC_{50} values for each fraction were significantly different than that of BHA, and required lower concentrations to achieve a 50% quenching of all radicals. The average estimated EC_{50} value among fractions A through H was 28.6 μg/mL, which reveals a slightly higher radical scavenging effect when compared to the peanut skins used in the 2007 study by J. Wang et al (30.8 μg/mL). Again, this could be due to the differences in the phenolic profiles between the Gregory line and peanut from other cultivars. The BHA treatment achieved an estimated EC_{50} value of 50.4 μg/mL, indicating that peanut skin fractions exhibited a 43% average increase in antioxidant activity over that of BHA.

CONCLUSION

The use of methanol proved to be an efficient solvent for the extraction of phenolic-based antioxidant compounds from peanut skins, resulting in high extraction

yields when compared studies which used other forms of solvents (Huang et al., 2003; Nepote et al., 2005; Wang et al., 2007). Methanol also could prove to be a cost effective method for the extraction of these compounds, since it could be easily recovered during evaporation, and reused for further extractions. Addition of methanolic extracts to a Toyopearl SEC column resulted in the separation of phenolic compounds based on different size classes (fractions A through H). Analysis of total phenolics in these fractions using the FC method revealed an even distribution of different types of phenolic compounds relative to molecule size. Further antioxidant capacity studies, using the DPPH radical scavenging activity method, revealed that compounds contained within each fraction exhibit antioxidant capabilities that far exceed that of BHA. This indicates that the structures contained in each of these fractions can be utilized as a viable antioxidant source, and have the ability to replace synthetic antioxidants (such as BHA) with those that are naturally-derived. Further research conducted in this particular study aims to determine (via HPLC-MS^n) which compounds are responsible for the given antioxidant effects exhibited by each fraction (see Chapter 3). In addition to the possible applications in food systems, these compounds could have significant human health implications, since their powerful oxy-radical scavenging effects could help reduce oxidative-induced cell damage. Determining which compounds contribute to antioxidant activity also could lead to the discovery of new compounds, those that may exhibit other important pharmaceutical and nutraceutical attributes.

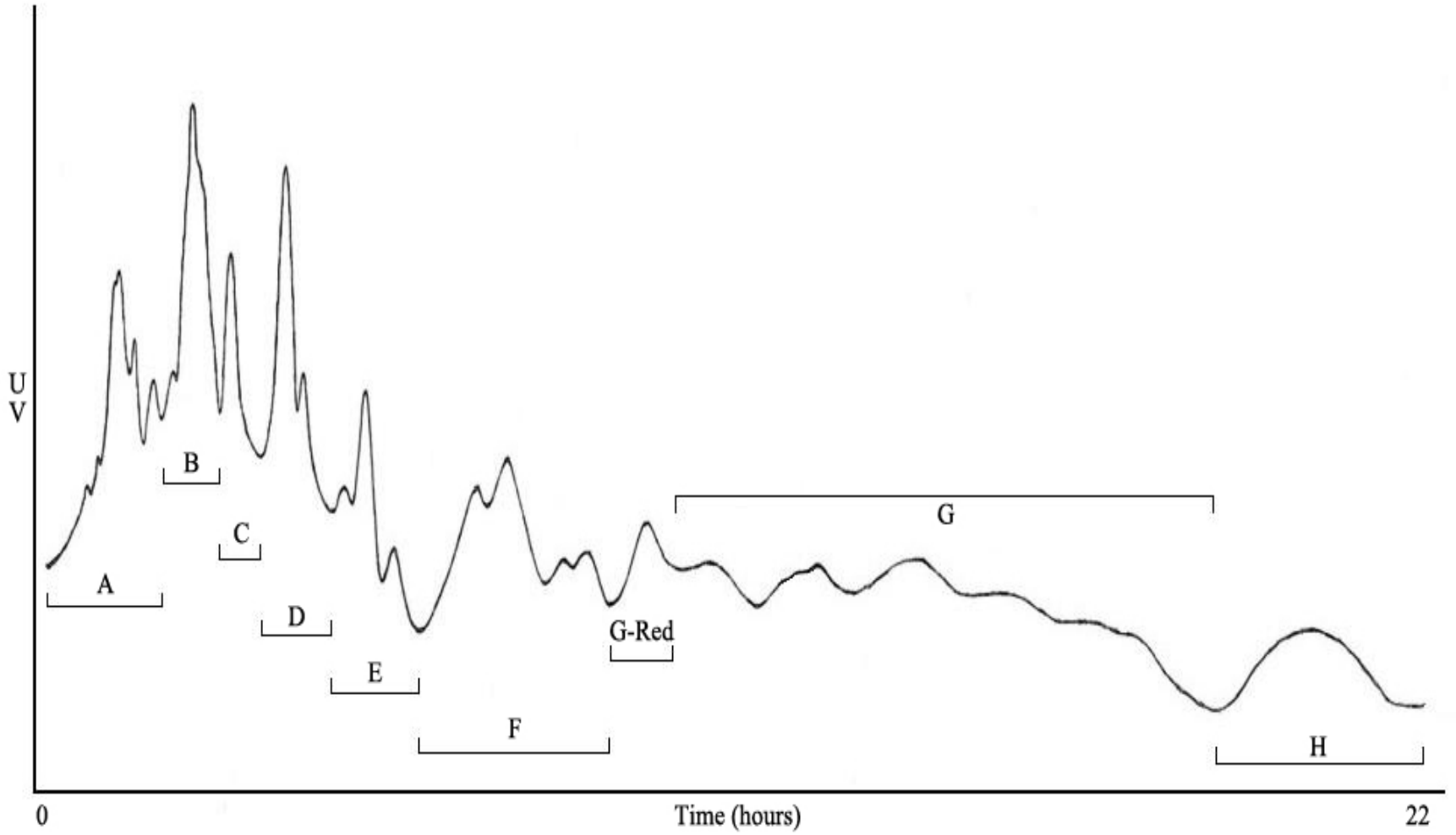

Figure 2. Size Exclusion Chromatography (SEC) of Raw Peanut Skin Extract Using Toyopearl HW-40S – SEC of peanut skin raw extract from Gregory peanut line. Figure represents time (t) from 0 to 22 hours (length of the sample run), versus UV intensity at 280nm. Peanut skin fractions obtained from SEC are indicated (A, B, C, D, E, F, G-Red, G, H), which were used for further analysis.

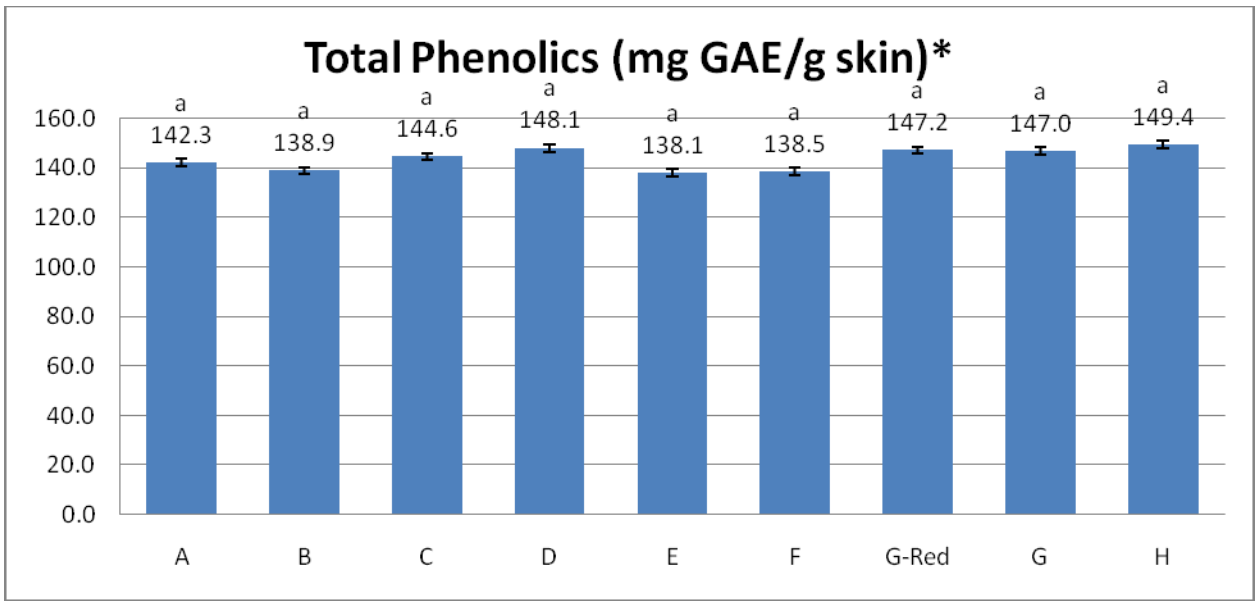

Figure 3. Total Phenolics using Folin-Ciocalteu Method: for Fractions A though H (obtained from Toyopearl Size Exclusion Chromatography) of raw peanut skin extract for Gregory peanut line. *Data represents the means of three replicates, and bars indicate ± standard deviations (n=3). Total phenolics concentration expressed as mg Gallic Acid Equivalent per gram peanut skin (GAE/g). Values with same letters are not significantly different at $P<0.05$.

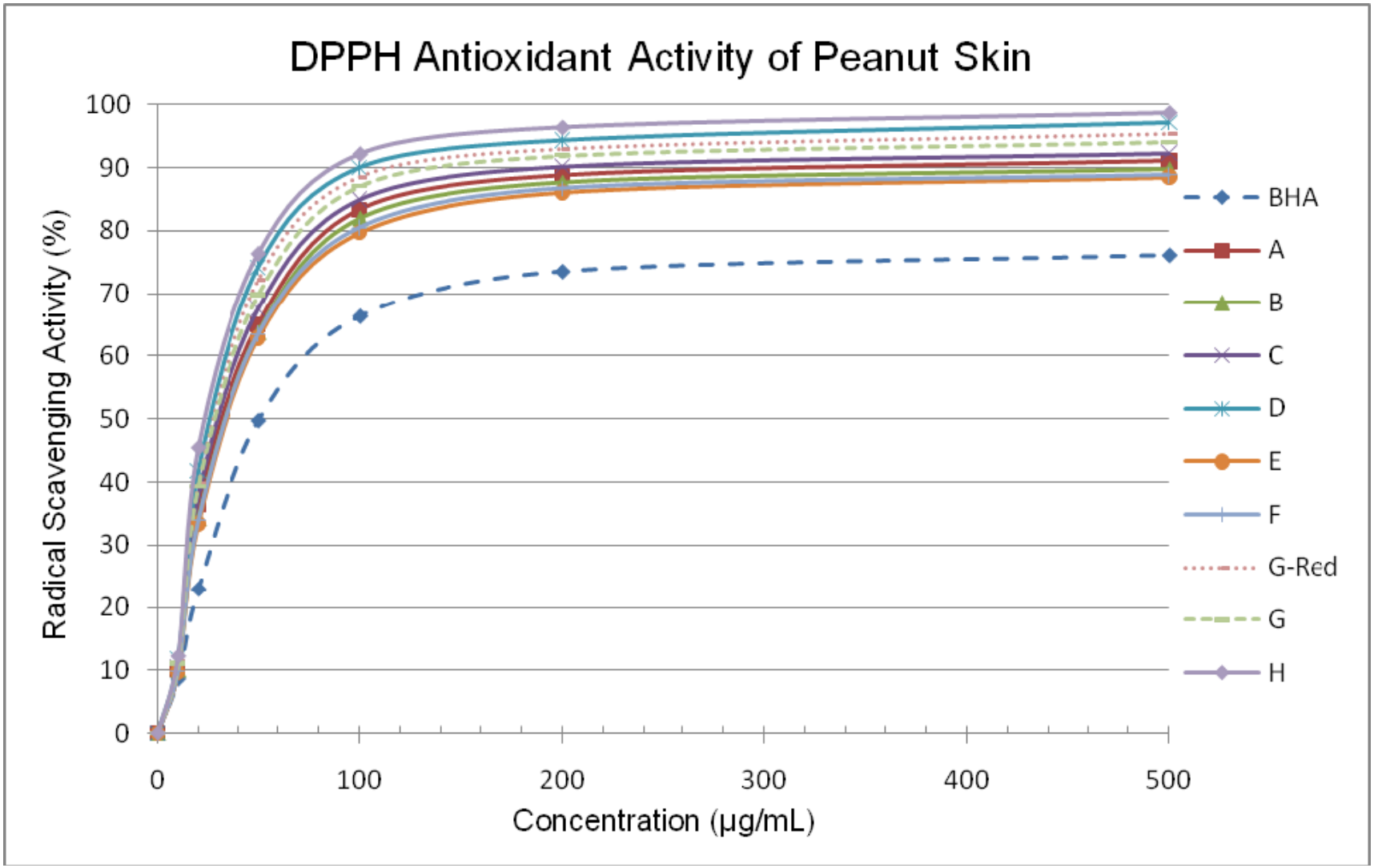

Figure 4. DPPH Scavenging Capacity of Peanut Skin Fractions Obtained from Toyopearl SEC – Percent (%) scavenging Capacity of DPPH radical for Gregory line peanut skin extract (fractions A though H) versus BHA at various concentrations (10-500µg/mL).

REFERENCES

Blois, M. S. (1958). Antioxidant determinations by the use of stable free radical. *Nature, 181*, 1199-1200.

Engelhardt, U. (2001). Flavonoids-analysis. *Crit. Rev. Food Sci. Nutr., 41*, 398-399.

Fitzpatrick, D. F., Fleming, R. C., Bing, B., Maggi, D. A., and O'Malley, R. M. (2000). Isolation and characterization of endothelium-dependent vasorelaxing compounds from grape seeds. *J. Agric. Food Chem., 48*, 6384-6390.

Duh, P. D., Yeh, D. B., and Yen, G. C. (1992). Extraction and identification of an antioxidative component from peanut hulls. *J. Am. Oil Chem. Soc., 69*(8), 814-818.

Huang, S. C., Yen, G. C., Chang, L. W., Yen, W. J., and Duh, P. D. (2003). Identification of an antioxidant, ethyl protocatechuate, in peanut seed testa. *J. Agric. Food Chem., 51*, 2380-2383.

Lou, H., Yamazaki, Y., Saski, T., Uchida, M., Tanaka, H. and Oka, S. (1999). A-type proanthocyanidins from peanut skins. *Phytochemistry, 51*, 297-308.

Lou, H., Yuan, H., Ma, B., Ren, D., Ji, M., and Oka, S. (2004). Polyphenols from peanut skins and their free radical-scavenging effects. *Phytochemistry, 65*, 2391-2399.

Lou, H., Yuan, H., Yamazaki, Y., Sasaki, T., and Oka, S. (2001). Alkaloids and flavanoids from peanut skins. *Planta Med., 67*, 345-349.

Nepote, V., Gross, N. R., and Guzman, C. A. (2005). Optimization of extraction of phenolic antioxidants from peanut skins. *J. Sci. Food Agric., 85*, 33-38.

Nepote, V., Mestrallet, M. G., and Grosso, N. R. (2004). Natural antioxidant effect from peanut skins in honey-roasted peanuts. *J. Food Sci., 69*, S295-S300.

Scalbert, A., Manach, C., Morand, C., and Rémésy, C. (2005). Dietary polyphenols and the prevention of diseases. *Crit. Rev. Food Sci. Nutr., 45*, 287-306.

Singleton, V. L. and Rossi, J. A. (1965). Colorimetry of total phenolics with phosphotungstic acid reagents. *Am. J. Enol. Vitic., 16*, 2349-2351.

Soares, J. R., Dins, T. C., Cunha, A. P., and Ameida, L. M. (1997). Antioxidant activity of some extracts of *Thymus zygis*. *Free Radical Res., 26*, 469-478.

Wang, J., Yuan, X., Jin, Z., Tian, Y., and Song, H. (2007). Free radical and reactive oxygen species scavenging activities of peanut skins extract. *Food Chem., 104*, 242-250.

Yen, G. C. and Duh, P. D. (1995). Antioxidant activity of methanolic extracts of peanut hulls from various cultivars. *J. Am. Oil Chem. Soc., 72*, 1065-1067.

Yu, J., Ahmedna, M., and Goktepe, I. (2005). Effects of processing methods and extraction solvents on concentration and antioxidant activity of peanut skin phenolics. *Food Chem., 90*, 199-206.

CHAPTER III: IDENTIFICATION OF PHENOLIC COMPOUNDS IN PEANUT SKIN EXTRACT USING HPLC WITH NEGATIVE MODE ION TRAP MS^n AND ELECTROSPRAY IONIZATION

ABSTRACT

The analysis of phenolic compounds often is performed using some form of high performance liquid chromatography (HPLC) coupled with mass spectrometry (MS) detection. However, the use of electrospray ionization (ESI) and ion trap MS^n (MS/MS/MS) offers better detection over tradition first-order MS techniques. This study utilized negative mode (-)ESI-HPLC-MS^n to identify phenolic-based compounds in nine fractions obtained from size-exclusion chromatography (SEC) of raw methanolic peanut skin extract. The study was designed to determine if previously undiscovered phenolic antioxidant compounds are present in peanut skins, and also to identify if structures exist that exhibit pharmaceutical/nutraceutical properties. Two separate HPLC method were developed to offer maximum separation and reduce co-elution. A total of 314 phenolic-based structures were identified or tentatively identified, the majority of which are newly discovered compounds that have never been previously detected in peanut skins. HPLC Method 1 identified 219 unique compounds, while HPLC Method 2 offered better separation (due to mobile phase and column differences), resulting in the detection of 95 additional structures. Most identified compounds were hydroxy- or methoxy- substituted phenolics. These structures included numerous phenolic acids, coumarins, chalcones, stilbenes, flavonoids, flavonoid-glycosides, oligomeric flavonoids (including A and B type procyanidin dimers, trimers, and tetramers), biflavonoids, and flavonoids with various types of attached side-groups. Many of the compounds identified are known to have powerful oxyradical scavenging effects, which agrees with previous studies conducted (on these fractions) which indicate high antioxidant activities. In addition, many of the detected compounds have been previously reported (in literature) to exhibit numerous beneficial chemical and biological activities, including the treatment of various human health-related conditions.

INTRODUCTION

The majority of prior studies on peanut skin extracts have involved the use of some form of High Performance Liquid Chromatography (HPLC) system, including a variety of detection methods such as UV-VIS and mass spectrometry (MS) (Lou et al., 1999, 2001; Yu et al., 2005, 2006). However, several issues exist when attempting to use these methods when analyzing compounds from these types of extracts. First, problems often arise from co-elution, where multiple compounds have the same (or similar) retention times. The utilization of UV-VIS detection alone will not provide the necessary mode of qualitative analysis, since many phenolic-based compounds will exhibit identical (or partially overlapping) HPLC retention times due to their polar natures. Second, the use of standard (non MS^n) mass spectrometry techniques, such as electron impact (EI) and time-of-flight (TOF), often will provide inconclusive results. This is due to the fact that when using a (non-MS^n) mass spectrometer, many phenolic and flavonoid-based compounds that exhibit identical molecular weights will sometimes have indistinguishable fragmentation patterns.

Many bioflavanoids exist as flavonoid-glycosides, which makes MS identification even more difficult when using non-MS^n methods. The use of standard MS techniques only offers a first stage of fragmentation, resulting in the cleavage of just the flavonoid aglycone from the sugar moiety (Cuyckens and Claeys 2004). The lack of further dissociation leaves only the m/z of the flavonoid monomer, of which many can exist at any given molecular weight. For example, several m/z 447 $(M-H)^-$ flavonoid-glycosides exist, including kaempferol-glucoside and luteolin-glucoside derivatives. The utilization of a single-step MS technique will only remove the glucose sugar from the flavonoid aglycone. Upon cleavage, the remaining m/z 285 $(M-H)^-$ represents the flavonoid (aglycone) monomer, of which luteolin and kaempferol both

exhibit this same 286 amu molecular weight. Without further fragmentation of the flavonoid aglycone, the proper identification of this monomer would not be possible. In addition, many flavonoids that share the same molecular weight will sometimes follow similar dissociation schemes (in the initial fragmentation step), making identification difficult when using a standard MS (non-MS^n) method. The further fragmentation of identical molecular weight flavonoid compounds (exhibited by MS^n instrumentation capable of MS/MS or MS/MS/MS) often will show differences in fragmentation pathways, making positive identification possible.

As previously mentioned, the large number of compounds typically exhibited in plant extracts often causes the co-elution of multiple compounds during HPLC separation, making identification impossible with single-step mass spectrometers. This can be circumvented by the use of advanced MS instruments (such as Ion Trap MS^n), since they may be tuned to simultaneously identify multiple compounds at different molecular weight ranges. For these reasons, the use of such MS^n techniques is critical for the proper identification of phenolic-based compounds in extremely flavonoid-rich extracts (such as in the case of peanut skins). This type of method has never been performed in the analysis of peanut skin extracts, and could result in the discovery of novel phenolic and flavonoid-based compounds.

One of the primary objectives of this study is to use HPLC-MS^n (ESI-Ion Trap MS) for the possible identification of compounds in peanut skin extracts that have never been previously reported, since the use of MS^n (MS/MS/MS) may allow for the detection of compounds that could not be recognized using other analytical methods. The ultimate goal of utilizing HPLC-ESI-MS^n is not only to identify structures which have known antioxidant activity, but also determine if compounds are present which exhibit specific biological activities from a pharmaceutical or nutraceutical standpoint. This study also may show that compounds which

have been previously shown to exist in peanut skins are actually different structures altogether, since past researchers have only used raw molecular weights and/or inconclusive fragmentation data (obtained from non-MS^n mass spectrometers) as a means for identification of these phenolic-based compounds.

MATERIALS AND METHODS

Preliminary experiments using HPLC-UV on raw peanut skin extracts (without any preparatory separations, such as Toyopearl SEC) revealed this plant source contains a large number of compounds (Figure A.1). This discovery indicated that in order to properly identify these compounds, the need for multiple HPLC methods (along with a preparatory separation technique, i.e., Toyopearl SEC) would be required to both maximize resolution/separation and decrease co-elution. Therefore, two separate HPLC-MS^n methods (designated as HPLC Method 1, and HPLC Method 2) were utilized for the identification of compounds in peanut skin fractions (A through H) obtained from Toyopearl Size Exclusion Chromatography. For both HPLC methods, a Thermo Finnigan LCQ HPLC-MS^n (MS/MS) Ion Trap mass spectrometer with electrospray ionization (ESI) was used. The instrument incorporated an Agilent (Palo Alto, CA) 1100 series G1312A binary pump, with a Rheodyne 7125 manual injector (25 μL injection loop). Separations for HPLC Method 1 were carried out using a Waters (Ireland) Nova-Pak C18 (3.9 x 150 mm; 60A; 4 μm) reverse phase column, plus a C18 guard column. The solvent system comprised of two mobile phase parts: (A) 0.5% glacial acetic acid in water, and (B) 0.5% glacial acetic acid in methanol. The solvent gradient parameters were as follows: elution rate of 0.8 mL/min, with %(B) = 0% (0 – 2 minutes), 4.75% (5 minutes), 30.88% (15 minutes), 74.7% (42 minutes), 95% (52 – 70 minutes), and 100% (80 – 100 minutes). UV detection was

conducted at 280nm for detection of bioflavanoids, using an Agilent 1100 G1314A UV/Vis detector (Applied Biosystems Model 785A Programmable Absorbance Detector). Samples then were analyzed using ESI-MS^n in negative ionization mode, with the following parameters: sheath gas (N_2) = 60; auxiliary gas (N_2) = 5; spray voltage 3.3kV; capillary temperature 250°C; cap voltage = 15; tube lens offset = 0V. Base peak ranges used for (-)ESI-MS^n consisted of two parameters, utilizing an initial scanning range of m/z 125-600 $(M-H)^-$ ions, with a source induced dissociation (SID) voltage of 1.0V (sid=1.0). The second scan range encompassed ions of m/z 590-2000 $(M-H)^-$, with an SID voltage of 2.0V (sid=2.0). In the case of both 'sid=1.0' and 'sid=2.0' scan ranges, further MS^n (i.e., isolation and dissociation) was dependent on the most intense ion in each scan range. MS^n first is defined by the detection of the most intense ion in the normal mass spectra (ms spectra), of which MS/MS is then performed on this parent ion (resulting in an ms2 sepctra). The most intense ion in the ms2 spectra then undergoes further dissociation, with the resulting ion fragments shown in the ms3 spectra (MS/MS/MS). Data dependent settings of the LCQ ion trap were as follows: MS^n=2,3; 5u isolation window; normalized collision energy 42.5% (CID); and activation Q (Mathieu q parameter) = 0.3. All samples of peanut skin extracts, including fractions A through H obtained from Toyopearl SEC, were continually stored at -80°C (from the point of SEC completion, to the time of HPLC injection). All sample runs including the standard mix, and peanut skin fractions A through H (obtained from Toyopearl SEC), were injected using a 20µL sample volume.

HPLC Method 2 was conducted in an attempt to offer improved chromatographic separation and resolution in comparison to HPLC method 1. Separations for HPLC Method 2 were carried out using a Waters (Ireland) Atlantis dC18 (2.1 x 150 mm; 3 µm) column, plus a 2mm x 4mm Phenomenex C18 guard column. The solvent system comprised of two mobile

phase parts: (A) 0.3% glacial acetic acid in water, and (B) 0.3% alacial acetic acid in methanol. The solvent gradient parameters were as follows: elution rate of 0.8 mL/min, with %(B) = 0% (0 minutes), 20% (7 minutes), 70% (70 minutes), and 95% (80-100 minutes). UV detection was conducted at 280nm for maximum detection of bioflavanoids, using an Agilent 1100 G1314A UV/Vis detector (Applied Biosystems model 785A programmable absorbance detector). Samples then were analyzed using ESI-MS^n in negative ionization mode, with the following parameters: sheath gas (N_2) = 65; auxiliary gas (N_2) = 3; spray voltage 3.3kV; capillary temperature 250°C; cap voltage = 15; tube lens offset = 0V. Base peak ranges used for (-)ESI-MS^n consisted of three parameters, utilizing an initial scanning range of m/z 125-250 $(M-H)^-$ ions, with an SID voltage of 1.0V (sid=1.0). The second scan range encompassed ions of m/z 230-410 $(M-H)^-$, with an SID voltage of 2.0V (sid=2.0). The final scan range analyzed ions of m/z 400-2000 $(M-H)^-$, with an SID voltage of 3.0V (sid=3.0). In all three cases of 'sid=1.0', 'sid=2.0', and 'sid=3.0' scan ranges, further MS^n (i.e., isolation and dissociation) was dependent on the most intense ion in each scan range. As in the case of HPLC Method 1, MS^n first is defined by the detection of the most intense ion in the normal mass spectra (ms spectra), of which MS/MS is then performed on this parent ion (resulting in an ms2 sepctra). The most intense ion in the ms2 spectra then undergoes further dissociation, with the resulting ion fragments shown in the ms3 spectra (MS/MS/MS). Data dependant settings of the LCQ ion trap were as follows: MS^n=2,3; 5u isolation window; normalized collision energy 42.5% (CID); and activation Q (Mathieu q parameter) = 0.3. All samples of peanut skin extracts, including fractions A through H obtained from Toyopearl SEC, were continually stored at -80°C (from the point of SEC completion, to the time of HPLC injection). All sample runs including the standard mix, and peanut skin fractions A through H (obtained from Toyopearl SEC), were injected using

a 20µL sample volume.

A standard mix was prepared to aid in the identification of unknown compounds. These standard compounds included: p-coumaric acid (para-hydroxycinnamic acid), gallic acid (3,4,5-trihydroxybenzoic acid), caffeic acid, ferulic acid, flavone, resveratrol, kaempferol (3,4',5,7-tetrahydroxyflavone), luteolin (3',4',5,7-tetrahydroxyflavone), eriodictyol (3',4',5,7-tetrahydroxy-flavanone), catechin, epicatechin, hesperitin (3',5,7-Trihydroxy-4'-methoxyflavanone), quercetin (3,3',4',5,7-pentahydroxyflavone), gallocatechin, epigallocatechin, quercetin dihydrate, chlorogenic acid, epicatechin gallate, catechin gallate, quercetrin (quercetin-3-O-rhamnoside), epigallocatechin gallate, gallocatechin gallate, and procyanidin B3 dimer. The "standard mix" UV chromatogram and normal mass spectra TIC (Total Ion Chromatogram – indicating the base peaks for the most intense ions) can be seen in Figure A.2 and A.3. Figure A.4 shows UV versus TICs for the MS^n (ms, ms2, and ms3) of individual standard compounds in the standard mix. The top TIC in this figure shows the full MS of the most intense (parent) ions in the normal mass spectra. The second TIC reveals the most intense ions formed in the ms2 spectra (MS/MS), while the third TIC shows the most intense ions formed in the ms3 spectra (MS/MS/MS). The bottom chromatogram shows the UV (280nm) that corresponds to the base peaks in the normal mass spectra. An example showing the ion spectra for each TIC base peak (ms, ms2, and ms3) is seen in Figure A.5, which indicates the MS^n ion fragmentation pattern for the epicatechin standard (at RT 16.53). The dissociation pathways which correspond to the ions in these spectra can be seen in Figure A.6. The standard mix for HPLC Method 2 can be seen in Figure A.39. The MS^n spectra for numerous additional standard compounds were provided by Jodie Johnson from the University of Florida Mass Spectrometry Laboratory (Gainesville, FL). In the case of all compounds (including those in both the standard mix and peanut skin fractions from

Toyopearl SEC), discovery of the molecular ion for each structure was determined by the presence of adduct ions found in the normal mass spectra, which are commonly formed when conducting (-)ESI-MS. Based on the modifier used in the solvent system for this study, which allows for deprotonation to occur during negative mode ionization, these adducts include acetate (59-60 amu) and sodium acetate (82 amu). Other adduct ions used for molecular ion identification included chlorine (35 or 37 amu), and ions produced by the formation of low-intensity dimers (of the molecular ion in question) during the electrospray process. Further identification of unknown structures was accomplished either by matching UV retention times (with the aforementioned standards), or by using the ion fragmentation pathways of known standards to assist in the interpretation of unknown compounds. The interpretation of ion spectra also was accomplished by following the dissociation patterns that are common to phenolic acids and bioflavonoids, known as retro-Diels-Alder (RDA) reactions. In addition, several software packages were used to aid in the identification of unknown compounds, including Thermo-Finnigan QualBrowser, the National Institute of Standards and Technology (NIST) 2005 Mass Spectral Database (and included tools such as MS Interpreter, Isotope Calculator, and MS Search), the Automated Mass Spectral Deconvolution and Identification System (AMDIS ver. 2.64), and MS fragmentation tools from ACD/Labs v12.0 and ChemBioDraw Ultra v11.0 (ChemBioOffice 2008). Other tools included web resources such as the NIST Chemistry WebBook (online mass spectral database), PubChem, and ChemBioFinder.

RESULTS AND DISCUSSION

Fraction A - HPLC Method 1

A total of 53 compounds were identified in peanut skin Fraction A obtained from Toyopearl SEC (Table 1). UV chromatograms and TICs for each scan range can be seen in Figures A.7 through A.9. Compound 1-A1 at RT 1.69 (min) exhibited a high UV intensity and ion relative abundance. An intense ion at m/z 401 $(M-H)^-$ was noted in the normal mass spectra, along with a sodium acetate $[(M-H)+CH_3COONa]^-$ adduct ion at m/z 483. Dissociation of the m/z 401 ion yielded an intense m/z 341 ion in the ms2 spectra, which revealed the presence of an acetate $[M+CH_3COO]^-$ adduct (due to the 60 amu neutral loss). Further fragmentation of the m/z 341 ion produced the following fragments in the ms3 spectra: m/z 179 (the most intense ion), 161, 143, and 119. The m/z 179 ion indicated a neutral loss of 162 amu, which proves the existence of a glucose (or galactose) monosaccharide side-group. The fragmentation scheme of the remaining 180 amu molecular weight compound follows the dissociation pathway of a dihydroxy-cinnamic acid. An example of such a compound is 3,4-dihydroxycinnamic acid (a.k.a caffeic acid) (Figure 1). Therefore, compound 1-A1 is most likely a dihydroxycinnamic acid, with a glucose (or galactose) side-unit.

Compound 2-A1 at RT 7.78 (min) exhibited an intermediate UV intensity, but a low relative ion abundance. An intense m/z 443 $(M-H)^-$ ion in the normal mass spectra dissociated to yield an m/z 383 ion in the ms2 spectra. The resulting 60 amu neutral loss showed the presence of an acetate $[(M-H)+CH_3COOH]^-$ adduct ion (confirming m/z 383 as the molecular ion). Further dissociation of the m/z 383 ion produced an intense m/z 237 ion in the ms3 spectra, which indicates the presence of a terminal rhamnose sugar (due to the 146 amu neutral loss). An additional m/z 161 ion fragment was found in the ms3 ion spectra, revealing that the m/z 237

$(M-H)^-$ compound is most likely a monohydroxy-flavone or isoflavone. The fragmentation pattern agrees with any possible flavone or isoflavone where the hydroxyl group resides on either the A or C flavonoid ring. Possible flavones compounds (and their isoflavone derivatives) include: 3-hydroxyflavone (a.k.a. flavonol), 5-hydroxyflavone (a.k.a. primuletin), 6-hydroxy-flavone, and 7-hydroxyflavone (Figure 2). The likelihood of compound 2-A1 being a mono-hydroxyflavone was also confirmed by matching ion spectra using the NIST 05 Mass Spectral Database. Other possible explanations for the fragmentation pattern of compound 2-A1 (although less likely than the mono-hydroxyflavone scenario) is the presence of the following methoxy-chalcone compounds: 4'-methoxychalcone (Figure 3) and 4-methoxychalcone. Similarities to these chalcone compounds were also confirmed using the NIST 05 database.

Compound 3-A1 at RT 8.54 showed an intermediate UV intensity, but a low relative ion abundance. The m/z 301 $(M-H)^-$ molecular ion dissociated to form the following fragments in the ms2 and ms3 spectra: m/z 285, 217, 167, 150, and 126. This fragmentation scheme follows the dissociation pathway for the compound known as 3',4',5,5',7-pentahydroxyflavone (a.k.a. tricetin) (Figure 4).

Compound 4-A1 at RT 8.69 (min) exhibited an intermediate UV intensity, but a low relative ion abundance. The m/z 379 $(M-H)^-$ molecular ion was confirmed by the presence of an acetate $[M+CH_3COO]^-$ adduct ion at m/z 439 (60 amu difference). Dissociation of the molecular ion formed the following ions in the ms2 spectra: m/z 363, 361, 350, 336, 335 (the most intense ion), 318/317, 291/290, 218/217, and 202. The predictive fragmentation patterns for the compound known as 4,4'-dihydroxy-3,3'-(2-methoxyethylidene) dicoumarin (a.k.a. dicoumoxyl) (Figure 5) nearly follows the exact dissociation pathway for compound 4-A1. A similar

dicoumarin compound with complimentary fragmentation ions was also found using the NIST 05 database (although, it had one less hydroxyl and methyl group), which supports this finding.

Compound 5-A1 at RT 8.84 (min) had a high UV response at 280nm, and gave an intense ion of m/z = 395 $(M-H)^-$ in the normal mass spectra. Further ms2 fragmentation yielded an m/z = 335 ion, showing a neutral loss of 60 amu, which is indicative of an acetate $[M+CH_3COO]^-$ adduct ion. Therefore, the molecular ion in this case is m/z = 335 $(M-H)^-$. An additional intense ion in the ms2 spectra included m/z 319. Further fragmentation of the m/z 335 ion gave ms3 product ions of m/z = 291, 273, 247, and 173. This follows the possible fragmentation pathway of the compound known as 3,3'-methylenebis[4-hydroxycoumarin] (a.k.a. dicoumarin) (Figure 6). In addition, a NIST 05 database search of the ms2 spectra confirmed a high probability that the compound is a dicoumarin. NIST 05 showed significant matches with the compound coumarin-6-(7-hydroxycoumarin-8-yl)-7-methoxy, which further supports the likelihood that compound 5-A1 is one of the aforementioned dicoumarin-based compounds.

Compound 6-A1 at RT 9.90 (min) gave both a low UV intensity and ion relative abundance. An intense m/z 457 $(M-H)^-$ ion was found in the normal mass spectra. This ion dissociated to form an m/z 397 ion in the ms2 spectra, indicating a neutral loss of 60 amu, which signifies the presence of an acetate $[(M-H)+CH_3COOH]^-$ adduct. This confirms m/z 397 $(M-H)^-$ as the molecular ion. The molecular ion dissociated to yield the following ms2 ion fragments: m/z 251 (most intense ion), 235, 163, 161, and 143. The m/z 251 ion indicates a neutral loss of 146 amu, revealing the presence of a rhamnose sugar side-group. Additional fragments in the ms3 spectra indicate that the compound is most likely 3-methoxyflavone (Figure 7). A possible match of the spectra for this compound was also confirmed using the NIST 05 database. Therefore, compound 6-A1 is most likely a 3-methoxyflavone with a rhamnose sugar side-group.

Compound 7-A1 at RT 10.20 (min) exhibited both a low UV intensity and ion relative abundance. The molecular ion was confirmed at m/z 215 $(M-H)^-$ due to the presence of acetate $[M+CH_3COO]^-$ and sodium acetate $[(M-H)+CH_3COONa]^-$ adduct ions at m/z 276 and 298 respectively. The molecular ion dissociated to yield m/z 198, 172, and 157. This follows the possible fragmentation scheme for the compound (or a derivative of) 6-hydroxy-2-naphthalenepropanoic acid (a.k.a. allenolic acid) (Figure 8). A similar compound, known as 2,3-napthalenedicarboxylic acid, was identified via a NIST 05 Mass Spectral Database search. Although compound 7-A1 is most likely not 6-hydroxy-2-naphthalenepropanoic acid (a.k.a. allenolic acid) or 2,3-napthalenedicarboxylic acid (since they are synthetized compounds), it does however show structural similarities to both these compounds based on the fragmentation scheme. This resemblance yields dissociation pathways with parallel fragmentation characteristics, which supports the theory that compound 7-A1 is possibly a derivative of allenolic acid.

Compound 13-A1 at RT 14.07 (min) exhibited a low UV response, and relatively low ion intensity. The most intense ion in the normal mass spectra (m/z 397 $(M-H)^-$) dissociated to form an intense m/z 337 $(M-H)^-$ ion in the ms2 spectra. The 60 amu difference indicates the presence of an acetate $[(M-H)+CH_3COOH]^-$ adduct, which confirms m/z 337 as the molecular ion. Other major ion fragments in the ms2 spectra include m/z 321 and 251. The fragmentation pattern somewhat follows the dissociation characteristics of a chromone-based compound, however, the ion fragments are more indicative of a compound similar in structure to 4'-hydroxy-7-methoxy-6-(3-methyl-2-butenyl)-flavanone (a.k.a. bavachinin A). The possible presence of this compound (or a close derivative of this compound) was further supported by the NIST 05 MS

database, which matched a similar structure with nearly identical fragmentation characteristics (an isoflavone derivative known as hydroxywighteone).

Compound 17-A1 at RT 17.01 gave an intermediate UV intensity, and low relative ion abundance. An m/z 167 $(M-H)^-$ molecular ion was seen in the normal mass spectra, although, no adduct ions were present. The molecular ion dissociated to yield the following ms2 ion fragments: m/z 152, 151, 137, 123, 121, 109, and 108. According to the NIST 05 database, this follows the exact fragmentation fingerprint for the compound known as vanillic acid. In addition, it shows extreme similarity to the predictive dissociation scheme for homogentisic acid (Figure 9).

Compound 18-A1 at RT 17.42 (min) exhibited a low UV intensity, but a high ion relative abundance. An intense m/z 475 $(M-H)^-$ ion in the normal mass spectra underwent collision-induced dissociation (CID) to yield an m/z 415 ion in the ms2 spectra. The 60 amu difference indicates the presence of an acetate $[(M-H)+CH_3COOH]^-$ adduct ion, which confirms m/z 415 as the molecular ion. The molecular ion then dissociated to yield an ms3 ion of m/z 269, which signifies the loss of a 146 amu rhamnose sugar. An additional m/z 161 fragment was seen in the ms3 spectra, which indicates that the m/z 269 compound could be one of several structures. Compounds which match this 270 amu molecular weight, while also exhibiting an m/z 161 fragment, include various dihydroxy-methoxy-chalcones, trihydroxy-flavones, trihydroxy-isoflavones, and hydroxy-methoxyflavanones. An example of such a compound is 3',4',7-trihydroxyflavone (Figure 10). Therefore, compound 18-A1 is most likely one of the aforementioned classes of compounds, along with an attached rhamnose sugar group.

Compound 21-A1 at RT 19.04 (min) exhibited a low UV intensity, but an intermediate-ranged ion relative abundance. A molecular ion was found at m/z 443 $(M-H)^-$, although no

adduct ions were confirmed. The parent ion dissociated to yield an m/z 299 ion in the ms2 spectra. This indicated a 144 amu neutral loss, which reveals the possible presence of a coumaroyl side-group. Further fragmentation of the m/z 299 ms2 ion produced an m/z 137 ion in the ms3 spectra, which indicates the presence of a 162 amu glucose (or galactose) unit. The remaining m/z 137 ion is most likely a hydroxybenzoic acid derivative (such as 2-hydroxybenzoic acid, 3-hydroxybenzoic acid, or 4-hydroxybenzoic acid). Therefore, compound 21-A1 is most likely a glucose-linked hydroxybenzoic acid, with a coumaroyl acyl side-group.

Compound 22-A1 at RT 19.42 (min) revealed a low UV intensity, but an intermediate ion relative abundance. An intense m/z 595 $(M-H)^-$ was found in the normal mass spectra, which dissociated to yield an m/z 535 ion in the ms2 spectra. The 60 amu difference indicated the presence of an acetate $[(M-H)+CH_3COOH]^-$ adduct ion, which confirmed m/z 535 as the molecular ion. Further fragmentation of the m/z 535 molecular ion produced the following daughter ions in the ms3 spectra: m/z 389 and 227. The m/z 389 indicated a neutral loss of 146 amu, indicative of a rhamnose sugar. Furthermore, the m/z 227 fragments yielded a neutral loss of 308 amu, which reveals the presence of a rutinose (6-O-alpha-L-rhamnosyl-D-glucose) disaccharide. The remaining m/z 227 ion fragment is most likely a resveratrol aglycone base-unit. Therefore, compound 22-A1 is tentatively identified as resveratrol, with a rutinose sugar side-group.

Compound 23-A1 at RT 19.94 (min) showed both an intermediate-to-high UV intensity and relative ion abundance. The m/z 173 molecular ion $(M-H)^-$ was confirmed by the presence of acetate $[(M-H)+CH_3COOH]^-$ adduct ion at m/z 232 (59 amu difference). The molecular ion dissociated to form ms2 ion fragments of m/z 155, 143, 142, 129, 111, 109, 83, and 81. This closely follows the predictive fragmentation pathway for shikimic acid (Figure 11). The

fragmentation fingerprint was also confirmed using the NIST 05 Mass Spectral Database. The presence of this compound at high concentrations makes sense, given that shikimic acid is the precursor to the formation of flavonoid structures.

Compound 24-A1 at RT 20.21 (min) exhibited a low UV response, but a high ion intensity. The molecular ion is assumed to be m/z 595 $(M-H)^-$, although no adduct ions were seen in the normal mass spectra. Dissociation of the molecular ion resulted in ms2 and ms3 spectra with the following ion fragments: m/z 579, 535, 487, 389, 367, 271, 263, 251, and 225. Two compounds which follow this possible fragmentation scheme (and exhibited this 596 amu molecular weight) include eriodictyol-7-neohesperidoside (a.k.a. neoeriocitrin) and eriodictyol 7-O-rutinoside (a.k.a. eriocitrin) (Figure 12).

Compound 25-A1 at RT 21.83 (min) gave both a low UV response and ion intensity. The molecular ion was noted at m/z 579 $(M-H)^-$, although no adduct ions were visible. The most intense ms2 ion formed included m/z 285. The neutral loss difference between the molecular ion (m/z 579) and the m/z 285 daughter ion was equal to 294 amu, revealing the presence of either a sambubiose (2-O-beta-D-xylosyl-D-glucose) or lathyrose (2-O-beta-D-xylosyl-D-galactose) disaccharide sugar. Further dissociation of m/z 285 yielded the following ms3 ion fragments: m/z 267, 257, 241, 217, 213, 201, and 175. This follows the exact fragmentation fingerprint for the flavonoid luteolin. Therefore, compound 25-A1 is identified as luteolin, plus either a sambubiose or lathyrose disaccharide side-group.

Compound 26-A1 at RT 24.26 gave a weak UV response, and a relatively weak MSn ion intensity. An additional compound (Compound 28-A1) with identical molecular weight and fragmentation characteristics was also found at RT 26.39, although, it had a much higher ion relative intensity. In both cases, a molecular ion was noted at m/z 243 $(M-H)^-$, confirmed by a

sodium acetate $[(M-H)+CH_3COONa]^-$ adduct ion at m/z 325 (82 amu difference). The molecular ion dissociated to yield an ms2 fragment of m/z 225. Other less intense ions were seen including m/z 201, 179, and 171. Further dissociation of the m/z 225 ms2 daughter ion yielded ms3 fragments of m/z 207, 197, 181, 163, 125, 109, 99, and 97. According the NIST 05 Mass Spectral Database, the dissociation pattern is similar to two coumarin-based compounds, known as 7-methoxy-8-isopentenylcoumarin (a.k.a. osthole) and 7-methoxy-6-isopentenylcoumarin (a.k.a. suberosin). In addition, predictive fragmentation indicates that this compound may also be either oxyresveratrol (Figure 13) or cedrecoumarin A (Figure 14).

Compound 27-A1 at RT 25.09 exhibited an intermediate UV intensity, but an extremely high relative ion abundance. This compound produced the highest ion response out of all Fraction A compounds, resulting in a compound which likely has the highest concentration in this fraction. An m/z 187 $(M-H)^-$ molecular ion was confirmed by the presence of an acetate $[(M-H)+CH_3COOH]^-$ adduct ion at m/z 246 (due to the 59 amu difference). The molecular ion dissociated to form the following ions in the ms2 spectra: m/z 169, 157, 151, 133, 125 (the most intense ion), and 97. The m/z 125 daughter fragment further dissociated to yield ms3 ion fragments of m/z 97, 83, 69, and 57. The fragmentation pattern of this compound is nearly identical to that of the standard for gallic acid (with regards to the m/z 125, 97, and 69 ion fragments). However, there is an 18 amu difference between the molecular weight of gallic acid (170 amu MW) and compound 27-A1 (188 amu MW). Several scenarios exist for the identification of compound 27-A1. First, the fragmentation pattern suggests this compound may be a phenolic acid with a structure similar to that of gallic acid. Also, the NIST 05 Mass Spectral Database revealed a high probability that compound 27-A1 may be a coumarin-based structure. In addition, there is also a possibility this compound (according to the NIST 05 Mass Spectral

Database) may be a structure similar to that of 5-hydroxy-2-methyl-1,4-naphtoquinone (a.k.a. plumbagin).

Compound 30-A1 at RT 30.46 exhibited an intermediate-range UV intensity and high relative ion abundance. A molecular ion was discovered at m/z 169 $(M-H)^-$ and confirmed by an acetate $[(M-H)+CH_3COOH]^-$ adduct ion at m/z 229 (59 amu difference), and a sodium acetate $[(M-H)+CH_3COONa]^-$ adduct at m/z 251 (82 amu difference). Fragmentation of the molecular ion produced ms2 ions of m/z 153 and 125, and further dissociation yielded an ms3 spectra with daughter ions of m/z 95, 83, 71, 57, and 55. Although the molecular weight is similar to that of gallic acid (3,4,5-trihydroxybenzoic acid), it is definitely not this compound due to slight differences in fragmentation characteristics. In addition, comparing the retention times of compound 30-A1 (RT 30.46) to the gallic acid standard (RT 5.49) indicate the two are not identical. However, the dissociation pattern suggests that these compounds are in fact similar (i.e., both are trihydroxy-benzoic acids). Predictive fragmentation indicates that compound 30-A1 is most likely 2,4,6-trihydroxybenzoic acid (Figure 15), or any other possible trihydroxybenzoic acid derivative where the hydroxy groups are not located at the 3-4-5 positions.

Compound 31-A1 at RT 31.46 (min) exhibited a low UV response, but a high ion intensity. A molecular ion was confirmed at m/z 719 $(M-H)^-$ due to the presence of an acetate $[(M-H)+CH_3COOH]^-$ adduct ion at m/z 779 (60 amu difference). Further dissociation of the molecular ion yielded an ms2 spectra with the most intense ion of m/z 659, and a low intensity ion at m/z 497. The continued dissociation of m/z 659 gave rise to fragments of m/z 539, 497, 479, and 377 (in the ms3 ion spectra). The m/z 539 fragment reveals a neutral loss of 180 amu, indicating the presence of a glucose (or galactose) sugar unit. According to the NIST 05 Mass

Spectral Database, the remaining fragments associated with the m/z 539 daughter ion are a near perfect match with the compound known as oleuropein.

Compound 34-A1 at RT 35.05 showed both a relatively strong UV response and ion relative abundance. The most intense ion was seen at m/z 557 $(M-H)^-$ in the normal mass spectra, which dissociated to yield an m/z 497 fragment in the ms2 spectra. The 60 amu neutral loss reveals the presence of an acetate $[M+CH_3COO]^-$ adduct ion, indicating m/z 497 as the molecular ion. The molecular ion dissociated to give an ms3 fragment of m/z 335, which the 162 amu neutral loss indicates the presence of single monosaccharide unit. Given the number of coumarin-based compounds which exist in this fraction (and also the discovery of m/z 335 coumarin compounds in other fractions), there is a likelihood that compound 34-A1 is any number of coumarin compounds with a 336 amu molecular weight. These compounds include: 6-(3-methylbut-2-enyl)-coumestrol (a.k.a. psoralidin), 3,3'-methylenebis[4-hydroxy-coumarin] (a.k.a. dicoumarin), lasiocephalin, and 6-(7-hydroxycoumarin-8-yl)-7-methoxy-coumarin.

Compound 35-A1 at RT 35.44 gave a both low UV intensity and ion relative abundance. The molecular ion was confirmed in the normal mass spectra at m/z 327 $(M-H)^-$ by the presence of several adduct ions including: acetate $[M+CH_3COO]^-$ at m/z 386 (59 amu difference), and sodium acetate $[(M-H)+CH_3COONa]^-$ at m/z 409 (82 amu difference). An additional compounds with the same molecular weight and similar fragmentation patterns were also found at RT 35.80 (compound 36-A1), RT 38.27 (compound 39-A1), RT 38.80 (compound 41-A1), and RT 43.98 (compound 47-A1). In all cases, dissociation of the molecular ion gave an ms2 ion spectra with fragments of m/z 309 (most intense), 221, 171, and 165. This follows the possible fragmentation pathway for the compound kaempferol-3,4',7-trimethyl-ether (Figure 16). The NIST 05 Mass Spectral Database matched a similar compound (although the methoxy and hydroxy groups were

located a different positions) known as 3-hydroxy-4',5,7-trimethoxyflavone. Therefore, these compounds are most likely various derivatives of the aforementioned compounds (with methoxy and hydroxy groups located at different positions on the flavonoid A, B, and C rings).

Compound 43-A1 at RT 41.85 exhibited both a low UV response and ion intensity. The m/z 445 $(M-H)^-$ molecular ion dissociated to yield the following ions in the ms2 spectra: m/z 429, 416, 385 (the most intense ion), 383, 382, 367, 327, 325, 309, 293, 265, 249, and 194. Further dissociation of the m/z 385 ion produced the following fragments in the ms3 spectra: m/z 367, 354, 352, 341, 325, 311, and 309. The NIST 05 Mass Spectral Database produced a high probability match for the compounds vitexin and isovitexin. Although the fragmentation pattern in the NIST 05 Database gives insight into the characterization of compound 43-A1, this is however not a true match, since the molecular weights for vitexin (and isovitexin) is 432 amu. Several 446 amu compounds exist which exhibit structural similarities to vitexin and isovitexin. In addition, the possible fragmentation pathway for these compounds is nearly identical to that produced by compound 43-A1. These compounds include the following: 4',7-dihydroxy-6-methoxyisoflavone-7-D-glucoside (a.k.a. glycitin), baicalein-7-O-glucuronide, and biochanin A-7-glucoside (a.k.a. sissotrin) (Figures 17).

Fraction A - HPLC Method 2

The use HPLC method 2 exhibited better overall separation (than method 1), and in addition to all the structures identified in method 1, allowed the detection of compounds which were not otherwise seen in the first method. UV chromatograms and TICs for each scan range can be seen in Figures A.40 through A.41. A total of 8 additional compounds were identified in peanut skin Fraction A obtained from Toyopearl SEC (Table 2). These compounds mostly

included various types of phenolic acids. For example, compound 1-A2 was detected in extremely high concentrations (in both UV and ion intensity) from RT 4.08 to 14.26 (min), with a main peak finally appearing at RT 17.77. The m/z 239 $(M-H)^-$ molecular ion dissociated to form an m/z 179 fragment, indicating the presence of an acetate $[M+CH_3COO]^-$ adduct ion (60 amu difference). The m/z 179 $(M-H)^-$ molecular ion yielded fragments of m/z 161, 145, 117, 101, and 99. The fragmentation pattern appears to be that of a dihydroxycinnamic acid with a structure similar to 3,4-dihydroxycinnamic acid (a.k.a. caffeic acid) (Figure 18), however, the retention times do not match that of the caffeic acid standard (at RT 31.57). Therefore, compound 1-A2 is assumed to be a derivative of caffeic acid, possibly with hydroxyl units residing at different positions on the phenolic ring. The constant elution of this compound over a long retention time range could possibly be caused by either an extremely high concentration of a single dihydroxycinnamic structure, or possibly due to the presence of multiple dihydroxy-cinnamic acid derivatives.

Compound 2-A2 at RT 16.72 (min) exhibited an intermediate-to-high UV intensity, but a low relative ion abundance. An m/z 221 $(M-H)^-$ ion dissociated to yield an m/z 161 fragment, indicating the loss of acetate $[M+CH_3COO]^-$ adduct ion, and confirming m/z 161 as the molecular ion. Further fragmentation of the molecular ion yielded ion fragments of m/z 143 and 125. Possible compounds which produce an m/z 143 compound include coumarin-based structures, such as 3-hydroxycoumarin, 4-coumarinol, 7-hydroxycoumarin (a.k.a. umbelliferone) (Figure 19), and 4-hydroxycoumarin.

Compound 3A-2 at RT 40.05 (min) showed an intermediate-to-high UV intensity, but a high ion relative abundance. The m/z 173 molecular ion $(M-H)^-$ was confirmed by the presence of acetate $[(M-H)+CH_3COOH]^-$ adduct ion at m/z 232 (59 amu difference). The molecular ion

dissociated to form ms2 ion fragments of m/z 155, 143, 142, 129, 111, 109, 83, and 81. This closely follows the predictive fragmentation pathway for shikimic acid (Figure 11). The fragmentation fingerprint was also confirmed using the NIST 05 Mass Spectral Database. The presence of this compound at high concentrations makes sense, given that shikimic acid is the precursor to the formation of flavonoid structures.

In addition to compounds which were undetectable using the first method, method 2 often allowed the separation of multiple compounds with identical molecular weight and fragmentation attributes (i.e., compounds which only eluted once using method 1). The most viable explanation for this phenomenon is the presence of compounds with similar structural characteristics (while having the same molecular weight), or perhaps due to side-groups residing at different locations on the base-structure. For example, compound 4-A2 at RT 48.08 (min) exhibited an intermediate-to-high UV intensity, but a high ion relative abundance. An m/z 243 $(M-H)^-$ molecular ion dissociated to yield ms2 ion fragments of m/z 225, 201, 161, and 151. Additional compounds with identical molecular weights and fragmentation characteristics were also found at RT 49.51, 52.88, 53.57, and 54.54 (min). Two possible compounds which could theoretically exhibit such a dissociation pathway include cedrecoumarin A and oxyresveratrol (although, the fragmentation scheme more closely follows cedrecoumarin A) (Figures 13 and 14).

Compound 6-A2 at RT 54.67 (min) showed an intermediate UV intensity, and a high ion relative abundance. A molecular ion at m/z 241 $(M-H)^-$ dissociated to yield the following ion fragments in the ms2 spectra: m/z 225, 223, 205, 197, 179, and 161. Predictive fragmentation of a dihydroxy-flavan could produce this fragmentation fingerprint, such as 4',7-dihydroxyisoflavan (a.k.a. equol) (Figure 20). In addition, the NIST 05 Mass Spectral Database produced spectra

matches from several similar flavandiol structures, including 4,4'-flavandiol and 4,7-flavandiol (a.k.a. 2-phenyl-4,7-chromanediol).

Compound 8-A2 at RT 60.30 (min) exhibited a somewhat low UV intensity, but a high ion relative abundance. A molecular ion was discovered at m/z 201 $(M-H)^-$, and dissociated to form ion fragments of m/z 183, 140, and 139 in the ms2 spectra. This follows the possible fragmentation pathway for various hydroxyfurocoumarin's, including 5-hydroxyfurocoumarin (a.k.a. bergaptrol) and 8-hydroxy-4'-5',6-7-furocoumarin (a.k.a. xanthotoxol) (Figure 21).

Fraction B - HPLC Method 1

A total of 24 compounds were identified in peanut skin Fraction B obtained from Toyopearl SEC (Table 3). UV chromatograms and TICs for each scan range can be seen in Figures A.10 through A.13. Compound 1-B1 at RT 8.78 (min) exhibited an extremely high UV intensity, and an intermediate ion relative abundance. The molecular ion was assumed to be at m/z 153 $(M-H)^-$, although, no adduct ions were observed. The parent ion dissociated to yield an m/z 109 fragment in the ms2 spectra. Further dissociation of this daughter ion produced ms3 ions of m/z 91 and 81. Almost all dihydroxybenzoic acid derivatives will follow this fragmentation pathway, including: 2,3-dihydroxybenzoic acid, 2,4-dihydroxybenzoic acid (a.k.a. β-resorcylic acid), 2,5-dihydroxybenzoic acid (a.k.a. gentisic acid), 3,4-dihydroxybenzoic acid (a.k.a. protocatechuic acid), and 3,5-dihydroxybenzoic acid (a.k.a. α-resorcylic acid). An example of the fragmentation pathway can be seen for 2,6-dihydroxybenzoic acid (a.k.a. γ-resorcylic acid) in Figure 22.

Compound 2-B1 at RT 11.07 (min) exhibited an intermediate UV intensity and ion relative abundance. An intense m/z 137 ion was assumed to be the molecular ion, although, no

adduct ions were observed. The parent ion dissociated to yield an ms2 spectra with the following ion fragments: m/z 119, 109, 108, 99, 95, 93, 81, 65, and 63. This follows the fragmentation pathway for all hydroxybenzoic acid derivatives, including: 3-hydroxybenzoic acid (a.k.a. m-salicylic acid), 4-hydroxybenzoic acid (a.k.a. p-salicylic acid), and 2-hydroxybenzoic acid (a.k.a. salicylic acid) (Figure 23). Another possible dissociation scheme includes compounds similar in structure to pyrocatechin monoethyl ether (Figure 24). Another compound (compound 3-B1) at RT 12.54 exhibited the same fragmentation characteristics, although, with an added glucose (or galactose) unit.

Compound 3-B1 at RT 12.54 (min) exhibited both a low UV and ion intensity response. The molecular ion, which exists at m/z 299 $(M-H)^-$, was confirmed by the presence of a sodium acetate $[(M-H)+CH_3COONa]^-$ adduct at m/z 381. Dissociation of the molecular ion yielded ms2 fragmentation which confirmed the presence of a glucose unit (162 amu neutral loss), due to an intense m/z 137 fragment. Further fragmentation of m/z 137 $(M-H)^-$ produced an m/z 93 ms3 fragment. This follows the possible dissociation scheme for various hydroxybenzoic acids, such as 2-hydroxybenzoic acid (a.k.a. salicylic acid) (Figure 23), 3-hydroxybenzoic acid (a.k.a. m-salicylic acid), and 4-hydroxybenzoic acid (a.k.a. p-salicylic acid). The ms2 and ms3 spectra were also a confirmed match with 4-hydroxybenzoic acid found in the NIST 05 Mass Spectral Database. Therefore, compound 3-B1 is identified as one of the aforementioned hydroxybenzoic acids, plus an added glucose (or galactose) monosaccharide side-group.

Compound 4-B1 at RT 12.98 (min) exhibited a low UV intensity, but an intermediate ion relative abundance. A molecular ion was noted at m/z 415 $(M-H)^-$, confirmed by a sodium acetate $[(M-H)+CH_3COONa]^-$ adduct ion at m/z 497 (82 amu difference). The molecular ion dissociated to yield an m/z 253 fragment in the ms2 spectra, revealing the presence of a glucose

(or galactose) unit due to the 162 amu neutral loss. Further dissociation of the m/z 253 daughter ion produced the following ms3 ion fragments: m/z 235, 202, 193, 160, 151, and 109. These fragments indicate the presence of a 254 amu flavonoid aglycone. Possible candidates of a compound with this molecular weight (and fragmentation pattern) include various derivatives of dihydroxyflavones and dihydroxyisoflavones. Examples of such compounds include 3,4'-dihydroxyflavone and 4',7-dihydroxyisoflavone (a.k.a. daidzein) (Figure 25).

Compound 5-B1 at RT 16.27 (min) exhibited both an intermediate UV intensity and ion relative abundance. An m/z 449 $(M-H)^-$ molecular ion was confirmed by the presence of an acetate $[M+CH_3COO]^-$ adduct ion at m/z 508, and a sodium acetate $[(M-H)+CH_3COONa]^-$ adduct ion at m/z 531. Dissociation of the molecular ion yielded an m/z 287 daughter fragment in the ms2 spectra, indicating the presence of a glucose (or galactose) side-group. Other ions noted in the ms2 spectra including m/z 431, 269, and 259. Further fragmentation of the m/z 287 fragment produced an ms3 spectra with the following ion fragments: m/z 269, 243, and 201. The most likely compound which follows this dissociation scheme is eriodictyol-7-glucoside (Figure 26). In addition to 3',4',5,7-tetrahydroxyflavanone (a.k.a. eriodictyol), several other 288 amu molecular weight flavonoids exist which could follow the dissociation pathway of the flavonoid aglycone monomer exhibited by compound 5-B1. These compounds include 2,3-dihydrofisetin (a.k.a. fustin) (Figure 27), 6-hydroxyapigenin, and dihydrokaempferol.

Fraction B contained numerous compounds which consisted of quercetin aglycones, along with various types of sugar-based side groups. These (poly)saccharide side-groups differed only by the number and type (i.e., pentose or hexose) of individual sugar units. For example, compound 7-B1 at RT 17.81 (min) exhibited both a low UV and ion intensity response. A molecular ion was discovered at m/z 933 $(M-H)^-$, and confirmed by a sodium acetate [(M-

H)+$CH_3COONa]^-$ adduct at m/z 1015 (82 amu difference). Dissociation of the molecular ion produced an ms2 ion of m/z 771, which designates a glucose (or galactose) sugar via a 162 amu difference. Further fragmentation of the m/z 771 ion gave rise to the following daughter ions in the ms3 spectra: m/z 591, 301, 300, 271, and 255. The neutral loss associated with the difference between m/z 771 and 591 equals 180 amu, identifying the presence of an additional glucose (or galactose) sugar. The neutral loss found between m/z 933 and 301 shows a difference of 632 amu, pinpointing the presence of two disaccharide units. The possible combination of disaccharides include one 324 amu disaccharide (sophorose, laminaribiose, or gentiobiose), plus an additional 308 amu disaccharide (rutinose). The ms3 ion fragments of m/z 301, 300, 271, and 255 are indicative of a quercetin aglycone with an O-glycosidic bond, which was verified by the standard for this compound. Therefore, this compound is most likely a quercetin-based monomer, plus two of the aforementioned disaccharides. Another example of a verified quercetin-glycoside includes compound 13-B1 at RT 19.66. This structure is made up of a quercetin aglycone monomer with a rutinose+glucose side-group. This compound can also be considered rutin or quercetin-3-O-rutinose (Figure 28), plus an additional glucose (or galactose).

Compound 9-B1 at RT 18.92 (min) exhibited both an intermediate UV intensity and ion relative abundance. An m/z 457 $(M-H)^-$ molecular ion was confirmed by the presence a sodium acetate $[(M-H)+CH_3COONa]^-$ adduct ion at m/z 539 (82 amu difference). The use of a single-step mass spectrometry technique (such as TOF-MS or EI-MS) could erroneously identify this structure as gallocatechin gallate (GCG) or epigallocatechin gallate (EGCG), since they have the same 458 amu molecular weight as compound 9-B1. However, the use of the current mult-stage MS/MS/MS (MSn) technique reveals that the fragmentation pathway of this compound is completely different than EGCG or GCG (according to the standards for these compounds). In

addition, the retention times for the GCG (RT 15.70) and EGCG (RT 17.44) standards do not match that of compound 9-B1 (at RT 18.92). Furthermore, a full scan of all fractions using both HPLC Method 1 and HPLC Method 2 (while utilizing a filter to pinpoint any 458 amu molecular weight compounds) revealed that neither GCG nor EGCG exists in any amount in the Gregory-line peanut skins. The lack of these compounds in peanut skins makes perfect sense, given that the existence of a galloyl-group (as seen with GCG and EGCG) requires the presence of gallic acid, which was also not detected in any amount in all fractions. In the case of compound 9-B1, the m/z 457 $(M-H)^-$ molecular ion dissociated to form the following product ions in the ms2 spectra: m/z 440, 311, 295, 293 (most abundant ion), 277, 221, 204, and 163. The presence of an m/z 295 $(M-H)^-$ ion fragment indicates a 162 amu neutral loss, revealing the presence of a glucose (or galactose) monosaccharide unit. The m/z 293 daughter ion underwent further dissociation to yield ms3 ion fragments of m/z 275, 219, 191, 187, 163, and 127. This follows the predictive fragmentation scheme for the compound 6-O-acetyldaidzin (Figure 29).

Compound 10-B1 at RT 19.34 exhibited a high UV intensity, and an intermediate-ranged relative ion abundance. A molecular ion was found at m/z 487 $(M-H)^-$, confirmed by a sodium acetate $[(M-H)+CH_3COONa]^-$ adduct ion at m/z 569 (82 amu difference). The molecular ion dissociated to yield an ms2 spectra with m/z 325 (most intense ion), 307, 293, 193, and 179 ion fragments. The m/z 325 ion indicates the existence of a glucose (or galactose) sugar unit, due to the 162 amu neutral loss. The m/z 325 daughter ion underwent further dissociation to yield m/z 193 (most intense ion), 149, and 134 ions in the ms3 spectra. The 132 amu neutral loss (between m/z 325 and 193) reveals the presence of a 132 amu xylose (or arabinose) sugar unit. The remaining fragments associated with m/z 193 (i.e., m/z 179, 149, and 134) follow the exact dissociation pattern of 3-methoxy-4-hydroxycinnamic acid (a.k.a. ferulic acid) (Figure 30),

which was confirmed by a ferulic acid standard. Therefore, compound 10-B1 is identified as ferulic acid, plus a 294 amu disaccharide side group (either sambubiose or lathyrose).

Compound 11-B1 at RT 19.39 gave both a high UV response and relative ion abundance. Although this compound is most likely a quercetin-glycoside, there is however a possibility that the aglycone may be a different flavonoid monomer. A molecular ion was noted at m/z 903 $(M-H)^-$, confirmed by an acetate $[M+CH_3COO]^-$ adduct ion at m/z 962 (59 amu difference) and a sodium acetate $[(M-H)+CH_3COONa]^-$ adduct ion at m/z 985 (82 amu difference). The molecular ion underwent collision-induced dissociation (CID), and yielded an ms2 fragment of m/z 741. Other less intense ions were seen including m/z 591, 463, and 447. Further dissociation of the m/z 741 ms2 daughter ion yielded ms3 fragments of m/z 609, 591, 463, 447, 301, 300, 271, and 255. The remaining fragments point to two possible scenarios regarding the identification of this compound, due to the dissociation pathway of the flavonoid aglycone monomer. First, the neutral loss associated with m/z 741 (from m/z 903) equals 162 amu, which is undoubtedly a glucose (or galactose) unit due to the extreme labile nature of glycosidic bonds. Further dissociation of m/z 741 yielded m/z 609, showing a neutral loss of 132 amu, which is indicative of a xylose (or arabinose) sugar unit. An additional fragment at m/z 463 revealed a neutral loss of 146 amu, which shows the presence of a rhamnose sugar unit. The last intense ion fragment of m/z 300-301 confirms a difference of 162 amu, indicating the presence of a second glucose (or galactose) unit. The remaining fragments (m/z's 271 and 255) possibly reveal the presence of a flavonoid aglycone with an m/z of 301 $(M-H)^-$, which is most likely quercetin with either a 7-D-glucoside (Figure 31) or 4'-O-glucoside linkage. This fragmentation scheme would tentatively identify the compound as quercetin with the following sugar sidegroups: glucose(galactose) + rhamnose + xylose(arabinose) + glucose(galactose), or simply lathyrose (or

sambubiose) plus rutinose. The second possible fragmentation pathway begins with the loss of glucose (162 amu) from m/z 903 $(M-H)^-$, yielding the m/z 741 daughter ion. Further dissociation of m/z 741 yields an m/z 609 fragment (132 amu neutral loss), revealing a xylose or arabinose sugar. Further fragmentation gives a daughter ion at m/z 447, with a difference of 162 amu signifying a glucose or galactose sugar. Further loss of one more xylose/arabinose unit yields 315 amu, which would reveal the presence of either 6-methoxyluteolin (aka nepetin), 3-methylquercetin (a.k.a. isorhamnetin), 4'-methoxyquercetin (a.k.a. tamarixetin), or 7-methylquercetin (a.k.a. rhamnetin). The possible presence of one of these m/z 315 flavonoids is further supported by the fragments seen at m/z 300, 271 and 255, although, the dissocation pathway is most similar to that of the methoxy-flavone called isorhamnetin. In addition to isorhamnetin, the NIST 05 Database also revealed close matches for other methoxy-flavones, including 3',4',5,6-tetrahydroxy-7-methoxy-flavone (a.k.a. pedalitin), which further supports the theory that the aglycone may possibly be a methoxy-flavonoid. Therefore, the second possible identification of this compound includes one of these aforementioned m/z 315 compounds (most likely isorhamnetin), plus the following sugar side-groups: glucose(galactose) + xylose(arabinose) + glucose(galactose) + xylose(arabinose), or simply sambubiose (or lathyrose) plus another sambubiose (or lathyrose).

Compound 14-B1 at RT 20.14 exhibited a high UV intensity, and an intermediate-ranged relative ion abundance. A molecular ion was found at m/z 137 $(M-H)^-$, confirmed by a sodium acetate $[(M-H)+CH_3COONa]^-$ adduct ion at m/z 219 (82 amu difference). The molecular ion dissociated to yield an ms2 spectra with ion fragments of m/z 119, 109, 108, 93, and 65. This follows the possible dissociation scheme for various hydroxybenzoic acids, such as 2-hydroxybenzoic acid (a.k.a. salicylic acid) (Figure 23), 3-hydroxybenzoic acid (a.k.a. m-salicylic

acid), and 4-hydroxybenzoic acid (a.k.a. p-salicylic acid). A search of the ms2 spectra using the NIST 05 Mass Spectral Database produced a perfect match for 4-hydroxybenzoic acid (a.k.a. p-salicylic acid).

As in the previous case regarding quercetin aglycone monomers, Fraction B contained numerous compounds which consisted of isorhamnetin aglycones with various types of sugar-based side groups. These (poly)saccharide side-groups differed only by the number and type (i.e., pentose or hexose) of individual sugar units. For example, compound 15-B1 at RT 21.49 (min) exhibited both a very high UV and ion intensity response. A molecular ion was discovered at m/z 785 $(M-H)^-$, and confirmed by an acetate $[(M-H)+CH_3COOH]^-$ adduct ion at m/z 844 (59 amu difference). Dissociation of the molecular ion produced an ms2 ion of m/z 605, which designates a glucose (or galactose) sugar via a 180 amu difference. The most intense ion in the ms2 spectra was found at m/z 315 $(M-H)^-$, which reveals a neutral loss of 470 amu (from the m/z 785 molecular ion). The 470 amu difference indicates the presence of a 308 amu rutinose (6-O-alpha-L-rhamnosyl-D-glucose) disaccharide sugar, plus an additional 162 amu glucose (or galactose) monosaccharide unit. Additional (less intense) ion fragments in the ms2 spectra included m/z 299 and 271. Further fragmentation of the m/z 315 ion gave rise to the following daughter ions in the ms3 spectra: m/z 300, 299, 285, 271, 243, and 177. The ms3 ion fragments (along with the m/z 315, 299, and 271 daughter ions found in the ms2 spectra) indicate the presence of an isorhamnetin aglycone monomer (Figure 32). Therefore, compound 15-B1 is identified as isorhamnetin-3-O-rutinoside, plus an additional glucose (or galactose) sugar. This finding is further supported by an identical discovery by (Lou et al., 2001) who used NMR analysis to confirm the presence of isorhamnetin-3-O-[2-O-β-glucopyranosyl-6-O-α-rhamnopyranosyl]-β-glucopyranoside in peanut skins. Another example of a verified

isorhamnetin-glycoside includes compound 16-B1 at RT 22.18. In this case, the m/z 639 $(M-H)^-$ molecular ion underwent collision-induced dissociation (CID) to yield an m/z 315 isorhamnetin monomer. In this case, the structure is made up of an isorhamnetin aglycone monomer with one of the following dissacharide side-groups (due to the 324 amu neutral loss): laminaribiose (3-O-beta-D-glucosyl-d-glucose), gentiobiose (6-O-beta-D-glucosyl-D-glucose), or sophorose (2-O-beta-D-glucosyl-d-glucose). The final isorhamnetin-based structure was compound 18-B1, and was detected at RT 23.31. This compound exhibited an m/z 755 $(M-H)^-$ molecular ion, which underwent collision-induced dissociation (CID) to yield an m/z 315 isorhamnetin monomer. The 440 amu neutral loss indicates the presence of a 308 amu rutinose (6-O-alpha-L-rhamnosyl-D-glucose) disaccharide, plus an additional 132 amu xylose (or arabinose) monosaccharide. Again, an identical compound (isorhamnetin-3-O-[2-O-β-xylopyranosyl-6-O-α-rhamnopyranosyl]-β-glucopyranoside) was reported by (Lou et al., 2001) by means of NMR analysis.

Compound 19-B1 at RT 24.54 exhibited both an intermediate UV intensity and ion relative abundance. An m/z 463 $(M-H)^-$ molecular ion was confirmed by the presence of a sodium acetate $[(M-H)+CH_3COONa]^-$ adduct ion at m/z 545 (82 amu difference). The molecular ion dissociated to yield an ms2 spectra with ion fragments of m/z 301 (most intense ion), 283, 257, and 234. The m/z 301 ion fragment indicates a neutral loss of 162 amu (a glucose or galactose sugar). Further dissociation of the m/z 301 ion produced the following ions in the ms3 spectra: m/z 286, 271, 256, 241, 217, 164, and 151. This follows the exact dissociation pathway for the compound 3',5,7-trihydroxy-4'-methoxyflavanone (hesperitin) (Figure 33). Confirmation of hesperitin was also conducted by matching MS/MS Ion Trap standards run in this study.

Compound 20-B1 at RT 27.59 exhibited both an intermediate UV response and ion relative abundance. A molecular ion was identified at m/z 461 $(M-H)^-$ due to the presence of a

chlorine $[M+Cl^-]^-$ adduct ion at m/z 500 (37 amu difference). The molecular ion dissociated to form ms2 spectra with an intense ion at m/z 299, and less intense ions at m/z 284, 255, and 227. The neutral loss associated with the m/z 299 ion fragment yields 162 amu, indicative of a glucose (or galactose) sugar unit. The m/z 299 daughter fragment underwent further dissociation to produce an intense m/z 284 ion in the ms3 spectra. Other less intense ions included m/z 267, 243, 178, 151, and 119. The 15 amu loss (methyl group) between the m/z 299 ion and the ms3 daughter fragment indicates the likely presence of a methoxy group. Dissociation pathways based on obtained fragmentation data of standards for this study indicate a high probability that the compound is 5,7,4'-trihydroxy-3'-methoxy-flavone (a.k.a. chrysoeriol), specifically with regards to the m/z 284, 256, and 151 fragments. However, it has also been shown that chrysoeriol (Figure 34) exhibits dissociation patterns which are nearly identical to that of diosmetin (aka luteolin-4'-methyl ether). In addition, these two compounds elute at nearly the same retention times under similar chromatographic conditions, which supports the theory that the other compound may possibly be diosmetin. Although fragmentation data for the standards of these compounds was obtained, definitive matches are only possible by running the actual standards to determine UV retention times (which were not available for this research). Although the aglycone in compound 20-B1 is most likely one of the two aforementioned compounds, the lack of definitive proof for identification opens the possibility that the aglycone may in fact be one of many other 300 amu flavonoid compounds which exhibited similar fragmentation pathways (specifically with regards to the m/z 284 and 227 daughter ions). The dissociation pathway follows the predictive fragmentation patterns for numerous bioflavonoids with 300 amu molecular weights, including: 3',5,7-trihydroxy-4'-methoxyisoflavone (a.k.a. pratensein), 4',5,7-trihydroxy-6,8-dimethylflavanone (a.k.a. farresol or cyrtopterinetin), 4',5,7-

trihydroxy-6-methoxyisoflavone (a.k.a. tectorigenin) (Figure 35), psi-tectorigenin, 4'-hydroxy-5,7-dimethoxyflavanone, 8-methoxy-iso-scutellargin, 3,7-dihydroxy-2-(4-hydroxy-3-methoxy-phenyl)-4-benzopyrone (a.k.a. geraldol), and kaempferol 4'-methyl ether (a.k.a. kaempferide). Therefore, compound 20-B1 is one of the aforementioned flavonoid aglycones, with an attached glucose (or galactose) monosaccharide side-unit.

Compound 21-B1 at RT 49.11 exhibited both a high UV intensity and ion relative abundance. A molecular ion at m/z 435 $(M-H)^-$ was confirmed by the presence of a sodium acetate $[(M-H)+CH_3COONa]^-$ adduct ion at m/z 517 (82 amu difference). The parent ion dissociated to form the following ion fragments in the ms2 spectra: m/z 420 (the most intense ion), 378, 366, 351, 312, 299, and 271. The m/z 420 further dissociated to yield ms3 fragments of m/z 405, 377, 351, 338, 309, 298, 283, 270, 259, and 188. Predictive fragmentation patterns indicate that compound 21-B1 may be similar in structure to a compound known as orotinichalcone (Figure 36). In addition, a search of the NIST 05 Mass Spectral Database revealed a similar structure (2'-O-methylcajanone) with analogous fragmentation patterns. Several other compounds with similar fragmentation patterns were detected at RT 50.90 and 53.00 (min). As in the case with the previous structure, the NIST 05 Database showed possible matches to various chalcone, chromone, and chromene-based compounds.

Fraction B - HPLC Method 2

The use HPLC method 2 exhibited better overall separation (than method 1), and in addition to all the structures identified in method 1, allowed the detection of compounds which were not otherwise seen in the first method. UV chromatograms and TICs for each scan range can be seen in Figures A.42 through A.43. A total of 27 additional compounds were identified in

peanut skin Fraction B obtained from Toyopearl SEC (Table 4). For example, compound 2-B2 at RT 17.08 (min) exhibited a high UV intensity, and an intermediate-ranged ion relative abundance. An m/z 403 $(M-H)^-$ molecular ion was confirmed by the presence of an acetate $[M+CH_3COO]^-$ adduct ion at m/z 463. The molecular ion dissociated to yield the following ions in the ms2 spectra: m/z 357, 293, 271 (most intense ion), 240, 191, 177, 161, and 149. Further dissociation of the m/z 271 daughter fragment yielded ms3 ions of m/z 181, 161, 151, 113, 109, 101, 100, and 97. Although some of these fragments (m/z 177 and 151 $M-H^-$) would indicate the presence of a terminal rhamnose sugar unit along with a naringenin aglycone (as shown by fragmentation patterns of standards), the dissociation scheme also follows that of a compound known as 2',3,4,4'-tetrahydroxychalcone (a.k.a. butein) (plus a terminal rhamnose monosaccharide unit) (Figure 37).

Compound 5-B2 at RT 22.01 exhibited a high UV intensity, but a low relative ion abundance. An intense m/z 419 $(M-H)^-$ ion was found in the normal mass spectra, but no adduct ions were noted. Dissociation of this ion produced an intense m/z 359 ion in the ms2 spectra, yielding a 60 amu neutral loss. This would indicate the presence of an acetate $[M+CH_3COO]^-$ adduct ion, revealing m/z 359 as the molecular ion. Additional less intense ions in the ms2 spectra included m/z 289, 177, and 152. Further dissociation of the m/z 359 ion led to the following ion fragments in the ms3 spectra: m/z 342/341, 297, 289, 273, 247, 231, 207/206, 191, 165, and 153. Prediction of the fragmentation scheme indicates that the dissociation pathway is nearly identical to a compound known as 3',5,7-trihydroxy-4',5',6-trimethoxyisoflavone (a.k.a. irigenin) (Figure 38). However, the fragmentation patterns may also follow other trihydroxy-trimethoxy-flavonoid derivatives. In addition, a spectral search using the NIST 05 Database indicated ion fragments similar to 3-hydroxy-3',4',5,7-tetramethoxy-flavanone. The NIST 05

search also yielded a flavonoid compound known as 3-hydroxy-3',4',7,8-tetramethoxy-flavanone (although it produced slightly less similar fragment matches).

Compound 10-B2 at RT 33.65 (min) exhibited a low UV and ion intensity. The molecular ion at m/z 479 $(M-H)^-$ dissociated to yield an ms2 ion of m/z 317, which signify the loss of a 162 amu glucose (or galactose) unit. Other less intense ion fragments in the ms2 spectra included m/z 299, 289, 258, and 179. Further dissociation of the m/z 317 daughter ion resulted in ms3 fragments with m/z's 284, 268, and 176. The m/z 317 fragment indicates the molecular weight (318 amu) of the flavonoid aglycone. The remaining ions follow the most likely fragmentation patterns for the following m/z 317 $(M-H)^-$ flavonoid compounds: 3,3',4',5,5',7-hexahydroxyflavone (a.k.a. myricetin) (Figure 39), 3,3',4',5,6,7-hexahydroxy-flavone (a.k.a. quercetagetin), and 3,3',4',5,7,8-hexahydroxyflavone (a.k.a. gossypetin). Similarities in the ion fragmentation of these three compounds were also confirmed using the NIST 05 Mass Spectral Database. Therefore, compound 10-B2 is most likely one of the three aforementioned compounds, with a glucoside side-group. An example of such a compound is gossypetin-8-glucoside (a.k.a. gossypin) (Figure 40).

Compound 13-B2 at RT 39.35 (min) exhibited an intermediate UV intensity and ion relative abundance. A molecular ion was found at m/z 331 $(M-H)^-$, and was confirmed by the presence of an acetate $[M+CH_3COO]^-$ adduct ion at m/z 391. The molecular ion dissociated to yield the following ion fragments in the ms2 spectra: m/z 315, 299 (most intense ion), 287, 271, 255, and 179. The m/z 299 underwent further dissociation to yield the following ion fragments in the ms2 spectra: m/z 271, 256, 239, 227, 215, 187, 179, 151, and 124. According to the NIST 05 Mass Spectral Database, these ion fragments follow the exact dissociation pathway for the following chromanediol compounds: 2-(3,4-demethoxyphenyl)-7-methoxy-3,4-chromanediol,

and 7,8-dimethoxy-2-(4-methoxyphenyl)-3,4-chromanediol. NIST 05 also produced an additional match for 5,6,8,3',4'-pentahydroxy-7-methoxyflavone, however, the existence of this compound is less likely due to fewer matching fragments in the ion spectra. A similar compound (compound 19-B2) with nearly identical fragmentation patterns was found at RT 50.03, although the molecular weight was 364 amu (m/z 363 $(M-H)^-$). The 32 amu difference indicates that compound 19-B2 is a structure which is identical to the aforementioned chromanediol's, except for the addition of one methoxy group.

Compound 14-B2 at RT 42.64 (min) exhibited both an intermediate UV intensity and ion relative abundance. An m/z 389 $(M-H)^-$ molecular ion dissociated to yield the following ions in the ms2 spectra: m/z 374, 341 (the most intense ion), 323, 303, 195, and 193. The m/z 374 ion fragment indicates a loss of 15 amu (CH_3) from the molecular ion, indicating the possible presence of a methoxy group. Further dissociation of the m/z 341 daughter ion produced the following fragments in the ms3 spectra: m/z 326, 309, 297, 295, 250, and 233. Ion fragments m/z 326, 309, and 295 each indicate a loss of 15 amu (CH_3) from the m/z 341 daughter fragment, revealing the possible presence of three additional methoxy groups (totaling four methoxy groups). This follows the exact dissociation pattern for the trihydroxy-tetramethoxy-flavone compound known as gardenin E (Figure 41). In addition, the NIST 05 Database indicated a similar fragmentation scheme for the compound known as 3',5,7-trihydroxy-4',5',6,8-tetramethoxy-flavone (a.k.a. scaposin), which further supports the theory that compound 14-B2 is a trihydroxy-tetramethoxy-flavone.

Compound 17-B2 at RT 46.47 (min) exhibited both a high UV intensity and ion relative abundance. The m/z 301 $(M-H)^-$ molecular ion dissociated to yield ion fragments of m/z 283, 271, 257 (the most intense ion), 255, and 218 in the ms2 spectra. Further dissociation of the m/z

257 daughter ion produced the following fragments in the ms3 spectra: m/z 242, 229, 215, 213, 211, 199, 189, 187, 171, and 147. Except for one major missing ion (m/z 286), this follows almost the exact dissociation pathway for the flavonoid compound known as 3',5,7-trihydroxy-4'-methoxyflavanone (a.k.a. hesperitin). It was further confirmed that Compound 17-B2 was not in fact hesperitin, due to the comparison of a non-matching retention time exhibited by the standard for this compound. Other flavonoids exist (with a 302 amu molecular weight) which could also follow a similar dissociation pathway, including: 2',3,4',5,7-pentahydroxyflavone (a.k.a. morin) (Figure 42), 3,3',4',5',7-pentahydroxyflavone (a.k.a. robinetin) (Figure 43), and 3',4',5,5',7-pentahydroxyflavone (a.k.a. tricetin).

Compound 18-B2 at RT 47.03 (min) exhibited both a high UV intensity and ion relative abundance. The molecular ion was confirmed at m/z 311 $(M-H)^-$ due to the presence of an acetate $[M+CH_3COO]^-$ adduct ion at m/z 361. The molecular ion underwent collision-induced dissociation (CID) to yield an intense ion fragment at m/z 179 in the ms2 spectra. The 132 amu neutral loss indicates the presence of a terminal rhamnose monosaccharide unit. Further dissociation of the m/z 179 daughter ion produced an m/z 135 fragment, indicative of 3,4-dihydroxycinnamic acid (a.k.a. caffeic acid) (Figure 44). Therefore, compound 18-B2 is identified as caffeic acid, plus a terminal rhamnose monosaccharide side-group.

Compound 25-B2 at RT 66.41 (min) exhibited an intermediate UV intensity, but a high ion relative abundance. An m/z 399 $(M-H)^-$ molecular ion dissociated to yield daughter fragments of m/z 384 (the most intense ion), 323, and 308 in the ms2 spectra. Further dissociation of the m/z 384 fragment produced the following ions in the ms3 spectra: m/z 370, 366, 341, 326, 309, 308, 298, 297, 283, 281, 269, 268, and 251. This follows the exact predictive fragmentation scheme for the compound torosaflavone A (Figure 45). However, the

NIST 05 Mass Spectral Database produced a similar spectral match for 2-[2-[3,5-dihydroxyphenyl]ethenyl]-5-hydroxy-chromone.

Compound 26-B2 at RT 80.91 (min) exhibited an intermediate UV intensity, but a high ion relative abundance. The molecular ion (at m/z 367) dissociated to yield the following ion fragments in the ms2 spectra: m/z 352, 349, 337, 297 (most intense ion), 282, and 270. The m/z 297 ion fragment further dissociated to form m/z 282 and 267 in the ms3 spectra. This fragmentation pathway follows the exact dissociation scheme for the compound known as glycycoumarin (Figure 46).

Compound 27-B2 at RT 86.62 showed both a high UV intensity and ion relative abundance. The m/z 351 molecular ion dissociated to form an intense m/z 336 ion fragment, along with less intense m/z 296 and 281 ion fragments. The m/z 336 daughter ion underwent further dissociation to yield the following fragments in the ms3 spectra: m/z 319 and 281 (the most intense ion). This fragmentation fingerprint follows the possible dissociation pathway for the compound pongagallone A (Figure 47).

Fraction C - HPLC Method 1

A total of 35 compounds were identified in peanut skin Fraction C obtained from Toyopearl SEC (Table 5). UV chromatograms and TICs for each scan range can be seen in Figures A.14 through A.17. Compound 2-C1 at RT 8.05 (min) had a high UV response at 280nm, and gave an ms1 parent ion of m/z = 349 $(M-H)^-$. Further ms2 fragmentation yielded an m/z = 267 ion, showing a neutral loss of 82 amu, which is indicative of a sodium acetate adduct $[(M-H)+CH_3COONa]^-$. Therefore, the molecular ion in this case is m/z = 267. Further fragmentation gave ms3 product ions of m/z = 150 and 134. This follows the possible $(M-H)^-$

fragmentation pathway of several different compounds including 2',4'-dimethoxychalcone, 7-methoxyflavonol, 3-hydroxy-7-methoxy-flavone, and 3-hydroxy-6-methoxyflavone (Figure 48). In addition, a NIST 05 database search of the ms2 spectra confirmed a high probability that the compound is most likely a flavonoid with a methoxy group, which further supports the likelihood that compound 2-C1 is possibly one of the aforementioned flavonoid-based compounds.

Compound 3-C1 at RT 8.51 (min) also gave a high UV response, although, it exhibited a weak ion intensity. Ions produced included $(M-H)^-$ m/z 517, 493, and 435, with m/z 435 being the most intense ion. Ions at m/z = 517 and 493 signify sodium acetate $[(M-H)+CH_3COONa]^-$ and acetate $[(M-H)+CH_3COOH]^-$ adduct ions respectively, giving positive confirmation of a molecular ion at m/z = 435. The $(M-H)^-$ molecular ion of m/z = 435 yielded ms2 ion fragments of 417, 399, 375, 357, 345, 333, 315, and 289 (m/z). The 417 and 399 fragments both signify neutral losses of 18 amu, indicative of water. The m/z 375, 345, 333, and 315 fragments show losses of 60, 90, 102, and 120 amu respectively. These numbers reveal characteristic product ions which are typically associated with the cross-ring cleavages of sugars. Also, the loss of one (or two) water molecules is often noted in the CID spectrum of monosaccharides (Cuyckens and Claeys, 2004). In addition, the m/z = 289 $(M-H)^-$ fragment shown in the ms2 spectra gives a neutral loss of 146, signifying the possible presence of a terminal rhamnose unit, with a glycosidic O-linkage. Further fragmentation resulted in an ms3 ion spectra with daughter ions which are common to catechin and/or epicatechin (m/z = 245 and 205). Although there is a possibility that compound 3-C1 may be a catechin or epicatechin with a coumaroyl acylated side-group (denoted by a neutral loss of 146), it is however unlikely due to the characteristic O-glycosidic fragmentation patterns exhibited by this compound (Figure 49). Therefore, based on

the typical positions in which sugar units attach to a flavonoid aglycone, compound 3-C1 is tentatively identified as one of the following flavonoid-O-glycosides: catechin-3-O-rhamnoside, catechin-5-O-rhamnoside, or catechin-7-O-rhamnoside (or their epicatechin derivatives).

Compound 4-C1 at RT 12.31 (min) showed a weak UV response, with medium ion intensity. Several possible scenarios exist for the identification of compound 4-C1, since the MSn spectra were extremely complicated. One could assume the molecular ion to be one of two possible ions, since adduct ions were not easily interpreted. One scenario offers a fragmentation scheme with the molecular ion at m/z 419, and the other at m/z 359. First, the normal mass spectra gave an intense ion at m/z 419 $(M-H)^-$, along with a possible sodium acetate $[(M-H)+CH_3COONa]^-$ adduct at m/z 501 (due to the 82 amu difference). If in fact m/z 419 is the parent ion, then it dissociated to form ms2 fragments of m/z 401, 359, 341, 329, and 289. The most intense ms2 ion (m/z 359) dissociated to form a plethora of ms3 fragments. These ions included m/z 341, 331, 315, 297, 289, 273, 255, 247, 245, 235, 227, 205, 203, 187, 161, and 151. The specific fragmentation scheme of m/z 419 offers several possibilities regarding identification of compound 4-C1. The first possibility is a type of hydroxy-hexamethoxy-flavone, or derivative of, since the position of the lone hydroxyl group is unknown (and would likely require NMR to determine the exact location). A similar hexamethoxy-flavone compound (3,3',4',5,5',7-hexamethoxyflavone) was matched with similar fragments by searching the ms2 spectra with the NIST 05 database, which further supports this theory (although, it exhibited one less hydroxyl group). In addition, the neutral loss associated with the ion fragments reveals consecutive losses of water (18 amu) and numerous methoxy (31 amu) groups. For example, the ms3 fragments of m/z 297, 235, and 205 reveal respective losses of 62 (two methoxy groups), 124 (four methoxy groups), and 155 (five methoxy groups) amu from their m/z 359 ms2

daughter ion. Again, these losses support the possible presence of this class of compound. A second possibility for the m/z 419 scenario points to the presence of a stilbene-based compound, with a sugar side-group. The ion fragments of m/z 359, 329, and 315 represent neutral losses of 60, 90, and 104 amu respectively. These neutral losses commonly indicate the presence of a monosaccharide unit. Furthermore, the remaining fragments point to the possibility that compound 4-C1 is similar in structure to 4'-methoxy-3,3',5-stilbenetriol 3-glucoside (Figure 50), which itself is very similar to resveratrol (since it exhibits a resveratrol base unit). The presence of a fragment at m/z 227 (which matches the molecular weight of resveratrol) also supports this theory. Other possibilities for m/z 419, although less likely, are the compounds (or derivatives of) 3'-benzyloxy-5,7-dihydroxy-3,4'-dimethoxyflavone (Figure 51) and isopomiferin (Figure 52). The second fragmentation scheme scenario would present the molecular ion at m/z 359, which is the most intense ms2 ion. This is possible since the most intense ion in the normal mass spectra is m/z 419, which would indicate that the 60 amu loss associated with m/z 359 is possibly an acetate $[M+CH_3COO]^-$ adduct ion (and thereby possibly confirming m/z 359 as the molecular ion instead of m/z 419). If this is in fact the case, then the m/z 359 parent ion dissociated to form the ms3 fragments mentioned above. Based on this dissociation pattern (and the number of confirmed methoxy groups), a possible candidate for compound 4-C1 would be 3',5,7-trihydroxy-4',5',6-trimethoxyisoflavone (or a derivative of), also known as irigenin (Figure 53). According to the NIST 05 database, other possible candidates include the following methoxy-flavonoids: 3-hydroxy-3',4',5,7-tetramethoxy-flavanone, 3-hydroxy-3',4',7,8-tetramethoxy-flavanone, and 5,6,3'-trihydroxy-3,7,4'-trimethoxy-flavone (a.k.a. oxyanin B). One last scenario cannot be ruled out for the identification of compound 4-C1. The ms2 spectra shows a fragment of m/z 289, with further ms3 fragments of m/z 245, 227, 205, 203, 187, 161, and 151. This

follows the exact fragmentation scheme for catechin and/or epicatechin, which could point to compound 4-C1 being this flavonoid base unit, with an unknown 130 amu side-group.

Compound 5-C1 at RT 13.37 (min) exhibited both a low UV and ion intensity response. The ion at m/z 399 $(M-H)^-$ dissociated to yield an ms2 ion of m/z 339, with a difference indicating acetate $[M+CH_3COO]^-$ via a neutral loss of 60 amu. Therefore, the m/z 339 is most likely the molecular ion. Another intense ms2 ion of m/z 177 $(M-H)^-$ was observed, which reveals the presence of a glucose unit due to a loss of 162 amu from the m/z 339 molecular ion. Further dissociation yielded ms3 fragmentation which confirmed the presence of a glucose unit (m/z = 162), due to m/z fragments of 134, 120, and 90 (which are common fragments produced by cross-ring cleavages of sugars). Dissociation of m/z 177 $(M-H)^-$ revealed ms3 fragmentation patterns which could indicate the possible presence of (one of) many different compounds. Various derivatives of methoxy-cinnamic acids, benzoic acids, propionic acids, and propenoic acids are all possible candidates. Examples of these compounds include the following (or similar derivatives): chroman-2-carboxylic acid, 3-chromane-carboxylic acid, and 4-methoxycinnamic acid. Furthermore, the NIST 05 Database revealed a high probability that this compound is in fact 6,7-dihydroxycoumarin-6-glucoside (a.k.a. esculin). This is also supported by predicting the possible fragments generated by common structural cleavages during dissociation. The presence of this compound would not be out of the ordinary, since it is commonly found in the skins and bark of chestnuts. Other possible derivatives of this compound, which could also prove to be compound 5-C1, include 6,7-dihydroxycoumarin-7-glucoside (a.k.a. cichoriin) and 7,8-dihydroxycoumarin 7-β-D-glucoside (a.k.a. daphnetin-7-O-glucoside, or simply daphnin).

Compound 6-C1 at RT 14.42 (min) exhibited an extremely low UV response, and relatively low ion intensity. Ions in the normal mass spectrum include the most intense ion of

m/z 437 $(M-H)^-$, and a low intensity ion at m/z 518 (indicating a sodium acetate aduct). The molecular ion at m/z 437 dissociated to form two major ms2 fragments at m/z 347 and 289. The m/z 289 fragment conveys a neutral loss of 148 amu, which could be indicative of a trans-cinnamic acid acyl group. This is further supported by the 90 amu loss associated with the m/z 347 fragment, which would indicate a C_7H_6 loss common to cinnamic acids. Further dissociation of m/z 289 resulted in ms3 ions which follow the fragmentation scheme for catechin and/or epicatechin. Therefore, this compound is tentatively identified as a catechin (or epicatechin), with a trans-cinnamic acid side-group. An additional compound (compound 9-C1) with the same molecular ion and fragmentation pattern exists at RT 15.17 min. The presence of two compounds (at different retention times) with identical MS fragmentation characteristics is possibly due to the existence of trans-cinnamic acid side-groups residing at different positions on the flavonoid aglycone.

Compound 7-C1 at RT 14.88 (min) exhibited a low UV and ion intensity. The molecular ion at m/z 641 $(M-H)^-$ dissociated to yield ms2 ions of m/z 479 and 317, which signify the loss of two 162 amu glucose units. Further dissociation of the m/z 479 daughter ion resulted in ms3 fragments with m/z 317, 300, 299, 209, 191, and 176. The m/z 317 fragment indicates the presence of the second glucose unit (i.e., its 162 amu difference from m/z 479), and also reveals the molecular weight of the flavonoid aglycone. The remaining ions follow the most likely fragmentation patterns for the following m/z 317 $(M-H)^-$ flavonoid compounds: 3,3',4',5,5',7-hexahydroxyflavone (a.k.a. myricetin), 3,3',4',5,6,7-hexahydroxyflavone (a.k.a. quercetagetin) (Figure 54), and 3,3',4',5,7,8-hexahydroxyflavone (a.k.a. gossypetin). Similarities in the ion fragmentation of these three compounds were also confirmed using the NIST 05 Mass Spectral

Database. Therefore, compound 7-C1 is most likely one of the three aforementioned compounds, with a diglucoside side-group.

Compound 8-C1 at RT 15.06 (min) showed both low UV and ion intensity, with the most intense ion at m/z 319 $(M-H)^-$. Other ions found in the normal mass spectrum include m/z 401 and 378, indicating sodium acetate $[(M-H)+CH_3COONa]^-$ and acetate $[(M-H)+CH_3COOH]^-$ adducts respectively, which confirmed m/z 319 as the molecular ion. The m/z 319 molecular ion dissociated to form ms2 ions at m/z 287, 197 (the most intense ion), and 165 $(M-H)^-$. The m/z 197 ms2 daughter ion dissociated to form an m/z 165 ion in the ms3 spectra. The m/z 287 ms2 fragment indicates the loss of 32 amu, which is commonly indicative of a methoxy group. Further losses indicate fragmentation which follows the dissociation pattern for the compound oureatacatechin (Figure 55), which has a similar structure to catechin and epicatechin, but with an added methoxy group.

Compound 10-C1 at RT 15.24 (min) exhibited both a strong UV response and high ion intensity. The molecular ion, which exists at m/z 639 $(M-H)^-$, was confirmed by the presence of acetate $[M+CH_3COO]^-$ and sodium acetate $[(M-H)+CH_3COONa]^-$ adducts at m/z 699 and 722 respectively. Dissociation of the molecular ion resulted in m/z 477 and 315 ms2 product ions. As in the case with compound 7-C1 at RT 14.88, this was due to the loss of two glucose units (162 amu each). Further fragmentation resulted in ms3 ions with m/z 315, 300, and 271. This follows the fragmentation patterns for the flavonoid isorhamnetin, as seen in previous the standard for this compound. In addition, the common presence of isorhamnetin among various plant types makes it the most likely aglycone for compound 10-C1. However, the ms3 ion fingerprint could also result from the fragmentation of several other possible compounds including 6-methoxyluteolin (aka nepetin), 4'-methoxyquercetin (a.k.a. tamarixetin), and 7-

methylquercetin (a.k.a. rhamnetin) (Figures 56). In addition to isorhamnetin, the NIST 05 Database also revealed close matches for other methoxy-flavones, including 3',4',5,6-tetrahydroxy-7-methoxy-flavone (a.k.a. pedalitin), which further supports the theory that the aglycone is in fact a methoxy-flavonoid. Unfortunately, the MSn fragmentation patterns for these compounds are nearly identical, and the position of the methoxy group cannot be determined without performing NMR analysis. In addition, the lack of standards for these compounds prevented positive identification via UV rentention times. Therefore, compound 10-C1 is tentatively identified to contain one of the aforementioned flavonoid aglycones, with a diglucoside side-group.

Compound 11-C1 at RT 15.56 (min) gave both a low UV response and ion intensity. The molecular ion was noted at m/z 551 $(M-H)^-$ due to an acetate $[M+CH_3COO]^-$ adduct at m/z 611. The most intense ms2 ion formed included m/z 389. The neutral loss difference between the molecular ion (m/z 551) and the m/z 389 daughter ion was equal to 162 amu, revealing the presence of glucose. Further dissociation of m/z 389 yielded an ms3 ion of m/z 227, which also gave a neutral loss of 162 amu, signifying a second glucose unit. It is possible that the remaining m/z 227 is resveratrol. Other ms3 ions would also indicate such a compound (including m/z 341, 193, and 161), as noted with the fragmentation scheme of resveratrol-3-β-mono-D-glucoside (Figure 57). Therefore, it is hypothesized that Compound 11-C1 consists of a reveratrol aglycone base unit, with a diglucoside side-group. This dissacharides is most likely either laminaribiose (3-O-beta-D-glucosyl-d-glucose) or gentiobiose (6-O-beta-D-glucosyl-D-glucose), since they are the most common diglucoside side-groups found on flavonoid and stilbene aglycones.

Compound 12-C1 at RT 19.70 exhibited both a low UV and ion intensity response. A molecular ion was discovered at m/z 757 $(M-H)^-$, and confirmed by a sodium acetate $[(M-H)+CH_3COONa]^-$ adduct at m/z 839 (82 amu neutral loss) and a chlorine $[Cl^-]$ adduct at m/z 793. Dissociation of the molecular ion produced an ms2 ion of m/z 595, which designates a glucose(galactose) sugar via a 162 amu difference. Further fragmentation in the ms3 spectra gave rise to daughter ions of m/z 463, 301, 300, 271, and 255. The neutral loss associated with the difference between m/z 595 and 463 equals 132 amu, identifying the presence of a xylose (or arabinose) sugar. An additional neutral loss found between m/z 463 and 301 shows a difference of 162 amu, pinpointing the presence of another glucose (or galactose) unit. The ms3 ion fragments of m/z 301, 300, 271, and 255 are indicative of quercetin with an O-glycosidic bond, as shown by the standard obtained for this compound. This compound is most likely a quercetin-based monomer, plus the following trisaccharide: glucose (or galactose) + xylose (or arabinose) + glucose (or galactose) (or simply stated, either a sambubiose or lathyrose sugar plus an additional glucose/galactose).

Compound 13-C1 at RT 19.89 (min) exhibited a relatively strong UV response, but low ion intensity. A molecular ion was confirmed at m/z 477 $(M-H)^-$ due to a sodium acetate $[(M-H)+CH_3COONa]^-$ adduct ion at m/z 559 (resulting in an 82 amu neutral loss), and an acetate $[(M-H)+CH_3COOH]^-$ adduct ion at m/z 536 (59 amu neutral loss). Further dissociation of the molecular ion yielded an ms2 spectra with the most intense ion of m/z 315, and a low intensity ion at m/z 300. The neutral loss associated with m/z 315 equals 162 amu, revealing the presence of a single glucose unit. The continued dissociation of m/z 315 gave rise to fragments at m/z 300, 271, 256, and 151 (in the ms3 ion spectra). As seen by the fragmentation patterns of obtained standards, this dissociation scheme closely follows the ion spectra for the flavonoid

isorhamnetin. Therefore, it is hypothesized that this compound is most likely isorhamnetin-3-glucoside. However (as mentioned above), although the presence of the ms3 daughter ions follow a striking similarity to that of isorhamnetin, it is possible that the flavonoid aglycone may also be either 6-methoxyluteolin (a.k.a. nepetin), 4'-methoxyquercetin (a.k.a. tamarixetin), or 7-methylquercetin (a.k.a. rhamnetin) (since they also show similar if not identical fragmentation schemes to that of isorhamnetin). In addition to isorhamnetin, the NIST 05 Database also revealed close matches for other methoxy-flavones, including 3',4',5,6-tetrahydroxy-7-methoxy-flavone (a.k.a. pedalitin), which further supports the theory that the aglycone is in fact a methoxy-flavonoid (although, based on its common appearance in many plants, isorhamnetin is the most likely aglycone).

Compound 14-C1 at RT 20.03 showed a relatively strong UV response, however, it exhibited a low ion intensity in the normal mass spectra. The most intense ion was seen at m/z 177 $(M-H)^-$, which is assumed to be the molecular ion (although no adduct ions were present). The molecular ion dissociated to give ms2 fragments of m/z 151, 149, 133, 109, and 89 (with 133 being the most intense ion fragment). Further fragmentation of m/z 133 yielded ms3 fragments of m/z 123, 105, 104, 91, and 89. Based on the fragmentation pathway (Figure 58), there is a strong possibility that this compound is a methoxycinnamic acid (such as 4-methoxycinnamic acid). However, the fragmentation scheme also closely follows that of a chroman-carboxylic acid derivative (chroman-2-carboxylic acid) (Figure 59). The possible presence of this compound makes sense, since chroman serves as part of the base structure for many flavonoid compounds. According to the NIST 05 Database, other strong candidates for compound 14-C1 include dihydroxy-coumarins (including derivatives such as 6,7-dihydroxycoumarin and 7,8-dihydroxycoumarin).

Compound 15-C1 at RT 20.81 exhibited both a strong UV response and ion intensity, which would indicate a high concentration of this particular compound in Fraction C. The molecular ion was confirmed in the normal mass spectra at m/z 741 $(M-H)^-$ by the presence of several adduct ions including: chlorine $[M+Cl^-]$ at m/z 776 (35 amu), acetate $[M+CH_3COO]^-$ at m/z 801 (60 amu), and sodium acetate $[(M-H)+CH_3COONa]^-$ at m/z 822. The m/z 741 molecular ion underwent collision-induced dissociation (CID) to yield an ms2 spectra with ion fragments of m/z 609, 591, 475, 301, 300, 271, and 255. Further dissociation of m/z 300 led to m/z 271, 255, 179, 169, and 151 ion fragments in the ms3 spectra. The ms2 spectra showed the most intense ion at m/z 300, revealing a neutral loss of 440. This 440 amu difference indicates the presence of a trisaccharide consisting of one 6-carbon pentose sugar (rhamnose at 146 amu), one 5-carbon pentose sugar (xylose or arabinose at 132 amu), and one 6-carbon hexose sugar (glucose or galactose at 162 amu). Fragmentation pathways in both the ms2 and ms3 ion spectra indicate the possible presence of a quercetin base structure. Therefore, this compound is likely to be quercetin with a trisaccharide side-group containing xylose(arabinose) + rhamnose + glucose(galactose). This is in agreement with previous research by (Lou et al., 2001) who reported the presence of quercetin-3-O-[2-O-β-glucopyranosyl-6-O-α-rhamnopyranosyl]-β-glucopyranoside at the same molecular weight (and confirmed the stereochemistry via NMR).

Compound 16-C1 at RT 21.29 exhibited an extremely weak UV signal strength and low ion abundance. The molecular ion was noted at m/z 595 $(M-H)^-$, confirmed by the presence of a chlorine $[M+Cl^-]$ adduct at m/z 631. Dissociation of the m/z 595 parent ion yielded an ms2 spectra with ion fragments of m/z 445, 301 (most intense), 300, 271, and 255. The 294 amu neutral loss associated with (the difference between) m/z 595 and 301 reveals the presence of either the dissacharide sambubiose (2-O-beta-D-xylosyl-D-glucose) or lathyrose (2-O-beta-D-

xylosyl-D-galactose). Further fragmentation of m/z 301 yielded an ms3 spectra with ion fragments of m/z 271, 255, 179, 169, and 151. These daughter ions point to the likely presence of quercetin. Therefore, this compound is most likely quercetin-3-arabinoglucoside (a.k.a. peltatoside), due to the quercetin aglycone base-unit with the dissacharide side-group (Figure 60). However, several other compounds exist which have the ability to follow a similar fragmentation scheme, including eriodictyol-7-neohesperidoside (a.k.a. neoeriocitrin) and eriodictyol-7-O-rutinoside (a.k.a. eriocitrin) (Figure 12).

Compound 17-C1 at RT 21.95 exhibited an extremely weak UV intensity, and an extremely low relative ion abundance. A molecular ion was noted at m/z 771 $(M-H)^-$ in the normal mass spectra. This molecular ion was confirmed by the presence of several adduct ions at m/z 806 (chlorine $[M+Cl^-]$), 831 (acetate $[M+CH_3COO]^-$), and 853 (sodium acetate $[(M-H)+CH_3COONa]^-$). The molecular ion dissociated via CID to form ms2 ions with m/z 609 (most intense ion), 463, and 301. The noted 162 amu neutral loss difference between the molecular ion (m/z 771) and main ms2 fragment (m/z 609) indicates the presence of glucose (or galactose). In addition, the loss between ms2 ion fragments m/z 609 and m/z 463 show the presence of a rhamnose sugar (146 amu). Further loss between ms2 fragments m/z 463 and m/z 301 $(M-H)^-$ point to the presence of both a second glucose unit (due to additional loss of 162 amu), and the possible existence of quercetin. The ms2 ion spectra was searched using the NIST (National Institute of Standards and Technology) Mass Spectral Database, and the software returned a 99% probability match delphinidin-3-rutinoside. However, comparing the ms2 spectra of compound 17-C1 to the delphinidin standard revealed differences which rule out this anthocyanin as a possible match. Fragmentation of daughter ion m/z 609 led to ms3 ion spectra with fragments m/z 301, 300, 271, and 255. These daughter ions most likely confirm the presence of a quercetin

aglycone. Therefore, compound 17-C1 is tentatively identified as quercetin with the following trisaccharide side-group: glucose (or galactose) + rhamnose + glucose (or galactose). The most likely configuration (based on the formation seen in other flavonoid glycosides) would be a rutinoside sugar, plus an added glucose unit.

Compound 18-C1 at RT 23.68 exhibited both an extremely high UV intensity and ion abundance, indicating a very high concentration of this particular compound. Ions produced in the normal mass spectra include the most intense ion of m/z 609 $(M-H)^-$, and a less intense ion at m/z 691, which indicates the presence of a sodium acetate $[(M-H)+CH_3COONa]^-$ adduct ion (due to the 82 amu neutral loss). Therefore, the molecular ion in this case is confirmed at m/z 609. Dissociation of the molecular ion formed ms2 spectra fragments of m/z 301, 300, 271, and 255. The 308 amu neutral loss difference between the m/z 609 molecular ion and the m/z 301 ms2 ion reveal the presence of a rutinose disaccharide side-group (6-O-alpha-L-rhamnosyl-D-glucose). Dissociation of the most intense ms2 ion (at m/z 301/300) yielded ms3 fragments of m/z 271, 255, 179, and 151, which indicate the presence of quercetin with an O-glycosidic bond (confirmed via the quercitrin standard). Therefore, this compound is most likely a quercetin aglycone with a rutinoside sugar side-group, and the most probable candidate for such a compound is rutin (or quercetin-3-O-rutinoside).

Compound 19-C1 at RT 26.19 exhibited both a very high UV intensity and relative ion abundance. The molecular ion was confirmed at m/z 593 $(M-H)^-$, with a sodium acetate $[(M-H)+CH_3COONa]^-$ adduct ion at m/z 676, and an acetate adduct ion at m/z 653. The parent molecular ion dissociated to form an ms2 daughter fragment of m/z 285. This fragment was the result of a 308 amu neutral loss, which indicates the presence of a rutinose sugar (6-O-alpha-L-rhamnosyl-D-glucose). Further dissociation of m/z 285 yielded the following fragments in the

ms3 spectra: m/z 267, 257, 255, 243, 241, 239, 229, 213, 199, 197, 169, 163, 153, 151, and 135. This fragmentation pattern follows the pathway for the compounds luteolin and keampferol (both of which have an $M\text{-}H^-$ m/z of 285). According to the standards, there are only trace differences between the fragmentation schemes of these two compounds. This makes sense, since the only structural difference is the placement of a single hydroxyl unit (C-ring position 3 for kaempferol, versus B-ring position 3' for luteolin). Both compounds exhibited ions at m/z 267, 257, 243, and 213, however, luteolin yields high intensity ions at m/z 241, 217, 199, 197, and 175 (which these fragments are either not seen in kaempferol, or not seen at a high intensity). In the case of kaempferol, ions exist (which are either not seen in luteolin, or at least not in high intensity) at m/z 255, 239, 229, and 169. By looking at the ms3 fragments for compound 19-C1, it can be seen that fragmentation attributes of both luteolin and kaempferol exist, making positive identification difficult. Since the fragmentation fingerprint matches that of both the luteolin and kaempferol standard, it is theorized that these two rutinose-linked flavonoid aglycones are simultaneously co-eluting. This isn't completely unlikely, since luteolin and kaempferol are very similar structures, and although their monomers elute at different retention times on a C-18 column, the added rutinose dissacharide side-group added to both structures may react to a C-18 column in nearly identical fashions. Therefore, compound 19-C1 is tentatively identified as either luteolin and/or kaempferol with an added rutinoside disaccharide side-group. Possible candidates include the following (one of each luteolin and kaempferol based structures): kaempferol-7-O-neohesperidoside, luteolin-7-O-neohesperidoside, kaempferol-3-O-rutinoside, luteolin-3-O-rutinoside, kaempferol-7-rutinoside (Figure 61), and luteolin-7-rutinoside.

Compound 22-C1 at RT 26.79 exhibited an extremely intense UV response at 280nm, and a mass spectra with an extremely high ion abundance. This represents the structure with the

highest concentration in Fraction C, and confirms that a very high quantity of this compound is found in peanut skins. The normal mass spectra showed the most intense ion at m/z 623 $(M-H)^-$, with low intensity adduct ions at m/z 659 $(M+Cl^-)$, 682 (acetate), and 705 (sodium acetate). These adducts confirmed a molecular ion at m/z 623. The molecular ion was further confirmed by the presence of a low intensity dimer ion at m/z 1247, which commonly forms during electrospray ionization. The appearance of such dimers is commonly used as an added technique for identifying molecular ions. The m/z 623 molecular ion dissociated to yield the following fragments in the ms2 spectra: m/z 315 (most intense ion), 300, 271, 255, and 243. The 308 amu neutral loss difference between m/z 623 and 315 reveal the presence of a rutinose (6-O-alpha-L-rhamnosyl-D-glucose) disaccharide sugar. Further dissociation of m/z 315 produced a spectra with ms3 ions of m/z 300, 271, and 255. This fragmentation scheme follows the pattern for the isorhamnetin, however (as previously mentioned), the ms3 ion fingerprint could also result from the fragmentation of several other possible compounds including 6-methoxyluteolin (a.k.a. nepetin), 4'-methoxyquercetin (a.k.a. tamarixetin), and 7-methylquercetin (a.k.a. rhamnetin) (Figure 56). The most likely candidate for compound 22-C1 is isorhamnetin-3-O-rutinoside (Figure 62), since most sugars attach at the 3 position on the flavonoid C-ring (Cuyckens and Claeys, 2004). Other possible (but less likely) candidates include 4'-methylquercetin-7-O-rutinoside, iso-rhamnetin-3-O-neohesperidoside, and iso-rhamnetin 3-O-robinobioside.

Compound 23-C1 at RT 28.46 gave both low UV and ion intensity. The most intense ion was found at m/z 407 $(M-H)^-$, and was confirmed to be the molecular ion by the presence of an acetate $[(M-H)+CH_3COOH]^-$ adduct ion at m/z 466 (59 amu loss), and a sodium acetate $[(M-H)+CH_3COONa]^-$ adduct ion at m/z 489 (82 amu loss). The m/z 407 parent ion dissociated to form an ms2 spectra with ion fragments of m/z 389, 379, 363, 297, 285 (most intense ms2 ion

fragment), 283, 269, 257, 256, 255, and 243. The m/z 285 fragment further dissociated to yield ms3 ion fragments of m/z 257, 255, 241, 213, 201, and 175. Several possible scenarios exist regarding the identification of this compound via prediction of the fragmentation scheme. In the first scenario, the most intense ion in the ms2 spectra (m/z 285) produced a neutral loss difference of 122 amu from the m/z 407 parent ion, which could possibly indicate the presence of a benzoic acid derivative side-group. This is further supported by the m/z 363 fragment, which represents a neutral loss of 44 amu, and indicates the possible loss of a carboxylic acid. Ion fragments in the ms3 spectra indicate the possible existence of either a luteolin or keampferol flavonoid base unit (based on fragmentation patterns of their standards). Therefore, this compound may possibly be either one of the aforementioned flavonoids, with an added benzoic acid acylated side-group. A second scenario exists based on the dissociation scheme, which would possibly identify the compound as remangiflavanone (Figure 63). A third prediction for the possible identification of compound 23-C1 is sophora-flavanone (Figure 64).

Compound 24-C1 at RT 28.75 exhibited a weak UV response, and a low ion relative abundance. Another compound at RT 29.66 (compound 25-C1) exhibited identical fragmentation patterns to compound 24-C1, but demonstrated nearly double the ion abundance. The most intense ion in the normal mass spectra for both compounds was m/z 283 $(M-H)^-$, and is assumed to be the molecular ion (although no adduct ions exist). In both cases, the molecular ion dissociated to form an m/z 268 fragment in the ms2 spectra, which the 15 amu loss is most likely caused by the loss of a methyl group (and typically indicates the presence of a methoxy group). Further fragmentation led to an ms3 spectra with ion fragments of m/z 240, 239, 224, and 211. According to obtained standards, these ion fragments closely follow the exact dissociation pathways for 5,7-dihydroxy-4'-methoxyisoflavone (aka biochanin A or genistein 4-

methyl Ether), 4',5-dihydroxy-7-methoxyisoflavone (aka prunetin), and 5,7-dihydroxy-4'-methoxyflavone (aka acacetin or apigenin-4'-methyl ether). However, it appears to more closely follow the ion fragmentation for both biochanin A and prunetin, since acacetin appears to have a much weaker 223/224 fragment than the other two compounds. Although compounds 24-C1 and 25-C1 are most likely one of the two aforementioned compounds, the fragmentation scheme (with the m/z 268 daughter ion) also compares to numerous other flavonoid monomers at m/z 283 $(M-H)^-$ which exhibit similar structural characteristics. These compounds include the following: 5-dihydroxy-7-methoxyflavone (a.k.a. 7-methoxyapigenin), 4',7-dihydroxy-6-methoxy-isoflavone (a.k.a. glycitein), 5,6-dihydroxy-7-methoxyflavone (a.k.a. negletein or balcalein-7-methyl ether) (Figure 56), 5,7-dihydroxy-6-methoxyflavone (a.k.a. oroxylin), and 5,7-methoxyflavanone. In addition, the NIST 05 database gave high probability spectra matches for methoxy flavones, including 5,7-dihydroxy-8-methoxyflavone (a.k.a. vogonin) and 4',5-dihydroxy-7-methoxyflavone (a.k.a. genkwanin). Also, the existence of an m/z 268 daughter ion has the potential to follow the fragmentation scheme for chalcone-based compounds, including 2'-hydroxy-3,4-dimethoxychalcone and 2'-hydroxy-4',6'-dimethoxy-chalcone (Figure 66). Unfortunately, standards for these compounds were not used for this research (preventing positive identification by means of matching UV retention times), therefore, compounds 24-C1 and 25-C1 can only be tentatively identified via fragmentation data from past literature, and/or MS^n interpretation through fragmentation prediction.

Compound 26-C1 at RT 32.68 exhibited both a low UV response and ion relative abundance. Another similar compound at RT 33.43 had the same molecular weight and fragmentation characteristics, although, it showed a slightly higher UV response (and an intermediate-ranged ion relative abundance). In both cases, a molecular ion was identified at m/z

299 $(M-H)^-$ due to the presence of an acetate $[M+CH_3COO]^-$ adduct at m/z 359 and a sodium acetate $[(M-H)+CH_3COONa]^-$ adduct at m/z 381. The molecular ion dissociated to form ms2 spectra with an intense ion at m/z 284 (for both compounds). The 15 amu loss (methyl group) between the molecular ion and the ms2 daughter fragment indicates the possible presence of a methoxy group. In the case of compound 26-C1, further dissociation formed ms3 ion fragments of m/z 284/283, 266, 256, 240, 228/227, 212/211, 200, 193, 183, 165, 150, and 137. For the other compound at RT 33.43, further fragmentation of m/z 284 yielded ms3 fragments of m/z 267, 256, 239, 227, 215, 199, 173, and 151. Although the dissociation patterns are extremely similar, slight variations in fragment ions (along with slightly different retention times) reveal that these are in fact two separate compounds. Dissociation pathways based on obtained fragmentation data of standards for this study indicate a high probability that the compound is 5,7,4'-trihydroxy-3'-methoxy-flavone (a.k.a. chrysoeriol), specifically with regards to the m/z 284, 256, and 151 fragments. However, it has also been shown that chrysoeriol (Figure 34) exhibits dissociation patterns which are nearly identical to that of diosmetin (aka luteolin-4'-methyl ether). In addition, these two compounds elute at nearly the same retention times under similar chromatographic conditions, which supports the theory that the other compound may possibly be diosmetin. Although fragmentation data for the standards of these compounds was obtained, definitive matches are only possible by running the actual standards to determine retention times (which were not available for this research). Although these compounds are most likely the two aforementioned structures, the lack of definitive proof for identification opens the possibility that these compounds may in fact be other flavonoid or chalcone compounds, which exhibited similar fragmentation pathways (specifically with regards to the m/z 284 and 227 daughter ions). Possible flavonoid compounds include: 3',5,7-trihydroxy-4'-methoxyisoflavone

(a.k.a. pratensein), 4',5,7-trihydroxy-6,8-dimethylflavanone (a.k.a. farresol or cyrtopterinetin), 4',5,7-trihydroxy-6-methoxyisoflavone (a.k.a. tectorigenin) (Figure 35), psi-tectorigenin, 4'-hydroxy-5,7-dimethoxyflavanone, 8-methoxy-iso-scutellargin, 3,7-dihydroxy-2-(4-hydroxy-3-methoxyphenyl)-4-benzopyrone (a.k.a. geraldol), and kaempferol 4'-methyl ether (a.k.a. kaempferide). Possible chalcone compounds include: 2',4'-dihydroxy-3',6'-dimethoxychalcone, 2',4-dihydroxy-4',6'-dimethoxychalcone (Figure 67), 2',6'-dihydroxy-3',4'-dimethoxychalcone, and 2',6'-dihydroxy-4,4'-dimethoxychalcone.

Compound 27-C1 at RT 34.15 (min) showed a low UV intensity, but an intermediate-range relative ion abundance. A molecular ion was found with an m/z of 329 $(M-H)^-$, and a sodium acetate $[(M-H)+CH_3COONa]^-$ adduct ion at m/z 411 (82 amu difference). The parent ion fragmented to form m/z 314 (most intense ion) and 299 in the ms2 spectra. These two fragments each correspond to a 15 amu loss, each indicative of a methyl (CH_3) group, and most likely reveal the presence of two methoxy groups. Further dissociation yielded the following fragments in the ms3 spectra: m/z 299, 286, 285, 271, 257, and 243. Based on obtained standards for this study, the compound isorhamnetin-3-methoxy follows this specific fragmentation scheme (Figure 68). Although this structure is most likely the aforementioned compound, other possibilities do in fact exist based on the dissociation pathway (specifically with regards to fragments m/z 314 and 299). Since it would be difficult to determine the positions of the two methoxy groups with MS/MS alone, one possibility (for other compound matches) is the placement of the methoxy groups at different positions. Examples of such compounds are 3',4',5-trihydoxy-6,7-dimethoxyflavone (a.k.a. circiliol), irisflavone A (Figure 69), irisflavone D, and 3',5,7-trihydroxy-3',4'-dimethoxyflavone (a.k.a. quercetin 3,4'-dimethyl ether). The NIST 05 Database revealed similar compounds (based on matching similar spectra), which supports the

theory of a dimethoxy-flavonoid. These compounds include: 5,6,4'-trihydoxy-7,8-dimethoxy-flavone, 5,8,4'-trihydoxy-6,7-dimethoxyflavone, 7,3',4'-trihydoxy-5,6-dimethoxyflavone, 3',4',5-trihydoxy-3,7-dimethoxyflavone (a.k.a. quercetin 3,7-dimethyl ether), 3',4',5-trihydoxy-3',7-dimethoxyflavone (a.k.a. quercetin 3',7-dimethyl ether), and 4',5,7-trihydroxy-3,3'-dimethoxyflavone (a.k.a. quercetin 3,3'-dimethyl ether). Another possible structure would be similar to those mentioned above, however, with one added methoxy group (and therefore, one less hydroxyl group). Examples of these compounds include kaempferol-3,7,4'-trimethylether, and kaempferol-3,4',7-trimethyl ether (Figure 70). One final possibility with regards to similar dissociation patterns exists with a chalcone-based structure. An example of this compound is 3',6'-dihydroxy-2',4',5'-trimethoxychalcone (Figure 71), or a derivative of this compound.

Compound 28-C1 at RT 39.41 (min) exhibited an extremely low UV and ion intensity. The normal mass spectra revealed two intense ions at m/z 369 and 339, which makes it difficult to identify the molecular ion. Pinpointing the molecular ion becomes even more difficult given that each of these intense ions appear to exhibit attached sodium acetate $[(M-H)+CH_3COONa]^-$ adducts at m/z 421 and 451. The most logical explanations would be either the presence of two co-eluting compounds, or perhaps collision-induced dissociation before or after the electrospray source. The most likely scenario is the latter, since the ms2 and ms3 spectra appear to contain fragments from only one compound. In addition, the difference in molecular weight between the two intense ions found in the normal mass spectra is 30 amu, which would indicate the presence of a methoxy group (and could easily dissociate via CID). Therefore, it is believed that the molecular ion is most likely m/z 369, which underwent source CID to present an m/z 339 fragment in the normal mass spectra. The molecular ion then yielded ms2 ion fragments of m/z 295, 251, 245, 233, 219, and 177. Upon losing the methoxy group (and therefore yielding m/z

339), the m/z 177 fragment indicates the loss of a 162 amu glucose unit. Further dissociation produced ms3 ion fragments of m/z 209, 191, 177, 176, 175, 151, 150, 134, and 133. Based on the fragmentation scheme (Figures 72), compound 28-C1 is tentatively identified as fraxetin-8-glucoside (a.k.a. fraxin or fraxoside).

Compound 29-C1 at RT 39.85 (min) exhibited a low UV intensity, and an intermediate-level ion relative abundance. The normal mass spectra revealed an intense m/z 353 $(M-H)^-$ ion, and a less intense ion at m/z 435. The 82 amu difference between these two ions reveals the presence of a sodium acetate adduct $[(M-H)+CH_3COONa]^-$, which verifies that m/z 353 is a molecular ion. Dissociation of the parent ion led to the following daughter ions in the ms2 spectra: m/z 335, 309, 297 (most intense ion), 284, 253, 240, and 175. The m/z 297 daughter fragment further dissociated to form ms3 ions of m/z 269, 256, 255, 253, 227, 225, 211, and 161. The molecular weight matches that of chlorogenic acid, however, the UV retention time of compound 29-C1 does not correlate to the standard for this phenolic acid. In addition, although the dissociation pathway shows some similarity to that of the chlorogenic acid standard, the differences in ion fragmentation rules out this compound as a possible match. The fragmentation scheme shows a striking similarity to other compounds which don't have the same molecular weight as compound 29-C1, which could give insight into its structural characteristics. The dissociation pathway of the flavonoid chrysoeriol (and other flavonoids with MWs of 300 which have methoxy-groups) yields very similar ions to this structure, including its major fragments of m/z 284, 256, 255, and 227. The NIST 05 Mass Spectral Database also revealed several flavonoid compounds with methoxy-groups (although with different MW's) which had similar ion fragments. These compounds include: 2-(2-acetoxy-3-methoxyphenyl)-3-methoxy-4H-chromen-4-one, 7-hydroxy-3-methoxy-2-p-methoxyphenyl-4H-chromen-4-one, and 2-(3-

hydroxy-4-methoxyphenyl)-3-methoxy-4H-chromen-4-one. Although compound 29-C1 is definitely not one of these aforementioned compounds (since they have different molecular weights), the similarities in fragmentation schemes indicate that not only is this structure a flavonoid-based compound, but it also may be a derivative of one of these compounds. A NIST 05 search also identified two flavonoid-based compounds with MW's which matched that of compound 29-C1, with fragmentation patterns which were similar. These compounds were the following: 7-hydroxy-2-(4-hydroxyphenyl)-5-methoxy-8-(3-methyl-2-butenyl)-2,3-dihydro-4H-chromen-4-one, and 3,5,7,8-tetra-hydroxy-6-(3-methyl-2-butenyl)-2-phenyl-4H-chromen-4-one. Another possibility for the identification of compound 29-C1 is a structure similar to glycycoumarin (although, with one less methyl group), since the fragmentation pathways are comparable (Figure 46). There are several other flavonoid-based compounds which exhibit even more similarities (than any of the previously mentioned compounds) to their fragmentation schemes when compared to this compound. These structures include glycyrrh-iso-flavone, iso-licoflavonol, lico-iso-flavanone, and lico-iso-flavone A. An example of the predictive fragmentation pathway for these compounds can be seen by lico-iso-flavone A in Figure 73. Therefore, it is theorized that compound 29-C1 is most likely one of these four compounds.

Three closely eluting compounds (at RT's 40.71, 42.72, and 43.39), with identical molecular weights, exhibited extremely similar fragmentation pathways. First, compound 30-C1 at RT 40.71 showed an extremely weak UV intensity, and a low ion relative abundance. The molecular ion was confirmed at m/z 367 $(M-H)^-$ due to the presence of an acetate $[(M-H)+CH_3COOH]^-$ adduct at m/z 426. Dissociation of the molecular ion yielded ms2 fragments of m/z 352, 349, 337 (most intense ion), 322, and 296. Further fragmentation of the m/z 337 daughter ion yielded ms3 fragments of m/z 322 and 296. Second, compound 32-C1 at RT 42.72

exhibited an intermediate-ranged UV intensity, and a high ion relative abundance. The m/z 367 $(M-H)^-$ molecular ion was identified by the presence of a sodium acetate $[(M-H)+CH_3COONa]^-$ adduct at m/z 449 (82 amu difference). The m/z 367 molecular ion dissociated to yield ion fragments of m/z 352 (the most intense ion), 312, 309, and 297. The m/z 352 fragment dissociation to form the following ions in the ms3 spectra: m/z 338, 324, 309, 297, 281, 271, 253, and 161. Finally, compound 33-C1 at RT 43.39 exhibited a low UV intensity, and an intermediate-ranged ion relative abundance. The m/z 367 $(M-H)^-$ molecular ion was identified by the presence of the two following adduct ions: Chlorine $[M+Cl^-]^-$ at m/z 404 (37 amu difference), and sodium acetate $[(M-H)+CH_3COONa]^-$ at m/z 449 (82 amu difference). The molecular ion dissociated to form an intense m/z 352 ion in the ms2 spectra. Other low-intensity ions were observed at m/z 309 and 297. The m/z 352 ms2 daughter ion dissociated to form ms3 fragments of m/z 309 and 297. Although slight differences can be seen in the fragmentation patterns of these three compounds, the dissociation pathways exhibit characteristics which closely resemble that of glycycoumarin (Figure 46), and glycyrrh-iso-flavanone.

Compound 31-C1 at RT 41.58 exhibited both an extremely low UV intensity and ion relative abundance. The normal mass spectra showed an intense m/z 281 $(M-H)^-$ ion, and low intensity ions at m/z 341 and 363. The two low-intensity ions represent acetate $[M+CH_3COO]^-$ and sodium acetate $[(M-H)+CH_3COONa]^-$ respectively, which in turn verifies the molecular ion at m/z 281. The molecular ion dissociated to form an intense m/z 266 ion fragment in the ms2 spectra. The loss associated with m/z 266 (from the parent m/z 281 molecular ion) is indicative of a methyl group fragment (15 amu), and most likely reveals the presence of a methoxy group. Further dissociation yielded an ms3 spectra with m/z 266, 238, 237, 210, 196, 194, and 138. The 282 amu molecular weight could indicate many compound possibilities, including dimethoxy-

flavones, dimethoxy-isoflavones, hydroxy-methoxy-methylflavones, and hydroxy-methoxy-methyl-isoflavones. The m/z 266 ms2 ion fragment follows the dissociation pathway of almost every one of these compound classes, since initial fragmentation yields the loss of a methyl group. However, the remaining fragments mostly follow the dissociation scheme of a dimethoxyflavone, of which there are many types. This includes the following dimethoxyflavones: 2',3'-dimethoxyflavone, 2',4'-dimethoxyflavone, 3,5-dimethoxy-flavone, 3,7-dimethoxyflavone, 3',4'-dimethoxyflavone, 3',6-dimethoxyflavone, 4',5-dimethoxyflavone, 4',6-dimethoxyflavone, 4',7-dimethoxyflavone, 6,7-dimethoxy-flavone, and 7,8-dimethoxy-flavone. Of these dimethoxyflavones, the compounds which most closely following the fragmentation scheme of compound 31-C1 is 2',3'-dimethoxyflavone (Figure 74) and 7,8-dimethoxyflavone.

Two compounds, compound 34-C1 at RT 47.29 and compound 35-C1 at RT 48.12, exhibited identical molecular weights, and nearly identical fragmentation patterns. Compound 34-C1 exhibited an intermediate-ranged UV intensity, and a very high ion relative abundance. Conversely, compound 35-C1 exhibited both an extremely high UV intensity and ion relative abundance. The molecular ion for both compounds was identified at m/z 351 $(M-H)^-$ due to the presence of a chlorine $[M+Cl^-]^-$ adduct ion at m/z 387, and a sodium acetate $[(M-H)+CH_3COONa]^-$adduct ion at m/z 433. The molecular ion in both compounds dissociated to form ms2 fragments of m/z 336 (most intense ion), 296, and 281 (although, compound 35-C1 had a higher intensity m/z 281 ion). The m/z 336 ms2 ion was the result of a 15 amu loss (CH_3), and is a common indicator of the presence of a methyl and/or methoxy group. In the case of compound 34-C1, the m/z 336 daughter ion underwent further dissociation to yield ms3 ions of m/z 321, 317, 307, 293 (the most intense ion), 281 (second most intense ion), 267, 253, 243, 237,

219, 213, and 188. On the other hand, compound 35-C1 yielded ms3 ions of m/z 321, 318, 308, 293, 281, 266, 253, 249, 227, and 216. In contrast (to compound 34-C1), compound 35-C1 gave a more intense ms3 ion at m/z 281, and the second most intense ion at m/z 293, which comparatively flip-flopped ion intensities in the ms3 spectra. The nearly identical dissociation pathways (and the close retention times) indicate that these compounds are practically identical, although, they likely have functional groups at different locations on the main structures. According to the NIST 05 database, two possibilities exist regarding the identification of these compounds. First, the dicoumarin known as daphnoretin not only shares the same molecular weight (352 amu), but also exhibits extremely similar fragmentation patterns. A second compound, known as 5-O-methyllupiwighteone, also has the same molecular weight and fragmentation characteristics. Two other compounds exist at this molecular weight which would follow extremely similar predictive fragmentation patterns: pongagallone A (Figure 47), and sophora-iso-flavone A.

Fraction C - HPLC Method 2

The use HPLC Method 2 exhibited better overall separation (than method 1), and in addition to all the compounds identified in method 1, allowed the detection of compounds which were not otherwise seen in the first method. UV chromatograms and TICs for each scan range can be seen in Figures A.44 through A.45. A total of 34 additional compounds were identified in peanut skin Fraction C obtained from Toyopearl SEC (Table 6). In addition to compounds which were undetectable using the first method, method 2 often allowed the separation of multiple compounds with identical molecular weight and fragmentation attributes (i.e., compounds which only eluted once using method 1). The most viable explanation for this

phenomenon is the presence of compounds with similar structural characteristics (while having the same molecular weight), or perhaps due to side-groups residing at different locations on the base-structure. For example, compound 3-C1 at RT 8.51 (MW = 436 amu) eluted once using method 1, however, the enhanced separation exhibited in method 2 revealed the presence of two compounds with these identical molecular weights and dissociation attributes (at RT's 18.67 and 20.87). In the case of HPLC Method 2, these compounds exhibited a high UV intensity, but a somewhat low ion relative abundance. The fragmentation characteristics (as explained in HPLC Method 1 for Fraction C) reveal that these compounds may be two different catechin and/or epicatechin base units, with rhamnoside groups residing at different locations on the flavonoid aglycone. Possible candidates for each of these two compounds include the following: catechin-3-O-rhamnoside, catechin-5-O-rhamnoside, or catechin-7-O-rhamnoside (or their epicatechin derivatives) (Figure 49).

Another instance in which HPLC Method 2 offered better separation involves compound 8-C1 (MW = 320, or m/z 319 $M-H^-$), found at RT 15.06 with HPLC Method 1. The utilization of HPLC Method 2 enabled the separation of two distinct compounds (as opposed to one of these 320 amu compounds in Method 1) with the same monoisotopic mass and fragmentation pattern as compound 8-C1. When using Method 2, both of these compounds (compound 2-C2 at RT 27.34, and compound 4-C2 at 30.29) exhibited a high UV intensity and ion relative abundance. As explained above, compound 8-C1 (HPLC Method 1) was identified as oureatacatechin, which has a similar structure to catechin and epicatechin, but with an added methoxy group. The most likely explanation for the presence of two of these compounds (with identical MW's and fragmentation pathways) when utilizing Method 2, is the presence of the methoxy group at a different location on one of the flavonoid rings. Method 2 also revealed the presence of a third

m/z 319 $(M-H)^-$ compound, although, the fragmentation patterns were different than the oureatacatechin-like compounds. This compound (compound 9-C2 at RT 37.80) exhibited a low UV intensity and ion relative abundance. The molecular ion was confirmed at m/z 319 based on the presence of adducts at m/z 355 (chlorine), 378 (acetate), and 401 (sodium acetate). The molecular ion dissociated to form the following ion fragments in the ms2 spectra: m/z 302, 289, 287, 286, 275, and 273. Although there are some similarities in the possible fragmentation patterns of the compound known as 4'-O-methyl-epigallocatechin, is it more likely that this compound is possibly 3,3',4',5,5',7-hexahydroxyflavanone (a.k.a. dihydromyricetin) (Figure 75).

A third example of multiple eluting structures (with identical molecular weights) exists with compound 26-C1 at RT 32.68 (MW = 300, or m/z 299 $M-H^-$) using HPLC Method 1. The use of HPLC Method 2 allowed the separation of four distinct compounds with this exact molecular weight and similar fragmentation scheme (as opposed to only one compound detected in method 1). This included the following compounds: compound 23-C2 at RT 59.12 (with low UV intensity, and low ion abundance), compound 25-C2 at RT 62.67 (with low UV intensity, and low ion abundance), compound 27-C2 at RT 68.47 (with low UV, and intermediate ion abundance), and compound 29-C2 at RT 70.39 (with low UV, and intermediate ion abundance). Based on the fragmentation patterns, at least two of these compounds are most likely chrysoeriol and diosmetin. Therefore, the remaining two 300 amu compounds which exist in this fraction may each be one of the following compounds (based on their dissociation schemes): pratensein, farresol (or cyrtopterinetin), tectorigenin, psi-tectorigenin, 4'-hydroxy-5,7-dimethoxy-flavanone, 8-methoxy-iso-scutellargin, geraldol, kaempferide, 2',4'-dihydroxy-3',6'-dimethoxychalcone, 2',4-dihydroxy-4',6'-dimethoxychalcone, 2',6'-dihydroxy-3',4'-dimethoxy-chalcone, and 2',6'-dihydroxy-4,4'-dimethoxychalcone. As explained previously, the similarities in fragmentation

patterns make it difficult to determine exactly which (out of the group listed) are actually present, and only the use of specific standards can achieve proper confirmation via UV retention time (or NMR analysis).

One final example of how HPLC Method 2 exhibited better separation can be seen with compound 27-C1 at RT 34.15 (MW = 330 amu, or m/z 329 $M\text{-}H^-$) when using HPLC Method 1. In the case of HPLC Method 2, a total of three compounds with this exact molecular weight and fragmentation scheme were found (compound 24-C2 at RT 62.07, compound 28-C2 at RT 69.72, and compound 30-C2 at RT 71.54). Compound 24-C2 exhibited a low UV intensity and ion relative abundance, however, compounds 28-C2 and 30-C2 both exhibited low UV intensity with intermediate-to-high relative ion abundance. According to obtained standards, at least one of these three compounds is most likely isorhamnetin-3-methoxy (Figure 68). Each of the other two structures are possibly one of the following compounds: 3',4',5-trihydoxy-6,7-dimethoxyflavone (a.k.a. circiliol), irisflavone A (Figure 69), irisflavone D, 3',5,7-trihydroxy-3',4'-dimethoxyflavone (a.k.a. quercetin 3,4'-dimethyl ether), kaempferol-3,7,4'-trimethylether, kaempferol-3,4',7-trimethyl ether, and 3',6'-dihydroxy-2',4',5'-trimethoxychalcone. Another m/z 329 $(M\text{-}H)^-$ compound was found at RT 49.77 (compound 20-C2), and although it exhibited similar fragmentation patterns to the previous compounds, differences in the dissociation pathway were noted. Compound 20-C2 revealed an extremely low UV intensity and ion relative abundance. An acetate $[M+CH_3COO]^-$ adduct ion was found at m/z 389, which confirmed the m/z 329 molecular ion. The molecular ion dissociated to form ms2 fragments of m/z 314, 312, 301, 296, 281, 257, 255, 206, 193 (the most intense ion fragment), 178, 164, and 150. The m/z 193 ion underwent further dissociation to yield ms3 ion fragments of 178, 177, 165, 164, and 150. Although many of the aforementioned compounds produce a number of these fragments

during dissociation, the compound irisflavone D can predicatively produce virtually all of these ions (Figure 76).

The use of HPLC Method 2 allowed the detection of many compounds which were not found using Method 1. The first of these structures is compound 1-C2 at RT 21.18, which exhibited a high UV intensity, but a low relative ion abundance. The molecular ion was identified at m/z 327 $(M-H)^-$ by the presence of an acetate $[M+CH_3COO]^-$ adduct ion at m/z 387, and a sodium acetate $[(M-H)+CH_3COONa]^-$ adduct ion at m/z 409. The molecular ion dissociated to form ms ions of m/z 309, 289, 283, 267, 165 (most intense), and 161. The most intense ms2 ion was found at m/z 165, which reveals a neutral loss of 162 amu (from the m/z 327 parent ion), and indicates the presence of a glucose/galactose unit. Further dissociation of the m/z 165 ion formed fragments 141, 137, and 121. The most likely scenario for the identification of compound 1-C2 is the presence of an m/z 165 $(M-H)^-$ compound, with a sugar side-group. A possible candidate of such a compound, which has both a 166 amu MW and follows the ms3 fragmentation pattern, is any derivative of o-hydrocoumaric acid (Figure 77). Therefore, compound 1-C2 may possibly be an O-glycosidic bound derivative of such an acid. Two other possible structures exist which exhibit these fragmentation characteristics (and also have sugar conjugates), although the aglycones are not acids. These compounds include androsin and betuloside (Figure 78). Additionally, compound 1-C2 may also possibly be one of these aforementioned compounds (or a derivative thereof).

Another compound which was detectable in Method 2 (but not Method 1) was compound 3-C2 at RT 29.22. This compound exhibited both an intermediate-ranged UV intensity and ion abundance. An intense ion was found in the normal mass spectra at m/z 641 $(M-H)^-$, and is assumed to be the molecular ion (although no adduct ions were found). The parent ion

underwent collision-induced dissociation (CID) to yield ms2 fragments of m/z 479 (the most intense ion), 477, and 315. The m/z 477 and 315 fragments indicate the loss of two sugar units (due to the 164 and 162 amu losses), revealing the presence of a rhamnose and glucose sugar. In addition, the combined loss (326 amu) reveals the presence of a rutinose disaccharide (6-O-alpha-L-rhamnosyl-D-glucose). Further dissociation of the m/z 479 ms2 fragment produced the following ions in the ms3 spectra: m/z 317, 315 (most intense ion), 300, 299, 257, 256, and 214. The flavonoid aglycone in this case is m/z 315 $(M-H)^-$, and according to the standards, the dissociation pathway closely follows that of isorhamnetin. This would tentatively identify this compound as isorhamnetin with an O-rutinoside conjugate. Unfortunately, the position of the disaccharide cannot be determined, although, in most cases they reside at the 3 position on the flavonoid C-ring. Although the flavonoid base unit is most likely isorhamnetin (based on literature data), the ms3 ion fingerprint could also result from the fragmentation of several other possible compounds with molecular weights of 316 amu. These compounds include 6-methoxyluteolin (a.k.a. nepetin), 4'-methoxyquercetin (a.k.a. tamarixetin), and 7-methyl-quercetin (a.k.a. rhamnetin). These compounds differ in their methoxy group location on the flavonoid structure. Unfortunately, the MS^n fragmentation patterns for these compounds are nearly identical, and the position of the methoxy group cannot be determined without performing NMR analysis. In addition, the lack of standards for these compounds prevented positive identification via UV retention times.

Compound 5-C2 at RT 33.06 was also found using HPLC Method 2 specifically, and exhibited a high UV intensity and intermediate ion abundance. An intense m/z 611 $(M-H)^-$ ion can be seen in the normal mass spectra, although no adduct ions were present. The most intense ion in the ms2 spectra was m/z 551 (a neutral loss of 60 amu from m/z 611), and suggests that

the difference is an acetate $[M+CH_3COO]^-$ adduct. Therefore, this identifies m/z 551 $(M-H)^-$ as the molecular ion. Other fragments found in the ms2 spectra include m/z 389 and 227. The ion fragment m/z 389 represents a neutral loss of 162 amu (glucose/galactose), and an additional (162 amu) sugar is lost as indicated by ion fragment m/z 227. One structure which could exhibit these fragmentation characteristics is a compound called monotropein (who's aglycone moiety is m/z 227), although, with an added sugar unit. Another possibility for the identification of compound 5-C2, is that the remaining m/z 227 is the compound resveratrol. An example of such a compound is resveratrol-3-β-mono-D-glucoside (Figure 57). Therefore, in this case, compound 5-C2 would be identified as resveratrol, with a disaccharide side-group.

Although HPLC Method 1 was unable to detect any compounds with a 304 amu molecular weight, HPLC Method 2 was able to identify numerous structures within this monoisotopic mass range. The first of these compounds, compound 6-C2 at RT 33.34, exhibited an intermediate UV intensity and low ion relative abundance. A molecular ion was confirmed at m/z 303 $(M-H)^-$ by the presence of an acetate $[M+CH_3COO]^-$ adduct at m/z 363. The molecular parent ion dissociated to form ms2 fragments of m/z 285, 271, 259 (most intense), 244, 219, 217, 204, 163, and 137. Further dissociation of the m/z 259 ms3 ion led to the following fragments in the ms3 spectra: m/z 246, 244, and 228. Another compound with a nearly identical fragmentation scheme was found at RT 40.54. It also showed an intermediate UV intensity and low ion relative abundance. The m/z 303 $(M-H)^-$ molecular ion for this particular compound was verified by the presence of an acetate $[M+CH_3COO]^-$ adduct at m/z 363. Based on the spectra of obtained standards, these two compounds follow the exact fragmentation pathway for both 3'-O-methylcatechin (Figure 79) and/or 4'-O-methylcatechin. A third m/z 303 $(M-H)^-$ compound (compound 8-C2) was detected at RT 36.16, and exhibited an intermediate UV intensity and low

ion relative abundance. Compound 8-C2 had similar (but not identical) fragmentation characteristics to that of compound 6-C2 at RT 33.34. The m/z 303 $(M-H)^-$ molecular ion was confirmed by the presence of an acetate $[M+CH_3COO]^-$ adduct at m/z 363. The molecular ion dissociated to form the following fragments in the ms2 spectra: m/z 287 (the most intense fragment), 275, 266, 261, 259, 217, 215, and 179. The m/z 287 ion found in the ms2 spectra underwent further dissociation to yield ms3 fragments of m/z 272 and 259. Although this compound does not appear to be either 3'-O-methylcatechin or 4'-O-methylcatechin, it does however closely follow the fragmentation pathway of other possible m/z 303 flavonoid compounds (which was confirmed using the NIST 05 Mass Spectral Database). These compounds include dihydroquercetin (a.k.a. taxifolin) (Figure 80) and dihydrorobinetin, which are similar in structure (except for the placement of a single hydroxyl group). Several other m/z 303 $(M-H)^-$ compounds which also closely follow the fragmentation scheme of taxifolin and dihydrorobinetin were found at RT 41.25 (min) and RT 42.86 (min). Both compounds exhibited an intermediate UV intensity and low ion relative abundance, and had molecular ions confirmed by the presence of acetate $[M+CH_3COO]^-$ adducts at m/z 363. In both cases, the ms2 spectra yielded ion fragments of m/z 285, 276, 275, 274, 271, 259, 257, 245, 241, 219, 218, 199, 179, and 167 (which are consistent with taxifolin and dihydrorobinetin). The final m/z 303 $(M-H)^-$ compound was detected at RT 66.73 (min). It exhibited an extremely low UV intensity and ion relative abundance. The molecular ion was confirmed by the presence of a sodium acetate $[(M-H)+CH_3COONa]^-$ adduct ion at m/z 385. The m/z 303 parent ion dissociated to form ms2 fragments of m/z 285 (the most intense ion), 271, 260, 256, 244, 227, 223, and 185. The m/z 285 ms2 ion further dissociated to form an ms3 spectra with ions of m/z 257, 241, 198, and 197.

This fragmentation scheme closely follows the dissociation pathway for the methoxy-flavonoid compound known as 3-methoxy-3',4',5,7-flavantetrol (a.k.a. meciadanol) (Figure 81).

HPLC Method 2 revealed the presence of compound 7-C2 at RT 34.11, which exhibited a low UV intensity and ion relative abundance. An m/z 287 $(M-H)^-$ molecular ion was identified by the presence of the following two adduct ions: acetate $[M+CH_3COO]^-$ at m/z 347 (60 amu difference), and sodium acetate $[(M-H)+CH_3COONa]^-$ at m/z 369 (82 amu difference). Based on the 288 amu molecular weight, it would be expected that this compound would in fact be eriodictyol (since it is a common flavonoid). However, the fragmentation pathway and retention time does not match that of the eriodictyol standard. The m/z 287 $(M-H)^-$ molecular ion of compound 7-C2 dissociated to form ms2 fragment ions of m/z 269, 259, 245, 243 (most intense ion), 227, 205, 197, and 165. The m/z 243 ms2 ion underwent further dissociation to form ms3 fragments of m/z 227, 215, 203, 199, and 173. Compounds which may follow this fragmentation scheme include 2,3-dihydrofisetin (a.k.a. fustin), 6-hydroxyapigenin, and dihydrokaempferol (Figure 82). The NIST 05 Database also gave a high probability match for the flavanone compound fustin.

A compound was detected at RT 35.51 (min) which exhibited a low UV intensity, but a high ion relative abundance. Acetate $[M+CH_3COO]^-$ and sodium acetate $[(M-H)+CH_3COONa]^-$ adduct ions were found m/z 227 and 249 $(M-H)^-$ respectively, confirming m/z 167 $(M-H)^-$ as the molecular ion. The m/z 167 parent ion in the normal mass spectra dissociated to form the following ms2 fragments: m/z 152, 109, and 108. No ms3 fragments were detected. Several 168 amu (MW) compounds exist which could possibly yield these fragment ions. According to the NIST 05 database, the most likely match for this compound is 4-hydroxy-3-methoxybenzoic acid (a.k.a. vanillic acid), which is an intermediate in the formation of vanillin from ferulic acid

(Civolani et al, 2000; Lesage-Meessen et al., 1996). NIST 05 also revealed a high probably search hit for 3-hydroxy-4-methoxybenzoic acid (a.k.a. isovanillic acid). According to the NIST 05 database, the fragmentation patterns are also similar to that of 2-hydroxy-3-methoxybenzoic acid (a.k.a. o-vanillic acid), which is also an intermediate product in the two-step bioconversion of ferulic acid to vanillin (Lesage-Meessen et al., 1996). Additionally, NIST 05 also yielded search hits for homoprotocatechuic acid, 2-hydroxy-6-methoxybenzoic acid, orsellinic acid, and phloracetophenone. Predictive fragmentation also revealed compounds which are similar in structure to homogentisic acid (Figure 9), 6-methyl-β-resorcylic acid, and galloacetophenone.

Numerous compounds with molecular weights of 332 (m/z 331 $M-H^-$) were detected using HPLC Method 2, although, none were found using Method 1. Compound(s) 10-C2 consists of 12 total structures found at RTs 39.40, 40.17, 40.72, 41.42, 41.99, 42.68, 43.19, 44.02, 44.53, 44.84, 54.32, and 54.91. These compounds exhibited both intermediate-ranged UV intensities and relative ion abundances. The m/z 331 $(M-H)^-$ for each of these compounds was verified by either the presence of a chlorine $[M+Cl^-]^-$ or acetate $[M+CH_3COO]^-$ adduct ion. The twelve (nearly identical) structures which make up compound 10-C2 exhibited similar fragmentation schemes, although, slight variations in ms2 and ms3 daughter ion fragments were noted. This could indicate that these are in fact different compounds, as opposed to simply one slowly eluting compound (because of its affinity for the C-18 column). All compounds from RT 39.40 to 40.72 (min) dissociated to form the following ion fragments in the ms2 spectra: m/z 301, 300, 299 (most intense ion), 271, and 255. However, each of these compounds also exhibited their own other unique (less intense) ions. When comparing the unique ions among these compounds, the numbers in fact differed by a factor of 2 amu or less. This was also the case with the ms3 spectra, which although every compound revealed an m/z 271 fragment, they

also each exhibited other unique fragments (which were again very close regarding m/z). In the case of compounds detected from RT 41.42 through 44.84, each of these structures revealed the presence of m/z 301, 300, and 299 ms2 fragments, and an m/z 271 ms3 fragment. However, each of these compounds again showed their own other unique ion fragments in both the ms2 and ms3 spectra (which again only differ by several amu). This supports the concept (just as with the previously detected compounds from RT 39.40 to 40.72) that each of these structures are in fact only slightly different. In some cases regarding these spectra, a small m/z 315 ion fragment appears indicating a neutral loss which could reveal the presence of a methyl group (and therefore, possibly a methoxy group). In all cases, the presence of an m/z 299 fragment shows a neutral loss of 32 amu, which most likely indicates the existence of a methoxy group. Also, the presence of an m/z 301 fragment shows the difference of 15 amu, revealing the loss of two methyl groups (and therefore, possibly two methoxy groups). A flavonoid with a 332 amu molecular weight was identified in a prior study (Lou et al., 1999), which could possibly follow this overall fragmentation pathway. The presence of this compound, known as 3'4'5-tri-O-methylcatechin, would explain the various common ion fragments shown with these compounds. However, the occurrence of other unique fragments revealed in each of these individual compounds, could possibly be explained by the presence of the O-methyl groups residing at different locations on the flavonoid structure. Conversely, the compounds detected at RTs 54.32 and 54.91(min) exhibited a much different fragmentation scheme. In both cases, the m/z 331 molecular ion dissociated to form major ms2 fragments of m/z 316 and 314. However, each of these compounds formed other unique ms2 ion fragments (which only differed by 2 amu or less). This again reveals compounds which have the same molecular weight, but only slightly different fragmentation pathways. The m/z 316 ms2 fragments shown in both of these structures indicate

the loss of 15 amu, and could reveal the presence of a single methoxy group. According to the NIST 05 database, a compound known as 5,6,8,3',4'-pentahydroxy-7-methoxyflavone exhibits a similar fragmentation fingerprint (and also has only one methoxy group). Therefore, one of these two compounds may be the aforementioned structure, and the other compound a close derivative of this structure (in which the methoxy group is attached at a different location on the flavonoid base unit).

Two compounds (compound 11-C2 and 16-C2) were found using HPLC Method 2 which exhibited similar fragmentation patterns, although, their molecular weights were not identical. First, compound 11-C2 was found at RT 39.65, and gave an intermediate-ranged UV intensity, but low relative ion abundance. The molecular ion was identified at m/z 937 $(M-H)^-$, and confirmed by the presence of an acetate $[M+CH_3COO]^-$ adduct at m/z 997. The parent ion dissociated to form the following daughter fragments in the ms2 spectra: m/z 775 (the most intense ion), 579, 547, 417, and 389. The m/z 775 ms2 ion represents a neutral loss of 162 amu from the m/z 937 parent ion, and signifies the presence of a glucose (or galactose) sugar group. Further fragmentation of the m/z 775 ion fragment led to an ms3 spectra with ions of m/z 579 (the most intense ion), 389, and 372/371. The structure responsible for the loss of 196 amu between the m/z 775 (ms2) and 579 (ms3) main fragments could not be determined, although, it is most likely an unknown phenolic acid group. The remaining fragments which correspond to the m/z 579 compound follow a specific fragmentation path which is similar to that of amentoflavone-4',4",7-trimethyl ether (a.k.a. sciatopitysin) (Figure 83). Sciatopitysin is a dimer composed of a hydroxy-dimethoxy-flavonoid, and a dihydroxy-methoxy-flavonoid. The presence of such a compound is not surprising, given that many methoxy-flavonoids have been identified in this fraction alone. Therefore, compound 11-C2 is tentatively identified as

sciatopitysin, with both a sugar and (possibly) a phenolic acid side-group. Next, compound 16-C2 was found at RT 44.75, and exhibited both an intermediate UV intensity and ion relative abundance. A molecular ion for this structure was identified at m/z 775, and was confirmed by a chlorine $[M+Cl^-]^-$ adduct at m/z 811. The m/z 775 parent ion dissociated to form ms2 ions of m/z 579 (most intense ion), 389, and 372. As in the case of compound 11-C2, the reason for the 196 amu neutral loss between m/z 775 and 579 is unknown. Also, the fragmentation scheme of m/z 579 is identical to that shown with compound 11-C2 above. It is theorized that the base structure for compound 16-C2 is also amentoflavone-4',4",7-trimethyl ether (a.k.a. sciatopitysin) (Figure 83), with an unknown phenolic acid side-group.

Compound 12-C2 at RT 40.97 exhibited an intermediate UV intensity with a low relative ion abundance. An intense molecular ion was found in the normal mass spectra at m/z 479 $(M-H)^-$, and was confirmed by the presence of an acetate $[M+CH_3COO]^-$ adduct at m/z 539 (a 60 amu difference). The molecular ion underwent collision-induced dissociation (CID) to yield an m/z 317 daughter ion in the ms2 spectra. This daughter fragment represents a 162 amu difference, and indicates the presence of a sugar side-group. The m/z 317 ion further dissociated to produce the following fragments in the ms3 spectra: m/z 302, 300, 299, 287, 283, 272, 259, 257, 255, 179, 169, 151, and 149. The remaining ions follow the most likely fragmentation patterns for the following m/z 317 $(M-H)^-$ flavonoid compounds: 3,3',4',5,5',7-hexahydroxyflavone (a.k.a. myricetin), 3,3',4',5,6,7-hexahydroxyflavone (a.k.a. quercetagetin), and 3,3',4',5,7,8-hexahydroxy-flavone (a.k.a. gossypetin) (Figure 84). Similarities in the ion fragmentation of these three compounds were also confirmed using the NIST 05 Mass Spectral Database. Therefore, compound 12-C2 is most likely one of the three aforementioned compounds, with a glucoside (or galactoside) side-group.

Compound 14-C2 at RT 42.42 exhibited an intermediate UV Intensity, but a low ion relative abundance. The molecular ion of m/z 903 $(M-H)^-$ was confirmed by the presence of a sodium acetate $[(M-H)+CH_3COONa]^-$ adduct ion at m/z 985 (an 82 amu difference). The molecular ion underwent collision induced dissociation (CID) to yield an m/z 741 fragment in the ms2 spectra. This indicated a neutral loss of 162 amu, which revealed the presence of a glucose (or galactose) unit. The m/z 741 daughter ion further dissociated to form the following fragments in the ms3 spectra: m/z 609, 301, 300, 271, and 255. A neutral loss of 132 amu (from the m/z 741 ms2 fragment) is indicated by the occurrence of the m/z 609 fragment, and reveals the existence of a xylose sugar. The combined loss between the parent ion (m/z 903) and the m/z 609 fragment indicates a 294 amu neutral loss, which shows the presence of either a sambubiose (2-O-beta-D-xylosyl-D-glucose) or lathyrose (2-O-beta-D-xylosyl-D-galactose) disaccharide sugar. The continued loss between m/z 609 and m/z 301 yields a difference of 308 amu, which indicates the presence of a rutinose (6-O-alpha-L-rhamnosyl-D-glucose) disaccharide. The remaining fragments of the m/z 301 flavonoid base unit signify the dissociation pathway for quercetin. From the m/z 609 point in the dissociation pathway, the fragmentation pattern exactly follows that of rutin (a.k.a. quercetin-3-O-rutinoside). Therefore, compound 14-C2 is tentatively identified as rutin, plus either an additional sambubiose or lathyrose disscacharide side-group.

Compound 15-C2 at RT 43.77 revealed an intermediate UV intensity, but a low relative ion abundance. The normal mass spectra showed an intense ion at m/z 757 $(M-H)^-$, and low intensity ions at m/z 817 and 839 (indicating the presence of a 60 amu acetate $[M+CH_3COO]^-$ and 82 amu sodium acetate $[(M-H)+CH_3COONa]^-$ adduct ions). These adducts confirmed the molecular ion at m/z 757 $(M-H)^-$, which underwent collision-induced dissociation (CID) to yield an m/z 595 ms2 ion fragment. This daughter ion indicates a neutral loss of a 162 amu sugar unit

(glucose or galactose). Further dissociation produced ions of m/z 301, 300, 271, and 255 in the ms3 spectra, which the fragmentation pattern is indicative of quercetin. The 294 amu neutral loss between m/z 595 in the ms2 spectra, and the m/z 301 in the ms3 spectra, indicate the presence of either a sambubiose or lathyrose dissacharide. Therefore, compound 15-C2 consists of a quercetin flavonoid base-unit, with a trisaccharide side-group made up of a sambubiose (or lathyrose) + glucose (or galactose) sugar.

The use of HPLC Method 2 allowed the identification of three distinct flavonoid compounds with 318 amu molecular weights. First, a compound was detected at RT 43.70 (min) which exhibited an intermediate UV intensity, but a low relative ion abundance. The m/z 317 $(M-H)^-$ molecular ion was identified by the presence of the following two adduct ions: a 36 amu chlorine $[M+Cl^-]^-$ at m/z 353, and a 60 amu acetate $[M+CH_3COO]^-$ at m/z 377. The molecular ion dissociated to form the following ms2 ions: m/z 300 (most intense), 288, 272, 243, 191, and 181. The m/z 300 ms2 ion further dissociated to form an m/z 151 ms3 fragment. This follows the possible fragmentation pathway for the flavonoid known as 3,3',4',5,5',7-hexahydroxyflavone (a.k.a. myricetin). These ion fragments for myricetin were also verified using the NIST 05 Mass Spectral Database. Next, compound 17-C2 at RT 45.85 exhibited both an intermediate UV intensity and ion relative abundance. The m/z 317 $(M-H)^-$ molecular ion was confirmed by the existence of a chlorine $[M+Cl^-]^-$ adduct at m/z 353, an acetate $[M+CH_3COO]^-$ adduct at m/z 377, and a sodium acetate $[(M-H)+CH_3COONa]^-$ adduct at m/z 399. The molecular ion dissociated to yield the following ion fragments in the ms2 spectra: m/z 299 (most intense ion), 289, 284, 271, 245, 232, 193, 181, and 179. The m/z 299 ms2 daughter ion formed the following fragments in the ms3 spectra: m/z 284, 271, 255, 243, 231, 227, and 215. The dissociation pathway agrees with the predictive fragmentation scheme for the compound 3,3',4',5,7,8-hexahydroxyflavone

(a.k.a. gossypetin) (Figure 84). The ion fragmentation fingerprint for this compound was also verified using the NIST 05 Database. Finally, a compound was found at RT 47.51 which revealed both an intermediate UV intensity and ion relative abundance. The m/z 317 $(M-H)^-$ molecular ion was confirmed by the presence of the following adduct ions: chlorine $[M+Cl^-]^-$ at m/z 353, acetate $[M+CH_3COO]^-$ at m/z 376, and sodium acetate $[(M-H)+CH_3COONa]^-$ at m/z 399. The m/z 317 $(M-H)^-$ parent ion dissociated to yield an intense m/z 289 fragment in the ms2 spectra. Other ions seen in the ms2 included m/z 273, 245, 231, 207, 193, and 167. These ions follow the possible fragmentation scheme for the compound known as 3,3',4',5,6,7-hexahydroxyflavone (a.k.a. quercetagetin). As with the previous 318 amu compounds, the spectra was also verified using the NIST 05 Mass Spectral Database. The presence of these three structures supports the theory previously proposed for the identification of compound 7-C1 (Fraction C, HPLC Method 1) at RT 14.88, which appears to exhibit one of the three aforementioned compounds as a flavonoid aglycone base-unit.

Compound 18-C2 at RT 47.34 showed a m/z 347 $(M-H)^-$ molecular ion in the normal mass spectra, and was confirmed by an acetate $[(M-H)+CH_3COOH]^-$ adduct at m/z 407. The molecular ion dissociated to form the following ion fragments in the ms2 spectra: m/z 332, 319, 316, 315 (the most intense ion), 285, 271, 231, 219, 193, and 165. Further dissociation of m/z 315 yielded an ms3 spectra with the following ions: m/z 299, 285, 271, and 229 (most intense ion). The dissociation pathway is similar to that of the tetrahydroxy-methoxy flavonoids with 316 amu molecular weights, such as isorhamnetin. However, when compared to isorhamnetin, the 348 amu molecular weight of this compound would suggest it exhibites an extra methoxy group on the flavonoid structure (denoted by the 32 amu difference). This is further supported by ion fragments at m/z 316 and 285, which represent two consecutive 31 amu losses, and are

common indicators of existing methoxy groups. Therefore, compound 18-C2 may be a previously undiscovered tetrahydroxy-dimethoxy-flavonoid compound.

Compound 19-C2 at RT 47.92 exhibited both an intermediate UV intensity and ion relative abundance. The m/z 771 $(M-H)^-$ molecular ion was confirmed by the existence of a sodium acetate $[(M-H)+CH_3COONa]^-$ adduct at m/z 853. The m/z 771 parent ion underwent collision-induced dissociation (CID) to yield m/z 609 (most intense ion) and 463 fragments in the ms2 spectra. The m/z 609 fragment indicates the loss of 162 amu, revealing the presence of a glucose (or galactose) sugar unit. In addition, the m/z 463 fragment shows the existence of a rhamnose sugar unit (due to the 146 amu neutral loss). The m/z 609 ms2 fragment underwent further dissociation to yield ms3 ions of m/z 301, 300, and 271, which are indicative of the flavonoid quercetin. The m/z 301 ms3 fragment indicates a neutral loss of 308 amu (from the m/z 609 ms2 daughter ion), which reveals the presence of a rutinose (6-O-alpha-L-rhamnosyl-D-glucose) dissacharide. Therefore, compound 19-C2 is a quercetin-trisaccharide which consists of quercetin as the flavonoid base-unit, with an additional rutinose + glucose (or galactose) side-group.

Compound 21-C2 at RT 52.34 exhibited both a low UV intensity and ion relative abundance. The m/z 343 $(M-H)^-$ molecular ion was confirmed in the normal mass spectra by the presence of a chlorine $[M+Cl^-]^-$ adduct at m/z 379 (36 amu difference). The molecular ion dissociated to form the following ion fragments in the ms2 spectra: m/z 329, 327, 315 (most intense ion), 313, 297, 282, 271, 229, 227, 165, and 149. Further dissociation of the m/z 315 ms2 fragment yielded the following ions in the ms3 spectra: m/z 297, 273, 271, 247, 229, 227, 206, 177, and 165. Several flavonoid compounds exist which could follow this dissociation pathway, all of which are dihydroxy-trimethoxy-flavones. These compounds include 3',5-

dihydroxy-4',6,7-trimethoxyflavone (a.k.a. eupatorin), 5,7-dihydroxy-3',4',5'-trimethoxy-flavone, gossypetin 3,3',4',7-tetramethyl ether (Figure 85), irisflavone B, and xanthomicrol. Of these compounds, the predictive dissociation pathway reveals fragments which yield the most similarities to that of 5,7-dihydroxy-3',4',5'-trimethoxyflavone and irisflavone B. The NIST 05 Database also confirmed that the fragmentation characteristics (shown above) conform to that of various dihydroxy-trimethoxy-flavones.

Two distinct compounds with 356 amu molecular weights were found using HPLC Method 2, both of which had similar fragmentation characteristics. First, compound 22-C2 at RT 54.72 exhibited both a low UV intensity and ion relative abundance. The m/z 355 $(M-H)^-$ molecular ion was confirmed by the presence of a chlorine $[M+Cl^-]^-$ adduct at m/z 391 (a 36 amu difference). The molecular ion dissociated to form numerous ion fragments in the ms2 spectra, including m/z 340, 339, 337, 327, 323, 313, 312, 298, 292, 285, 231, 219 (the most intense ms2 fragment), 218, 195, and 193. The m/s 219 daughter fragment underwent further dissociation to yield the following ions in the ms3 spectra: m/z 204, 191, 190, 177, and 176. The m/z 285 fragment in the ms2 spectra reveals a neutral loss of 70 amu, and could indicate the presence of a C_5H_{10} (3-methylbutyl) side-group. The remaining fragments appear to be the dissociation pathway of an m/z 285 flavonoid compound. A candidate for such a compound is cudraflavanone B (or a derivative thereof) (Figure 86), which exhibits a total of four hydroxy and one methylbutyl group [4',5,6',7-tetrahydroxyflavanone-6-(3-methylbutyl)]. A similar compound with nearly identical fragmentation characteristics was verified using the NIST 05 Database, although, that particular flavonoid structure exhibited slightly different structural characteristics. That compound, known as 5-methoxy-4',7-dihydroxy-flavanone-8-(3-methylbutyl), shows two hydroxy and one methoxy group, instead of the four hydroxy groups

exhibited by cudraflavanone B (that is, in addition to the 3-methylbutyl side-group existing on both compounds). One last compound (or derivative of) exists which could possibly exhibit a similar dissociation pathway to compound 22-C2, although, its prevalence is less likely due to fewer matching ion fragments (via interpretation of possible ion fragments). This compound is known as 2-carbethoxy-5,7-dihydroxy-4'-methoxyisoflavone. Next, compound 31-C2 at RT 74.49 exhibited a low UV intensity, but intermediate relative ion abundance. The m/z 355 $(M-H)^-$ molecular ion was confirmed by the presence of a chlorine $[M+Cl^-]^-$ adduct at m/z 391 (a 36 amu difference). The molecular ion dissociated to form the following fragments in the ms2 spectra: m/z 337, 324, 310, 295, 293, 251, 237, 219 (most intense ion), 193, 175, 162, 157, and 136. The m/z 219 daughter ion underwent further dissociation to form the following ms3 ion fragments: m/z 175, 151, 149, 133, and 107. As in the case with compound 22-C2, the fragments yielded by compound 31-C2 follow the dissociation pathway for any of the three aforementioned compounds.

Compound 26-C2 at RT 64.81 showed an extremely low UV intensity, and a low relative ion abundance. A molecular ion was noted at m/z 285 $(M-H)^-$, which was confirmed by the presence of an acetate $[M+CH_3COO]^-$ adduct ion at m/z 345, and a sodium acetate $[(M-H)+CH_3COONa]^-$ adduct at m/z 367. The molecular ion dissociated to form the following ion fragments in the ms2 spectra: m/z 268, 257, 243, 241 (most intense), 217, 199, 175, and 151. The m/z 241 daughter ion underwent further dissociation to yield ms3 fragments of m/z 227, 213, 211, 201, and 199. This fragmentation scheme follows the exact dissociation pathway for the flavonoid 3',4',5,7-tetrahydroxyflavone (a.k.a. luteolin). In addition to the matching fragmentation pattern, this structure was also confirmed by the matching retention time for the luteolin standard.

Compound 32-C2 at RT 76.69 revealed both a low UV intensity and ion relative abundance. A molecular ion was discovered at m/z 887 $(M-H)^-$, confirmed by the presence of acetate $[M+CH_3COO]^-$ and sodium acetate $[(M-H)+CH_3COONa]^-$ adducts at m/z 947 and 970 respectively. The m/z 887 molecular ion underwent collision-induced dissociation to yield an ms2 spectra with ion fragments at m/z 490, 463, 317 and 285 (the most intense ion fragment). The noted difference between the m/z 463 and 317 ion fragments indicates a 146 amu neutral loss, revealing the presence of a rhamnose sugar. In addition, the neutral loss associated with the m/z 285 ion fragment yields a 602 amu neutral loss, which indicates the existence of two monosaccharide units. The possible monosaccharide units (whose sum equals 602 amu) include one 308 amu rutinose (6-O-alpha-L-rhamnosyl-D-glucose) unit, plus either a 294 amu lathyrose (2-O-beta-D-xylosyl-D-galactose) unit, or a 294 amu sambubiose (2-O-beta-D-xylosyl-D-glucose) unit. The m/z 285 daughter ion found in the ms2 spectra underwent further dissociation to yield the following fragments in the ms3 spectra: m/z 267, 257, 243, 241, 217, 213, 201, and 164. This fragmentation scheme follows the exact dissociation pattern for the flavonoid 3',4',5,7-tetrahydroxyflavone (a.k.a. luteolin) (confirmed via the luteolin standard). Therefore, compound 32-C2 is identified as luteolin, with rutinose and lathyrose (or sambubiose) side-groups.

Compound 33-C2 at RT 78.93 was detected using HPLC Method 2, and showed both a low UV intensity and ion relative abundance. An m/z 529 $(M-H)^-$ molecular ion was confirmed by the presence of a sodium acetate $[(M-H)+CH_3COONa]^-$ adduct at m/z 611. The molecular ion dissociated to form m/z 367 (the most intense fragment) and 352 ion fragments in the ms2 spectra. The 162 amu neutral loss associated with the m/z 367 daughter ion reveals the presence of a glucose (or galactose) side-group. Further fragmentation of m/z 367 yielded ions at m/z 352, 336, 324, 309, and 297. This fragmentation pathway follows the possible dissociation

scheme for the compound glycycoumarin (or derivative of) (Figure 46). Therefore, compound 33-C2 is tentatively identified as glycycoumarin (or a derivative thereof).

Compound 34-C2 at RT 79.92 exhibited both an intermediate UV intensity and ion relative abundance. An intense ion was found at m/z 339 $(M-H)^-$, and is assumed to be the molecular ion (although no adduct ions were detected). The m/z 339 parent ion dissociated to yield the following fragments in the ms2 spectra: m/z 251, 245, 233, 219 (the most intense ion), and 175. The m/z 219 daughter ion underwent further fragmentation to produce m/z 197, 191, 177, 176, 175, 163, 151, 149, and 133 ions in the ms3 spectra. The ion fragment at m/z 177 indicates a neutral loss of 162 amu, revealing the presence of a glucose (or galactose) unit. The overall dissociation scheme closely follows the predictive ion patterns from that of glycosidically bound dihydroxy-coumarins, including 6,7-dihydroxycoumarin-7-glucoside, 6,7-dihydroxy-coumarin-6-glucoside, and 7,8-dihydroxycoumarin-7-b-D-glucoside (Figure 87). Therefore, compound 34-C2 is tentatively identified as one of the aforementioned compounds (or a possible derivative thereof).

Fraction D - HPLC Method 1

A total of 38 compounds were identified in peanut skin Fraction D obtained from Toyopearl SEC (Table 7). UV chromatograms and TICs for each scan range can be seen in Figures A.18 through A.21. Fraction D contained high concentrations of flavonoid monomers, methoxy-flavonoids, methylated-flavonoids, flavonoid-glycosides, and a methoxy-flavonoid dimer. Several of the structures found in Fraction D have been previously reported in prior studies (such as catechin and epicatechin), however, a vast majority of these new compounds have not yet been shown to exist in peanut skins. Flavonoid monomers consisted of extremely

high amounts of catechin (compound 2-D1 at RT 13.14), epicatechin (compound 3-D1 at RT 16.44), and their O-methylated derivatives (compound 4-D1 at RT 19.09, compound 6-D1 at RT 21.14, and compound 13-D1 at RT 25.26). Other monomers included the identification of 318 amu flavonoid derivatives (compound 7-D1 at RT 21.84, and compound 8-D1 at RT 22.41) which appear to be catechin and/or epicatchin with an attached ethyl group (or two separate methyl groups on one or more flavonoid rings). Another possibility for the identification of these two structures includes a catechin or epicatechin base-unit, with two (of the five) hydroxyl units actually existing as methoxy units. The presence of catechin and epicatechin was confirmed by matching retention times with known standards. Methylated derivatives of catechin and epicatechin were identified either via fragmentation patterns revealed by obtained standards, or by interpretation of the dissociation pathway. The presence of a 316 amu structure was also detected (compound 16-D1 at RT 26.38), which follows the fragmentation pattern for 3-methylquercetin (a.k.a. isorhamnetin). This was confirmed by predictive fragmentation patterns (Figure 32), and the use of the NIST 05 Mass Spectral Database. The presence of this monomer compound is not surprising, given the vast number of isorhamnetin-based flavonoid glycosides which have been identified. Another m/z 315 $(M-H)^-$ compound was detected at RT 33.30 (compound 30-D1), which also follows a similar fragmentation scheme to that of isorhamnetin. Several other 316 amu molecular weight flavonoids exist which could follow this dissociation pattern, including: 6-methoxyluteolin (a.k.a. nepetin), 4'-methoxyquercetin (a.k.a. tamarixetin), and 7-methylquercetin (a.k.a. rhamnetin) (Figure 56).

Additional flavonoid monomers were detected in Fraction D which exhibited a 300 amu molecular weight (m/z 299 $(M-H)^-$). These structures include compound 28-D1 at RT 30.94, compound 29-D1 at RT 31.75, and compound 31-D1 at RT 33.54. All of these compounds

exhibited both a high UV response and ion relative abundance. In all cases, a molecular ion was identified at m/z 299 $(M-H)^-$ due to the presence of an acetate $[M+CH_3COO]^-$ adduct at m/z 359 and a sodium acetate $[(M-H)+CH_3COONa]^-$ adduct at m/z 381. The molecular ion dissociated to form ms2 spectra with an intense ion at m/z 284 (for all three compounds). The 15 amu loss (methyl group) between the molecular ion and the ms2 daughter fragment indicates the possible presence of a methoxy group. Further dissociation of m/z 284 (for all three compounds) formed an ms3 spectra with m/z 267, 256/255, and 227 ion fragments. Although the dissociation patterns for all three compounds are nearly identical, extremely slight variations in less intense fragment ions (along with slightly different retention times) reveal that these are in fact three separate compounds. Dissociation pathways based on obtained fragmentation data of standards for this study indicate a high probability that the compound is 5,7,4'-trihydroxy-3'-methoxy-flavone (a.k.a. chrysoeriol), specifically with regards to the m/z 284, 256, and 151 fragments. However, it has also been shown that chrysoeriol (Figure 34) exhibits dissociation patterns which are nearly identical to that of diosmetin (aka luteolin-4'-methyl ether). In addition, these two compounds elute at nearly the same retention times under similar chromatographic conditions, which supports the theory that the other compound may possibly be diosmetin. Although fragmentation data for the standards of these compounds was obtained, definitive matches are only possible by running the actual standards to determine UV retention times (which were not available for this research). Predictive fragmentation would indicate that the remaining compound is a different 300 amu molecular weight flavonoid which follows a similar fragmentation scheme, of which several exist. Although at least two of the three aforementioned compounds most likely chrysoeriol and diosmetin, the lack of standards for proper identification opens the possibility that these compounds may in fact be other flavonoid or chalcone

compounds, which exhibited similar fragmentation pathways (specifically with regards to the m/z 284 and 227 daughter ions). Possible flavonoid compounds include: 3',5,7-trihydroxy-4'-methoxyisoflavone (a.k.a. pratensein), 4',5,7-trihydroxy-6,8-dimethylflavanone (a.k.a. farresol or cyrtopterinetin), 4',5,7-trihydroxy-6-methoxyisoflavone (a.k.a. tectorigenin) (Figure 35), psi-tectorigenin, 4'-hydroxy-5,7-dimethoxyflavanone, 8-methoxy-iso-scutellargin, 3,7-dihydroxy-2-(4-hydroxy-3-methoxyphenyl)-4-benzopyrone (a.k.a. geraldol), and kaempferol 4'-methyl ether (a.k.a. kaempferide). Possible chalcone compounds include: 2',4'-dihydroxy-3',6'-dimethoxy-chalcone, 2',4-dihydroxy-4',6'-dimethoxychalcone, 2',6'-dihydroxy-3',4'-dimethoxychalcone, and 2',6'-dihydroxy-4,4'-dimethoxychalcone (Figure 67).

Compound 38-D1 at RT 38.07 is another example of a flavonoid monomer identified in Fraction D. This compound exhibited both an intermediate UV response and ion relative abundance. The most intense ion in the normal mass spectra was m/z 283 $(M-H)^-$, and was confirmed as the molecular ion by the presence of a sodium acetate $[(M-H)+CH_3COONa]^-$ adduct at m/z 365. The molecular ion dissociated to form an m/z 268 fragment in the ms2 spectra, which the 15 amu loss is most likely caused by the loss of a methyl group (and typically indicates the presence of a methoxy group). Further fragmentation led to an ms3 spectra with ion fragments of m/z 267, 240, 239, 226, 224, 223, 212, and 211. According to the standards, these ion fragments closely follow the exact dissociation pathways for 5,7-dihydroxy-4'-methoxyisoflavone (a.k.a. biochanin A or genistein 4-methyl ether), 4',5-dihydroxy-7-methoxyisoflavone (a.k.a. prunetin), and 5,7-dihydroxy-4'-methoxyflavone (a.k.a. acacetin or apigenin-4'-methyl ether). Although compound 38-D1 is most likely one of the aforementioned compounds, the fragmentation scheme (with the m/z 268 daughter ion) also compares to numerous other flavonoid monomers at m/z 283 $(M-H)^-$ which exhibit similar structural

characteristics. These compounds include the following: 5-dihydroxy-7-methoxyflavone (a.k.a. 7-methoxyapigenin), 4',7-dihydroxy-6-methoxy-isoflavone (a.k.a. glycitein), 5,6-dihydroxy-7-methoxyflavone (a.k.a. negletein or balcalein-7-methyl ether), 5,7-dihydroxy-6-methoxyflavone (a.k.a. oroxylin), and 5,7-methoxyflavanone (Figure 65). In addition, the NIST 05 database gave high probability spectra matches for methoxy flavones, including 5,7-dihydroxy-8-methoxyflavone (a.k.a. vogonin) and 4',5-dihydroxy-7-methoxyflavone (a.k.a. genkwanin). Also, the existence of an m/z 268 daughter ion has the potential to follow the fragmentation scheme for chalcone-based compounds, including 2'-hydroxy-3,4-dimethoxychalcone and 2'-hydroxy-4',6'-dimethoxychalcone (Figure 66). Unfortunately, standards for these compounds were not available for this research (preventing positive identification by means of matching UV retention times), therefore, compound 38-D1 can only be tentatively identified via fragmentation data from past literature, and/or MS^n interpretation through fragmentation prediction.

Additional flavonoid monomers identified in Fraction D can be found in Table 7. The vast majority of these compounds exhibited a high UV intensity and ion relative abundance. Some of these compounds include: 4',5,7-trihydroxy-3'-methoxyflavanone (a.k.a. homo-eriodictyol) (compound 25-D1 at RT 29.23), luteolin (a.k.a. 3',4',5,7-tetrahydroxyflavone) (compound 27-D1 at RT 30.43), and kaempferol-3,7-dimethoxy (compound 37-D1 at RT 37.81). These compounds were also identified by either matching retention times with those of standards, by matching of spectra via the NIST 05 Database, or prediction of fragmentation pathways.

A large number of high-concentration flavonoid glycosides were identified in fraction D (Table 7), all of which are based on the flavonoid monomers which have been detected in the peanut skins. For example, compound 5-D1 at RT 20.72 gave both a medium-to-high UV

response, and ion intensity in the normal mass spectra. The most intense ion was observed at m/z 477 $(M-H)^-$, and was confirmed to be the molecular ion due to the presence of a sodium acetate $[(M-H)+CH_3COONa]^-$ adduct ion at m/z 559 (82 amu difference). Dissociation of the molecular ion gave an ms2 ion spectra with fragments of m/z 315 (most intense), 314, 299, 271, and 247. The neutral loss associated with m/z 315 is equivalent to 162 amu, indicating the presence of glucose or galactose monosaccharide. Further fragmentation of m/z 315 yielded ions in the ms3 spectra including m/z 300, 299, 285, 245, 189, and 177, which follows the fragmentation pattern of isorhamnetin and its glycosidically-bound conjugate (Figure 88). This compound is most likely an isorhamnetin-glucoside derivative (such as isorhamnetin-3-glucoside), although the position of the glucose unit cannot be determined by MS/MS alone. Another m/z 477 compound (compound 15-D1) exists at RT 25.82, with a molecular ion confirmed by a sodium acetate $[(M-H)+CH_3COONa]^-$ adduct at m/z 559. Compound 15-D1 exhibits practically identical fragmentation attributes to that of compound 5-D1, and is most likely due to the presence of the sugar unit residing at a different location on the isorhamnetin base (when compared to compound 5-D1). Therefore, compound 15-D1 is either another isorhamnetin-glucose derivative, or less likely, the aglycone base unit is a different flavonoid (other than isorhamnetin) with the same 316 amu molecular weight (such as 6-methoxyluteolin a.k.a. nepetin, 4'-methoxyquercetin a.k.a. tamarixetin, or 7-methylquercetin a.k.a. rhamnetin). A final m/z 477 compound with identical fragmentation attributes was detected at RT 28.39. Again, this compound is most likely an isorhamnetin-based compound, with a glucose unit residing at a different position than the aforementioned compounds. The various locations of the glucose units on the isorhamnetin base-unit would account for the difference in HPLC elution time.

Another example of a Fraction D flavonoid-glycoside is compound 11-D1 at RT 23.73. This compound exhibited both an intermediate UV intensity and ion relative abundance. The molecular ion was confirmed at m/z 463 $(M-H)^-$ due to the presence of a sodium acetate $[(M-H)+CH_3COONa]^-$ adduct ion at m/z 545. The molecular ion underwent collision-induced dissociation (CID) to yield an intense m/z 301 daughter fragment in the ms2 spectra. The 162 amu neutral loss between the m/z 463 parent ion and the m/z 301 fragment indicate the existence of a glucose (or galactose) monosaccharide unit. The m/z 301 ion underwent further dissociation to produce the following ion fragments in the ms3 spectra: m/z 271, 255, 179, and 151. The dissociation scheme follows the exact fragmentation pattern of a quercetin aglycone. Therefore, compound 11-D1 is most likely a quercetin-based glycoside, such as isoquercetrin or hyperoside. An additional m/z 463 compound was detected at RT 24.42 (compound 12-D1), which showed an intermediate UV response, and a high relative ion abundance. The normal mass spectra showed an intense ion at m/z 463 $(M-H)^-$, and a low intensity ion at m/z 545. The m/z 545 ion reveals the presence of a sodium acetate $[(M-H)+CH_3COONa]^-$ adduct ion due to the difference (of 82 amu) between m/z 545 and 463. Therefore, m/z 463 is the molecular ion for this compound. The parent ion underwent collision-induced dissociation (CID) to yield an ms2 ion spectrum with an intense m/z 301 ion. The neutral loss associated with m/z 301 (from m/z 463) indicates the presence of a 162 amu hexose sugar (either glucose or galactose). Further fragmentation of m/z 301 produced an ms3 spectra with ions m/z 286 (most intense), 271, 256, 255, 241, 217, 201, 199, and 151. Based on the possible fragmentation schemes, the flavonoid aglycone is most likely quercetin, with an O-glycosidic linkage. Possible candidates for this compound include: quercetin-3-O-galactoside (a.k.a. hyperoside), quercetin-3-O-glucoside (a.k.a. isoquercitrin), quercetin-7-D-glucoside (a.k.a. gossypitrin or quercimeritrin), and

quercetin-4'-O-glucoside (a.k.a. spiraeoside). The dissociation pathways reveal that compound 12-D1 is most likely quercetin-4'-O-glucoside (a.k.a. spiraeoside), since it exhibits the most ion fragment matches to the MS^n spectra (Figure 89).

Additional flavonoid-glycosides identified in Fraction D can be found in Table 7. The vast majority of these compounds exhibited a high UV intensity and ion relative abundance. Some of these compounds include: Kaempferol-glucoside (compound 14-D1 at RT 25.56), isorhamnetin-3-methoxy-glucoside (or other m/z 329 $M-H^-$ aglycone)(compound 17-D1 at RT 26.64), chrysoeriol-glucoside (or other m/z 299 $M-H^-$ aglycone)(compound 20-D1 at RT 27.42), and luteolin-glucoside (compound 21-D1 at RT 27.80). These compounds were identified either by comparison to fragmentation standards, by matching of spectra via the NIST 05 Database, or prediction of fragmentation pathways.

Fraction D - HPLC Method 2

The use HPLC method 2 exhibited better overall separation (than method 1), however, the use of this method for Fraction D only allowed the detection of few additional compounds when compared to HPLC Method 1. UV chromatograms and TICs for each scan range can be seen in Figures A.46 through A.47. A total of 7 additional compounds were identified in peanut skin Fraction D obtained from Toyopearl SEC (Table 8). Compound 1-D2 at RT 43.10 exhibited a high UV intensity, and an intermediate relative ion abundance. An intense m/z 389 $(M-H)^-$ molecular ion was found in the normal mass spectra, and dissociated to form an m/z 227 ion in the ms2 spectra. The 162 amu neutral loss difference between the molecular ion and m/z 227 daughter fragment indicates the presence of a glucose (or galactose) monosaccharide side-group. The m/z 227 ion further dissociated to yield the following ion fragments in the ms3 spectra: m/z

185, 159, 157, and 143. This dissociation pattern follows the exact fragmentation scheme for the stilbene known as resveratrol. The fragmentation fingerprint was confirmed using a resveratrol standard. This was also further confirmed by matching the ms3 spectra with the known resveratrol fragmentation pattern using the NIST 05 Database. Therefore, compound 1-D2 is identified as a resveratrol aglycone, plus an additional glucose (or galactose) side-group.

HPLC Method 2 exhibited enough resolution to separate multiple 302 amu compounds which could not be identified using HPLC Method 1. The use of Method 1 allowed for the detection of two compounds with m/z 301 $(M-H)^-$, and in addition to those structures, Method 2 was able to separate four additional 302 amu compounds. Each of these compounds exhibited similar (but slightly different) fragmentation patterns, which is indicative of flavonoids at this given molecular weight. Standards for these compounds identified the presence of 2',3,4',5,7-pentahydroxyflavone (a.k.a. morin) (compound 2-D2 at RT 57.43) and 3',5,7-trihydroxy-4'-methoxyflavanone (a.k.a. hesperitin) (compound 5-D2 at RT 61.55). Two additional 302 amu molecular weight flavonoids were discovered at RT 60.03 and 60.69 (compounds 3-D2 and 4-D2). Based on the their similar dissociation patterns, these flavonoids are most likely 3,3',4',5',7-pentahydroxyflavone (a.k.a. robinetin) and 3',4',5,5',7-pentahydroxyflavone (a.k.a. tricetin).

The use of HPLC Method 2 also allowed for the identification of two 492 amu molecular weight compounds (compound 6-D2 at RT 72.98, and compound 7-D2 at RT 77.72). In both cases, the m/z 491 $(M-H)^-$ molecular ion was confirmed by the presence of a sodium acetate $[(M-H)+CH_3COONa]^-$ adduct ion at m/z 574. The molecular ion for both compounds dissociated to yield an intense m/z 287 fragment in the ms2 spectra. The 205/204 amu loss indicates the possible presence of a sinapoyl acyl side-group. Further dissociation of the m/z 287 daughter ion produced the following ion fragments in the ms3 spectra: m/z 269, 219, 165, and 161. This

fragmentation pattern follows the predictive pathway for the 288 amu compound known as 2,3-dihydrofisetin (a.k.a. fustin) (Figure 27). In addition, a search of the ms2 spectra using the NIST 05 Mass Spectral Database produced a high probability match for the compound known as 3,3',4',7-tetrahydroxyflavone (a.k.a. fisetin), which has a structure nearly identical to that of fustin. Therefore, compounds 6-D2 and 7-D2 are most likely fustin-based flavonoids, with sinapoyl acyl groups residing at different positions on the flavonoid structure.

Fraction E - HPLC Method 1

A total of 9 compounds were identified in peanut skin Fraction E obtained from Toyopearl SEC (Table 9). UV chromatograms and TICs for each scan range can be seen in Figures A.22 through A.24. Fraction E contained fewer compounds (and concentrations of compounds) when compared to all other fractions. It consisted of several flavonoid monomers, flavonoid-glycosides, and a flavonoid dimer. The first flavonoid monomer was compound 1-E1, found at RT 18.72. An m/z 349 $(M-H)^-$ molecular ion was confirmed by the presence of both an acetate $[(M-H)+CH_3COOH]^-$ adduct ion at m/z 408 (59 amu difference), and a sodium acetate $[(M-H)+CH_3COONa]^-$ adduct ion at m/z 431. The molecular ion dissociated to yield an ms2 spectra with ions of m/z 331 (the most intense ion) and 299. The m/z 331 daughter fragment underwent further dissociation to produce ms3 ions of m/z 300, 299, 287, 271, 179, and 151. Although this fragmentation pattern closely resembles the MS/MS spectra of many flavonoid and methoxy-flavonoid compounds (such as quercetin-based flavonoids and chromanediols), the 350 amu molecular weight does not coincide with any known flavonoids. For example, according to the NIST 05 Mass Spectral Database, compound 1-E1 exhibits almost the exact same dissociation pattern as 2-(3,4-dimethoxyphenyl)-7-methoxy-3,4-chromanediol. The only

difference between this structure and compound 1-E1 is an 18 amu difference in molecular weight. By predicting the known dissociation pathways in which flavonoids commonly follow, it is possible that this compound could be a previously undiscovered chromanediol structure called 2-(3,4-dimethoxyphenyl)-3,4-dihydro-2*H*-chromene-3,4,5,6,7-pentol (Figure 90). This new compound has almost the same structural characteristics as 2-(3,4-dimethoxyphenyl)-7-methoxy-3,4-chromanediol, except it exhibits one less methoxy group, and three additional hydroxy groups. A similar structure exists at RT 21.83 (compound 4-E1). This compound gave both an intermediate UV intensity and ion relative abundance. The m/z 363 $(M-H)^-$ molecular ion was confirmed by the presence of a sodium acetate $[(M-H)+CH_3COONa]^-$ adduct ion at m/z 445. The molecular ion dissociated to yield an ms2 spectra with ions of m/z 331 (the most intense ion) and 299. The m/z 331 daughter fragment underwent further dissociation to produce ms3 ions of m/z 300, 299, 287, 271, 179, and 151. Again, compound 4-E1 exhibits almost the exact same dissociation pattern as 2-(3,4-dimethoxyphenyl)-7-methoxy-3,4-chromanediol, however, in this case the only difference between this structure and compound 4-E1 is an 32 amu difference in molecular weight. By predicting the known dissociation pathways in which flavonoids commonly follow, it is possible that compound 4-E1 could be a previously undiscovered chromanediol structure called 2-(3,4-dimethoxyphenyl)-7-methoxy-3,4-dihydro-2*H*-chromene-3,4,5,6-tetrol (Figure 91). This new compound has almost the same structural characteristics as 2-(3,4-dimethoxyphenyl)-7-methoxy-3,4-chromanediol, except it exhibits two additional hydroxy groups.

Compound 6-E1 was another monomer discovered in Fraction E, which eluted at RT 25.90 with an intermediate UV intensity, but a high ion relative abundance. An intense m/z 347 $(M-H)^-$ ion was found in the normal mass spectra, which dissociated to yield an m/z 287 in the

ms2 spectra. The 60 amu neutral loss indicates the presence of an acetate $[M+CH_3COO]^-$ adduct ion, which confirms m/z 287 as the molecular ion. Further dissociation of the m/z 287 ion fragment produced m/z 269, 243, 225, 183, 169, 151, 135, and 125 in the ms3 spectra. Although this partially follows the dissociation scheme for several 288 amu flavonoids (such as 6-hydroxyapigenin), it more closely follows the predictive fragmentation scheme for dihydrokaempferol (Figure 82). However, the NIST 05 Mass Spectral Database yielded a high probability spectral match for the compound 3,3',4',7-tetrahydroxy-flavanone (a.k.a. 2,3-dihydrofisetin, or fustin). Therefore, compound 6-E1 is most likely one of the two aforementioned compounds.

Compound 7-E1 at RT 27.10 exhibited both an intermediate UV intensity and ion relative abundance. An intense m/z 285 $(M-H)^-$ ion was found in the normal mass spectra, and was confirmed to be the molecular ion by the presence of an acetate $[M+CH_3COO]^-$ and sodium acetate $[(M-H)+CH_3COONa]^-$ adduct ions at m/z 345 and 367 respectively. The molecular ion dissociated to form the following ion fragments in the ms2 spectra: m/z 257 (most intense ion), 229, 213, and 177. The m/z 257 daughter ion underwent further dissociation to yield the following fragments in the ms3 spectra: m/z 229, 213, 187, 172, and 151. Although this closely follows the dissociation pattern for the flavonoid compounds 3',4',5,7-tetrahydroxyflavone (a.k.a. luteolin) and 3,4',5,7-tetrahydroxyflavone (a.k.a. kaempferol), it does not however match the retention time for these known standards. Therefore, compound 7-E1 is a flavonoid compound other than these two aforementioned structures. The NIST 05 Mass Spectral database revealed fragment matches for several 286 amu flavonoids. These compounds include: 3,3',4',7-tetrahydroxyflavone (a.k.a. fisetin), 5-methoxy-3,7-dihydroxyflavanone, 2',3,4',5,7-penta-hydroxyflavone (a.k.a. datiscetin), 2'-hydroxygenistein, 7,8,2',4'-tetrahydroxy-isoflavone, 6-

hydroxyapigenin (a.k.a. scutellarin), 7,3',4',5'-tetrahydroxyisoflavone (a.k.a. baptigenin), isosakuranetin, naringen-7-methyl-ether (a.k.a. sakuranetin), and 5,7,2',4'-tetrahydroxy-isoflavone.

Compound 8-E1 at RT 29.32 represented the most abundant compound in Fraction E. It exhibited an extremely high UV intensity and ion relative abundance. A molecular ion was confirmed at m/z 301 $(M-H)^-$ due to the presence of a sodium acetate $[(M-H)+CH_3COONa]^-$ adduct ion at m/z 383. The molecular ion dissociated to yield m/z 273, 257, 179 and 151 daughter fragments in the ms2 spectra. Further dissociation yielded m/z 183, 169, and 151 fragments in the ms3 spectra. This follows the exact dissociation pathway for the flavonoid 3,3',4',5,7-pentahydroxyflavone (a.k.a. quercetin). This was confirmed by matching the UV retention time and fragmentation fingerprint with the standard for this compound.

Several flavonoid-glycosides were found in fraction E, including compound 3-E1 at RT 21.53, compound 5-E1 at RT 25.31, and compound 9-E1 at RT 39.31. Compound 3-E1 and 5-E1 were both based on quercetin aglycones, with 162 amu glucose (or galactose) monosaccharide side-groups. Numerous possible compounds with this structural characteristic exist, since the sugar unit can reside at several different locations on the quercetin flavonoid structure. These compounds include: quercetin-3-glucoside (a.k.a. isoquercitrin), quercetin-3-galactoside (a.k.a. hyperoside), quercetin-7-D-glucoside (a.k.a. gossypitrin or quercimeritrin), and quercetin 4'-O-glucoside (a.k.a. spiraeoside). Standards for these compounds were not available, making it impossible to determine which of the aforementioned structures correspond to each of compound 3-E1 and 5-E1 (since these structures undergo nearly identical fragmentation pathways). Compound 9-E1 at RT 39.31 was an additional flavonoid-glycoside found in Fraction E, however, the aglycone was not quercetin. In the case of this compound, the

loss of a glucose (or galactose) sugar unit yielded an m/z 283 $(M-H)^-$ aglycone. MS/MS/MS of the m/z 283 compound produced m/z 255, 243, and 217 ion fragments. According to the NIST 05 Mass Spectral Database, this follows the possible fragmentation scheme for numerous dihydroxy-methoxy-flavones, dihydroxy-methoxy-isoflavones, and dimethoxy-flavanones.

A flavonoid dimer (compound 2-E1) was found at RT 20.80, and exhibited both an intermediate UV intensity and ion relative abundance. An m/z 575 $(M-H)^-$ molecular ion dissociated to yield ms2 daughter fragments of m/z 557, 449 (the most intense ion), 437, 408, 394, and 287. Further dissociation of the m/z 449 fragment produced the following ion fragments in the ms3 spectra: m/z 431, 287, and 243. This dissociation pathway follows the exact fragmentation scheme for an A-type proanthocyanidin dimer compound. Several possible positions exist in which the two flavonoid monomers can join (including A1, A2, A4, and A5'), however, proper identification of the attachment type would be difficult without a standard for comparison (or NMR analysis to determine the stereochemistry). An example of the dissociation pathway for such a compound can be seen in Figure 92.

Fraction E - HPLC Method 2

The use HPLC method 2 exhibited better overall separation (than method 1), however, the use of this method for Fraction E only allowed the detection of few additional compounds when compared to HPLC Method 1. However, Method 2 was in fact able to identify high concentrations of specific compounds in which Method 1 was unable to detect in any amount. UV chromatograms and TICs for each scan range can be seen in Figures A.48 through A.49. A total of 3 additional compounds were identified in peanut skin Fraction E obtained from Toyopearl SEC (Table 10). For example, compound 1-E2 was found at an extremely high UV

intensity and ion relative abundance. The concentration was high enough to cause compound 1-E2 to elute from RT 39.95 to 44.02 (min). The m/z 331 $(M-H)^-$ molecular ion was confirmed by the presence of an acetate $[M+CH_3COO]^-$ adduct at m/z 391. Dissociation of the molecular ion yielded the following ions in the ms2 spectra: m/z 301, 300, 299 (the most intense ion), 287, 271, 255, 179, and 151. Further dissociation of the m/z 299 daughter fragment led to the following ion fragments in the ms3 spectra: m/z 272, 271, 256, 255, 227, 179, and 155. The fragmentation pathway is nearly identical to that of 3-methylquercetin (a.k.a. isorhamnetin), however, a 16 amu difference exists between their molecular weights (332 amu for compound 1-E2 versus 316 amu for isorhamnetin). A limited number of possibilities exist for a flavonoid structure to have a 332 amu molecular weight. One known flavone compound exists (called 5,6,8,3',4'-pentahydroxy-7-methoxyflavone), however, it does not follow the same fragmentation pathway as compound 1-E2. One scenario would be a dihydoxy-dimethoxy-flavanone derivative similar to 3,5-dihydroxy-2-(4-hydroxy-3-methoxyphenyl)-7-methoxy-2,3-dihydro-4*H*-chromen-4-one (yielding a structure similar to that of isorhamnetin) (Figure 93), which could possibly be a newly undiscovered flavanone compound. Another possibility for compound 1-E2 is a chromanediol. The NIST 05 Mass Spectral Library showed a similar spectra for a 332 amu molecular weight compound called 2-(3,4-dimethoxyphenyl-7-methoxy-3,4-chromanediol.

Compound 2-E2 at RT 54.00 (min) showed an extremely high UV intensity and ion relative abundance. This compound exhibited the highest concentration out of all other structures in Fraction E, and reveals that compound 2-E2 is highly abundant in peanut skins. An intense m/z 287 $(M-H)^-$ ion was found in the normal mass spectra, and determined to be the molecular ion by the presence of acetate $[M+CH_3COO]^-$ and sodium acetate [(M-

H)+$CH_3COONa]^-$ adducts at m/z 347 and 369 (respectively). The molecular ion dissociated to yield an m/z 151 ion in the ms2 spectra. Further dissociation of this ion formed m/z 107 and 65 product ions in the ms3 spectra. Compound 2-E2 perfectly matches the retention time and fragmentation pattern for the standard of 3',4',5,7-tetrahydroxyflavanone (a.k.a. eriodictyol).

Compound 3-E2 at RT 61.28 exhibited both an intermediate UV intensity and ion relative abundance. An intense m/z 285 $(M-H)^-$ ion was found in the normal mass spectra, and was confirmed to be the molecular ion by the presence of an acetate $[M+CH_3COO]^-$ and sodium acetate $[(M-H)+CH_3COONa]^-$ adduct ions at m/z 345 and 367 respectively. The molecular ion dissociated to form the following ion fragments in the ms2 spectra: m/z 257 (most intense ion), 256, 229, 213, and 175. The m/z 257 daughter ion underwent further dissociation to yield the following fragments in the ms3 spectra: m/z 239, 229, 213, 171, and 157. Although this closely follows the dissociation pattern for the flavonoid compounds 3',4',5,7-tetrahydroxyflavone (a.k.a. luteolin) and 3,4',5,7-tetrahydroxyflavone (a.k.a. kaempferol), it does not however match the retention time for these known standards. Therefore, compound 3-E2 is a flavonoid compound other than these two aforementioned structures. The NIST 05 Mass Spectral database revealed fragment matches for several 286 amu flavonoids. These compounds include: 3,3',4',7-tetrahydroxyflavone (a.k.a. fisetin), 5-methoxy-3,7-dihydroxyflavanone, 2',3,4',5,7-penta-hydroxyflavone (a.k.a. datiscetin), 2'-hydroxygenistein, 7,8,2',4'-tetrahydroxy-isoflavone, 6-hydroxyapigenin (a.k.a. scutellarin), 7,3',4',5'-tetrahydroxyisoflavone (a.k.a. baptigenin), isosakuranetin, naringen-7-methyl-ether (a.k.a. sakuranetin), and 5,7,2',4'-tetrahydroxy-isoflavone.

Fraction F - HPLC Method 1

A total of 20 compounds were identified in peanut skin Fraction F obtained from Toyopearl SEC (Table 11). UV chromatograms and TICs for each scan range can be seen in Figures A.25 through A.27. Fraction F contained high concentrations of flavonoid dimers, along with several monomers which have never been reported to exist in peanut skins. Extremely high UV intensities and ion relative abundances reveal that peanut skins contain very high concentrations of these compounds. Several of the dimer structures found in Fraction F have been previously reported in prior studies (based on catechin and/or epicatechin), however, the use of Toyopearl Size-Exclusion Chromatography (SEC) allowed for the separation of different dimeric classes. The result was the ability to detect multiple types of dimers which have been previously unreported, due to the enhanced separation exhibited by first using an HPLC preparatory method such as Toyopearl SEC. Multiple instances of dimers with identical molecular weights were found, although the fragmentation patterns were slightly different. This phenomenon can be explained by the presence of various dimeric classes, including different IFB (inter-flavonoid bond) linkages for both A-type proanthocyanidin and B-type procyanidin dimers (along with their branched and linear derivatives). Another explanation for the detection of many instances of similar dimers is the different possibilities of catechin and epicatechin combinations. For example, a dimer can exist as catechin-epicatechin, epicatechin-catechin, catechin-catechin, and epicatechin-epicatechin. The detection of these numerous compounds would not be possible without the use of a prepratory method (such as SEC), since proper separation via HPLC would be unlikely due to co-elution.

A flavonoid dimer (compound 1-F1) was found at RT 6.92, and exhibited an intermediate UV intensity, but a low ion relative abundance. An m/z 575 $(M-H)^-$ molecular ion dissociated to

yield ms2 daughter fragments of m/z 557, 531, 513, 449, 423 (the most intense ion), and 407. Further dissociation of the m/z 423 fragment produced the following ion fragments in the ms3 spectra: m/z 387, 379, 361, 298, 285, and 269. This dissociation pathway follows the exact fragmentation scheme for an A-type proanthocyanidin dimer compound. Although the presence of certain fragments show identical ions to the A-type proanthocyanidin dimer found in Fraction E, slight differences in less intense ions do however exist. This reveals that Compound 1-F1 is a different proanthocyanidin dimer derivative to the one found in the previous fraction. Additional proanthocyanidin dimers were also detected at RT 23.03 (compound 15-F1) and RT 23.60 (compound 16-F1), which also exhibited many identical ion fragments (with some variations in less intense ions). This reveals that peanut skins contain multiple derivatives of A-type proanthocyanidin dimers which exhibit different types of IFB (inter-flavonoid bond) linkages. Several possible IFB positions exist in which the two flavonoid monomers can join (including A1, A2, A4, and A5'), however, proper identification of the attachment type would be difficult without a standard for comparison (or NMR analysis to determine the stereochemistry). An example of the dissociation pathway for such a compound can be seen in Figure 94.

Numerous m/z 577 $(M-H)^-$ B-type procyanidin dimers were detected in Fraction F, including compound 2-F1 at RT 10.11, compound 3-F1 at RT 10.84, compound 4-F1 at RT 11.43, compound 5-F1 at 11.97, compound 12-F1 at RT 19.45, and compound 13-F1 at RT 20.06. The ion fragmentation pattern and UV retention time for compound 4-F1 at RT 11.43 perfectly matched the standard for a procyanidin B3 dimer. The remaining compounds also had matching dissociation pathways (except for subtle differences in minor ion fragments), although, the UV retention times were different. This reveals that the remaining compounds are in fact B-type procyanidin dimers, however, the different HPLC elutions times can be explained by the

variations in IFB linkages (i.e., B1, B2, B3, etc.), branch types (i.e., linear versus branched), and the combination/order of catechin and epicatechin monomers which make up the dimer structure (Figure 95).

Several 592 amu molecular weight (m/z 591 $(M-H)^-$) compounds were detected in Fraction F, each of which constitutes a newly undiscovered flavonoid dimer. These structures include Compound 6-F1 (at RT 13.90), Compound 8-F1 (at RT 15.73), and Compound 10-F1 (at RT 16.14). Each of these compounds exhibited identical fragmentation patterns, except for minor differences in low intensity ions. The dissociation pathway and neutral losses are similar to the standard for the procyanidin B3 dimer, which yield the fragmentation of two catechin/epicatechin monomers. This can easily be deduced by the presence of an m/z 289 $(M-H)^-$ ion fragment, which yields a neutral loss of 288 amu from the parent ion. However, in the case of these compounds, the 288 amu neutral loss of a catechin/epicatechin yields an m/z 303 $(M-H)^-$ ion fragment, which is indicative of a O-methylated catechin (or O-methylated epicatechin). In addition, a search of the ms3 ion spectra using the NIST 05 Mass Spectral Database produced a match for a trihydroxy-methoxy-flavonoid, which further supports the theory that one of the monomers exhibits a methoxy group. Therefore, these compounds are most likely dimers comprised of a catechin or epicatechin monomer, along with an O-methylated catechin/epicatchin monomer. The different retention times of these compounds can be explained by the different possibilities regarding both the linkage positions and the various combinations of catechin/epicatechin monomers (and their O-methylated derivatives).

Numerous 574 amu molecular weight (m/z 573 $(M-H)^-$) dimers were detected in Fraction F, including compound 7-F1 at RT 14.73, compound 9-F1 at RT 15.87, compound 11-F1 at RT 16.80, and compound 14-F1 at 20.21. In each case, dissociation of the molecular ion produced

an ms2 spectra with ion fragments of m/z 555, 529, 447 (the most intense ion fragment), and 285. Further dissociation of the m/z 447 daughter ion yield the following product ions in the ms3 spectra: m/z 285 (most intense ion), 271, 246, and 177. Although the compound appears to be a dimer composed of a catechin/epicatechin monomer plus an additional m/z 285 $(M-H)^-$ monomer (such as luteolin or kaempferol), it however more closely follows the fragmentation scheme for a different dimeric compound. The dissociation pathway follows the exact predictive fragmentation pattern for a procyanidin dimer (Figure 96), although, with monomer structures which differ slightly when compared to the normal catechin and/or epicatechin monomers. In this case, the monomer units look identical to catechin and/or epicatechin, except for a double bond between the 2 and 3 carbons on the flavonoid C-ring. This would account for the reduction in total molecular weight when compared to other typical catechin/epicatechin dimers (i.e., 574 amu for this series of compounds, versus 576, 578, and 590 amu for other typical catechin/epicatechin dimers). The different retention times exhibited by these compounds can be explained by the various possibilities in which these monomers are able to form dimeric compounds, since many unique derivatives are capable based on the different positions in which the monomers are able to attach on the flavonoid rings.

Two 424 amu (m/z 423 $(M-H)^-$) molecular weight compounds were found in Fraction F, both of which exhibited an intermediate UV intensity and ion relative abundance. Compounds 17-F1 and 20-F1 (at RT's 25.82 and 38.09 respectively) were both confirmed by the presence of a sodium acetate $[(M-H)+CH_3COONa]^-$ adduct ion at m/z 505. The fragmentation patterns for both compounds were nearly identical, except for small differences in low intensity ions. In the case of both compounds, the molecular ion dissociated to yield the following product ions in the ms2 spectra: m/z 405, 355, 341, 313, 301, 299 (the most intense ion), 285, 271, and 259. Again,

in both cases, the m/z 299 daughter ion underwent further dissociation to produce ms3 ions of m/z 283 and 271. These ion fragments follow the exact dissociation pathway for three known flavanone compounds: Remangiflavanone B, euchrestaflavanone B, and sophoraflavanone G (Figure 97). Each of these flavanones follows nearly the same fragmentation scheme. Therefore, compounds 17-F1 and 20-F1 are each most likely one of the three aforementioned compounds.

Compound 18-F1 at RT 27.32 (min) exhibited both an intermediate UV intensity and ion relative abundance. An m/z 587 $(M-H)^-$ molecular ion dissociated to form the following ion fragments in the ms2 spectra: m/z 451 (the most intense ion), 435, 421, 391, 377, 301, 299, and 270. The m/z 451 daughter ion underwent further fragmentation to yield ms3 ions at m/z 423, 407, 405, 383, 341, 325, 299, 287, and 257. The predictive fragmentation pathway for the biflavanone compound kolaflavanone follows this exact dissociation scheme (Figure 98). Therefore, compound 18-F1 is most likely kolaflavanone, or a similar derivative of this compound.

One flavonoid glycoside was detected in Fraction F at RT 31.86. Compound 19-F1 exhibited an intermediate UV intensity and ion relative abundance. An m/z 447 $(M-H)^-$ molecular ion was confirmed by the presence of both an acetate $[(M-H)+CH_3COOH]^-$ and sodium acetate $[(M-H)+CH_3COONa]^-$ adducts at m/z 506 and 529 respectively. Collision-induced dissociation (CID) yielded ms2 ion fragments of m/z 429, 403, 337, 325, 323, 296, 295, 283, and 268. Further fragmentation produced an ms3 spectra with the following ion fragments: m/z 324, 307, 297, 295, 281, 266, and 251. The 179 amu loss of an O-glycosidic sugar unit yielded the remaining 268 amu aglycone. It is difficult to properly identify compound 19-F1, given that many 448 amu flavonoid glycosides exist which follow this same fragmentation

pathway. An example of a compound which closely follows this dissociation scheme is 3,4',5,7-tetrahydroxyflavone-3-glucoside (a.k.a. astragalin) (Figure 99). However, positive identification is impossible, since no standards were available, and the following compounds also follow similar dissociation schemes to that of compound 19-F1: 4',5-dihydroxy-7-methoxyflavanone-5-glucoside (a.k.a. sakuranin), isoorientin, kaempferol-3-glucoside, kaempferol-7-glucoside, luteolin-4'-glucoside, luteolin-8-C-glucoside (a.k.a. lutexin or orientin), luteolin-7-b-D-glucopyranoside, and luteolin-5-glucoside.

Fraction F - HPLC Method 2

The use HPLC method 2 exhibited better overall separation (than method 1), however, the use of this method for Fraction E only allowed the detection of few additional compounds when compared to HPLC Method 1. UV chromatograms and TICs for each scan range can be seen in Figures A.50 through A.51. A total of 3 additional compounds were identified in peanut skin Fraction F obtained from Toyopearl SEC (Table 12). The presence of a high concentration 316 amu structure was detected (compound 1-F2 at RT 19.48) at a very high UV intensity and ion relative abundance. An m/z 315 $(M-H)^-$ molecular ion dissociated to form m/z 297 (the most intense ion), 271, and 231 ion fragments in the ms2 spectra. Further dissociation of the m/z 297 daughter ion yielded an ms3 product ion of m/z 269. Several 316 amu molecular weight flavonoids can follow the dissociation pathway associated with the m/z 297 ion fragment, including: 6-methoxyluteolin (a.k.a. nepetin), 4'-methoxyquercetin (a.k.a. tamarixetin), and 7-methylquercetin (a.k.a. rhamnetin) (Figure 100). The NIST 05 Mass Spectral Database found several other 316 amu flavonoids which are capable of an m/z 297 (and/or an additional m/z 269 or 271) ion fragment, including 5,7-dimethoxy-2-(4-methoxyphenyl)-4-chromanol, 2-(3,4-

dimethoxyphenyl)-6-methyl-3,4-chromanediol, 3',4',5,6-tetrahydroxy-7-methoxyflavone (a.k.a. pedalitin), and 5,6,8,4'-tetrahydroxy-7-methoxyflavone.

Two 320 amu molecular weight compounds (compounds 2-F2 and 3-F2) were detected at RTs 27.49 and 30.59 (min). In both cases, an m/z 319 $(M-H)^-$ molecular ion was confirmed by the presence of an acetate $[M+CH_3COO]^-$ and sodium acetate $[(M-H)+CH_3COONa]^-$ adducts at m/z 379 and 401 respectively. Dissociation of the molecular ion yielded m/z 287, 197 (the most intense ion), 165, 153, and 125 in the ms2 spectra. Further fragmentation of the m/z 197 daughter ion produced an m/z 165 ion in the ms3 spectra. This dissociation scheme follows the exact fragmentation pathway for the compound oureatacatechin (Figure 55). Therefore, at least one of these compounds is oureatacatechin, or both of these structures are derivatives of oureatacatechin.

Fraction G-Red - HPLC Method 1

A total of 12 compounds were identified in peanut skin Fraction G-Red obtained from Toyopearl SEC (Table 13). UV chromatograms and TICs for each scan range can be seen in Figures A.28 through A.30. Fraction G-Red contained high concentrations of different types of flavonoid dimers. Extremely high UV intensities and ion relative abundances reveal that peanut skins contain very high concentrations of these compounds. Several of the dimer structures found in Fraction G-Red have been previously reported (based on catechin and/or epicatechin), however, the use of Toyopearl Size-Exclusion Chromatography (SEC) allowed for the separation of different dimeric classes. The result was the ability to detect multiple types of dimers which have been previously unreported, due to the enhanced separation exhibited by first using an HPLC preparatory method such as Toyopearl SEC. Multiple instances of dimers with identical

molecular weights were found, although the fragmentation patterns were slightly different. This phenomenon can be explained by the presence of various dimeric classes, including different IFB (inter-flavonoid bond) linkages for both A-type proanthocyanidin and B-type procyanidin dimers (along with their branched and linear derivatives). Another explanation for the detection of many instances of similar dimers is the different possibilities of catechin and epicatechin combinations. For example, a dimer can exist as catechin-epicatechin, epicatechin-catechin, catechin-catechin, and epicatechin-epicatechin. The detection of these numerous compounds would not be possible without the use of a prepratory method (such as SEC), since proper separation via HPLC would be unlikely due to co-elution factors.

Numerous m/z 577 $(M-H)^-$ B-type procyanidin dimers were detected in Fraction G-Red, including compound 1-Gr1 at RT 10.89, compound 2-Gr1 at RT 11.27, compound 3-Gr1 at RT 12.90, compound 4-Gr1 at 13.84, and compound 5-Gr1 at RT 16.00. UV and ion relative abundances ranged from low to extremely high. These compounds had nearly identical dissociation pathways (except for subtle differences in minor ion fragments), and matched the ion fragments exhibited by the B-type procyanidin dimer standard. This reveals that these compounds are in fact B-type procyanidin dimers, however, the different HPLC elutions times can be explained by the variations in IFB linkages (i.e., B1, B2, B3, etc.), branch types (i.e., linear versus branched), and the combination/order of catechin and epicatechin monomers which make up the dimer structure (Figures 101 and 102).

A flavonoid dimer (compound 6-Gr1) was found at RT 16.51 (min), and exhibited an extremely strong UV intensity and ion relative abundance. An m/z 575 $(M-H)^-$ molecular ion dissociated to yield ms2 daughter fragments of m/z 449 (the most intense ion), 423, 407, 289, and 285. Further dissociation of the m/z 449 fragment produced the following ion fragments in

the ms3 spectra: m/z 287 and 285. This dissociation pathway follows the exact fragmentation scheme for an A-type proanthocyanidin dimer compound. An additional A-type proantho-cyanidin dimer (compound 8-Gr1) was also detected at RT 18.32 (min), which exhibited many identical ion fragments (with some variations in less intense ions). This reveals that peanut skins contain multiple derivatives of A-type proanthocyanidin dimers which exhibit different types of IFB (inter-flavonoid bond) linkages. Several possible IFB positions exist in which the two flavonoid monomers can join (including A1, A2, A4, and A5'), however, proper identification of the attachment type would be difficult without a standard for comparison (or NMR analysis to determine the stereochemistry). An example of the dissociation pathway for such a compound can be seen in Figure 92.

Numerous 574 amu molecular weight (m/z 573 $(M-H)^-$) dimers were detected in Fraction F, including compound 7-Gr1 at RT 18.01, compound 9-Gr1 at RT 19.17, and compound 10-Gr1 at RT 21.12. These compounds ranged from low UV and ion abundances (low concentrations), to extremely high concentrations. In each case, dissociation of the molecular ion produced an ms2 spectra with ion fragments of m/z 555, 529, and 447 (the most intense ion fragment). Further dissociation of the m/z 447 daughter ion yield the following product ions in the ms3 spectra: m/z 285 (most intense ion), and 271. Although the compound appears to be a dimer composed of a catechin/epicatechin monomer plus an additional m/z 285 $(M-H)^-$ monomer (such as luteolin or keampferol), it however more closely follows the fragmentation scheme for a different dimeric compound. The dissociation pathway follows the exact predictive frag-mentation pattern for a procyanidin dimer (Figure 96), although, with monomer structures which differ slightly when compared to the normal catechin and/or epicatechin monomers. In this case, the monomer units look identical to catechin and/or epicatechin, except for a double bond

between the 2 and 3 carbons on the flavonoid C-ring. This would account for the reduction in total molecular weight when compared to other typical catechin/epicatechin dimers (i.e., 574 amu molecular weight for this series of compounds, versus 576, 578, and 590 amu for other typical catechin/epicatechin dimers). The different retention times exhibited by these compounds can be explained by the various possibilities in which these monomers are able to form dimeric compounds, since many unique derivatives are capable based on the different positions in which the monomers are able to attach on the flavonoid rings. Similar compounds were identified in the previous fraction (Fraction F), although, these compounds most likely have different IFB linkages.

Two 556 amu molecular weight compounds were found in Fraction G-Red, which have never previously been detected in peanut skins. Both compounds 11-Gr1 (at RT 38.21) and 12-Gr1 (at RT 39.79) exhibited an intermediate UV intensity and ion relative abundance. An m/z 555 $(M-H)^-$ molecular ion dissociated to yield ms2 daughter ions of m/z 445, 433 (the most intense ion), 403, 390, 283, 271, and 243. Further fragmentation of the m/z 433 ion produced the following ions in the ms3 spectra: m/z 404, 389, 361, 283, 269, 255, and 243. This follows the exact dissociation pathway for two 556 amu flavonoid dimers known as hegoflavone A (Figure 103) and morelloflavone (Figure 104). Both of these dimers are comprised of IFB linked naringenin and luteolin monomers, but attached at different positions on the flavonoid structure. Given each of these dimers exhibit identical fragmentation pathways, it would therefore be impossible to determine which corresponds (to compound 11-Gr1 and 12-Gr1) without the use of standards.

Fraction G-Red - HPLC Method 2

The use HPLC method 2 exhibited better overall separation (than method 1), however, the use of this method for Fraction G-Red only allowed the detection of few additional flavonoid compounds when compared to HPLC Method 1. UV chromatograms and TICs for each scan range can be seen in Figures A.52 through A.53. A total of 4 additional compounds were identified in peanut skin Fraction G-Red obtained from Toyopearl SEC (Table 14). Compound 1-Gr2 at RT 62.40 exhibited a high UV intensity and ion relative abundance. An m/z 301 $(M-H)^-$ molecular ion was confirmed by the presence of acetate $[(M-H)+CH_3COOH]^-$ and sodium acetate $[(M-H)+CH_3COONa]^-$ adduct ions at m/z 360 and 383 respectively. The UV retention time and dissociation pathway perfectly matches the standard for the flavonoid compound 3',5,7-trihydroxy-4'-methoxyflavanone (a.k.a. hesperitin). The presence of another flavonoid monomer was detected at RT 63.10 (compound 2-Gr2), which exhibited a 316 amu molecular weight. This compound also revealed a high UV intensity and ion relative abundance. Several 316 amu molecular weight flavonoids exist which could follow this dissociation pattern, including: 6-methoxyluteolin (a.k.a. nepetin), 4'-methoxyquercetin (a.k.a. tamarixetin), and 7-methyl-quercetin (a.k.a. rhamnetin) (Figures 56 and 100).

Compound 3-Gr2 at RT 64.81 showed a high UV intensity and relative ion abundance. A molecular ion was noted at m/z 285 $(M-H)^-$, which was confirmed by the presence of an acetate $[M+CH_3COO]^-$ adduct ion at m/z 345, and a sodium acetate $[(M-H)+CH_3COONa]^-$ adduct at m/z 367. The molecular ion dissociated to form the following ion fragments in the ms2 spectra: m/z 268, 257, 243, 241 (most intense), 217, 199, 175, and 151. The m/z 241 daughter ion underwent further dissociation to yield ms3 fragments of m/z 227, 213, 211, 201, and 199. This fragmentation scheme follows the exact dissociation pathway for the flavonoid 3',4',5,7-

tetrahydroxyflavone (a.k.a. luteolin). In addition to the matching fragmentation pattern, this structure was also confirmed by the matching UV retention time for the luteolin standard.

Compound 4-Gr2 at RT 70.41 exhibited both a low UV response, but an intermediate ion relative abundance. A molecular ion was identified at m/z 299 $(M-H)^-$ due to the presence of a sodium acetate $[(M-H)+CH_3COONa]^-$ adduct at m/z 381. The molecular ion dissociated to form ms2 spectra with an intense ion at m/z 284 (for both compounds). The 15 amu loss (methyl group) between the molecular ion and the ms2 daughter fragment indicates the possible presence of a methoxy group. In the case of compound 4-Gr2, further dissociation formed ms3 ion fragments of m/z 284, 256, 227, and 163. Dissociation pathways based on obtained fragmentation data of standards for this study indicate a high probability that the compound is 5,7,4'-trihydroxy-3'-methoxy-flavone (a.k.a. chrysoeriol), specifically with regards to the m/z 284, 256, and 151 fragments. However, it has also been shown that chrysoeriol (Figure 34) exhibits dissociation patterns which are nearly identical to that of diosmetin (aka luteolin-4'-methyl ether). In addition, these two compounds elute at nearly the same retention times under similar chromatographic conditions, which supports the theory that the other compound may possibly be diosmetin. Although fragmentation data for the standards of these compounds was obtained, definitive matches are only possible by running the actual standards to determine UV retention times (which were not available for this research). Although compound 4-Gr2 is most likely one of the two aforementioned compounds, the lack of definitive proof for identification opens the possibility that these compounds may in fact be other flavonoid or chalcone compounds, which exhibited similar fragmentation pathways (specifically with regards to the m/z 284 and 227 daughter ions). Possible flavonoid compounds include: 3',5,7-trihydroxy-4'-methoxyisoflavone (a.k.a. pratensein), 4',5,7-trihydroxy-6,8-dimethylflavanone (a.k.a. farresol or

cyrtopterinetin), 4',5,7-trihydroxy-6-methoxyisoflavone (a.k.a. tectorigenin) (Figure 35), psi-tectorigenin, 4'-hydroxy-5,7-dimethoxyflavanone, 8-methoxy-iso-scutellargin, 3,7-dihydroxy-2-(4-hydroxy-3-methoxyphenyl)-4-benzopyrone (a.k.a. geraldol), and kaempferol 4'-methyl ether (a.k.a. kaempferide). Possible chalcone compounds include: 2',4'-dihydroxy-3',6'-dimethoxy-chalcone, 2',4-dihydroxy-4',6'-dimethoxychalcone, 2',6'-dihydroxy-3',4'-dimethoxychalcone, and 2',6'-dihydroxy-4,4'-dimethoxychalcone (Figure 67).

Fraction G - HPLC Method 1

A total of 19 compounds were identified in peanut skin Fraction G obtained from Toyopearl SEC (Table 15). UV chromatograms and TICs for each scan range can be seen in Figures A.31 through A.34. Compounds detected in Fraction G using Method 1 consisted of numerous instances of flavonoid trimers and tetramers, along with several monomeric flavonoids which have never been previously reported in peanut skins. The extremely strong UV intensities and ion relative abundances exhibited by these structures reveal that peanut skins contain very high concentrations of these compounds. The use of Toyopearl Size-Exclusion Chromatography (SEC) allowed for the separation of many polymeric flavonoid structures via HPLC. The result was the ability to detect multiple types of trimers and tetramers which have been previously unreported, due to the enhanced separation exhibited by first using an HPLC preparatory method such as Toyopearl SEC. Multiple instances of trimers and tetramers with identical molecular weights were detected, which exhibited similar fragmentation schemes regarding the high intensity ion fragments, although the fragmentation patterns were slightly different for less intense daughter ions. This phenomenon can be explained by the presence of various trimer and tetramer derivatives which are attached in different manners (i.e., various branched and linear

forms), and the type/position of the incorporated linkages (for example, an A-type interflavanic linkage). Another explanation for the detection of many instances of similar dimers/tetramers is the numerous possibilities of catechin and epicatechin combinations. For example, a trimer can exist as catechin-epicatechin-catechin, epicatechin-catechin-catechin, catechin-catechin-catechin, etc. Therefore, based on the numerous variables involved in the formation of these structures, a vast amount of possible forms may exist. The detection of these abundant compounds would not be possible without the use of a prepratory method (such as SEC), since proper separation via HPLC would be unlikely due to co-elution factors.

Numerous 864 amu molecular weight trimers were found with UV and ion abundances which ranged from weak to extremely high. These structures included Compound 1-G1 at RT 10.00 (min), Compound 2-G1 at RT 10.83, Compound 3-G1 at RT 11.41, Compound 4-G1 at RT 11.80, Compound 5-G1 at RT 12.72, Compound 6-G1 at RT 14.31, Compound 7-G1 at RT 15.33, Compound 8-G1 at RT 15.42, Compound 9-G1 at RT 15.86, and Compound 11-G1 at RT 16.86. According to previous work conducted by Gu et al. (2003) using Electrospray Ionization in negative mode, the fragmentation scheme of these structures (revealed by the most intense ions) suggest they are various derivatives of catechin/epicatechin trimers with a single A-type interflavanic linkage (IFL). An A-type IFL refers to the form of linkage between the flavanol units, which is exhibited by an added ether bond between the C-2 of one monomer, and the O-7 of another monomer (which is in addition to the common C4-C8 IFL bond, or the less common C4-C6 bond). Again, the multiple occurrences of these similar compounds at different retention times can be explained by the various positions of this A-type IFL (within the order of flavonoid monomers among the total trimer polymer), along with other factors such as branch type (i.e.,

linear versus branched), and the combination/order of catechin and epicatechin monomers which make up the trimer structure (Figure 105).

The same previously explained theory holds true for the various tetramer compounds detected in Fraction G. Although these compounds eluted at different retention times, they did however exhibit nearly identical dissociation pathways (except for subtle differences in minor ion fragments). Flavonoid tetramers with 1152 amu molecular weights were detected at RT 16.39 (Compound 10-G1), RT 19.17 (Compound 12-G1), and RT 19.95 (Compound 13-G1). The UV intensity and ion relative abundance for these structures ranged from intermediate to extremely high, revealing a high concentration of these compounds in peanut skins. Again, according to Gu et al. (2003), the high intensity ion fragments indicate that these compounds also exhibit a single A-type interflavanic linkage (IFL). The presence of specific ion fragments (such as m/z 863 $(M-H)^-$, 861, 575, and 573) can give insight into the position of one or more A-type IFL sites. Both Compound 10-G1 (RT 16.39) and 12-G1 (RT 19.17) exhibited high intensity m/z 863 and 575 $(M-H)^-$ ion fragments, which are indicative of the following A-type IFL binded catechin/epicatechin tetramer structure: (Cat)Epi--(Cat)Epi--(Cat)Epi--A(IFL)--(Cat)Epi. On the other hand, compound 13-G1 at RT 19.95 showed a high intensity m/z 861 $(M-H)^-$ ion fragment, which reveals the presence of the following A-type IFL binded catechin/epicatechin tetramer structure: (Cat)Epi--A(IFL)--(Cat)Epi--(Cat)Epi--(Cat)Epi.

A flavonoid dimer (compound 14-G1) was found at RT 21.64, and exhibited an intermediate UV intensity and ion relative abundance. An m/z 575 $(M-H)^-$ molecular ion dissociated to yield ms2 daughter fragments of m/z 557, 531, 513, 449, 423 (the most intense ion), and 407. Further dissociation of the m/z 423 fragment produced the following ion fragments in the ms3 spectra: m/z 387, 325, 297, 287, 285, and 269. This dissociation pathway

follows the exact fragmentation scheme for an A-type proanthocyanidin dimer compound (Appledoorn et al., 2009). Although the presence of certain fragments show identical ions to the A-type proanthocyanidin dimer found in previous fractions, slight differences in less intense ions do however exist. This reveals that compound 14-G1 is a different proanthocyanidin dimer derivative to the one found in the previous fractions. This reveals that peanut skins contain multiple derivatives of A-type proanthocyanidin dimers which exhibit different types of IFB (inter-flavonoid bond) linkages. Several possible IFB positions exist in which the two flavonoid monomers can join (including A1, A2, A4, and A5'), however, proper identification of the attachment type would be difficult without a standard for comparison (or NMR analysis to determine the stereochemistry).

Compound 15-G1 at RT 23.51 exhibited an intermediate UV intensity, but a high ion relative abundance. An intense m/z 589 $(M-H)^-$ molecular ion was found in the normal mass spectra, which dissociated to yield product ions of m/z 571, 560, 466, 463 (the most intense ion), 421, 404, 343, 303, and 285 in the ms2 spectra. The m/z 463 daughter ion underwent further dissociation to form the following ms3 ion fragments: m/z 435, 353, 341, 312, 302, 285, 269, 259, and 229. This dissociation scheme follows the exact predictive fragmentation pathway for the biflavanone known as manniflavanone (Figure 106).

Compound 18-G1 at RT 30.21 (min) exhibited both an intermediate UV intensity and ion relative abundance. A similar 588 amu molecular weight compound was found in Fraction F, although, it exhibited a slightly different fragmentation pattern (and the UV retention times differed by 1 minute). In the case of this compound in Fraction G, an m/z 587 $(M-H)^-$ molecular ion dissociated to form the following ion fragments in the ms2 spectra: m/z 569, 477, 464 (the most intense ion), 451, 407, 375, 313, 300, and 271. The m/z 464 daughter ion underwent

further fragmentation to yield ms3 ions at m/z 437, 392, 313, 311, 300, 299, 287, 269, 254, and 163. The predictive fragmentation pathway for the biflavanone compound kolaflavanone follows this exact dissociation scheme (Figure 107). Therefore, compound 18-G1 is most likely kolaflavanone, or a similar derivative of this compound.

A 424 amu molecular weight compound was detected in Fraction G, which exhibited a low UV intensity and ion relative abundance. The m/z 423 $(M-H)^-$ molecular ion for compound 19-G1 (at RT 39.35) was confirmed by the presence of a sodium acetate $[(M-H)+CH_3COONa]^-$ adduct ion at m/z 505. The fragmentation pattern was nearly identical to that of two other 424 amu molecular weight compounds found in fraction F, except for small variations in low intensity ions, and a different UV retention time. As in the case of the previous compounds found in Fraction F, the molecular ion dissociated to yield the following product ions in the ms2 spectra: m/z 405, 355, 341, 313, 301, 299 (the most intense ion), 285, 271, and 259. The m/z 299 daughter ion underwent further dissociation to produce ms3 ions of m/z 283 and 271. These ion fragments follow the exact dissociation pathway for three known flavanone compounds: remangiflavanone B, euchrestaflavanone B, and sophoraflavanone G (Figure 97). Each of these flavanones follows nearly the same fragmentation scheme. Therefore, compound 19-G1 is most likely one of the three aforementioned structures.

Fraction G - HPLC Method 2

The use HPLC Method 2 exhibited better overall separation (than method 1), however, the use of this method for Fraction G only allowed the detection of few additional compounds when compared to HPLC Method 1. UV chromatograms and TICs for each scan range can be seen in Figures A.54 through A.55. A total of 4 additional compounds were identified in peanut

skin Fraction G obtained from Toyopearl SEC (Table 16). Several 862 amu molecular weight compounds were detected using method 2, which could not be found using Method 1. Compound 1-G2 (at RT 37.98) and compound 2-G2 (at RT 44.27) both exhibited extremely high UV intensities and ion relative abundances, and therefore exist at extremely high concentrations in peanut skins. In both cases, an m/z 861 $(M-H)^-$ molecular ion was confirmed by the presence of an acetate $[(M-H)+CH_3COOH]^-$ adduct ion at m/z 920, and a low intensity dimer at m/z 1723. The molecular ion dissociated to yield the following daughter ions in the ms2 spectra: m/z 735, 720, 718, 709 (the most intense ion), 694, 451, 435, and 375. Further fragmentation produced ms3 ion fragments of m/z 584, 411, and 285. This fragmentation fingerprint follows the exact predictive dissociation pathway for a flavonoid trimer with two A-type IFL linkages. The basic structure for this compound would be: (Cat)Epi--A(IFL)--(Cat)Epi--A(IFL)--(Cat)Epi. An example of a compound such as this is aesculitannin C (Figure 108). This was further confirmed by fragmentation literature for polymeric flavonoid compounds by Gu et al. (2003). A similar 862 amu molecular weight structure was found at RT 44.27 (compound 2-G2), which had a fragmentation pattern with identical high intensity ions (although some differences in low intensity ions were noted). This compound was also confirmed as a flavonoid trimer with two A-type linkages, although, the difference in retention time between these two compounds is most likely a function of the possible combinations of catechin/epicatchin monomers within the structure. Fragmentation data gathered from previous work done by Gu et al also allowed the confirmation of a flavonoid tetramer with 2 A-type IFL bond sites. Compound 3-G2 at RT 49.14 (which showed a high UV intensity and ion relative abundance) exhibited an m/z 1149 $(M-H)^-$ molecular ion. The presence of specific ion fragments (such as m/z 863 $(M-H)^-$, 861, 575, and 573) can give insight into the position of one or more A-type IFL sites. According to this prior

study (by Gu et al), compound 3-G2 revealed product ions which are indicative of the following flavonoid tetramer: (Cat)Epi--A(IFL)--(Cat)Epi--A(IFL)--(Cat)Epi--(Cat)Epi.

Compound 4-G2 at RT 58.73 represented the last flavonoid monomer detected in all fractions A through H. An m/z 319 $(M-H)^-$ molecular ion was confirmed by the presence of an acetate $[M+CH_3COO]^-$ adduct ion at m/z 379. The molecular ion dissociated to yield ms2 product ions of m/z 301, 286, 183 (most intense ion), and 151. This follows the predictive fragmentation scheme for the flavonoid compound 3,3',4',5,5',7-hexahydroxyflavanone (a.k.a. dihydromyricetin) (Figure 109).

Fraction H - HPLC Method 1

A total of 13 compounds were identified in peanut skin Fraction H obtained from Toyopearl SEC (Table 17). UV chromatograms and TICs for each scan range can be seen in Figures A.35 through A.38. Compounds detected in Fraction H using Method 1 consisted of numerous instances of flavonoid trimers and tetramers. The extremely strong UV intensities and ion relative abundances exhibited by these structures reveal that peanut skins contain very high concentrations of these compounds. The use of Toyopearl size-exclusion chromatography (SEC) allowed for the separation of many polymeric flavonoid structures via HPLC. The result was the ability to detect multiple types of trimers and tetramers which have been previously unreported, due to the enhanced separation exhibited by first using an HPLC preparatory method such as Toyopearl SEC. Multiple instances of trimers and tetramers with identical molecular weights were detected, which exhibited similar fragmentation schemes regarding the high intensity ion fragments, although the fragmentation patterns were slightly different for less intense daughter ions. This phenomenon can be explained by the presence of various trimer and tetramer

derivatives which are attached in different manners (i.e., linear versus top/middle/bottom branched forms), and the type/position of the incorporated linkages (for example, an A-type interflavanic linkage). Another explanation for the detection of many instances of similar dimers/tetramers is the numerous possibilities of catechin and epicatechin combinations. For example, a trimer can exist as catechin-epicatechin-catechin, epicatechin-catechin-catechin, catechin-catechin-catechin, etc. Therefore, based on the numerous variables involved in the formation of these structures, a vast amount of possible derivatives may exist. The detection of these abundant compounds would not be possible without the use of a prepratory method (such as SEC), since proper separation via HPLC would be unlikely due to co-elution.

Numerous m/z 1151 $(M-H)^-$ catechin/epicatchin tetramers were detected in Fraction H. Although these compounds eluted at different retention times, they did however exhibit nearly identical dissociation pathways (except for subtle differences in minor ion fragments). In addition, these compounds had similar high intensity ion fragments compared to the tetramers found in the previous Fraction G, however, slight variations in these ions (along with different HPLC elution times) reveal that these compounds are in fact different tetramer derivatives. Flavonoid tetramers with 1152 amu molecular weights were detected at RT 12.06 (compound 1-H1), RT 12.67 (compound 2-H1), RT 13.93 (compound 4-H1), and RT 15.51 (compound 6-H1). The UV intensity and ion relative abundance for these structures were extremely high, revealing a high concentration of these compounds in peanut skins. According to previous work conducted by Gu et al. (2003) using Electrospray Ionization in negative mode, the fragmentation scheme of these structures (revealed by the most intense ions) suggest they are various derivatives of catechin/epicatechin tetramers with a single A-type interflavanic linkage (IFL). An A-type IFL refers to the form of linkage between the flavanol units, which is exhibited by an

added ether bond between the C-2 of one monomer, and the O-7 of another monomer (which is in addition to the common C4-C8 IFL bond, or the less common C4-C6 bond). Again, the multiple occurrences of these similar compounds at different retention times can be explained by the various positions of this A-type IFL (within the order of flavonoid monomers among the total tetramer polymer), along with other factors such as branch type (i.e., linear versus top/middle/bottom branched), and the combination/order of catechin and epicatechin monomers which make up the tetramer structure. (Figure 110). The presence of specific ion fragments (such as m/z 863 $(M-H)^-$, 861, 575, and 573) can give insight into the position of one or more A-type IFL sites. According to the fragmentation literature (Gu et al), an 1152 amu tetramer with high intensity m/z 861 and 573 $(M-H)^-$ ion fragments will have a structure of (Cat)Epi--A(IFL)--(Cat)Epi--(Cat)Epi--(Cat)Epi. These daughter ions were yielded by compound 1-H1 (at RT 12.06) and compound 2-H1 (at RT 12.67), which indicate the position of the A-type IFL binding site for these structures. On the other hand, compound 4-H1 at RT 13.93 showed high intensity m/z 863 and 573 $(M-H)^-$ ion fragments, which reveals the presence of the following A-type IFL binded catechin/epicatechin tetramer structure: (Cat)Epi--(Cat)Epi--A(IFL)--(Cat)Epi--(Cat)Epi. Furthermore, using the fragmentation theories outlined by Gu et al, compound 6-H1 (at RT 15.51) exhibited ion fragments of m/z 851 and 575, which indicate the presence of the following tetramer structure with two A-type IFL binding sites: (Cat)Epi--A(IFL)--(Cat)Epi--(Cat)Epi--A(IFL)--(Cat)Epi. Another tetramer was detected at RT 18.04 (compound 8-H1), which exhibited an 1148 amu molecular weight. When comparing various flavonoid tetramers with A-type IFL binding sites, the presence of each additional A-type IFL is revealed by the loss of 2 amu to the total molecular weight of the compound (because of the loss of a hydrogen for each of the two C-C bonds). This indicates that compound 8-H1 is a catechin/epicatechin tetramer, with

three total A-type IFL binding sites. Therefore, the tetramer structure in this case is: (Cat)Epi--A(IFL)--(Cat)Epi--A(IFL)--(Cat)Epi--A(IFL)--(Cat)Epi.

Two unique compounds were identified at RT 13.41 (compound 3-H1) and 18.41 (compound 9-H1). Both of these structures had 876 amu molecular weights, and exhibited nearly identical dissociation pathways. The neutral losses associated with most of the high intensity ion fragments reveal that this compound is a flavonoid trimer which is similar to an 862 amu molecular weight trimer. In the case of an 862 amu molecular weight catechin/epicatechin trimer (with two A-type IFL binding sites), an m/z 571 $(M-H)^-$ ion fragment exhibits a neutral loss of 290 amu from the m/z 861 parent ion. The 290 amu loss is indicative of the presence of one (of the three) catechin/epicatechin monomer units. In the case of compounds 3-H1 and 9-H1, the m/z 571 $(M-H)^-$ ion fragment yields a neutral loss of 304 amu from the m/z 875 $(M-H)^-$ parent ion. This indicates that these compounds are both flavonoid trimers (with two A-type IFL binding sites) which consist of two catechin/epicatechin monomer units, along with one 304 amu flavonoid monomer unit. The most likely candidate for this 304 amu compound is either 3'-O-methylcatechin or 4'-O-methylcatechin. A similar situation exists with compound 5-H1 at RT 14.22, which has an 1166 amu molecular weight. Interpretation of the neutral losses for this compound reveals only one possible solution regarding the identification of this tetramer structure. First, compound 5-H1 consists of three catechin/epicatechin units connected by two A-type IFL binding sites (as previously explained above for the 862 amu molecular weight compound). The remaining 304 amu flavonoid monomer fulfills the remainder of the tetramer polymer, and as in the case with the 876 amu compound, is most likely either 3'-O-methylcatechin or 4'-O-methylcatechin. These novel flavonoid trimer and tetramer compounds

which contain an O-methylated catechin are newly discovered compounds in this plant source, since they have never been previously reported to exist in peanut skins.

Several 862 amu molecular weight compounds were detected using HPLC Method 1, including compound 10-H1 (at RT 18.74), compound 11-H1 (at RT 19.41), compound 12-H1 (at RT 21.68), and compound 13-H1 (at RT 22.95). All of these structures exhibited extremely high UV intensities and ion relative abundances, and therefore exist at extremely high concentrations in peanut skins. In all cases, an m/z 861 $(M-H)^-$ molecular ion was confirmed by the presence of an acetate $[(M-H)+CH_3COOH]^-$ adduct ion at m/z 920, and a low intensity sextamer (i.e., electrospray-induced dimer of the timer) at m/z 1723. The molecular ion dissociated to yield the following daughter ions in the ms2 spectra: m/z 825, 735, 709, and 571. In some cases, the most intense ion in the ms2 spectra was m/z 735, while in other instances the most intense daughter fragments was m/z 709. Further fragmentation of the most intense ms2 ion fragment produced ms3 ions of m/z 571 and 285. As seen in the previous fraction (G), this fragmentation fingerprint follows the exact predictive dissociation pathway for a flavonoid trimer with two A-type IFL linkages. The basic structure for this compound would be: (Cat)Epi--A(IFL)--(Cat)Epi--A(IFL)--(Cat)Epi. An example of a compound such as this is aesculitannin C (Figure 108). This was further confirmed by fragmentation literature for polymeric flavonoid compounds by Gu et al. (2003). The differences in retention time among these four compounds are most likely a function of the possible combinations of catechin/epicatchin monomers within the structure.

Fraction H - HPLC Method 2

The use HPLC Method 2 exhibited better overall separation (than method 1), however, the use of this method for Fraction G only allowed the detection of few additional compounds when compared to HPLC Method 1. UV chromatograms and TICs for each scan range can be seen in Figures A.56 through A.57. A total of 5 additional compounds were identified in peanut skin Fraction H obtained from Toyopearl SEC (Table 18). All of these compounds consisted of 864 amu molecular weight flavonoid trimers which exhibited strong UV intensities and ion relative abundances. These structures included compound 1-H2 at RT 21.52 (min), compound 2-H2 at RT 24.03, compound 3-H2 at RT 27.86, compound 4-H2 at RT 32.36, and compound 5-H2 at RT 35.21. According to previous work conducted by Gu et al. (2003) using Electrospray Ionization in negative mode, the fragmentation scheme of these structures (revealed by the most intense ions) suggest they are various derivatives of catechin/epicatechin trimers with a single A-type interflavanic linkage (IFL). An A-type IFL refers to the form of linkage between the flavanol units, which is exhibited by an added ether bond between the C-2 of one monomer, and the O-7 of another monomer (which is in addition to the common C4-C8 IFL bond, or the less common C4-C6 bond). Similar 864 amu molecular weight trimer compounds were detected in the previous fraction (G), however, they exhibited different HPLC UV retention times. The multiple occurrences of these similar compounds at different retention times can be explained by the various positions of this A-type IFL (within the order of flavonoid monomers among the total trimer polymer), along with other factors such as branch type (i.e., linear versus branched), and the combination/order of catechin and epicatechin monomers which make up the trimer structure (Figure 105).

CONCLUSION

This study was designed to determine if previously undiscovered phenolic antioxidant compounds are present in peanut skin fractions obtained from Toyopearl size exclusion chromatography (SEC), and also to identify the possible existence of structures which may have pharmaceutical/nutraceutical properties. The use of an ESI-HPLC (negative mode Ion Trap MS^n) technique was utilized to better understand the phenolic profile of peanut skin extracts. Although preliminary HPLC-UV studies indicated the presence of enormous amounts of compounds in raw peanut skin extracts, previous studies have only identified a handful of compounds from this plant source (Lou et al., 1999, 2001, 2004; Yu et al., 2005). The utilization of a (-)ESI-HPLC-MS^n method (HPLC Method 1) for this study enabled the successful identification of two hundred and nineteen compounds in peanut skin fractions A through H (obtained from Toyopearl SEC). However, the development of a second (-)ESI-HPLC-MS^n method (which incorporated the use of a different column and HPLC-MS^n parameters) not only identified the same compounds detected in HPLC Method 1, but also allowed for the discovery of ninety five additional compounds in these fractions. This not only reveals that the (-)ESI-HPLC-MS^n parameters used for HPLC Method 2 offered improved separation and detection of phenolic-based compounds in peanut skins (over HPLC Method 1), but also showed that these settings can be custom tailored to better analyze specific bioflavonoid classes within this plant source.

The success of HPLC Method 2 was partially due to the use of three separate SID (Source Induced Dissociation) scan ranges, which allowed for improved detection of compounds of different sizes and classes (as opposed to two scan ranges used in HPLC Method 1). Most phenolic acids fall into the m/z 125-250 $(M-H)^-$ range, while most bioflavonoid monomers have

molecular weights which would categorize them into the m/z 230-410 range. Furthermore, most flavonoid-glycosides, dimers, trimers, and tetramers fall into the m/z 400-2000 range. The use of three SID ranges allowed for the simultaneous and systematic separation of these phenolic classes during analysis, making detection and identification easier. This method offers a significant improvement over HPLC Method 1, since the use of only two SID scan ranges caused an overlap in the aforementioned classes of compounds. Only the most intense ions in each scan range are detected and analyzed, causing less intense ions to be ejected from the ion trap. For example, HPLC Method 1 utilized scan ranges of m/z 125-600 and m/z 590-2000. Many types of phenolic compounds are encompassed in the m/z 125-600 range, including phenolic acids, bioflavanoid monomers, flavonoid-glycosides, and flavonoid dimers (proanthocyanidins and procyanidins). If two compounds elute at similar retention times, with one structure existing as a flavonoid-glycoside exhibiting a 464 amu molecular weight (while the other structure existing as a phenolic acid compound having a 164 amu molecular weight), then the compound with the lower molecular weight will go undetected (and will not undergo further MS^n in the ion trap). This undesirable phenomenon was overcome by setting the instrument parameters to three SID scan ranges (as in the case of HPLC Method 2), which allowed for the simultaneous analysis of compounds from various size ranges, regardless of whether they have overlapping retention times. The incorporation of this method proved extremely useful for the analysis of peanut skin extracts, given the vast amounts of co-eluting compounds in each SEC fraction.

The vast majority of the 314 identified compounds have never been previously reported to exist in peanut skin extracts. Many of these compounds were positively identified as a single structure based on its unique fragmentation pathway. However, many phenolic-based compounds among similar classes (i.e., phenolic acids, flavones, isoflavones, flavonols,

flavanones, chalcones, etc.) will share identical molecular weights, and often follow extremely similar fragmentation patterns during dissociation in an ion trap mass spectrometer. For example, methoxyflavonoids chrysoeriol and diosmetin both exhibit 300 amu molecular weights (m/z 299 $M\text{-}H^-$), and elute at nearly the same HPLC retention time under identical chromatographic conditions. These two methoxyflavonoids have structures which are nearly indistinguishable, except for the position of the methoxy group on the flavonoid B-ring. In addition, the MS^n (MS/MS/MS) fragmentation scheme for these compounds is nearly identical, making positive identification difficult. This theory holds true for many other phenolic-based compounds (even between similar classes), because of the numerous derivatives which are capable of being formed at any given molecular weight. Therefore, many cases existed (for the identification of structures in peanut skin fractions A through H) where compounds were "tentatively identified" as being one possible compound out of a group of structures. The obvious reason for offering several compounds for the purpose of identification is due to the fact that more than one structure exists which is capable of following the same dissociation pathway. In these situations where multiple compounds share both molecular weight and fragmentation attributes, only the use of standards would allow for full identification of structures via matching HPLC-UV retention times. Unfortunately, the large quantity of standards required to fully classify these "tentatively identified" compounds were not available for this study.

In a situation similar to that explained above, many compounds which exhibit the same molecular weight (and fragmentation patterns) were identified in one or more fractions, but with different retention times. This is due to the multiple possible derivatives which are capable in each individual class of phenolic compounds (i.e., flavonoids, chalcones, phenolic acids, etc.). For example, a flavone existing with a 302 amu molecular weight may have many possible

structure variations due to the numerous locations in which hydroxyl units can reside on the flavonoid rings. These compounds include the following 302 amu molecular weight flavones: quercetin, hesperitin, morin, robinetin, tricetin, and homoeriodictyol. Numerous 302 amu compounds (which belong to the same flavone phenolic class) were detected in multiple peanut skin fractions at different retention times. The number of distinct 302 amu compounds identified reveals that every possible aforementioned flavone derivative (with this given molecular weight) exists in peanut skins. These various compounds were found in both the monomer form, and also in their flavonoid-glycoside forms. This phenomenon also existed with various other flavonoid (and/or other phenolic compound) classes, where numerous distinct structures were identified with the same molecular weight. For example, numerous flavonoid compounds exist in nature which exhibit a 300 amu molecular weight, including chrysoeriol, diosmetin, kaempferide, geraldol, pratensein, farresol, tectorigenin, and psi-tectorigenin. The vast number of distinct 300 amu compounds detected among the various peanut skin fractions shows that most (if not all) of these compounds exist in this plant source. As in the case with the 302 amu structures, some of these existed as flavonoid-glycosides (in addition to their monomer counterparts). Other examples existed with the detection of numerous identical molecular weight phenolic-compounds, such as in the case of 316 amu, 288 amu, 286 amu, and 284 amu compounds. This reveals that the majority of possible phenolic (flavonoid, chalcone, ect.) derivatives for each individual molecular weight exist in peanut skins. This phenomenon also holds true for the various detected flavonoid-glycosides which exhibited identical molecular weights (and similar fragmentation patterns), but were revealed at different retention times. For example, numerous 464 amu flavonoid glycosides were found among the different fractions, indicating that many flavonoid-glycosides with identical molecular weights exist in peanut skins

(such as isoquercetrin, hyperoside, gossypitrin, and spiraeoside). Another example where numerous flavonoid-glycosides were detected for a given molecular weight included 448 amu compounds, which are encompassed by various luteolin and kaempferol derivatives.

Compounds detected among the various peanut skin fractions (obtained from Toyopearl SEC) generally followed a trend from low-to-high molecular weight for each consecutive fraction (A through H). Phenolic acids were detected in early fractions (A and B), but were also discovered in small concentrations in each consecutive fraction. Phenolic-based monomers (flavonoids, chalcones, chromanes, chromenes, etc.), as well as their sugar-linked derivatives, were generally found in fractions A through E. Higher molecular weight compounds, such as oligomeric procyanidins (OPC) structures consisting of flavonoid dimers (including numerous novel biflavonoids), trimers, and tetramers, were generally found in fractions F through H.

The use of HPLC Method 1 allowed for the identification of 53 compounds in Fraction A, while HPLC Method 2 detected the presence of 8 additional compounds in this fraction (Tables 1 and 2). These structures mostly consisted of small-to-intermediate size compounds (168 to 720 amu) which were comprised of phenolic acids (such as cinnamic and benzoic derivatives), stilbene-derivatives (resveratrol-based), coumarin-based compounds, and chalcone-based structures. A large number of additional distinct phenolic acids existed in Fraction A which could not be identified (and were therefore not reported), due to difficulties in interpreting their fragmentation pathways. Other compounds in Fraction A included flavonoids (or isoflavonoids) with one or more hydroxy and/or methoxy group(s). Many of these compounds were bound by sugar side groups consisting of mono- or disaccharides, such as in the case of various glycosylated flavonoids (and possibly their glycosylated iso-flavonoid derivatives). Most of these structures are less known flavonoid compounds, and have never been reported to

exist in peanut plant parts. However, some of the glycosylated flavonoids found in Fraction A incorporate aglycones which are widely recognized in bioflavanoid research, such as eriodictyol and luteolin. Fraction A revealed the highest number of individual compounds when compared to all other fractions obtained from Toyopearl SEC, however, these compounds were generally not present in extremely high concentrations.

A total of 24 compounds were identified in Fraction B using HPLC Method 1 (Table 3). The utilization of HPLC Method 2 allowed for the detection of 27 additional compounds (Table 4). These structures ranged from small-to-intermediate size compounds (138 to 934 amu), and mostly consisted of numerous phenolic acids (benzoic and cinnamic acid derivatives), chalcones, chromones, chromenes, chromanediols, and flavonoids (or isoflavonoids) with one or more hydroxyl and/or methoxy group(s). As in the case of Fraction A, most of these compounds are newly discovered in peanut skins. Numerous high concentration flavonoid-glycosides were also detected in Fraction B, of which most had aglycones consisting of quercetin, eriodictyol, isorhamnetin, and hesperitin.

Fraction C consisted of 69 total compounds, of which 35 were detected using HPLC Method 1, and 34 were identified using HPLC Method 2 (Tables 5 and 6). Many of these compounds were flavonoids (or isoflavonoids) with one or more hydroxyl or methoxy groups. As in the case of previous fractions, many of these compounds have never been previously reported in peanut skins. Numerous high-concentration flavonoid-glycosides were also found, many consisting of aglycones which are more commonly found to exist as flanvoid glycosides (such as quercetin, isorhamnetin, luteolin, and kaempferol). However, several of these flavonoid-glycosides are made up of uncommon aglycone moieties which have never been reported to exist in peanut skins (such as fraxetin, myricetin, quercetagetin, gossypetin, and

fraxetin). Other detected compounds include various coumarin-based structures.

The use of HPLC Method 1 allowed for the identification of 15 compounds in Fraction D, while HPLC Method 2 detected the presence of 7 additional compounds in this fraction (Tables 7 and 8). Fraction E contained a total of 12 compounds, of which 9 were identified using HPLC Method 1, and 3 using HPLC Method 2 (Tables 9 and 10). The compounds identified in Fractions D and E included extremely high concentrations of flavonoid monomers and flavonoid-glycosides. Several of these compounds have been previously reported in numerous studies (such as catechin, epicatechin, and quercetin), however, the majority of the remaining compounds have never been determined to exist in peanut skins. Some of these monomers included diosmetin, chrysoeriol, homoeriodictyol, morin, robinetin, and tricetin. Flavonoid-glycosides included isoquercitrin, hyperoside, gossypitrin, and spiraeosdie. The large number of these identified high-concentration compounds indicates the wide range of diverse flavonoid compounds which reside in this plant source. Several researchers have attempted to analyze the flavonoid profile of peanut skins, however, these studies did not incorporate a method (such as Toyopearl SEC coupled with HPLC ion trap MS^n) which is capable of fully recognizing these types of structures.

A total of 20 compounds were identified in Fraction F using HPLC Method 1, while HPLC Method 2 detected the presence of 3 additional compounds in this fraction (Tables 11 and 12). Fraction G-Red contained a total of 16 compounds, of which 12 were identified using HPLC Method 1, and 4 using HPLC Method 2 (Tables 13 and 14). Although several flavonoid-based monomers were detected in these fractions (such as luteolin and hesperitin), the majority of the compounds identified consisted of extremely high concentrations of flavonoid dimers. Most of these dimer structures were numerous B-type procyanidins, which indicates that many

dimeric flavonoid-based derivatives exist in peanut skins containing multiple combinations of catechin/epicatechin monomers in various linear and branched forms. Several A-type proanthocyanidin dimers were also discovered, revealing that numerous catechin/epicatechin derivatives of these structures are also present.

The use of HPLC Method 1 allowed for the identification of 19 compounds in Fraction G, while HPLC Method 2 detected the presence of 4 additional compounds in this fraction (Tables 15 and 16). Fraction H contained a total of 18 compounds, of which 13 were identified using HPLC Method 1, and 5 using HPLC Method 2 (Tables 17 and 18). These fractions consisted mainly of numerous catechin/epicatechin trimers and tetramers at extremely high concentrations. The vast number of unique trimers and tetramers indicates that many derivatives exist in peanut skins, mainly due to the multiple combinations which are possible with oligomeric procyanidins (OPC's). These derivatives consist of various branch forms (linear vs branched), along with the order of catechin versus epicatechin within the flavonoid polymer.

The vast number of phenolic-based compounds identified in this study reveals that peanut skins are possibly one of the most phenolic-rich and diverse plant sources ever studied. The majority of these compounds are known to exhibit powerful antioxidant activity, indicating that peanut skins could be used as a novel source for the extraction of natural antioxidant and preservative components. This proves the capability that peanut skins, which had been previously viewed as a by-product (or waste-product) of the peanut industry, can become a value-added commodity and revenue stream for peanut farmers.

Numerous compounds were detected which have been reported to exhibit specific chemical, biological, nutraceutical, and pharmaceutical attributes (Table 19). This indicates the possibility that peanut skins could be utilized as a novel source for the extraction of compounds

which have the potential to treat ailments such as cardiovascular disease and various forms of cancer. All of these factors showcase the need for future research into the biological effects of components contained within peanut skins. Future research could use this study as a template, to further narrow down the numerous compounds which were tentatively identified (many of which have significant antioxidant and biological effects).

Table 1: Detected Compounds in Fraction A using HPLC Method 1. Indicates Compound Number (CMPD #), Molecular Weight (MW) in atomic mass units (amu), Retention Time (RT) in minutes (min), Mass Spec Base Peak Identification (BP-ID) showing negative mode ionization $[M-H]^-$ (indicates the type of ion which forms the Base Peak. Base Peak refers to the most abundant ion in the mass spectrum), Parent ion (P^-) m/z after $[M-H]^-$ ionization (indicates the Base Peak in the normal mass spectra), Base Peak of the daughter ion (D-BP) (i.e., the most abundant ion in the daughter spectrum), MS/MS or MS/MS/MS product ions (MS^3), and the arithmetic difference in m/z between the parent ion and individual daughter ions (P-Di). Bold donates most abundant ion in the given spectra.

CMPD	MW	RT	BP-ID	P-	==>	D-BP	Other Daughter Ions								Possible Structure ID(s)
1-A1	402	1.69	[M-H]-	401	==>	341									Dihydroxy-cinnamic Acid (such as 3,4-Dihydroxycinnamic acid (Caffeic Acid)) plus a single glucose sugar unit
					P-Di	60									
			MS^3	341	==>	281	**179**	161	149	143	131	125	119		
					P-Di	60	162	180	192	198	210	216	222		
2-A1	444	7.78	[M-H]-	443	==>	383									Hydroxy-flavone, or isoflavone (such as Flavonol, Primuletin, or 6- or 7-Hydroxyflavone), or Methoxy-Chalcone plus a single rhamonse sugar unit
					P-Di	60									
			MS^3	383	==>	355	299	247	**237**	229	179	163	161		
					P-Di	28	84	136	146	154	204	220	222		
3-A1	302	8.54	[M-H]-	301	==>	241	217								3',4',5,5',7-Pentahydroxyflavone (a.k.a. Tricetin)
					P-Di	60	84								
			MS^3	241	==>	218	199	197	150	138	126				
					P-Di	23	42	44	91	103	115				
4-A1	380	8.69	[M-H]-	379	==>	361	335	299	217						4,4'-Dihydroxy-3,3'-(2-methoxy-ethylidene)-dicoumarin (a.k.a. Dicoumoxyl)
					P-Di	18	44	80	162						
			MS^3	361	==>	291	**272**	271	255						
					P-Di	70	89	90	106						
5-A1	396	8.84	[M-H]-	395	==>	335	319								3,3'-Methylenebis[4-hydroxycoumarin] (a.k.a. Dicoumarin), or Coumarin-6-(7-hydroxycoumarin-8-yl)-7-methoxy
					P-Di	60	76								
			MS^3	335	==>	317	**291**	275	273	249	247	229	201	173	
					P-Di	18	44	60	62	86	88	106	134	162	
6-A1	458	9.90	[M-H]-	457	==>	397									3-Methoxyflavone, with a rhamnose sugar side-group
					P-Di	60	457	457	457						
			MS^3	397	==>	355	335	265	**251**	235	163	161	143		
					P-Di	42	62	132	146	162	234	236	254		
7-A1	217	10.20	[M-H]-	216	==>	198									6-Hydroxy-2-naphthalenepropanoic Acid (a.k.a. Allenolic Acid)
					P-Di	18									
			MS^3	154	==>										
					P-Di										
8-A1	398	11.56	[M-H]-	397	==>	379	**351**	337	333	315	307	305	289	287	UNKOWN, perhaps Coumaroylquinic Acid derivative
					P-Di	18	46	60	64	82	90	92	108	110	
			MS^3	379	==>	279	277	273	**259**	253	249	241	197	187	
					P-Di	100	102	106	120	126	130	138	182	192	
9-A1	382	11.86	[M-H]-	381	==>	335	**321**	299	217						UNKOWN, according to NIST, similar to Chromone, 2-[2-(3,5-diacetoxy-phenyl)ethyl]-3-methyl
					P-Di	46	60	82	164						
			MS^3	321	==>	273	219	191	**137**						
					P-Di	48	102	130	184						
10-A1	396	12.16	[M-H]-	395	==>	337	321	319	307	293					UNKOWN, perhaps Coumaroylquinic Acid derivative. According to NIST, this may be a Chromone derivative
					P-Di	58	74	76	88	102					
			MS^3	337	==>	305	**293**	291	275	261	231				
					P-Di	32	44	46	62	76	106				
11-A1	300	12.47	[M-H]-	299	==>	137									Reported in Fraction B due to higher concentrations present
					P-Di	162									
			MS^3	137	==>	93									
					P-Di	44									
12-A1	398	13.05	[M-H]-	397	==>	337	293	251							UNKOWN, perhaps Coumaroylquinic Acid derivative. According to NIST, this may be a Chromone derivative
					P-Di	60	104	146							
			MS^3	337	==>	293	275	249	231	219					
					P-Di	44	62	88	106	118					
13-A1	398	14.07	[M-H]-	397	==>	337	321	251							Flavanone compound similar to Bavachinin A. May also be isoflavone derivative similar to a compound known as Hydroxywighteone
					P-Di	60	76	146							
			MS^3	337	==>	293	275	231							
					P-Di	44	62	106							
14-A1	396	15.58	[M-H]-	395	==>	321									UNKNOWN, NIST suggests a Chromone derivative
					P-Di	74									
			MS^3	321	==>	303	277	259	247	233	**203**				
					P-Di	18	44	62	74	88	118				
15-A1	396	15.88	[M-H]-	395	==>	321									UNKNOWN, NIST suggests a Chromone derivative
					P-Di	74									
			MS^3	321	==>	303	**277**	259	247	233	203				
					P-Di	18	44	62	74	88	118				

Table 1: (cont.)

CMPD	MW	RT	BP-ID	P-	==>	D-BP	Other Daughter Ions								Possible Structure ID(s)
16-A1	378	16.30	[M-H]-	377	==>	333	315	297	289	271	259	229	201		UNKNOWN
					P-Di	44	62	80	88	106	118	148	176		
			MS^3	333	==>	303	**289**	287	271	269	219	213	193	187	
					P-Di	30	44	46	62	64	114	120	140	146	
17-A1	168	17.01	[M-H]-	167	==>	152	109	108							Either Vanillic Acid, Homogentisic Acid, Hydroxy-methoxy-benzoic Acid, Homoprotocatechuic Acid, Orsellinic Acid, or Resorcylic Acid derivative
					P-Di	15	58	59							
			MS^3	152	==>	123	**109**	108							
					P-Di	29	43	44							
18-A1	476	17.42	[M-H]-	475	==>	415									Rhamnose sugar plus either a trihydroxyflavone, trihydroxyiso-flavone, hydroxy-methoxy-flavanone, or dihydroxy-methoxy-chalcone
					P-Di	60									
			MS^3	415	==>	299	**269**	247	161	158					
					P-Di	116	146	168	254	257					
19-A1	240	17.98	[M-H]-	239	==>	179									Dihydroxy-benzoic Acid (such as Caffeic Acid), less a 60 amu acetate adduct ion
					P-Di	60									
			MS^3	179	==>	161	159	87							
					P-Di	18	20	92							
20-A1	188	18.43	[M-H]-	187	==>	125									Benzoic Acid derivative, fragments similar to Caffeic Acid
					P-Di	62									
			MS^3	125	==>	97	81	57							
					P-Di	28	44	68							
21-A1	444	19.04	[M-H]-	443	==>	425	341	305	**299**						Glucose-linked Hydroxy-benzoic Acid, with Coumaroyl acyl side-group
					P-Di	18	102	138	144						
			MS^3	299	==>	137									
					P-Di	162									
22-A1	596	19.42	[M-H]-	595	==>	535									Resveratrol, plus rutinose sugar side-group
					P-Di	60									
			MS^3	535	==>	443	**389**	307	247	227	187				
					P-Di	92	146	228	288	308	348				
23-A1	174	19.94	[M-H]-	173	==>	155	143	142	129	**111**	109	102	83	81	Shikimic Acid
					P-Di	18	30	31	44	62	64	71	90	92	
			MS^3	111	==>	83	57								
					P-Di	28	54								
24-A1	596	20.21	[M-H]-	595	==>	579	535								Eriodictyol-7-neohesperidoside (a.k.a. neoeriocitrin), or Eriodictyol 7-O-rutinoside (a.k.a. Eriocitrin)
					P-Di	16	60								
			MS^3	535	==>	487	**389**	367	271	263	251	225			
					P-Di	48	146	168	264	272	284	310			
25-A1	580	21.83	[M-H]-	579	==>	411	**285**								Luteolin, plus either a sambubiose or lathyrose disaccharide side-group
					P-Di	168	294								
			MS^3	285	==>	267	257	**241**	217	213	201	175	163	147	
					P-Di	18	28	44	68	72	84	110	122	138	
26-A1	244	24.26	[M-H]-	243	==>	225	181								Either 7-methoxy-8-isopentenyl-coumarin (Osthole), 7-methoxy-6-iso-pentenylcoumarin (Suberosin), Oxy-resveratrol, or Cedrecoumarin A
					P-Di	18	62								
			MS^3	225	==>	207	181	163	99	97					
					P-Di	18	44	62	126	128					
27-A1	188	25.09	[M-H]-	187	==>	169	157	151	125	97					Either a Benzoic Acid derivative (similar to Gallic Acid), or Coumarin-like structure, or 5-Hydroxy-2-methyl-1,4-naphtoquinone (a.k.a. Plumbagin).
					P-Di	18	30	36	62	90					
			MS^3	125	==>	97	83	69	57						
					P-Di	28	42	56	68						
28-A1	244	26.39	[M-H]-	243	==>	225	207								Either 7-methoxy-8-isopentenyl-coumarin (Osthole), 7-methoxy-6-iso-pentenylcoumarin (Suberosin), Oxy-resveratrol, or Cedrecoumarin A
					P-Di	18	36								
			MS^3	225	==>	207	181	163	97						
					P-Di	18	44	62	128						
29-A1	242	28.24	[M-H]-	241	==>	223	**197**	179	161						Sinnapic Acid-like (plus water)
					P-Di	18	44	62	80						
			MS^3	223	==>	179	161	153	151	137	125	123	111	95	
					P-Di	44	62	70	72	86	98	100	112	128	
30-A1	170	30.46	[M-H]-	169	==>	125									2,4,6-Trihydroxybenzoic acid (or other Trihydroxybenzoic acid derivative)
					P-Di	44									
			MS^3	125	==>	95	83	**71**	57						
					P-Di	30	42	54	68						
31-A1	720	31.46	[M-H]-	719	==>	659	497								Oleuropein, plus additional glucose sugar unit
					P-Di	60	222								
			MS^3	659	==>	581	**539**	497	479	437	425	395	377	377	
					P-Di	78	120	162	180	222	234	264	282	282	
32-A1	462	34.00	[M-H]-	461	==>	401									Possible Hexamethoxyflavone (such 3',4',5,5',6,7-Hexamethoxyflavone)
					P-Di	60									
			MS^3	401	==>	327	**309**								
					P-Di	74	92								

Table 1: (cont.)

CMPD	MW	RT	BP-ID	P-	==>	D-BP	Other Daughter Ions								Possible Structure ID(s)
33-A1	326	34.81	[M-H]-	325	==>	307	289								Fragments similar to 5-Hydroxy-4',7-dimethoxy-6,8-dimethylflavone (a.k.a. Eucalyptin), and 5,7-Dimethoxy-3-(4'-methoxyphenyl)-4-methylcoumarin
					P-Di	18	36								
			MS^3	307	==>	289	235	185	137	121					
					P-Di	18	72	122	170	186					
34-A1	558	35.05	[M-H]-	557	==>	497									Coumarin compound, such as Psoralidin, Dicoumarin, Lasiocephalin, or 6-(7-hydroxycoumarin-8-yl)-7-methoxy-coumarin, plus a glucose unit
					P-Di	60									
			MS^3	497	==>	335									
					P-Di	162									
35-A1	328	35.44	[M-H]-	327	==>	309	291	239	171						Compound similar to: Kaempferol-3,4',7-trimethyl ether, or 3-hydroxy-4',5,7-trimethoxyflavone
					P-Di	18	36	88	156						
			MS^3	309	==>	291	251	171							
					P-Di	18	58	138							
36-A1	328	35.80	[M-H]-	327	==>	309	291	239	229	221	211	209	171	165	Compound similar to: Kaempferol-3,4',7-trimethyl ether, or 3-hydroxy-4',5,7-trimethoxyflavone
					P-Di	18	36	88	98	106	116	118	156	162	
			MS^3	309	==>	291	253	227	125						
					P-Di	18	56	82	184						
37-A1	464	36.08	[M-H]-	463	==>	403									UNKNOWN
					P-Di	60									
			MS^3	403	==>	329	311	211							
					P-Di	74	92	192							
38-A1	330	37.70	[M-H]-	329	==>	309	291	229	211	209	185	171			UNKNOWN, possible Hydroxy-trimethoxy-flavanone
					P-Di	20	38	100	118	120	144	158			
			MS^3	309	==>	305	**291**	191							
					P-Di	4	18	118							
39-A1	328	38.27	[M-H]-	327	==>	309	291	229	211	209	185	171			Compound similar to: Kaempferol-3,4',7-trimethyl ether, or 3-hydroxy-4',5,7-trimethoxyflavone
					P-Di	18	36	98	116	118	142	156			
			MS^3	309	==>	305	**291**	191							
					P-Di	4	18	118							
40-A1	330	38.44	[M-H]-	329	==>	309	291	229	211	209	185	171			UNKNOWN, possible Hydroxy-trimethoxy-flavanone
					P-Di	20	38	100	118	120	144	158			
			MS^3	309	==>	305	**291**	191							
					P-Di	4	18	118							
41-A1	328	38.80	[M-H]-	327	==>	309	**307**	291	289	229	213	201	171		Compound similar to: Kaempferol-3,4',7-trimethyl ether, or 3-hydroxy-4',5,7-trimethoxyflavone
					P-Di	18	20	36	38	98	114	126	156		
			MS^3	309	==>	305	291	289	245	209	191	171	163	137	
					P-Di	4	18	20	64	100	118	138	146	172	
42-A1	326	40.71	[M-H]-	325	==>	307									Fragmentation similar to Eucalyptin
					P-Di	18									
			MS^3	307	==>	289	209	125							
					P-Di	18	98	182							
43-A1	446	41.85	[M-H]-	445	==>	385									Either 4',7-Dihydroxy-6-methoxy-isoflavone-7-D-glucoside (Glycitin), Biochanin-A-7-glucoside (Sissotrin), or Baicalein-7-O-glucuronide
					P-Di	60									
			MS^3	385	==>	311	293								
					P-Di	74	92								
44-A1	360	42.08	[M-H]-	359	==>	311	**291**	289	223	209	183	125			UNKOWN, fragmentation pattern similar to 3',5,7-Trihydroxy-4',5',6-trimethoxyisoflavone (aka Irigenin)
					P-Di	48	68	70	136	150	176	234			
			MS^3	311	==>	305	**273**	271	255	247	217	197	189	163	
					P-Di	6	38	40	56	64	94	114	122	148	
45-A1	360	42.49	[M-H]-	359	==>	341	**323**	171	169						UNKOWN, fragmentation pattern similar to 3',5,7-Trihydroxy-4',5',6-trimethoxyisoflavone (aka Irigenin)
					P-Di	18	36	188	190						
			MS^3	341	==>	291	193	169	153	151	149				
					P-Di	50	148	172	188	190	192				
46-A1	312	43.66	[M-H]-	311	==>	293	223								3,5,7-Trimethoxyflavone (according to NIST 05 Database)
					P-Di	18	88								
			MS^3	293	==>	275	247	235	221	149	141				
					P-Di	18	46	58	72	144	152				
47-A1	328	43.98	[M-H]-	327	==>	309	291								Compound similar to: Kaempferol-3,4',7-trimethyl ether, or 3-hydroxy-4',5,7-trimethoxyflavone
					P-Di	18	36								
			MS^3	309	==>	291	289	247	245	209	193	155	153		
					P-Di	18	20	62	64	100	116	154	156		
48-A1	310	44.37	[M-H]-	309	==>	293	291	209							Fragmentation similar to Maxima-Isoflavone A
					P-Di	16	18	100							
			MS^3	293	==>	275	273	257	247	215	193	185	165	149	
					P-Di	18	20	36	46	78	100	108	128	144	
49-A1	312	44.37	[M-H]-	311	==>	293	291	209							Fragmentation similar to Maxima-Isoflavone G, and Maxima-Isoflavone E
					P-Di	18	20	102							
			MS^3	293	==>	275	273	257	247	215	193	185	165	149	
					P-Di	18	20	36	46	78	100	108	128	144	

Table 1: (cont.)

CMPD	MW	RT	BP-ID	P-	==>	D-BP	Other Daughter Ions								Possible Structure ID(s)
50-A1	314	45.31	[M-H]-	313	==>	295	201	171							Fragmentation similar to Pectolinarigenin
					P-Di	18	112	142							
			MS^3	295	==>	183	181	171	165	155	153	137	127	125	
					P-Di	112	114	124	130	140	142	158	168	170	
51-A1	314	49.57	[M-H]-	313	==>	295									Fragmentation similar to Pectolinarigenin
					P-Di	18									
			MS^3	295	==>	277	275	251	151	141	127	111			
					P-Di	18	20	44	144	154	168	184			
52-A1	402	49.82	[M-H]-	401	==>	341	313	289	274	260					UNKNOWN
					P-Di	60	88	112	127	141					
			MS^3	341	==>	324	314	310	306	295	282	265	166		
					P-Di	17	27	31	35	46	59	76	175		
53-A1	272	53.55	[M-H]-	271	==>	253	225								UNKNOWN
					P-Di	18	46								
			MS^3	253	==>	221	201	195	83						
					P-Di	32	52	58	170						

Table 2: Detected Compounds in Fraction A using HPLC Method 2. Indicates Compound Number (CMPD #), Molecular Weight (MW) in atomic mass units (amu), Retention Time (RT) in minutes (min), Mass Spec Base Peak Identification (BP-ID) showing negative mode ionization $[M-H]^-$ (indicates the type of ion which forms the Base Peak. Base Peak refers to the most abundant ion in the mass spectrum), Parent ion (P^-) m/z after $[M-H]^-$ ionization (indicates the Base Peak in the normal mass spectra), Base Peak of the daughter ion (D-BP) (i.e., the most abundant ion in the daughter spectrum), MS/MS or MS/MS/MS product ions (MS^3), and the arithmetic difference in m/z between the parent ion and individual daughter ions (P-Di). Bold donates most abundant ion in the given spectra.

CMPD	MW	RT	BP-ID	P-	==>	D-BP	Other Daughter Ions							Structure ID
1-A2	240	4.08	[M-H]-	239	==>	179								Dihydroxycinnamic Acid(s)
		to			P-Di	60								
		17.77	MS^3	179	==>	161	145	141	125	117	101	99	91	
					P-Di	18	34	38	54	62	78	80	88	
2-A2	222	16.72	[M-H]-	221	==>	161								Coumarin-based compound, such as 3-Hydroxycoumarin, 4-Coumarinol, 4-Hydroxycoumarin, or 7-Hydroxycoumarin (Umbelliferone)
					P-Di	60								
			MS^3	161	==>	143	125							
					P-Di	18	36							
3-A2	174	40.05	[M-H]-	173	==>	155	143	142	129	111	109	102	83	81
					P-Di	18	30	31	44	62	64	71	90	92
			MS^3	111	==>									Shikimic Acid
					P-Di									
4-A2	244	48.08	[M-H]-	243	==>	225								Cedrecoumarin A, and Oxyresveratrol
		49.51			P-Di	18								
		52.88	MS^3	225	==>									
		53.57			P-Di									
5-A2	188	50.96	[M-H]-	187	==>	169	157	151	125	97				Either a Benzoic Acid derivative (similar to Gallic Acid), or Coumarin-like structure, or 5-Hydroxy-2-methyl-1,4-naphtoquinone (a.k.a. Plumbagin).
					P-Di	18	30	36	62	90				
			MS^3	169	==>									
					P-Di									
6-A2	242	54.67	[M-H]-	241	==>	223	205	197	179	161				Either a Dihydroxyflavan, such as 4',7-Dihydroxyisoflavan (a.k.a. Equol), or a Flavandiol such as 4,4'-flavandiol or 4,7-flavandiol
					P-Di	18	36	44	62	80				
			MS^3	223	==>									
					P-Di									
7-A2	170	57.53	[M-H]-	169	==>	153	**125**	83	71					2,4,6-Trihydroxybenzoic acid (or other Trihydroxybenzoic acid derivative)
					P-Di	16	44	86	98					
			MS^3	307	==>									
					P-Di									
8-A2	202	60.30	[M-H]-	201	==>	183	**139**							Hydroxyfurocoumarin, such as 5-Hydroxyfurocoumarin (Bergaptrol) and 8-Hydroxy-4'-5',6-7-furocoumarin (a.k.a. Xanthotoxol)
					P-Di	18	62							
			MS^3	183	==>									
					P-Di									

Table 3: Detected Compounds in Fraction B using HPLC Method 1. Indicates Compound Number (CMPD #), Molecular Weight (MW) in atomic mass units (amu), Retention Time (RT) in minutes (min), Mass Spec Base Peak Identification (BP-ID) showing negative mode ionization $[M-H]^-$ (indicates the type of ion which forms the Base Peak. Base Peak refers to the most abundant ion in the mass spectrum), Parent ion (P^-) m/z after $[M-H]^-$ ionization (indicates the Base Peak in the normal mass spectra), Base Peak of the daughter ion (D-BP) (i.e., the most abundant ion in the daughter spectrum), MS/MS or MS/MS/MS product ions (MS^3), and the arithmetic difference in m/z between the parent ion and individual daughter ions (P-Di). Bold donates most abundant ion in the given spectra.

CMPD	MW	RT	BP-ID	P-	==>	D-BP	Other Daughter Ions								Structure ID
1-B1	154	8.78	[M-H]-	153	==>	109									Dihydroxybenzoic Acid, such as Resorcylic Acid, Gentisic Acid, and Protocatechuic Acid
					P-Di	44									
			MS^3	109	==>	91	81								
					P-Di	18	28								
2-B1	138	11.07	[M-H]-	137	==>	119	109	93	81	65					Hydroxybenzoic Acid, such as various Salicylic Acid derivatives. Also, this compound may be Pyrocatechin-Monoethyl-Ether
					P-Di	18	28	44	56	72					
			MS^3	119	==>										
					P-Di										
3-B1	300	12.54	[M-H]-	299	==>	137									Either Hydroxybenzoic Acid or Pyrocatechin-Monoethyl-Ether, plus an added glucose or galactose side-group
					P-Di	162									
			MS^3	137	==>	**93**									
					P-Di	44									
4-B1	416	12.98	[M-H]-	415	==>	313	253								Dihydroxyflavone (such as 3,4'-Dihydroxyflavone) or Dihydroxy-isoflavone (such as Daidzein), plus glucose (or galactose) unit
					P-Di	102	162								
			MS^3	313	==>	**253**	235	203	193	151	109				
					P-Di	60	78	110	120	162	204				
5-B1	450	16.27	[M-H]-	449	==>	287	269	259	179						Likely Eriodictyol-7-glucoside, but aglycone may also be either Fustin, Hydroxyapigenin, or Dihydrokeampferol
					P-Di	162	180	190	270						
			MS^3	287	==>	259	243	215	201	199	187	175	157	125	
					P-Di	28	44	72	86	88	100	112	130	162	
6-B1	474	17.08	[M-H]-	473	==>	311	293	179							Trisaccharide: Two glucose (or galactose) units, plus one xylose (or arabinose) unit
					P-Di	162	180	294							
			MS^3	311	==>	179	149	135							
					P-Di	132	162	176							
7-B1	934	17.81	[M-H]-	933	==>	771									Quercetin Glycoside. Sugar group consists of Rutinose plus added dissacharide (either Sophorose, Gentiobiose, or Laminaribiose)
					P-Di	162									
			MS^3	771	==>	753	625	609	591	549	408	367	343	301	
					P-Di	18	146	162	180	222	363	404	428	470	
8-B1	164	18.32	[M-H]-	163	==>	119									p-Hydroxycinnamic Acid (a.k.a. p-Coumaric Acid)
					P-Di	44									
			MS^3	119	==>										
					P-Di										
9-B1	458	18.92	[M-H]-	457	==>	440	311	295	**293**	277	221	204	163		6-O-Acetyldaidzin
					P-Di	17	146	162	164	180	236	253	294		
			MS^3	293	==>	275	219	191	187	179	163	155	139	127	
					P-Di	18	74	102	106	114	130	138	154	166	
10-B1	488	19.34	[M-H]-	487	==>	325	307	293							Ferulic Acid, plus a disaccharide side group (either sambubiose or lathyrose)
					P-Di	162	180	194							
			MS^3	325	==>	193	149	113							
					P-Di	132	176	212							
11-B1	904	19.39	[M-H]-	903	==>	741									Quercetin plus rutinose and lathyrose (or sambubiose), or Isorhamnetin plus combination of 2 sambubiose's (or lathyrose's)
					P-Di	162									
			MS^3	741	==>	723	609	591	573	343	327	**300**	271	255	
					P-Di	18	132	150	168	398	414	441	470	486	
12-B1	904	19.39	[M-H]-	903	==>	741									Quercetin plus rutinose and lathyrose (or sambubiose), or Isorhamnetin plus combination of 2 sambubiose's (or lathyrose's)
					P-Di	162									
			MS^3	741	==>	723	609	591	573	545	475	355	343	337	
					P-Di	18	132	150	168	196	266	386	398	404	
13-B1	772	19.66	[M-H]-	771	==>	609	591	573	505	465	447	301	300	271	Quercetin Glycoside. Sugar group consists of Rutinose plus added glucose (or galactose)
					P-Di	162	180	198	266	306	324	470	471	500	
			MS^3	609	==>	283	273	271	255	244	229	199	179	151	
					P-Di	326	336	338	354	365	380	410	430	458	
14-B1	138	20.14	[M-H]-	137	==>	93									Hydroxybenzoic Acid, such as 3-Hydroxybenzoic Acid or 4-Hyrdoxybenzoic Acid
					P-Di	44									
			MS^3	93	==>										
					P-Di										
15-B1	786	21.49	[M-H]-	785	==>	753	623	605	519	423	357	339	**315**	314	Isorhamnetin-3-O-rutinoside, plus additional glucose (or galactose)
					P-Di	32	162	180	266	362	428	446	470	471	
			MS^3	753	==>	301	300	299	287	285	272	271	256	247	
					P-Di	452	453	454	466	468	481	482	497	506	

Table 3: (cont.)

CMPD	MW	RT	BP-ID	P-	==>	D-BP	Other Daughter Ions								Structure ID
16-B1	640	22.18	[M-H]-	639	==>	477	459	357	339	316	315	314	300	299	Isorhamnetin plus disaccharide side-group (either laminaribiose getiobiose, or sophorose)
					P-Di	162	180	282	300	323	324	325	339	340	
			MS^3	477	==>	301	300	299	287	285	272	271	259	256	
					P-Di	176	177	178	190	192	205	206	218	221	
17-B1	474	23.01	[M-H]-	473	==>	311	293								Trisaccharide: 2 glucose units plus 1 xylose unit
					P-Di	162	180								
			MS^3	311	==>	**179**	149	135							
					P-Di	132	162	176							
18-B1	756	23.31	[M-H]-	755	==>	723	623	605	577	489	**315**	314	300	271	Isorhamnetin plus rutinose disaccharide, plus additional xylose (or arabinose) sugar
					P-Di	32	132	150	178	266	440	441	455	484	
			MS^3	723	==>	301	300	299	285	271	257	247	241	183	
					P-Di	422	423	424	438	452	466	476	482	540	
19-B1	464	24.54	[M-H]-	463	==>	301									Hesperitin plus glucose (or galactose)
					P-Di	162									
			MS^3	301	==>	287	286	271	256	217	183	164	151		
					P-Di	14	15	30	45	84	118	137	150		
20-B1	462	27.59	[M-H]-	461	==>	299									Flavonoid (either Chrysoeriol, Diosmetin, or other 300 amu flavonoid), plus monosaccharide unit (glucose or galactose)
					P-Di	162									
			MS^3	299	==>	284									
					P-Di	15									
21-B1	436	49.11	[M-H]-	435	==>	420	378	351	312	299	271				Chalcone, Chromone, or Chromene-based compound. Similar to Orotinichalcone and 2'-O-Methylcajanone
					P-Di	15	57	84	123	136	164				
			MS^3	420	==>	405	377	351	338	309	298	283	270	259	
					P-Di	15	43	69	82	111	122	137	150	161	
22-B1	436	50.90	[M-H]-	435	==>	365									Chalcone, Chromone, or Chromene-based compound. Similar to Orotinichalcone and 2'-O-Methylcajanone
					P-Di	70									
			MS^3	365	==>	350	321	310	295						
					P-Di	15	44	55	70						
23-B1	420	53.00	[M-H]-	419	==>	404	364	361	349	321					Chalcone, Chromone, or Chromene-based compound
					P-Di	15	55	58	70	98					
			MS^3	404	==>	361	349	305	256						
					P-Di	43	55	99	148						
24-B1	420	53.36	[M-H]-	419	==>	404	364	335	296	281	229				Chalcone, Chromone, or Chromene-based compound. Possible 5-O-Methyllupiwighteone
					P-Di	15	55	84	123	138	190				
			MS^3	404	==>	361	349	335	294	293	282	281	269	253	
					P-Di	43	55	69	110	111	122	123	135	151	

Table 4: Detected Compounds in Fraction B using HPLC Method 2. Indicates Compound Number (CMPD #), Molecular Weight (MW) in atomic mass units (amu), Retention Time (RT) in minutes (min), Mass Spec Base Peak Identification (BP-ID) showing negative mode ionization $[M-H]^-$ (indicates the type of ion which forms the Base Peak. Base Peak refers to the most abundant ion in the mass spectrum), Parent ion (P^-) m/z after $[M-H]^-$ ionization (indicates the Base Peak in the normal mass spectra), Base Peak of the daughter ion (D-BP) (i.e., the most abundant ion in the daughter spectrum), MS/MS or MS/MS/MS product ions (MS^3), and the arithmetic difference in m/z between the parent ion and individual daughter ions (P-Di). Bold donates most abundant ion in the given spectra.

CMPD	MW	RT	BP-ID	P-	==>	D-BP	Other Daughter Ions								Structure ID
1-B2	240	3.84	[M-H]-	239	==>	179	161								Dihydroxycinnamic Acid (with acetate adduct)
					P-Di	60	78								
			MS^3	179	==>	161	159	141	125	117	103	87			
					P-Di	18	20	38	54	62	76	92			
2-B2	404	17.08	[M-H]-	403	==>	357	293	271	191	177	161	161			2',3,4,4'-Tetrahydroxychalcone (a.k.a. Butein) plus rhamnose sugar, **or** possibly Naringenin plus rhamnose monosaccharide unit
					P-Di	46	110	132	212	226	242	242			
			MS^3	271	==>	181	**161**	151	113	109	101	100	97		
					P-Di	90	110	120	158	162	170	171	174		
3-B2	240	18.98	[M-H]-	239	==>	179									Dihydroxycinnamic Acid (with acetate adduct)
					P-Di	60									
			MS^3	179	==>	161									
					P-Di	18									
4-B2	316	20.11	[M-H]-	315	==>	297	**271**	227	153						316 amu Flavonoid, such as Isorhamnetin, Nepetin, Tamaraxetin, or Rhamnetin
					P-Di	18	44	88	162						
			MS^3	271	==>	227									
					P-Di	44									
5-B2	420	22.01	[M-H]-	419	==>	359	289								Trihydroxy-trimethoxy-flavanoid, such as Irigenin. Also may be a Hydroxy-tetramethoxy-flavanoid
					P-Di	60	130								
			MS^3	359	==>	341	331	315	273	247	231	217	209	153	
					P-Di	18	28	44	86	112	128	142	150	206	
6-B2	626	27.78	[M-H]-	625	==>	463									Quercetin-diglucoside
					P-Di	162									
			MS^3	463	==>	301	191	176							
					P-Di	162	272	287							
7-B2	450	29.05	[M-H]-	449	==>	287	269	259							Fustin (2,3-Dihydrofisetin), plus glucose (or galactose) monosaccharide side group
					P-Di	162	180	190							
			MS^3	287	==>	259	180								
					P-Di	28	107								
8-B2	640	31.07	[M-H]-	639	==>	477	315								Isorhamnetin-diglucoside
					P-Di	162	324								
			MS^3	477	==>	409	315	300	271	256					
					P-Di	68	162	177	206	221					
9-B2	152	32.77	[M-H]-	151	==>	107	93								o-Homosalicylic Acid
					P-Di	44	58								
			MS^3	107	==>										
					P-Di										
10-B2	480	33.65	[M-H]-	479	==>	317	299	289	258	179					Either Myricetin, Quercetagetin, or Gossypetin, plus a glucose (or galactose) side-group. Possible Gossypetin-8-glucoside (Gossypin)
					P-Di	162	180	190	221	300					
			MS^3	299	==>	284	268	176							
					P-Di	15	31	123							
11-B2	334	33.90	[M-H]-	333	==>	315	289	271	229	164	151				Unkown flavonoid: Isorhamnetin-like fragmentation, but with added 18 amu (water)
					P-Di	18	44	62	104	169	182				
			MS^3	315	==>	297	271	245	229	205	177	165	149		
					P-Di	18	44	70	86	110	138	150	166		
12-B2	288	35.75	[M-H]-	287	==>	259	243	201	159	127					Dihydrokaempferol
					P-Di	28	44	86	128	160					
			MS^3	259	==>	241	215	187	173	151	125				
					P-Di	18	44	72	86	108	134				
13-B2	332	39.35	[M-H]-	331	==>	315	299	287	271	255	179				Chromanediol compound, such as: 2-(3,4-Demethoxyphenyl)-7-methoxy-3,4-chromanediol, or 7,8-Dimethoxy-2-(4-methoxyphenyl)-3,4-chromanediol
					P-Di	16	32	44	60	76	152				
			MS^3	299	==>	271	256	239	227	215	187	179	151	124	
					P-Di	28	43	60	72	84	112	120	148	175	
14-B2	390	42.64	[M-H]-	389	==>	374	341	323	303	195	193	165			Trihydroxy-tetramethoxy-flavone, such as Gardenin E, or 3',5,7-trihydroxy-4',5',6,8-tetramethoxy-flavone (a.k.a. Scaposin)
					P-Di	15	48	66	86	194	196	224			
			MS^3	341	==>	326	309	297	295	282	265	250	233		
					P-Di	15	32	44	46	59	76	91	108		
15-B2	178	44.16	[M-H]-	177	==>	151	149	135	133	123	109	89	65		3-Methoxycinnamic Acid
					P-Di	26	28	42	44	54	68	88	112		
			MS^3	151	==>										
					P-Di										

Table 4: (cont.)

CMPD	MW	RT	BP-ID	P-	==>	D-BP	Other Daughter Ions									Structure ID
16-B2	478	44.33	[M-H]-	477	==>	315	299	271	247							Isorhamnetin-glucoside
					P-Di	162	178	206	230							
			MS^3	315	==>	300	299	286	269	231						
					P-Di	15	16	29	46	84						
17-B2	302	46.47	[M-H]-	301	==>	283	271	257	255							Pentahydroxyflavone, such as Morin, Robinetin, or Tricetin
					P-Di	18	30	44	46							
			MS^3	257	==>	242	229	215	213	211	199	189	187	171		
					P-Di	15	28	42	44	46	58	68	70	86		
18-B2	312	47.03	[M-H]-	311	==>	179	149	131								Caffeic acid, plus a terminal rhamnose monosaccharide side-group
					P-Di	132	162	180								
			MS^3	179	==>	135										
					P-Di	44										
19-B2	364	50.03	[M-H]-	363	==>	331	299	283	272	227	195	163				Chromanediol derivative, similar to Compound 13-B2, but with extra 32 amu (methoxy group)
					P-Di	32	64	80	91	136	168	200				
			MS^3	331	==>	299	195	180								
					P-Di	32	136	151								
20-B2	372	54.08	[M-H]-	371	==>	353	341	327	309	235	191					Syringin
					P-Di	18	30	44	62	136	180					
			MS^3	353	==>	338	207									
					P-Di	15	146									
21-B2	300	54.57	[M-H]-	299	==>	299										300 amu MW flavonoid, such as Chrysoeriol, Diosmetin, Kaempferide, Geraldol, Pratensein, or Tectorigenin
					P-Di	0										
			MS^3	299	==>	284										
					P-Di	15										
22-B2	478	56.47	[M-H]-	477	==>	315	314	300	285	271	243					Isorhamnetin (or other 316 amu flavonoid), plus glucose or galactose side-group
					P-Di	162	163	177	192	206	234					
			MS^3	315	==>	300	286	285	271	257	243	151				
					P-Di	15	29	30	44	58	72	164				
23-B2	304	57.15	[M-H]-	303	==>	285	257	243	201							304 amu flavonoid, such as 3'-O-Methylcatechin, 4'-O-Methyl-catechin, Taxifolin, or Dihydrorobinetin
					P-Di	18	46	60	102							
			MS^3	285	==>	270	257	241	215	163	149					
					P-Di	15	28	44	70	122	136					
24-B2	284	63.25	[M-H]-	283	==>	268	255	217	190							Either Prunetin, Biochanin A, or Acacetin
					P-Di	15	28	66	93							
			MS^3	268	==>	240	239	211	185							
					P-Di	28	29	57	83							
25-B2	400	66.41	[M-H]-	399	==>	384	323	308								Either Torosaflavone A, or Chromone compound such as 2-[2-[3,5-dihydroxyphenyl]ethenyl]-5-hydroxy-chromone
					P-Di	15	76	91								
			MS^3	384	==>	370	366	356	341	326	309	308	298	297		
					P-Di	14	18	28	43	58	75	76	86	87		
26-B2	368	80.91	[M-H]-	367	==>	352	349	337	**297**	282	270					Glycycoumarin
					P-Di	15	18	30	70	85	97					
			MS^3	297	==>	**282**	267	254								
					P-Di	15	30	43								
27-B2	352	86.62	[M-H]-	351	==>	**336**	296	281								Pongagallone A
					P-Di	15	55	70								
			MS^3	336	==>	319	293	**281**								
					P-Di	17	43	55								

Table 5: Detected Compounds in Fraction C using HPLC Method 1. Indicates Compound Number (CMPD #), Molecular Weight (MW) in atomic mass units (amu), Retention Time (RT) in minutes (min), Mass Spec Base Peak Identification (BP-ID) showing negative mode ionization $[M-H]^-$ (indicates the type of ion which forms the Base Peak. Base Peak refers to the most abundant ion in the mass spectrum), Parent ion (P^-) m/z after $[M-H]^-$ ionization (indicates the Base Peak in the normal mass spectra), Base Peak of the daughter ion (D-BP) (i.e., the most abundant ion in the daughter spectrum), MS/MS or MS/MS/MS product ions (MS^3), and the arithmetic difference in m/z between the parent ion and individual daughter ions (P-Di). Bold donates most abundant ion in the given spectra.

CMPD	MW	RT	BP-ID	P-	==>	D-BP	Other Daughter Ions								Structure ID
1-C1	135	3.41	[M-H]-	134	==>	107	92								UNKNOWN
					P-Di	27	42								
			MS^3	107	==>										
					P-Di										
2-C1	350	8.05	[M-H]-	349	==>	267	167								Either 2',4'-dimethoxychalcone, 7-methoxyflavonol, 3-hyrdoxy-7-methoxyflavone, or 3-hydroxy-6-methoxyflavone
					P-Di	82	182								
			MS^3	267	==>	151	**150**	149	134	126					
					P-Di	116	117	118	133	141					
3-C1	436	8.51	[M-H]-	435	==>	417	399	375	357	345	**333**	315	289		Catechin or Epicatechin with O-rhamnoside sugar side-group (such as catechin-3-O, 5-O, or 7-O-rhamnoside)
					P-Di	18	36	60	78	90	102	120	146		
			MS^3	333	==>	**315**	289	271	245	229	223	205			
					P-Di	18	44	62	88	104	110	128			
4-C1	420	12.31	[M-H]-	419	==>	401	359	289							Either a Methoxy-flavonoid, a Stilbene-glycoside, a Benzyl-oxyflavone, or a (cat)epicatechin with an unknown side-group
					P-Di	18	60	130							
			MS^3	359	==>	341	331	315	297	289	279	273	269	255	
					P-Di	18	28	44	62	70	80	86	90	104	
5-C1	400	13.37	[M-H]-	399	==>	339	177								Penolic acid (such as 4-Methoxy-cinnamic Acid) or coumarin-linked glycoside, such as Esculin, Cichoriin, and Daphnin
					P-Di	60	222								
			MS^3	339	==>	183	177	167	153	150	**149**	135	134	**133**	
					P-Di	156	162	172	186	189	190	204	205	206	
6-C1	438	14.42	[M-H]-	437	==>	347	289								Catechin or Epicatechin with a trans-Cinnamic Acid side-group
					P-Di	90	148								
			MS^3	347	==>	329	**289**	245	225	205	177	167	161	139	
					P-Di	18	58	102	122	142	170	180	186	208	
7-C1	642	14.88	[M-H]-	641	==>	479	317								Myricetin, Quercetagetin, or Gossypetin, with a diglucoside side-group
					P-Di	162	324								
			MS^3	479	==>	317	299	271	257	249	229	209	191	179	
					P-Di	162	180	208	222	230	250	270	288	300	
8- C1	320	15.06	[M-H]-	319	==>	287	**197**	165							Oureatacatechin
					P-Di	32	122	154							
			MS^3	197	==>	165									
					P-Di	32									
9-C1	438	15.17	[M-H]-	437	==>	347	317	289							Catechin or Epicatechin with a trans-Cinnamic Acid side-group
					P-Di	90	120	148							
			MS^3	347	==>	329	**289**	245	225	207	205	167	151	125	
					P-Di	18	58	102	122	140	142	180	196	222	
10-C1	640	15.24	[M-H]-	639	==>	477	315								316 amu MW flavonoid such as Isorhamnetin, Tamarixetin, Nepetin, Rhamnetin, or Pedalitin, plus a diglucoside side-group
					P-Di	162	324								
			MS^3	477	==>	409	315	300	299	271	247	229	213	175	
					P-Di	68	162	177	178	206	230	248	264	302	
11-C1	552	15.56	[M-H]-	551	==>	389	227								Resveratrol, plus diglucoside side-group
					P-Di	162	324								
			MS^3	389	==>	227									
					P-Di	162									
12-C1	758	19.70	[M-H]-	757	==>	595									Quercetin, plus trisaccharide side-group (sambubiose or lathyrose, plus additional glucose or galactose)
					P-Di	162									
			MS^3	595	==>	301	300	271	255	243	215	300	271	255	
					P-Di	294	295	324	340	352	380	295	324	340	
13-C1	478	19.89	[M-H]-	477	==>	315	300								316 amu MW flavonoid such as Isorhamnetin, Tamarixetin, Nepetin, Rhamnetin, or Pedalitin, plus glucose or galactose side-group
					P-Di	162	177								
			MS^3	315	==>	301	**300**	271	256	247	230	151			
					P-Di	14	15	44	59	68	85	164			
14-C1	178	20.03	[M-H]-	177	==>	149	**133**	109	89						Methoxycinnamic Acid, Chroman-carboxylic acid, or Dihydroxy-coumarin
					P-Di	28	44	68	88						
			MS^3	133	==>	123	105	104	91	89					
					P-Di	10	28	29	42	44					
15-C1	742	20.81	[M-H]-	741	==>	609	591	475	325	301	300	271	255		Quercetin, with trisaccharide side-group (xylose/arabinose plus rhamnose plus glucose/galactose)
					P-Di	132	150	266	416	440	441	470	486		
			MS^3	609	==>	271	255	179	169	151					
					P-Di	338	354	430	440	458					

Table 5: (cont.)

CMPD	MW	RT	BP-ID	P-	==>	D-BP	Other Daughter Ions								Structure ID
16-C1	596	21.29	[M-H]-	595	==>	475	445	301	**300**	271	255				Quercetin with disaccharide side-group (most likely Peltatoside).
					P-Di	120	150	294	295	324	340				
			MS^3	307	==>	271	255	243	227	203	179	169			
					P-Di	36	52	64	80	104	128	138			
17-C1	772	21.95	[M-H]-	771	==>	609	463	301							Quercetin with trisaccharide side-group (rutinose plus glucose or galactose)
					P-Di	162	308	470							
			MS^3	609	==>	301	300	271	255						
					P-Di	308	309	338	354						
18-C1	610	23.68	[M-H]-	609	==>	343	301	300	273	271	255	243	229		Rutin (Quercetin-3-O-rutinoside)
					P-Di	266	308	309	336	338	354	366	380		
			MS^3	301	==>	271	257	255	179	151	121				
					P-Di	30	44	46	122	150	180				
19-C1	594	26.19	[M-H]-	593	==>	285	255								Kaemperfol and/or Luteolin, plus disaccharide side-group (either rutinoside or neohesperidoside)
					P-Di	308	338								
			MS^3	285	==>	285	267	**257**	255	241	239	229	223	213	
					P-Di	0	18	28	30	44	46	56	62	72	
20-C1	594	26.19	[M-H]-	593	==>	447	327	**285**	257	229					Kaemperfol and/or Luteolin, plus disaccharide side-group (either rutinoside or neohesperidoside)
					P-Di	146	266	308	336	364					
			MS^3	285	==>	285	267	257	255	241	239	229	213		
					P-Di	0	18	28	30	44	46	56	72		
21-C1	478	26.28	[M-H]-	477	==>	357	315	**314**	299	285	271	257	243		316 amu MW flavonoid such as Isorhamnetin, Tamarixetin, Nepetin, Rhamnetin, or Pedalitin, plus glucose or galactose side-group
					P-Di	120	162	163	178	192	206	220	234		
			MS^3	314	==>	300	286	285	271	257	243				
					P-Di	14	28	29	43	57	71				
22-C1	624	26.79	[M-H]-	623	==>	315	300	271	255	243					316 amu MW flavonoid such as Isorhamnetin, Tamarixetin, Nepetin, Rhamnetin, or Pedalitin, plus rutinoside sugar side-group
					P-Di	308	323	352	368	380					
			MS^3	315	==>	301	300	299	287	271	255	163			
					P-Di	14	15	16	28	44	60	152			
23- C1	408	28.46	[M-H]-	407	==>	389	297	**285**	283	256	255	243			Either a Benzoic Acid-linked Luteolin or Keampferol, or possibly Remangiflavanone or Sophoraflavanone
					P-Di	18	110	122	124	151	152	164			
			MS^3	285	==>	257	255	241	227	213	201	153			
					P-Di	28	30	44	58	72	84	132			
24-C1	284	28.75	[M-H]-	283	==>	269	268								Either Biochanin A, Prunetin, or Acacetin. Also possibility this may be other 284 amu MW flavonoid.
					P-Di	14	15								
			MS^3	269	==>	267	241	**240**	239	224	211	196	184		
					P-Di	2	28	29	30	45	58	73	85		
25-C1	284	29.66	[M-H]-	283	==>	269									Either Biochanin A, Prunetin, or Acacetin. Also possibility this may be other 284 amu MW flavonoid.
					P-Di	14									
			MS^3	269	==>	268	241	240	239	224	223	212	211	195	
					P-Di	1	28	29	30	45	46	57	58	74	
26-C1	300	32.68	[M-H]-	299	==>	284									Chrysoeriol, Diosmetin, or other 300 amu MW flavonoid (such as Geraldol, Tectorigenin, Kaempferide, Pratensein, Farresol, etc.)
					P-Di	15									
			MS^3	284	==>	256	228	211	200	193	165	150	137		
					P-Di	28	56	73	84	91	119	134	147		
27-C1	330	34.15	[M-H]-	329	==>	314	299								Likely a Trihydroxy-dimethoxy-flavone (such as Isorhamnetin-3-methoxy), or a Hydroxy-trimethoxy-flavone
					P-Di	15	30								
			MS^3	314	==>	300	299	286	285	271	257	243			
					P-Di	14	15	28	29	43	57	71			
28-C1	370	39.41	[M-H]-	369	==>	339	295	251	245	233	219	177			Fraxetin-8-glucoside (a.k.a. Fraxin or Fraxoside)
					P-Di	30	74	118	124	136	150	192			
			MS^3	219	==>	209	191	177	176	175	151	150	134	133	
					P-Di	10	28	42	43	44	68	69	85	86	
29-C1	354	39.85	[M-H]-	353	==>	335	309	**297**	284	253	240	175			Possible Glycyrrh-isoflavone, Lico-isoflavanone, Lico-iso-flavone A, or iso-Licoflavonol.
					P-Di	18	44	56	69	100	113	178			
			MS^3	297	==>	269	256	255	253	227	225	211	161		
					P-Di	28	41	42	44	70	72	86	136		
30-C1	368	40.71	[M-H]-	367	==>	352	349	**337**	322						Either Glycycoumarin or Glycyrrh-isoflavanone
					P-Di	15	18	30	45						
			MS^3	337	==>	322	296								
					P-Di	15	41								
31-C1	282	41.58	[M-H]-	281	==>	266	261	253	233						Dimethoxyflavone (such as 2',3'-Dimethoxyflavone or 7,8-Dimethoxyflavone)
					P-Di	15	20	28	48						
			MS^3	266	==>	238	237	222	210	196	194	182	166	138	
					P-Di	28	29	44	56	70	72	84	100	128	
32-C1	368	42.72	[M-H]-	367	==>	352	312	309	297						Either Glycycoumarin or Glycyrrh-isoflavanone
					P-Di	15	55	58	70						
			MS^3	352	==>	338	324	309	297	281	271	253	161		
					P-Di	14	28	43	55	71	81	99	191		

Table 5: (cont.)

CMPD	MW	RT	BP-ID	P-	==>	D-BP	Other Daughter Ions		Possible Structure ID(s)
33-C1	368	43.39	[M-H]-	367	==>	352			Either Glycycoumarin or Glycyrrh-isoflavanone
					P-Di	15			
			MS^3	352	==>	309	297		
					P-Di	43	55		
34-C1	352	47.29	[M-H]-	351	==>	336	296		Either 5-O-Methyllupiwighteone, Daphnoretin, Pongagallone A, or Sophora-iso-flavone A
					P-Di	15	55		
			MS^3	336	==>	293	281		
					P-Di	43	55		
35-C1	352	48.12	[M-H]-	351	==>	336	296	281	Either 5-O-Methyllupiwighteone, Daphnoretin, Pongagallone A, or Sophora-iso-flavone A
					P-Di	15	55	70	
			MS^3	336	==>	293	281		
					P-Di	43	55		

Table 6: Detected Compounds in Fraction C using HPLC Method 2. Indicates Compound Number (CMPD #), Molecular Weight (MW) in atomic mass units (amu), Retention Time (RT) in minutes (min), Mass Spec Base Peak Identification (BP-ID) showing negative mode ionization $[M-H]^-$ (indicates the type of ion which forms the Base Peak. Base Peak refers to the most abundant ion in the mass spectrum), Parent ion (P^-) m/z after $[M-H]^-$ ionization (indicates the Base Peak in the normal mass spectra), Base Peak of the daughter ion (D-BP) (i.e., the most abundant ion in the daughter spectrum), MS/MS or MS/MS/MS product ions (MS^3), and the arithmetic difference in m/z between the parent ion and individual daughter ions (P-Di). Bold donates most abundant ion in the given spectra.

CMPD	MW	RT	BP-ID	P-	==>	D-BP	Other Daughter Ions							Possible Structure ID(s)
1-C2	328	21.18	[M-H]-	327	==>	309	283	267	165	161				o-Hydrocoumaric Acid, plus glucose (or galactose) sugar side-group
					P-Di	18	44	60	162	166				
			MS^3	165	==>	141	137	121	69					
					P-Di	24	28	44	96					
2-C2	320	27.34	[M-H]-	319	==>	301	287	275	269	**197**	165	125		Oureatacatechin
					P-Di	18	32	44	50	122	154	194		
			MS^3	197	==>	165								
					P-Di	32								
3-C2	642	29.22	[M-H]-	641	==>	479	477	315						Isorhamnetin (or other flavonoid at 316 amu, such as Nepetin, Tamarixetin, or Rhamnetin), plus an O-rutinoside disaccharide side-group
					P-Di	162	164	326						
			MS^3	479	==>	317	315	300	299	257	256	214		
					P-Di	162	164	179	180	222	223	265		
4-C2	320	30.29	[M-H]-	319	==>	301	287	275	269	**197**	165	125		Oureatacatechin
					P-Di	18	32	44	50	122	154	194		
			MS^3	197	==>	165								
					P-Di	32								
5-C2	612	33.06	[M-H]-	611	==>	551	449	389	227					Either Monotropein, or Resveratrol-disaccharide (two glucose or galactose units)
					P-Di	60	162	222	384					
			MS^3	551	==>	449	389							
					P-Di	102	162							
6-C2	304	33.34	[M-H]-	303	==>	285	259	244	219	217	204			**Identical CMPD also detected at RT 40.54.** Identified as 3'-O-Methylcatechin, and 4'-O-Methylcatechin
					P-Di	18	44	59	84	86	99			
			MS^3	259	==>	246	244	228	217	175				
					P-Di	13	15	31	42	84				
7-C2	288	34.11	[M-H]-	287	==>	259	243	227	205	197	165			Either 2,3-Dihydrofisetin (a.k.a. Fustin), 6-Hydroxyapigenin, or Dihydrokaempferol
					P-Di	28	44	60	82	90	122			
			MS^3	259	==>	227	**215**	203	199	173				
					P-Di	32	44	56	60	86				
8-C2	304	36.16	[M-H]-	303	==>	287	275	266	261					**Similar 304 amu compounds also found at RT's 41.25, 42.86, & 66.73**. Compounds include Taxifolin, Dihydrobinetin, and Meciadanol.
					P-Di									
			MS^3	287	==>	272								
					P-Di									
9-C2	320	37.80	[M-H]-	319	==>	302	289	287	286	**275**	273			3,3',4',5,5',7-Hexahydroxyflavanone (a.k.a. Dihydromyricetin)
					P-Di	17	30	32	33	44	46			
			MS^3	275	==>									
					P-Di									
10-C2	332	39.40	[M-H]-	331	==>	299	271	255	179					**Also at RT's 39.40, 40.17, 40.72, 41.42, 41.99, 42.68, 43.19, 44.02, 44.53, 44.84, 54.32, and 54.91**. Pentahydroxy-Methoxy-flavone & Tri-O-Methylcatechin derivatives
					P-Di	32	60	76	152					
			MS^3	299	==>	271	257							
					P-Di	28	42							
11-C2	938	39.65	[M-H]-	937	==>	775	693	579	547	475	389			Amentoflavone-4',4",7-trimethyl Ether (a.k.a. Sciatopitysin), plus both a glucose (or galactose) sugar and unknown phenolic acid side-groups
					P-Di	162	244	358	390	462	548			
			MS^3	775	==>	727	638	579	389	371	341	327		
					P-Di	48	137	196	386	404	434	448		
12-C2	480	40.97	[M-H]-	479	==>	317	273	255	217					Hexahydroxy-flavone (such as Myricetin, Quercetagetin, or Gossypetin), plus a glucose (or galactose) sugar side-group
					P-Di	162	206	224	262					
			MS^3	317	==>	302	301	287	272	259	169	151		
					P-Di	15	16	30	45	58	148	166		
13-C2	304	42.35	[M-H]-	303	==>	285	271							UNKNOWN BIOFLAVONOID
					P-Di	18	32							
			MS^3	271	==>	243	227	215	199	157				
					P-Di	28	44	56	72	114				
14-C2	904	42.42	[M-H]-	903	==>	741								Rutin (a.k.a. Quercetin-3-O-rutinoside), plus additional sambubiose (or lathyrose) disscaharide side-group
					P-Di	162								
			MS^3	741	==>	609	591	475	301	300	271	255		
					P-Di	132	150	266	440	441	470	486		
15-C2	758	43.77	[M-H]-	757	==>	595								Quercetin, plus trisaccharide side-group [consisting of sambubiose (or lathyrose) disaccharide, plus an added glucose (or galactose) sugar]
					P-Di	162								
			MS^3	595	==>	301	300	271	243	227	203			
					P-Di	294	295	324	352	368	392			
16-C2	776	44.75	[M-H]-	775	==>	727	640	606	579	389	372	341		Amentoflavone-4',4",7-trimethyl Ether (a.k.a. Sciatopitysin), plus an unknown phenolic acid side-group
					P-Di	48	135	169	196	386	403	434		
			MS^3	727	==>	385								
					P-Di	342								

Table 6: (cont.)

CMPD	MW	RT	BP-ID	P-	==>	D-BP	Other Daughter Ions								Possible Structure ID(s)
17-C2	318	45.85	[M-H]-	317	==>	299	289	271	231	193	181				**Compounds also detected at RT's 43.70 & 47.51.** Identified as Myricetin, Gossypetin, and Quercetagetin
					P-Di	18	28	46	86	124	136				
			MS^3	299	==>	284	271	231	215						
					P-Di	15	28	68	84						
18-C2	348	47.34	[M-H]-	347	==>	332	319	316	315	285	271	231	219	193	UNKNOWN flavonoid, possibly a newly discovered tetrahydroxy-dimethoxy-flavonoid
					P-Di	15	28	31	32	62	76	116	128	154	
			MS^3	315	==>	299	285	271	229	165					
					P-Di	16	30	44	86	150					
19-C2	772	47.92	[M-H]-	771	==>	609	463								Quercetin, plus trisaccharide side-group [consisting of a rutinose disaccharide, plus an added glucose (or galactose) sugar]
					P-Di	162	308								
			MS^3	609	==>	301	300	271	213						
					P-Di	308	309	338	396						
20-C2	330	49.77	[M-H]-	329	==>	314	312	301	296	281	257	255	206	**193**	Irisflavone D
					P-Di	15	17	28	33	48	72	74	123	136	
			MS^3	193	==>	178	177	165	164	150					
					P-Di	15	16	28	29	43					
21-C2	344	52.34	[M-H]-	343	==>	329	327	315	313	297	282	271	229	227	Dihydroxy-trimethoxy-flavone (such as Irisflavone B)
					P-Di	14	16	28	30	46	61	72	114	116	
			MS^3	315	==>	297	273	271	247	229	227	206	177	165	
					P-Di	18	42	44	68	86	88	109	138	150	
22-C2	356	54.72	[M-H]-	355	==>	340	339	337	327	323	313	312	298	292	Cudraflavanone B, **or** 2-Carbethoxy-5,7-dihydroxy-4'-methoxyisoflavone, **or** 5-methoxy-4',7-dihydroxy-flavanone-8-(3-methylbutyl), **or** derivative of these.
					P-Di	15	16	18	28	32	42	43	57	63	
			MS^3	219	==>	204	191	190	177	176					
					P-Di	15	28	29	42	43					
23-C2	300	59.12	[M-H]-	299	==>	284									Chrysoeriol, Diosmetin, or other 300 amu MW flavonoid (such as Geraldol, Tectorigenin, Kaempferide, Pratensein, Farresol, etc.)
					P-Di	15									
			MS^3	284	==>	256	228	211	200	193	165	150	137		
					P-Di	28	56	73	84	91	119	134	147		
24-C2	330	62.07	[M-H]-	329	==>	314	299								Trihydroxy-dimethoxy-flavone (such as Isorhamnetin-3-methoxy), or a Hydroxy-trimethoxy-flavone
					P-Di	15	30								
			MS^3	314	==>	300	299	286	285	271	257	243			
					P-Di	14	15	28	29	43	57	71			
25-C2	300	62.67	[M-H]-	299	==>	284									Chrysoeriol, Diosmetin, or other 300 amu MW flavonoid (such as Geraldol, Tectorigenin, Kaempferide, Pratensein, Farresol, etc.)
					P-Di	15									
			MS^3	284	==>	256	228	211	200	193	165	150	137		
					P-Di	28	56	73	84	91	119	134	147		
26-C2	286	64.81	[M-H]-	285	==>	267	257	243	**241**	217	199	175	151	133	3',4',5,7-Tetrahydroxyflavone (a.k.a. Luteolin)
					P-Di	18	28	42	44	68	86	110	134	152	
			MS^3	241	==>										
					P-Di										
27-C2	300	68.47	[M-H]-	299	==>	284									Chrysoeriol, Diosmetin, or other 300 amu MW flavonoid (such as Geraldol, Tectorigenin, Kaempferide, Pratensein, Farresol, etc.)
					P-Di	15									
			MS^3	284	==>	256	228	211	200	193	165	150	137		
					P-Di	28	56	73	84	91	119	134	147		
28-C2	330	69.72	[M-H]-	329	==>	314	299								Trihydroxy-dimethoxy-flavone (such as Isorhamnetin-3-methoxy), or a Hydroxy-trimethoxy-flavone
					P-Di	15	30								
			MS^3	314	==>	300	299	286	285	271	257	243			
					P-Di	14	15	28	29	43	57	71			
29-C2	300	70.39	[M-H]-	299	==>	284									Chrysoeriol, Diosmetin, or other 300 amu MW flavonoid (such as Geraldol, Tectorigenin, Kaempferide, Pratensein, Farresol, etc.)
					P-Di	15									
			MS^3	284	==>	256	228	211	200	193	165	150	137		
					P-Di	28	56	73	84	91	119	134	147		
30-C2	330	71.54	[M-H]-	329	==>	314	299								Trihydroxy-dimethoxy-flavone (such as Isorhamnetin-3-methoxy), or a Hydroxy-trimethoxy-flavone
					P-Di	15	30								
			MS^3	314	==>	300	299	286	285	271	257	243			
					P-Di	14	15	28	29	43	57	71			
31-C2	356	74.49	[M-H]-	355	==>	337	324	310	295	293	251	237	219	193	Cudraflavanone B, **or** 2-Carbethoxy-5,7-dihydroxy-4'-methoxyisoflavone, **or** 5-methoxy-4',7-dihydroxy-flavanone-8-(3-methylbutyl), **or** derivative of these.
					P-Di	18	31	45	60	62	104	118	136	162	
			MS^3	219	==>	175	151	149	133	107					
					P-Di	44	68	70	86	112					
32-C2	888	76.69	[M-H]-	887	==>	490	463	317	285						3',4',5,7-Tetrahydroxyflavone (a.k.a. Luteolin), with rutinose and lathyrose (or sambubiose) side-groups
					P-Di	397	424	570	602						
			MS^3	285	==>	267	257	243	241	217	213	201	164		
					P-Di	18	28	42	44	68	72	84	121		
33-C2	530	78.93	[M-H]-	529	==>	367	352	329	219						Glycycoumarin (or a derivative of)
					P-Di	162	177	200	310						
			MS^3	367	==>	352	336	324	309	297					
					P-Di	15	31	43	58	70					
34-C2	340	79.92	[M-H]-	339	==>	251	245	233	219	175					Glycosidically-bound Dihydroxy-Coumarin, such as 6,7-Dihydroxycoumarin-7-glucoside (or any possible derivative of)
					P-Di	88	94	106	120	164					
			MS^3	219	==>	197	175	151	133						
					P-Di	22	44	68	86						

Table 7: Detected Compounds in Fraction D using HPLC Method 1. Indicates Compound Number (CMPD #), Molecular Weight (MW) in atomic mass units (amu), Retention Time (RT) in minutes (min), Mass Spec Base Peak Identification (BP-ID) showing negative mode ionization $[M-H]^-$ (indicates the type of ion which forms the Base Peak. Base Peak refers to the most abundant ion in the mass spectrum), Parent ion (P^-) m/z after $[M-H]^-$ ionization (indicates the Base Peak in the normal mass spectra), Base Peak of the daughter ion (D-BP) (i.e., the most abundant ion in the daughter spectrum), MS/MS or MS/MS/MS product ions (MS^3), and the arithmetic difference in m/z between the parent ion and individual daughter ions (P-Di). Bold donates most abundant ion in the given spectra.

CMPD	MW	RT	BP-ID	P-	==>	D-BP	Other Daughter Ions								Possible Structure ID(s)
1-D1	327	7.86	[M-H]-	326	==>	266	134								Either a Hydroxy-Methoxy-Flavone, a Methoxy-Flavonol, or a Dimethoxy-Chalcone, with acetate adduct ion.
					P-Di	60	192								
			MS^3	266	==>	**134**	107								
					P-Di	132	159								
2-D1	290	13.14	[M-H]-	289	==>	245	205	179	165	151	137	123	109		Catechin
					P-Di	44	84	110	124	138	152	166	180		
			MS^3	245	==>	227	**203**	187	161	135					
					P-Di	18	42	58	84	110					
3-D1	290	16.44	[M-H]-	289	==>	245	205	179	165	161	151	137	125	109	Epicatechin
					P-Di	44	84	110	124	128	138	152	164	180	
			MS^3	245	==>	227	**203**	187	161	135	123	109			
					P-Di	18	42	58	84	110	122	136			
4-D1	304	19.09	[M-H]-	303	==>	285	177	125							3'-O-Methylcatechin, or 4'-O-Methylcatechin (or their epicatechin derivatives)
					P-Di	18	126	178							
			MS^3	285	==>	257	243	241	217	201	199	177	175	161	
					P-Di	28	42	44	68	84	86	108	110	124	
5-D1	478	20.72	[M-H]-	477	==>	**315**	**314**	**300**	**299**	285	**271**	247	175		Isorhamnetin-glucoside derivative (such as Isorhamnetin-3-glucoside)
					P-Di	162	163	177	178	192	206	230	302		
			MS^3	315	==>	301	300	**299**	285	269	245	227	205		
					P-Di	14	15	16	30	46	70	88	110		
6-D1	364	21.14	[M-H]-	363	==>	345	313	299	281	255	169				A Tetra-O-methylcatechin or Tetra-O-methylepicatechin derivative with additional 18 amu (water)
					P-Di	18	50	64	82	108	194				
			MS^3	345	==>	330	315	314	313	299	286	285	284	271	
					P-Di	15	30	31	32	46	59	60	61	74	
7-D1	318	21.84	[M-H]-	317	==>	299	289	273	271	255	247	245	233	231	Catechin (or Epicatechin) with two added methyl groups (possibly located either on a flavonoid ring, or existing as methoxy groups)
					P-Di	18	28	44	46	62	70	72	84	86	
			MS^3	289	==>	229	227	225	217	205	203	201	189	187	
					P-Di	60	62	64	72	84	86	88	100	102	
8-D1	318	22.41	[M-H]-	317	==>	289	273	231	229	125					Catechin (or Epicatechin) with two added methyl groups (possibly located either on a flavonoid ring, or existing as methoxy groups)
					P-Di	28	44	86	88	192					
			MS^3	289	==>	275	**274**	271	257	245	230	203	185	183	
					P-Di	14	15	18	32	44	59	86	104	106	
9-D1	448	22.84	[M-H]-	447	==>	285									Luteolin-glucoside (such as Luteolin-7-O-glucoside)
					P-Di	162									
			MS^3	285	==>	267	257	243	241	229	223	217	213	201	
					P-Di	18	28	42	44	56	62	68	72	84	
10-D1	520	22.99	[M-H]-	519	==>	461	299								Either 3',5,7-Trihydroxy-4'-methoxy-iso-flavone-3'-O-beta-glucopyranoside, **or** 8-Glycosyl-4',5,7-trihydroxy-3'-methoxy-flavone (Scoparoside), w/ acetate adduct
					P-Di	58	220								
			MS^3	461	==>	299									
					P-Di	162									
11-D1	464	23.73	[M-H]-	463	==>	301	300								Quercetin-based glycoside, such as Isoquercetrin or Hyperoside
					P-Di	162	163								
			MS^3	307	==>	271	257	255	239	229	193	183	**179**	167	
					P-Di	36	50	52	68	78	114	124	128	140	
12-D1	464	24.42	[M-H]-	463	==>	301									Quercetin-glycoside, such as Isoquercitrin, Hyperoside, Gossypitrin, or Spiraeoside
					P-Di	162									
			MS^3	301	==>	287	**286**	**271**	**256**	240	225	203	183	153	
					P-Di	14	15	30	45	61	76	98	118	148	
13-D1	346	25.26	[M-H]-	345	==>	330	328	315	314	**313**	300	299	285	281	Either 3,4',5,7-Tetrahydroxy-3',5'-dimethoxyflavone (a.k.a. Syringetin), or Tetra-O-methylcatechin (or Tetra-O-methylepicatechin)
					P-Di	15	17	30	31	32	45	46	60	64	
			MS^3	313	==>	300	299	286	**285**	282	271	269	253	239	
					P-Di	13	14	27	28	31	42	44	60	74	
14-D1	448	25.56	[M-H]-	447	==>	285									Keampferol-glucoside
					P-Di	162									
			MS^3	285	==>	267	257	243	241	239	229	217	213	211	
					P-Di	18	28	42	44	46	56	68	72	74	
15-D1	478	25.82	[M-H]-	477	==>	**315**	300								Isorhamnetin (or other 316 amu Flavonoid, such as Tamarixetin, Nepetin, or Rhamnetin) with a glucose or galactose side-group
					P-Di	162	177								
			MS^3	315	==>	301	**300**	287	272	271	255	243	215	191	
					P-Di	14	15	28	43	44	60	72	100	124	

Table 7: (cont.)

CMPD	MW	RT	BP-ID	P-	==>	D-BP	Other Daughter Ions								Possible Structure ID(s)
16-D1	316	26.38	[M-H]-	315	==>	301	**300**	299	286	285	272	271	247	243	3-Methylquercetin (a.k.a. Isorhamnetin)
					P-Di	14	15	16	29	30	43	44	68	72	
			MS^3	300	==>	283	282	272	271	256	244	243	**232**	230	
					P-Di	17	18	28	29	44	56	57	68	70	
17-D1	492	26.64	[M-H]-	491	==>	477	**476**	329	314	313	299				Isorhamnetin-3-methoxy-glucoside (or other m/z 329 M-H$^-$ aglycone)
					P-Di	14	15	162	177	178	192				
			MS^3	476	==>	314	**313**	299	298	285	281	270	242	227	
					P-Di	162	163	177	178	191	195	206	234	249	
18-D1	572	26.91	[M-H]-	571	==>	419	285								Biflavone (such as Hegoflavone)
					P-Di	152	286								
			MS^3	419	==>	257									
					P-Di	162									
19-D1	272	27.03	[M-H]-	271	==>	253	227								Resveratrol plus C3H7 or COOH
					P-Di	18	44								
			MS^3	253	==>	185	183	159	157	143					
					P-Di	68	70	94	96	110					
20-D1	462	27.42	[M-H]-	461	==>	301	300	**299**	284						Chrysoeriol-glucoside (or other m/z 299 M-H$^-$ aglycone)
					P-Di	160	161	162	177						
			MS^3	299	==>	285	**284**	179	151						
					P-Di	14	15	120	148						
21-D1	448	27.80	[M-H]-	447	==>	285									Luteolin-glucoside
					P-Di	162									
			MS^3	285	==>	270	267	257	243	241	217	201	199	175	
					P-Di	15	18	28	42	44	68	84	86	110	
22-D1	478	28.39	[M-H]-	477	==>	315									Isorhamnetin (or other 316 amu Flavonoid, such as Tamarixetin, Nepetin, or Rhamnetin) with a glucose or galactose side-group
					P-Di	162									
			MS^3	315	==>	300									
					P-Di	15									
23-D1	302	28.66	[M-H]-	301	==>	287	**286**	271	256	151					Either 3,3',4',5',7-Pentahydroxyflavone (a.k.a. Robinetin), **or** 3',4',5,5',7-Pentahydroxyflavone (a.k.a. Tricetin)
					P-Di	14	15	30	45	150					
			MS^3	286	==>	271	241	183	169	164	151	150	136	107	
					P-Di	15	45	103	117	122	135	136	150	179	
24-D1	580	29.12	[M-H]-	579	==>	339									Amentoflavone-4',4'',7-trimethyl Ether (a.k.a. Sciatopitysin)
					P-Di	240									
			MS^3	339	==>	324	311	297	295						
					P-Di	15	28	42	44						
25-D1	302	29.23	[M-H]-	301	==>	286	258	257	251	242	217	183	177	165	4',5,7-Trihydroxy-3'-methoxyflavanone (a.k.a. Homoeriodictyol)
					P-Di	15	43	44	50	59	84	118	124	136	
			MS^3	286	==>	183	169	135	134	107	83				
					P-Di	103	117	151	152	179	203	286	286	286	
26-D1	330	29.67	[M-H]-	329	==>	314	299								Isorhamnetin-3-methoxy
					P-Di	15	30								
			MS^3	314	==>	300	299	271	255	242	230	227	217	215	
					P-Di	14	15	43	59	72	84	87	97	99	
27-D1	286	30.43	[M-H]-	285	==>	267	257	243	241	239	217	213	201	199	Luteolin (a.k.a. 3',4',5,7-Tetrahydroxyflavone)
					P-Di	18	28	42	44	46	68	72	84	86	
			MS^3	267	==>	213	203	201	199	198	197	185	177	173	
					P-Di	54	64	66	68	69	70	82	90	94	
28-D1	300	30.94	[M-H]-	299	==>	284									300 amu flavonoid, such as Diosmetin, Chrysoeriol, Pratensein, Farresol, Tectorigenin, Geraldol, and Kaempferide
					P-Di	15	299	299	299						
			MS^3	284	==>	267	**256**	**255**	239	227	211	200	199	183	
					P-Di	17	28	29	45	57	73	84	85	101	
29-D1	300	31.75	[M-H]-	299	==>	284									300 amu flavonoid, such as Diosmetin, Chrysoeriol, Pratensein, Farresol, Tectorigenin, Geraldol, and Kaempferide
					P-Di	15									
			MS^3	284	==>	267	**256**	**255**	239	227	211	200	195	188	
					P-Di	17	28	29	45	57	73	84	89	96	
30-D1	316	33.30	[M-H]-	315	==>	300									316 amu flavonoid, such as Nepetin, Tamarixetin, and Rhamnetin
					P-Di	15									
			MS^3	300	==>	283	271	255	243	227	216	211	199	183	
					P-Di	17	29	45	57	73	84	89	101	117	
31-D1	300	33.54	[M-H]-	299	==>	284									300 amu flavonoid, such as Diosmetin, Chrysoeriol, Pratensein, Farresol, Tectorigenin, Geraldol, and Kaempferide
					P-Di	15									
			MS^3	284	==>	256									
					P-Di	28									
32-D1	312	34.01	[M-H]-	311	==>	293	267	255	241	201					Maxima-IsoFlavone-E
					P-Di	18	44	56	70	110					
			MS^3	241	==>	223	213	199	173	155	145				
					P-Di	18	28	42	68	86	96				

Table 7: (cont.)

CMPD	MW	RT	BP-ID	P-	==>	D-BP	Other Daughter Ions								Possible Structure ID(s)
33-D1	286	34.57	[M-H]-	285	==>	270									286 amu flavonoid: either Isosakuranetin, Licochalcone B, Homobutein, Sakuranetin, or Sappanchalcone
					P-Di	15									
			MS^3	270	==>	255	183	169	151						
					P-Di	15	87	101	119						
34-D1	314	34.71	[M-H]-	313	==>	298	283								Either Kaempferol-3,7-dimethoxy, **or** 5,7-dihydroxy-4',6-dimethoxyflavone (a.k.a. Pectolinarigenin)
					P-Di	15	30								
			MS^3	298	==>	283	269	267							
					P-Di	15	29	31							
35-D1	448	36.78	[M-H]-	447	==>	267									Hydroxy-methoxyflavone, plus glucose (or galactose)
					P-Di	180									
			MS^3	267	==>	239	227	225							
					P-Di	28	40	42							
36-D1	314	36.93	[M-H]-	313	==>	298									Either Kaempferol-3,7-dimethoxy, **or** 5,7-dihydroxy-4',6-dimethoxyflavone (a.k.a. Pectolinarigenin)
					P-Di	15									
			MS^3	298	==>	283	255								
					P-Di	15	43								
37-D1	314	37.81	[M-H]-	313	==>	298									Either Kaempferol-3,7-dimethoxy, **or** Kaempferol-3,7-dimethoxy
					P-Di	15									
			MS^3	298	==>	281	270	269	243	242	226	198			
					P-Di	17	28	29	55	56	72	100			
38-D1	284	38.07	[M-H]-	283	==>	268									Biochanin A, Prunetin, Acacetin, or other 284 amu flavonoid (such as Glycitein, Negletein, Oroxylin, Vogonin, or Genkwanin)
					P-Di	15									
			MS^3	268	==>	267	240	239	226	224	223	212	211	195	
					P-Di	1	28	29	42	44	45	56	57	73	

Table 8: Detected Compounds in Fraction D using HPLC Method 2. Indicates Compound Number (CMPD #), Molecular Weight (MW) in atomic mass units (amu), Retention Time (RT) in minutes (min), Mass Spec Base Peak Identification (BP-ID) showing negative mode ionization $[M-H]^-$ (indicates the type of ion which forms the Base Peak. Base Peak refers to the most abundant ion in the mass spectrum), Parent ion (P^-) m/z after $[M-H]^-$ ionization (indicates the Base Peak in the normal mass spectra), Base Peak of the daughter ion (D-BP) (i.e., the most abundant ion in the daughter spectrum), MS/MS or MS/MS/MS product ions (MS^3), and the arithmetic difference in m/z between the parent ion and individual daughter ions (P-Di). Bold donates most abundant ion in the given spectra.

CMPD	MW	RT	BP-ID	P-	==>	D-BP	Other Daughter Ions							Possible Structure ID(s)
1-D2	390	43.10	[M-H]-	389	==>	227								Resveratrol, plus a glucose (or galactose) side-group
					P-Di	162								
			MS^3	227	==>	185	159	157	143					
					P-Di	42	68	70	84					
2-D2	302	57.43	[M-H]-	301	==>	284	283	257	165					2',3,4',5,7-Pentahydroxyflavone (a.k.a. Morin)
					P-Di	17	18	44	136					
			MS^3	283	==>	268	255	252	240					
					P-Di	15	28	31	43					
3-D2	302	60.03	[M-H]-	301	==>	286	271	257	241	164	151			Either 3,3',4',5',7-Pentahydroxyflavone (a.k.a. Robinetin), **or** 3',4',5,5',7-Pentahydroxyflavone (a.k.a. Tricetin)
					P-Di	15	30	44	60	137	150			
			MS^3	283	==>	269	228	180	164	151				
					P-Di	14	55	103	119	132				
4-D2	302	60.69	[M-H]-	301	==>	286	257	242	217	177	165	151		Either 3,3',4',5',7-Pentahydroxyflavone (a.k.a. Robinetin), **or** 3',4',5,5',7-Pentahydroxyflavone (a.k.a. Tricetin)
					P-Di	15	44	59	84	124	136	150		
			MS^3	283	==>	267	259	242	212	176	151			
					P-Di	16	24	41	71	107	132			
5-D2	302	61.55	[M-H]-	301	==>	286	284	257	241	217	177	165	151	3',5,7-Trihydroxy-4'-methoxyflavanone (a.k.a. Hesperitin)
					P-Di	15	17	44	60	84	124	136	150	
			MS^3	283	==>	267	257	256	240	215	201	183	164	150
					P-Di	16	26	27	43	68	82	100	119	133
6-D2	492	72.98	[M-H]-	491	==>	287								Either 2,3-Dihydrofisetin (a.k.a. Fustin), **or** 3,3',4',7-tetrahydroxyflavone (a.k.a. Fisetin), with a sinapoyl acyl side-group.
					P-Di	204								
			MS^3	287	==>	269	245	243	219	165	161	125		
					P-Di	18	42	44	68	122	126	162		
7-D2	492	77.72	[M-H]-	491	==>	287								Either 2,3-Dihydrofisetin (a.k.a. Fustin), **or** 3,3',4',7-tetrahydroxyflavone (a.k.a. Fisetin), with a sinapoyl acyl side-group.
					P-Di	204								
			MS^3	287	==>	269	259	245	186	165	161	125		
					P-Di	18	28	42	101	122	126	162		

Table 9: Detected Compounds in Fraction E using HPLC Method 1. Indicates Compound Number (CMPD #), Molecular Weight (MW) in atomic mass units (amu), Retention Time (RT) in minutes (min), Mass Spec Base Peak Identification (BP-ID) showing negative mode ionization $[M-H]^-$ (indicates the type of ion which forms the Base Peak. Base Peak refers to the most abundant ion in the mass spectrum), Parent ion (P^-) m/z after $[M-H]^-$ ionization (indicates the Base Peak in the normal mass spectra), Base Peak of the daughter ion (D-BP) (i.e., the most abundant ion in the daughter spectrum), MS/MS or MS/MS/MS product ions (MS^3), and the arithmetic difference in m/z between the parent ion and individual daughter ions (P-Di). Bold donates most abundant ion in the given spectra.

CMPD	MW	RT	BP-ID	P-	==>	D-BP	Other Daughter Ions							Possible Structure ID(s)
1-E1	350	18.72	[M-H]-	349	==>	331	299							Newly discovered chromanediol: 2-(3,4-dimethoxyphenyl)-3,4-dihydro-2*H*-chromene-3,4,5,6,7-pentol
					P-Di	18	50							
			MS^3	331	==>	300	299	287	271	179	151			
					P-Di	31	32	44	60	152	180			
2-E1	576	20.80	[M-H]-	575	==>	557	449	437	408	394	287			A-type Proanthocyanidin dimer
					P-Di	18	126	138	167	181	288			
			MS^3	557	==>	431	287	243						
					P-Di	126	270	314						
3-E1	464	21.53	[M-H]-	463	==>	301								Either Isoquercitrin, Hyperoside, Gossypitrin, or Spiraeoside
					P-Di	162								
			MS^3	301	==>	183	179	169	151					
					P-Di	118	122	132	150					
4-E1	364	21.83	[M-H]-	363	==>	331								Newly discovered chromanediol: 2-(3,4-dimethoxyphenyl)-7-methoxy-3,4-dihydro-2*H*-chromene-3,4,5,6-tetrol
					P-Di	32								
			MS^3	331	==>	300	299	287	271	179	151			
					P-Di	31	32	44	60	152	180			
5-E1	464	25.31	[M-H]-	463	==>	301								Either Isoquercitrin, Hyperoside, Gossypitrin, or Spiraeoside
					P-Di	162								
			MS^3	301	==>	179	151							
					P-Di	122	150							
6-E1	348	25.90	[M-H]-	347	==>	287								Either Dihydrokeampferol, **or** 3,3',4',7-tetrahydroxy-flavanone (a.k.a. 2,3-Dihydrofisetin, or Fustin)
					P-Di	60								
			MS^3	287	==>	269	243	225	183	169	**151**	135	125	
					P-Di	18	44	62	104	118	136	152	162	
7-E1	286	27.10	[M-H]-	285	==>	257	229	213	177					Either Fisetin, Datiscetin, Scutellarin, Baptigenin, Sakuranetin, or a Tetrahydroxy-isoflavone
					P-Di	28	56	72	108					
			MS^3	257	==>	229	213	187	172	151				
					P-Di	28	44	70	85	106				
8-E1	302	29.32	[M-H]-	301	==>	179	151							3,3',4',5,7-Pentahydroxyflavone (a.k.a. Quercetin)
					P-Di	122	150							
			MS^3	179	==>	183	169	151						
					P-Di	-4	10	28						
9-E1	464	39.31	[M-H]-	463	==>	283								Either a Dihydroxy-methoxy-flavone, a Dihydroxy-methoxy-isoflavone, or a Dimethoxy-flavanone, with a glucose (or galactose) side-group
					P-Di	180								
			MS^3	283	==>	255	243	217						
					P-Di	28	40	66						

Table 10: Detected Compounds in Fraction E using HPLC Method 2. Indicates Compound Number (CMPD #), Molecular Weight (MW) in atomic mass units (amu), Retention Time (RT) in minutes (min), Mass Spec Base Peak Identification (BP-ID) showing negative mode ionization $[M-H]^-$ (indicates the type of ion which forms the Base Peak. Base Peak refers to the most abundant ion in the mass spectrum), Parent ion (P^-) m/z after $[M-H]^-$ ionization (indicates the Base Peak in the normal mass spectra), Base Peak of the daughter ion (D-BP) (i.e., the most abundant ion in the daughter spectrum), MS/MS or MS/MS/MS product ions (MS^3), and the arithmetic difference in m/z between the parent ion and individual daughter ions (P-Di). Bold donates most abundant ion in the given spectra.

CMPD	MW	RT	BP-ID	P-	==>	D-BP	Other Daughter Ions							Possible Structure ID(s)
1-E2	332	39.95	[M-H]-	331	==>	301	300	299	287	271	255	179	151	Possible new Dihydoxy-dimethoxy--flavanone: 3,5-dihydroxy-2-(4-hydroxy-3- methoxyphenyl)-7-methoxy -2,3-dihydro-4*H*-chromen-4-one
					P-Di	30	31	32	44	60	76	152	180	
			MS^3	299	==>	272	271	256	255	227	179	155		
					P-Di	27	28	43	44	72	120	144		
2-E2	288	54.00	[M-H]-	287	==>	269	199	183	161	151	135	107		3',4',5,7-Tetrahydroxyflavanone (a.k.a. Eriodictyol)
					P-Di	18	88	104	126	136	152	180		
			MS^3	151	==>	108	107	65						
					P-Di	43	44	86						
3-E2	286	61.28	[M-H]-	285	==>	257	229	213	163					Either Fisetin, Datiscetin, Scutellarin, Baptigenin, Sakuranetin, or a Tetrahydroxy-isoflavone
					P-Di	28	56	72	122					
			MS^3	257	==>	239	229	227	171	157				
					P-Di	18	28	30	86	100				

Table 11: Detected Compounds in Fraction F using HPLC Method 1. Indicates Compound Number (CMPD #), Molecular Weight (MW) in atomic mass units (amu), Retention Time (RT) in minutes (min), Mass Spec Base Peak Identification (BP-ID) showing negative mode ionization $[M-H]^-$ (indicates the type of ion which forms the Base Peak. Base Peak refers to the most abundant ion in the mass spectrum), Parent ion (P^-) m/z after $[M-H]^-$ ionization (indicates the Base Peak in the normal mass spectra), Base Peak of the daughter ion (D-BP) (i.e., the most abundant ion in the daughter spectrum), MS/MS or MS/MS/MS product ions (MS^3), and the arithmetic difference in m/z between the parent ion and individual daughter ions (P-Di). Bold donates most abundant ion in the given spectra.

CMPD	MW	RT	BP-ID	P-	==>	D-BP	Other Daughter Ions									Possible Structure ID(s)
1-F1	576	6.92	[M-H]-	575	==>	557	531	513	487	449	**423**	407	325			A-type Proanthocyanidin dimer
					P-Di	18	44	62	88	126	152	168	250			
			MS^3	423	==>	405	387	379	361	355	338	309	298	285		
					P-Di	18	36	44	62	68	85	114	125	138		
2-F1	578	10.11	[M-H]-	577	==>	451	425	407	289							B-type Procyanidin dimer
					P-Di	126	152	170	288							
			MS^3	425	==>	407	381	273								
					P-Di	18	44	152								
3-F1	578	10.84	[M-H]-	577	==>	451	425	407	289							B-type Procyanidin dimer
					P-Di	126	152	170	288							
			MS^3	425	==>	407	381	273								
					P-Di	18	44	152								
4-F1	578	11.43	[M-H]-	577	==>	559	451	**425**	407	299	289	246	217			Procyanidin B3 Dimer
					P-Di	18	126	152	170	278	288	331	360			
			MS^3	425	==>	407	381	357	339	297	273	162				
					P-Di	18	44	68	86	128	152	263				
5-F1	578	11.97	[M-H]-	577	==>	559	451	425	423	407	379	289				B-type Procyanidin dimer
					P-Di	18	126	152	154	170	198	288				
			MS^3	425	==>	407	381	361	297	273						
					P-Di	18	44	64	128	152						
6-F1	592	13.90	[M-H]-	591	==>	465	**439**	421	303							Flavonoid dimer consisting of a catechin (or epicatechin) monomer, bound to an O-methylated catechin (or epicatechin) monomer
					P-Di	126	152	170	288							
			MS^3	439	==>	421	395	287	271	259	243					
					P-Di	18	44	152	168	180	196					
7-F1	574	14.73	[M-H]-	573	==>	555	529	**447**	421	323	285	283				Procyanidin dimer
					P-Di	18	44	126	152	250	288	290				
			MS^3	447	==>	429	403	337	325	**285**	281	271	246	217		
					P-Di	18	44	110	122	162	166	176	201	230		
8-F1	592	15.73	[M-H]-	591	==>	465	455	**439**	421	303						Flavonoid dimer consisting of a catechin (or epicatechin) monomer, bound to an O-methylated catechin (or epicatechin) monomer
					P-Di	126	136	152	170	288						
			MS^3	439	==>	421	411	287	271	243						
					P-Di	18	28	152	168	196						
9-F1	574	15.87	[M-H]-	573	==>	555	529	511	**447**	421	285	283				Procyanidin dimer
					P-Di	18	44	62	126	152	288	290				
			MS^3	447	==>	429	403	337	325	**285**	281	243				
					P-Di	18	44	110	122	162	166	204				
10-F1	592	16.14	[M-H]-	591	==>	571	465	**439**	419	339	325	303	**285**			Flavonoid dimer consisting of a catechin (or epicatechin) monomer, bound to an O-methylated catechin (or epicatechin) monomer
					P-Di	20	126	152	172	252	266	288	306			
			MS^3	439	==>	421	419	301	287	285	283	271	243			
					P-Di	18	20	138	152	154	156	168	196			
11-F1	574	16.80	[M-H]-	573	==>	555	529	511	**447**	421	283					Procyanidin dimer
					P-Di	18	44	62	126	152	290					
			MS^3	447	==>	429	403	337	325	**285**	281	243	217			
					P-Di	18	44	110	122	162	166	204	230			
12-F1	578	19.45	[M-H]-	577	==>	451	425	407	289							B-type Procyanidin dimer
					P-Di	126	152	170	288							
			MS^3	425	==>	407	273									
					P-Di	18	152									
13-F1	578	20.06	[M-H]-	577	==>	451	425	407	289							B-type Procyanidin dimer
					P-Di	126	152	170	288							
			MS^3	425	==>	407	273									
					P-Di	18	152									
14-F1	574	20.21	[M-H]-	573	==>	555	529	511	487	471	447	421	283			Procyanidin dimer
					P-Di	18	44	62	86	102	126	152	290			
			MS^3	447	==>	429	403	385	361	343	337	325	285	279		
					P-Di	18	44	62	86	104	110	122	162	168		
15-F1	576	23.03	[M-H]-	575	==>	449	394	287	243							A-type Proanthocyanidin dimer
					P-Di	126	181	288	332							
			MS^3	394	==>	271	229									
					P-Di	123	165									

Table 11: (cont.)

CMPD	MW	RT	BP-ID	P-	==>	D-BP	Other Daughter Ions								Possible Structure ID(s)
16-F1	576	23.60	[M-H]-	575	==>	557	449	437	431	407	394	351	309	287	A-type Proanthocyanidin dimer
					P-Di	18	126	138	144	168	181	224	266	288	
			MS^3	449	==>	431	325	287	283						
					P-Di	18	124	162	166						
17-F1	424	25.82	[M-H]-	423	==>	405	355	341	313	301	**299**	285	271	259	Either Remangiflavanone B, Euchrestaflavanone B, or Sophoraflavanone G
					P-Di	18	68	82	110	122	124	138	152	164	
			MS^3	299	==>	283	271	243							
					P-Di	16	28	56							
18-F1	588	27.32	[M-H]-	587	==>	451	435	421	391	377	301	299	270		Kolaflavanone
					P-Di	136	152	166	196	210	286	288	317		
			MS^3	451	==>	423	407	405	383	341	325	299	287	257	
					P-Di	28	44	46	68	110	126	152	164	194	
19-F1	448	31.86	[M-H]-	447	==>	429	403	337	325	323	296	295	283	268	Flavonoid-glycoside: Possible aglycones include Astragalin, Orientin, Sakuranin, Kaempferol, and Luteolin
					P-Di	18	44	110	122	124	151	152	164	179	
			MS^3	323	==>	323	307	297	295	281	266	251			
					P-Di	0	16	26	28	42	57	72			
20-F1	424	38.09	[M-H]-	423	==>	405	379	355	313	299	285	271	259	217	Either Remangiflavanone B, Euchrestaflavanone B, or Sophoraflavanone G
					P-Di	18	44	68	110	124	138	152	164	206	
			MS^3	299	==>	271	255	242	227						
					P-Di	28	44	57	72						

Table 12: Detected Compounds in Fraction F using HPLC Method 2. Indicates Compound Number (CMPD #), Molecular Weight (MW) in atomic mass units (amu), Retention Time (RT) in minutes (min), Mass Spec Base Peak Identification (BP-ID) showing negative mode ionization $[M-H]^-$ (indicates the type of ion which forms the Base Peak. Base Peak refers to the most abundant ion in the mass spectrum), Parent ion (P^-) m/z after $[M-H]^-$ ionization (indicates the Base Peak in the normal mass spectra), Base Peak of the daughter ion (D-BP) (i.e., the most abundant ion in the daughter spectrum), MS/MS or MS/MS/MS product ions (MS^3), and the arithmetic difference in m/z between the parent ion and individual daughter ions (P-Di). Bold donates most abundant ion in the given spectra.

CMPD	MW	RT	BP-ID	P-	==>	D-BP	Other Daughter Ions				Possible Structure ID(s)
1-F2	316	19.48	[M-H]-	315	==>	297	271	231			Either 6-methoxyluteolin (aka Nepetin), or a methoxyquercetin (i.e. Rhamnetin or Tamarixetin), or a Tetrahydroxy--methoxyflavone (such as Pedalitin)
					P-Di	18	44	84			
			MS^3	297	==>	269	253	227			
					P-Di	28	44	70			
2-F2	320	27.49	[M-H]-	319	==>	287	197	161	125		Oureatacatechin (or a derivative of)
					P-Di	32	122	158	194		
			MS^3	197	==>	165					
					P-Di	32					
3-F2	320	30.59	[M-H]-	319	==>	287	197	165	153	125	Oureatacatechin (or a derivative of)
					P-Di	32	122	154	166	194	
			MS^3	197	==>	165					
					P-Di	32					

Table 13: Detected Compounds in Fraction G-Red using HPLC Method 1. Indicates Compound Number (CMPD #), Molecular Weight (MW) in atomic mass units (amu), Retention Time (RT) in minutes (min), Mass Spec Base Peak Identification (BP-ID) showing negative mode ionization $[M-H]^-$ (indicates the type of ion which forms the Base Peak. Base Peak refers to the most abundant ion in the mass spectrum), Parent ion (P^-) m/z after $[M-H]^-$ ionization (indicates the Base Peak in the normal mass spectra), Base Peak of the daughter ion (D-BP) (i.e., the most abundant ion in the daughter spectrum), MS/MS or MS/MS/MS product ions (MS^3), and the arithmetic difference in m/z between the parent ion and individual daughter ions (P-Di). Bold donates most abundant ion in each spectra.

CMPD	MW	RT	BP-ID	P-	==>	D-BP	Other Daughter Ions								Possible Structure ID(s)
1-Gr1	578	10.89	[M-H]-	577	==>	451	425	407	289						B-type Procyanidin dimer
					P-Di	126	152	170	288						
			MS^3	425	==>	407	297	273							
					P-Di	18	128	152							
2-Gr1	578	11.27	[M-H]-	577	==>	451	425	407	289						B-type Procyanidin dimer
					P-Di	126	152	170	288						
			MS^3	425	==>	407	297	273							
					P-Di	18	128	152							
3-Gr1	578	12.90	[M-H]-	577	==>	559	451	425	407	289					B-type Procyanidin dimer
					P-Di	18	126	152	170	288					
			MS^3	425	==>	407	381	339	299	273	211	187			
					P-Di	18	44	86	126	152	214	238			
4-Gr1	578	13.84	[M-H]-	577	==>	559	451	425	407	289					B-type Procyanidin dimer
					P-Di	18	126	152	170	288					
			MS^3	425	==>	407	381	339	299	273	211	187			
					P-Di	18	44	86	126	152	214	238			
5-Gr1	578	16.00	[M-H]-	577	==>	559	451	425	407	289	287				B-type Procyanidin dimer
					P-Di	18	126	152	170	288	290				
			MS^3	425	==>	407	381	341	273						
					P-Di	18	44	84	152						
6-Gr1	576	16.51	[M-H]-	575	==>	539	**449**	423	407	289	285				A-type Proanthocyanidin dimer
					P-Di	36	126	152	168	286	290				
			MS^3	449	==>	405	325	287	285	243					
					P-Di	44	124	162	164	206					
7-Gr1	574	18.01	[M-H]-	573	==>	529	511	**447**	421	283					Procyanidin dimer
					P-Di	44	62	126	152	290					
			MS^3	447	==>	429	403	325	**285**	242	201				
					P-Di	18	44	122	162	205	246				
8-Gr1	576	18.32	[M-H]-	575	==>	539	449	423	289	285					A-type Proanthocyanidin dimer
					P-Di	36	126	152	286	290					
			MS^3	447	==>	325	287	285							
					P-Di	122	160	162							
9-Gr1	574	19.17	[M-H]-	573	==>	555	529	511	447	421	323	283			Procyanidin dimer
					P-Di	18	44	62	126	152	250	290			
			MS^3	447	==>	429	385	361	337	325	285	271	243	227	
					P-Di	18	62	86	110	122	162	176	204	220	
10-Gr1	574	21.12	[M-H]-	573	==>	529	447	283							Procyanidin dimer
					P-Di	44	126	290							
			MS^3	447	==>	429	403	337	285						
					P-Di	18	44	110	162						
11-Gr1	556	38.21	[M-H]-	555	==>	445	433	403	390	323	283				Either Hegoflavone A, or Morelloflavone
					P-Di	110	122	152	165	232	272				
			MS^3	433	==>	404	389	361	283	269	255	243			
					P-Di	29	44	72	150	164	178	190			
12-Gr1	556	39.79	[M-H]-	555	==>	445	433	403	390	323	283				Either Hegoflavone A, or Morelloflavone
					P-Di	110	122	152	165	232	272				
			MS^3	433	==>	404	389	361	283	269	255	243			
					P-Di	29	44	72	150	164	178	190			

Table 14: Detected Compounds in Fraction G-Red using HPLC Method 2. Indicates Compound Number (CMPD #), Molecular Weight (MW) in atomic mass units (amu), Retention Time (RT) in minutes (min), Mass Spec Base Peak Identification (BP-ID) showing negative mode ionization $[M-H]^-$ (indicates the type of ion which forms the Base Peak. Base Peak refers to the most abundant ion in the mass spectrum), Parent ion (P^-) m/z after $[M-H]^-$ ionization (indicates the Base Peak in the normal mass spectra), Base Peak of the daughter ion (D-BP) (i.e., the most abundant ion in the daughter spectrum), MS/MS or MS/MS/MS product ions (MS^3), and the arithmetic difference in m/z between the parent ion and individual daughter ions (P-Di). Bold donates most abundant ion in each spectra.

CMPD	MW	RT	BP-ID	P-	==>	D-BP	Other Daughter Ions								Possible Structure ID(s)
1-Gr2	302	62.40	[M-H]-	301	==>	286	283	258	257	242	217	199	179		3',5,7-Trihydroxy-4'-methoxyflavanone (a.k.a. Hesperitin)
					P-Di	15	18	43	44	59	84	102	122		
			MS^3	286	==>	242	215	201	199						
					P-Di	44	71	85	87						
2-Gr2	316	63.10	[M-H]-	315	==>	283									Either 6-methoxyluteolin (aka Nepetin), 4'-methoxyquercetin (aka Tamarixetin), or 7-methylquercetin (aka Rhamnetin)
					P-Di	32									
			MS^3	283	==>	255	239	227	215	211					
					P-Di	28	44	56	68	72					
3-Gr2	286	64.81	[M-H]-	285	==>	267	257	243	**241**	217	213	199	175	151	3',4',5,7-Tetrahydroxyflavone (a.k.a. Luteolin)
					P-Di	18	28	42	44	68	72	86	110	134	
			MS^3	241	==>	224	213	199							
					P-Di	17	28	42							
4-Gr2	300	70.41	[M-H]-	299	==>	**284**	217								Chrysoeriol, Diosmetin, or other 300 amu MW flavonoid (such as Geraldol, Tectorigenin, Kaempferide, Pratensein, Farresol, etc.)
					P-Di	15	82								
			MS^3	284	==>	**256**	227	217	212	163	151				
					P-Di	28	57	67	72	121	133				

Table 15: Detected Compounds in Fraction G using HPLC Method 1. Indicates Compound Number (CMPD #), Molecular Weight (MW) in atomic mass units (amu), Retention Time (RT) in minutes (min), Mass Spec Base Peak Identification (BP-ID) showing negative mode ionization $[M-H]^-$ (indicates the type of ion which forms the Base Peak. Base Peak refers to the most abundant ion in the mass spectrum), Parent ion (P^-) m/z after $[M-H]^-$ ionization (indicates the Base Peak in the normal mass spectra), Base Peak of the daughter ion (D-BP) (i.e., the most abundant ion in the daughter spectrum), MS/MS or MS/MS/MS product ions (MS^3), and the arithmetic difference in m/z between the parent ion and individual daughter ions (P-Di). Bold donates most abundant ion in the given spectra.

CMPD	MW	RT	BP-ID	P-	==>	D-BP	Other Daughter Ions									Possible Structure ID(s)
1-G1	864	10.00	[M-H]-	863	==>	**711**	693	575	559	449						Catechin/Epicatech trimer with single A-type Inter-Flavanic Linkage (IFL)
					P-Di	152	170	288	304	414						
			MS^3	711	==>	693	559									
					P-Di	18	152									
2-G1	864	10.83	[M-H]-	863	==>	**711**	693	575	559	449						Catechin/Epicatech trimer with single A-type Inter-Flavanic Linkage (IFL)
					P-Di	152	170	288	304	414						
			MS^3	711	==>	693	559	403								
					P-Di	18	152	308								
3-G1	864	11.41	[M-H]-	863	==>	**711**	693	575	559	449						Catechin/Epicatech trimer with single A-type Inter-Flavanic Linkage (IFL)
					P-Di	152	170	288	304	414						
			MS^3	711	==>	693	559	541								
					P-Di	18	152	170								
4-G1	864	11.80	[M-H]-	863	==>	711	693	**575**	559	449						Catechin/Epicatech trimer with single A-type Inter-Flavanic Linkage (IFL)
					P-Di	152	170	288	304	414						
			MS^3	575	==>	557	539	449	423	407	325	289	285	541		
					P-Di	18	36	126	152	168	250	286	290	34		
5-G1	864	12.72	[M-H]-	863	==>	711	693	**575**	559	449						Catechin/Epicatech trimer with single A-type Inter-Flavanic Linkage (IFL)
					P-Di	152	170	288	304	414						
			MS^3	575	==>	557	539	449	423	407	327	289	285			
					P-Di	18	36	126	152	168	248	286	290			
6-G1	864	14.31	[M-H]-	863	==>	**711**	693	575	573	559	451	411				Catechin/Epicatech trimer with single A-type Inter-Flavanic Linkage (IFL)
					P-Di	152	170	288	290	304	412	452				
			MS^3	711	==>	693	567	559	541	525	407					
					P-Di	18	144	152	170	186	304					
7-G1	864	15.33	[M-H]-	863	==>	711	**693**	575	559	449						Catechin/Epicatech trimer with single A-type Inter-Flavanic Linkage (IFL)
					P-Di	152	170	288	304	414						
			MS^3	693	==>	657	525	449	403							
					P-Di	36	168	244	290							
8-G1	864	15.42	[M-H]-	863	==>	**711**	693	575	559	449						Catechin/Epicatech trimer with single A-type Inter-Flavanic Linkage (IFL)
					P-Di	152	170	288	304	414						
			MS^3	711	==>	693	559	541	403							
					P-Di	18	152	170	308							
9-G1	864	15.86	[M-H]-	863	==>	711	**693**	575								Catechin/Epicatech trimer with single A-type Inter-Flavanic Linkage (IFL)
					P-Di	152	170	288								
			MS^3	693	==>	657	525	449	403							
					P-Di	36	168	244	290							
10-G1	1152	16.39	[M-H]-	1151	==>	863	**575**	539	449	423	407					Catechin/Epicatech tetramer with one A-type Inter-Flavanic Linkage (IFL): (Cat)Epi--(Cat)Epi--(Cat)Epi--A(IFL)--(Cat)Epi
					P-Di	288	576	612	702	728	744					
			MS^3	575	==>	557	539	449	423	407	289	285				
					P-Di	18	36	126	152	168	286	290				
11-G1	864	16.86	[M-H]-	863	==>	711	693	**575**	559	539						Catechin/Epicatech trimer with single A-type Inter-Flavanic Linkage (IFL)
					P-Di	152	170	288	304	324						
			MS^3	575	==>	557	539	449	423	407	391	289	285	245		
					P-Di	18	36	126	152	168	184	286	290	330		
12-G1	1152	19.17	[M-H]-	1151	==>	863	**575**	539	449	423	407					Catechin/Epicatech tetramer with one A-type Inter-Flavanic Linkage (IFL): (Cat)Epi--(Cat)Epi--(Cat)Epi--A(IFL)--(Cat)Epi
					P-Di	288	576	612	702	728	744					
			MS^3	575	==>	557	539	449	423	407	289	285				
					P-Di	18	36	126	152	168	286	290				
13-G1	1152	19.95	[M-H]-	1151	==>	861	**575**	539	423							Catechin/Epicatech tetramer with one A-type Inter-Flavanic Linkage (IFL): (Cat)Epi--A(IFL)--(Cat)Epi--(Cat)Epi--(Cat)Epi
					P-Di	290	576	612	728							
			MS^3	575	==>	557	539	449	423	289	285					
					P-Di	18	36	126	152	286	290					
14-G1	576	21.64	[M-H]-	575	==>	557	539	465	**449**	423	407	369	327	297		A-type Proanthocyanidin dimer
					P-Di	18	36	110	126	152	168	206	248	278		
			MS^3	449	==>	405	387	325	297	**287**	285	269	267	243		
					P-Di	44	62	124	152	162	164	180	182	206		
15-G1	590	23.51	[M-H]-	589	==>	571	560	466	463	421	404	343	303	285		Manniflavanone (a biflavanone)
					P-Di	18	29	123	126	168	185	246	286	304		
			MS^3	463	==>	435	353	341	312	302	285	269	259	229		
					P-Di	28	110	122	151	161	178	194	204	234		

Table 15: (cont.)

CMPD	MW	RT	BP-ID	P-	==>	D-BP	Other Daughter Ions								Possible Structure ID(s)
16-G1	560	24.74	[M-H]-	559	==>	433	423	407	289	269					UNKNOWN Biflavanoid. Exhibits one catechin (or epicatechin) monomer, attached to a second unknown 270 amu monomer
					P-Di	126	136	152	270	290					
			MS^3	433	==>	323	311	309	297	281	271	269			
					P-Di	110	122	124	136	152	162	164			
17-G1	560	27.71	[M-H]-	559	==>	433	407	289	269						UNKNOWN Biflavanoid. Exhibits one catechin (or epicatechin) monomer, attached to a second unknown 270 amu monomer
					P-Di	126	152	270	290						
			MS^3	433	==>	323	311	309	297	281	271	269			
					P-Di	110	122	124	136	152	162	164			
18-G1	588	30.21	[M-H]-	587	==>	569	477	**464**	451	407	375	313	300	271	Kolaflavanone (a biflavanone)
					P-Di	18	110	123	136	180	212	274	287	316	
			MS^3	464	==>	437	392	313	311	300	299	287	269	254	
					P-Di	27	72	151	153	164	165	177	195	210	
19-G1	424	39.35	[M-H]-	423	==>	405	379	341	313	299	271	259			Either Remangiflavanone B, Euchrestaflavanone B, or Sophoraflavanone G
					P-Di	18	44	82	110	124	152	164			
			MS^3	299	==>	271	255	242	225	214					
					P-Di	28	44	57	74	85					

Table 16: Detected Compounds in Fraction G using HPLC Method 2. Indicates Compound Number (CMPD #), Molecular Weight (MW) in atomic mass units (amu), Retention Time (RT) in minutes (min), Mass Spec Base Peak Identification (BP-ID) showing negative mode ionization $[M-H]^-$ (indicates the type of ion which forms the Base Peak. Base Peak refers to the most abundant ion in the mass spectrum), Parent ion (P^-) m/z after $[M-H]^-$ ionization (indicates the Base Peak in the normal mass spectra), Base Peak of the daughter ion (D-BP) (i.e., the most abundant ion in the daughter spectrum), MS/MS or MS/MS/MS product ions (MS^3), and the arithmetic difference in m/z between the parent ion and individual daughter ions (P-Di). Bold donates most abundant ion in each spectra.

CMPD	MW	RT	BP-ID	P-	==>	D-BP	Other Daughter Ions								Possible Structure ID(s)
1-G2	862	37.98	[M-H]-	861	==>	735	720	718	709	694	451	435	375		Catechin/Epicatech trimer with two A-type Inter-Flavanic Linkages (IFL): (Cat)Epi--A(IFL)--(Cat)Epi--A(IFL)--(Cat)Epi
					P-Di	126	141	143	152	167	410	426	486		
			MS^3	709	==>	584	411	285							
					P-Di	125	298	424							
2-G2	862	44.27	[M-H]-	861	==>	844	735	709	693	675	627	575	571	376	Catechin/Epicatech trimer with two A-type Inter-Flavanic Linkages (IFL): (Cat)Epi--A(IFL)--(Cat)Epi--A(IFL)--(Cat)Epi
					P-Di	17	126	152	168	186	234	286	290	485	
			MS^3	571	==>	411									
					P-Di	160									
3-G2	1150	49.14	[M-H]-	1149	==>	997	864	725	573						Catechin/Epicatech tetramer with two A-type Inter-Flavanic Linkages (IFL): (Cat)Epi--A(IFL)--(Cat)Epi--A(IFL)--(Cat)Epi--(Cat)Epi
					P-Di	152	285	424	576						
			MS^3	997	==>	573									
					P-Di	424									
4-G2	320	58.73	[M-H]-	319	==>	287	183	151							3,3',4',5,5',7-Hexahydroxyflavanone (a.k.a. Dihydromyricetin)
					P-Di	32	136	168							
			MS^3	183	==>	169	151								
					P-Di	14	32								

Table 17: Detected Compounds in Fraction H using HPLC Method 1. Indicates Compound Number (CMPD #), Molecular Weight (MW) in atomic mass units (amu), Retention Time (RT) in minutes (min), Mass Spec Base Peak Identification (BP-ID) showing negative mode ionization $[M-H]^-$ (indicates the type of ion which forms the Base Peak. Base Peak refers to the most abundant ion in the mass spectrum), Parent ion (P^-) m/z after $[M-H]^-$ ionization (indicates the Base Peak in the normal mass spectra), Base Peak of the daughter ion (D-BP) (i.e., the most abundant ion in the daughter spectrum), MS/MS or MS/MS/MS product ions (MS^3), and the arithmetic difference in m/z between the parent ion and individual daughter ions (P-Di). Bold donates most abundant ion in the given spectra.

CMPD	MW	RT	BP-ID	P-	==>	D-BP	Other Daughter Ions						Possible Structure ID(s)
1-H1	1152	12.06	[M-H]-	1151	==>	981	861	829	573	529			Catechin/Epicatech tetramer with one A-type Inter-Flavanic Linkage (IFL): (Cat)Epi--A(IFL)--(Cat)Epi--(Cat)Epi--(Cat)Epi
					P-Di	170	290	322	578	622			
			MS^3	981	==>	829	692	530					
					P-Di	152	289	451					
2-H1	1152	12.67	[M-H]-	1151	==>	981	861	829	709	573			Catechin/Epicatech tetramer with one A-type Inter-Flavanic Linkage (IFL): (Cat)Epi--A(IFL)--(Cat)Epi--(Cat)Epi--(Cat)Epi
					P-Di	170	290	322	442	578			
			MS^3	861	==>	709	569	451					
					P-Di	152	292	410					
3-H1	876	13.41	[M-H]-	875	==>	857	813	723	571	527			Flavonoid trimer with two A-type IFL linkages. Two monomers consist of catechin (or epicatechin), while the other is an O-methylated-(Cat)Epi.
					P-Di	18	62	152	304	348			
			MS^3	723	==>	679	512	423	353				
					P-Di	44	211	300	370				
4-H1	1152	13.93	[M-H]-	1151	==>	981	863	711	573				Catechin/Epicatech tetramer with one A-type Inter-Flavanic Linkage (IFL): (Cat)Epi--(Cat)Epi--A(IFL)--(Cat)Epi--(Cat)Epi
					P-Di	170	288	440	578				
			MS^3	863	==>	711	573	451					
					P-Di	152	290	412					
5-H1	1166	14.22	[M-H]-	1165	==>	1013	999	847	727	591			Flavonoid tetramer with two A-type IFL linkages. Three of the monomers consist of (Cat)Epi, with the last being an O-methylated-(Cat)Epi.
					P-Di	152	166	318	438	574			
			MS^3	999	==>	847	424	285					
					P-Di	152	575	714					
6-H1	1152	15.51	[M-H]-	1151	==>	981	862	861	711	693	575		Catechin/Epicatech tetramer with two A-type Inter-Flavanic Linkages (IFL): (Cat)Epi--A(IFL)--(Cat)Epi--(Cat)Epi--A(IFL)--(Cat)Epi
					P-Di	170	289	290	440	458	576		
			MS^3	711	==>	**693**	559						
					P-Di	18	152						
7-H1	860	16.28	[M-H]-	859	==>	707	569	443					UNKNOWN trimer, most likely with two A-type IFL linkages
					P-Di	152	290	416					
			MS^3	707	==>	569	433						
					P-Di	138	274						
8-H1	1148	18.04	[M-H]-	1147	==>	995	857	571					Catechin/Epicatech tetramer with three A-type IFL Linkages: (Cat)Epi--A(IFL)--(Cat)Epi--A(IFL)--(Cat)Epi--A(IFL)--(Cat)Epi
					P-Di	152	290	576					
			MS^3	995	==>								
					P-Di								
9-H1	876	18.41	[M-H]-	875	==>	857	839	723	571	557	463		Flavonoid trimer with two A-type IFL linkages. Two monomers consist of catechin (or epicatechin), while the other is an O-methylated-(Cat)Epi.
					P-Di	18	36	152	304	318	412		
			MS^3	857	==>	731	571						
					P-Di	126	286						
10-H1	862	18.74	[M-H]-	861	==>	825	735	709	571				Catechin/Epicatech trimer with two A-type Inter-Flavanic Linkages (IFL): (Cat)Epi--A(IFL)--(Cat)Epi--A(IFL)--(Cat)Epi
					P-Di	36	126	152	290				
			MS^3	825	==>								
					P-Di								
11-H1	862	19.41	[M-H]-	861	==>	825	735	709	571				Catechin/Epicatech trimer with two A-type Inter-Flavanic Linkages (IFL): (Cat)Epi--A(IFL)--(Cat)Epi--A(IFL)--(Cat)Epi
					P-Di	36	126	152	290				
			MS^3	709	==>	571	541	523	448	285			
					P-Di	138	168	186	261	424			
12-H1	862	21.68	[M-H]-	861	==>	825	735	709	571				Catechin/Epicatech trimer with two A-type Inter-Flavanic Linkages (IFL): (Cat)Epi--A(IFL)--(Cat)Epi--A(IFL)--(Cat)Epi
					P-Di	36	126	152	290				
			MS^3	709	==>	571							
					P-Di	138							
13-H1	862	22.95	[M-H]-	861	==>	825	735	709	693	571	449		Catechin/Epicatech trimer with two A-type Inter-Flavanic Linkages (IFL): (Cat)Epi--A(IFL)--(Cat)Epi--A(IFL)--(Cat)Epi
					P-Di	36	126	152	168	290	412		
			MS^3	735	==>	699	583	445					
					P-Di	36	152	290					

Table 18: Detected Compounds in Fraction H using HPLC Method 2. Indicates Compound Number (CMPD #), Molecular Weight (MW) in atomic mass units (amu), Retention Time (RT) in minutes (min), Mass Spec Base Peak Identification (BP-ID) showing negative mode ionization $[M-H]^-$ (indicates the type of ion which forms the Base Peak. Base Peak refers to the most abundant ion in the mass spectrum), Parent ion (P^-) m/z after $[M-H]^-$ ionization (indicates the Base Peak in the normal mass spectra), Base Peak of the daughter ion (D-BP) (i.e., the most abundant ion in the daughter spectrum), MS/MS or MS/MS/MS product ions (MS^3), and the arithmetic difference in m/z between the parent ion and individual daughter ions (P-Di). Bold donates most abundant ion in the given spectra.

CMPD	MW	RT	BP-ID	P-	==>	D-BP	Other Daughter Ions		Possible Structure ID(s)
1-H2	864	21.52	[M-H]-	863	==>	711	693	575	Catechin/Epicatech trimer with single A-type Inter-Flavanic Linkage (IFL)
					P-Di	152	170	288	
			MS^3	711	==>				
					P-Di				
2-H2	864	24.03	[M-H]-	863	==>	711	575	449	Catechin/Epicatech trimer with single A-type Inter-Flavanic Linkage (IFL)
					P-Di	152	288	414	
			MS^3	711	==>				
					P-Di				
3-H2	864	27.86	[M-H]-	863	==>	711	693	575	Catechin/Epicatech trimer with single A-type Inter-Flavanic Linkage (IFL)
					P-Di	152	170	288	
			MS^3	711	==>				
					P-Di				
4-H2	864	32.36	[M-H]-	863	==>	575	423		Catechin/Epicatech trimer with single A-type Inter-Flavanic Linkage (IFL)
					P-Di	288	440		
			MS^3	575	==>				
					P-Di				
5-H2	864	35.21	[M-H]-	863	==>	711	693	575	Catechin/Epicatech trimer with single A-type Inter-Flavanic Linkage (IFL)
					P-Di	152	170	288	
			MS^3	711	==>				
					P-Di				

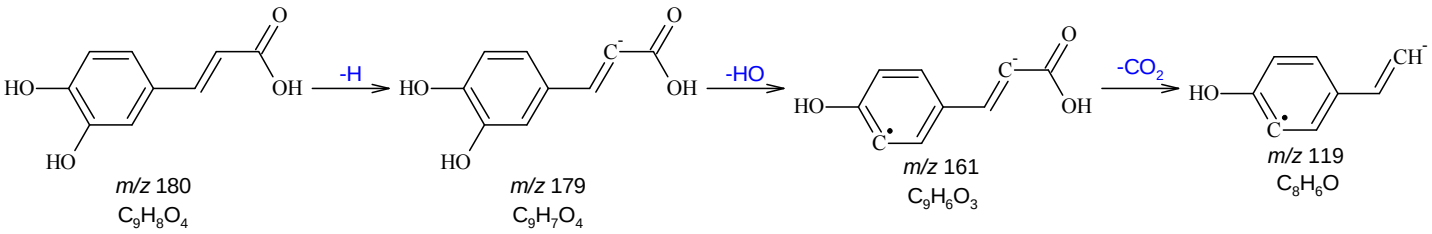

Figure 1: Fragmentation Scheme for 3,4-Dihydroxycinnamic Acid (a.k.a Caffeic Acid)

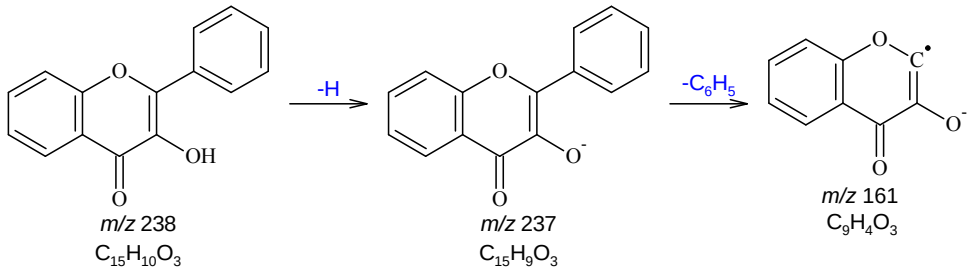

Figure 2: Fragmentation Scheme for 3-Hydroxyflavone (a.k.a. Flavonol)

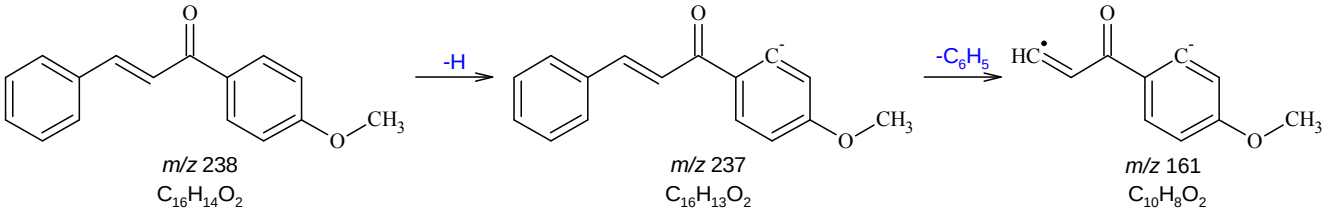

Figure 3: Fragmentation Scheme for 4'-Methoxychalcone

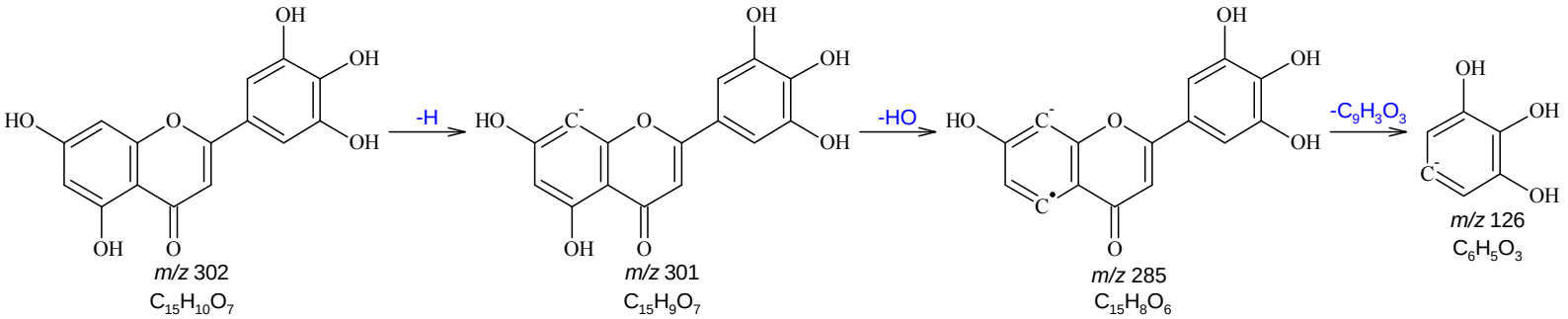

Figure 4: Fragmentation Scheme for 3',4',5,5',7-Pentahydroxyflavone (a.k.a. Tricetin)

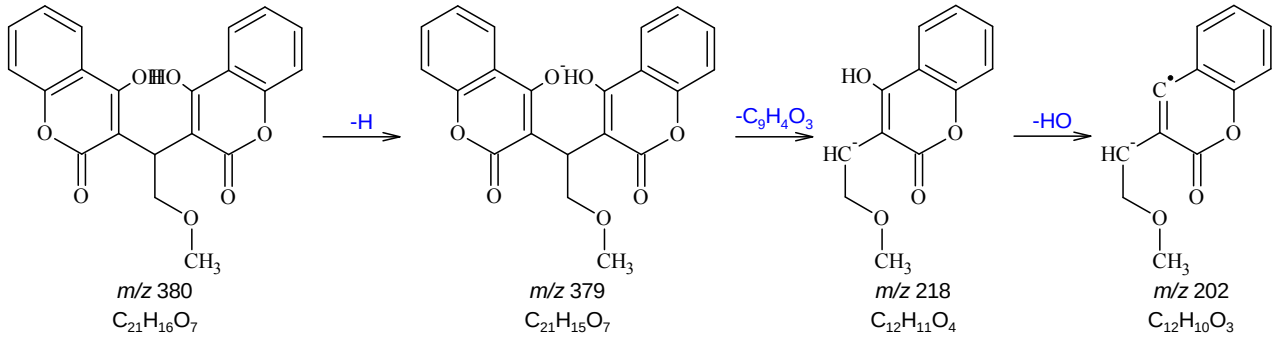

Figure 5: Fragmentation Scheme for 4,4'-Dihydroxy-3,3'-(2-methoxyethylidene) dicoumarin (a.k.a. Dicoumoxyl)

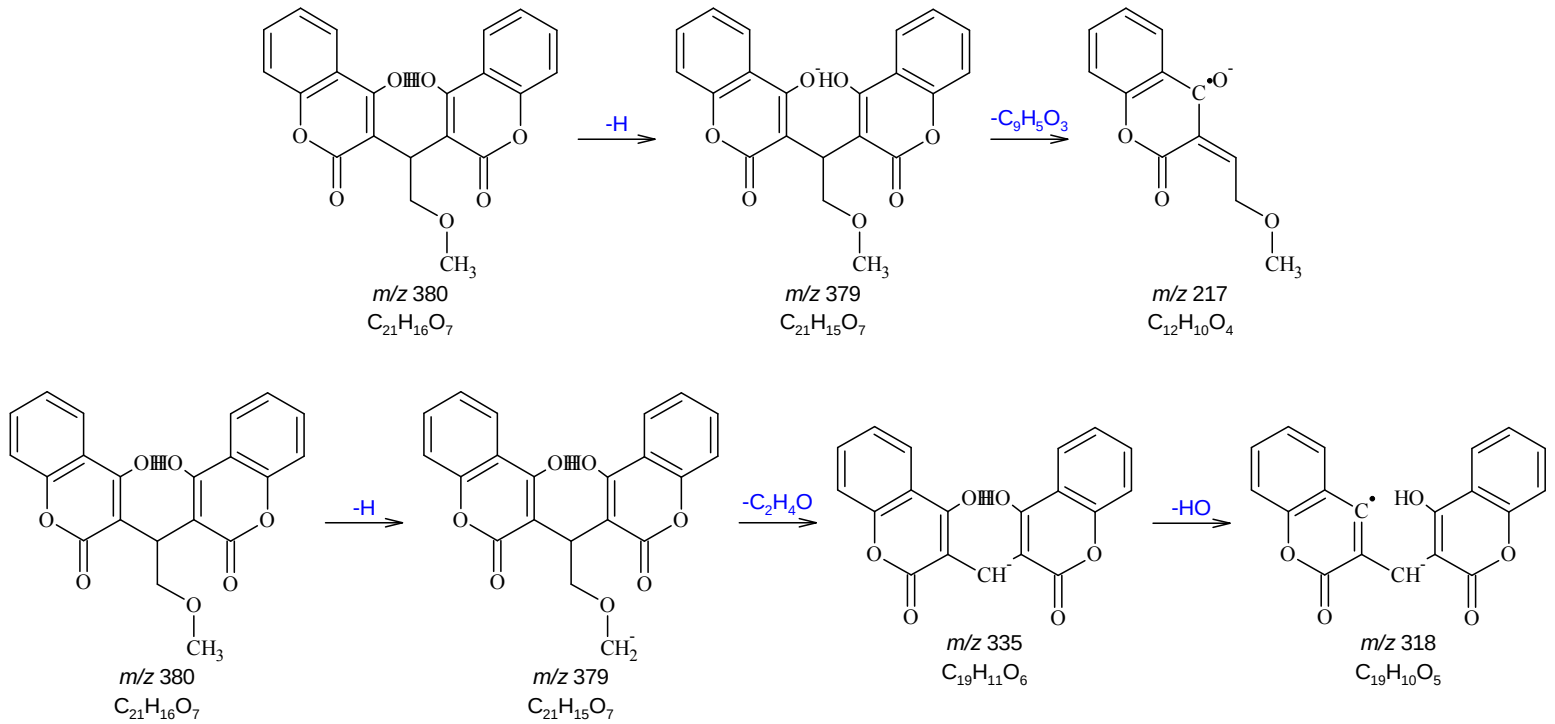

Figure 5 (cont.): Fragmentation Scheme for 4,4'-Dihydroxy-3,3'-(2-methoxyethylidene) dicoumarin (a.k.a. Dicoumoxyl)

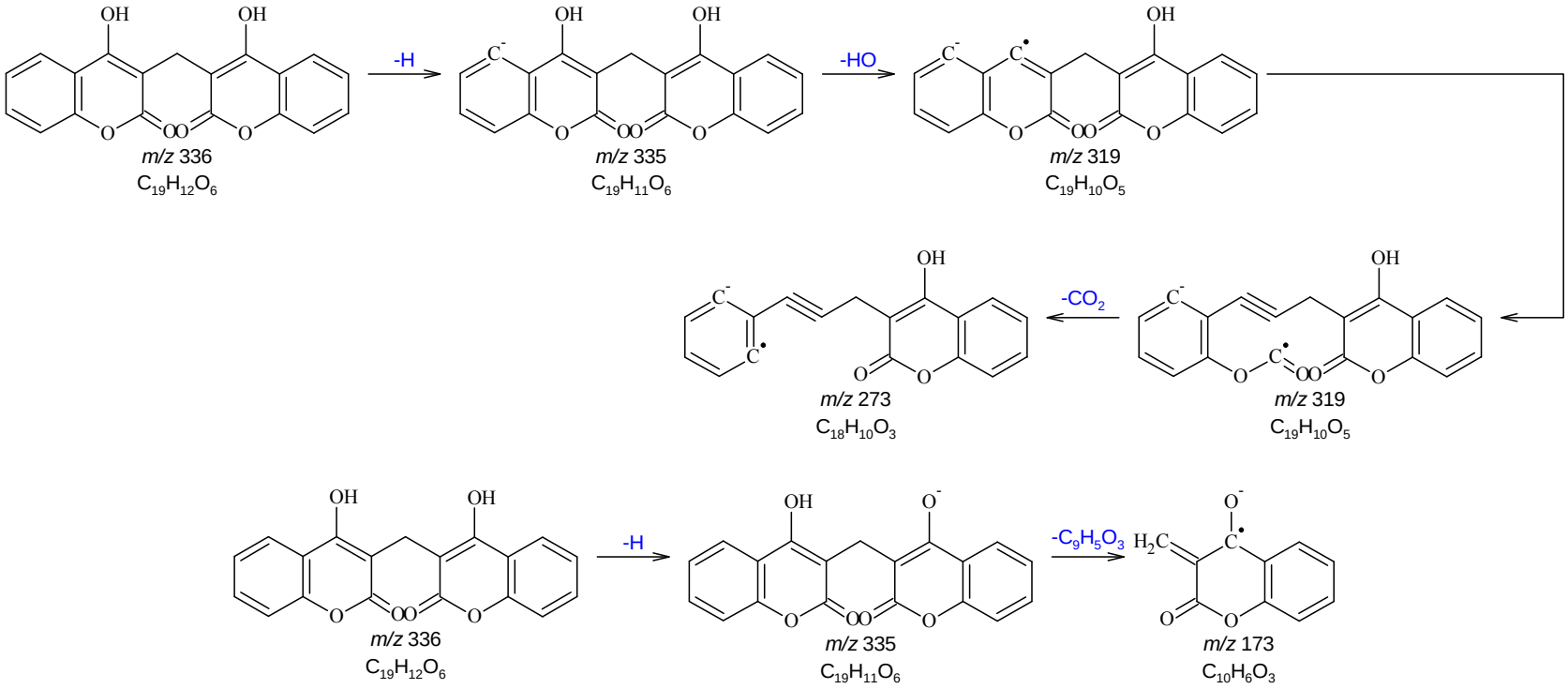

Figure 6: Fragmentation Scheme for 3,3'-Methylenebis[4-hydroxycoumarin] (a.k.a. Dicoumarin)

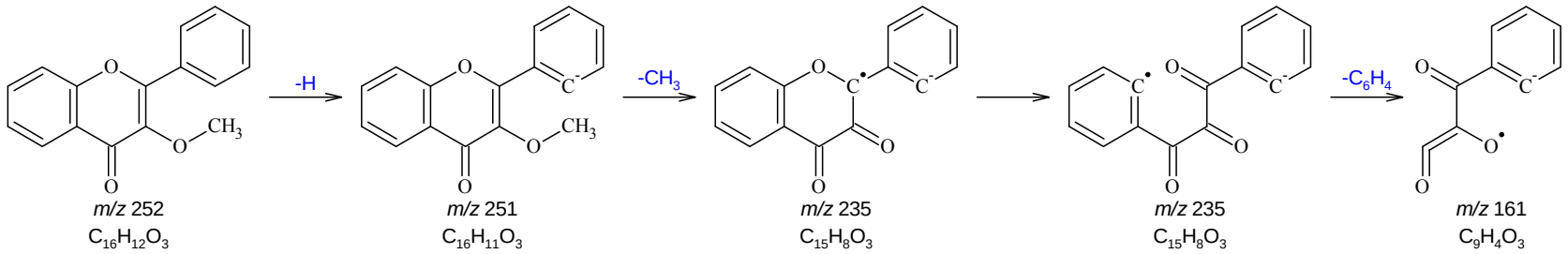

Figure 7: Fragmentation Scheme for 3-Methoxyflavone

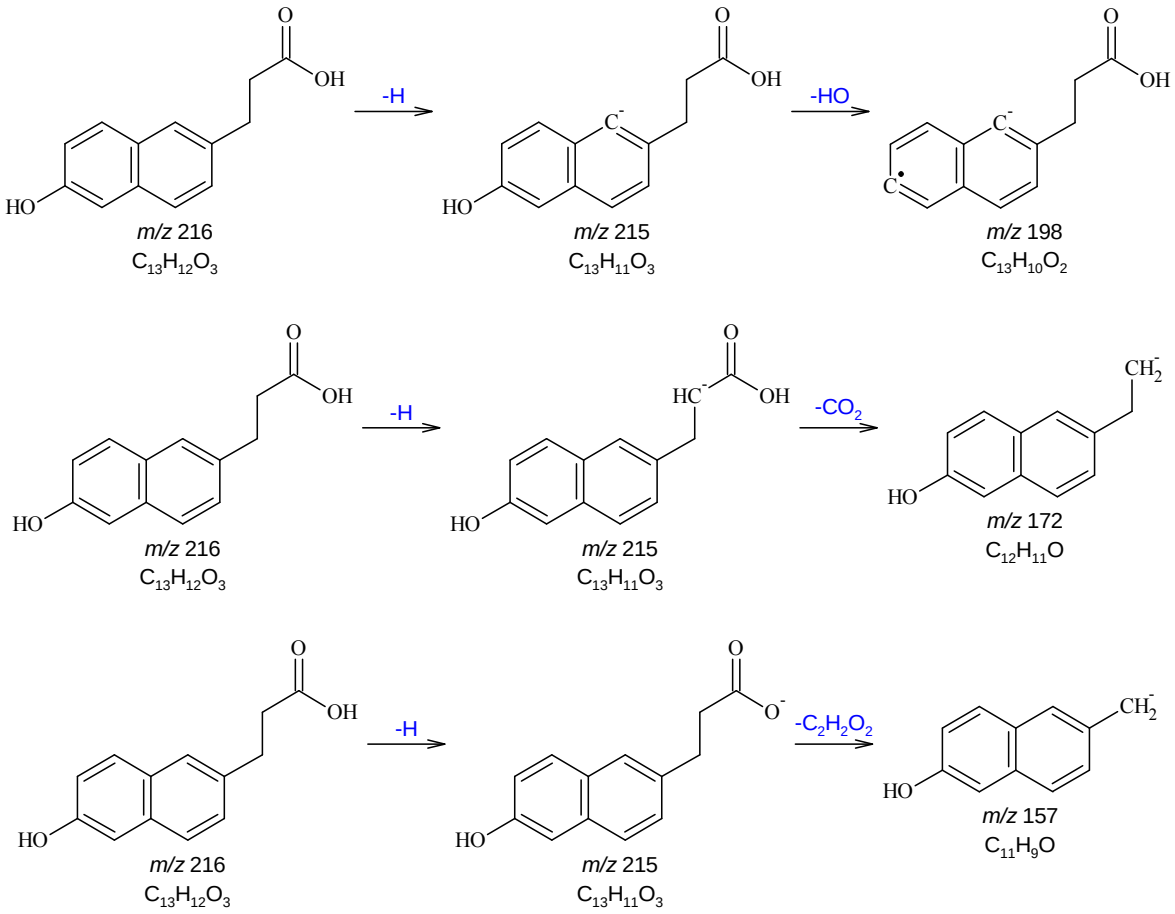

Figure 8: Fragmentation Scheme for 6-Hydroxy-2-naphthalenepropanoic Acid (a.k.a. Allenolic Acid)

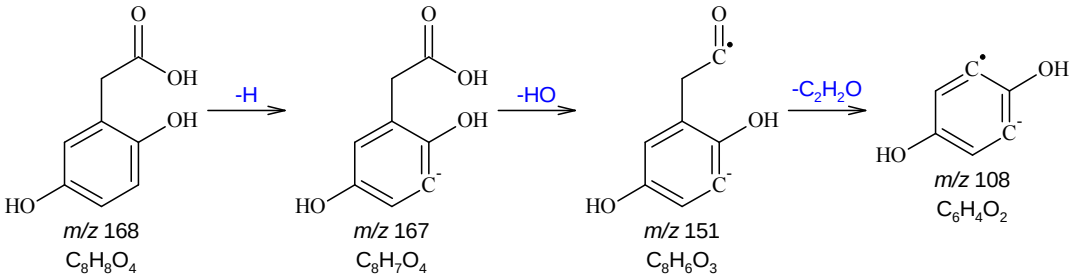

Figure 9: Fragmentation Scheme for Homogentisic Acid

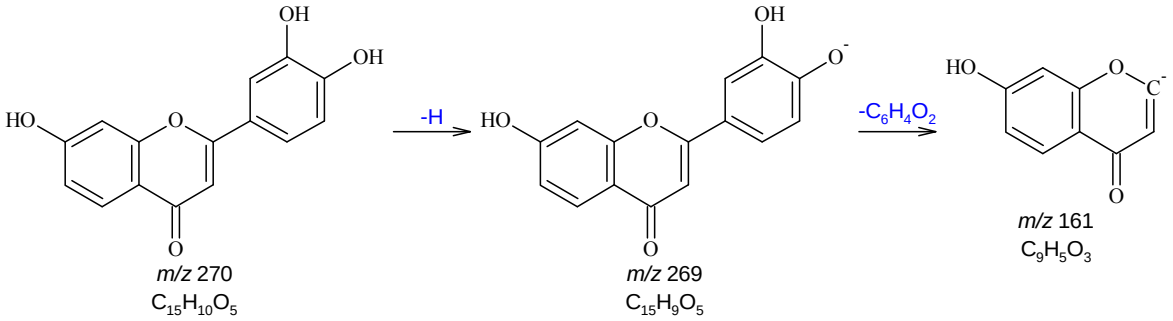

Figure 10: Fragmentation Scheme for 3',4',7-Trihydroxyflavone

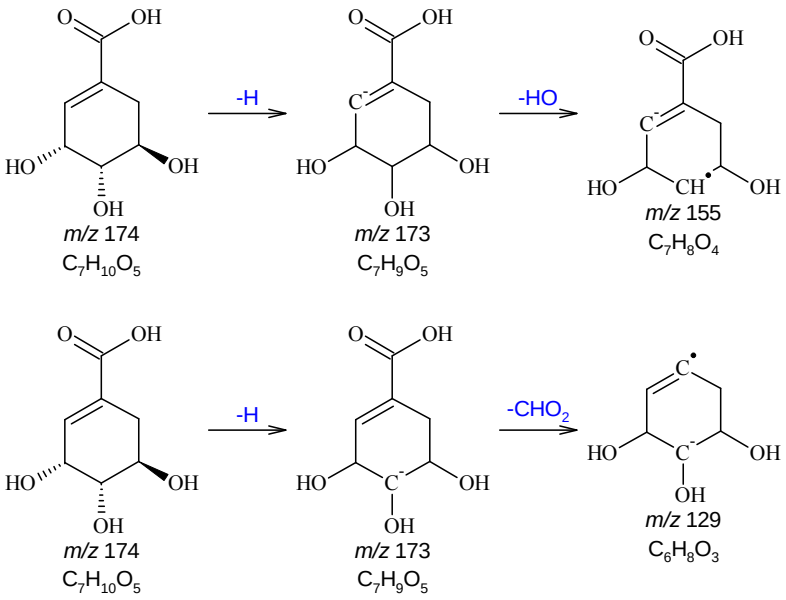

Figure 11: Fragmentation Scheme for Shikimic Acid

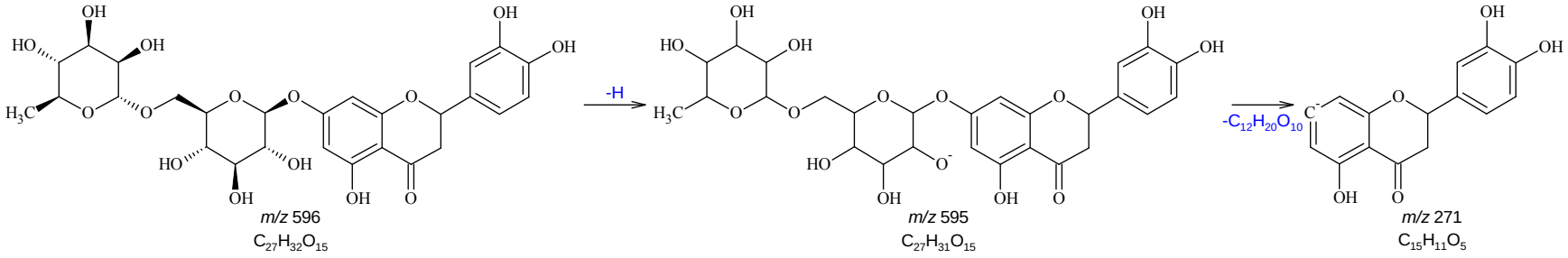

Figure 12: Fragmentation Scheme for Eriodictyol 7-O-rutinoside (a.k.a. Eriocitrin)

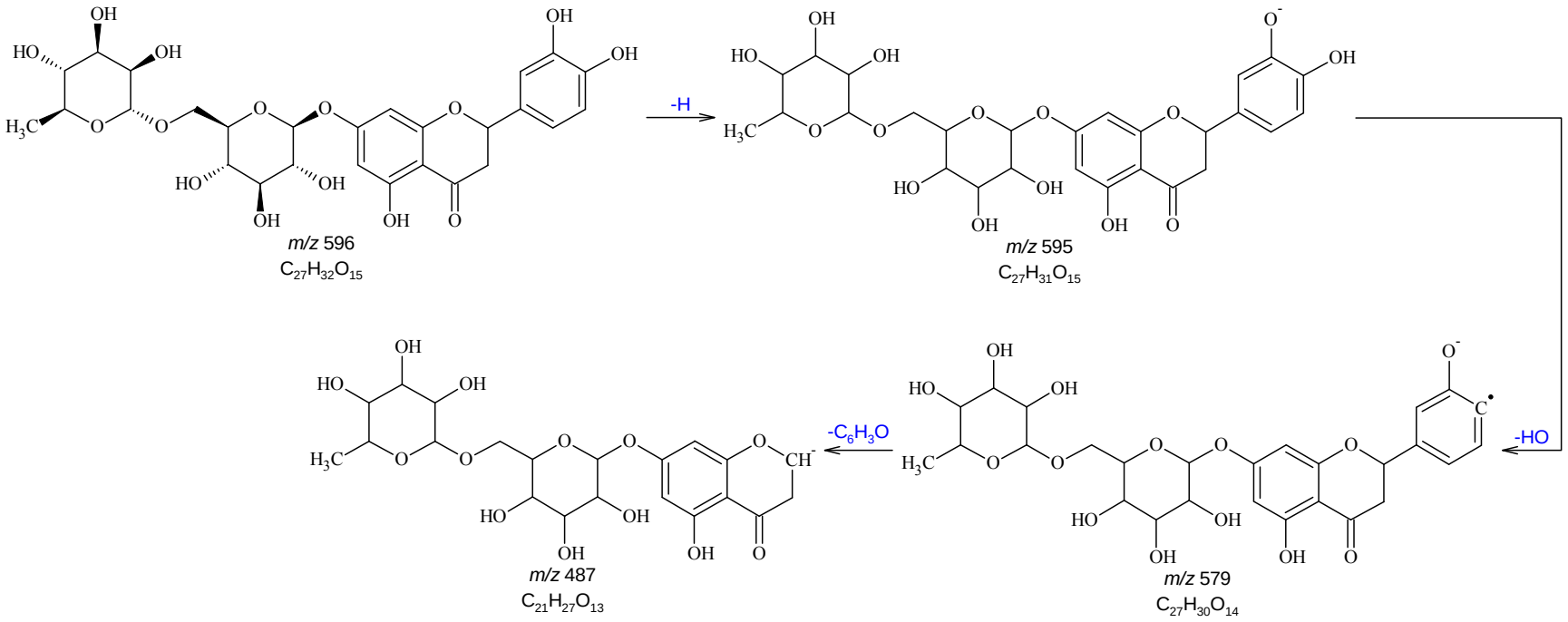

Figure 12 (cont.): Fragmentation Scheme for Eriodictyol 7-O-rutinoside (a.k.a. Eriocitrin)

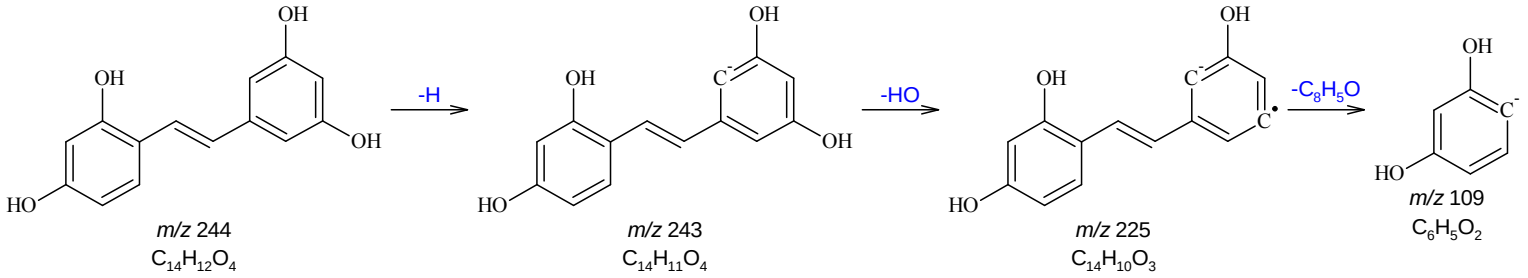

Figure 13: Fragmentation Scheme for Oxyresveratrol

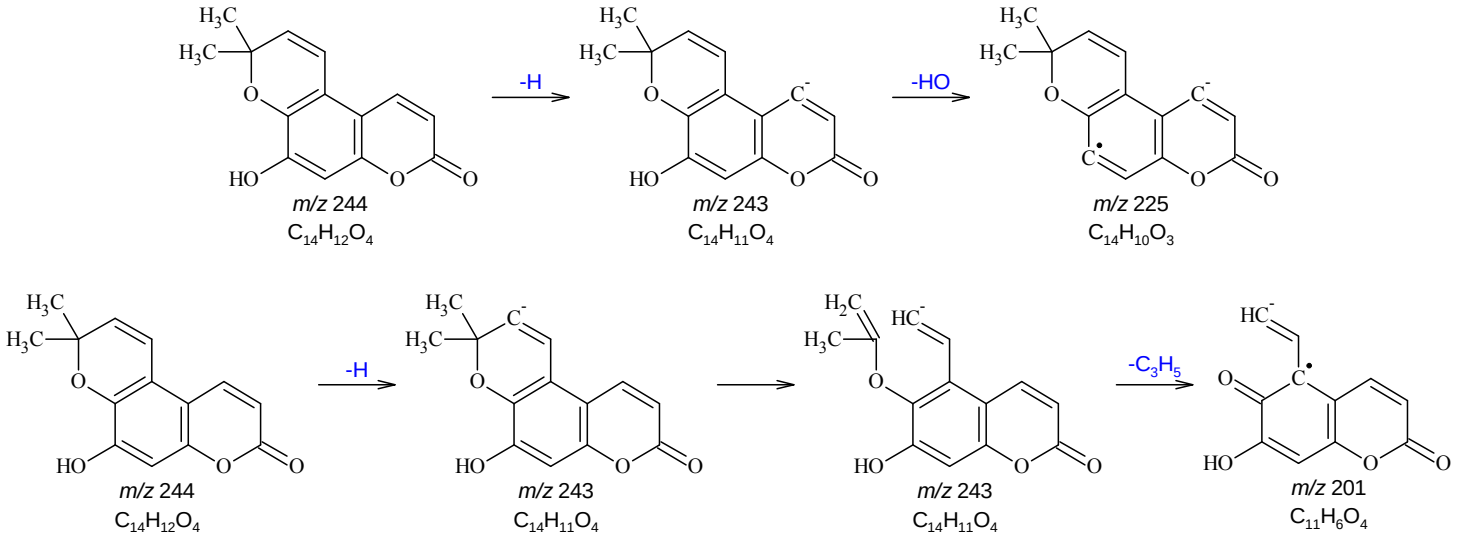

Figure 14: Fragmentation Scheme for Cedrecoumarin A

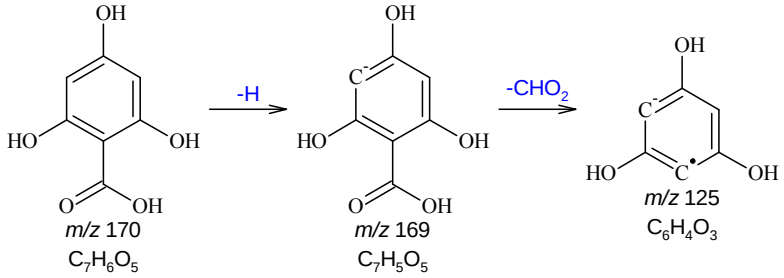

Figure 15: Fragmentation Scheme for 2,4,6-Trihydroxybenzoic Acid

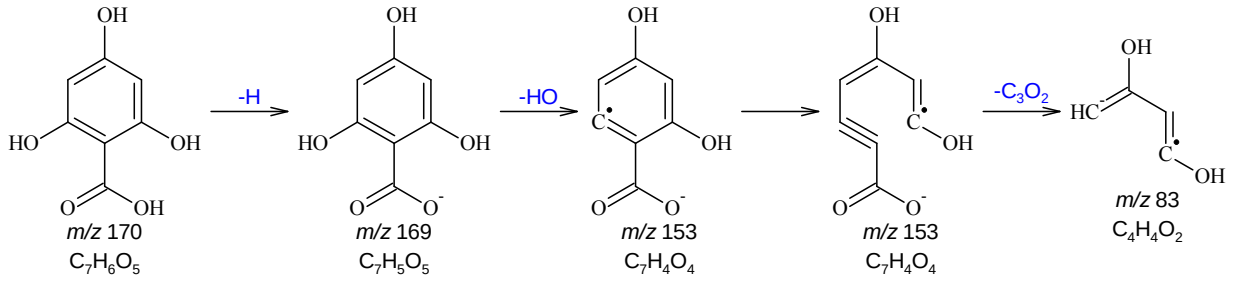

Figure 15 (cont.): Fragmentation Scheme for 2,4,6-Trihydroxybenzoic Acid

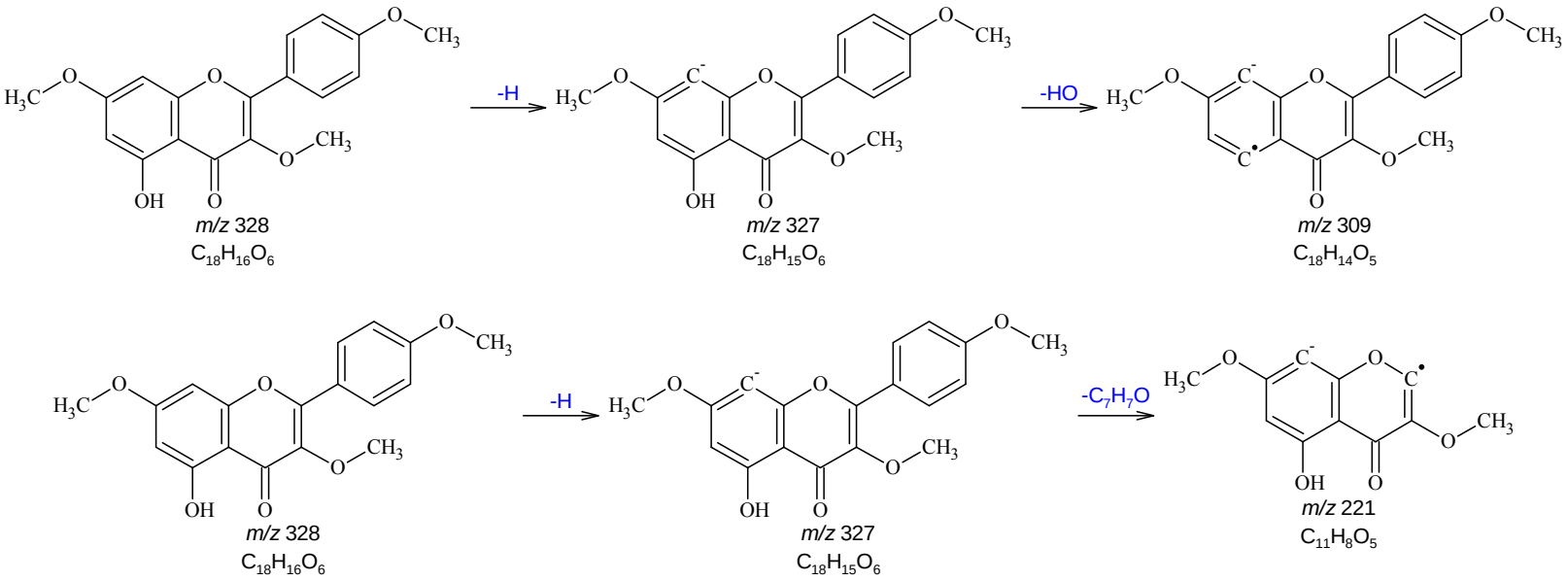

Figure 16: Fragmentation Scheme for Kaempferol-3,4',7-trimethyl Ether

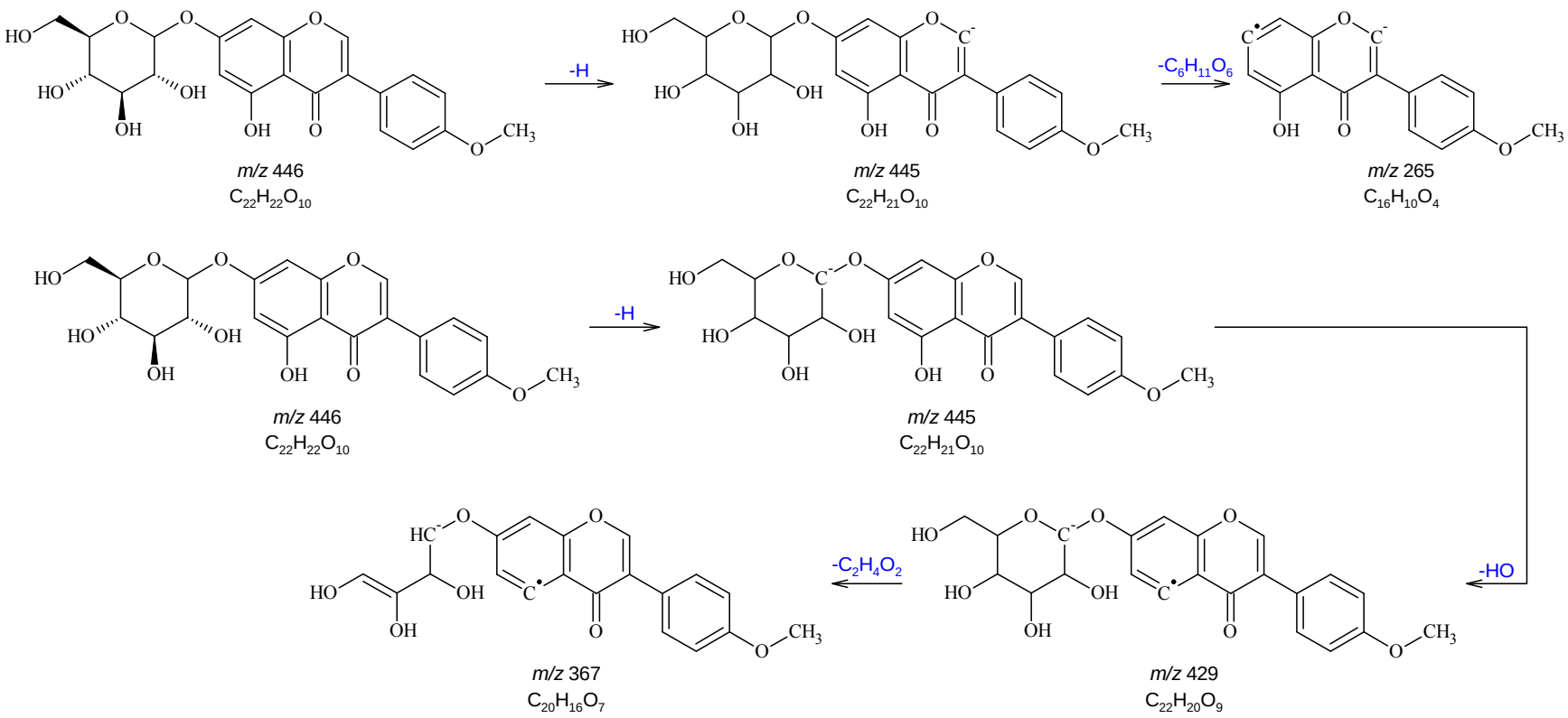

Figure 17: Fragmentation Scheme for Biochanin-A-7-glucoside (a.k.a. Sissotrin)

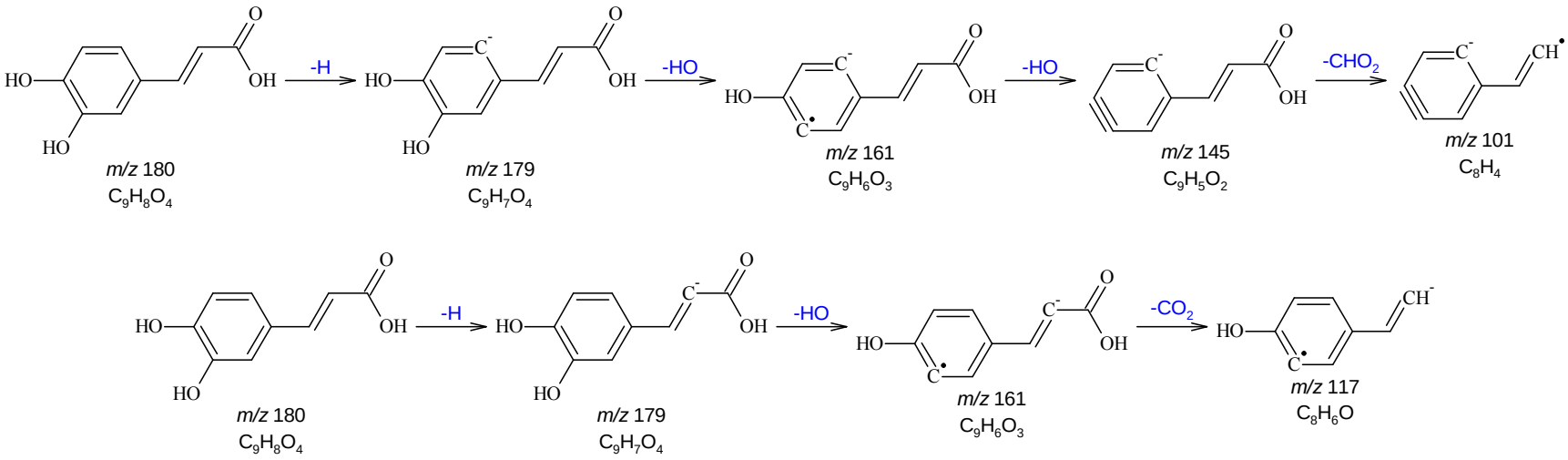

Figure 18: Fragmentation Scheme for 3,4-Dihydroxycinnamic Acid (a.k.a. Caffeic Acid)

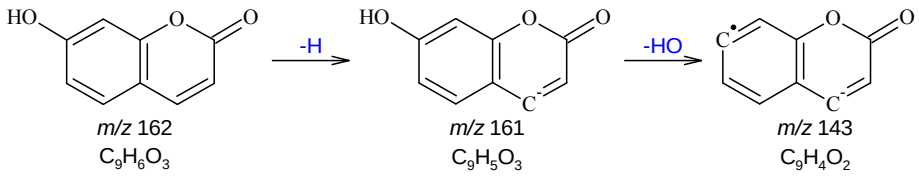

Figure 19: Fragmentation Scheme for 7-Hydroxycoumarin (a.k.a. Umbelliferone)

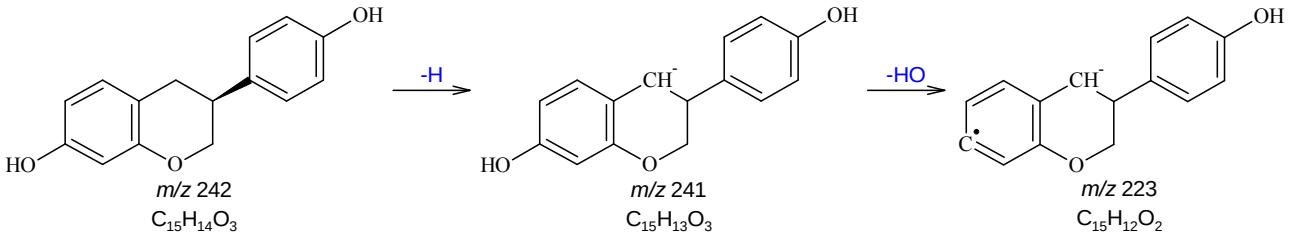

Figure 20: Fragmentation Scheme for 4',7-Dihydroxyisoflavan (a.k.a. Equol)

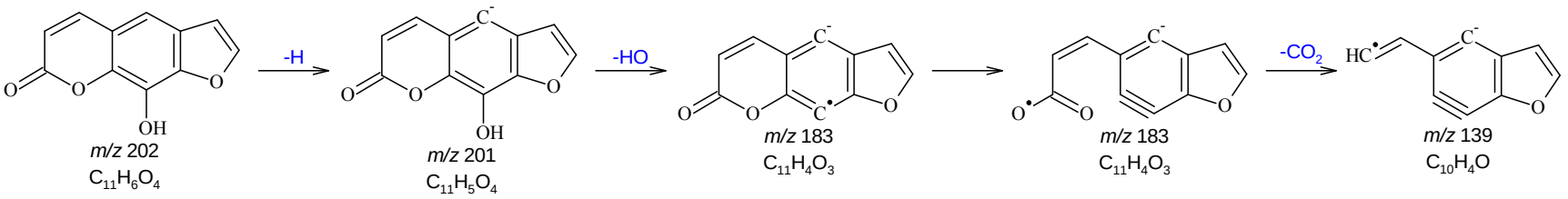

Figure 21: Fragmentation Scheme for 8-Hydroxy-4'-5',6-7-furocoumarin (a.k.a. Xanthotoxol)

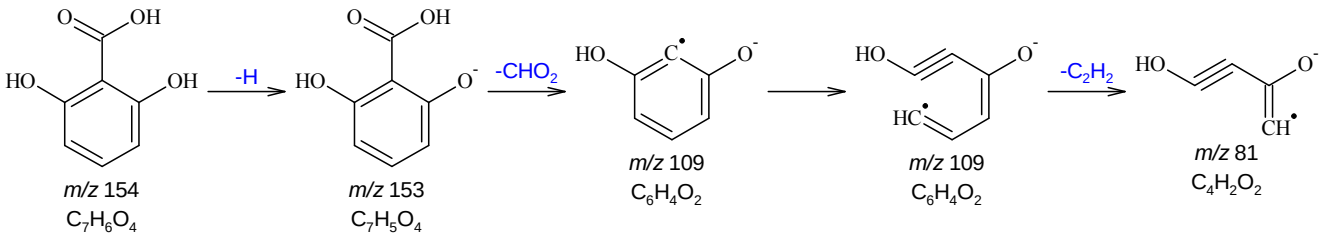

Figure 22: Fragmentation Scheme for 2,6-Dihydroxybenzoic Acid (a.k.a. g-Resorcylic Acid)

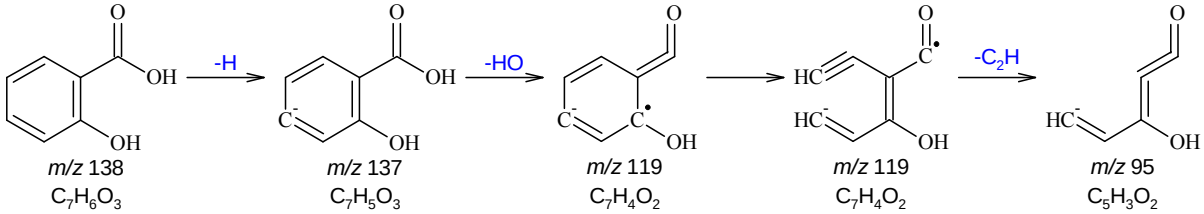

Figure 23: Fragmentation Scheme for 2-Hydroxybenzoic Acid (a.k.a. Salicylic Acid)

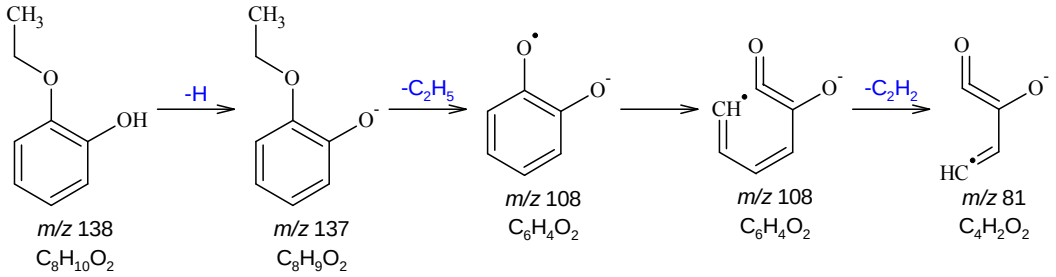

Figure 24: Fragmentation Scheme for Pyrocatechin Monoethyl Ether

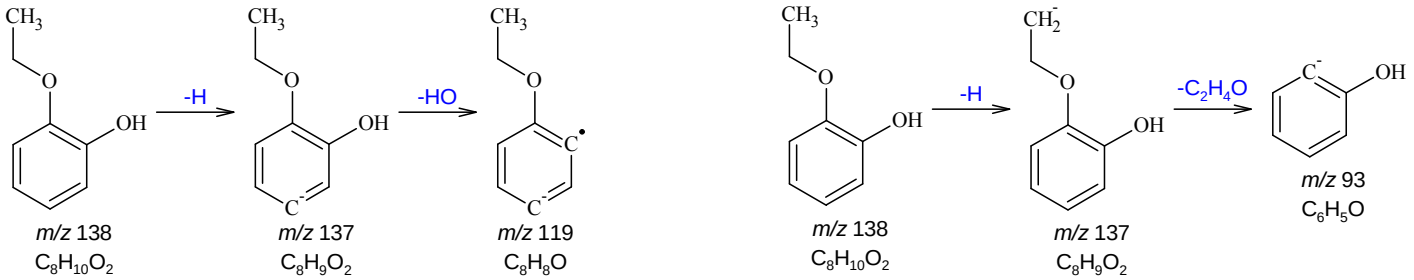

Figure 24 (cont.): Fragmentation Scheme for Pyrocatechin Monoethyl Ether

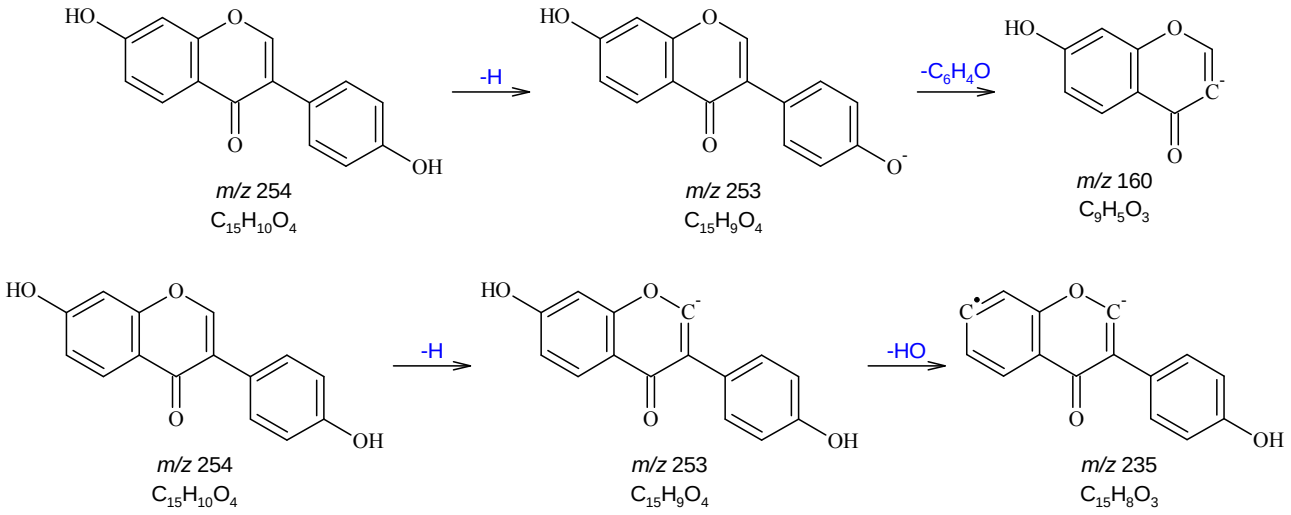

Figure 25: Fragmentation Scheme for 4',7-Dihydroxyisoflavone (a.k.a. Daidzein)

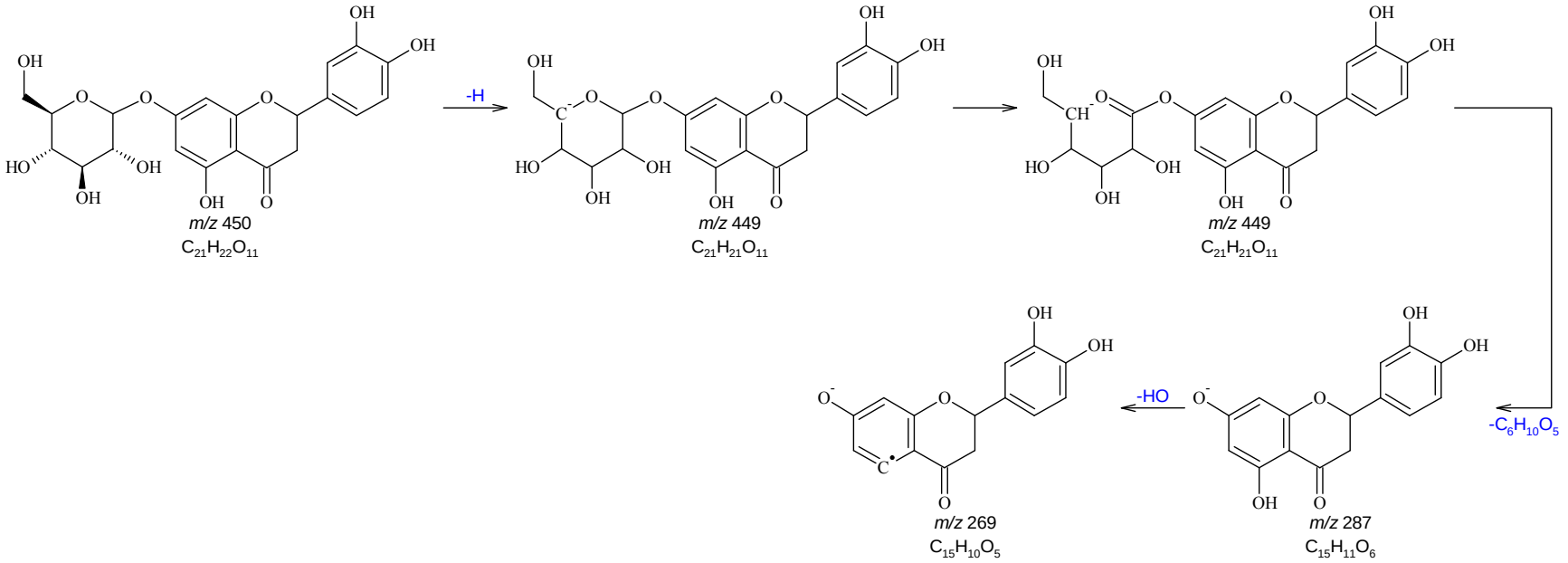

Figure 26: Fragmentation Scheme for Eriodictyol-7-glucoside

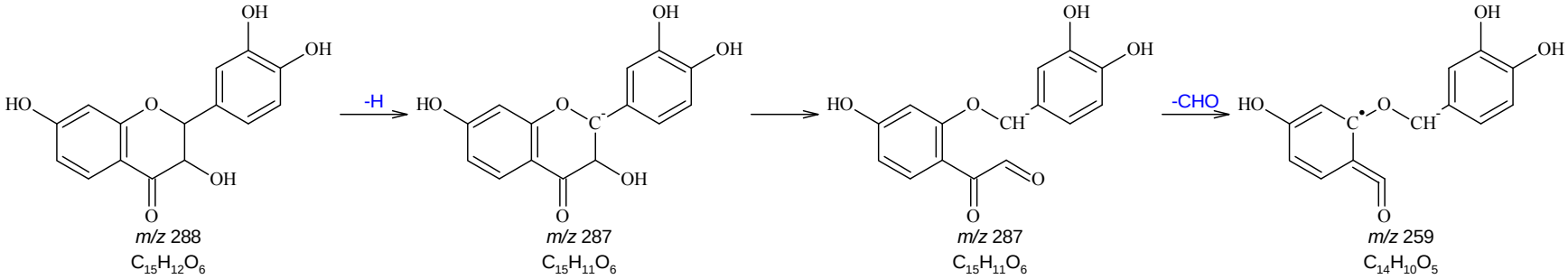

Figure 27: Fragmentation Scheme for 2,3-Dihydrofisetin (a.k.a. Fustin)

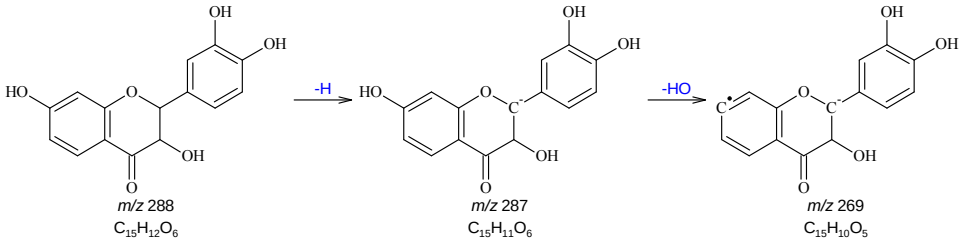

Figure 27 (cont.): Fragmentation Scheme for 2,3-Dihydrofisetin (a.k.a. Fustin)

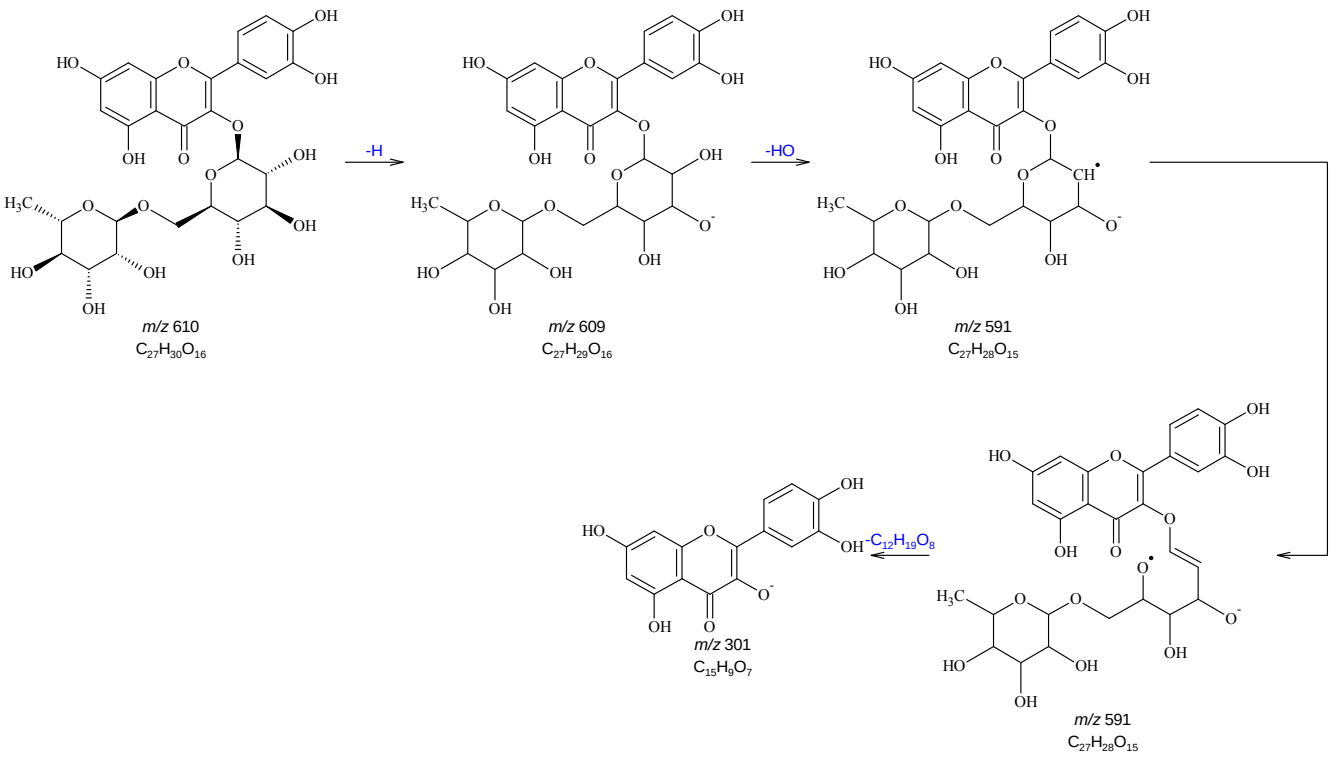

Figure 28: Fragmentation Scheme for Quercetin-3-O-rutinose (a.k.a. Rutin)

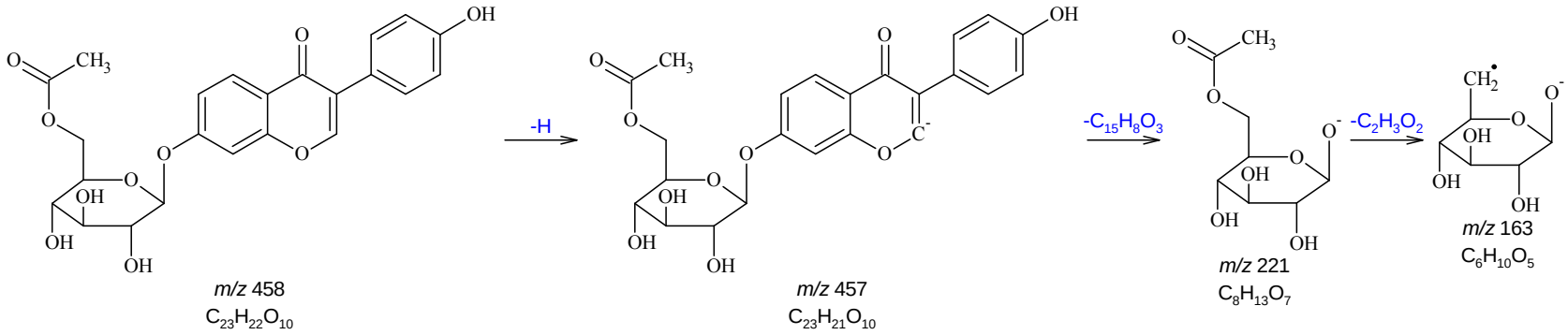

Figure 29: Fragmentation Scheme for 6-O-Acetyldaidzin

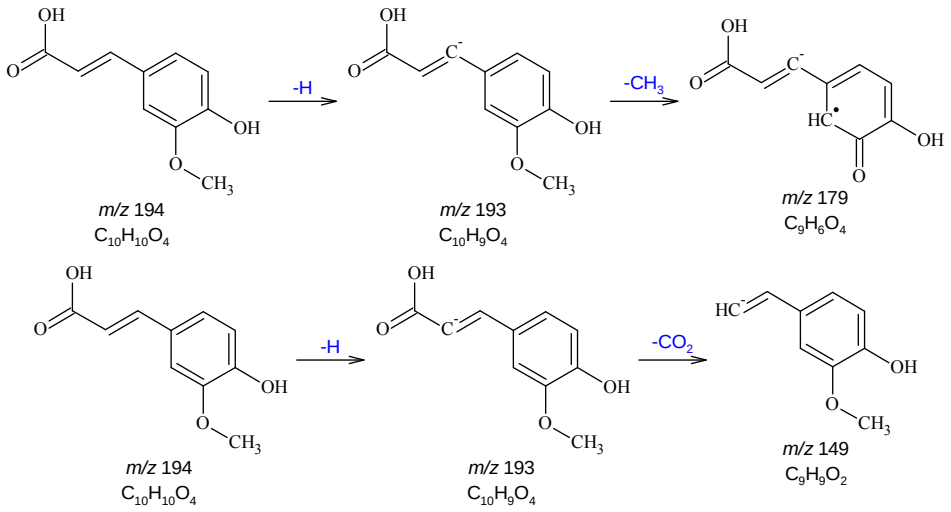

Figure 30: Fragmentation Scheme for 3-Methoxy-4-hydroxycinnamic Acid (a.k.a. Ferulic Acid)

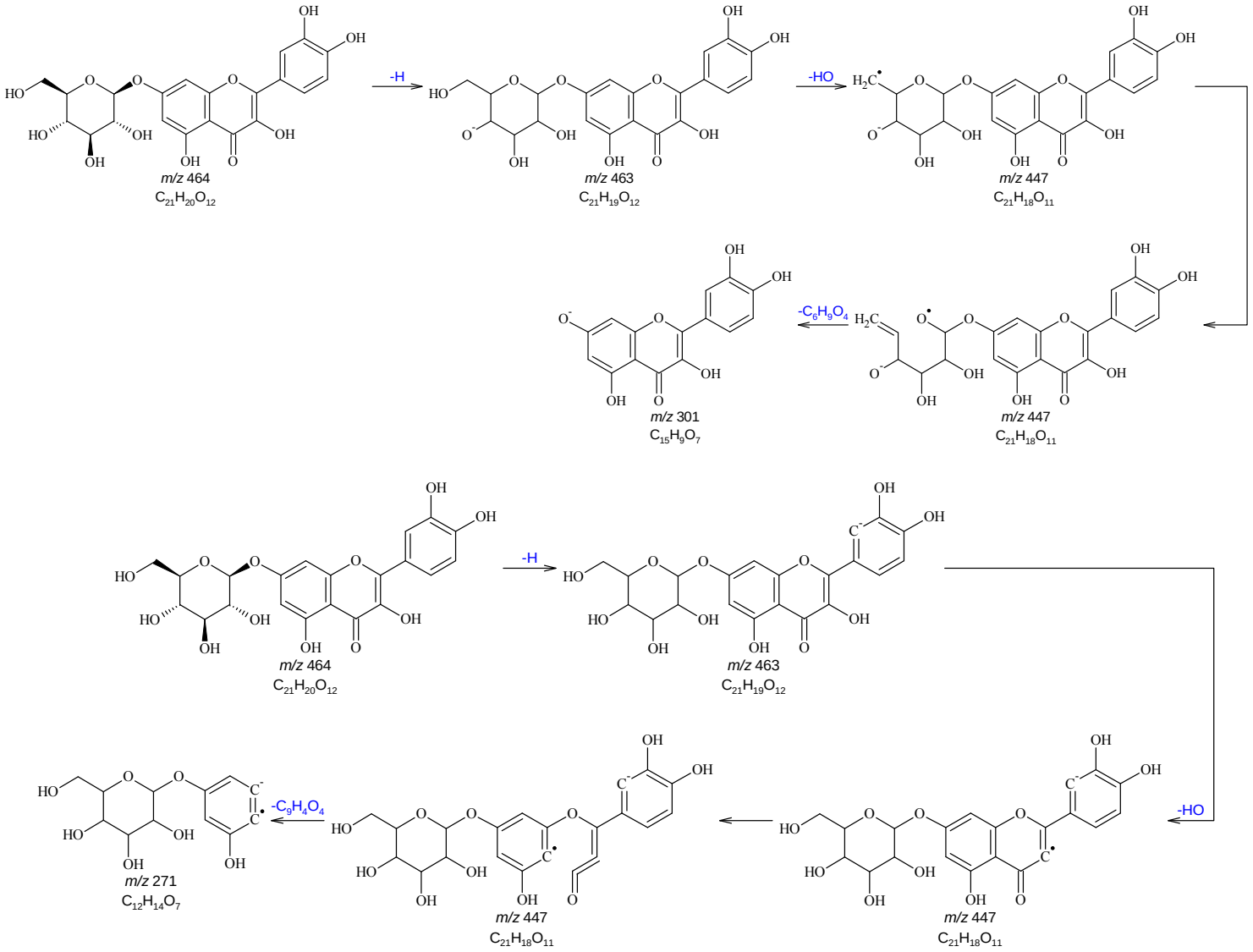

Figure 31: Fragmentation Scheme for Quercetin-7-D-glucoside

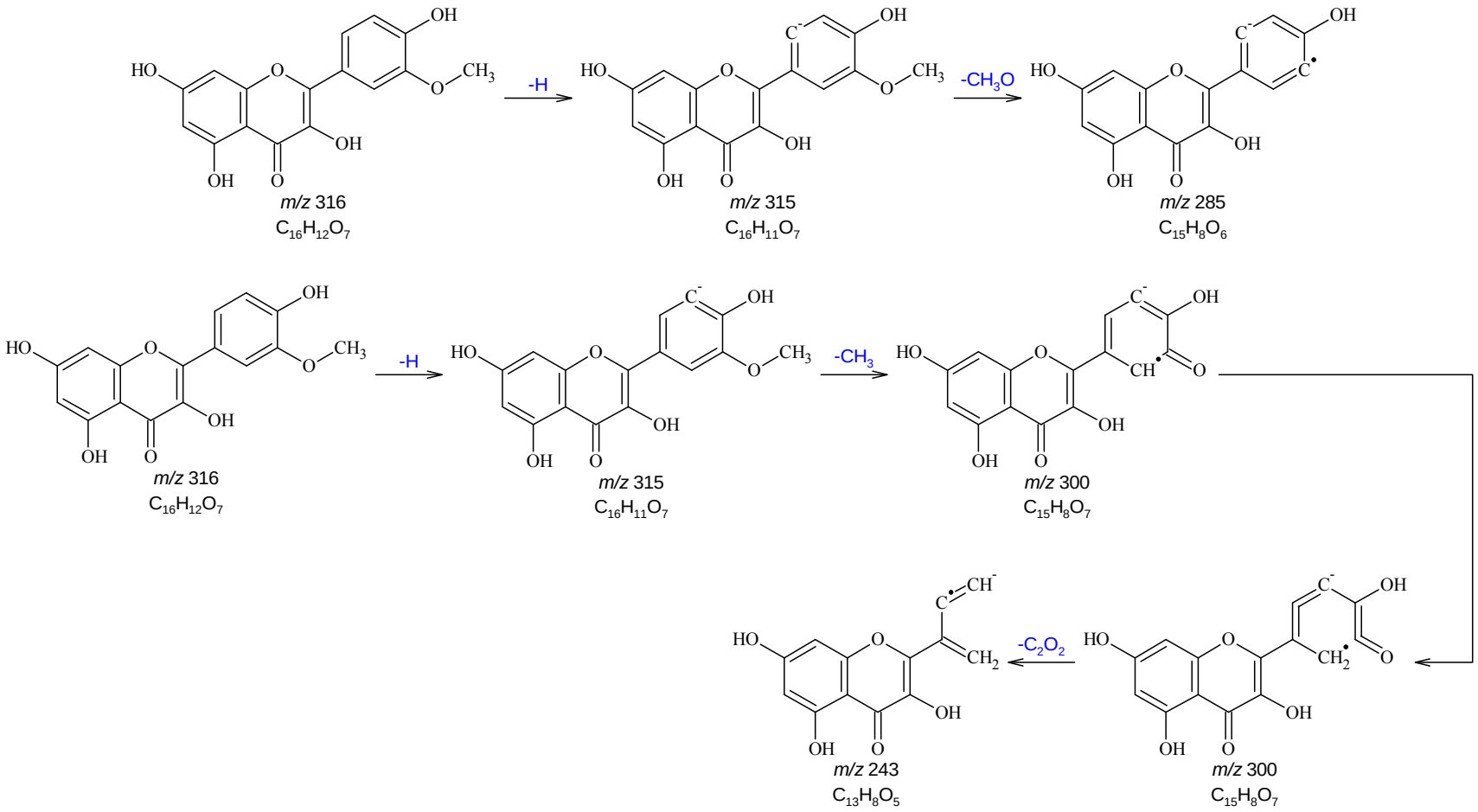

Figure 32: Fragmentation Scheme for 3-Methylquercetin (a.k.a. Isorhamnetin)

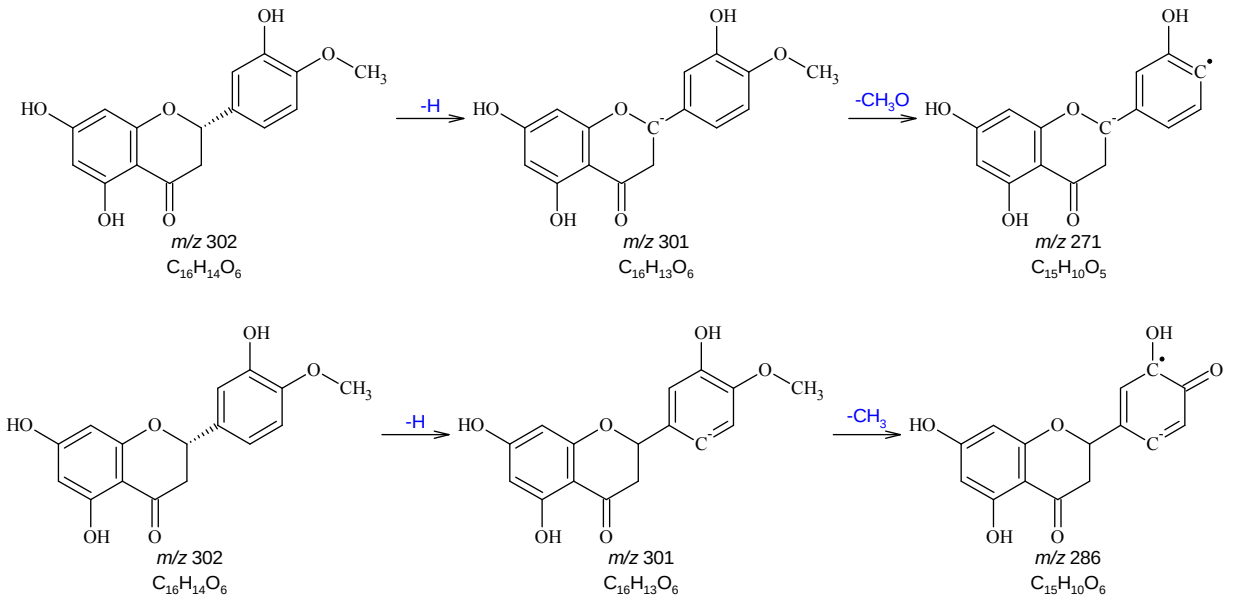

Figure 33: Fragmentation Scheme for 3',5,7-Trihydroxy-4'-methoxyflavanone (a.k.a. Hesperitin)

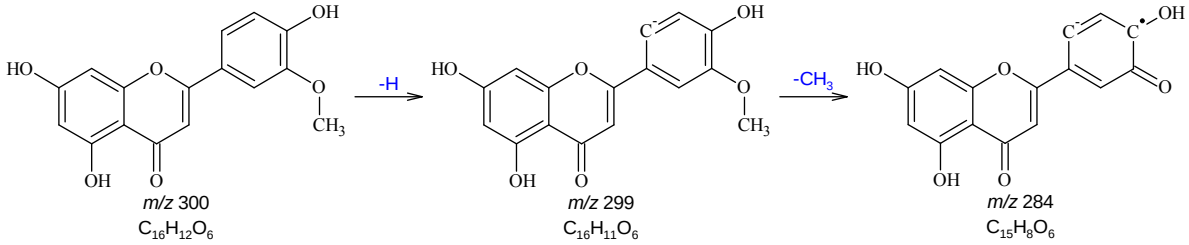

Figure 34: Fragmentation Scheme for 5,7,4'-Trihydroxy-3'-methoxyflavone (a.k.a. Chrysoeriol)

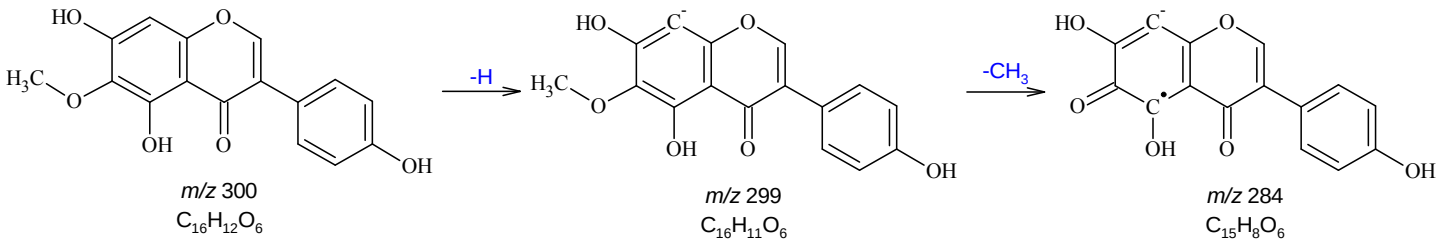

Figure 35: Fragmentation Scheme for 4',5,7-Trihydroxy-6-methoxyisoflavone (a.k.a. Tectorigenin)

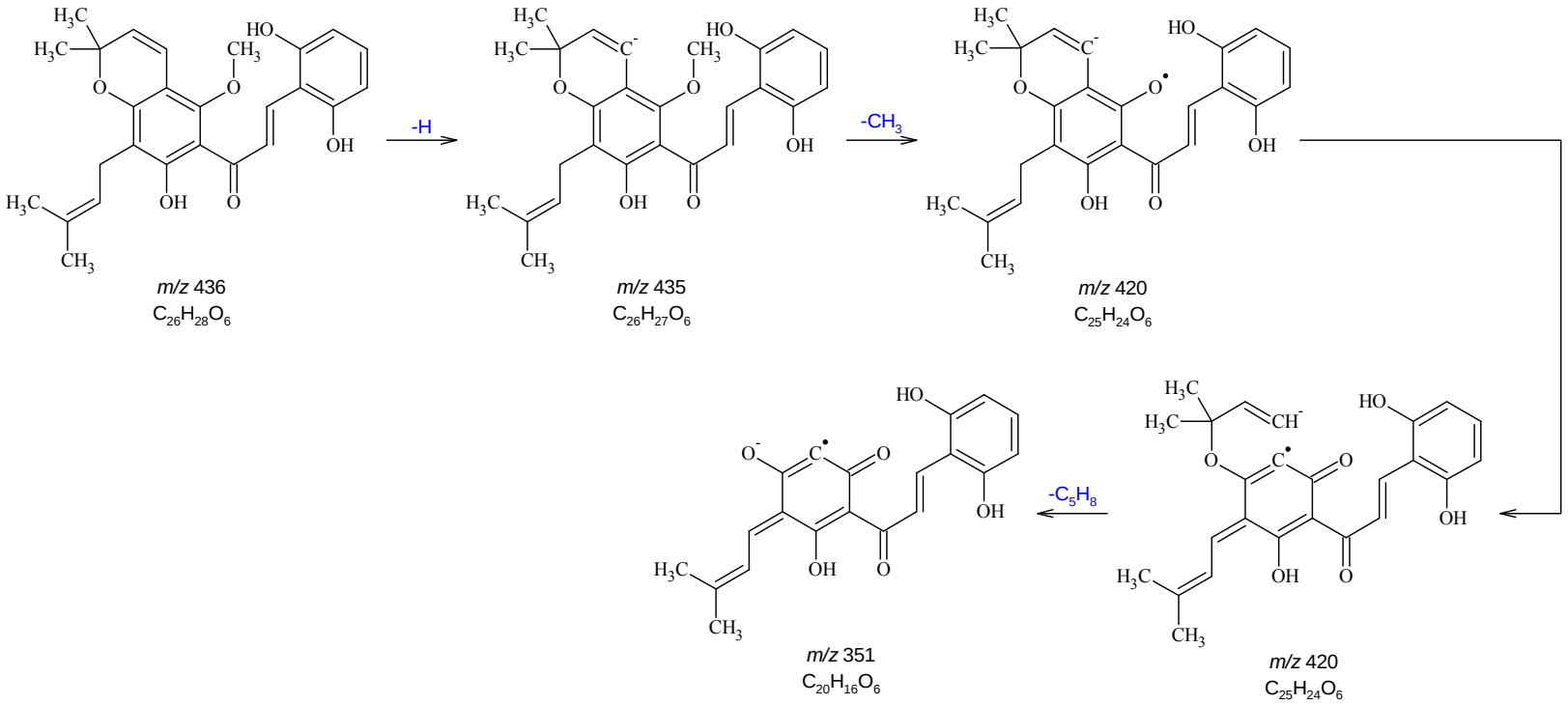

Figure 36: Fragmentation Scheme for Orotinichalcone

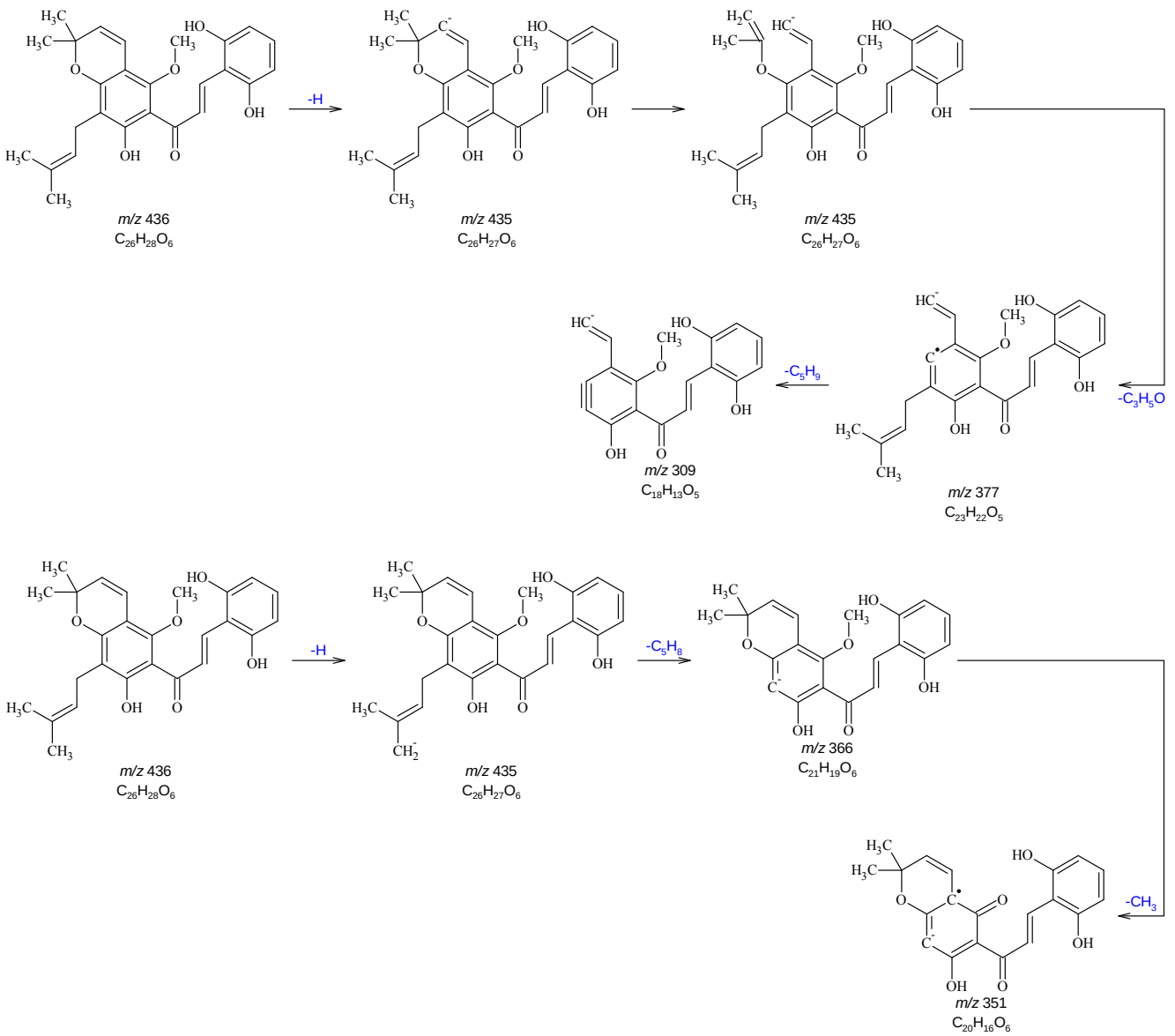

Figure 36 (cont.): Fragmentation Scheme for Orotinichalcone

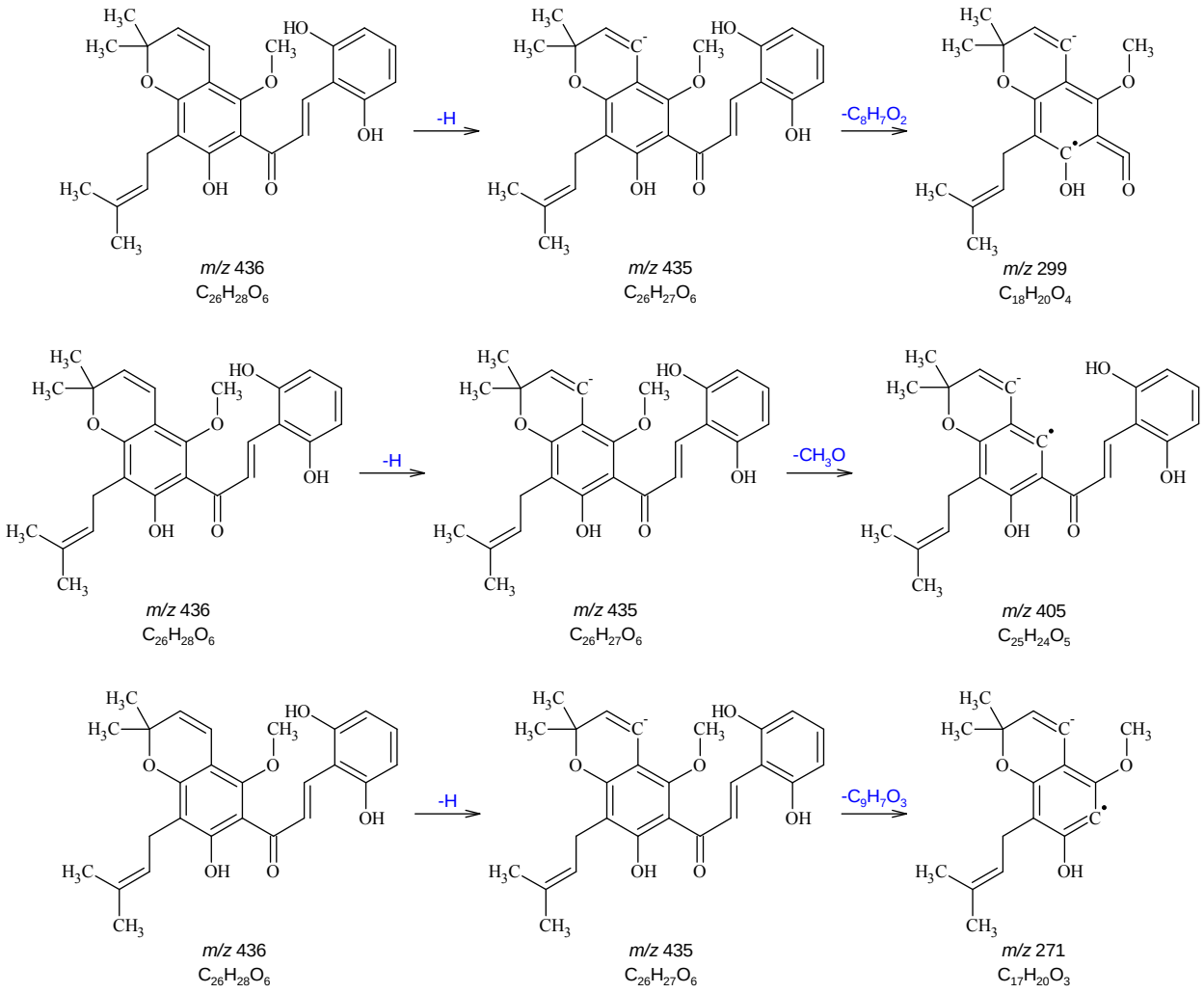

Figure 36 (cont.): Fragmentation Scheme Orotinichalcone

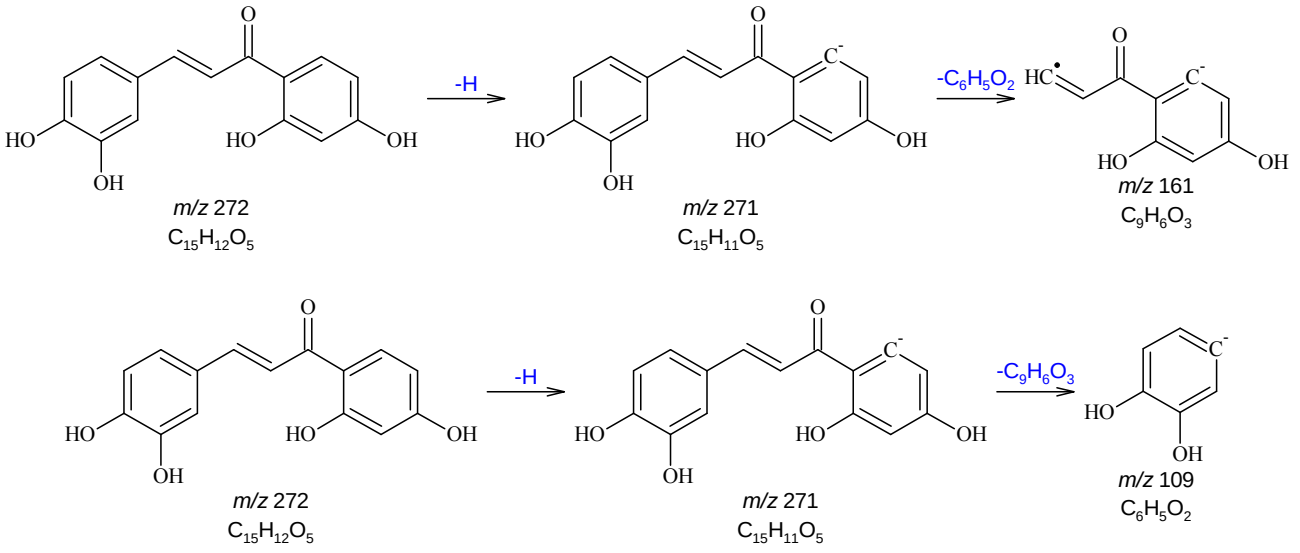

Figure 37: Fragmentation Scheme for 2',3,4,4'-Tetrahydroxychalcone (a.k.a. Butein)

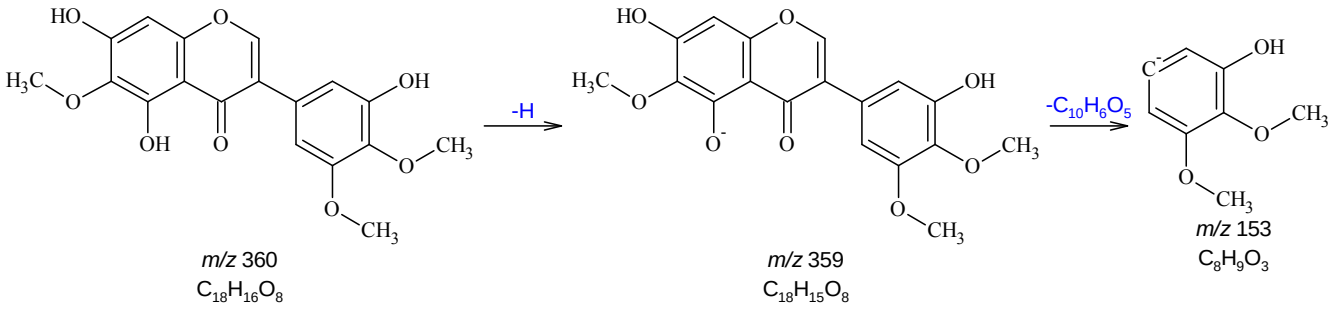

Figure 38: Fragmentation Scheme for 3',5,7-Trihydroxy-4',5',6-trimethoxyisoflavone (a.k.a. Irigenin)

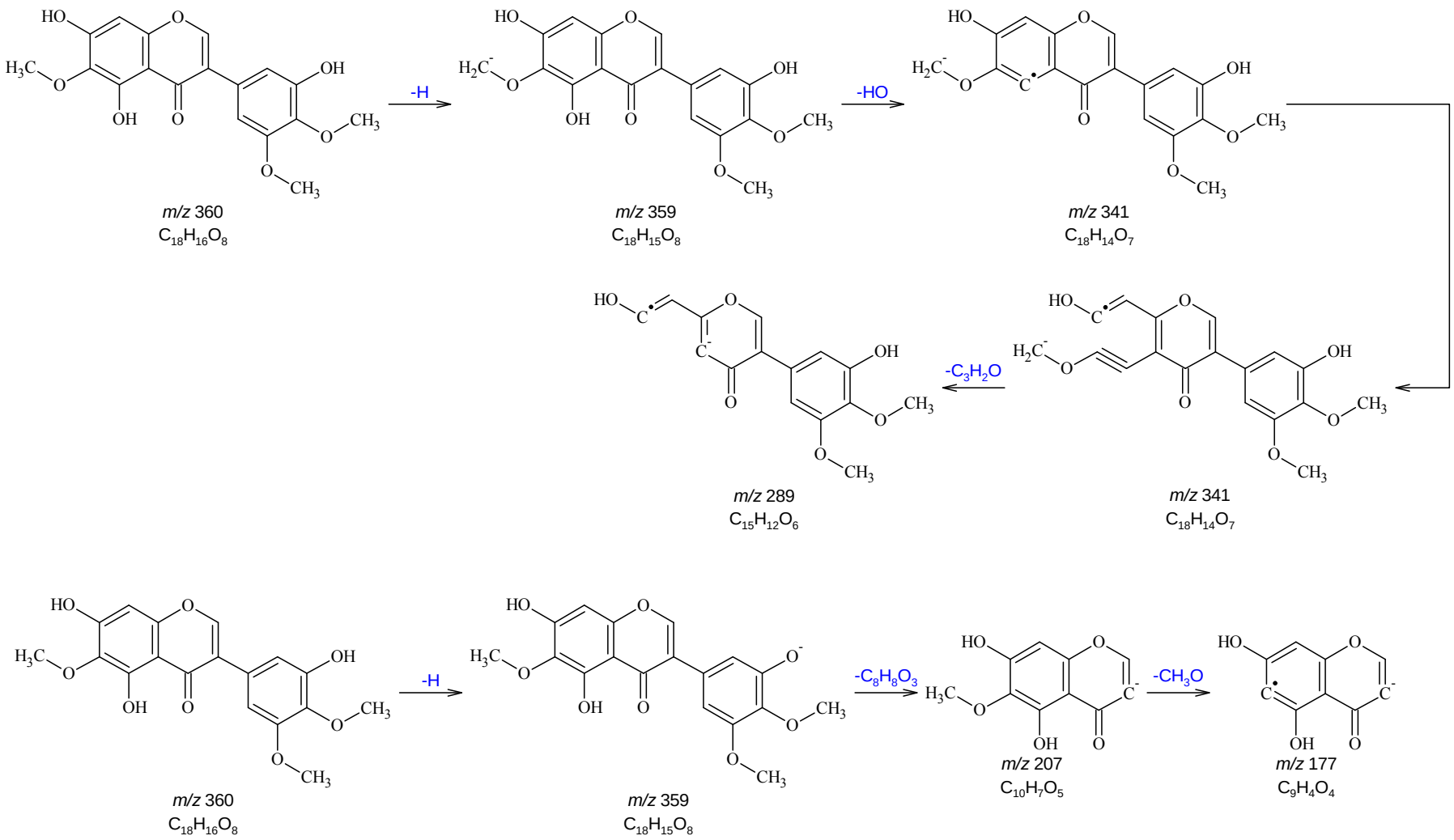

Figure 38 (cont.): Fragmentation Scheme for 3',5,7-Trihydroxy-4',5',6-trimethoxyisoflavone (a.k.a. Irigenin)

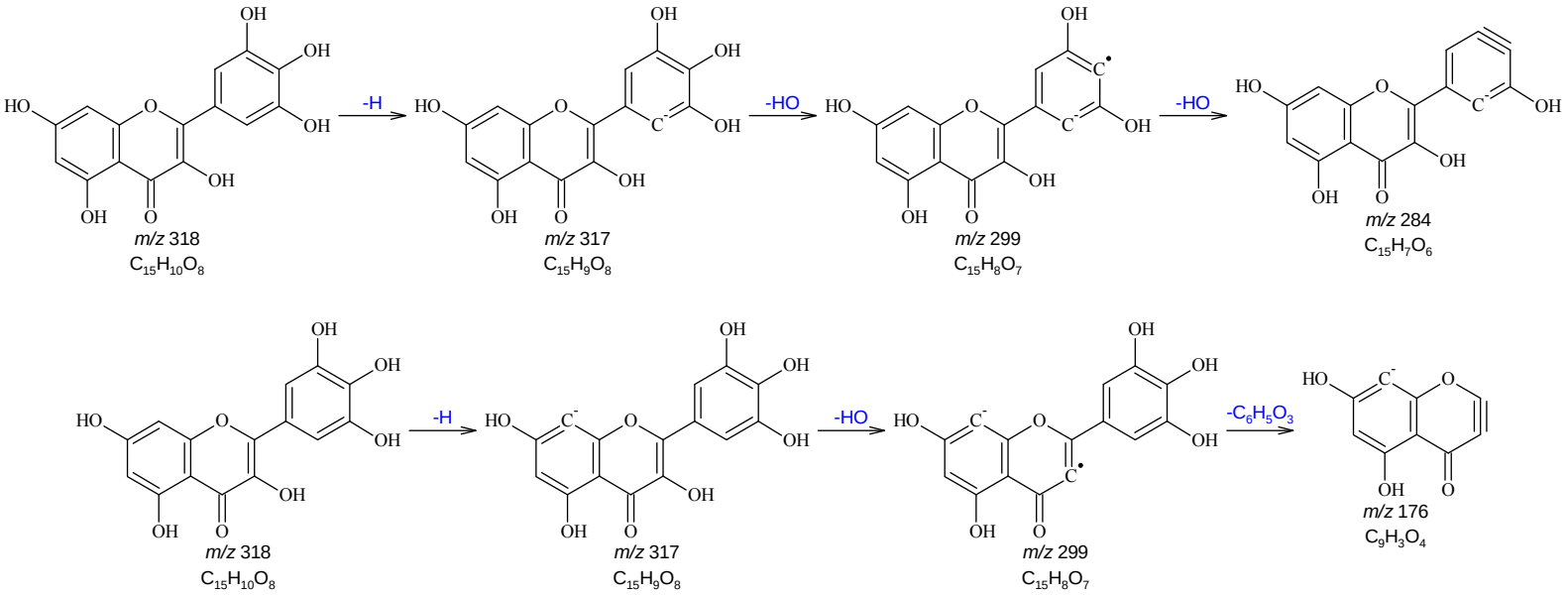

Figure 39: Fragmentation Scheme for 3,3',4',5,5',7-Hexahydroxyflavone (a.k.a. Myricetin)

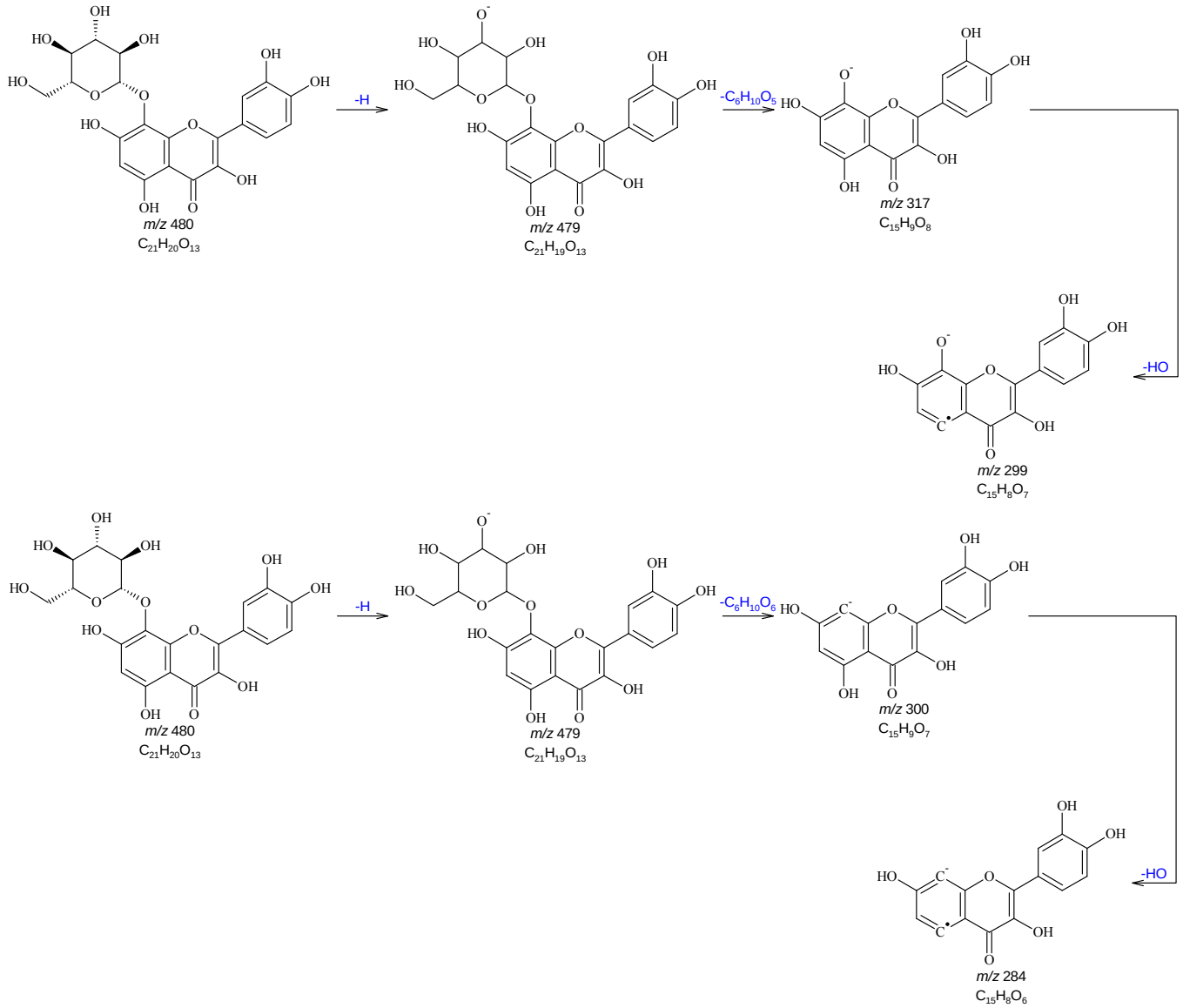

Figure 40: Fragmentation Scheme for Gossypetin-8-glucoside (a.k.a. Gossypin)

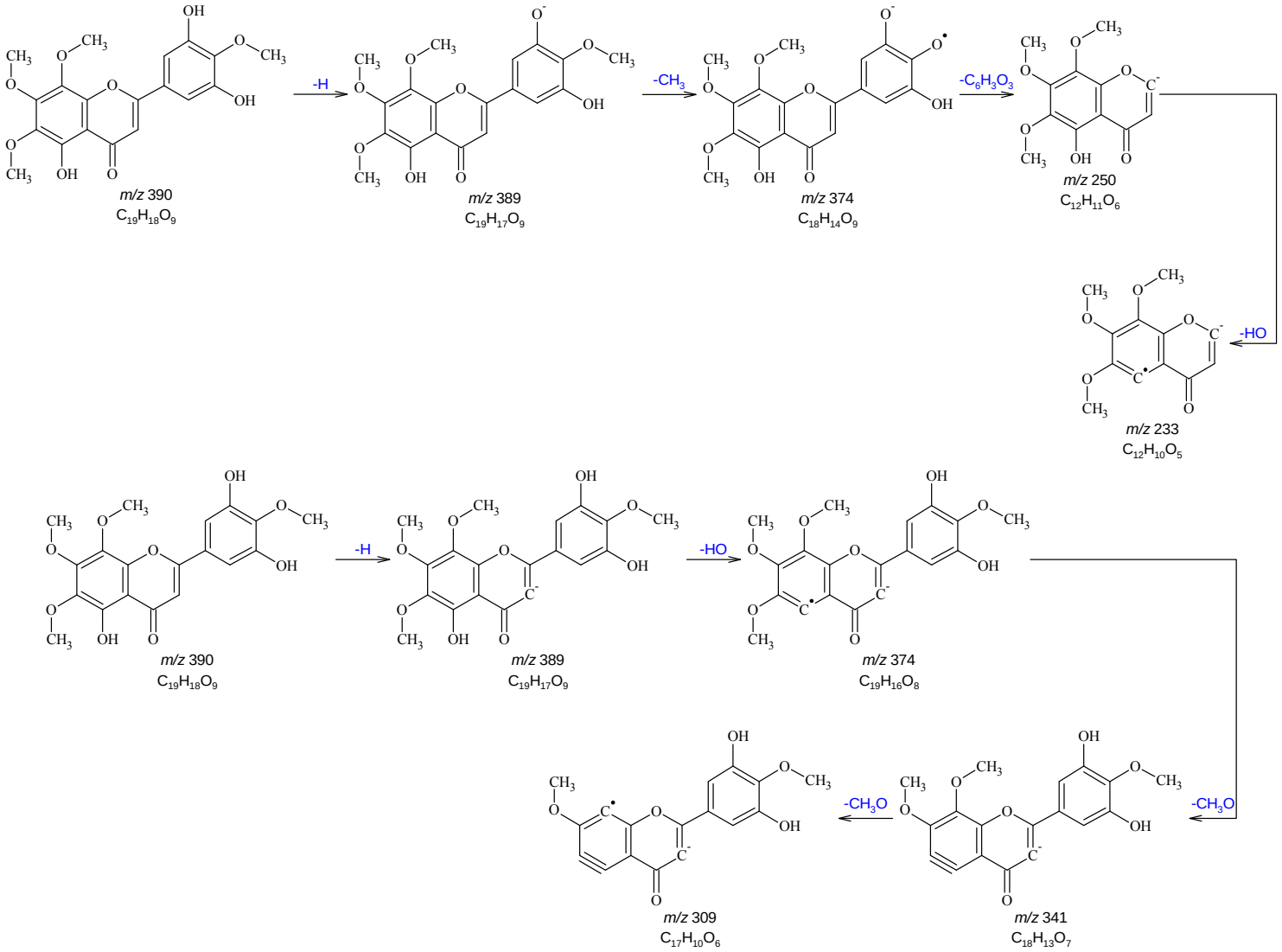

Figure 41: Fragmentation Scheme for Gardenin E

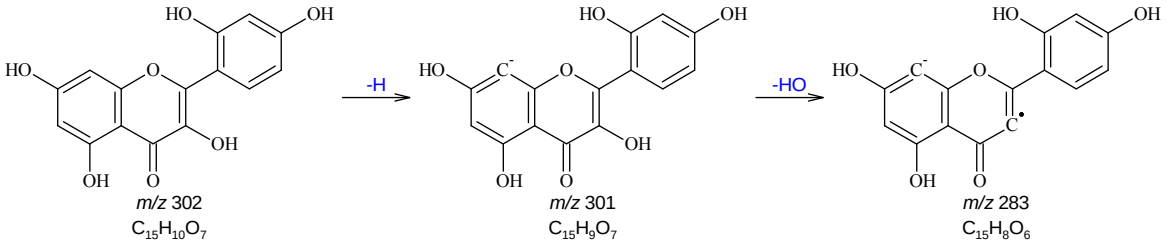

Figure 42: Fragmentation Scheme for 2',3,4',5,7-Pentahydroxyflavone (a.k.a. Morin)

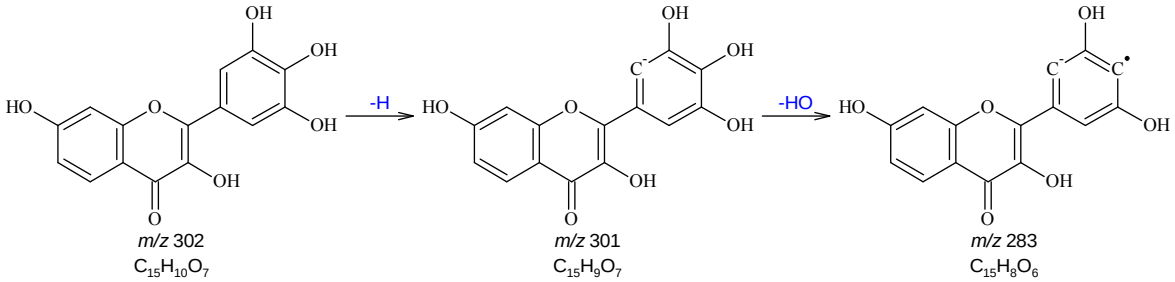

Figure 43: Fragmentation Scheme for 3,3',4',5',7-Pentahydroxyflavone (a.k.a. Robinetin)

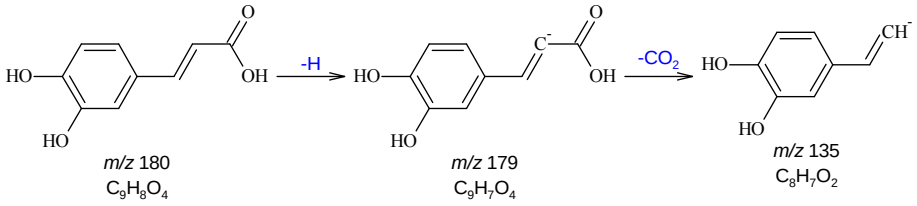

Figure 44: Fragmentation Scheme for 3,4-Dihydroxycinnamic Acid (a.k.a. Caffeic Acid)

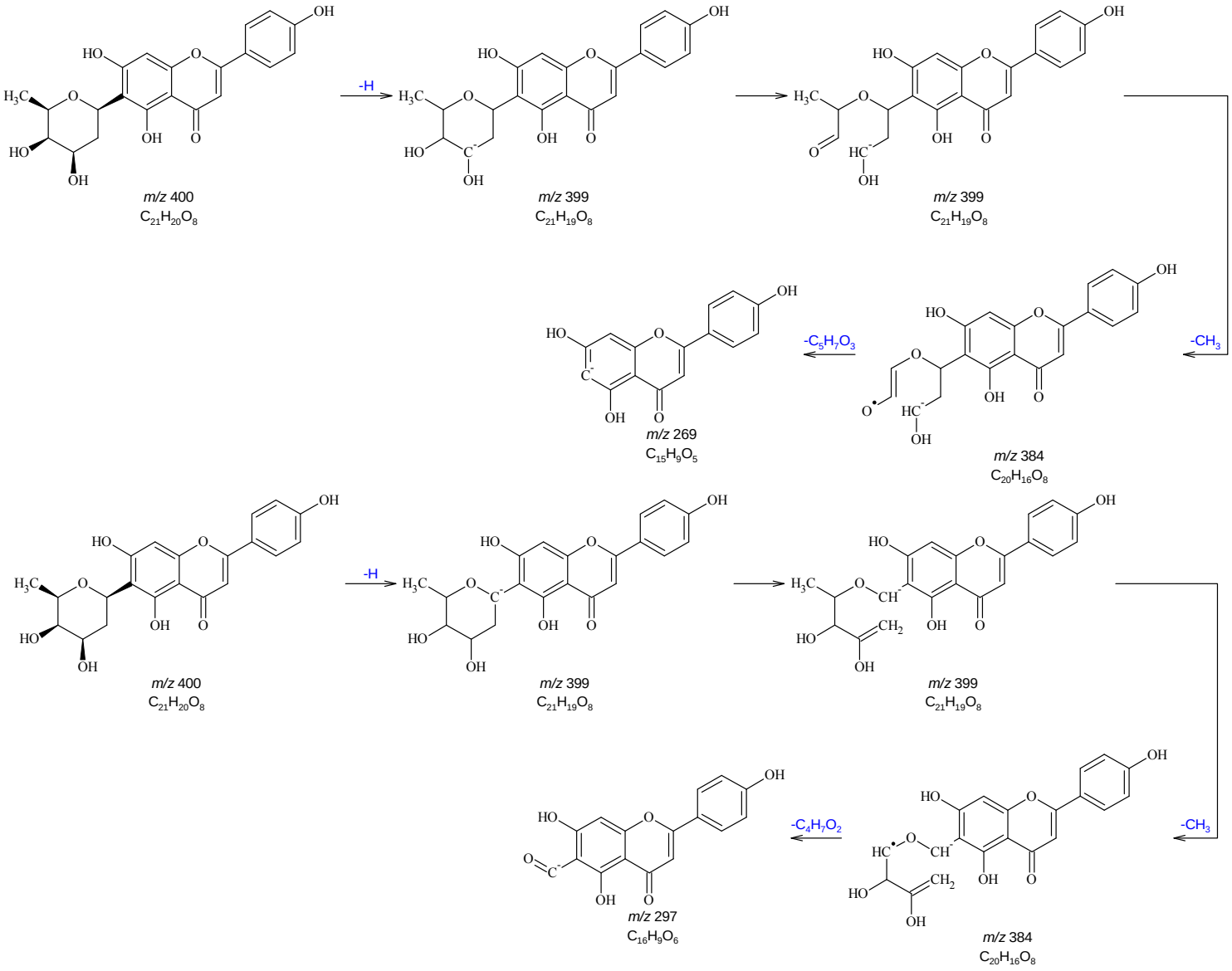

Figure 45: Fragmentation Scheme for Torosaflavone A

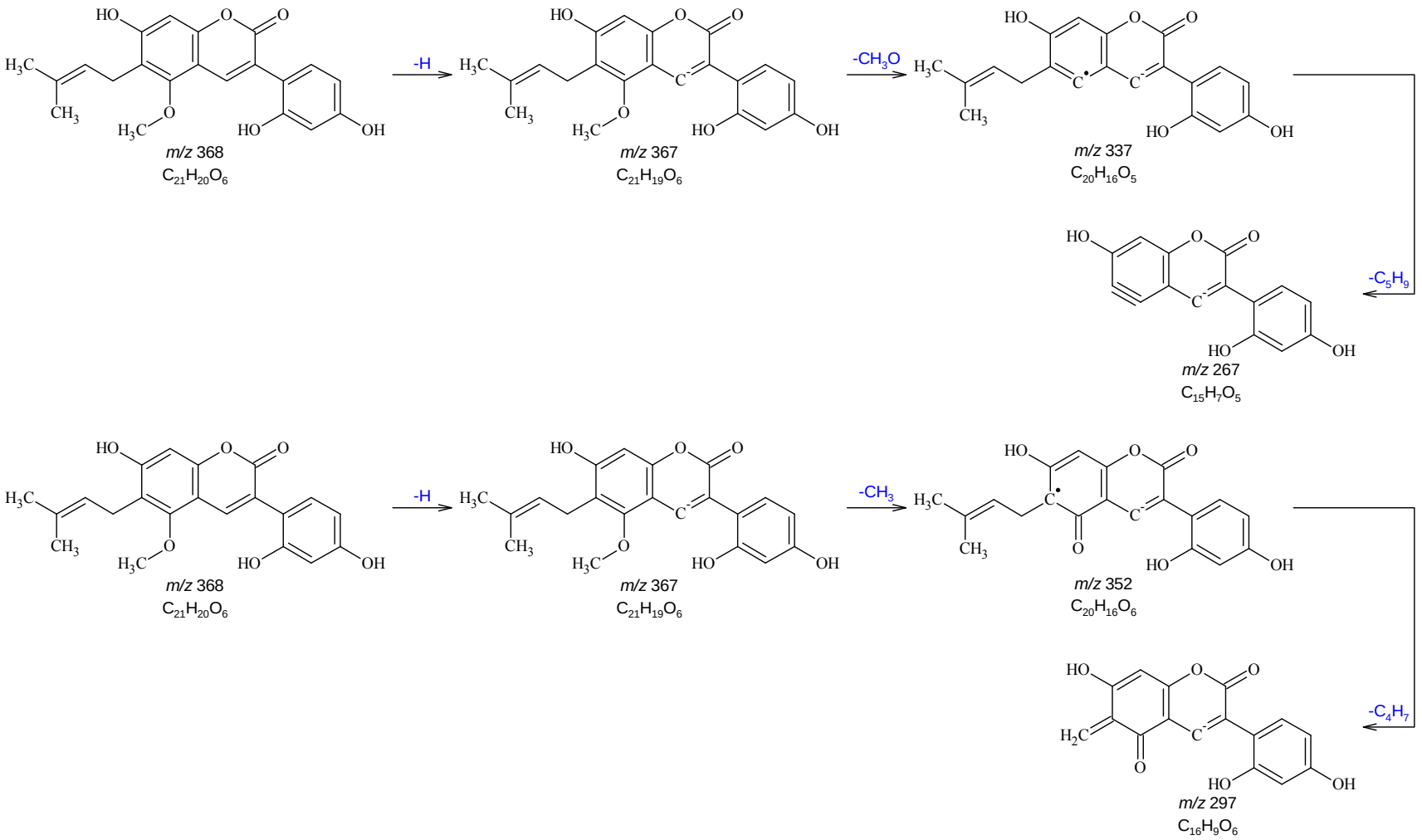

Figure 46: Fragmentation Scheme for Glycycoumarin

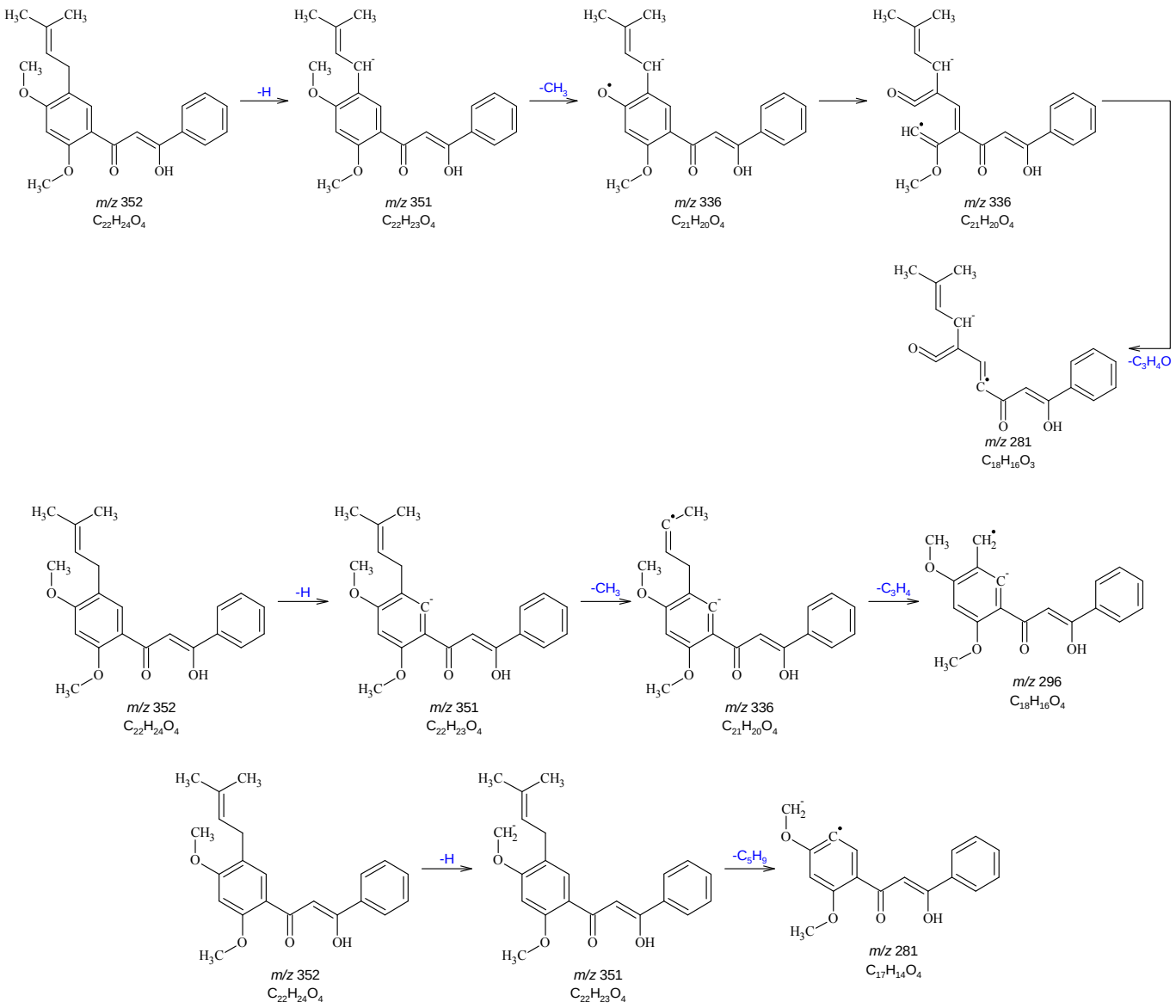

Figure 47: Fragmentation Scheme for Pongagallone A

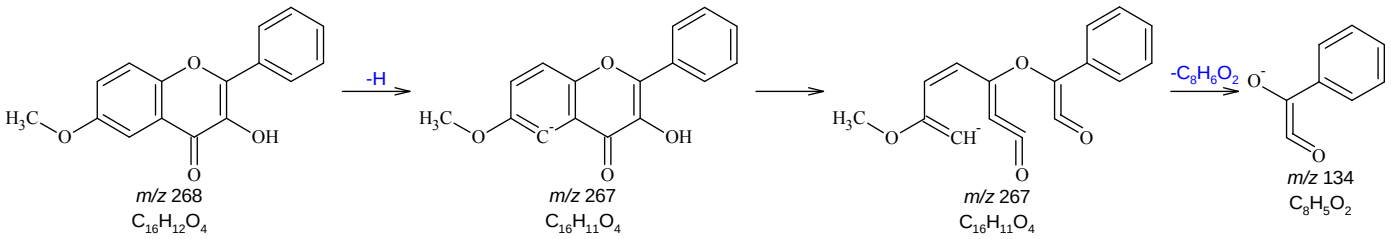

Figure 48: Fragmentation Scheme for 3-hydroxy-6-methoxyflavone

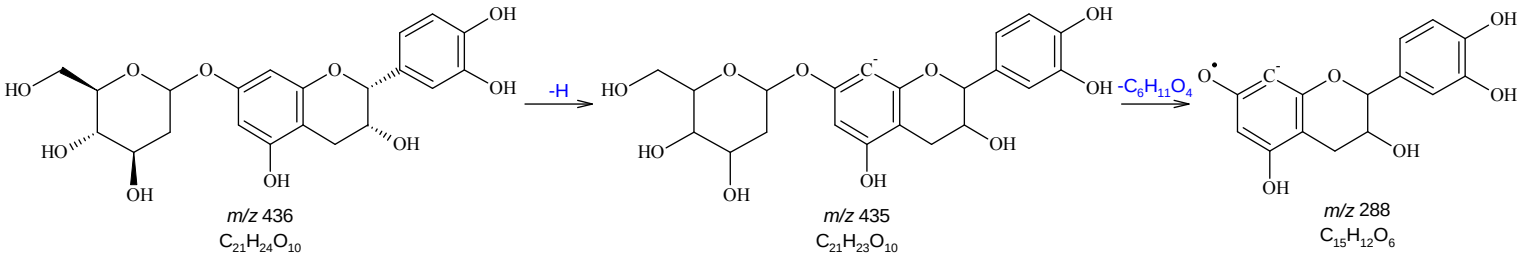

Figure 49: Fragmentation Scheme for Catechin-7-O-rhamnoside

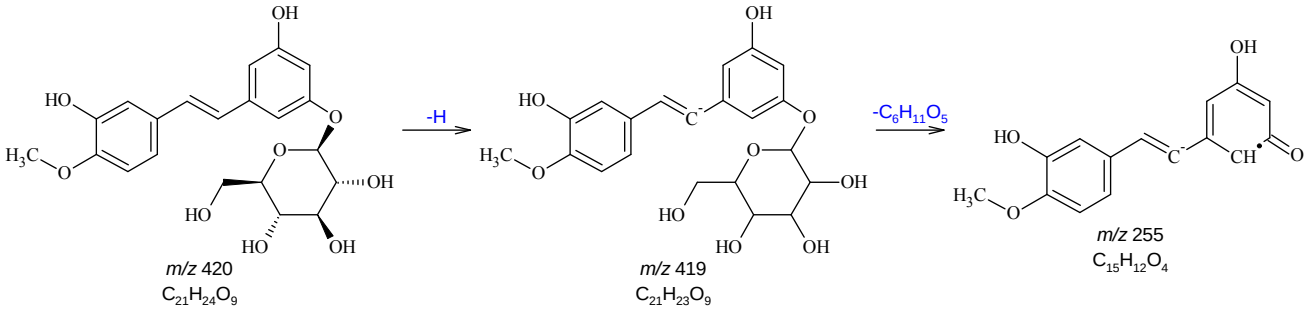

Figure 50: Fragmentation Scheme for 4'-Methoxy-3,3',5-stilbenetriol 3-Glucoside

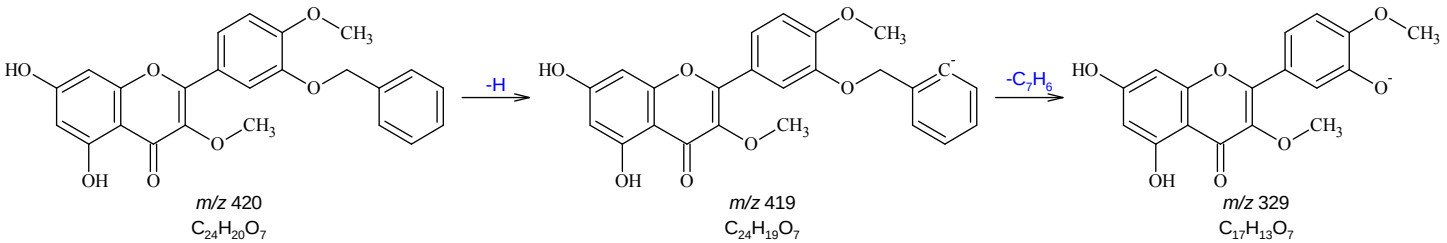

Figure 51: Fragmentation Scheme for 3'-Benzyloxy-5,7-dihydroxy-3,4'-dimethoxyflavone

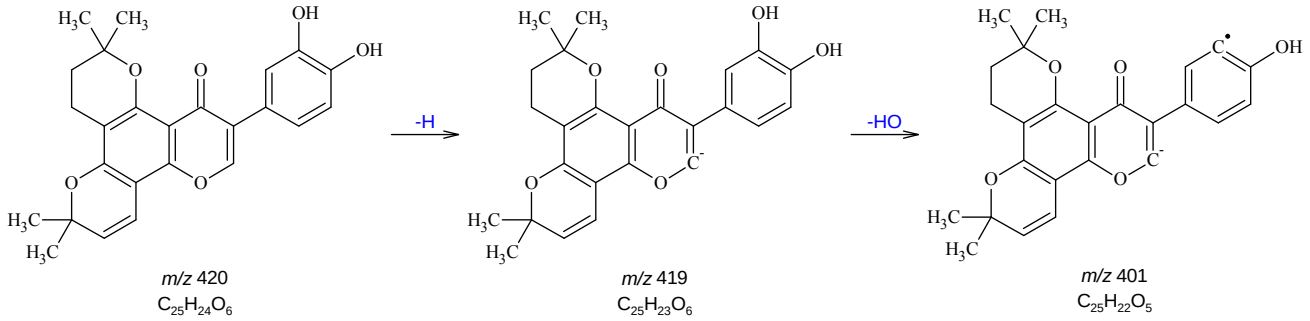

Figure 52: Fragmentation Scheme for Isopomiferin

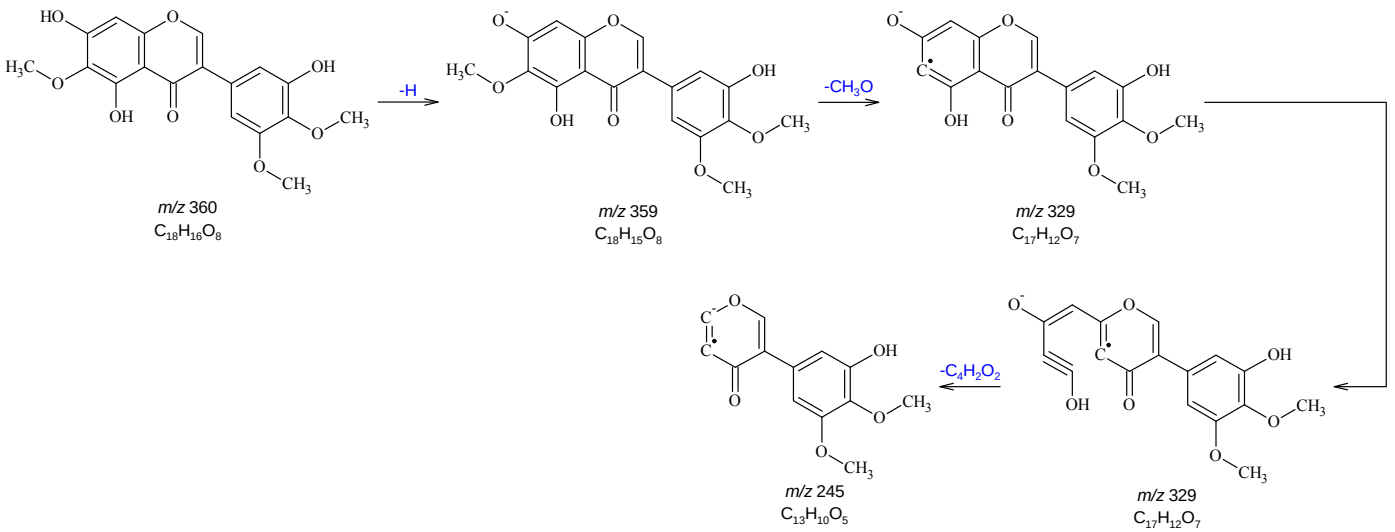

Figure 53: Fragmentation Scheme for 3',5,7-Trihydroxy-4',5',6-trimethoxyisoflavone (a.k.a. Irigenin)

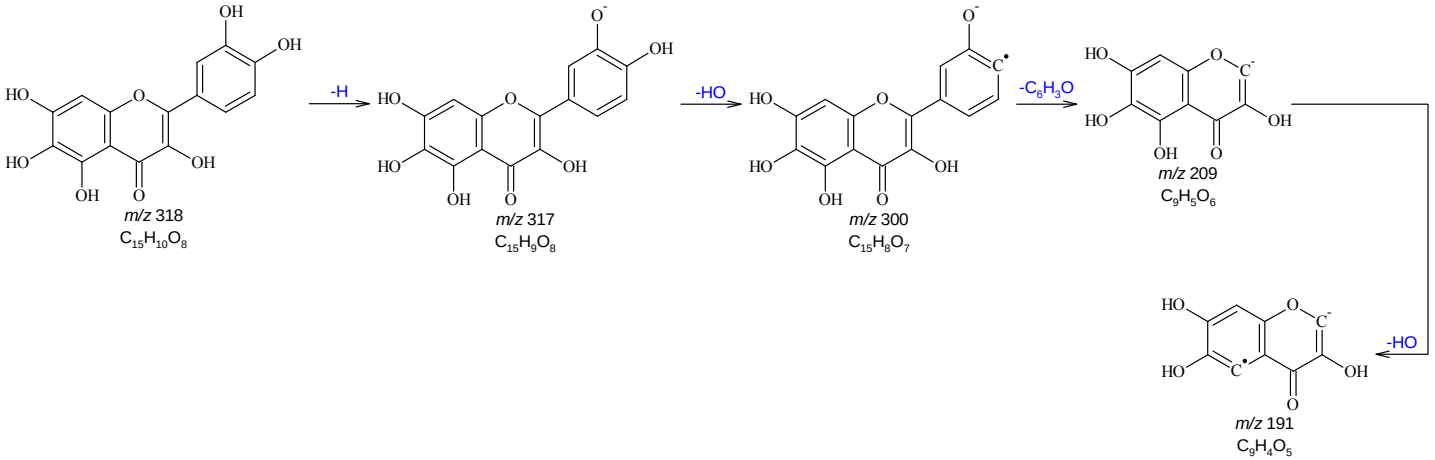

Figure 54: Fragmentation Scheme for 3,3',4',5,6,7-Hexahydroxyflavone (a.k.a. Quercetagetin)

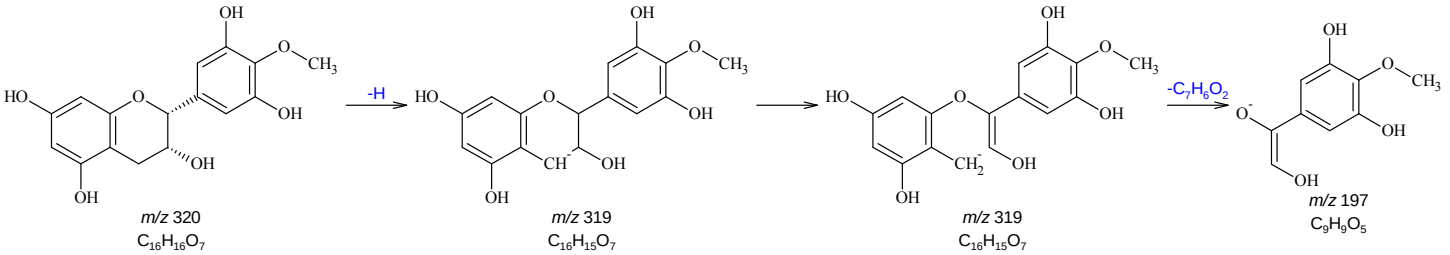

Figure 55: Fragmentation Scheme for Oureatacatechin

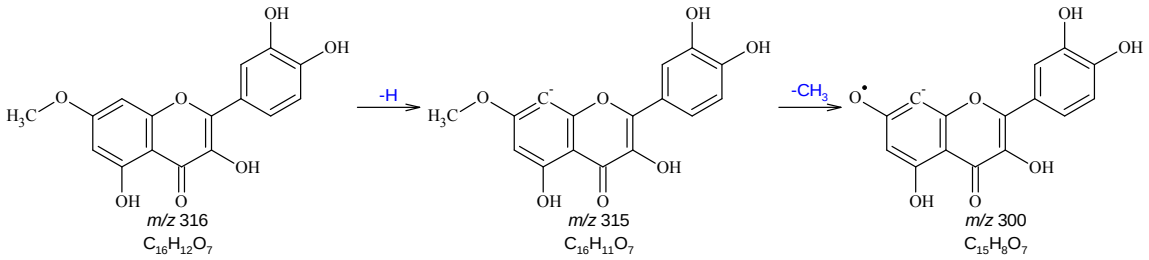

Figure 56: Fragmentation Scheme for 7-methylquercetin (a.k.a. Rhamnetin)

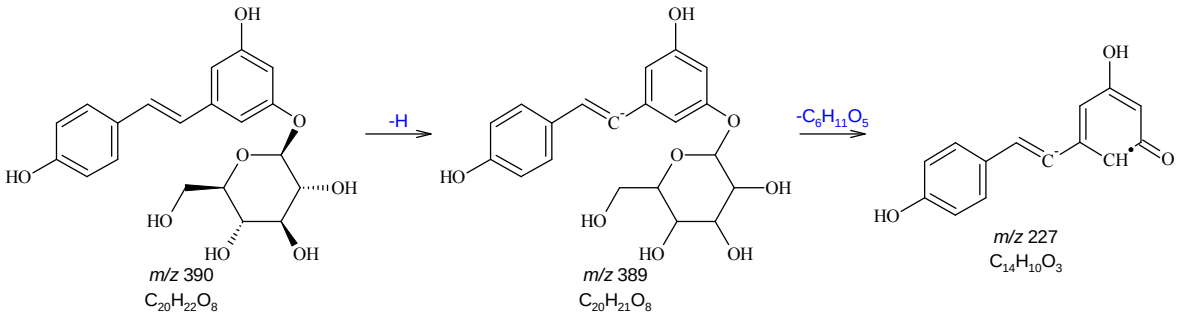

Figure 57: Fragmentation Scheme for Resveratrol-3-b-mono-D-glucoside

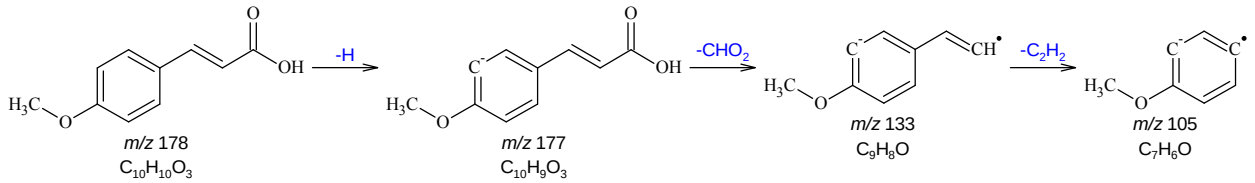

Figure 58: Fragmentation Scheme for 4-Methoxycinnamic Acid

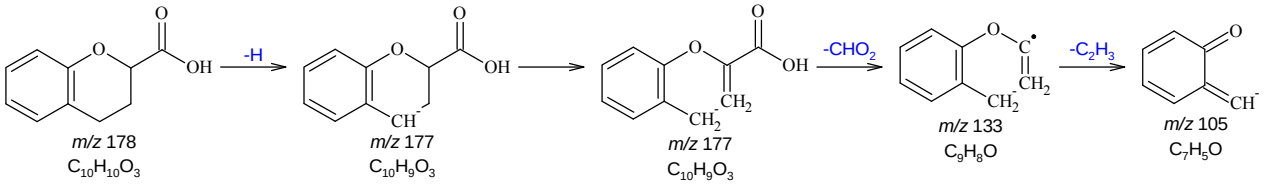

Figure 59: Fragmentation Scheme for Chroman-2-carboxylic Acid

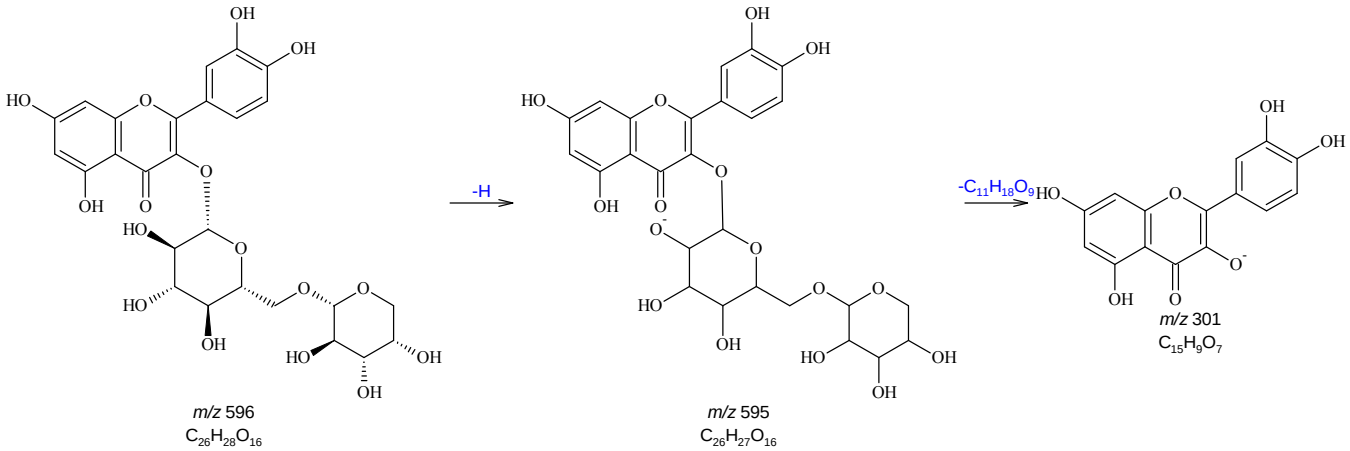

Figure 60: Fragmentation Scheme for Quercetin-3-arabinoglucoside (a.k.a. Peltatoside)

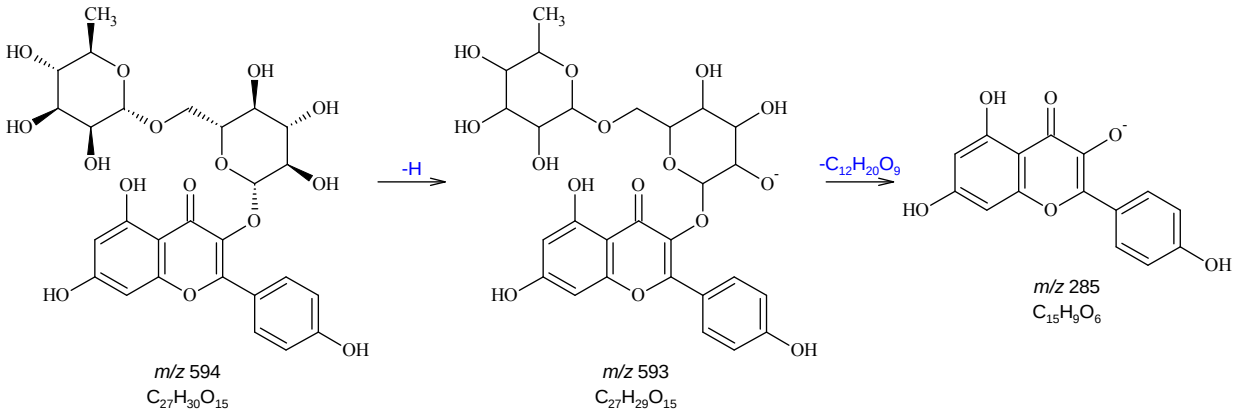

Figure 61: Fragmentation Scheme for Kaempferol-7-rutinoside

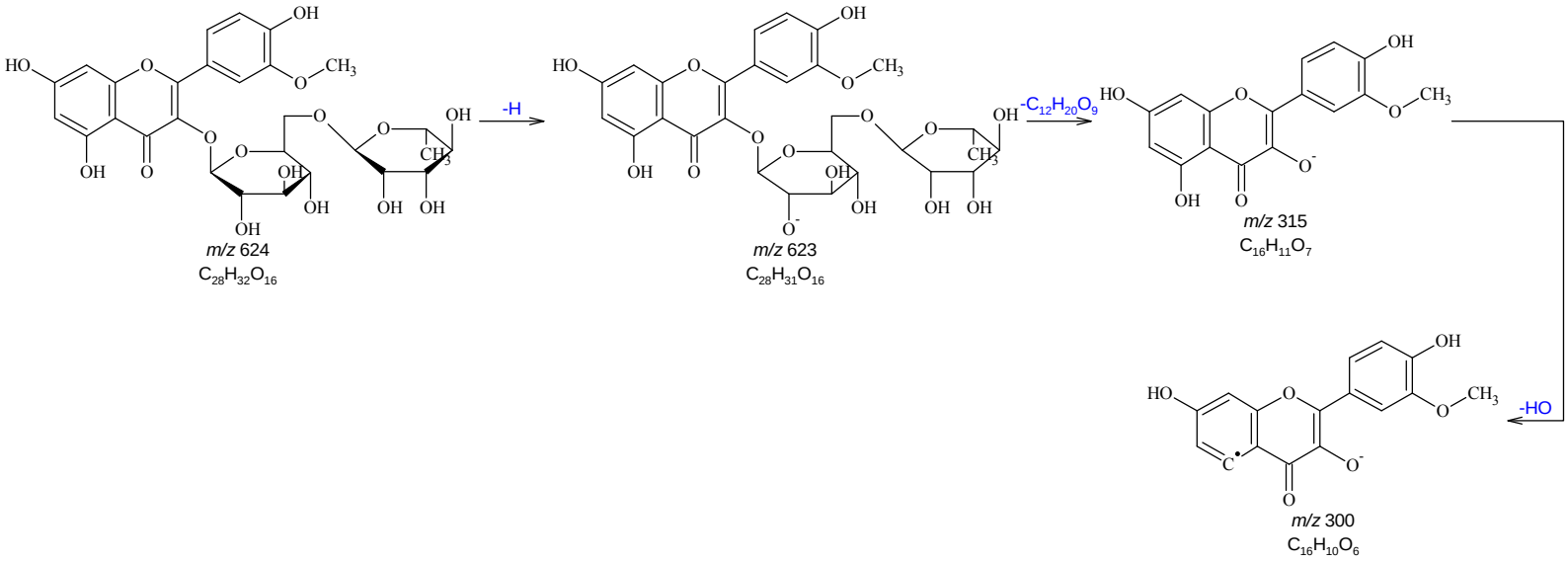

Figure 62: Fragmentation Scheme for Isorhamnetin-3-O-rutinoside

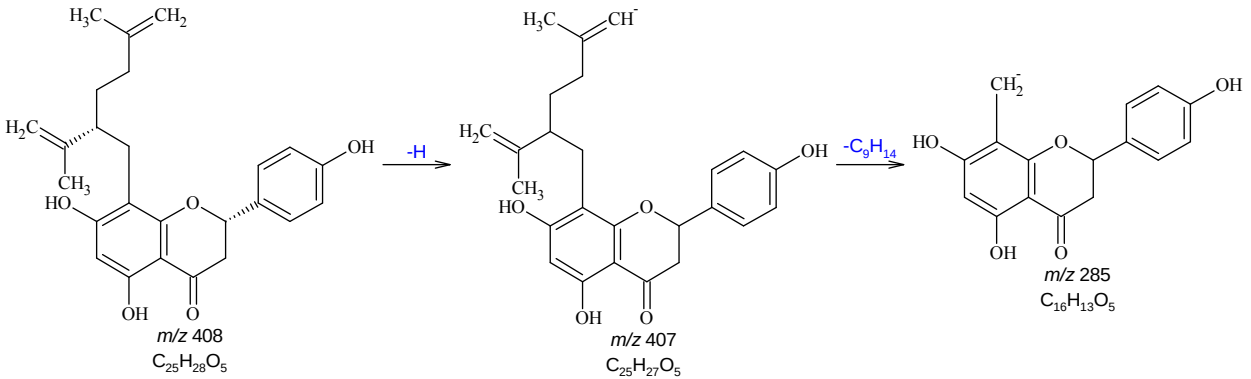

Figure 63: Fragmentation Scheme for Remangiflavanone

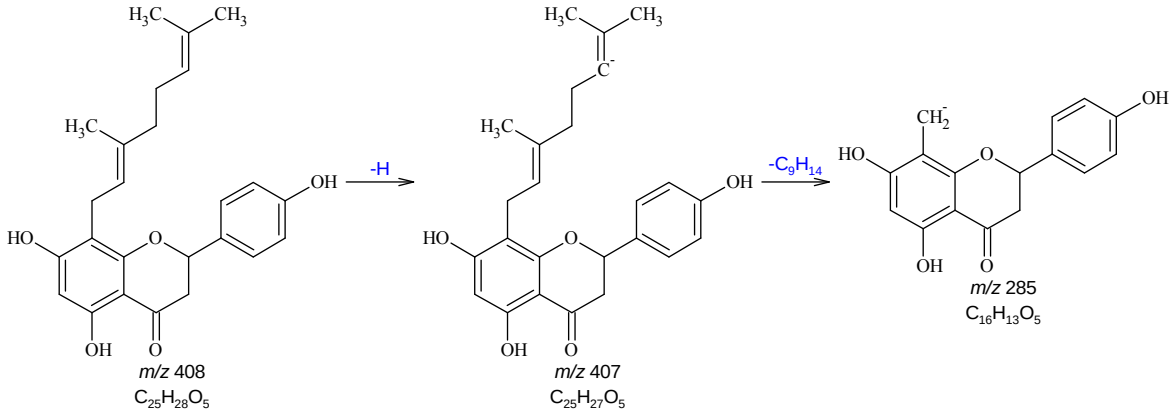

Figure 64: Fragmentation Scheme for Sophora-flavanone

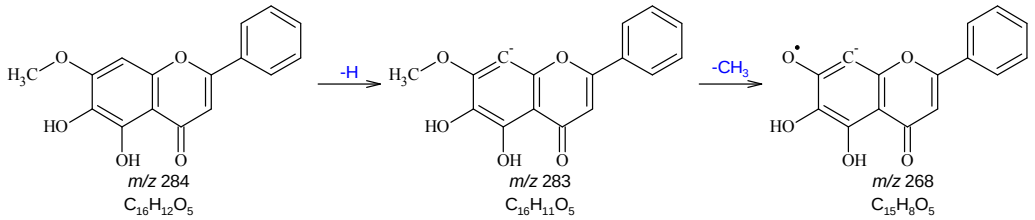

Figure 65: Fragmentation Scheme for 5,6-Dihydroxy-7-methoxyflavone (a.k.a. Negletein)

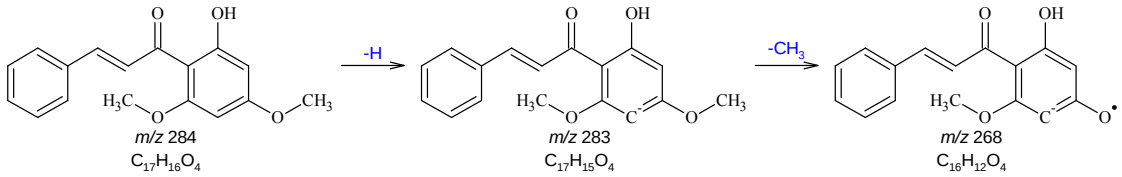

Figure 66: Fragmentation Scheme for 2'-Hydroxy-4',6'-dimethoxychalcone

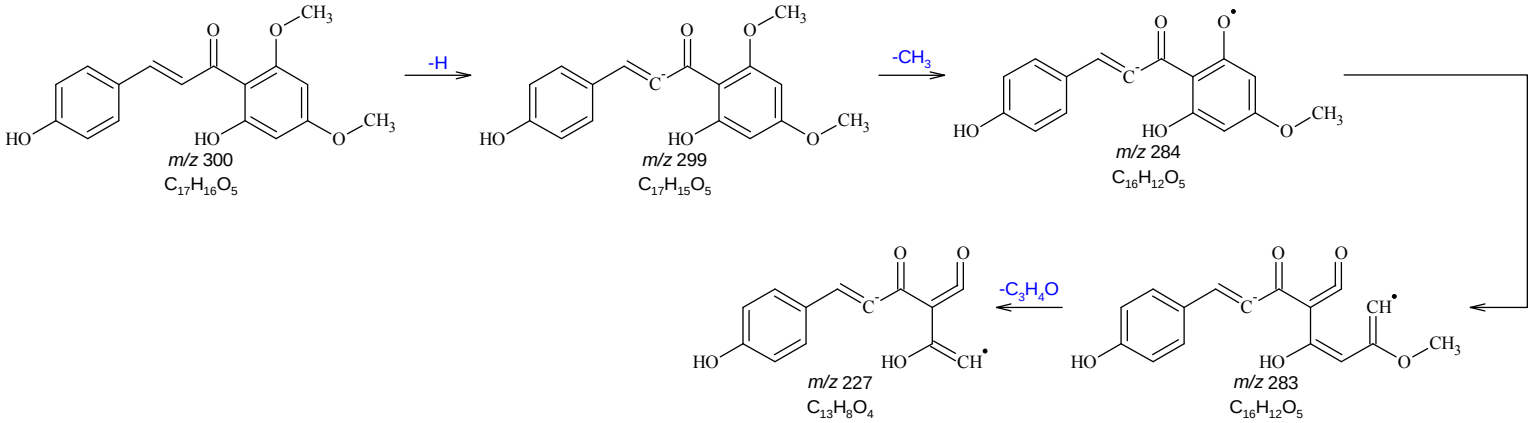

Figure 67: Fragmentation Scheme for 2',4-Dihydroxy-4',6'-dimethoxychalcone

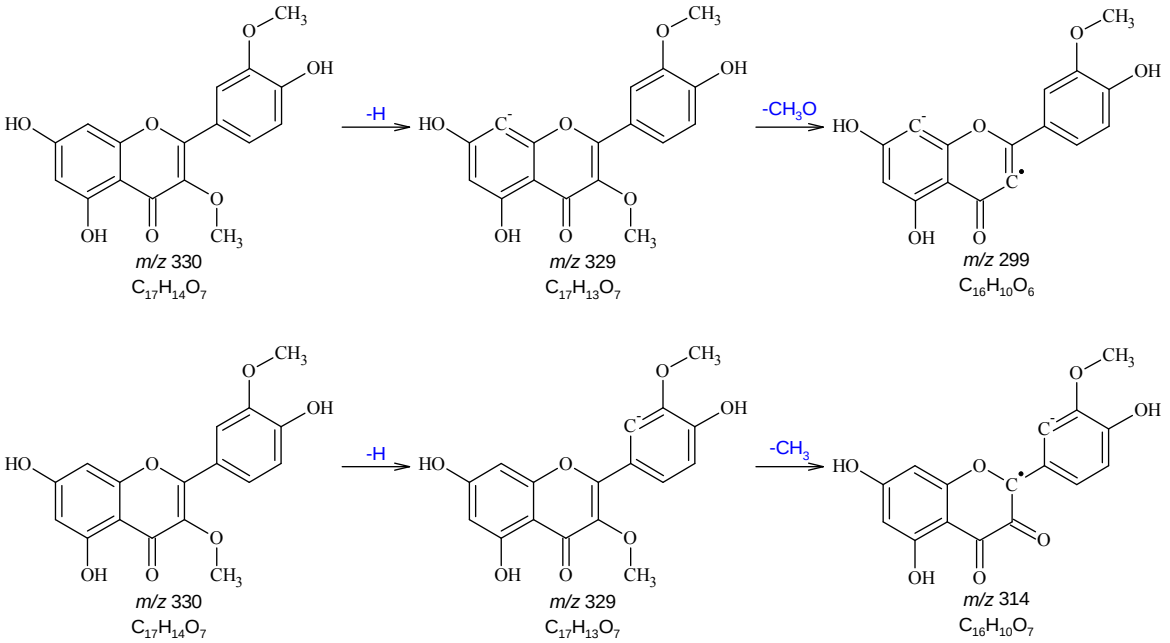

Figure 68: Fragmentation Scheme for Isorhamnetin-3-methoxy

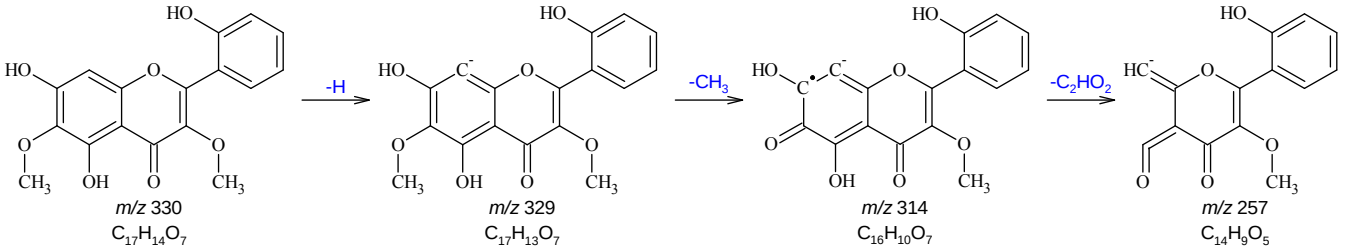

Figure 69: Fragmentation Scheme for Irisflavone A

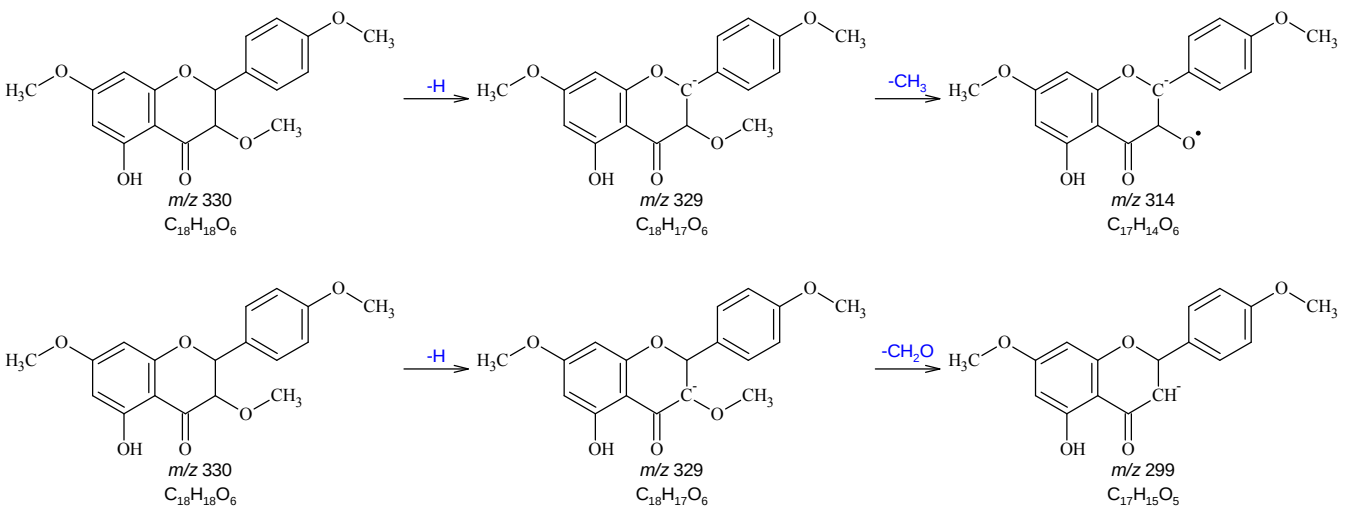

Figure 70: Fragmentation Scheme for Kaempferol-3,7,4'-Trimethylether

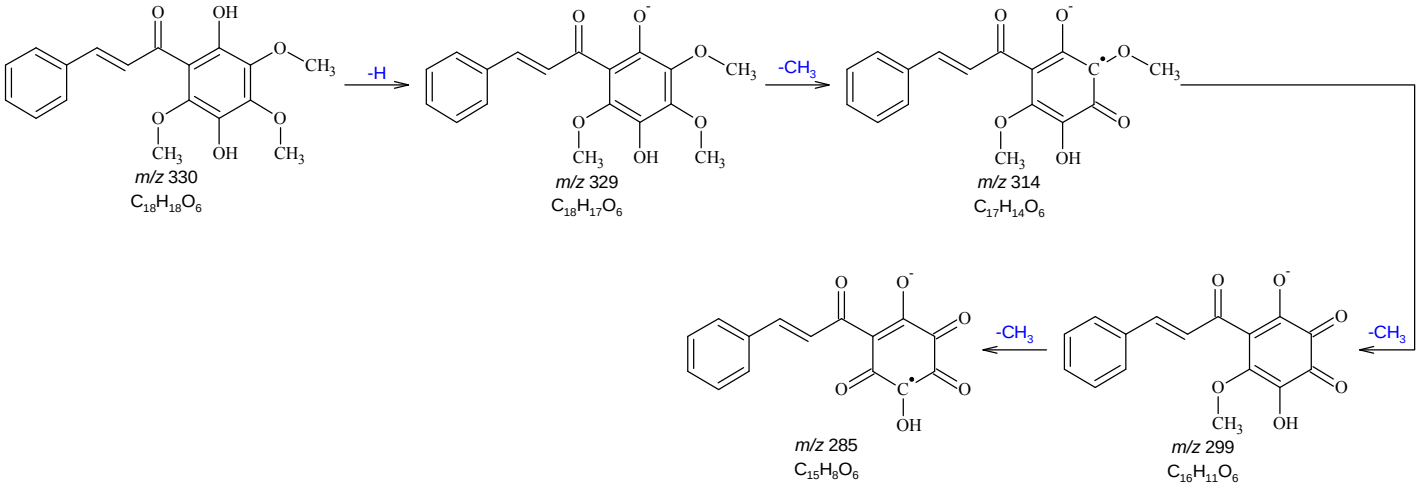

Figure 71: Fragmentation Scheme for 3',6'-Dihydroxy-2',4',5'-trimethoxychalcone

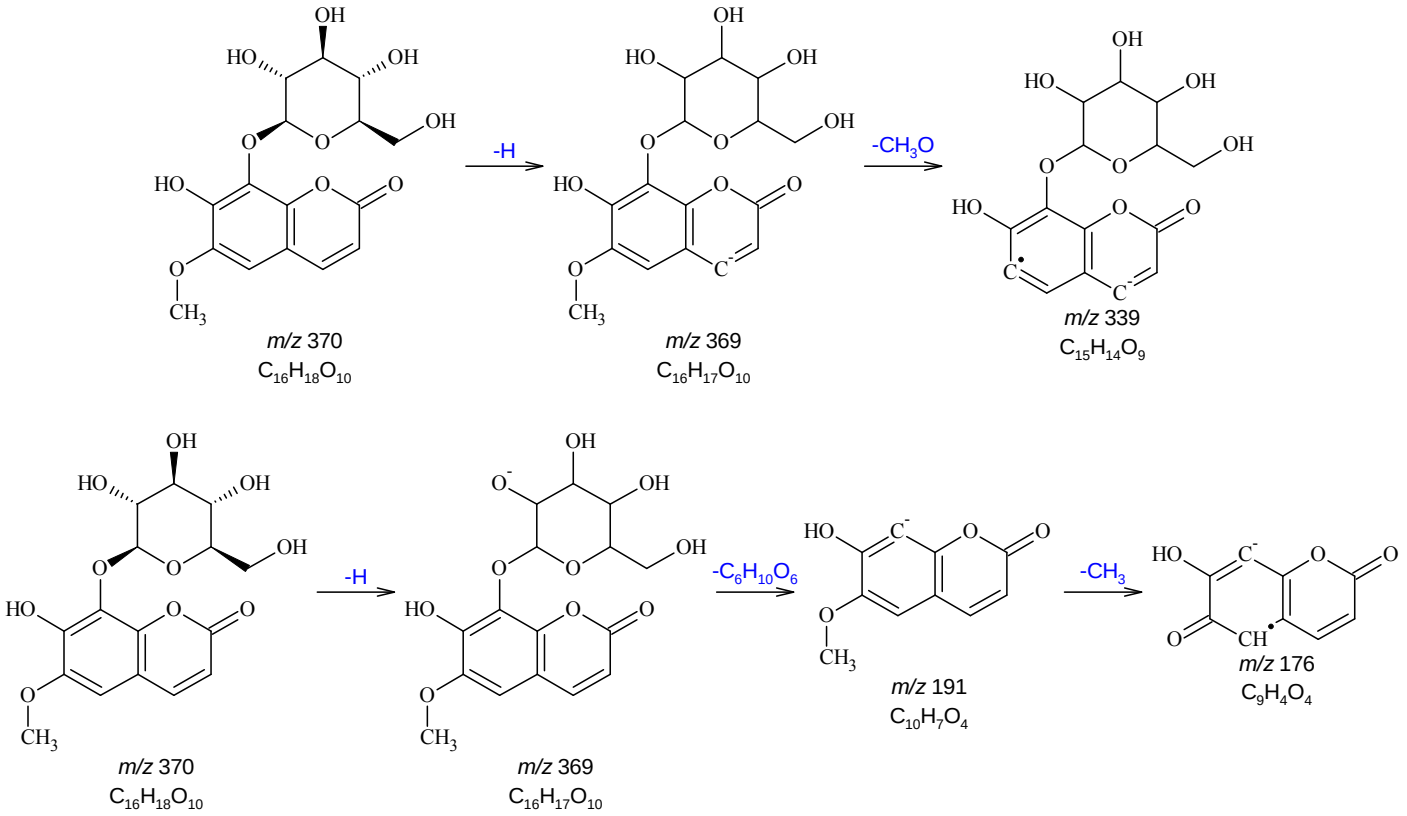

Figure 72: Fragmentation Scheme for Fraxetin-8-glucoside (a.k.a. Fraxin)

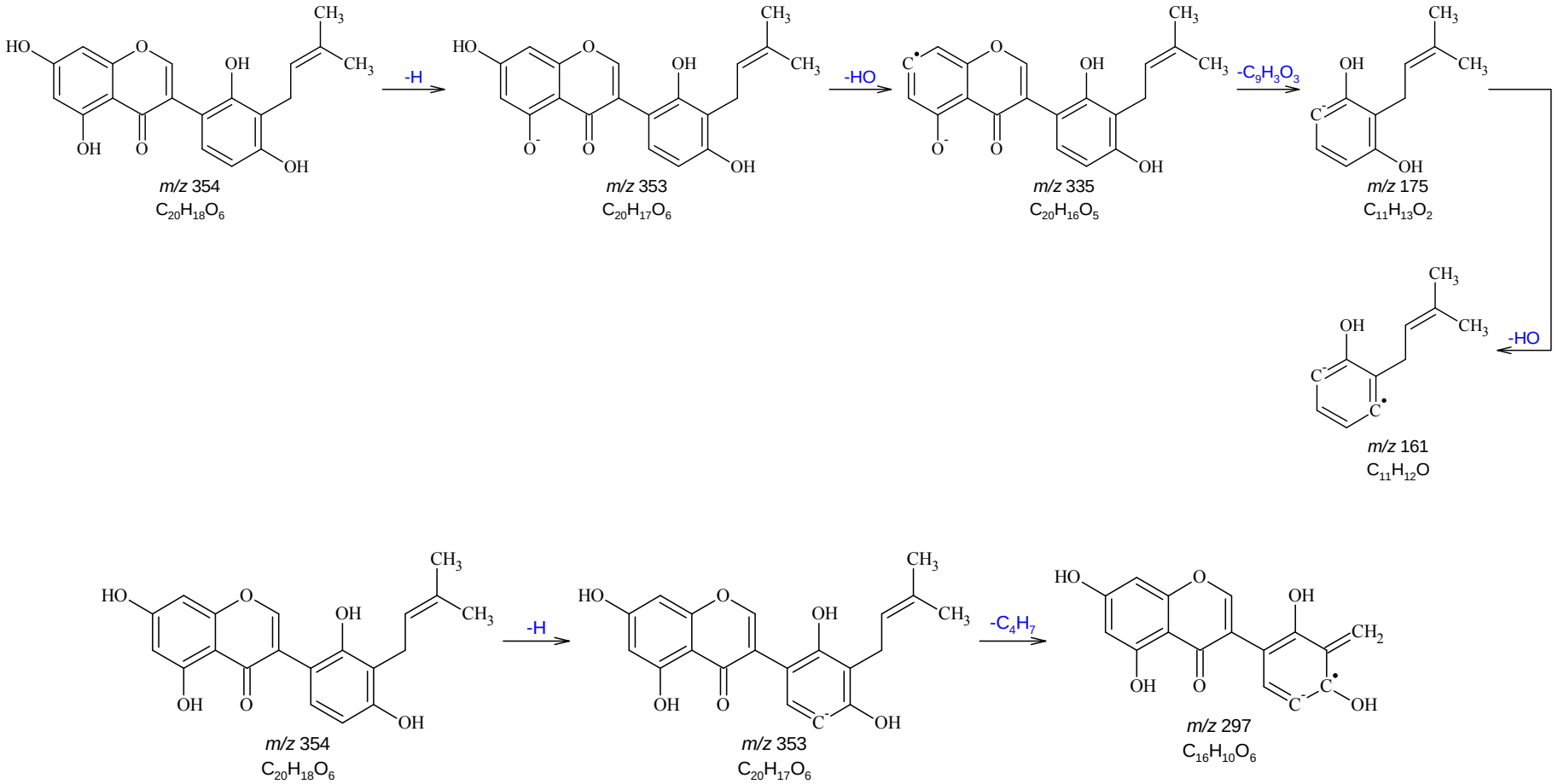

Figure 73: Fragmentation Scheme for Lico-iso-flavone A

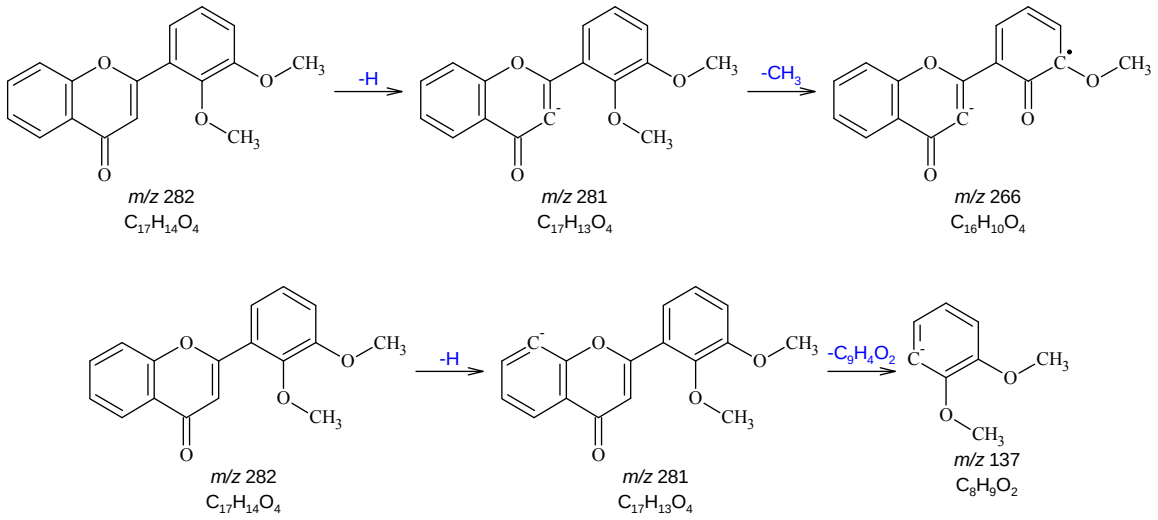

Figure 74: Fragmentation Scheme for 2',3'-Dimethoxyflavone

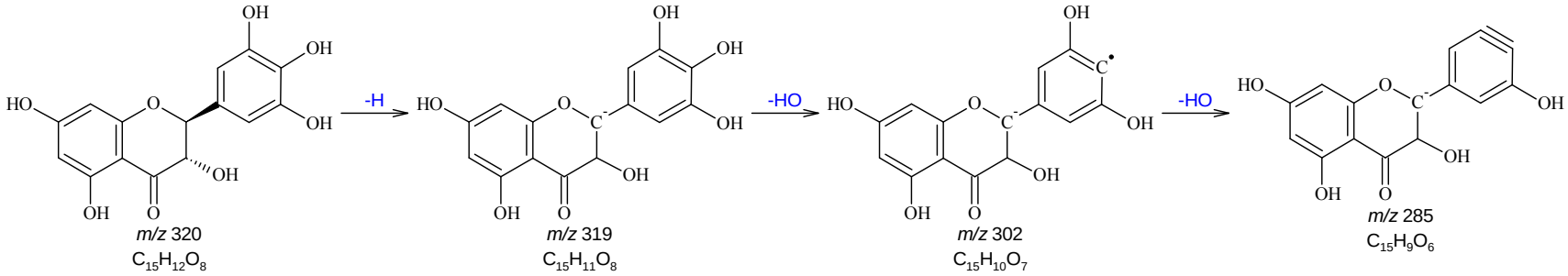

Figure 75: Fragmentation Scheme for 3,3',4',5,5',7-Hexahydroxyflavanone (a.k.a. Dihydromyricetin)

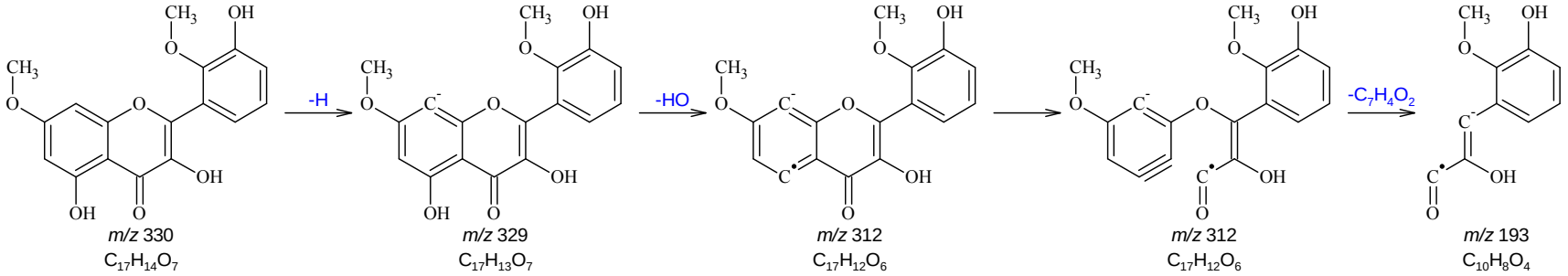

Figure 76: Fragmentation Scheme for Irisflavone D

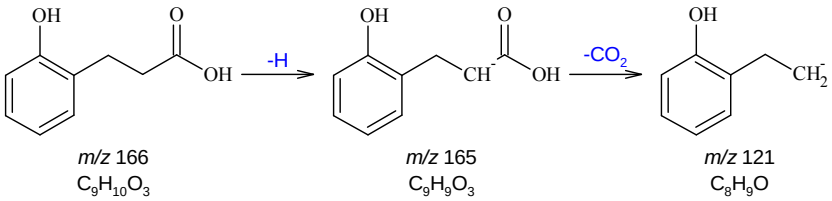

Figure 77: Fragmentation Scheme for o-Hydrocoumaric Acid

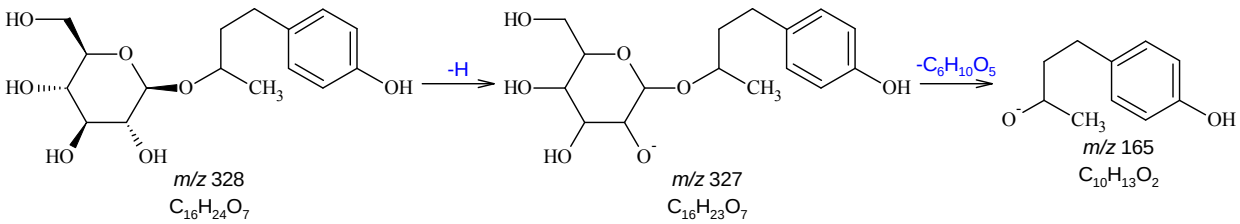

Figure 78: Fragmentation Scheme for Betuloside

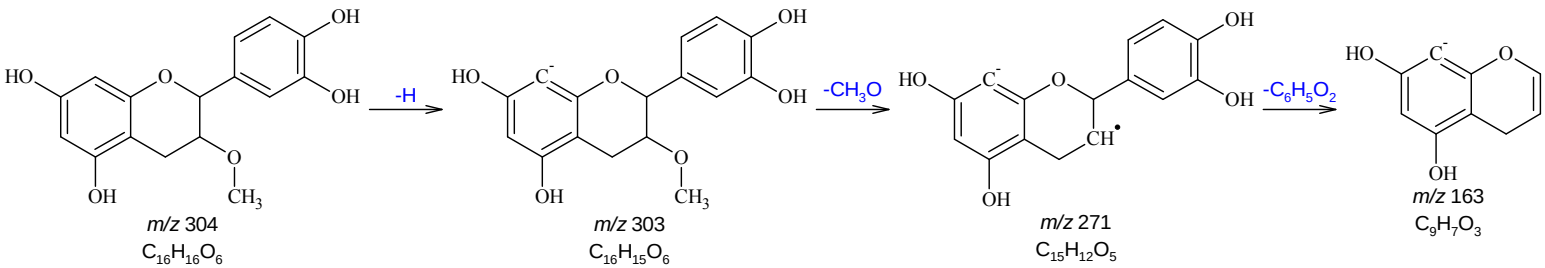

Figure 79: Fragmentation Scheme for 3'-O-Methylcatechin

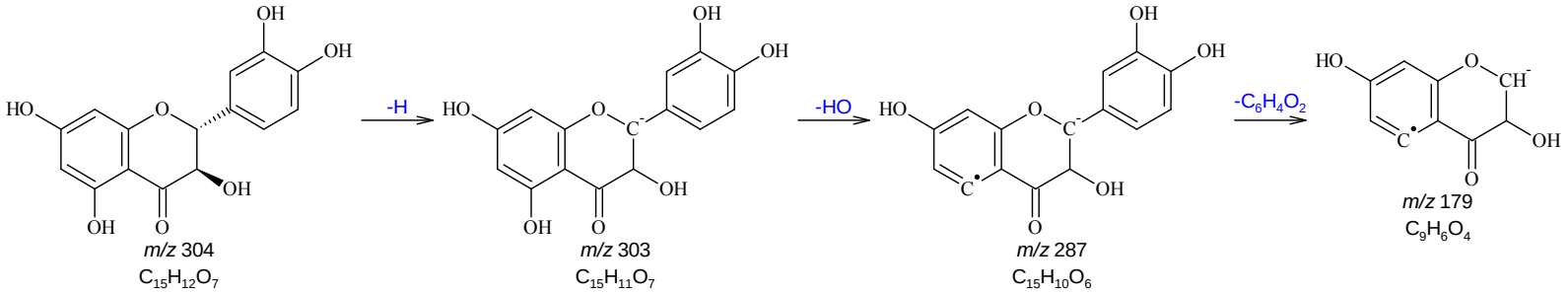

Figure 80: Fragmentation Scheme for Dihydroquercetin (a.k.a. Taxifolin)

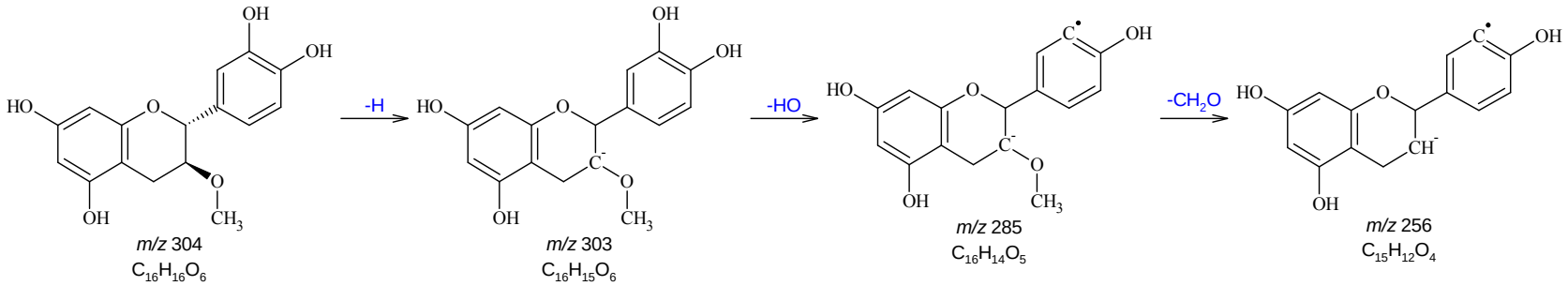

Figure 81: Fragmentation Scheme for 3-Methoxy-3',4',5,7-flavantetrol (a.k.a. Meciadanol)

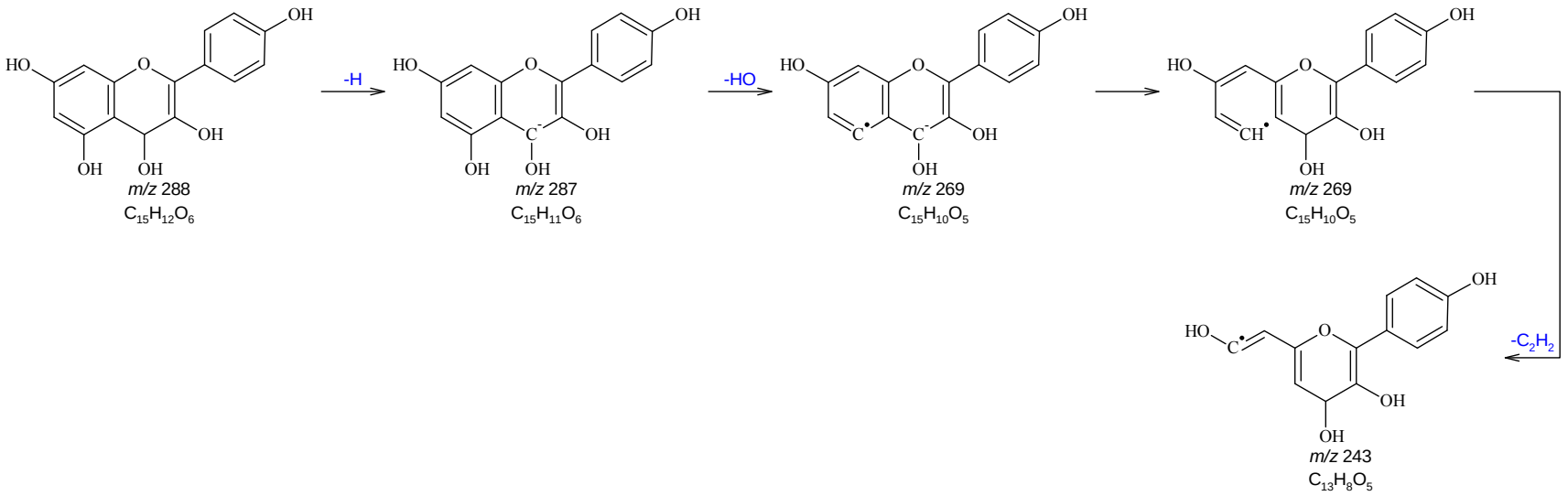

Figure 82: Fragmentation Scheme for Dihydrokaempferol

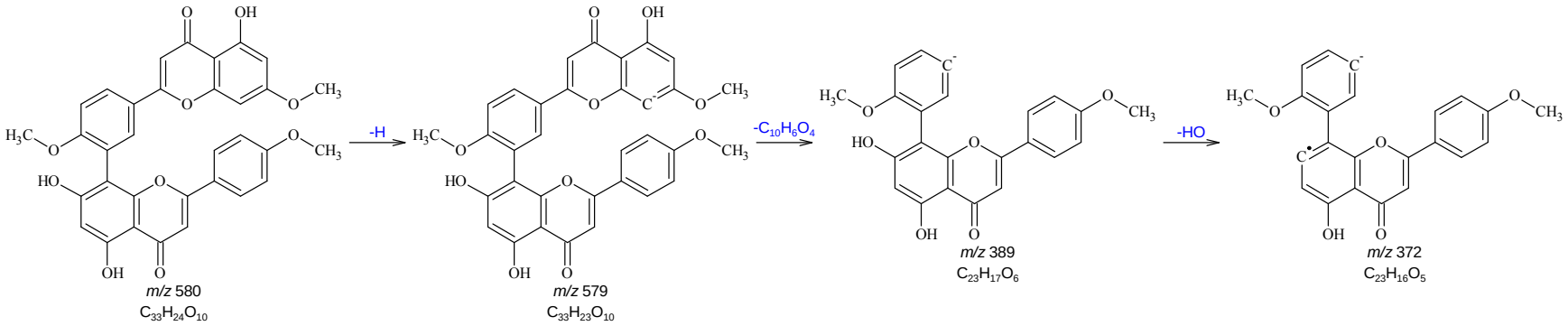

Figure 83: Fragmentation Scheme for Amentoflavone-4',4'',7-trimethyl Ether (a.k.a. Sciatopitysin)

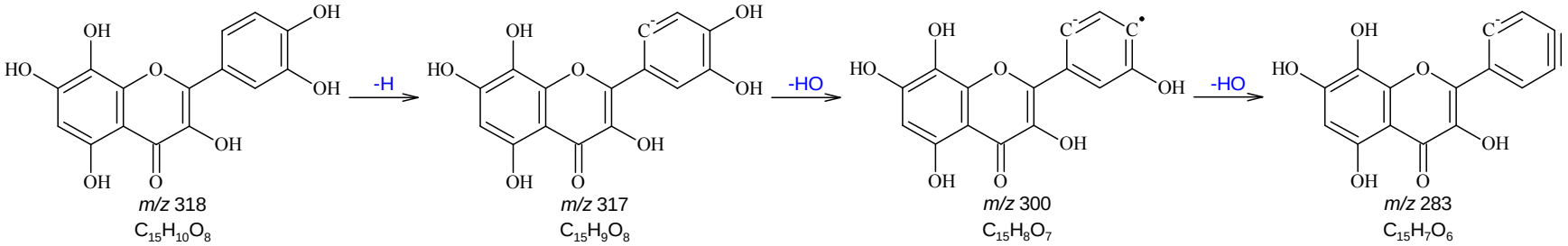

Figure 84: Fragmentation Scheme for 3,3',4',5,7,8-Hexahydroxyflavone (a.k.a. Gossypetin)

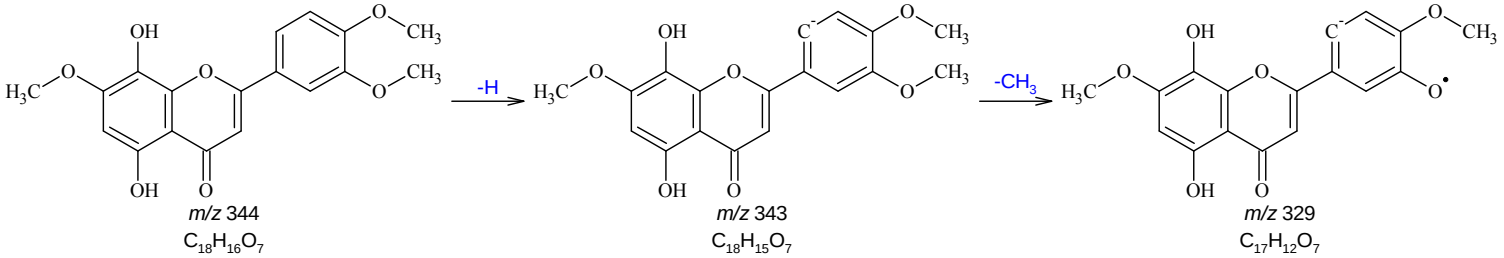

Figure 85: Fragmentation Scheme for Gossypetin 3,3',4',7-tetramethyl Ether

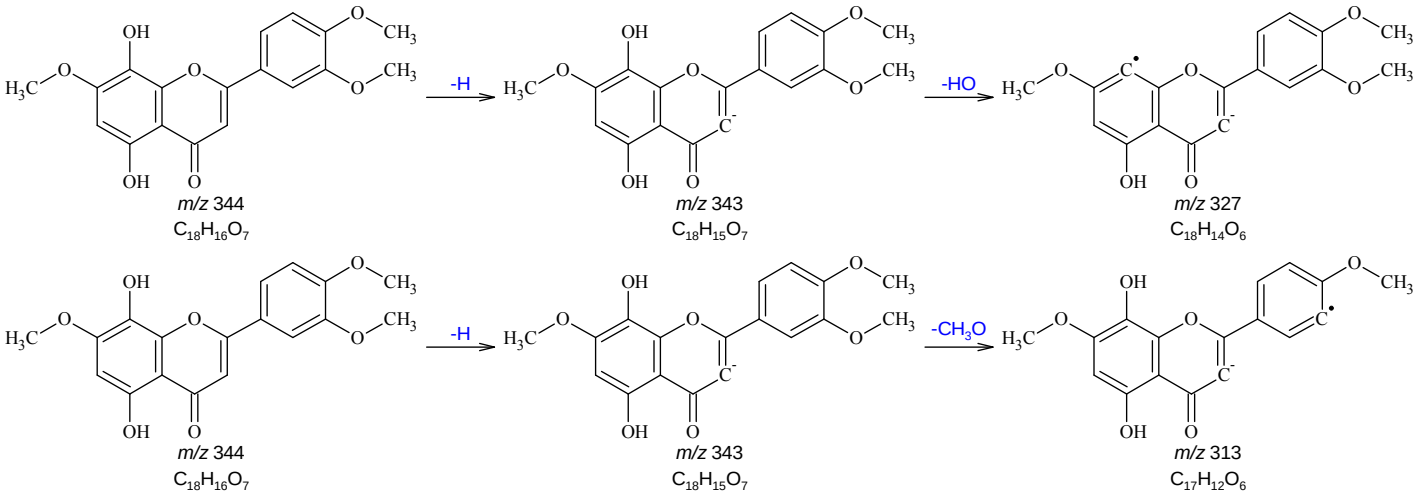

Figure 85 (cont.): Fragmentation Scheme for Gossypetin 3,3',4',7-tetramethyl Ether

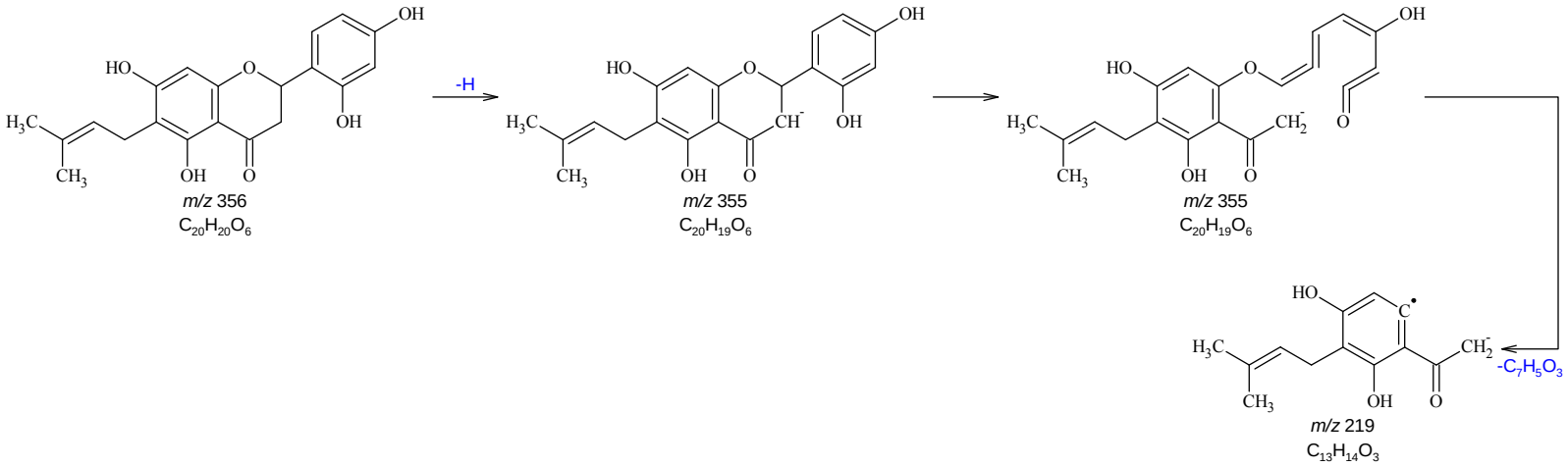

Figure 86: Fragmentation Scheme for Cudraflavanone B

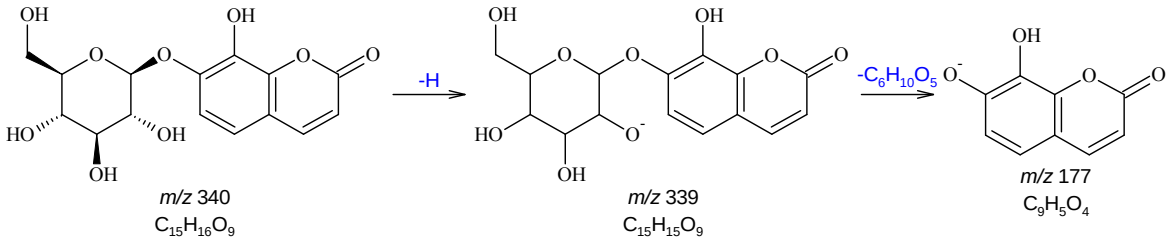

Figure 87: Fragmentation Scheme for 7,8-Dihydroxycoumarin-7-b-D-Glucoside

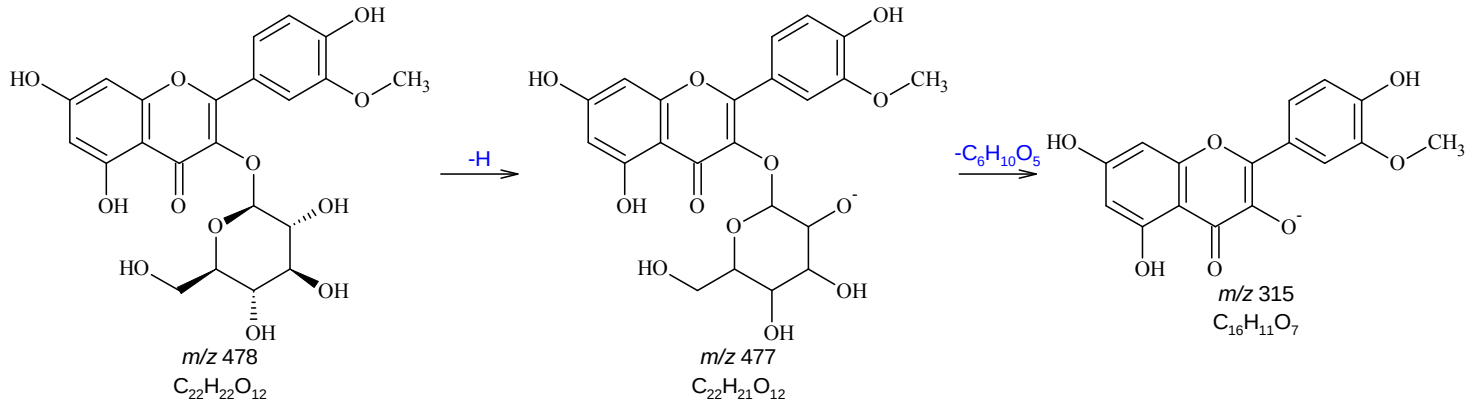

Figure 88: Fragmentation Scheme for Isorhamnetin-3-glucoside

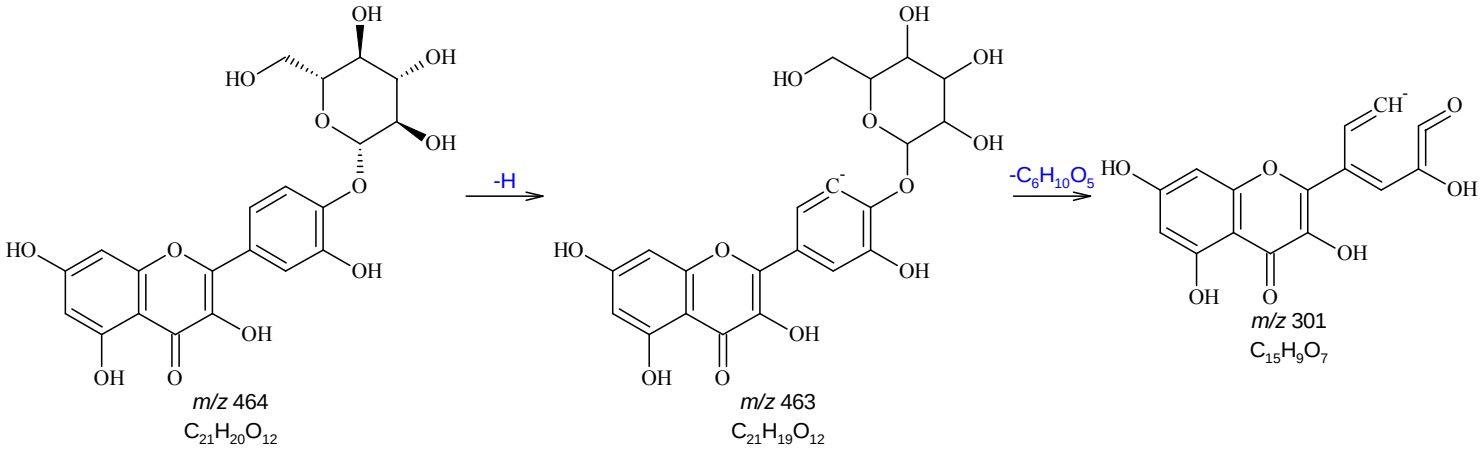

Figure 89: Fragmentation Scheme for Quercetin-4'-O-glucoside_(a.k.a. Spiraeoside)

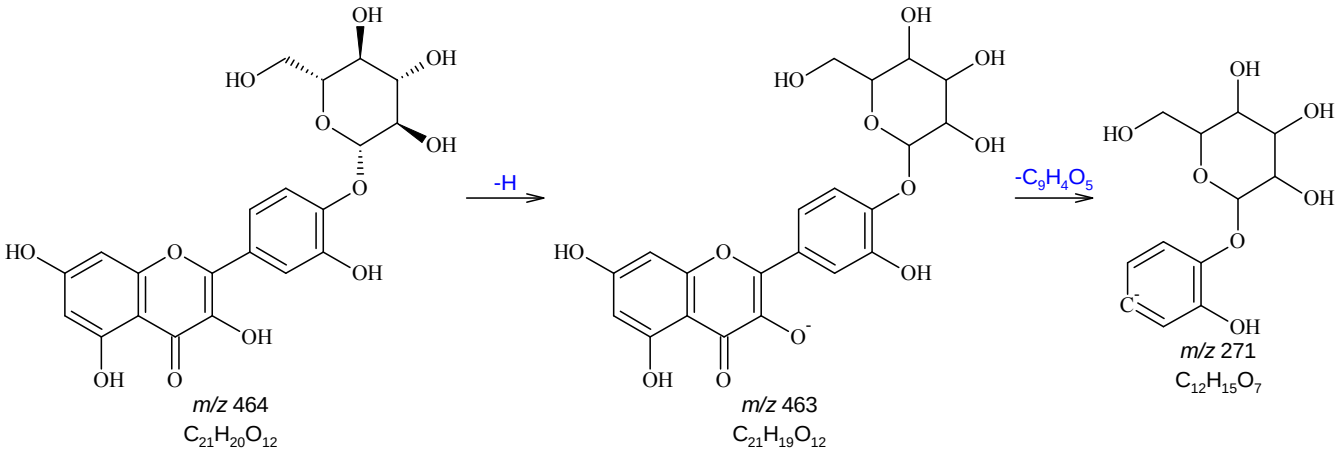

Figure 89 (cont.): Fragmentation Scheme for Quercetin-4'-O-glucoside (a.k.a. Spiraeoside)

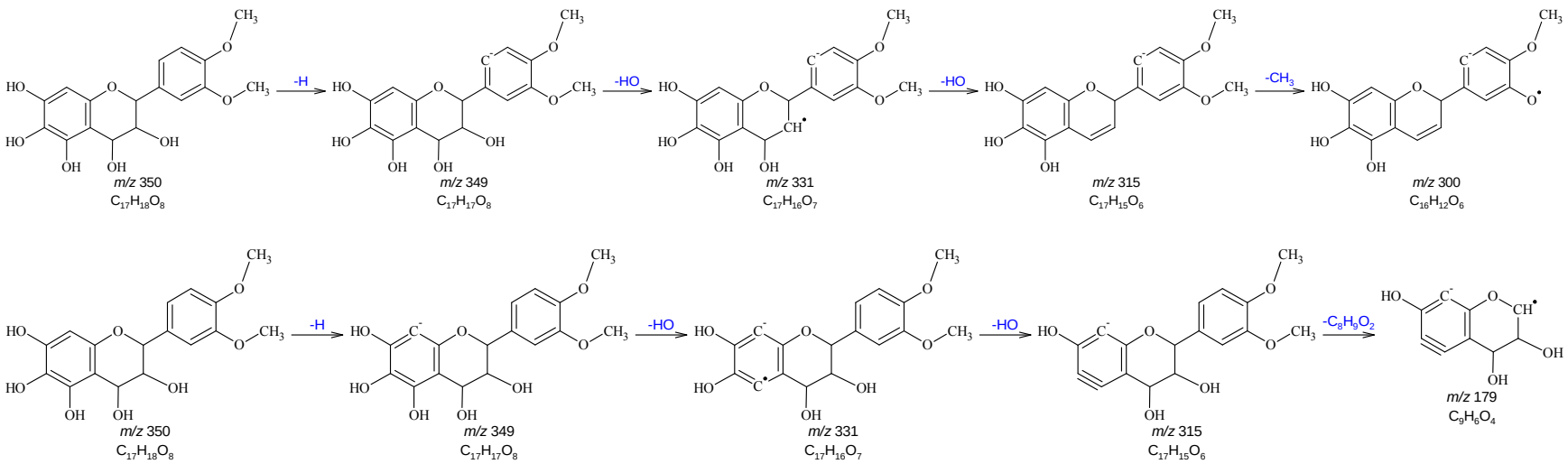

Figure 90: Fragmentation Scheme for 2-(3,4-dimethoxyphenyl)-3,4-dihydro-2*H*-chromene-3,4,5,6,7-pentol

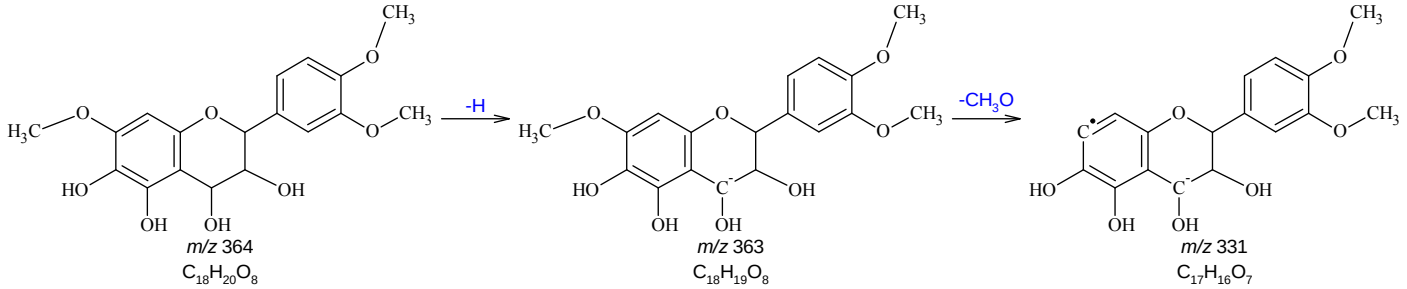

Figure 91: Fragmentation Scheme for 2-(3,4-dimethoxyphenyl)-7-methoxy-3,4-dihydro-2*H*-chromene-3,4,5,6-tetrol

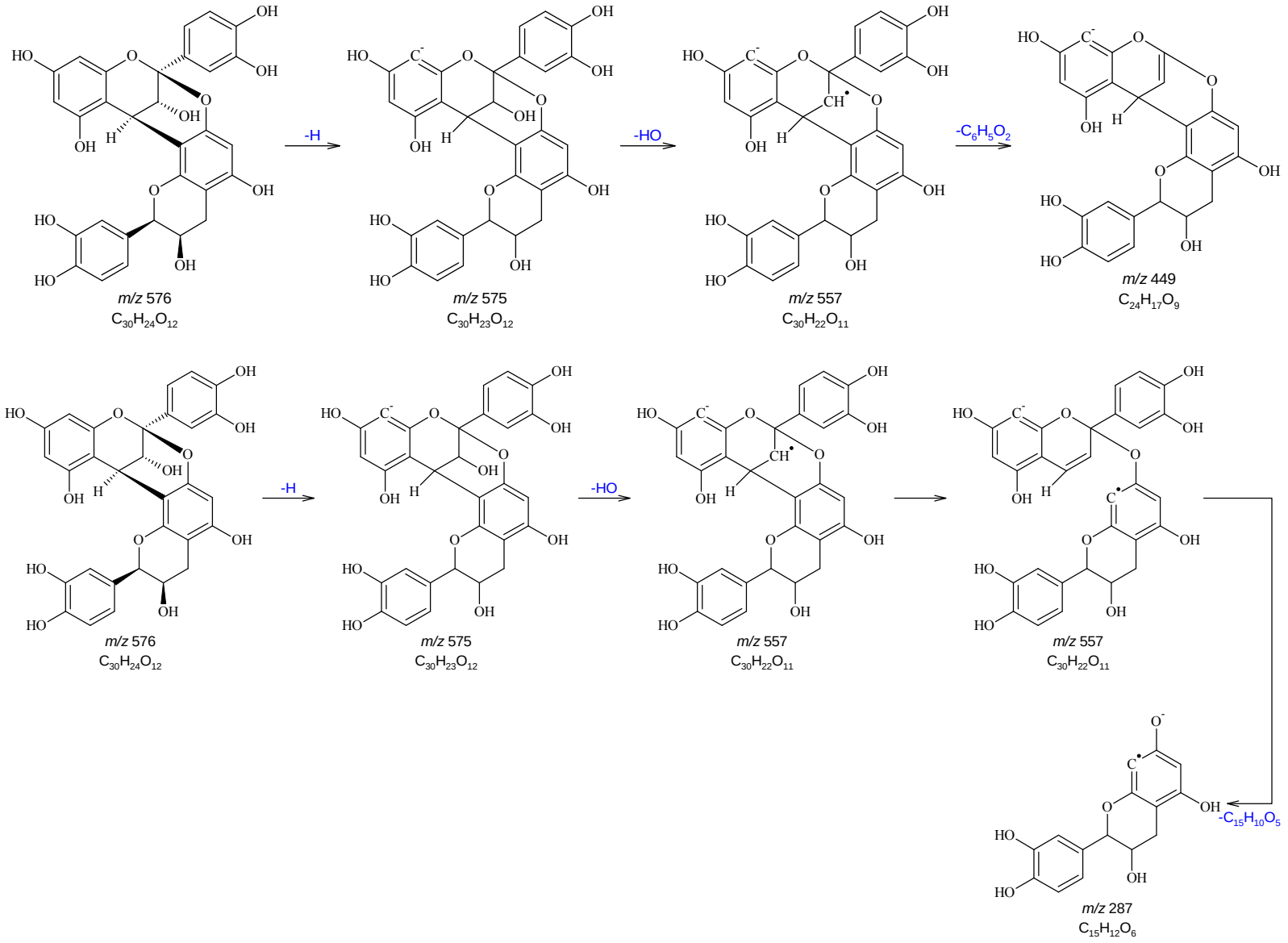

Figure 92: Fragmentation Scheme for Proanthocyanidin A2 Dimer

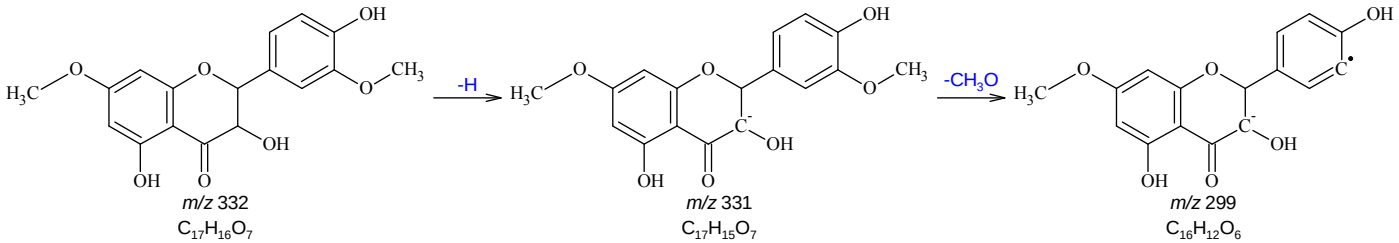

Figure 93: Fragmentation scheme for 3,5-dihydroxy-2-(4-hydroxy-3-methoxyphenyl)-7-methoxy-2,3-dihydro-4*H*-chromen-4-one

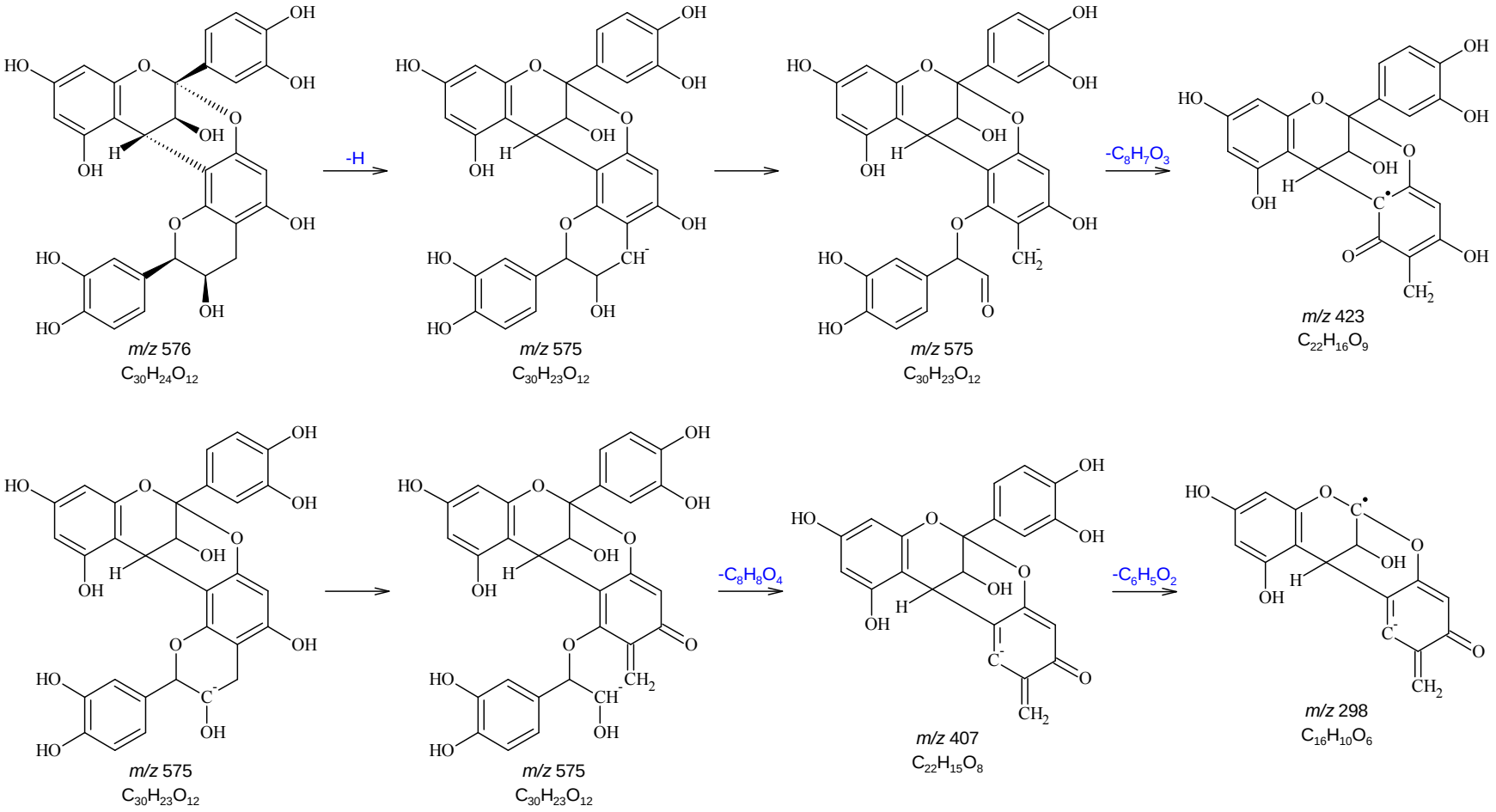

Figure 94: Fragmentation Scheme for Proanthocyanidin A5' Dimer

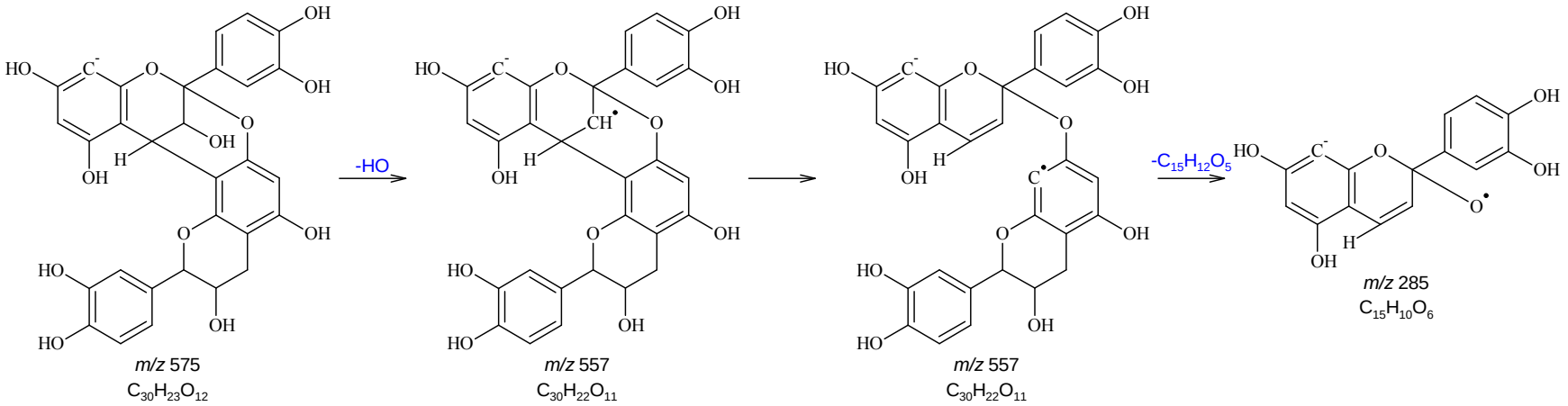

Figure 94 (cont.): Fragmentation Scheme for Proanthocyanidin A5' Dimer

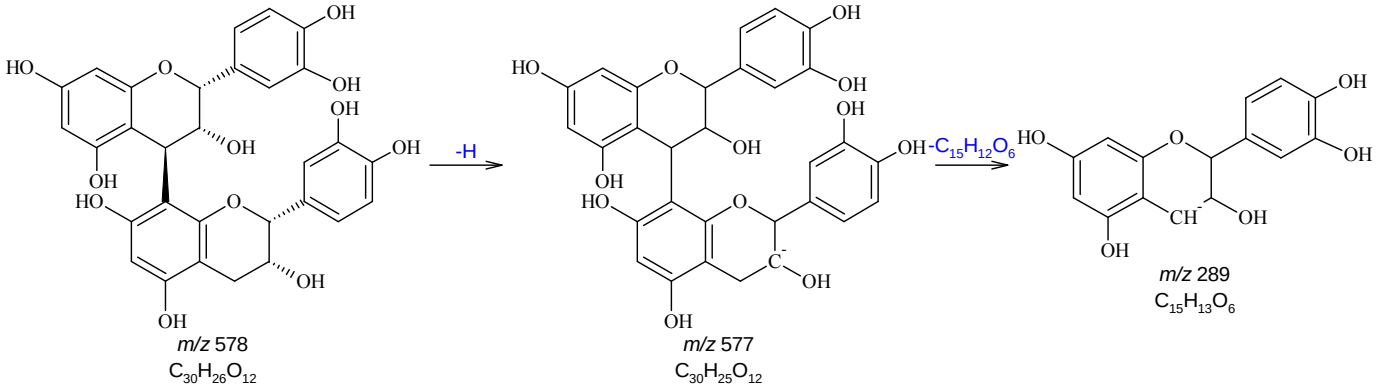

Figure 95: Fragmentation Scheme for Procyanidin B2 Dimer

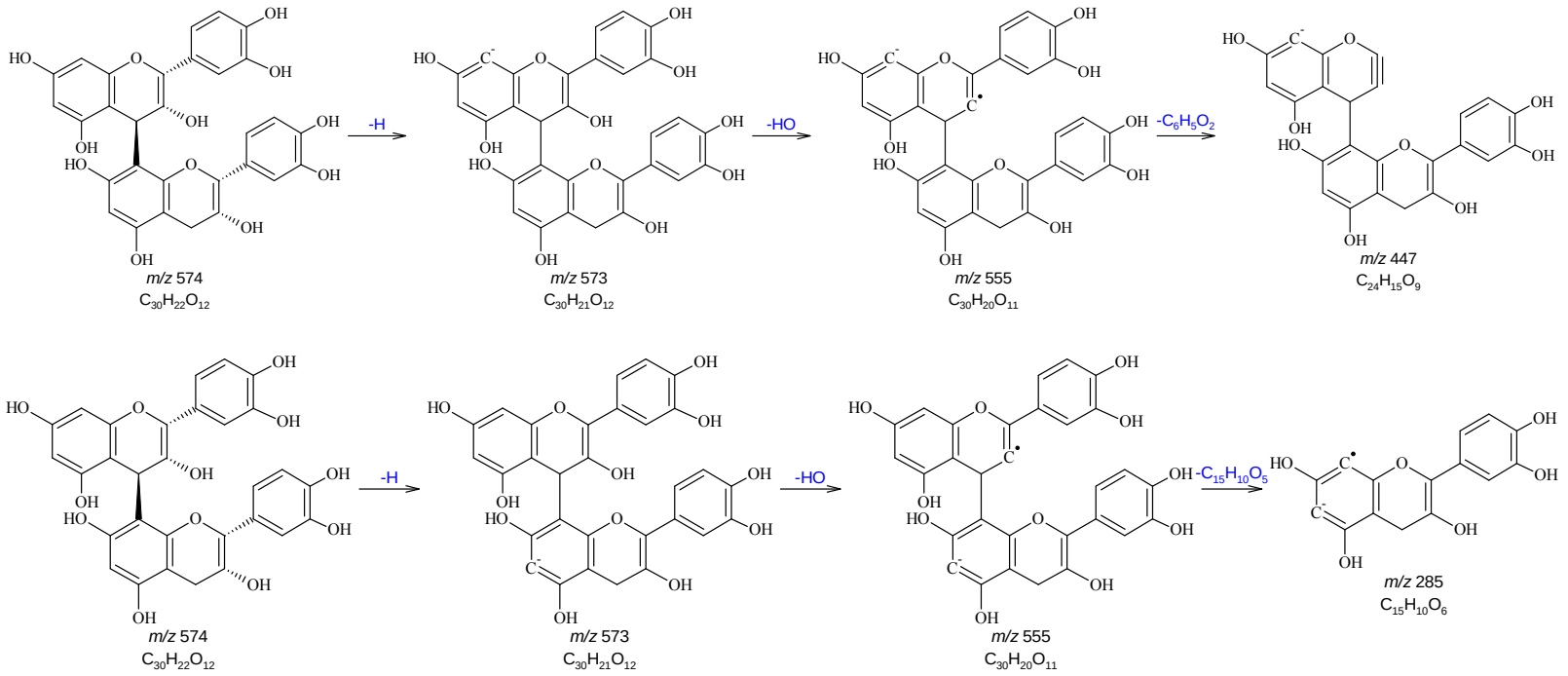

Figure 96: Fragmentation Scheme for Procyanidin B-type Dimer

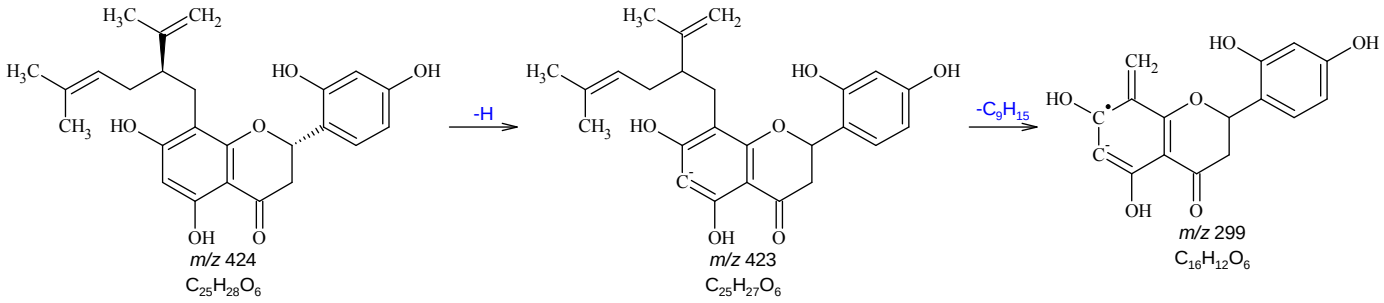

Figure 97: Fragmentation Scheme for Sophoraflavanone G

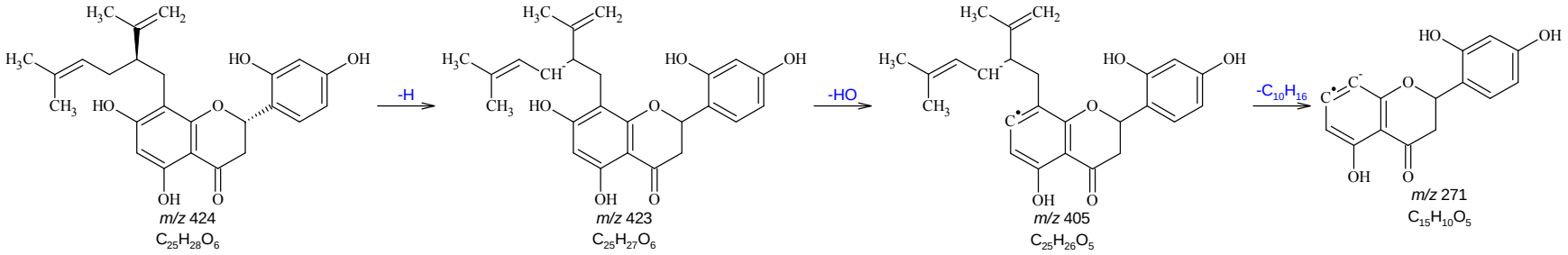

Figure 97 (cont.): Fragmentation Scheme for Sophoraflavanone G

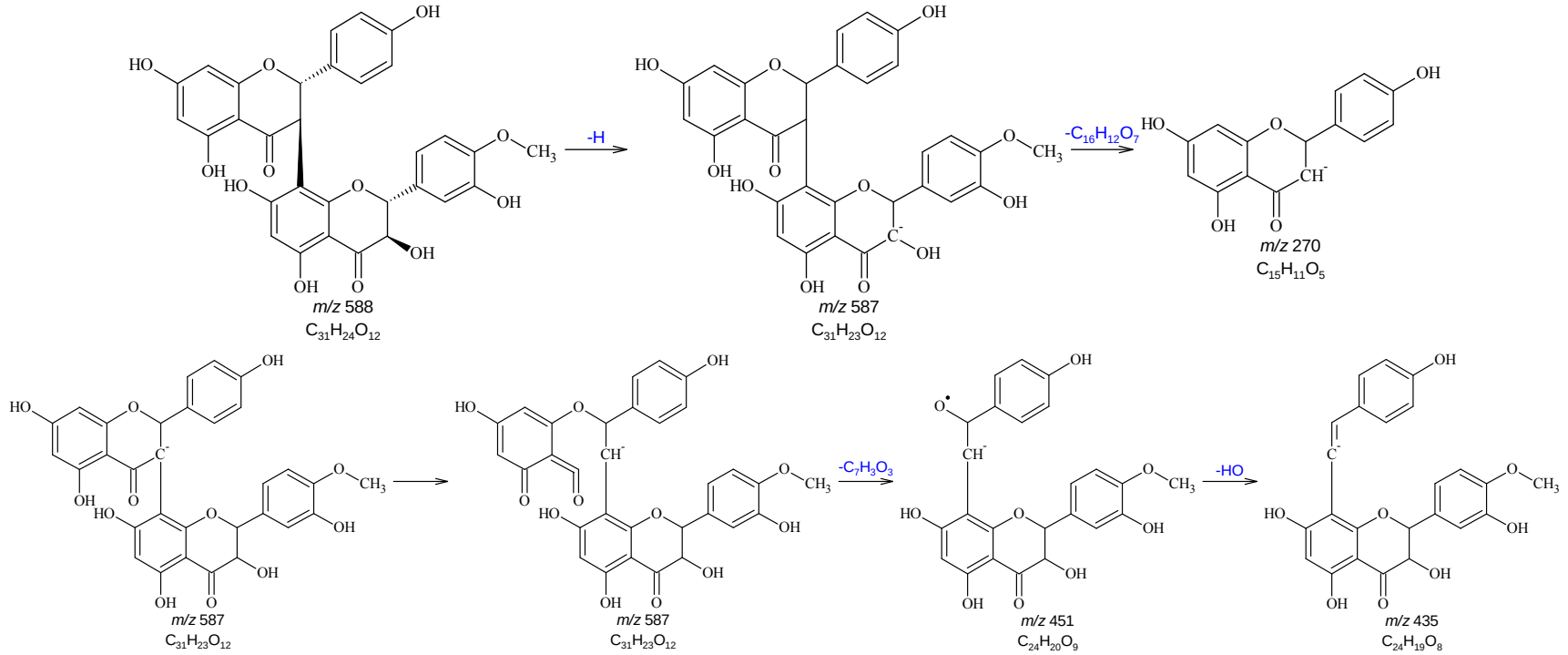

Figure 98: Fragmentation Scheme for Kolaflavanone

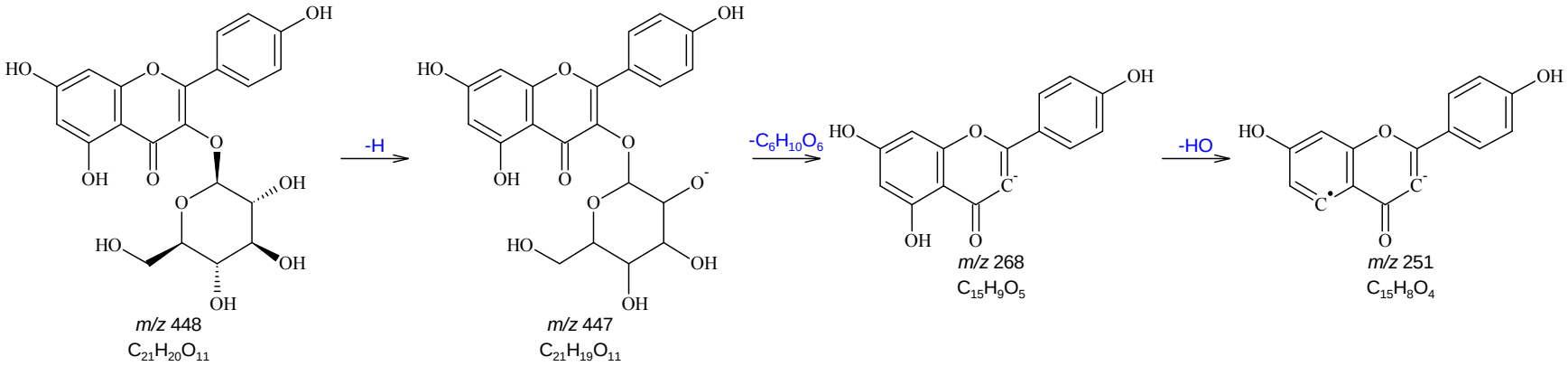

Figure 99: Fragmentation Scheme for 3,4',5,7-Tetrahydroxyflavone-3-glucoside (a.k.a. Astragalin)

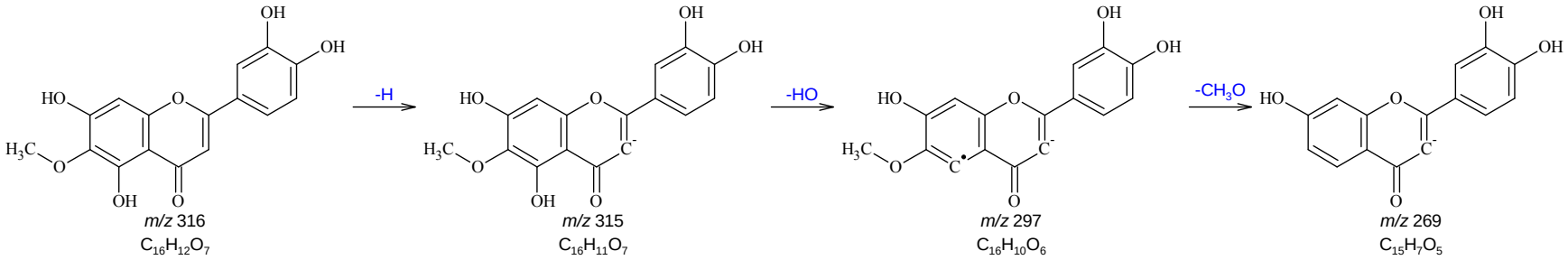

Figure 100: Fragmentation Scheme for 6-Methoxyluteolin (a.k.a. Nepetin)

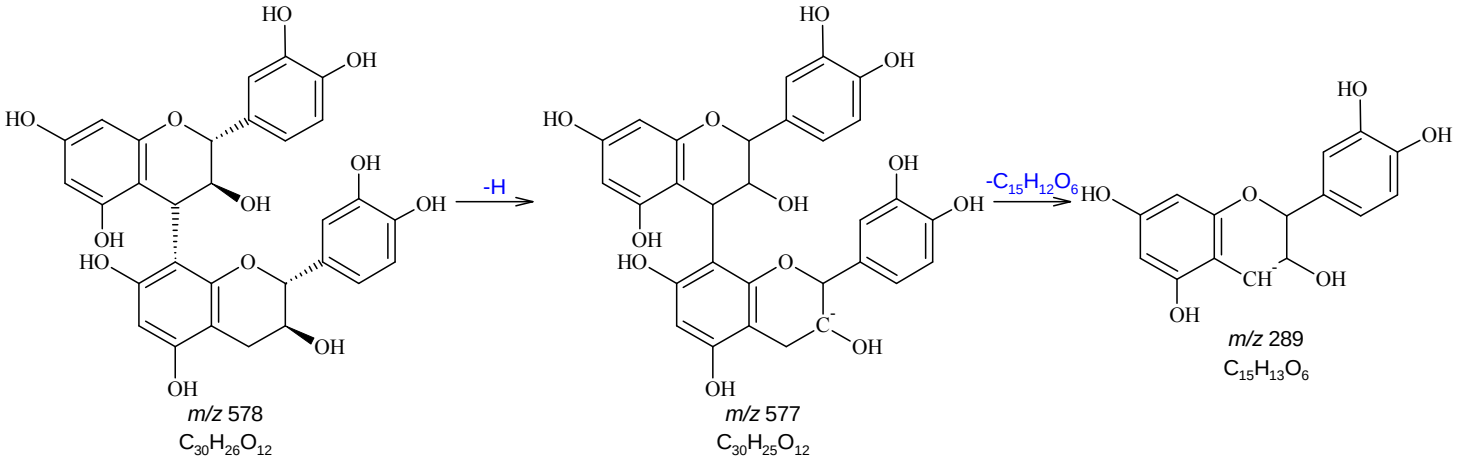

Figure 101: Fragmentation Scheme for Procyanidin B-type Dimer (Linear)

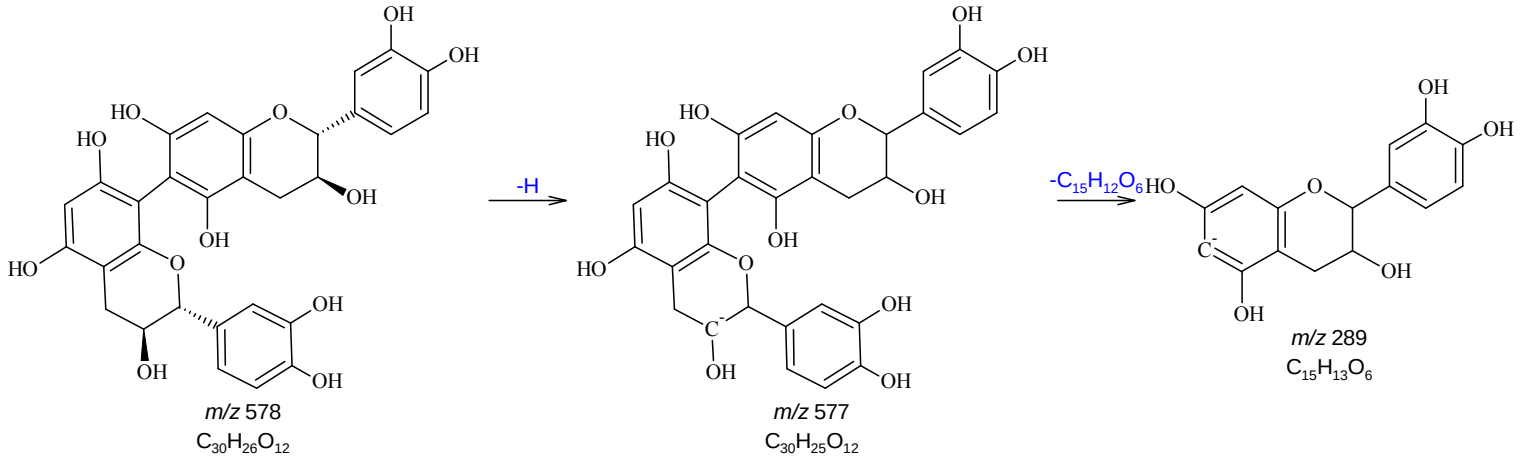

Figure 102: Fragmentation Scheme for Procyanidin B-type Dimer (Branched)

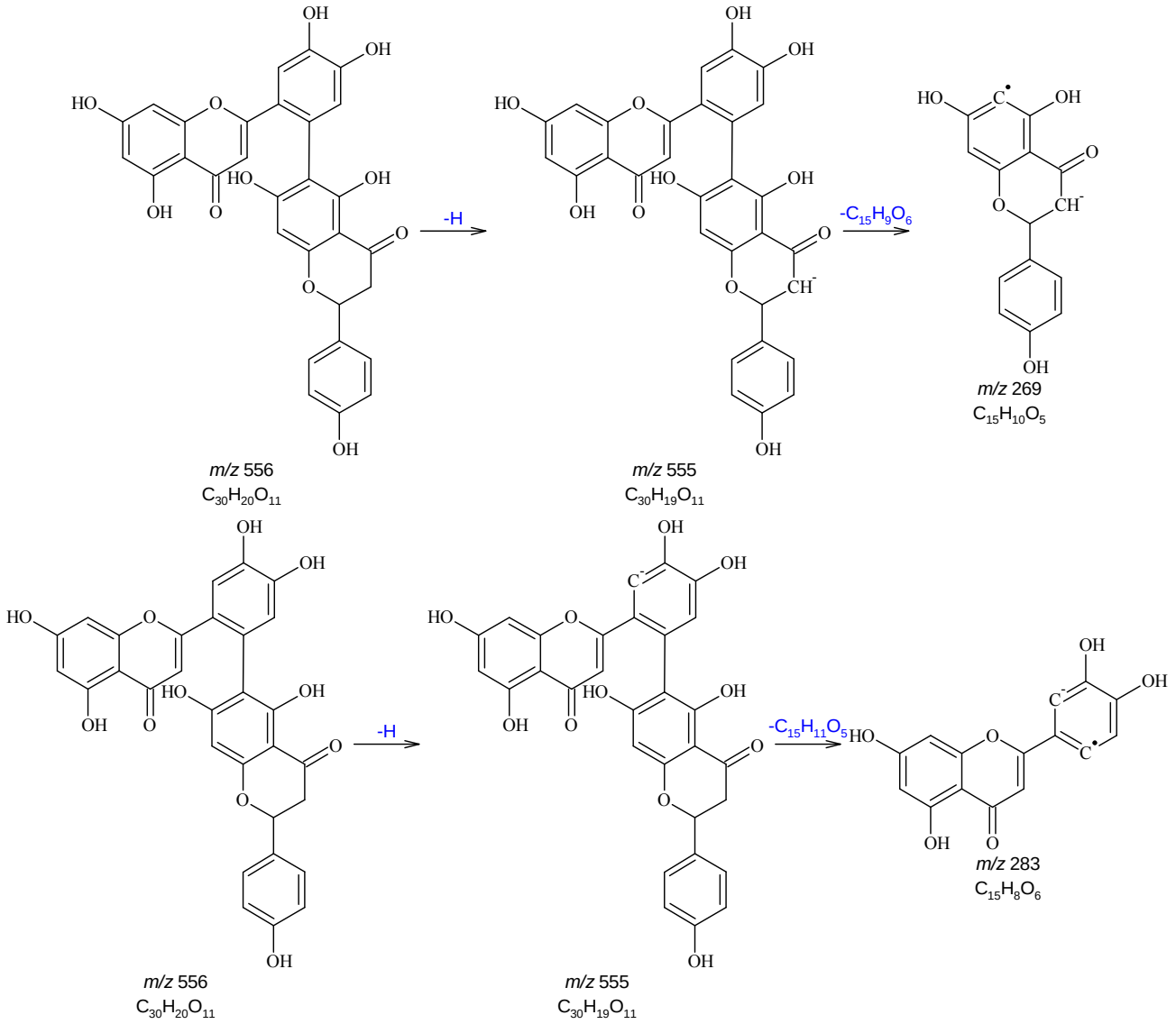

Figure 103: Fragmentation Scheme for Hegoflavone A

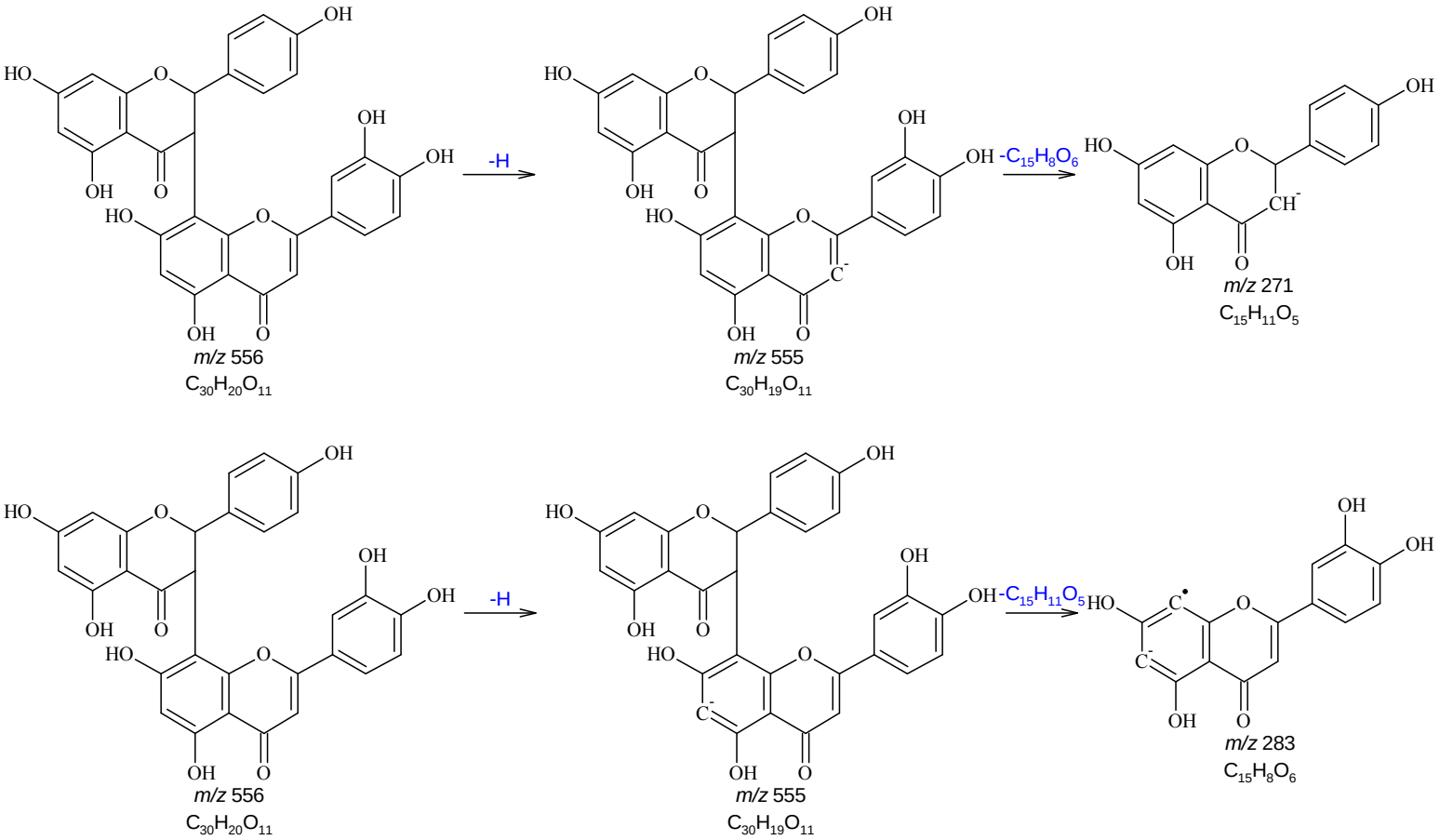

Figure 104: Fragmentation Scheme for Morelloflavone

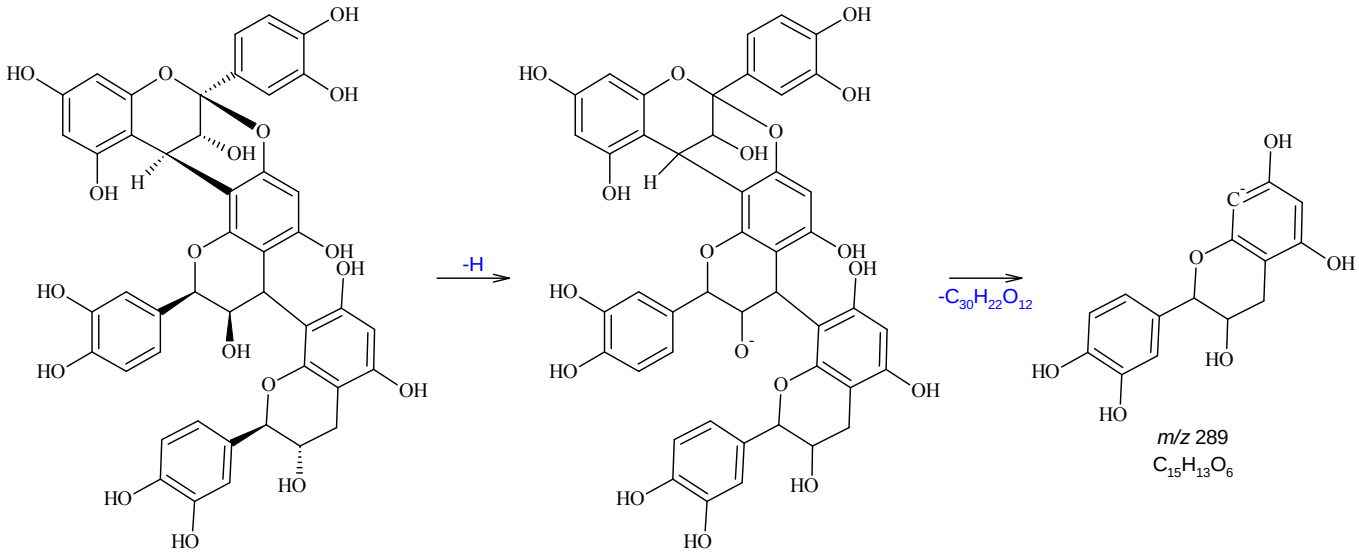

Figure 105: Fragmentation Scheme for Catechin/Epicatechin Trimer with Single A-type Interflavanic Linkage (IFL)

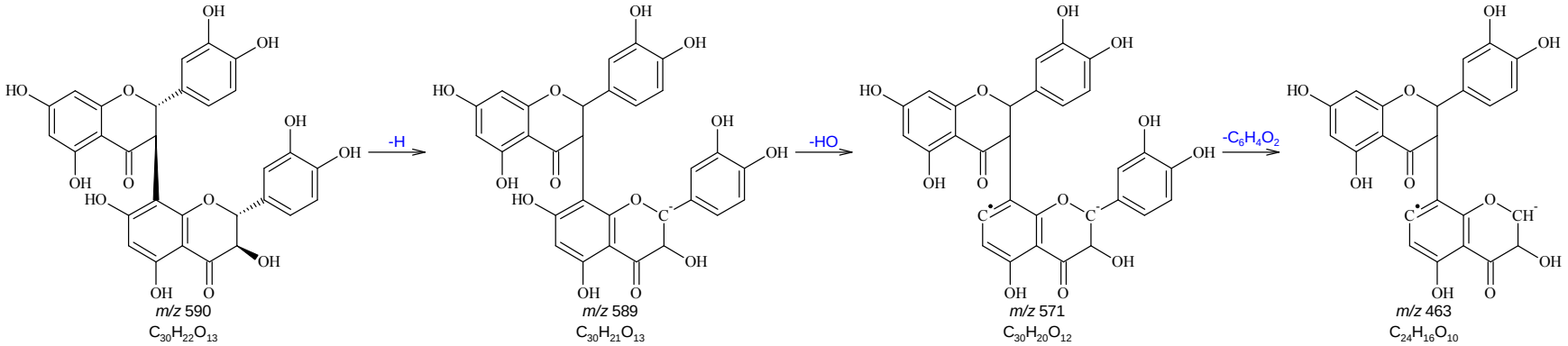

Figure 106: Fragmentation Scheme for Manniflavanone

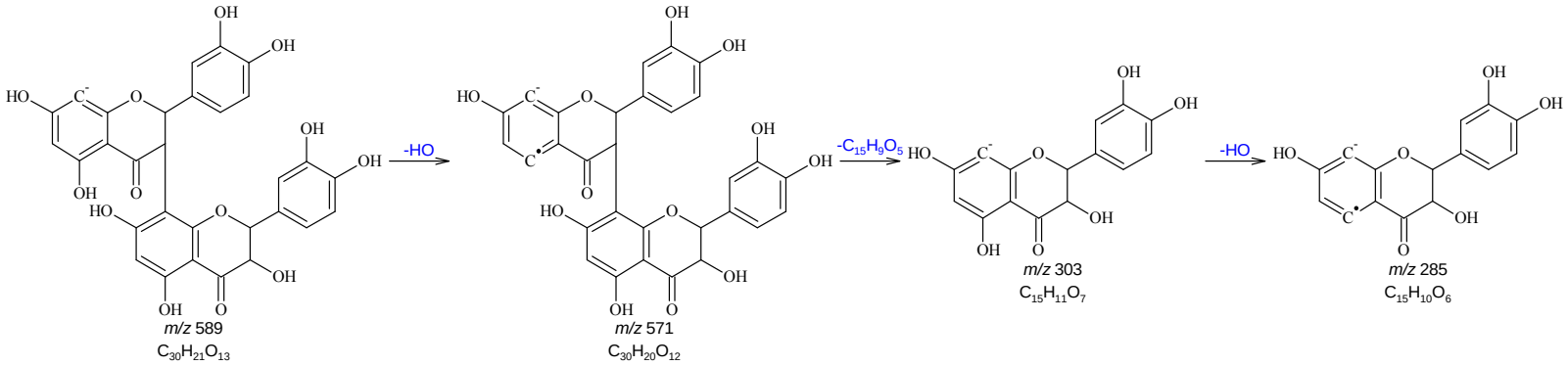

Figure 106 (cont.): Fragmentation Scheme for Manniflavanone

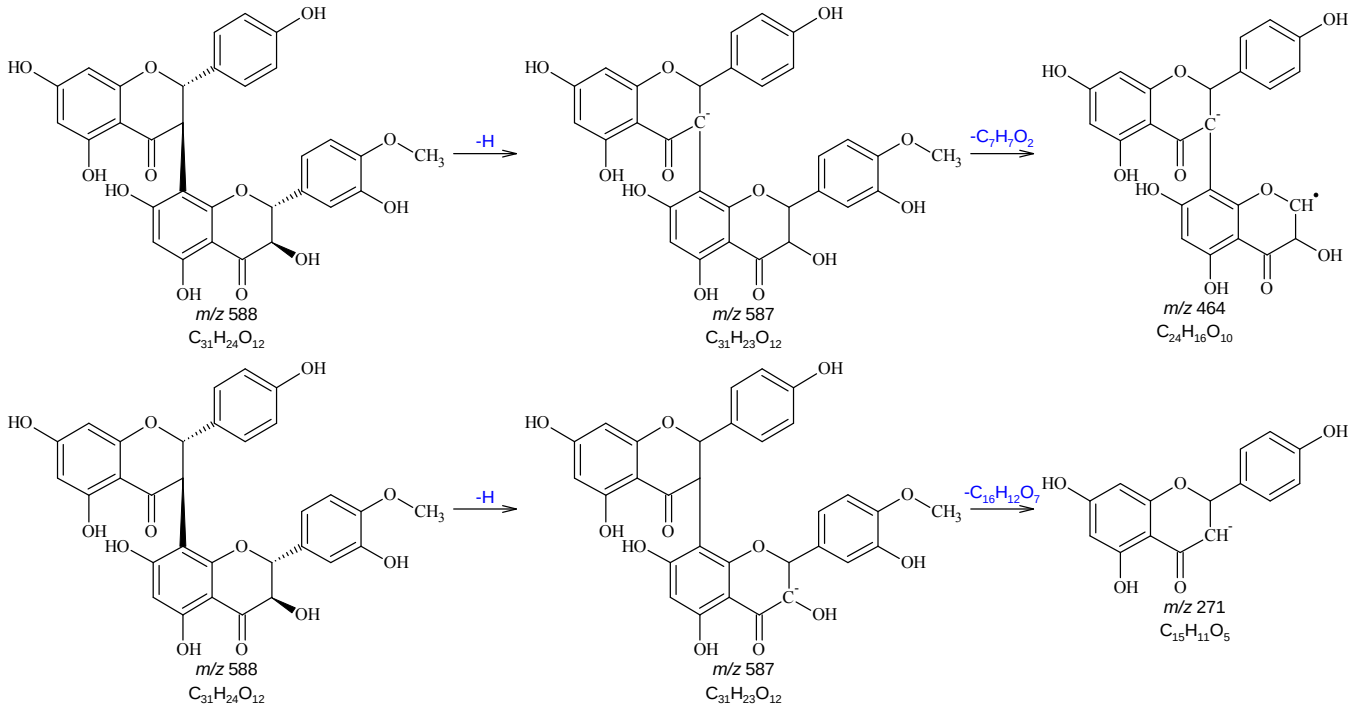

Figure 107: Fragmentation Scheme for Kolaflavanone

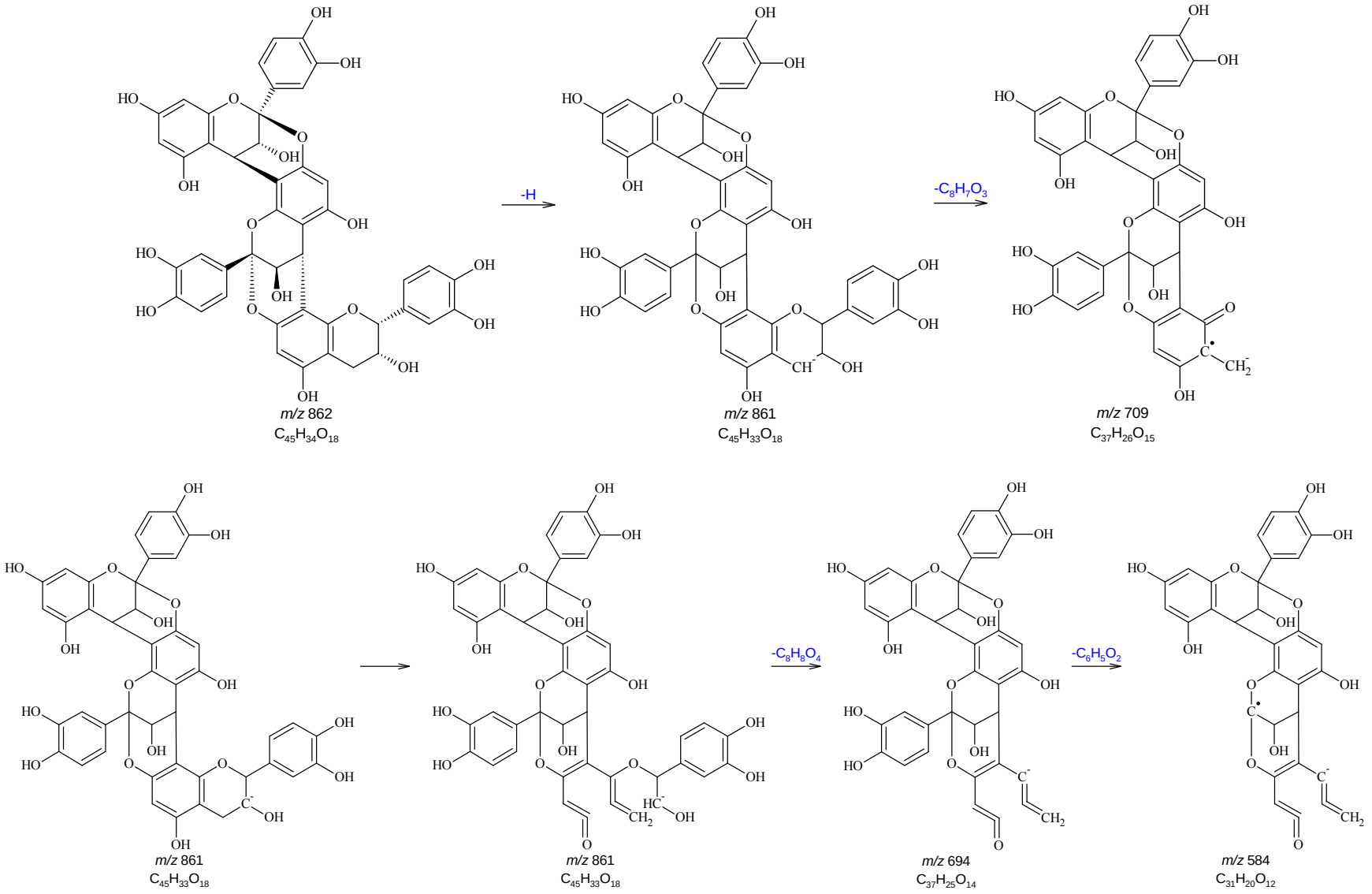

Figure 108: Fragmentation Scheme for Aesculitannin C

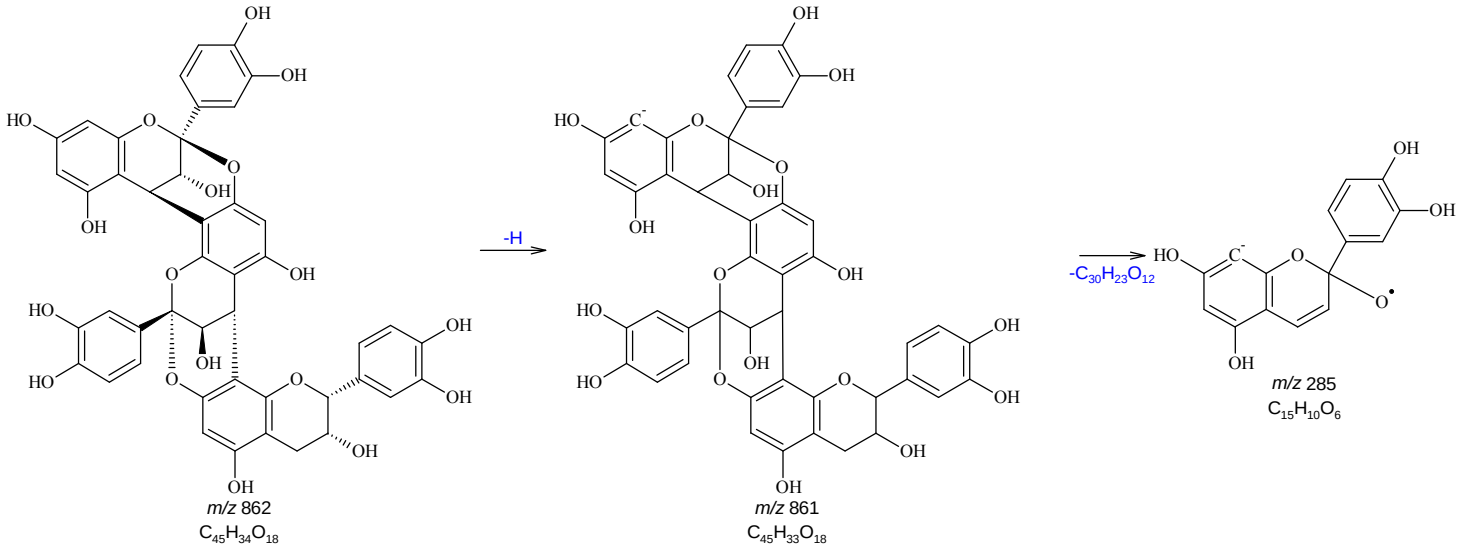

Figure 108 (cont.): Fragmentation Scheme for Aesculitannin C

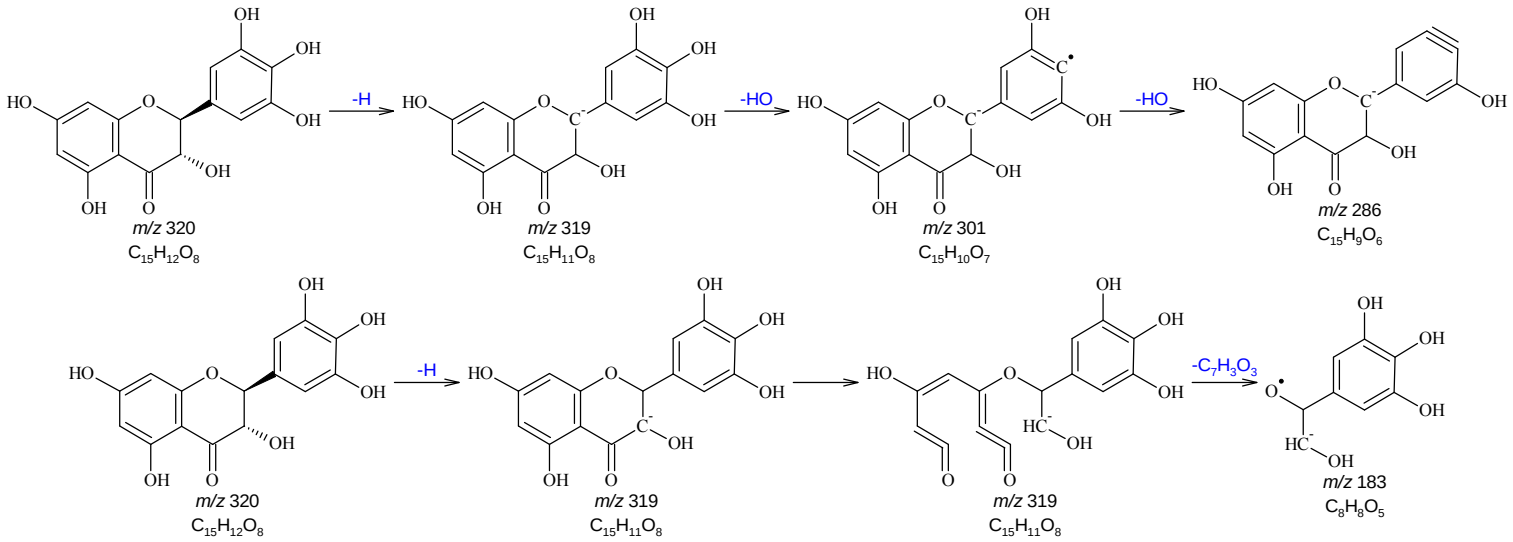

Figure 109: Fragmentation Scheme for 3,3',4',5,5',7-Hexahydroxyflavanone (a.k.a. Dihydromyricetin)

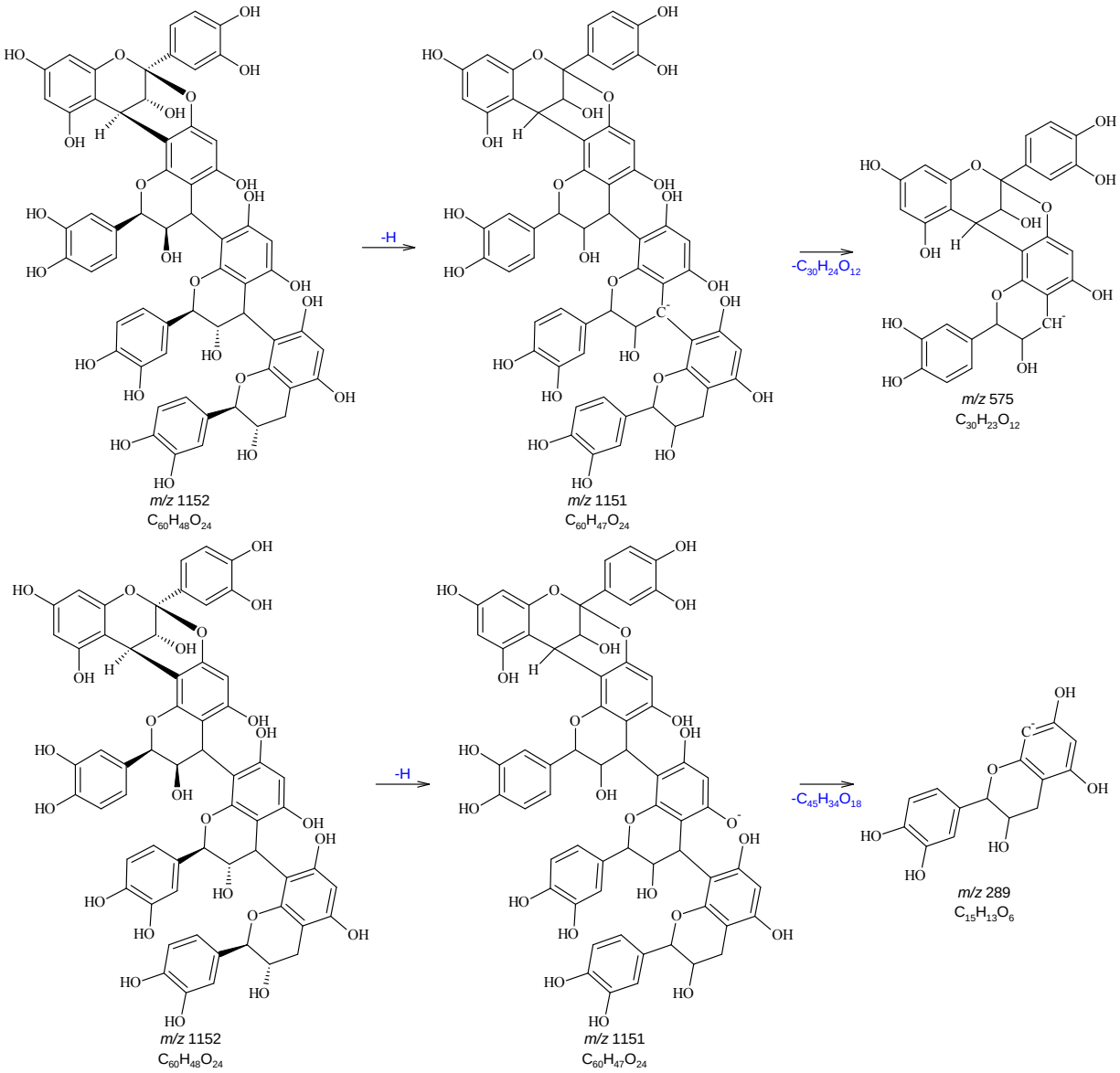

Figure 110: Fragmentation Scheme for Catechin/Epicatechin Tetramer with Single A-type Interflavanic Linkage (IFL)

Table 19: Biological Activities of Identified (and Tentatively Identified) Compounds Found in Peanut Skin Fractions

Compound Number	Compound Name	Biological Activity	Reference
Cinnamic Acids (including Methoxy- and Other Derivatives)			
1-A1, 19-A1, 18-B2	Caffeic Acid	Anticancer Activity Antiviral Activity Anti-Inflammatory Activity Immunomodulatory Properties Antimitogenic Activity	Kazumi et al., 1998 Grunberger et al., 1988 Grunberger et al., 1988 Grunberger et al., 1988 Natarajan et al., 1996
1-A1, 2-A1, 8-B1, 1-B2, 3-B2, 15-B2, 5-C1, 6-C1, 14-C1	Cinnamic Acids	Antibacterial Properties Antifungal Activity Inhibition of LDL Oxidation	Tonari et al., 2002 Bisogno et al., 2007 Lee et al., 2004
8-B1, 1-C2	p-Coumaric Acid	Antioxidant	Kristinová et al., 2009
10-B1	Ferulic Acid	Antioxidant Anti-Inflammatory Activity	Kristinová et al., 2009 Graf, 1992
Carboxylic Acids (including Methoxy- and Other Derivatives)			
14-C1	Chroman-2-Carboxylic Acid	Antioxidant	Tang and Liu, 2007
5-C2	Monotropein	Anti-Inflammatory Activity Analgesic	Jongwon et al., 2005 Jongwon et al., 2005
Benzoic Acids (including Methoxy- and Other Derivatives)			
1-B1	Protocatechuic Acid	Antioxidant Inhibition of LDL Oxidative Modification	Isanga and Zhang, 2007 Yen and Hsieh, 2002
1-B1	Resorcylic Acid	Estrogen-like Properties	Katzenellenbogan et al., 1979
2-B1	Salicylic Acid	Anti-Inflammatory Preventative Cancer Activity	Higgs et al., 1987 Paterson and Lawrence, 2001
Naphthoquinones (including Methoxy- and Other Derivatives)			
27-A1, 5-A2	Plumbagin	Apoptosis Activity Against Breast Cancer Cells Inhibition of Cancer Migration and Invasion Antimicrobial Activity Against Tuberculosis and Gonorrhoea	Ahmad et al., 2008 Shih et al., 2009 Kuete et al., 2009

Compound Number	Compound Name	Biological Activity	Reference
Stilbenes (including Methoxy- and Other Derivatives)			
26-A1, 28-A1, 4-A2	Oxyresveratrol	Anti-Herpes Simplex Virus Activity	Chuanasa et al., 2008
22-A1, 11-C1, 5-C2, 19-D1, 1-D2	Resveratrol	Antioxidant Inhibition of Cardiovascular Disease Cancer Preventative Activity Inhibition of LDL Oxidativion Estrogenic Activity Anti-Inflammatory	Olas and Wachowicz, 2002 Kris-Etherton et al., 2002 Francisco and Resurreccion, 2008 Frankel et al., 1993 Garvin et al., 2006 Rotondo et al., 1998
4-C1	Stilbenes	Antioxidant Anticancer Properties Antimutagen Properties (Detoxify Carcinogens) Anti-inflammatory Activity	Francisco and Resurreccion, 2008 Francisco and Resurreccion, 2008 Francisco and Resurreccion, 2008 Cassidy et al., 2000
Chalcones (including Methoxy- and Other Derivatives)			
2-A1, 18-A1	Methoxy-Chalcone	(Melanoma) Cancer Preventative Activity Antibacterial Activity Antifungal Activity	Kayo Henmi et al., 2009 Popova et al., 2001 Popova et al., 2001
2-B2	Butein	Antioxidant Anti-Inflammatory Activity Anticancer Activity Antifibrogenic Activity Vaxorelaxant Properties Antihepatoxic Activity (Liver Damage Prevention)	Cheng et al., 1998 Cheng et al., 1998 Samoszuk et al., 2005 Cheng et al., 1998 Yu et al., 1995 Woo et al., 2003
Coumarins (including Methoxy- and Other Derivatives)			
26-A1, 28-A1, 4-A1	Cedrecoumarin A	Vasorelaxant Properties	Rakotoarison et al., 2003
28-C1	Fraxin or Fraxoside	Antioxidant Anti-Inflammatory Preventative Cancer Activity	Whang et al., 2005 Klein-Galczinsky, 1999 Ivanovska et al., 1994

Compound Number	Compound Name	Biological Activity	Reference
26-B2, 30-C1, 32-C1, 33-C1, 33-C2	Glycycoumarin	Antiviral Activity Antispasmodic Properties Antibacterial Activity	Sekine-Osajima et al., 2009 Sato et al., 2006 Tanaka et al., 2001
26-A1, 28-A1	Osthole	Atherosclerosis Prevention Hepatic Lipid Suppression	Ogawa et al., 2007 Ogawa et al., 2007
26-A1, 28-A1	Suberosin	Anti-Inflammatory Activity	Chen et al., 2009
2-A2	Umbelliferone	Antiallergic Properties	Vasconcelos et al., 2009
8-A2	Xanthotoxol	Sedative Properties	Sethi et al., 1992
Dicoumarins (including Methoxy- and Other Derivatives)			
34-C1	Daphnoretin	Anticancer Activity	Liou et al., 2006
5-A1, 34-A1	Dicoumarin	Anticoagulant Properties	Zhou et al., 2009
4-A1	Dicoumoxyl	Anticoagulant Properties	Meriel et al., 1964
Coumestrols (including Methoxy- and Other Derivatives)			
34-A1	Psoralidin	Anticancer Activity	Kumar et al., 2009
Secoiridoids (including Methoxy- and Other Derivatives)			
31-A1	Oleuropein	Smooth Muscle Induction Activity Preventive Activity Against UVB Skin Damage Vasodilation Activity Antimicrobial Properties Inhibition of LDL Oxidation	Rocha et al., 2009 Kimura and Sumiyoshi, 2009 Visioli et al., 1998 Bisignano et al., 1999 Visioli and Galli, 1994
Coniferins (including Methoxy- and Other Derivatives)			
20-B2	Syringin	Glucose Regulator Hemostatic Properties	Niu et al., 2008 Wang, 1980
Flavans (including Glucosides, Methoxy- and Other Derivatives)			
3-C1, 2-D2	Catechin	Inhibition of LDL Oxidation Prevention of Plasma Oxidation Anticancer Activity Antimicrobial Properties	Andrikopolous et al., 2003 Lotito and Fraga, 1998 Kandil et al., 2002 Buzzini et al., 2007

Compound Number	Compound Name	Biological Activity	Reference
3-D1	Epicatechin	Antioxidant Anticancer Activity Antimicrobial Properties Antifungal Activity	Francisco and Resurreccion, 2008 Kandil et al., 2002 Buzzini et al., 2007 Narayana et al., 2001
23-B2, 6-C2, 4-D1	3'-O-Methylcatechin	Antioxidant Inhibition of Cell Death Preventative Cancer Activity Inhibition of LDL Oxidation	Spencer et al., 2001 Spencer et al., 2001 Ebeler et al., 2002 Cren-Olive et al., 2003
23-B2, 6-C2, 4-D1	4'-O-Methylcatechin	Preventative Cancer Activity Inhibition of LDL Oxidation	Ebeler et al., 2002 Cren-Olive et al., 2003
Isoflavans (including Glucosides, Methoxy- and Other Derivatives)			
6-A2	Equol	Therapeutic for Hormonal Conditions (Estrogenic Activity)	Setchell et al., 2009
Flavones (including Glucosides, Methoxy- and Other Derivatives)			
24-B2, 24-C1, 25-C1, 38-D1	Acacetin	Anticancer Activity	Hsu et al., 2004
5-B1, 7-C2	Apigenin	Anti-Hypertension Activity Heart Contraction Promotion Anti-Inflammatory Activity Antibacterial Activity Antiviral Activity Antifungal Activity	Narayana et al., 2001 Itoigawa et al., 1999 Narayana et al., 2001 Narayana et al., 2001 Narayana et al., 2001 Narayana et al., 2001
20-B1, 21-B2, 26-C1, 23-C2, 25-C2, 27-C2, 29-C2, 20-D1, 28-D1, 29-D1, 31-D1, 4-Gr2	Chrysoeriol	Antifungal Activity	Narayana et al., 2001
20-B1	Diosmetin	Anticancer Activity	Androutsopoulos et al., 2009
6-D2, 7-D2, 7-E1, 3-E2	Fisetin	Heart Contraction Promotion	Itoigawa et al., 1999

Compound Number	Compound Name	Biological Activity	Reference
10-B2	Gossypin	Anti-Anxiety Properties Sedative Properties Anti-Inflammatory Activity Analgesic Properties	Fernandez et al., 2009 Fernandez et al., 2009 Mada et al., 2009 Mada et al., 2009
11-D1, 12-D1, 3-E1, 5-E1	Hyperoside	Antioxidant	Liu et al., 2005
11-B1, 12-B1, 15-B1, 16-B1, 18-B1, 4-B2, 8-B2, 16-B2, 22-B2, 10-C1, 13-C1, 21-C1, 22-C1, 3-C2, 5-D1, 15-D1, 16-D1, 22-D1	Isohamnetin	Antioxidant Vasodilation Activity Anti-Inflammatory Anticancer Activity	Yokozawa et al., 2002 Pérez-Vizcaíno et al., 2002 Ahmed et al., 2005 Teng et al., 2006
19-F1	Kaempferol	Antioxidant Vasodilation Activity Heart Contraction Promotion Anti-Inflammatory Activity Antiallergic Properties Antiviral Activity Anticancer Activity	Francisco and Resurreccion, 2008 Pérez-Vizcaíno et al., 2002 Itoigawa et al., 1999 Narayana et al., 2001 Narayana et al., 2001 Narayana et al., 2001 Narayana et al., 2001
26-C2, 27-D1, 19-F1, 3-Gr2	Luteolin	Antioxidant Anti-Leukemic Activity Anti-Hypertensive Activity Vasorelaxant Properties Heart Contraction Promotion Anti-Inflammatory Activity Antiviral Activity	Francisco and Resurreccion, 2008 Chiang et al., 2003 Narayana et al., 2001 Narayana et al., 2001 Itoigawa et al., 1999 Narayana et al., 2001 Narayana et al., 2001

Compound Number	Compound Name	Biological Activity	Reference
17-B2, 2-D2	Morin	Antioxidant Heart Contraction Promotion Anti-Inflammatory Activity Antiallergic Properties Antiviral Activity Anticancer Activity	Narayana et al., 2001 Itoigawa et al., 1999 Narayana et al., 2001 Narayana et al., 2001 Narayana et al., 2001 Narayana et al., 2001
7-C1	Myricetin	Antioxidant Anti-Inflammatory Activity Antiallergic Properties Antiviral Activity Anticancer Activity	Francisco and Resurreccion, 2008 Narayana et al., 2001 Narayana et al., 2001 Narayana et al., 2001 Narayana et al., 2001
50-A1, 51-A1, 34-D1, 36-D1	Pectolinarigenin	Anti-Inflammatory Activity	Lim et al., 2008
2-A1	Primuletin	Antioxidant	Park et al., 2007
15-C2, 19-C2, 8-E1	Quercetin	Antioxidant Anticancer Activity Vasodilation Activity Anti-Inflammatory Activity Heart Contraction Promotion Antiallergic Properties Antiviral Activity	Francisco and Resurreccion, 2008 Francisco and Resurreccion, 2008 Pérez-Vizcaíno et al., 2002 Kobuchi et al., 1999 Itoigawa et al., 1999 Narayana et al., 2001 Narayana et al., 2001
4-B2, 10-C1, 13-C1, 21-C1, 22-C1, 3-C2, 15-D1, 22-D1, 30-D1, 1-F2, 2-Gr2	Rhamnetin	Antioxidant	Ratty, 1988
17-B2, 21-D1, 3-D2, 4-D2	Robinetin	Anticancer Activity	Birt et al., 1986

Compound Number	Compound Name	Biological Activity	Reference
18-C1	Rutin	Antioxidant Anti-Inflammatory Activity Antiallergic Properties Antiviral Activity Anticancer Activity Capillary and Vaso-Protectant	Francisco and Resurreccion, 2008 Guardia et al., 2001 Narayana et al., 2001 Narayana et al., 2001 Narayana et al., 2001 Levit et al., 1948
13-D1	Syringetin	Induction of Osteoblast Maturation Increases Bone Mass	Hsu et al., 2009a Hsu et al., 2009a
4-B2, 10-C1, 13-C1, 21-C1, 22-C1, 3-C2, 15-D1, 22-D1, 30-D1, 1-F2, 2-Gr2	Tamarixetin	Vasodilation Activity	Pérez-Vizcaíno et al., 2002
3-A1, 17-B2, 23-D1, 3-D2, 4-D2	Tricetin	Cancer Preventative Activity	Hsu et al., 2009b
Isoflavones (including Glucosides, Methoxy- and Other Derivatives)			
24-B2, 24-C1, 25-C1, 38-D1	Biochanin A	Antioxidant	Francisco and Resurreccion, 2008
4-B1	Daidzein	Antioxidant	Francisco and Resurreccion, 2008
38-D1	Glycitein	Estrogenic Activity	Song et al., 1999
43-A1	Glycitin	Osteonecrosis Prevention Enhancement of Spatial Working Memory	Li et al., 2005 Thorp et al., 2009
2-A1	Isoflavone	Anti-Inflammatory Activity Lower Dihydrotestosterone (DHT) Conc. in Men	D'Alessandro et al., 2003 Dillingham et al., 2005
29-C1	Lico-Isoflavone A	Inhibition of Lipid Oxidation	Toda and Shirataki, 2002
43-A1	Sissotrin	Inhibition of Arachidonic Acid	Kim and Yun-Choi, 2008
Flavanones (including Glucosides, Methoxy- and Other Derivatives)			
22-C2, 31-C2	Cudraflavanone B	Antifungal Activity	Fukai et al., 2003
9-C2, 4-G2,	Dihydromyricetin	Antiviral Activity (Specifically H1N1)	Roschek et al., 2009
24-A1	Eriocitrin	Antioxidant	Dorman et al., 2009

Compound Number	Compound Name	Biological Activity	Reference
24-A1, 5-B1, 2-E2	Eriodictyol	Vasodilation Activity	Ramón Sánchez de Rojas et al., 1999
17-F1, 20-F1, 19-G1	Euchrestaflavanone B	Preventative Cancer Activity	Kim et al., 2005
5-B1, 7-C2, 6-D2, 7-D2, 6-E1	Fustin	Inhibition of Neurotoxin (Parkinson's Disease)	Park et al., 2007
19-B1, 5-D2, 1-Gr2	Hesperitin	Antioxidant Anti-Inflammatory Vasodilation Activity Antibacterial Activity	Francisco and Resurreccion, 2008 Garg et al., 2001 Francisco et al., 2004 Narayana et al., 2001
33-D1	Isosakuranetin	Antihypertensive Properties Antifungal Activity	Maruyama et al., 2009 Sacco and Maffei, 1997
2-B2	Naringenin	Antioxidant Vasorelaxant Properties Antibacterial Activity Antiviral Activity Ulcer Preventative Activity	Francisco and Resurreccion, 2008 Narayana et al., 2001 Narayana et al., 2001 Narayana et al., 2001 Motilva et al., 1994
24-A1	Neoeriocitrin	Antimicrobial Activity	Mandalari et al., 2007
17-F1, 20-F1, 19-G1	Remangiflavanone B	Antimicrobial Properties	Deng et al., 2000
33-D1, 7-E1, 3-E2,	Sakuranetin	Antifungal Activity Anti-Inflammatory Preventative Allergy Activity	Pacciaroni Adel et al., 2008 Hernández et al., 2007 Ogawa et al., 2007
17-F1, 20-F1, 19-G1	Sophoraflavanone G	Antibacterial Properties	Cha et al., 2009
23-B2, 8-C2	Taxifolin	Antioxidant	Francisco and Resurreccion, 2008
Biflavones (including Glucosides, Methoxy- and Other Derivatives)			
11-Gr1, 12-Gr1	Morelloflavone	Anticancer Activity	Pang et al., 2009
11-C2	Sciatopitysin	Vasodilation Activity	Chung et al., 1982

Compound Number	Compound Name	Biological Activity	Reference
Biflavanones (including Glucosides, Methoxy- and Other Derivatives)			
18-F1, 18-G1	Kolaflavanone	Anti-Atherogenic Properties Antihepatoxic Activity (Liver Damage Prevention)	Adaramoye et al., 2005 Iwu, 1985
15-G1	Manniflavanone	Vascular Permeability and Fragility Treatment Prevention of Diabetes Mellitus Complications	Ferrari et al., 2003
Flavonoid Oligomers (including Glucosides, Methoxy- and Other Derivatives)			
2-E1, 1-F1, 15-F1, 16-F1, 6-Gr1, 8-Gr1, 14-G1	A-Type Proanthocyanidin Dimers	Insulin-Enhancing Activity Antibacterial Properties Immunomodulatory Properties Hemorrhage Protection	Anderson et al., 2004 Foo et al., 200 Lin et al., 2002 Lou et al., 1999
2-F1, 3-F1, 5-F1, 12-F1, 13-F1, 1-Gr1, 2-Gr1, 3-Gr1, 4-Gr1, 5-Gr1	B-Type Proanthocyanidin Dimers	Vasodilation Activity Inhibition of LDL Oxidation Anti-Inflammatory Activity Antimicrobial Properties Hair Growth Promotion	Karim et al., 2000 Pearson et al., 2001 Mao et al., 2000 Buzzini et al., 2007 Takahashi et al., 1999

References

Adaramoye, O. A., Nwaneri, V. O., Anyanwu, K. C., Farombi, E. O., and Emerole, G. O. (2005). Possible anti-atherogenic effect of kolaviron (a Garcinia kola seed extract) in hypercholesterolaemic rats. *Clinical and Experimental Pharmacology and Physiology, 32*(1-2), 40-46.

Ahmad, A., Banerjee, S., Zhiwei, W., Dejun, K., and Sarkar, F. H. (2008). Plumbagin-induced apoptosis of human breast cancer cells is mediated by inactiviation of NF-KB and Bcl-2. *J. Cell. Biochem., 105*(6), 1461-1471.

Ahmed, M. S., El Tanbouly, N. D., Islam, W. T., Sleem, A. A., and El Senousy, A. S. (2005). Antiinflammatory flavonoids from Opuntia dillenii (Ker-Gawl) Haw flowers growing in Egypt. *Phytotherapy Research, 19*(9), 807-809.

Anderson, R. A., Broadhurts, C. L., Polansky, M. M., Schmidt, W. F., Khan, A., Flanagan, V. P., Schoene, N. W., and Graves, D. J. (2004). Isolation and characterization of polyphenol type-A polymers from Cinnamon with insulin-like biological activity. *J. Agric. Food Chem., 52*, 65-70.

Andrikopoulos, N. K., Kaliora, A.C., Assimopoulou, A. N., and Papageorgiou, V. P. (2003). Inhibitory activity of minor polyphenolic and nonpolyphenolic constituents of olive oil against in vitro low density lipoprotein oxidation. *J. Med. Food, 5*, 1-7.

Androutsopoulos, V. P., Mahale, S., Arroo, R. R., and Potter, G. (2009). *Oncology Reports, 21*(6), 1525-1528.

Appledoorn, M. M., Sanders, M., Vincken, J.-P., Cheynier, V., Guernevé, C. L., Hollman, P. C. H., and Gruppen, H. (2009). Efficient isolation of procyanidin A-type dimers from peanut skins and B-type dimers from grape seeds. *Food Chem., 117*, 713-720.

Birt, D. F., Walker, B., Tibbels, M. G., and Bresnick, E. (1986). Anti-mutagenesis and anti-promotion by apigenin, robinetin, and indole-3-carbinol. *Carcinogenesis, 7*(6), 959-963.

Bisignano, G., Tomaino, A., Lo Cascio, R., Crisafi, G., Uccella, N., and Saija, A. (1999) On the in-vitro antimicrobial activity of oleuropein and hydroxytyrosol. *J. Pharm. Pharmacol., 51*(8), 971-974.

Bisogno, F., Mascoti, L., Sanchez, C., Garibotto, F., Giannini, F>, Kurina-Sanz, M., and Enriz, R. (2007). Structure-antifungal activity relationship of cinnamic acid derivatives. *J. Agric. Food Chem., 55*(26), 10635-10640.

Buzzini, P., Turchetti, B., Ieri, F., Goretti, M., Branda, E., Mulinacci, N., and Romani, A. (2007). Catechins and proanthocyanidins: Naturally occurring O-heterocylces with antimicrobial activity. *Top Heterocycl. Chem., 10*, 239-263.

Cassidy, A, Hanley, B., and Lamuela-Raventos, R. M. (2000). Isoflavones, lignans and stilbenes – origins, metabolism, and potential importance to human health. *J. Sci. Food Agric. 80*, 1044-1062.

Cha, J. D., Moon, S. E., Kim, J. Y., Jung, E. K., and Lee, Y. S. (2009). Antibacterial activity of sophoraflavanone G isolated from the roots of Sophora flavescens against methicillin-resistant Staphylococcus aureus. *Phytother. Res., 23*(9), 1326-1331.

Chen, Y.-C., Tsai, W.-J., Wu, M.-H., Lin, L.-C. And Kuo, Y.-C. (2009). Suberosin inhibits proliferation of human peripheral blood mononuclear cells through the modulation of the transcription factors NF-AT and NF-κB. *Br. J. Pharmacol., 150*(3), 298-312.

Cheng, Z. J., Kuo, S. C., Chan, S. C., Ko, F. N., and Teng, C. M. (1998). Antioxidant properties of butein isolated from Dalbergia odorifera. *Biochim. Biophys. Acta, 1392*(2-3), 291-299.

Chiang, L.-C., Chiang, W., Chang, M.-Y., Ng, L.-T., and Lin, C.-C. (2003). Antileukemic activity of selected natural products in Taiwan. *American Journal of Chinese Medicine, 31*(1), 37-46.

Choi, J., Lee, K.-T., Choi, M.-Y., Nam, J.-H., Jung, H.-J., Park, S.-K., and Park, H-J. (2005) Antiociceptive anti-inflammatory effect of monotropein isolated from the root of morinda officinlis. *Biol. Pharm. Bull. 28*(10), 1915-1918.

Chuanasa, T., Phromjai, J., Lipipun, V., Likhitwitayawuid, K., Suzuki, M., Pramyothin, P., Hattori, M., and Shiraki, K. (2008). Anti-herpes simplex virus (HSV-1) activity of oxyresveratrol derived from Thai medicinal plant: Mechanism of action and therapeutic efficacy on cutaneous HSV-1 infection in mice. *Antiviral Research, 80*(1), 62-70.

Chung, B. Y., Won, L. S., Lee, B. R., and Lee, C. H. (1982). A new chemical constituent of green leaves of Ginkgo biloba L. *Journal of the Korean Chemical Society, 26*(2), 95-98.

Civolani, C., Barghini, P., Roncetti, A. R., Ruzzi, M., Schiesser, A. (2000). Bioconversion of ferulic acid into vanillic acid by means of a vanillate-negative mutant of Pseudomonas fluorescens strain BF13. *Appl. Environ. Microbiol., 66*(6), 2311–2317.

Cren-Olive, C., Teissier, E., Duriez, P., and Rolando, C. (2003). Effect of catechin O-methylated metabolites and analogues on human LDL oxidation. *Free Radical Biol. Med., 34*(7), 850-855.

Cuyckens, F. and Caleys, M. (2004). Mass spectrometry in the structural analysis of flavonoids. *J. Mass Spectrom., 39*, 1-15.

D'Alessandro, T., Prasain, j., Benton, M. R., Botting, N., Moore, R., Darley-Usmar, V., Patel, R., and Barnes, S. (2003). Polyphenols, inflammatory response, and cancer prevention: Chlorination of isoflavones by human neutrophils. *J. Nutr. 133*, 3773S-3777S.

Deng, Y., Lee, J. P., Tianasoa-Ramamonjy, M., Snyder, J. K., Des Etages, S. A., Kanada, D., Snyder, M. P., and Turner, C. J. (2000). New antimicrobial flavanones from Physena madagascariensis. *J. Nat. Prod., 63*, 1082-1089.

Dillingham, B. L., McVeigh, B. L., Lampe, J. W., and Duncan, A. M. (2005). Soy protein isolates of varying isoflavone content exert minor effects on serum reproductive hormones in healthy young men. *J. Nutr., 135*, 584-591.

Dorman, H. J., Kosar, M., Baser, K. H., and Hiltunen, R. (2009). Phenolic profile and antioxidant evaluation of Metha x piperita L. (peppermint) extracts. *Natural Product Communications, 4*(4), 535-542.

Ebeler, S. E., Brenneman, C. A., Kim, G.-S., Jewell, W. T., Webb, M. R., Chacon-Rodriguez, L., MacDonald, E. A., Cramer, A. C., Levi, A., Ebeler, J. D., Islas-Trejo, A., Kraus, A., Hinrichs, S. H., and Clifford, A. J. (2002). Dietary catechin delays tumor onset in a transgenic mouse model. *Am. J. Clin. Nutr., 76*(4), 865-872.

Ferrari, J., Terreaux, C., Kurtán, T., Szikszai-Kiss, A., Antus, S., Msonthi, J. D., and Hostettmann, K. (2003). *Helv. Chim. Acta, 86*(8), 2768-2778.

Fernandez, S. P., Nguyen, M., Yow, T. T., Chu, C., Johston, G. A., Hanrahan, J. R., and Chebib, M. (2009). *Neurochem. Res., 34*(10), 1867-1875.

Foo, L. Y., Lu, Y., Howell, A. B., and Vorsa, N. (2000). The structure of cranberry proanthocyanidins which inhibit adherence of uropathogenic P-fimbriated Escherichia coli in vitro. *Phytochemistry,54*, 173-181.

Francisco, M. L. D. L. and Resurreccion, A. V. A. 2008. Functional components in peanuts. *Crit. Rev. Food Sci. Nutr., 48*(8), 715-746.

Frankel, E. N., Waterhouse, A. L. and Kinsella, J. E. (1993). Inhibition of human LDL oxidation by resveratrol. *Lancet, 341*,1103-1104.

Fukai, T., Yonekawa, M., Hou, A. J., Nomura, T., Sun, H. D., and Uno, J. (2003). Antifungal agents from the roots of Cudrania cochinchinensis against Candida, Cryptococcus, and Aspergillus species. *J. Nat. Prod., 66*(8), 1118-1120.

Garg, A., Garg, S., Zaneveld, L. J., and Singla, A. K. (2001). Chemistry and pharmacology of the citrus bioflavonoid hesperidin. *Phytother. Res., 15*(8), 655-669.

Garvin, S., Ollinger, K., and Dabrosin, C. (2006). Resveratrol induces apoptosis and inhibits angiogenesis in human breast cancer xenografts in vivo. *Cancer Letters, 231*, 113-122.

Graf, E. (1992). Antioxidant potential of ferulic acid. *Free Radic. Biol. Med., 13*(4), 435-448.

Grunberger, D., Banerjee, R., Eisinger, K., Oltz, K., Efros, E. M., Caldwell, M., Estevez, V. and Nakanishi, K. (1988) Preferential cytotoxicity on tumor cells by caffeic acid phenethyl ester isolated from propolis. *Experientia, 44*, 230-232.

Guardia, T., Rotelli, A. E., Juarez, A. O., and Pelzer, L. E. (2001). Anti-inflammatory properties of plant flavonoids. Effects of rutin, quercetin and hesperidin on adjuvant arthritis in rat. *Il Farmaco, 56*(9), 683-687.

Gu, L., Kelm, M. A., Hammerstone, J. F., Zhang, Z., Beecher, G., Holden, J., Haytowitz, D., and Prior, R. L. (2003). Liquid chromatographic/electrospray ionization mass spectrometric studies of proanthocyanidins in foods. *J. Mass Spectrom., 38*(12), 1272-1280.

Hernández, V., Recio, M. C., Máñez, S., Giner, R. M., and Ríos, J. L. (2007). Effects of naturally occurring dihydroflavonols from Inula viscosa on inflammation and enzymes involved in the arachidonic acid metabolism. *Life Sci., 81*(6), 480-488.

Higgs, G. A., Salmon, J. A., Henderson, B., and Vane, J. R. Pharmacokinetics of Aspirin and salicylate in relation to inhibition of arachidonate cyclooxygenase and anti-inflammatory activity. *Proc. Natl. Acad. Sci., 84*, 1417-1420.

Hsu, Y.-L, Kuo, P.-L., and Lin, C.-C. (2004). Acacetin inhibits the froliferation of Hep G2 by blocking cell cycle progression and inducing apoptosis. *Biochem. Pharmacol., 67*(5), 823-829.

Hsu, Y.-L., Liang, H.-L., Hung, C.-H., and Kuo, P.-L. (2009a). Syringetin, a flavonoid derivative in grape and wine, induces human osteoblast differentiation through bone morphogenetic protein-2/extracellular signal-regulated kinase 1/2 pathway. *Mol. Nutr. Food Res., 53*(11), 1452-1461.

Hsu, Y. L., Uen, Y. H., Chen, Y., Liang, H. L., and Kuo, P. L. (2009b). Tricetin, a dietary flavonoid, inhibits proliferation of human breast adenocarcinoma mcf-7 cells by blocking cell cycle progression and inducing apoptosis. *J. Agric. Food Chem., 57*(18), 8688-8695.

Isanga, J. and Zhang, G.-N. (2007). Biologically active components and nutraceuticals in peanuts and related products : review. *Food Reviews International, 23*, 123-140.

Itoigawa, M., Takeya, K., Ito, C., and Furu Kawa, H. (1999). Structure activity relationship of cardiotonic flavonoids in guinea pig papillary. *J. Ethnopharmacol., 65*, 267-272.

Ivanoyska, N., Yossifova, T., Vassileva, E., and Kostova, I. (1994). Effect of some hydroxycoumarins on complement-mediated hemolysis in human serum. *Methods Find Exp. Clin. Pharmacol., 16*, 557-562.

Iwu, M. M. (1985). Antihepatoxic constituents of Garcinia kola seeds. *Experientia, 41*(5), 699-700.

Kandil, F. E., Smith, M. A. L, Rogers, R. B., Pepin, M. F., Song, L. L., Pezzuto, J. M., and Seigler, D. S. (2002). Composition of a chemopreventive proanthocyanidin-rich fraction from cranberry fruits responsible for the inhibition of 12-O-tetradecanoyl phorbol-13-acetate (TPA)-induced ornithine decarboxylase (ODC) activity. *J. Agric. Food Chem., 50*, 1063-1069.

Karim, M., McCormick, K., and Kappagoda, C. T. (2000). Effects of cocoa procyanidins on endothelium-dependent relaxation. *J. Nutr., 130*, 2105S–2108S.

Katzenellenbogen, B. S., Katzenellenbogen, J. A., and Cai, D. M. (1979). Zearalenones: Characterization of the estrogenic potencies and receptor interactions of a series of fungal β-resorcylic acid lactones. *Endocrinology, 105*(1), 33-40.

Kayo Henmi, K., Hiwatashi, Y., Hikita, E., Toyama, N., and Hirano, T. (2009). Methoxy- and fluoro-chalcone derivatives arrest cell cycle progression and induce apoptosis in human melanoma cell A375. *Biol. Pharm. Bull., 32*(6), 1109-1113.

Kim, J. M. and Yun-Choi, H. S. (2008). Anti-platelet effects of flavonoids and flavonoid-glycosides from Sophora japonica. *Arch. Pharmacal Res., 31*(7), 886-890.

Kim, S.-H., Yoon, S.-H., Byong, W.-L., Ki, H. P., Young, H. K., and Bae, Y.-S. (2005). *Oncology Research., 15*(6), 327-332.

Kimura, Y. and Sumiyoshi, M. (2009). Olive leaf extract and its main component oleuropein prevent chronic ultraviolet B radiation-induced skin damage and carcinogenesis in hairless mice. *J. Nutr., 139*(11), 2079-2086.

Klein-Galczinsky, C. (1999). Pharmacological and clinical effectiveness of a fixed phytogenic combination trembling poplar (Populus tremula), true goldenrod (Solidago virgaurea) and ash (Fraxinus excelsior) in mild to moderate rheumatic complains. *Wien Med. Wochenschr, 149*, 248-253.

Kobuchi, H., Roy, S., Sen, C. K., Nguyen, H. G., and Packer, L. (1999). Quercetin inhibits inducible ICAM-1 expression in human endothelial cells through the JNK pathway. *Am. J. Physiol., 277*, C403-C411.

Kris-Etherton, P. M., Hecker, K. D., Bonanome, A., Coval, S. M., Binkoski, A. E., Hilpert, K. F., Griel, A. E., and Etherton, T. D. (2002). Bioactive compounds in foods: Their role in the prevention of cardiovascular disease and cancers. *Am. J. Med., 113*(9B), 71S-88S.

Kristinová, V., Mozuraityte, R., Storrø, I., and Rustad, T. (2009). *J. Agric. Food Chem., 57*(21), 10377-10385.

Kuete, V., Tangmouo, J. G., Marion Meyer, J. J., and Lall, N. (2009). Disopyrone, crassiflorone and plumbagin: three antimycobacterial and antigonorrhoeal naphthoquinones from two Diospyros spp. Int. J. Antimicrob. *Agents, 34*(4), 322-325.

Kumar, R., Sowmyalakshmi, S., Koduru, S., Pahari, P., Rohr, J., Kyprianou, N., and Damodaran, C. (2009). Psoralidin, an herbal molecule, inhibits phophatidylinositol 3-kinase-mediated akt signaling in androgen-independent prostate cancer cells. *Cancer Prevention Research, 2*, 234-243.

Lee, S., Han, J. M., Kim, H., Kim, E. Jeong, T. S., Lee, W. S., and Cho, K. H. (2004). Synthesis of cinnamic acid derivatives and their inhibitory effects on LDL-oxidation, acyl-CoA, cholesterol acyltransferase-1 and -2 activity, and decrease of HDL-particle size. *Bioorg. Med. Chem. Lett., 14*(18), 4677-4681.

Lesage-Meessen, L., Delattre, M., Haon, M., Thibault, J. F., Ceccaldi, B. C., Brunerie, P., Asther, M. (1996). A two-step bioconversion process for vanillin production from ferulic acid combining Aspergillus niger and Pycnoporus cinnabarinus. *J. Biotechnol., 50*(2-3), 107–113.

Levit, L., Cholst, M., King, R., and Handelsman, M. (1948). Rutin therapy for increased capillary fragility and retinopathy associated with diabetes mellitus. *Am. J. Med. Sci., 215*(2), 130-135.

Li, X.-H., Zhang, J.-C., Sui, S.-F., and Yang, M.-S. (2005). Effect of daidzin, genistin, and glycitin on osteogenic and adipogenic differentiation of bone marrow stromal cells and adipocytic transdifferentiation of osteoblasts. *Acta Pharmacol. Sin., 26*, 1081-1086.

Lim, H., Son, K. H., Chang, H. W., Bae, K., Kang, S. S., and Kim, H. P. (2008). Anti-inflammatory activity of pectolinarigenin and pectolinarin isolated from Cirsium chanroenicum. *Biol. Pharm. Bull., 31*(11), 2063-2067.

Lin, L. C., Kuo, Y.-C., and Chou, C.-J. (2002). Immunomodulatory proanthocyanidins from Ecdysanthera utilis. *J. Nat. Prod., 65*, 505-508.

Liou, Y. F., Hall, I. H., and Lee, K. H. (2006). Antitumor agents LIV: The effects of daphnoretin on in vitro protein synthesis of ehrlich ascites carcinoma cells and other tissues. *J. Pharm. Sci., 71*(7), 745-749.

Liu, Z., Tao, X., Zhang, C., Lu, Y., and Wei, D. (2005). Protective effects of hyperoside (quercetin-3-o-galactoside) to PC12 cells against cytotoxicity induced by hydrogen peroxide and tert-butyl hydroperoxide. Biomed. *Pharmacother., 59*(9), 481-490.

Lotito, S. B. and Fraga, C. G. (1998). Catechin prevents human plasma oxidation. *Free Radic. Biol. Med., 24*, 435-441.

Lou, H., Yamazaki, Y., Saski, T., Uchida, M., Tanaka, H. and Oka, S. (1999). A-type proanthocyanidins from peanut skins. *Phytochemistry, 51*, 297-308.

Lou, H., Yuan, H., Ma, B., Ren, D., Ji, M., and Oka, S. (2004). Polyphenols from peanut skins and their free radical-scavenging effects. *Phytochemistry, 65*, 2391-2399.

Lou, H., Yuan, H., Yamazaki, Y., Sasaki, T., and Oka, S. (2001). Alkaloids and flavanoids from peanut skins. *Planta Med., 67*, 345-349.

Mada, S. R., Metukuri, M. R., Burugula, L., Reddanna, P., and Krishna, D. R. (2009). Antiinflammatory and antinociceptive activities of gossypin and procumbentin – cyclooxygenase-2 (COX-2) inhibition studies. *Phytotherapy Research, 23*(6), 878-884.

Mandalari, G., Bennett, R. N., Bisignano, G., Trombetta, D., Saija, A., Faulds, C. B., Gasson, M. J., and Narbad, A. (2007). Antimicrobial activity of flavonoids extracted from bergamot (Citrus bergamia Risso) peel, a byproduct of the essential oil industry. *J. Appl. Microbiol., 103*(6), 2056-2064.

Mao, T., Van De Water, J., Keen, C. L., Schmitz, H., and Gershwin, M. (2000). Cocoa procyanidins and human cytokine transcription and secretion. *J. Nutr., 130*, 2093S–2099S.

Maruyama, H., Sumitou, Y., Sakamoto, T., Araki, Y., and Hara, H. (2009). Antihypertensive effects of flavonoids isolated from brazilian green propolis in spontaneously hypertensive rats. *Biol. Pharm. Bull., 32*(7), 1244-1250.

Meriel, P., Galinier, F., Bounhoure, J. P., and Gavalda, J. (1964). Use in cardiology of a new anticoagulant: Dicoumoxyl (1-bis-methoxy (4-hydroxy, 3-coumarinyl) 2,2-ethane). *Toulouse Med., 65*, 849-858.

Motilva, V., Alarcón de la Lastra, C., and Martin, M. J. (1994). Ulcer-protecting effects of naringenin on gastric lesions induced by ethanol in rat: role of endogenous prostaglandins. *J. Pharm. Pharmacol., 46*(2), 91-94.

Narayana, K. R., Reddy, M. S., Chaluvadi, M. R., and Krishna, D. R. (2001). Bioflavonoids classification, pharmacological, biochemical effects and therapeutic potential. *Indian Journal of Pharmacology, 33*, 2-16.

Natarajan, K., Singh, S., Burke, Jr., T. R., Grunberger, D., and Aggarwal, B. B. 1996. Caffeic acid phenetyl ester is a potent and specific inhibitor of activation of nuclear transcription factor NF-KB. *Proc. Natl. Acad. Sci., 93*, 9090-9095.

Niu, H. S., Liu, I. M., Cheng, J. T., Lin, C. L., and Hsu, F. L. (2008). Hypoglycemic effect of syringin from Eleutherococcus senticosus in Streptozotocin-induced diabetic rats. *Planta Med. 74*(2), 109-113.

Ogawa, H., Sasai, N., Kamisako, T., and Baba, K. 2007. Effects ofosthol on blood pressure and lipid metabolism in stroke-prone spontaneously hypertensive rats. *J. Ethnopharmacology, 112*(1), 26-31.

Ogawa, Y., Oku, H., Iwaoka, E., Iinuma, M., and Ishiguro, K. (2007). Allergy-preventive flavonoids from Xanthorrhoea hastilis. *Chem. Pharm. Bull., 55*(4): 675-678.

Olas, B. and Waschowicz, B. (2002). Resveratrol and vitamin C as antioxidants in blood platelets. *Thrombosis Research. 106*, 143-148.

Orallo, F., Alvarez, E., Basaran, H., and Lugnier, C. (2004). Comparative study of the vasorelaxant activity, superoxide-scavenging ability and cyclic nucleotide phosphodiesterase-inhibitory effects of hesperetin and hesperidin. *Naunyn-Schmiedeberg's Arch. Pharmacol., 370*(6), 452-463.

Pacciaroni Adel, V., Gette Mde, L., Derita, M., Ariza-Espinar, L., Gil, R. R., Zacchino, S. A., and Silva, G. L. (2008). Antifungal activity of Heterothalamus alienus metabolites. *Phytotherapy Research, 22*(4), 524-528.

Pang, X., Yi, T., Yi, Z., Cho S. G., Qu, W., Pinkaew, D., Fujise, K., and Liu, M. (2009). Morelloflavone, a biflavonoid, inhibits tumor angiogenesis by targeting rho GTPases and extracellular signal-regulated kinase signaling pathways. *Cancer Research 69*(2), 518-525.

Park, B. C., Lee, Y. S., Park, H. J., Kwak, M. K., Yoo, B. K., Kim, J. Y., and Kim J. A. (2007). Protective effects of fustin, a flavonoid from Rhus verniciflua Stokes, on 6-hydroxydopamin-induced neuronal cell death. *Exp. Mol. Med., 39*(3), 316-326.

Park, Y., Lee, S., and Lim, Y. (2007). Relationships between structures of hydroxyflavone derivatives and their anti-oxidative activities. In *Frontiers in the Convergence of Bioscience and Information Technologies* (pp. 43-47).

Paterson, J. R. and Lawrence, J. R. (2001). Salicylic acid: a link between aspirin, diet and the prevention of colorectal cancer. *Q. J. Med. 94*, 445-448.

Pearson, D. A., Schmitz, H.H., Lazarus, S. A., and Keen, C.L. (2001). Inhibition of in vitro low-density lipoprotein oxidation by oligomeric procyanidins present in chocolate and cocoas. In: L. Packer, *Methods in Enzymology*, (pp. 350-360). New York: Academic Press.

Pérez-Vizcaíno, F., Ibarra, M., Cogolludo, A. L., Duarte, J., Zaragozá-Arnáez, F., Morenol, L., López-López, G., and Tamargo, J. (2002). Endothelium-independent vasodilator effects of the flavonoid quercetin

and its methylated metabolites in rat conductance and resistance arteries. *J. Pharmacol. Exp. Ther., 302*(1), 66-72.

Popova, M., Bankova, V., Spassov, S., Tsvetkova, I., Naydenski, C., Silva, M. V., and Tsartsarova, M. (2001). New bioactive chalcones in propolis from El Salvador. *Z. Naturforsch., C: Biosci., 56*(7-8), 593-596.

Rakotoarison, O., Rabenau, I., Lobstein, A., Um, B. H., Schott, C., Anton, R., Randriantsoa, A., and Andriantsitohaina, R. (2003). Vasorelaxing properties and bio-guided fractionation of Cedrelopsis grevei. *Planta Med., 69*(2), 179-181.

Ramón Sánchez de Rojas, V., Somoza, B., Ortega, T., Villar, A. M., and Tejerina, T. (1999). Vasodilatory effect in rat aorta of eriodictyol obtained from Satureja obovata. Planta Med., 65(3), 234-238.
Ratty, A. K. Effects of flavonoids on nonenzymatic lipid peroxidation: structure-activity relationship. Biochem. *Med. Metabol. Biol., 39*, 67-79.

Rocha, B. S., Gago, B., Barbosa, R. M., and Laranjinha, J. (2009). Dietary polyphenols generate nitric oxide from nitrite in the stomach and induce smooth muscle relaxation. *Toxicology, 265*(1-2), 41-48.

Roschek, B., Fink, R. C., McMichael, M. D., Li, D. and Alberte, R. S. (2009). Elderberry flavonoids bind to and prevent H1N1 infection in vitro. *Phytochemistry, 70*(10), 1255-1261.

Rotondo, S., Rajtar, G., Manarini, S., Celardo, A., Rotillo, D., de Gaetano, G., Evangelista, V., and Cerletti, C. (1998). Effect of trans-resveratrol, a natural polyphenolic compound, on human polymorphonuclear leukocyte function. *Br. J. Pharmacol., 123*(8), 1691-1699.

Sacco, S. and Maffei, M. (1997). The effect of isosakuranetin (5,7-dihydroxy 4'-methoxy flavanone) on potassium umptake in wheat root segments. *Phytochemistry, 46*(2), 245-248.

Samoszuk, M., Tan, J., and Chorn, G. (2005). The chalcone butein from Rhus vernifciflua Stokes inhibits clonogenic growth of human breast cancer cells co-cultured with fibroblasts. *BMC Complement Altern. Med., 5*, 1-5.

Sata, Y., Akao, T., He, J. X., Nojima, H., Kuraishi, Y., Morota, T., Asano, T. and Tani, T. (2006). Glycycoumarin from Glycyrrhizae Radix acts as a potent antispasmodic through inhibition of phosphodiesterase 3. *J Ethnopharmacol., 105*(3), 409-414.

Sekine-Osajima, Y., Sakamoto, N., Nakagawa, M., Itsui, Y., Tasaka, M., Nishimura-Sakurai, Y., Chen, C. H., Suda, G., Mishima, K., Onuki, Y., Yamamoto, M., Maekawa, S., Enomoto, N., Kanai, T., Tsuchiya, K., and Watanabe, M. (2009). *Hepatology Research, 39*(1), 60-69.

Setchell, K. D., Zhao, X., Shoaf, S. E., and Ragland, K. (2009). The pharmacokinetics of S-(-)equol administered as SE5-OH tablets to healthy postmenopausal women. *J. Nutr., 139*(11), 2037-2043.

Sethi, O. P., Anand, K. K., and Gulati, O. D. (1992). Evaluation of xanthotoxol for central nervous system activity. *J. Ethnopharmacol., 36*(3), 239-247.

Shih, Y. W., Lee, Y. C., Wu, P. F., Lee, Y. B., and Chiang, T. A. Plumbagin inhibits invasion and migration of liver cancer HepG2 cells by decreasing productions of matrix metalloproteinase-2 and urokinase- plasminogen activator. *Hepatology Research, 39*(10), 998-1009.

Song, T. T., Hendrich, S., and Muphy, P. A. (1999). Estrogenic activity of glycitein, a soy isoflavone. *J. Agric. Food Chem., 47*(4), 1607-1610.
Spencer, J. P. E., Schroeter, H., Kuhnle, G., Srai, S. K. S., Tyrrell, R. M., Hahn, U., and Rice-Evans, C. (2001). Epicatechin and its in vivo metabolite, 3'-O-methyl epicatechin, protect human fibroblasts from oxidative-stress-induced cell death involving caspase-3 activation. *Biochem. J., 354*, 493-500.

Takahashi, T., Kamiya, T., Hasegawa, A., and Yokoo, Y. (1999). Procyanidins oligomers selectively and intensively promote proliferation of mouse hair epithelial cells in vitro and activate hair follicle growth in vivo. *J. Investigative Dermatology, 112*, 310-316.

Tanaka, Y., Kikuzaki, H., Fukuda, S., and Nakatani, N. (2001). Antibacterial compounds of licorice against upper airway respiratory tract pathogens. *J. Nutr. Sci. Vitaminol., 47*(3), 270-273.

Tang, Y. Z. and Liu, Z. Q. (2007). Insight into the free-radicial-scavenging mechanism of hydroxyl-substituent Schiff bases in the free-radical-induced hemolysis of erythrocytes. *Cell Biochem. Funct., 25*(6), 701-710.

Teng, B.-S., Lu, Y.-H., Wang, Z.-T., Tao, X.-Y., and Wei, D.-Z. (2006). In vitro anti-tumor activity of isorhamnetin isolated from Hippophae rhamnoides L. against BEL-7402 cells. *Pharmacol. Res., 54*(3), 186-194.

Thorp, A. A., Sinn, N., Buckley, J. D., Coates, A. M., and Howe, P. R. (2009). Soya isoflavone supplementation enhances spatial working memory in men. *Br. J. Nutr., 102*(9), 1348-1354.

Toda, S. and Shirataki, Y. (2002). Inhibitory effects of isoflavones in Sophora mooracrotiana on lipid peroxidation by superoxide. *Pharmaceutical Biology, 40*(6), 422-424.

Tonari, K., Mitsui, K., and Yonemoto, K. (2002). Structure and antibacterial activity of cinnamic acid related compounds. *J. Oleo Sci., 51*(4), 271-273.

Vasconcelos, J. F., Teixeira, M. M., Barbosa-Filho, J. M., Agra, M. F., Nunes, X. P., Giulietti, A. M, Riberiro-Dos-Santos, R., and Soares, M. B. (2009). Effects of umbelliferone in a murine model of allergic airway inflammation. *Eur. J. Pharmacol., 609*(1-3), 126-131.

Visioli, F., Bellosta, S., and Galli, C. (1998). Oleuropein, the bitter principle of olives, enhances nitric oxide production by mouse macrophages. *Life Sci., 62*(6), 541-546.

Visioli, F. and Galli, C. (1994). Oleuropein protects low density lipoprotein from oxidation. *Life Sci., 55*(24), 1965-1971.

Wang, M.S. (1980). Studies on the chemical constituents of Zu-Shi-Ma (Daphne giraldii) (III). *Chinese Traditional and Herbal Drugs, 11*(9), 389-390.

Woo, S. W., Lee, S. H., Kang, H.-C., Park, E.-J., Zhao, Y.-Z., Kim Y.-C., and Sohn, D. H. (2003). Butein suppresses myofibroblastic differentiation of rat hepatic stellate cells in primary culture. *J. Pharm. Pharmacol., 55*(3), 347-352.

Yagasaki, K., Furuse, T., and Miura, Y. (1998). Inhibitory effects of coffee and caffeic acid, 3,4-dihy-droxycinnamic acid, on the invasion of hepatoma cells. In *2nd International Electronic Conference on Synthetic Organic Chemistry*.

Yen, G. C. and Hsieh, C. L. (2002). Inhibitory effects of Du-zhong (Eucommia ulmoides Oliv.) against low-density lipoprotein oxidative modification. *Food Chem., 77*, 449-456.

Yokozawa, T., Kim, H. Y., Cho, E. J., Choi, J. S., and Chung, H. Y. (2002). Antioxidant effects of isorhamnetin 3,7-Di-O-β-d-glucopyranoside isolated from mustard leaf (Brassica juncea) in rats with Streptozotocin-induced diabetes. *J. Agric. Food Chem., 50*(19), 5490-5495.

Yu, J., Ahmedna, M., and Goktepe, I. (2005). Effects of processing methods and extraction solvents on concentration and antioxidant activity of peanut skin phenolics. *Food Chem., 90*, 199-206.

Yu, J., Ahmedna, M., Goktepe, I., and Dai, J. (2006). Peanut skin procyanidins:Composition and antioxidant activities as affected by processing. *J. Food Compos. Anal., 19*, 364-371.

Yu, S. M., Cheng, Z. J., and Kuo, S. C. (1995). Endothelium-dependent relaxation of rat aorta by butein, a novel cyclic AMP-specific phosphodiesterase inhibitor. *Eur. J. Pharmacol. 280*(1), 69-77.

Zhou, H. Y., Hong, J. L., Shu, P., Ni, Y. J., and Qin, M. J. A new dicoumarin and anticoagulant activity from Viola yedoensis Makino. *Filoterapia., 80*(5), 283-285.

SUMMARY

Prior to this research, the information available on the composition of polyphenols in peanut skins was incomplete. Previous studies had identified few compounds, in part due to the utilized analytical methodology. However, the vast number of phenolic-based compounds identified in this study reveals that peanut skins are possibly one of the most phenolic-rich and diverse plant sources ever studied. The majority of these compounds are known to exhibit powerful antioxidant activity, which was reported in this study by determining the antioxidant profile of the Gregory peanut line. This indicates that peanut skins could be used as a novel source for the extraction of natural antioxidant and preservative components. This proves the capability that peanut skins, which had been previously viewed as a by-product (or waste-product) of the peanut industry, can become a value-added commodity and revenue stream for peanut farmers.

Numerous compounds were detected which have been reported to exhibit specific chemical, biological, nutraceutical, and pharmaceutical attributes. This indicates the possibility that peanut skins could be utilized as a novel source for the extraction of compounds which have the potential to treat ailments such as cardiovascular disease, various forms of cancer, and other human health-related conditions. All of these factors showcase the need for future research into the biological effects of components contained within peanut skins. Future research could use this study as a template, to further narrow down the numerous compounds which were tentatively identified (many of which have significant antioxidant and biological effects).

APPENDIX

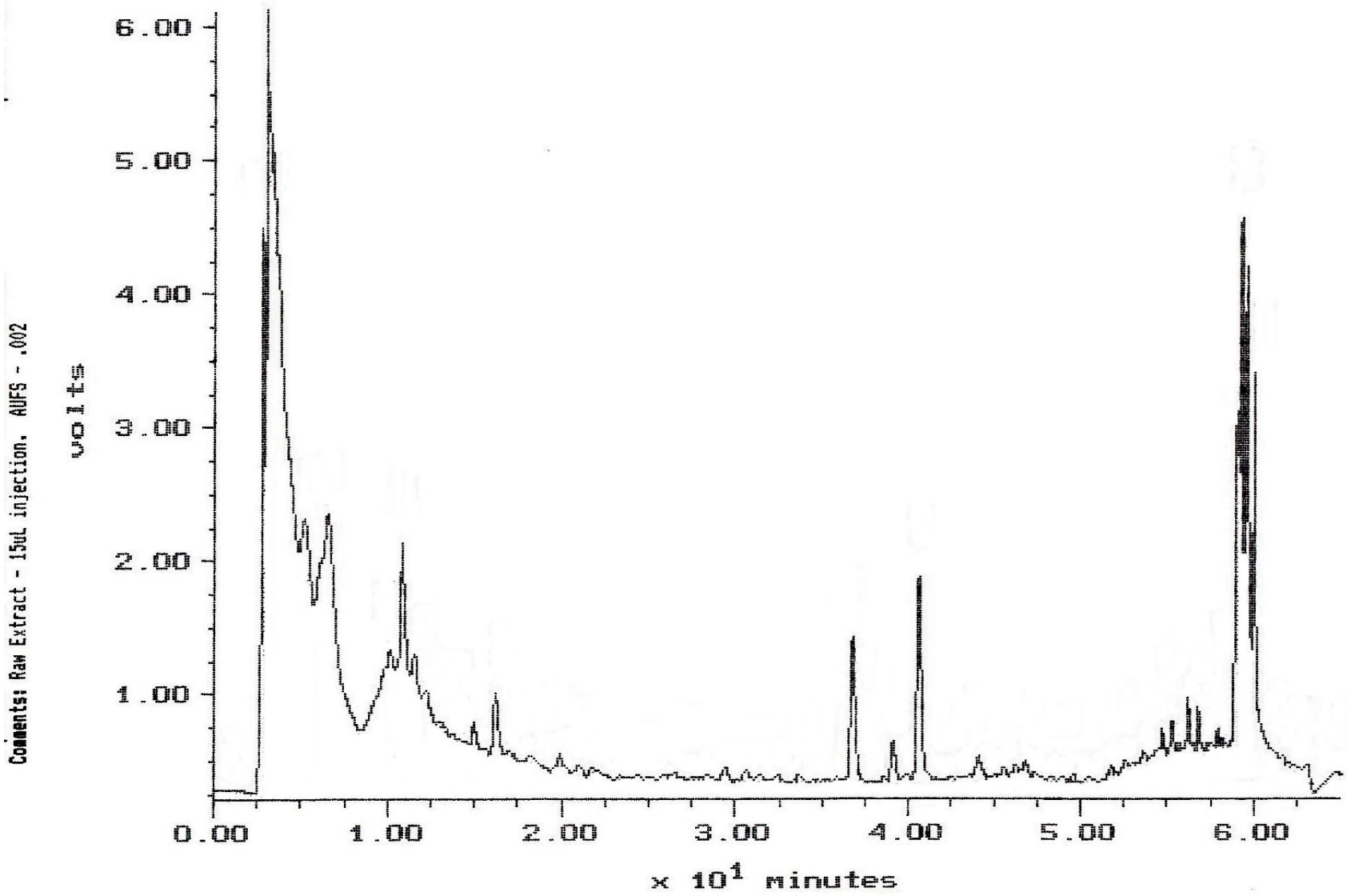

Figure A.1: HPLC-UV Chromatogram of Peanut Skin Raw Extract at 280nm.

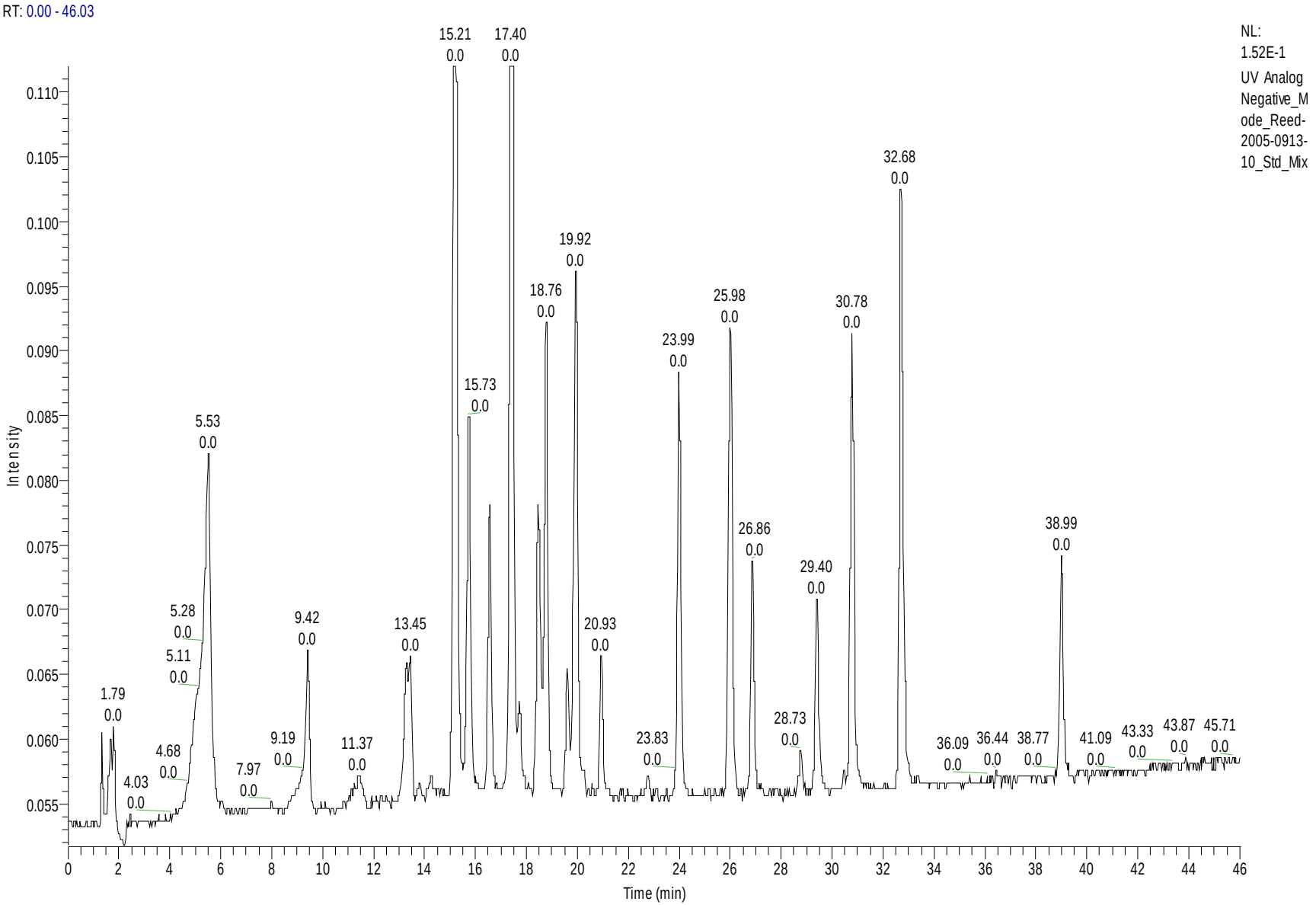

Figure A.2: HPLC-UV Chromatogram of Standard Mix at 280nm.

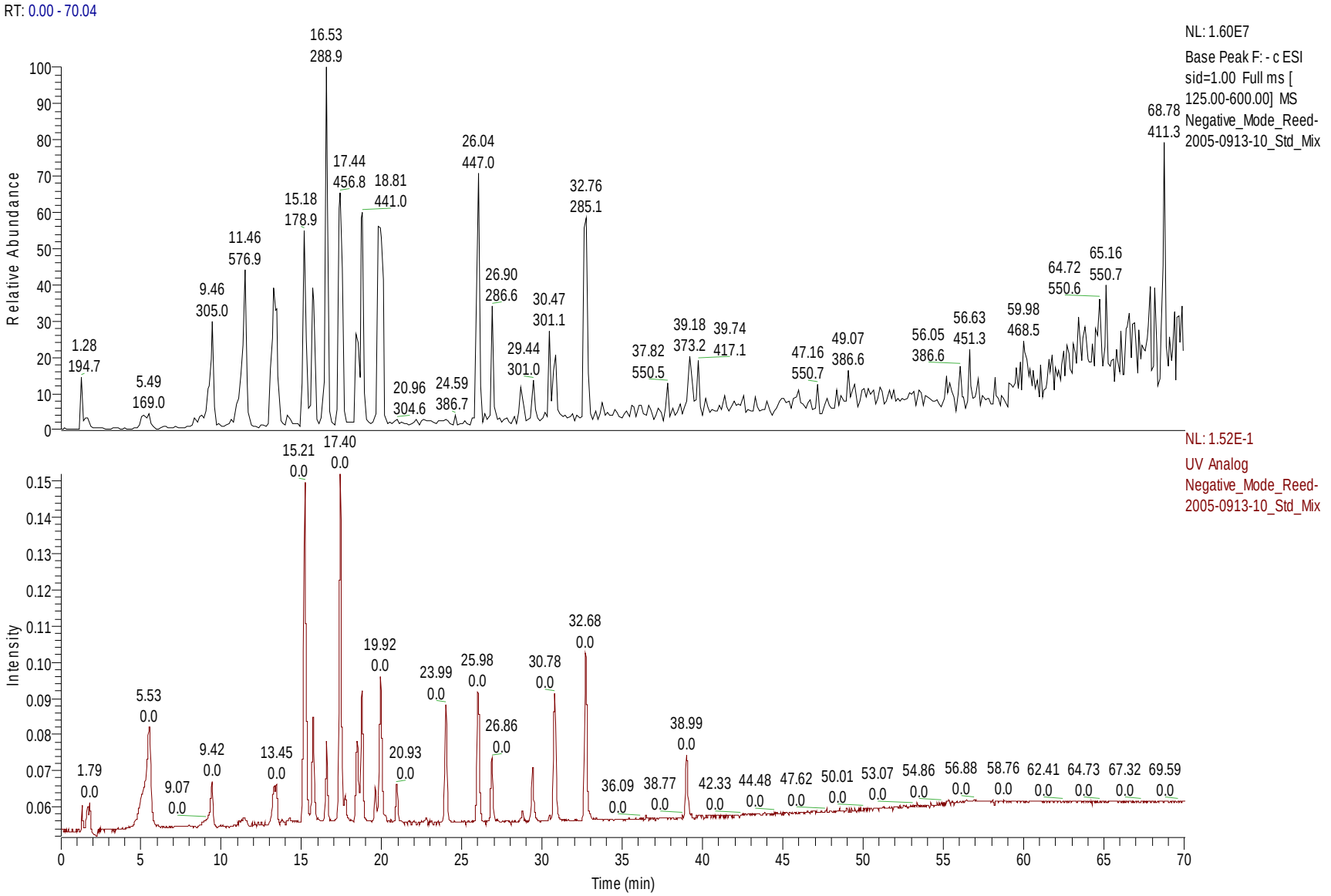

Figure A.3: Standard Mix: HPLC-UV Chromatogram (bottom) versus TIC [Total Ion Chromatogram – Showing the "ms" Normal Mass Spectra Base Peaks for the Most Intense Ions in SID=1.0 Scan Range (m/z 125-600 M-H$^-$)] (top).

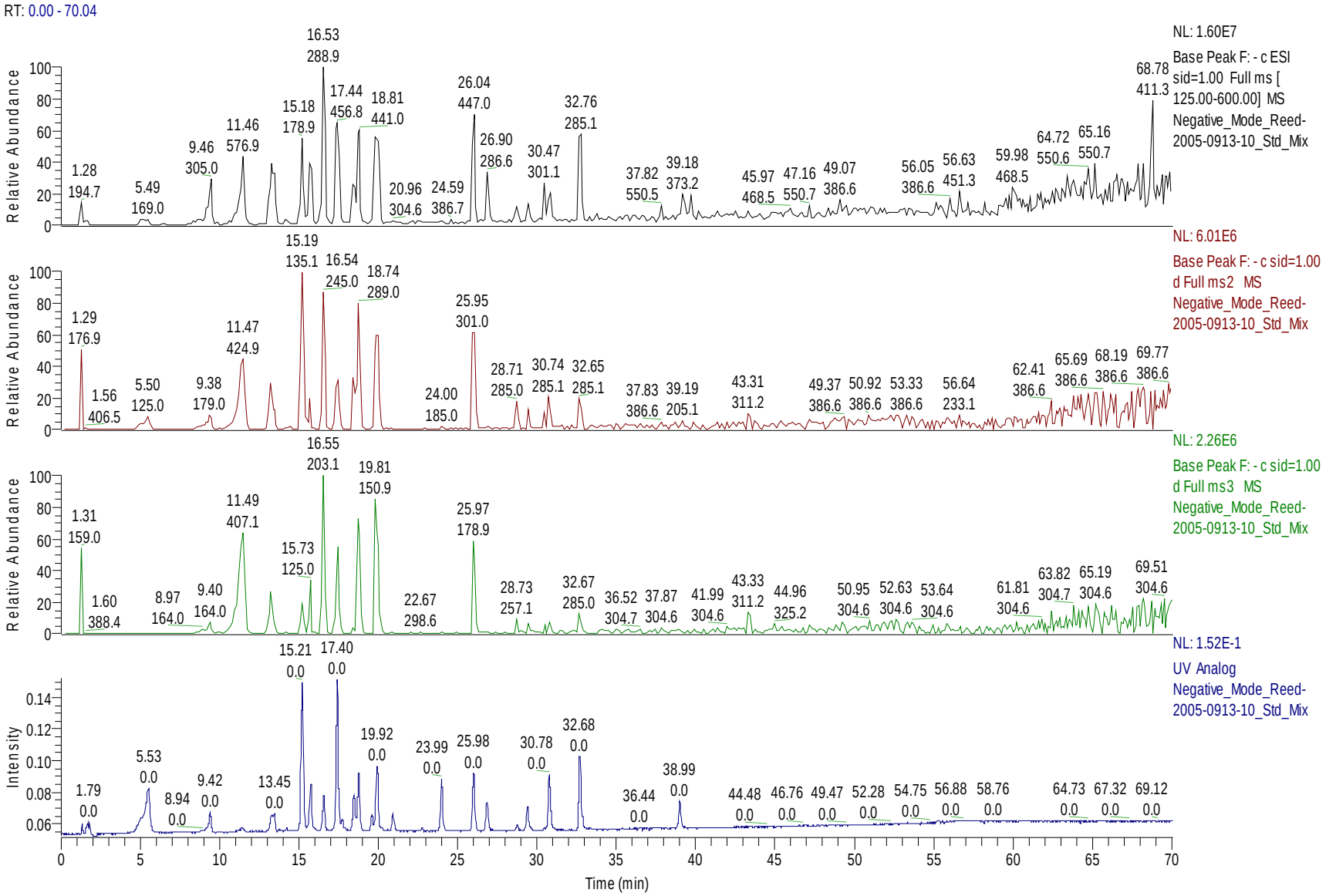

Figure A.4: Standard Mix: HPLC-UV Chromatogram (bottom) versus TIC's [Total Ion Chromatograms – Showing the "ms" Normal Mass Spectra (top), "ms2" (second), and "ms3" (third) Base Peaks for Most Intense Ions in SID=1.0 Scan Range (m/z 125-600 M-H$^-$)]

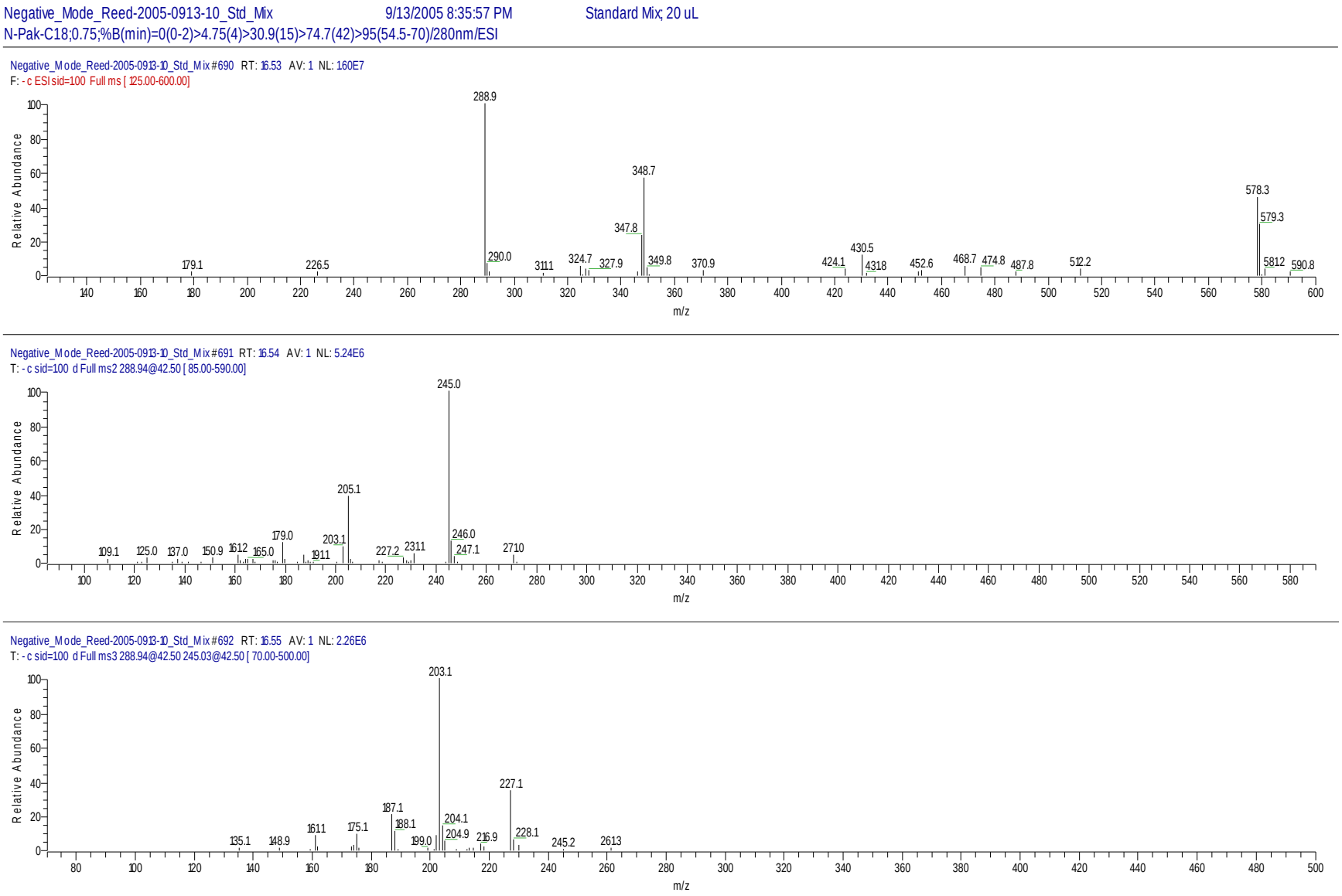

Figure A.5: Ion Spectra for Epicatechin – Showing the "ms" Normal Mass Spectra (top), "ms2" MS/MS Spectra (second), and "ms3" MS/MS/MS Spectra (bottom).

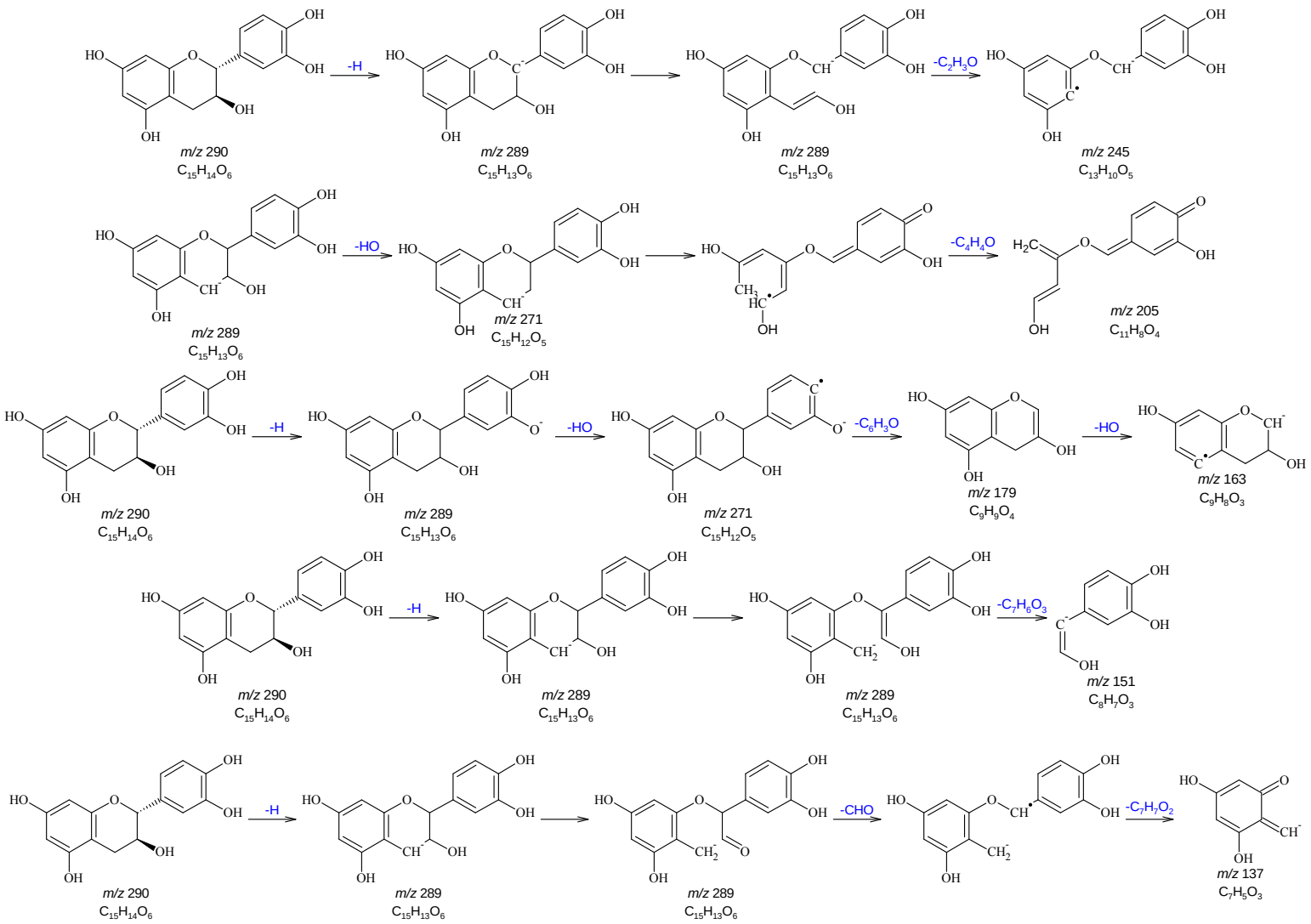

Figure A.6: Fragmentation Scheme for Epicatechin

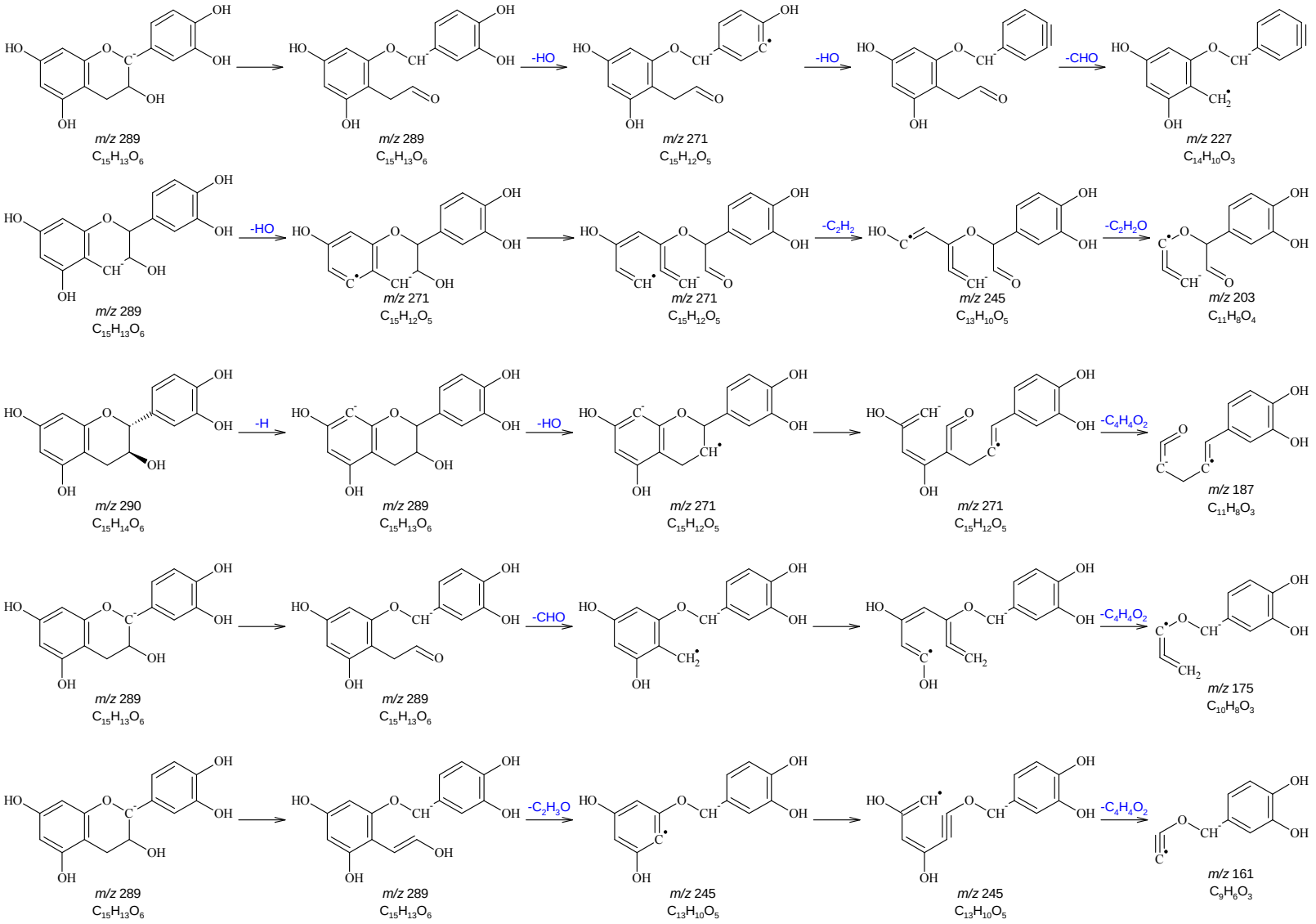

Figure A.6 (cont.): Fragmentation Scheme for Epicatechin

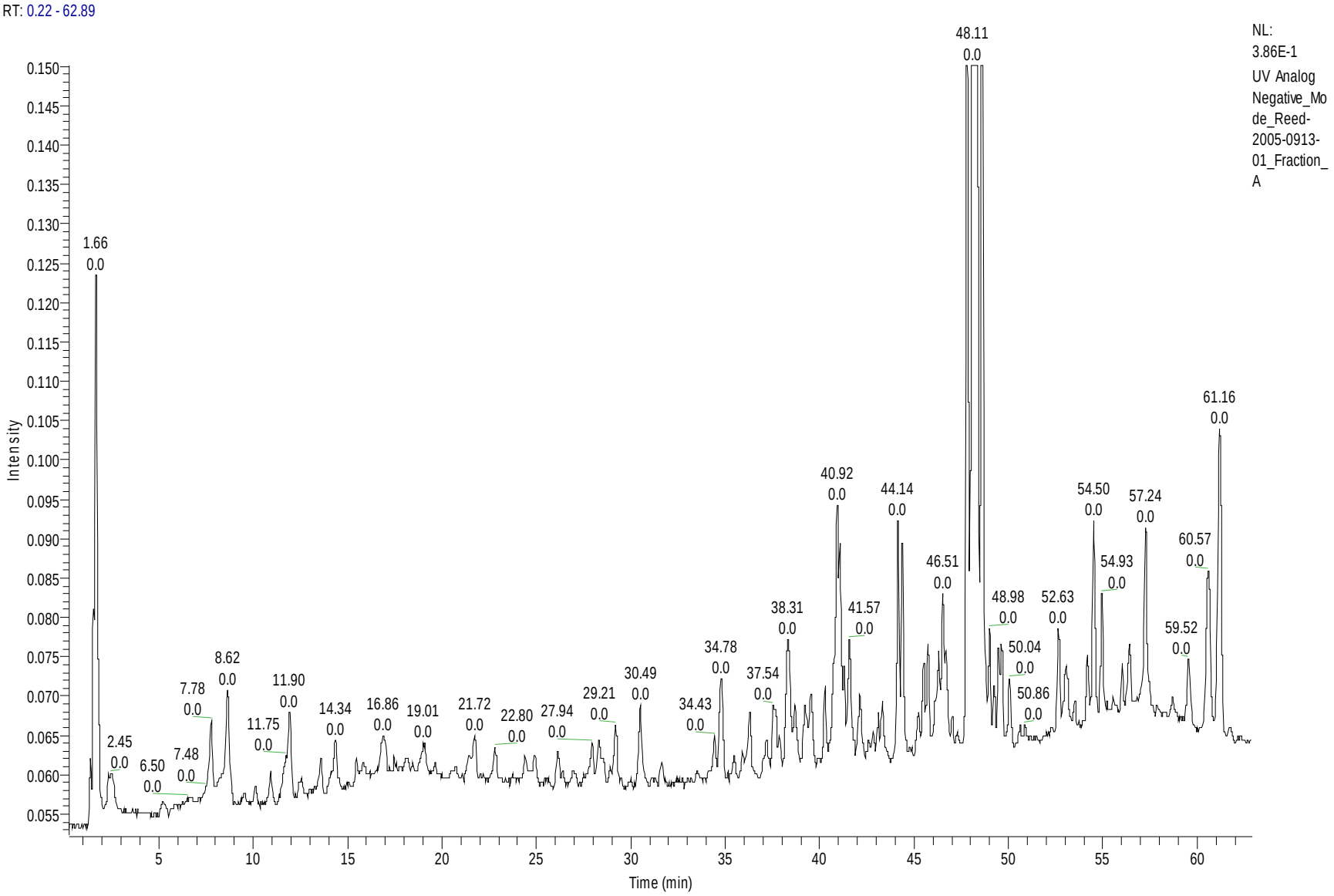

Figure A.7: HPLC-UV Chromatogram of Peanut Skin Fraction A (Obtained from Toyopearl Size Exclusion Chromatography) at 280nm.

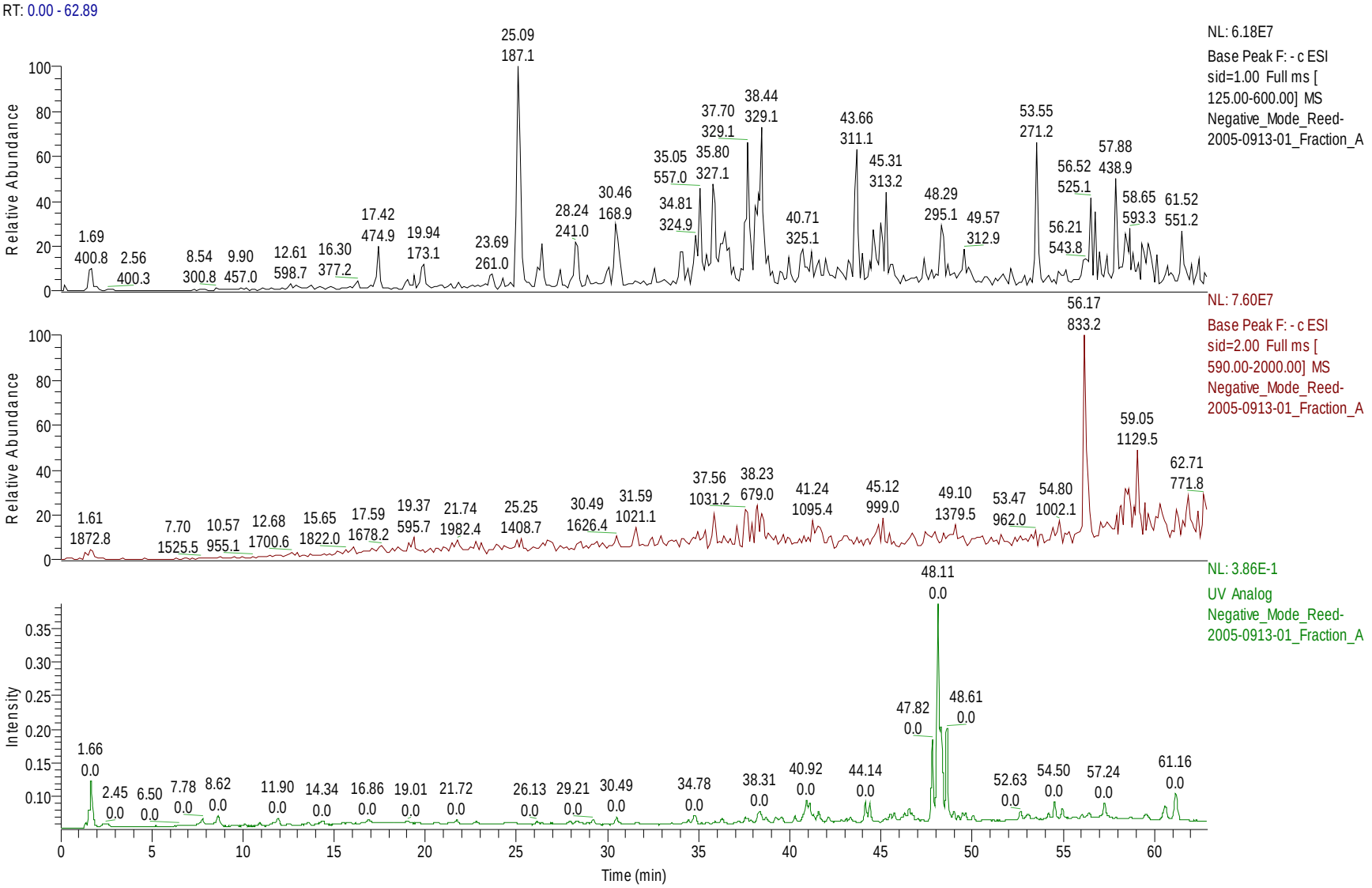

Figure A.8: Peanut Skin Fraction A: HPLC-UV Chromatogram (bottom) versus TIC's [Total Ion Chromatograms – Showing the "ms" Normal Mass Spectra Base Peaks for the Most Intense Ions in Both SID=1.0 Scan Range (m/z 125-600 M-H$^-$) (top) and SID=2.0 Scan Range (m/z 590-2000 M-H$^-$) (middle)].

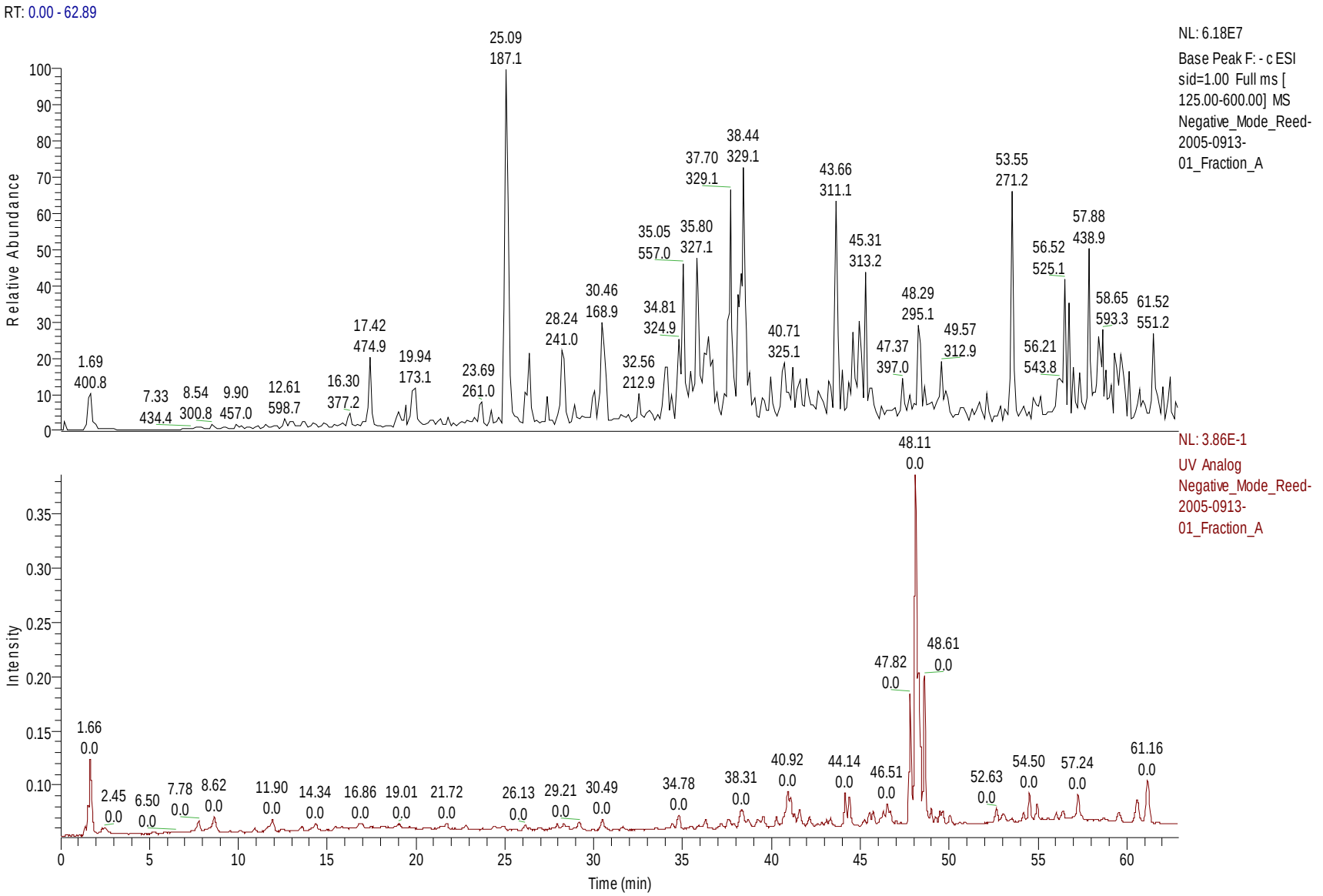

Figure A.9: Peanut Skin Fraction A: HPLC-UV Chromatogram (bottom) versus TIC [Total Ion Chromatogram – Showing the "ms" Normal Mass Spectra Base Peaks for the Most Intense Ions in SID=1.0 Scan Range (m/z 125-600 M-H$^-$)] (top).

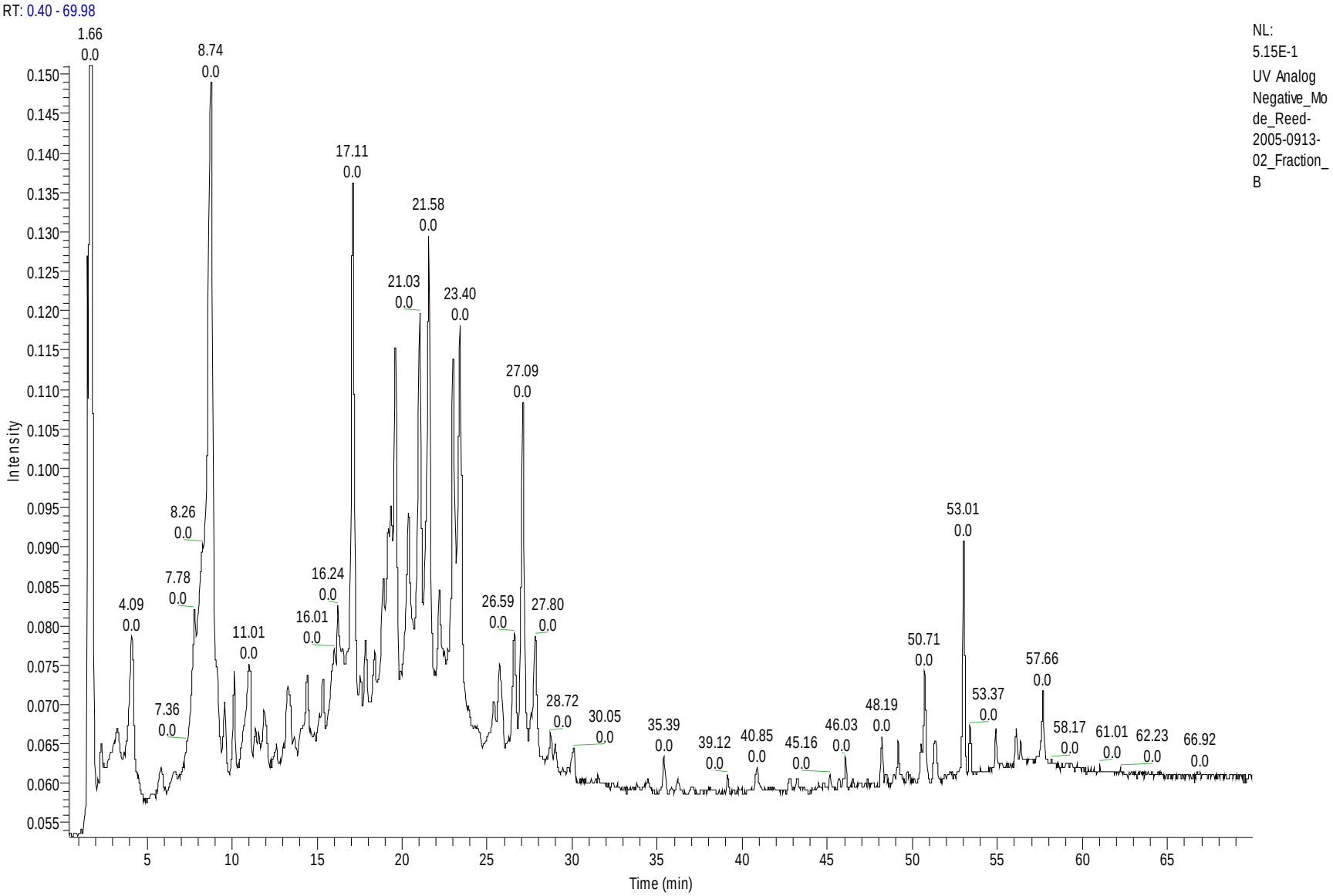

Figure A.10: HPLC-UV Chromatogram of Peanut Skin Fraction B (Obtained from Toyopearl Size Exclusion Chromatography) at 280nm.

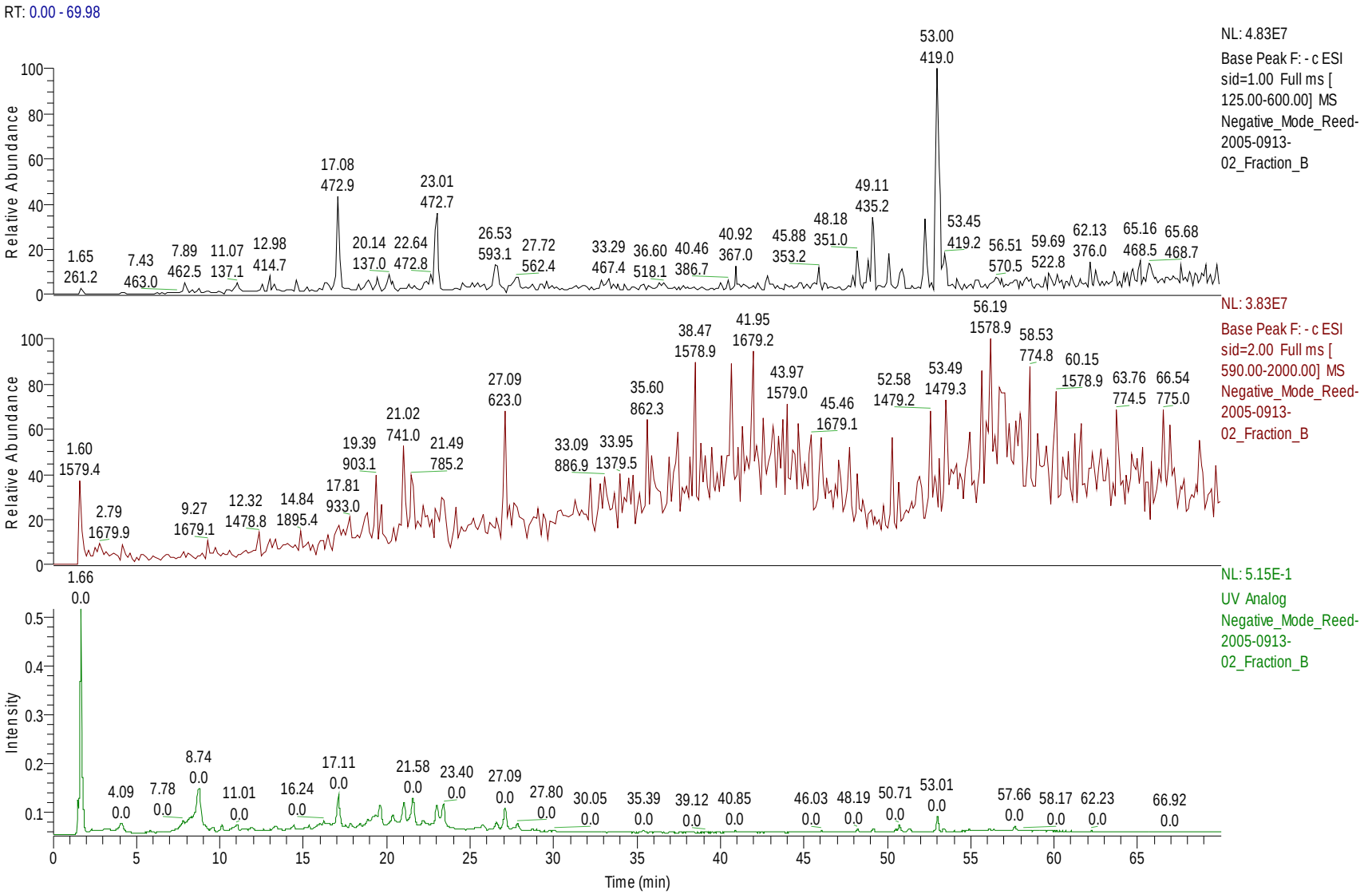

Figure A.11: Peanut Skin Fraction B: HPLC-UV Chromatogram (bottom) versus TIC's [Total Ion Chromatograms – Showing the "ms" Normal Mass Spectra Base Peaks for the Most Intense Ions in Both SID=1.0 Scan Range (m/z 125-600 M-H$^-$) (top) and SID=2.0 Scan Range (m/z 590-2000 M-H$^-$) (middle)].

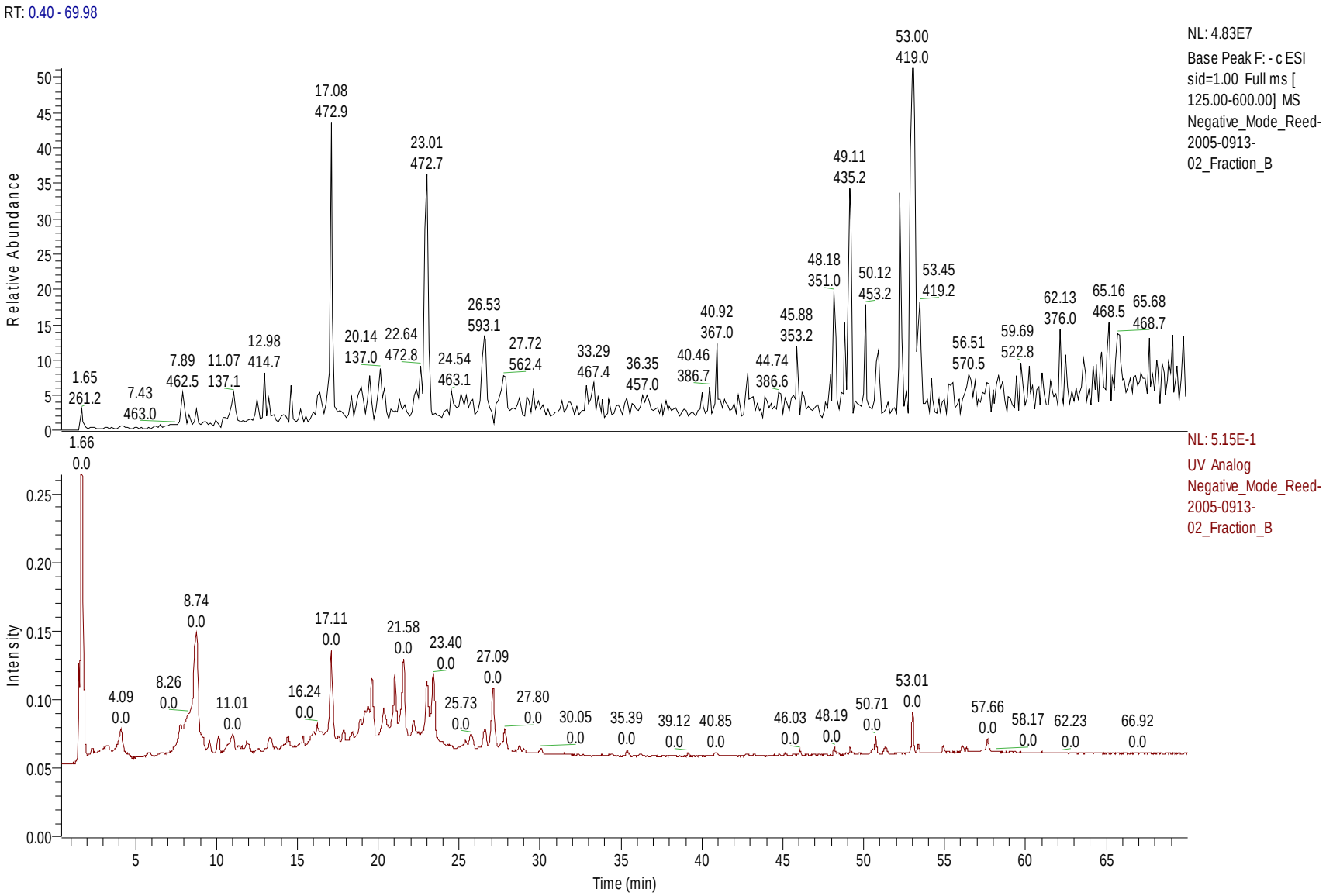

Figure A.12: Peanut Skin Fraction B: HPLC-UV Chromatogram (bottom) versus TIC [Total Ion Chromatogram – Showing the "ms" Normal Mass Spectra Base Peaks for the Most Intense Ions in SID=1.0 Scan Range (m/z 125-600 M-H$^-$)] (top).

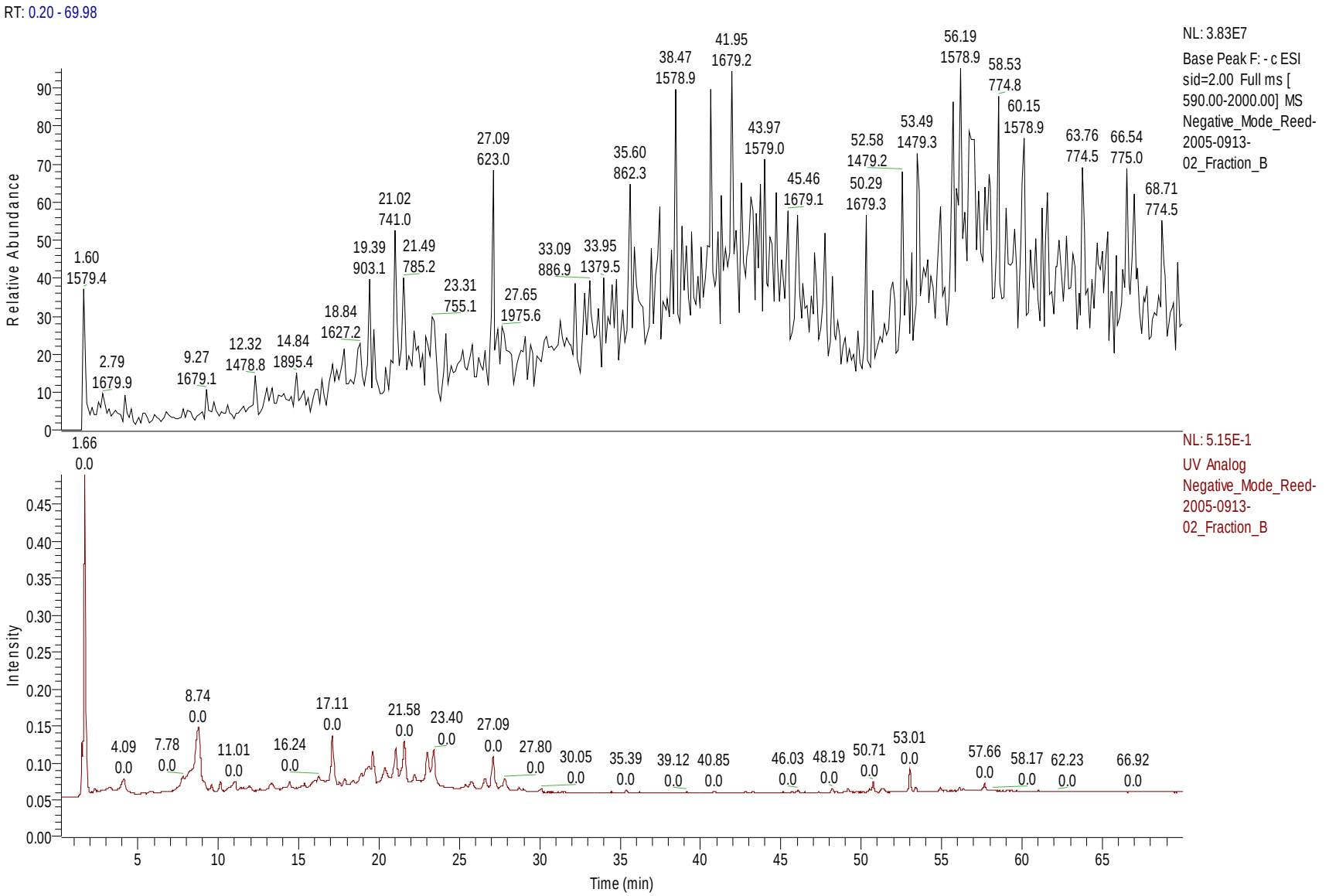

Figure A.13: Peanut Skin Fraction B: HPLC-UV Chromatogram (bottom) versus TIC [Total Ion Chromatogram – Showing the "ms" Normal Mass Spectra Base Peaks for the Most Intense Ions in SID=2.0 Scan Range (m/z 590-2000 M-H$^-$)] (top).

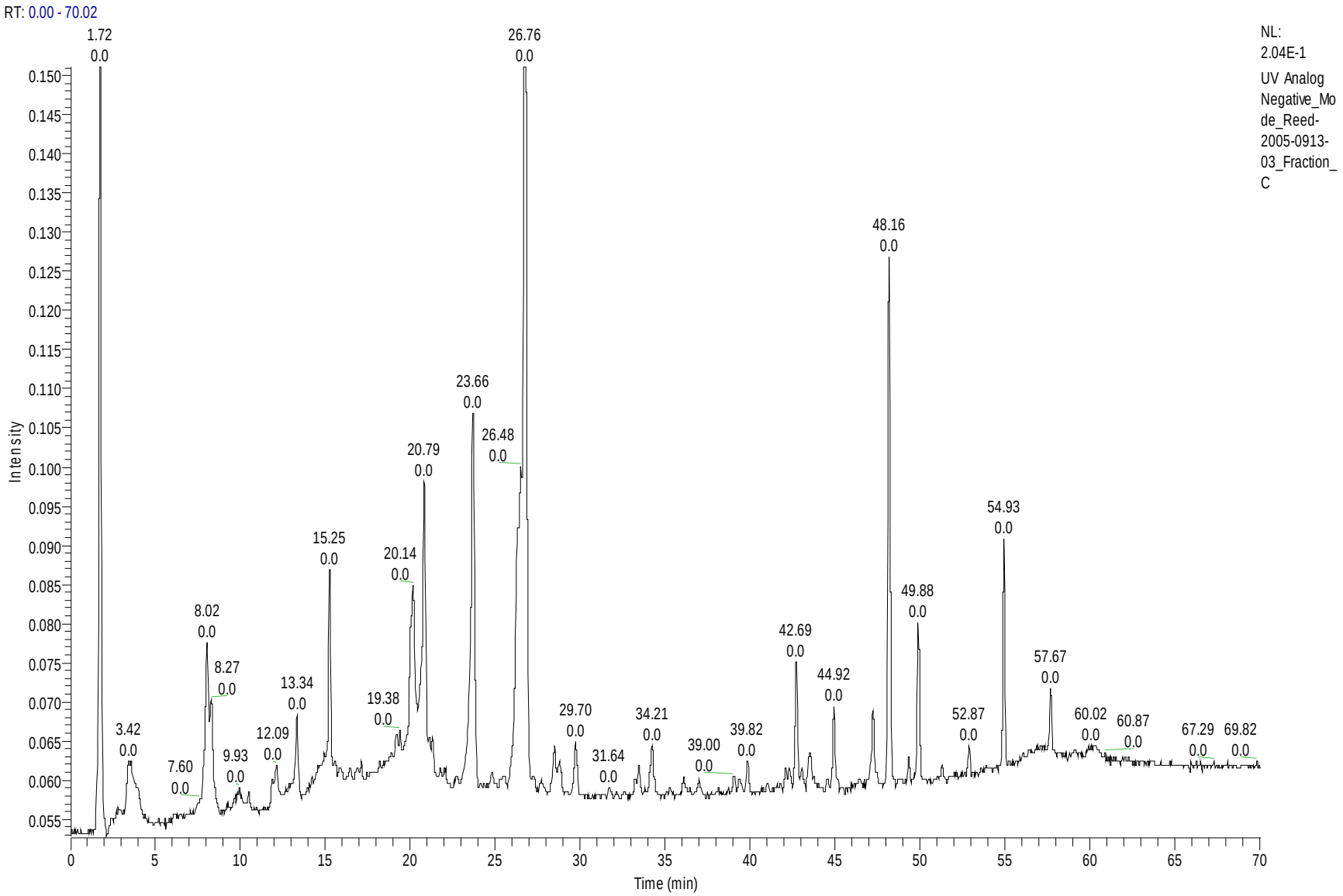

Figure A.14: HPLC-UV Chromatogram of Peanut Skin Fraction C (Obtained from Toyopearl Size Exclusion Chromatography) at 280nm.

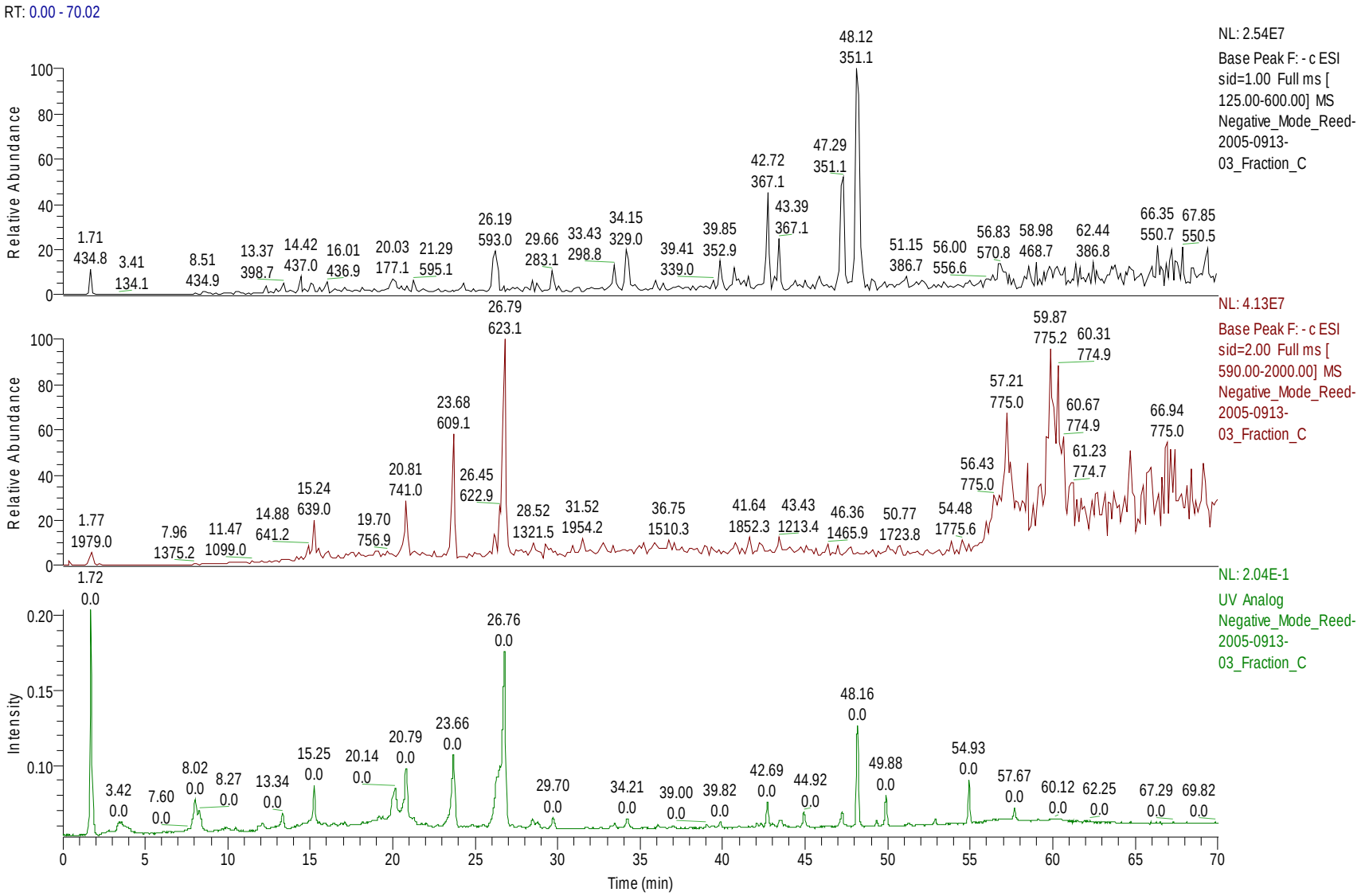

Figure A.15: Peanut Skin Fraction C: HPLC-UV Chromatogram (bottom) versus TIC's [Total Ion Chromatograms – Showing the "ms" Normal Mass Spectra Base Peaks for the Most Intense Ions in Both SID=1.0 Scan Range (m/z 125-600 M-H$^-$) (top) and SID=2.0 Scan Range (m/z 590-2000 M-H$^-$) (middle)].

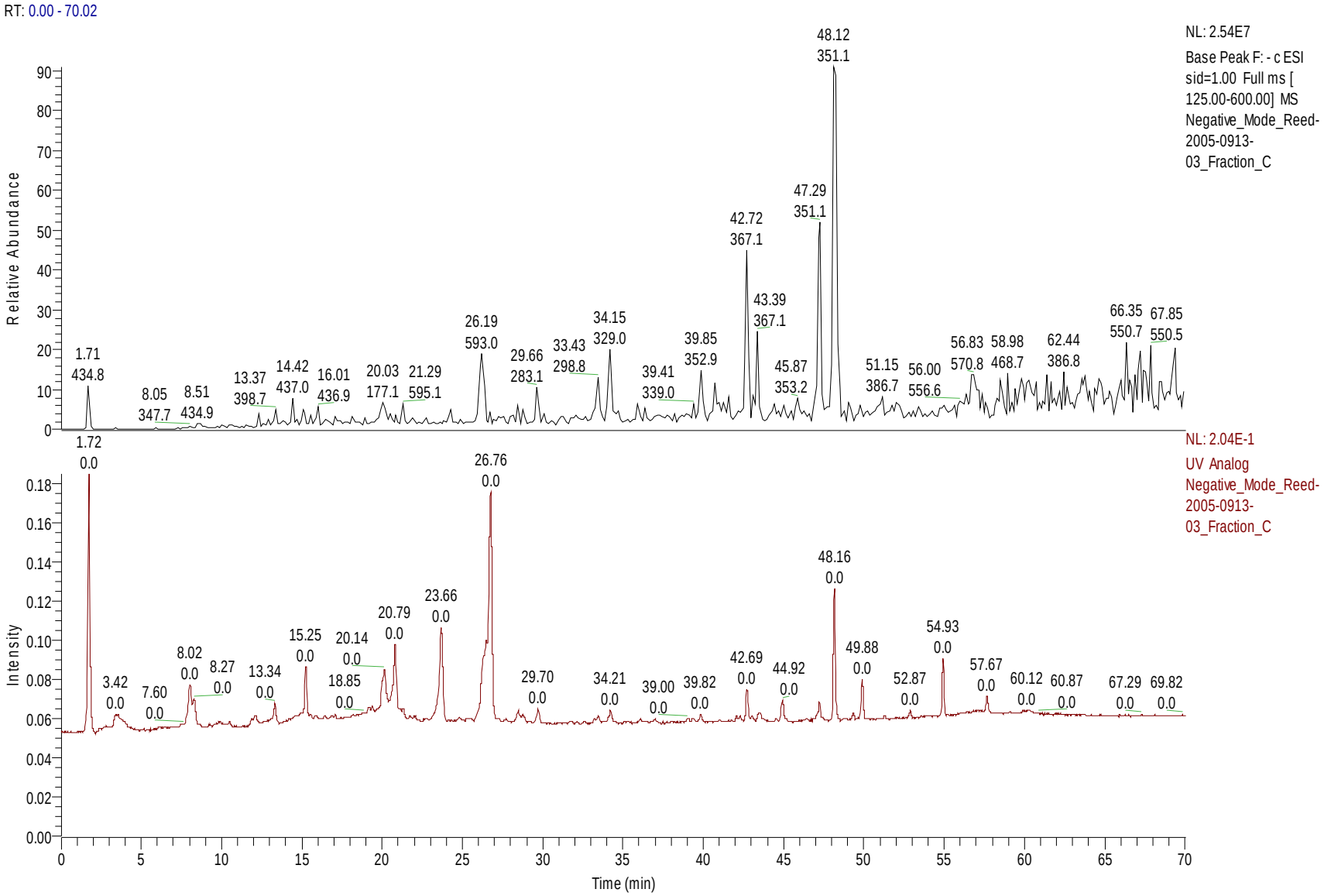

Figure A.16: Peanut Skin Fraction C: HPLC-UV Chromatogram (bottom) versus TIC [Total Ion Chromatogram – Showing the "ms" Normal Mass Spectra Base Peaks for the Most Intense Ions in SID=1.0 Scan Range (m/z 125-600 M-H$^-$)] (top).

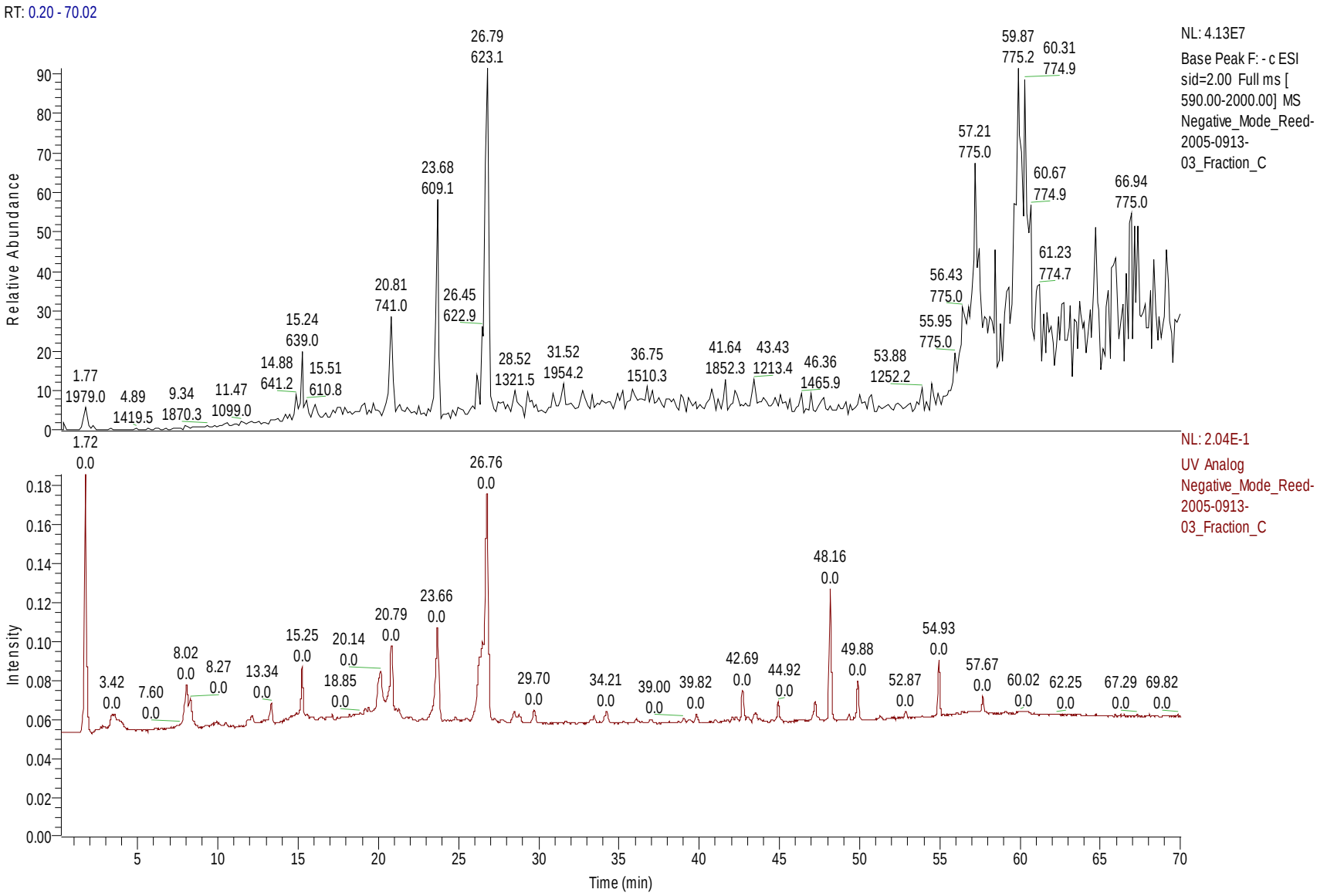

Figure A.17: Peanut Skin Fraction C: HPLC-UV Chromatogram (bottom) versus TIC [Total Ion Chromatogram – Showing the "ms" Normal Mass Spectra Base Peaks for the Most Intense Ions in SID=2.0 Scan Range (m/z 590-2000 M-H$^-$)] (top).

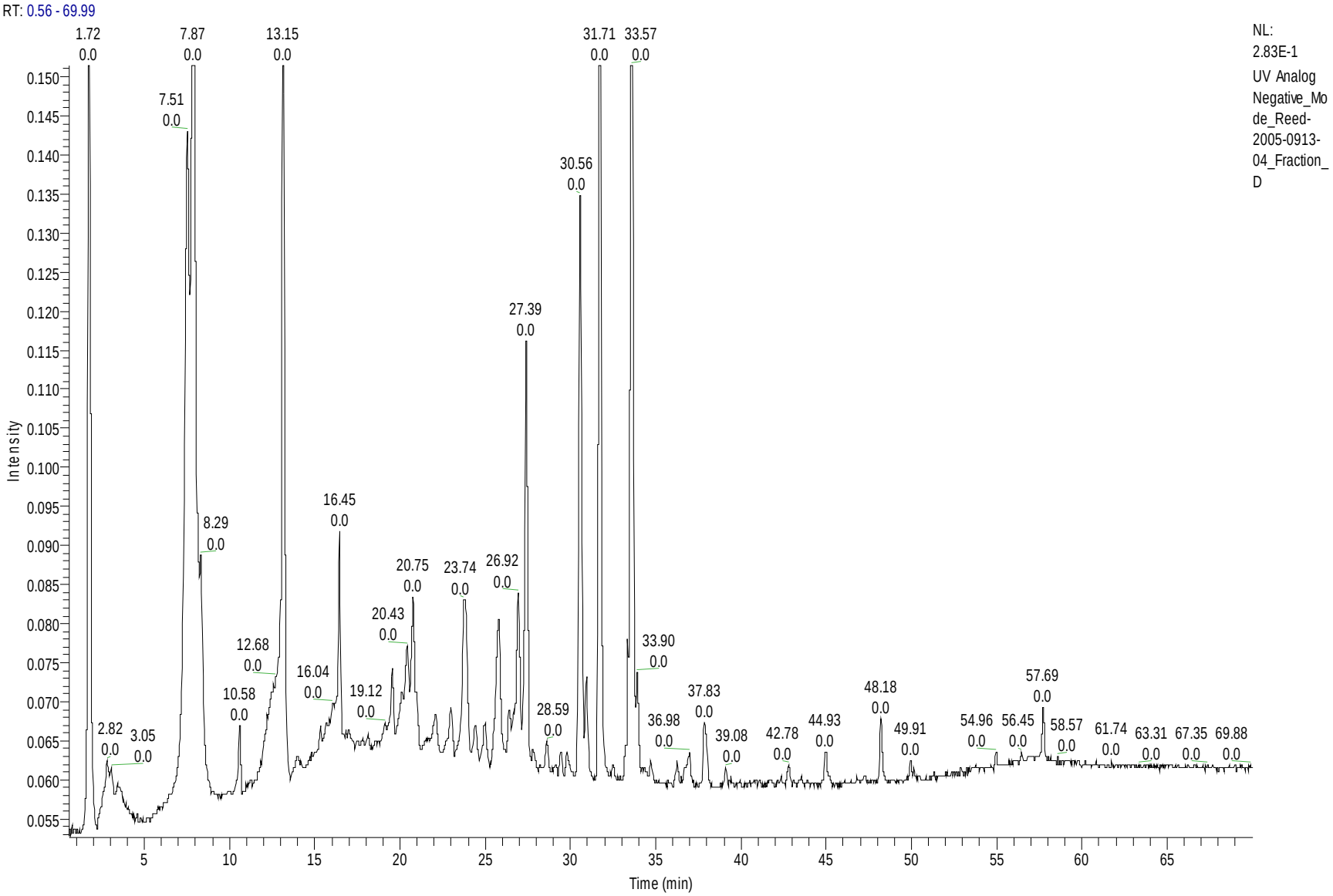

Figure A.18: HPLC-UV Chromatogram of Peanut Skin Fraction D (Obtained from Toyopearl Size Exclusion Chromatography) at 280nm.

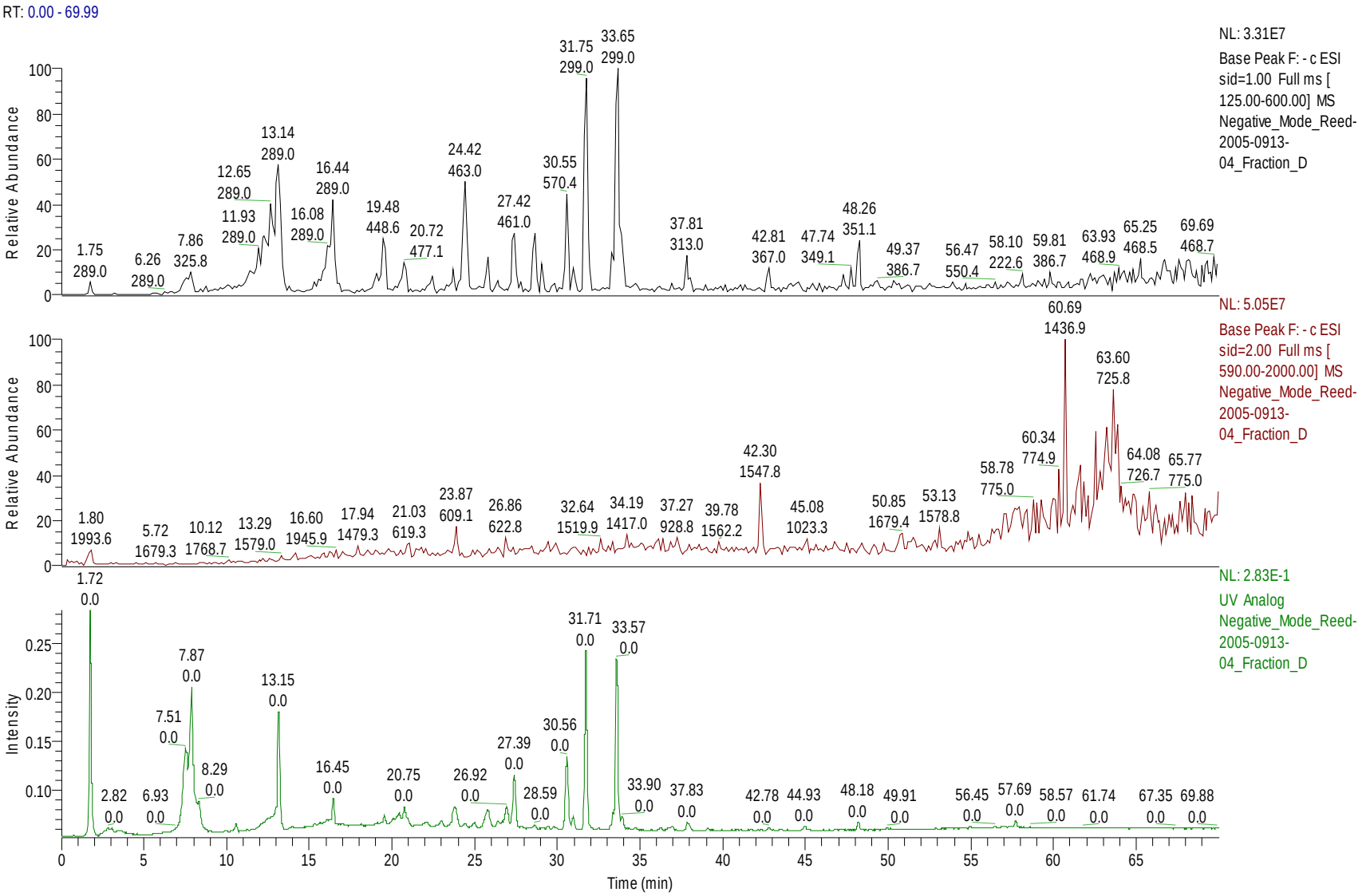

Figure A.19: Peanut Skin Fraction D: HPLC-UV Chromatogram (bottom) versus TIC's [Total Ion Chromatograms – Showing the "ms" Normal Mass Spectra Base Peaks for the Most Intense Ions in Both SID=1.0 Scan Range (m/z 125-600 M-H$^-$) (top) and SID=2.0 Scan Range (m/z 590-2000 M-H$^-$) (middle)].

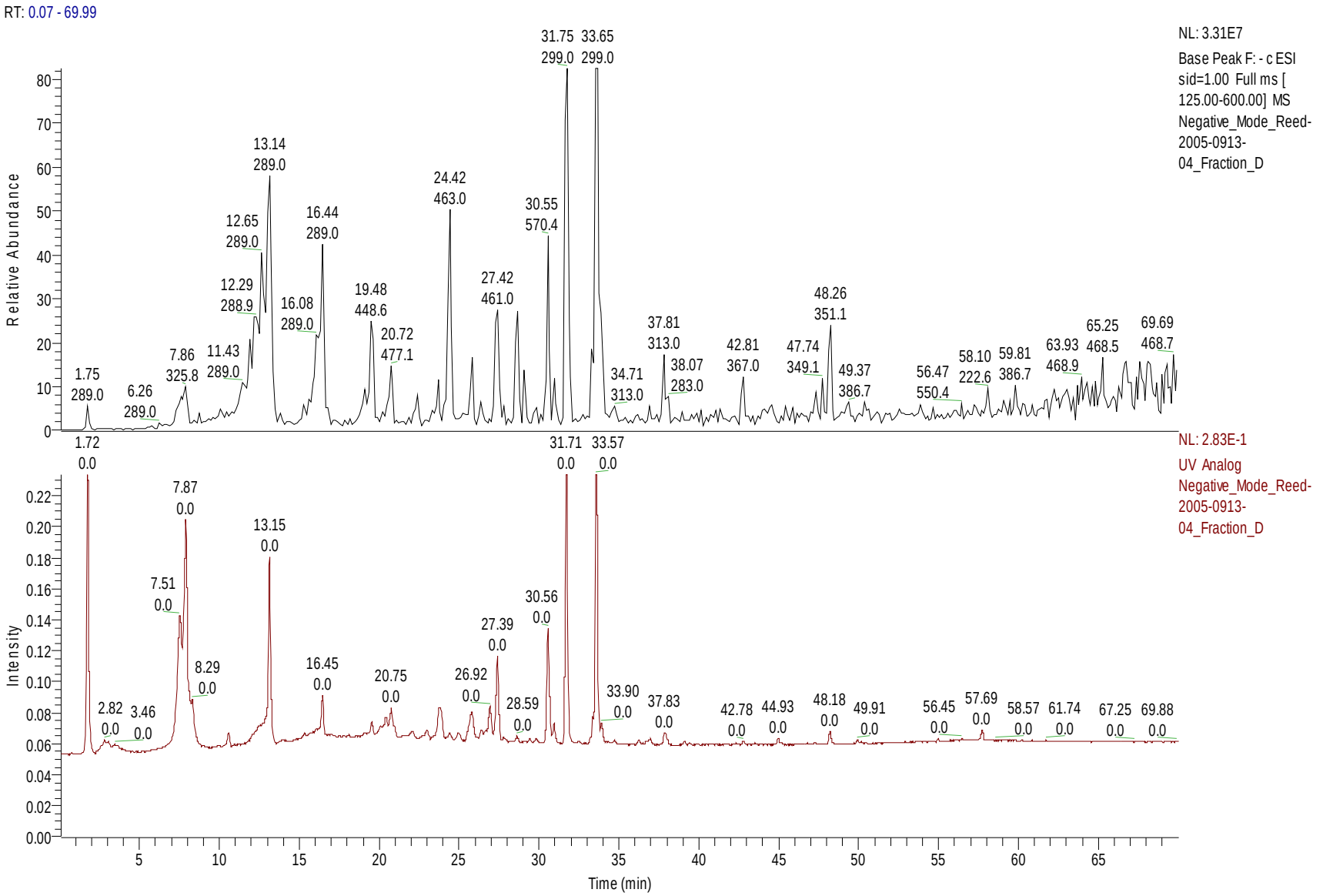

Figure A.20: Peanut Skin Fraction D: HPLC-UV Chromatogram (bottom) versus TIC [Total Ion Chromatogram – Showing the "ms" Normal Mass Spectra Base Peaks for the Most Intense Ions in SID=1.0 Scan Range (m/z 125-600 M-H$^-$)] (top).

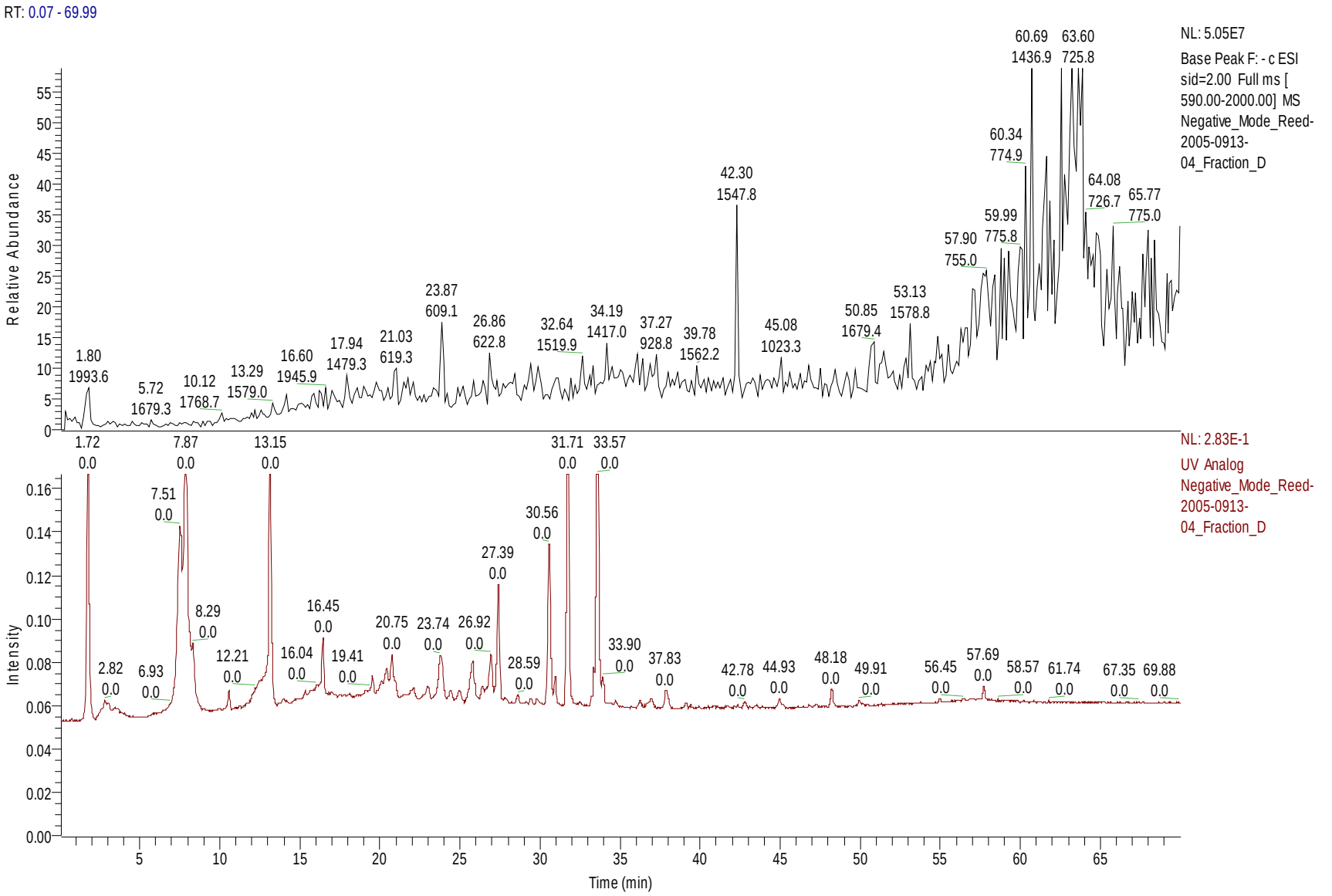

Figure A.21: Peanut Skin Fraction D: HPLC-UV Chromatogram (bottom) versus TIC [Total Ion Chromatogram – Showing the "ms" Normal Mass Spectra Base Peaks for the Most Intense Ions in SID=2.0 Scan Range (m/z 590-2000 M-H$^-$)] (top).

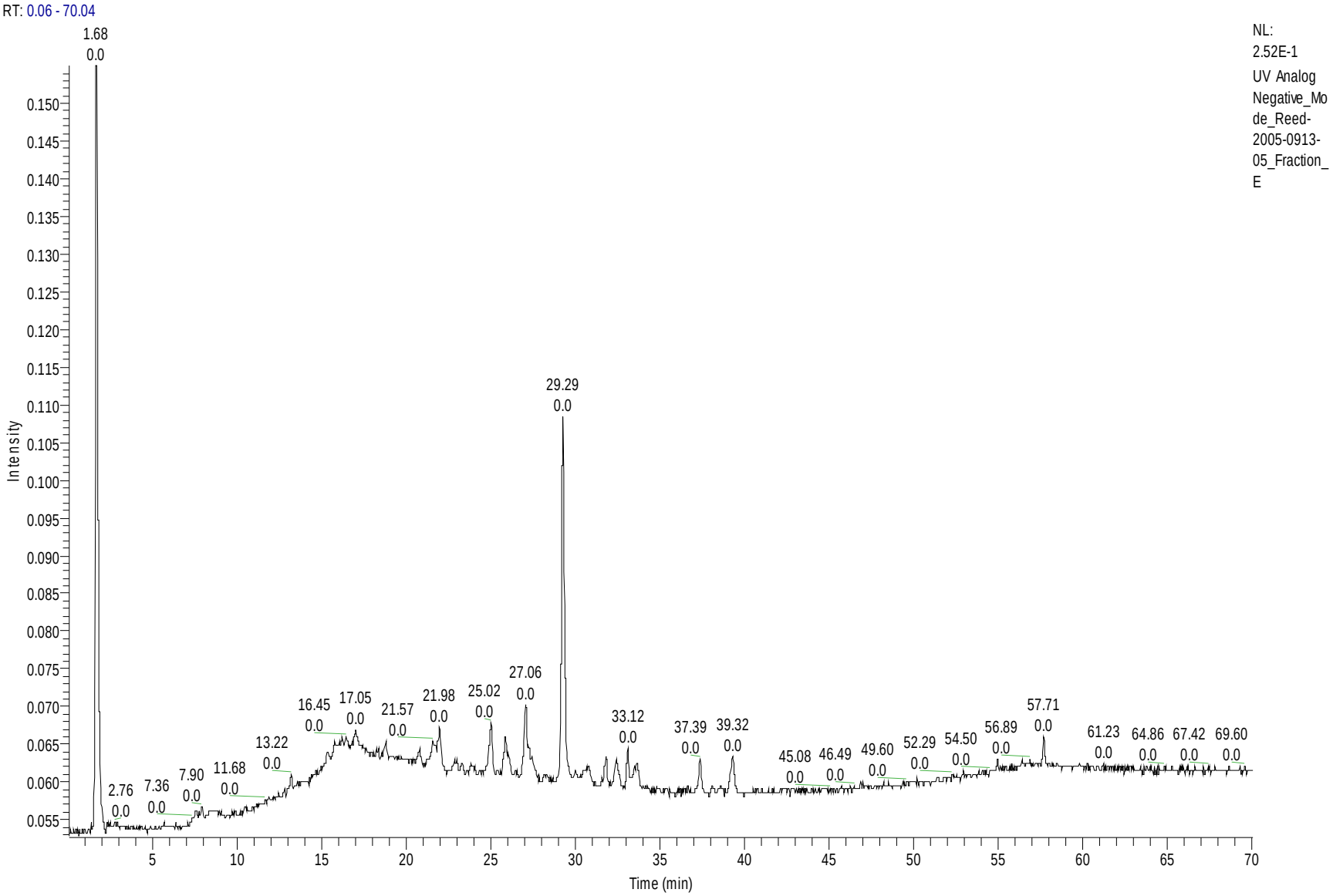

Figure A.22: HPLC-UV Chromatogram of Peanut Skin Fraction E (Obtained from Toyopearl Size Exclusion Chromatography) at 280nm.

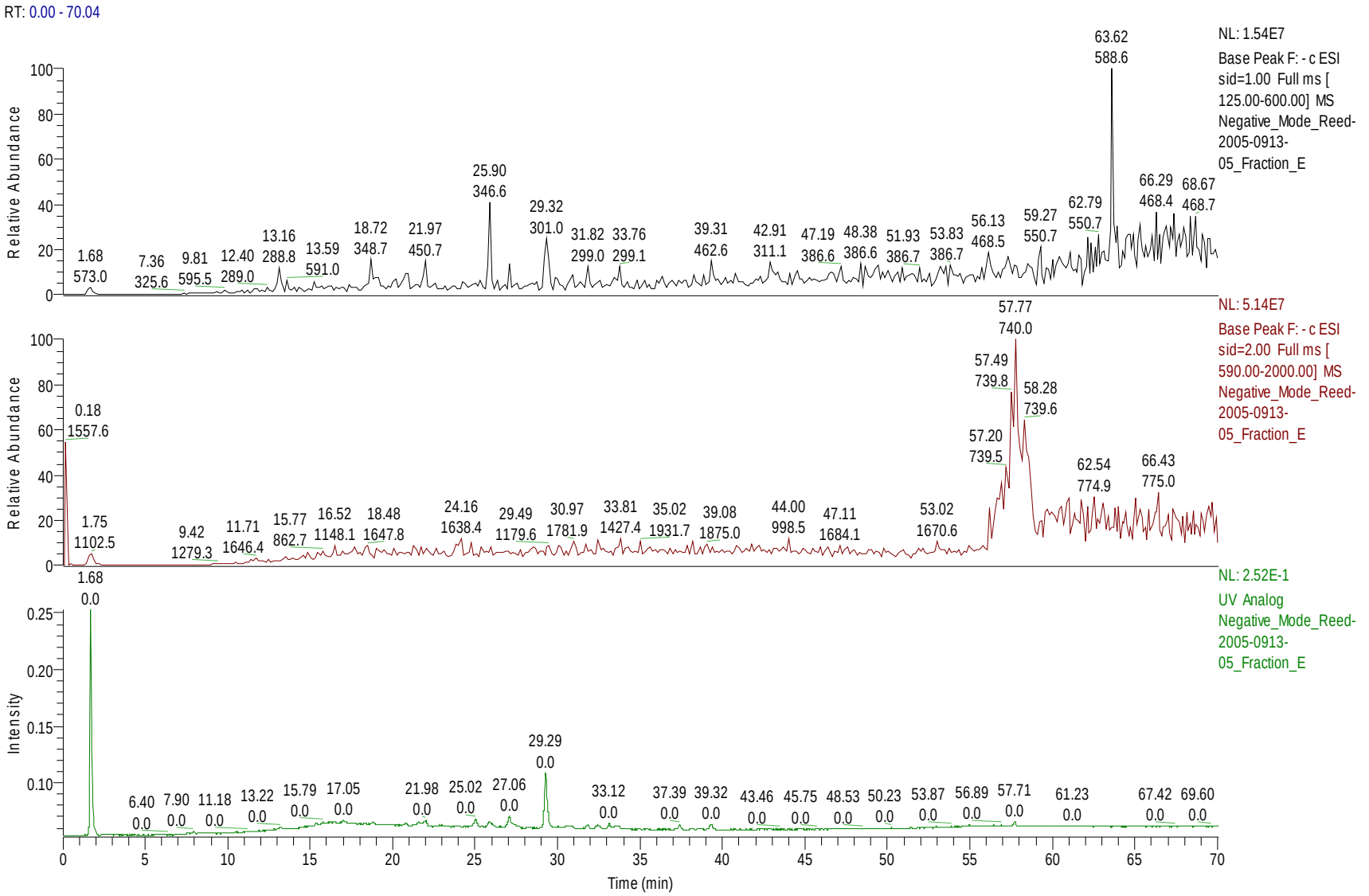

Figure A.23: Peanut Skin Fraction E: HPLC-UV Chromatogram (bottom) versus TIC's [Total Ion Chromatograms – Showing the "ms" Normal Mass Spectra Base Peaks for the Most Intense Ions in Both SID=1.0 Scan Range (m/z 125-600 M-H$^-$) (top) and SID=2.0 Scan Range (m/z 590-2000 M-H$^-$) (middle)].

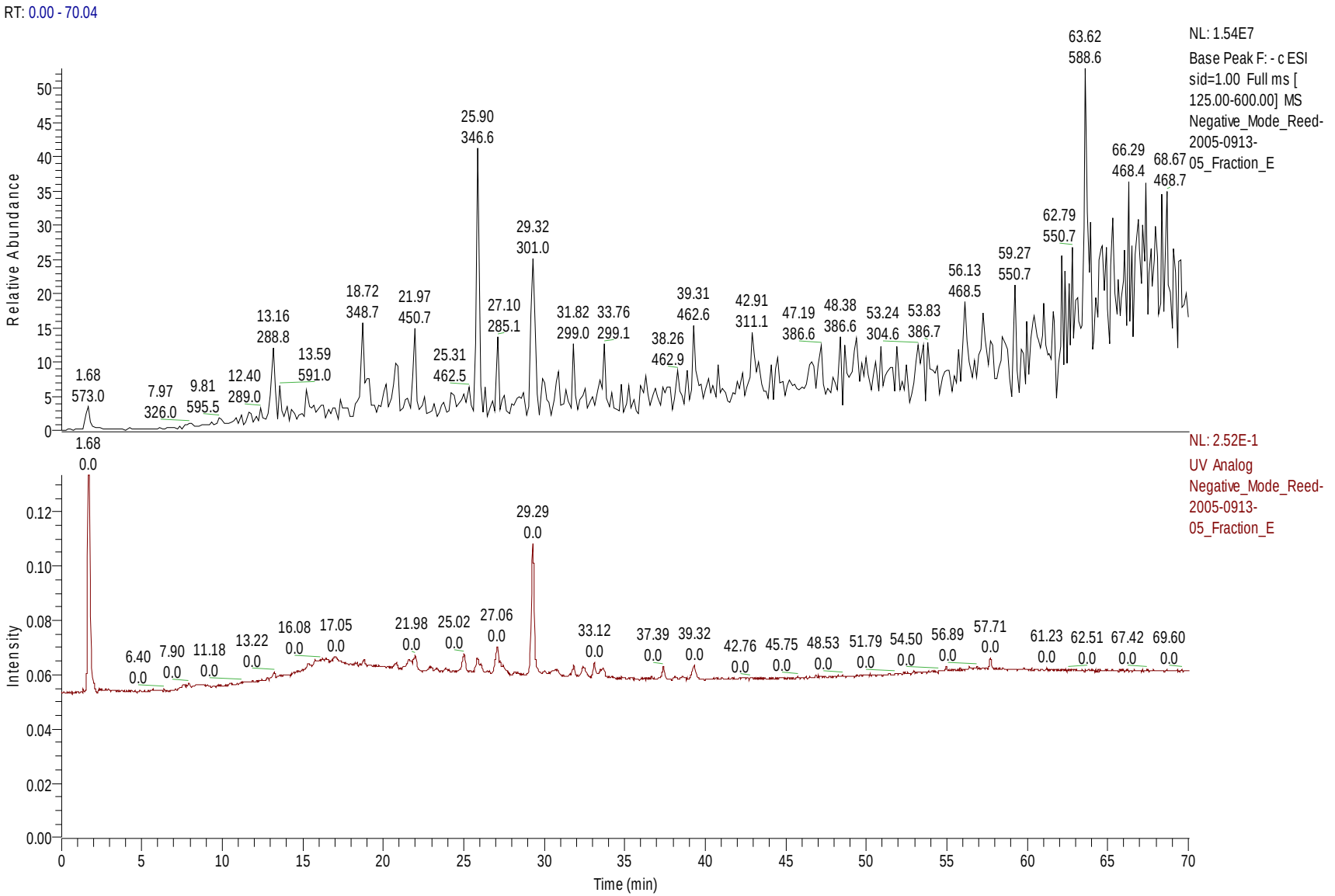

Figure A.24: Peanut Skin Fraction E: HPLC-UV Chromatogram (bottom) versus TIC [Total Ion Chromatogram – Showing the "ms" Normal Mass Spectra Base Peaks for the Most Intense Ions in SID=1.0 Scan Range (m/z 125-600 M-H$^-$)] (top).

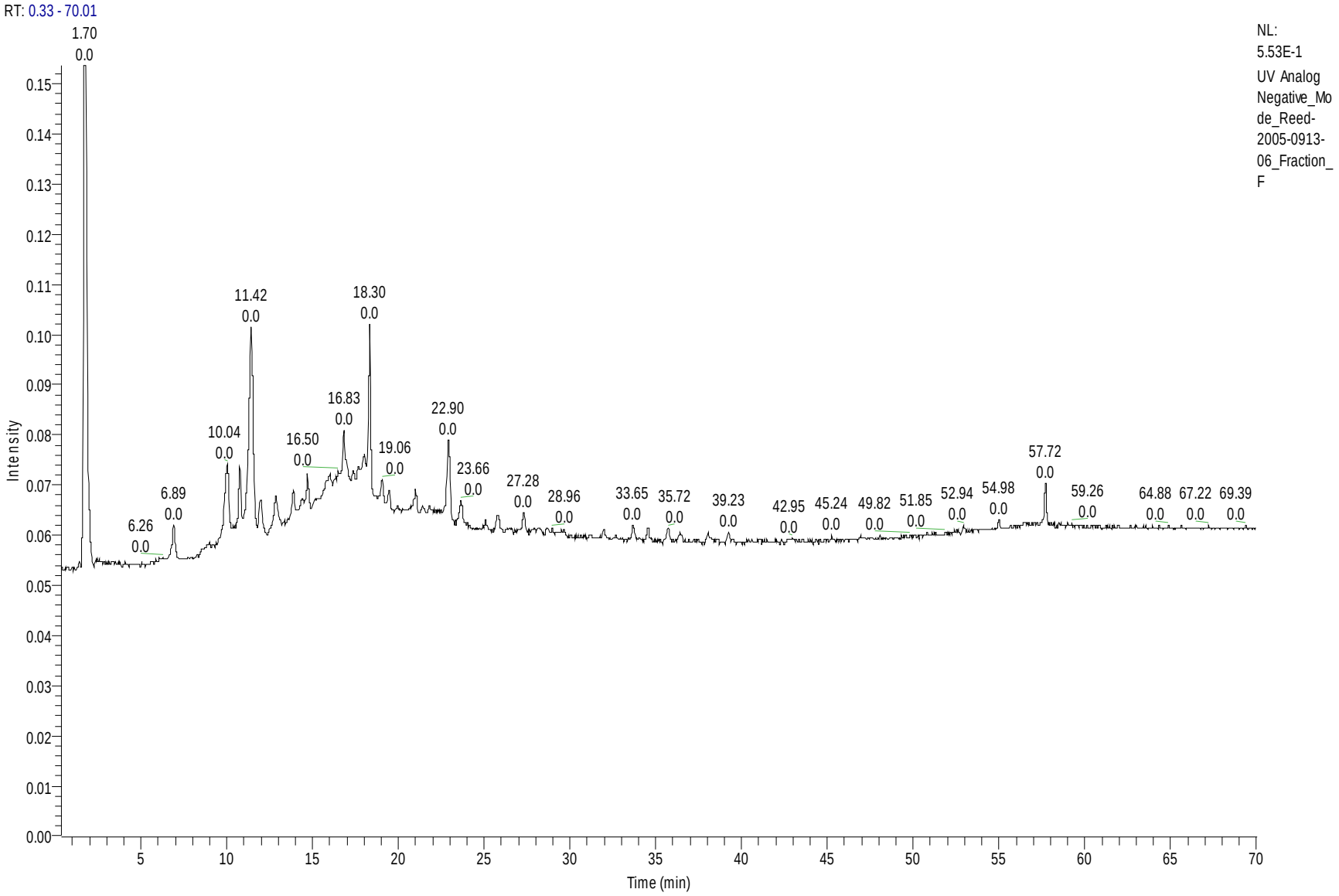

Figure A.25: HPLC-UV Chromatogram of Peanut Skin Fraction F (Obtained from Toyopearl Size Exclusion Chromatography) at 280nm.

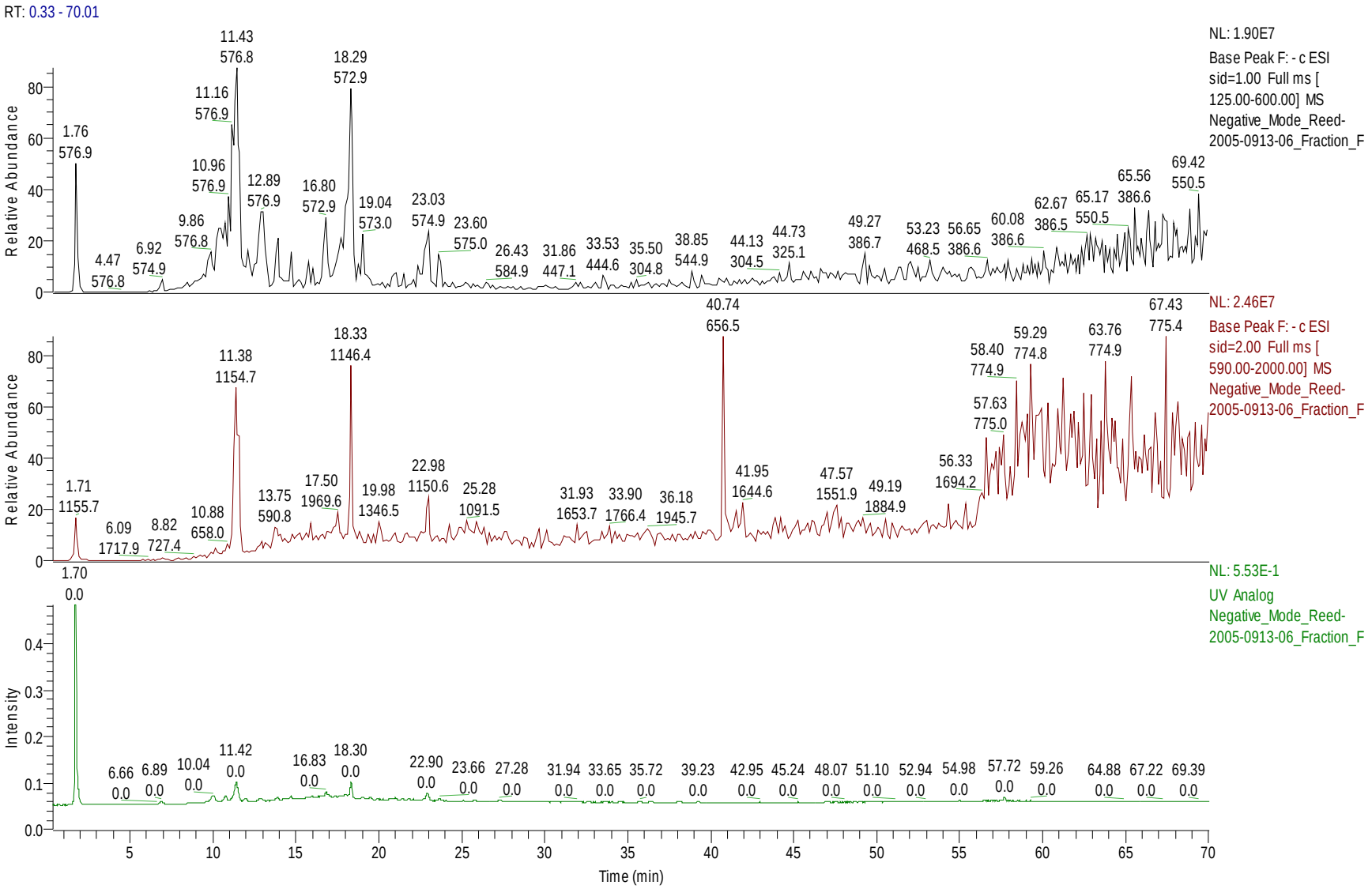

Figure A.26: Peanut Skin Fraction F: HPLC-UV Chromatogram (bottom) versus TIC's [Total Ion Chromatograms – Showing the "ms" Normal Mass Spectra Base Peaks for the Most Intense Ions in Both SID=1.0 Scan Range (m/z 125-600 M-H$^-$) (top) and SID=2.0 Scan Range (m/z 590-2000 M-H$^-$) (middle)].

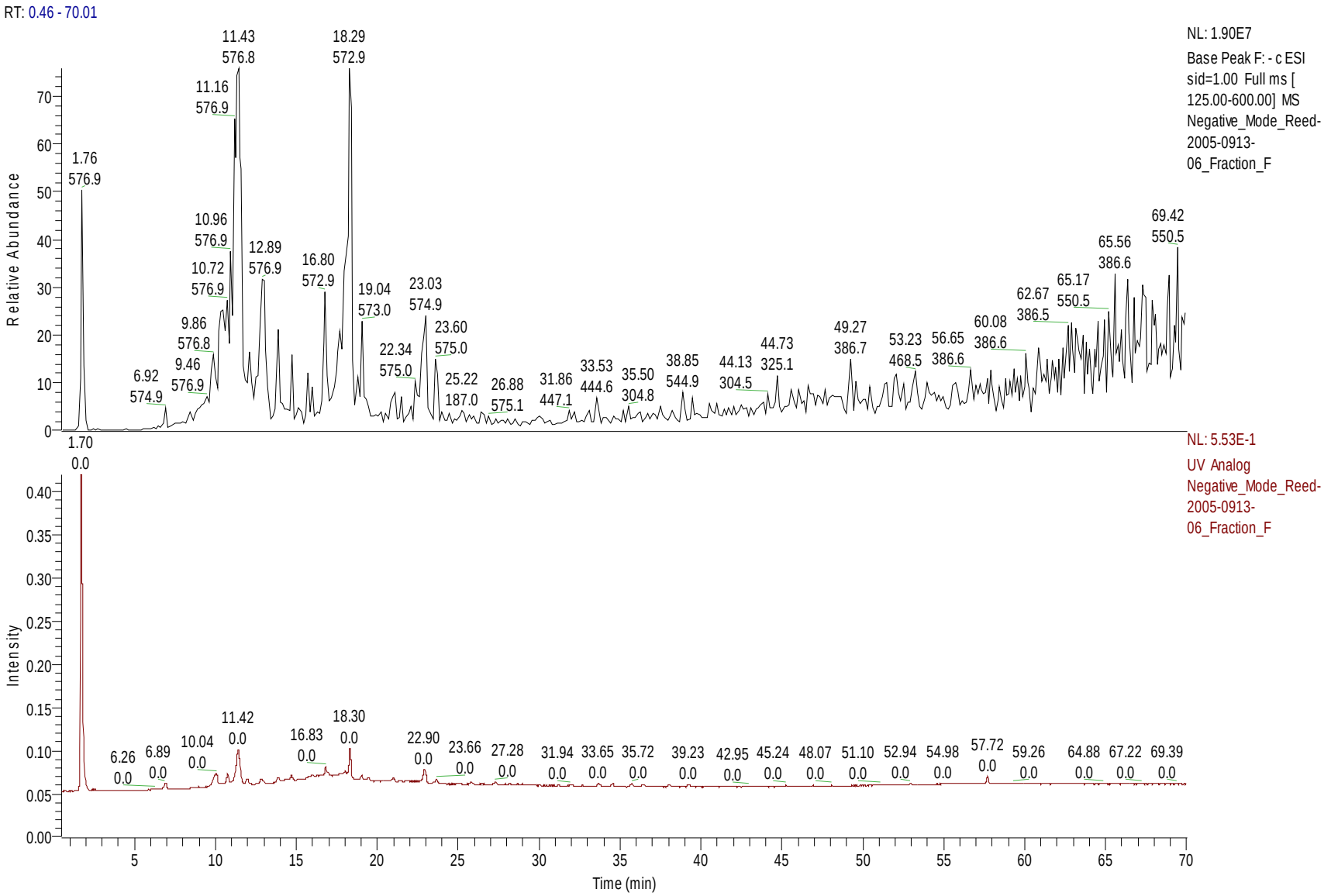

Figure A.27: Peanut Skin Fraction F: HPLC-UV Chromatogram (bottom) versus TIC [Total Ion Chromatogram – Showing the "ms" Normal Mass Spectra Base Peaks for the Most Intense Ions in SID=1.0 Scan Range (m/z 125-600 M-H$^-$)] (top).

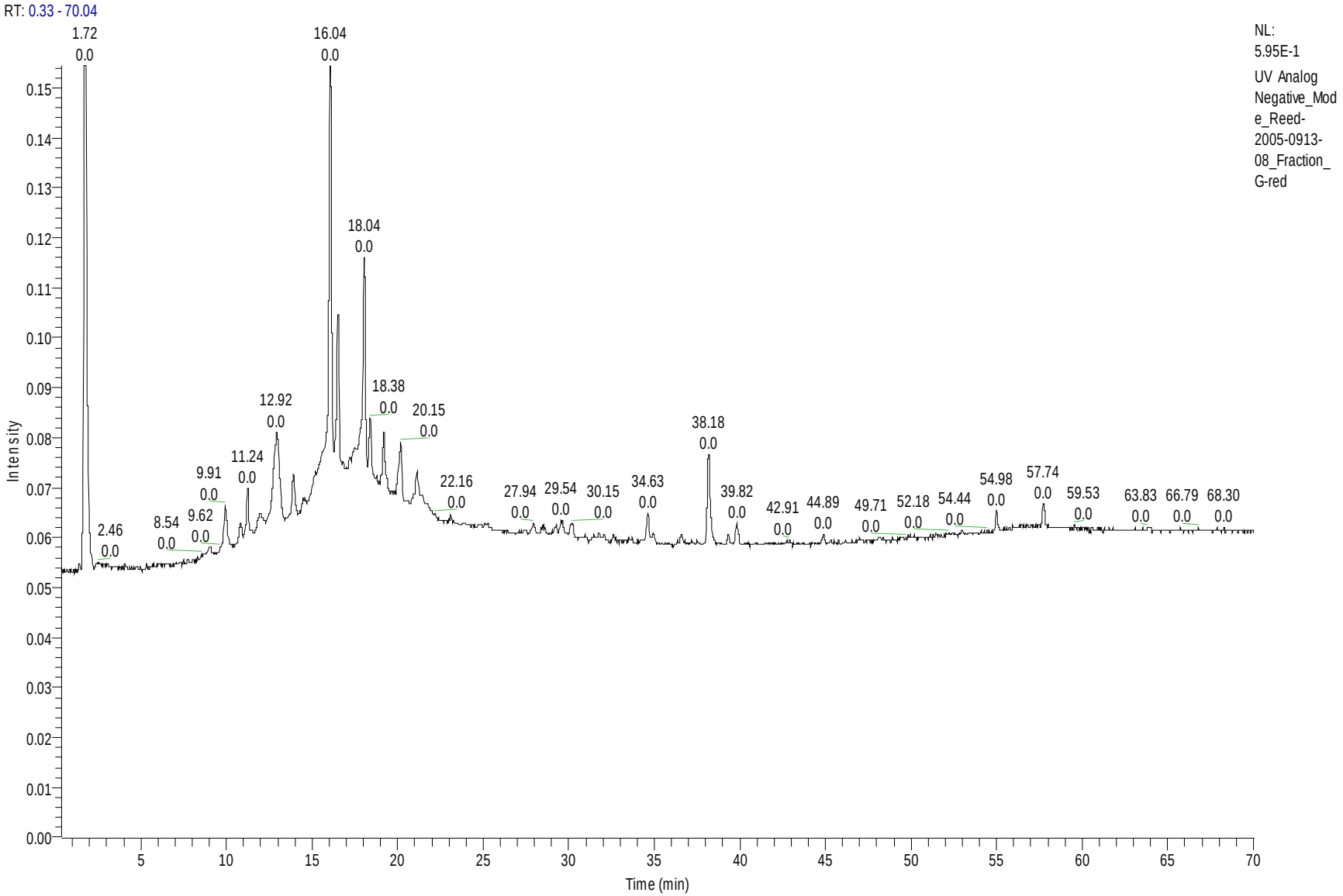

Figure A.28: HPLC-UV Chromatogram of Peanut Skin Fraction G-Red (Obtained from Toyopearl Size Exclusion Chromatography) at 280nm.

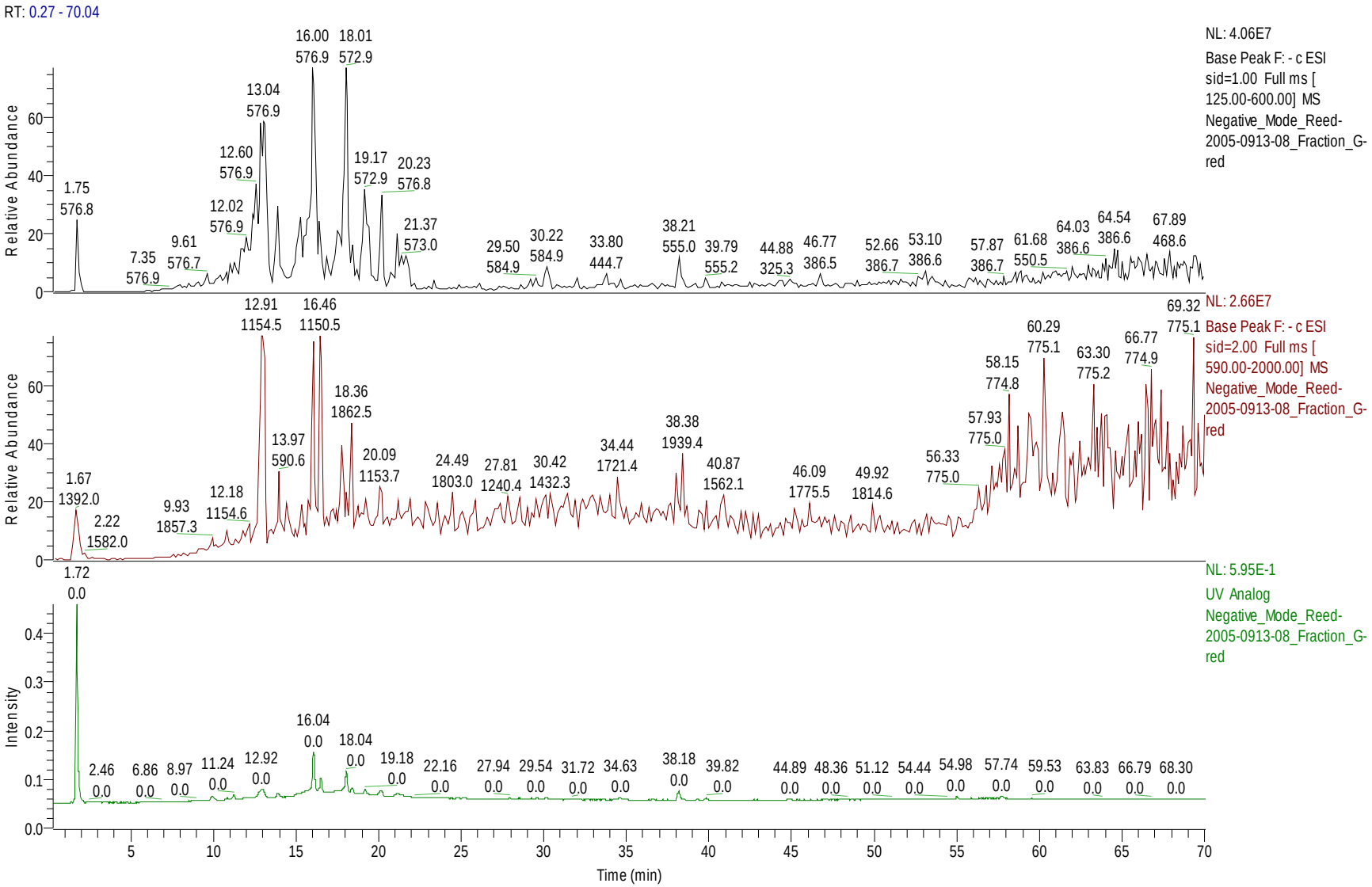

Figure A.29: Peanut Skin Fraction G-Red: HPLC-UV Chromatogram (bottom) versus TIC's [Total Ion Chromatograms – Showing the "ms" Normal Mass Spectra Base Peaks for the Most Intense Ions in Both SID=1.0 Scan Range (m/z 125-600 M-H$^-$) (top) and SID=2.0 Scan Range (m/z 590-2000 M-H$^-$) (middle)].

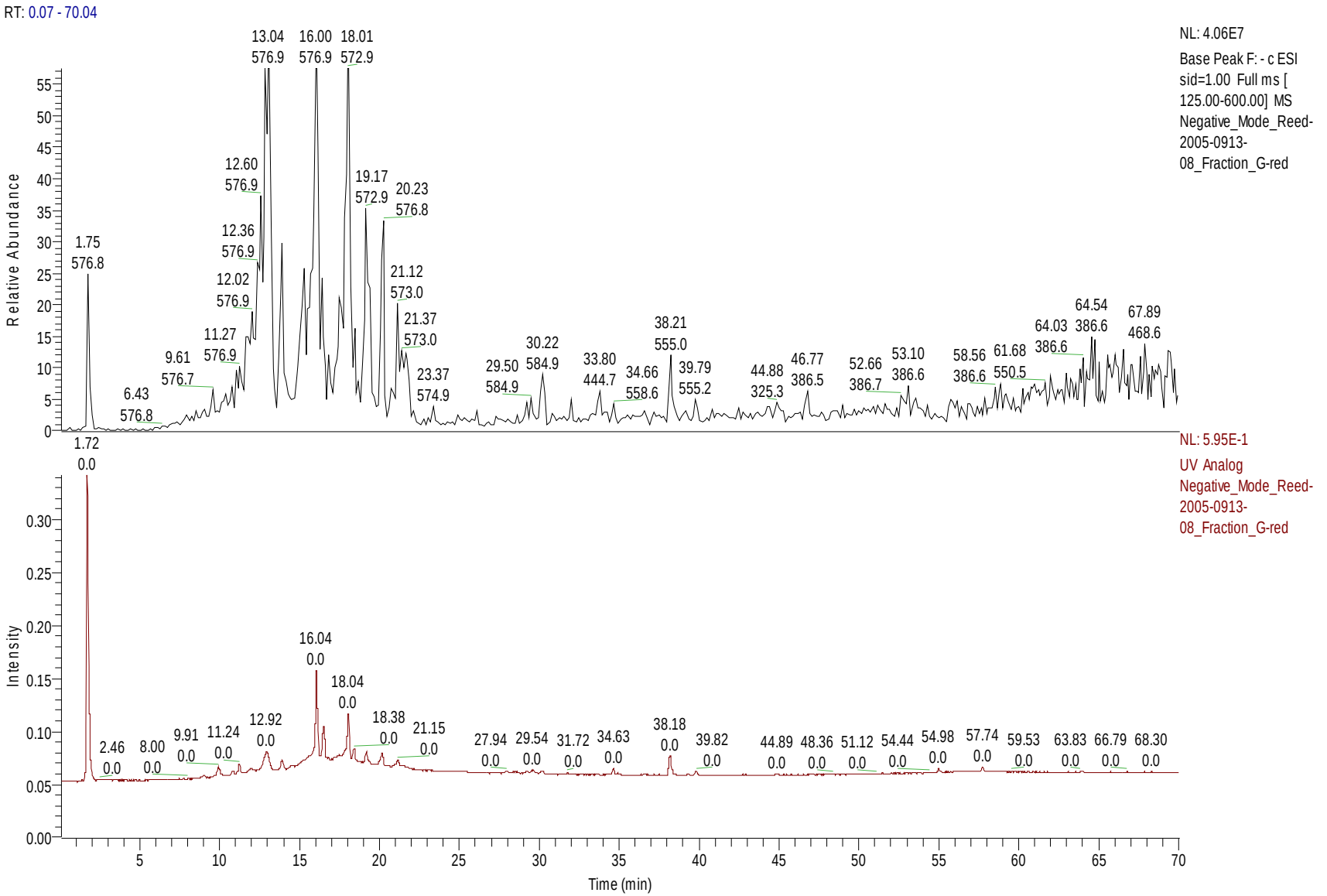

Figure A.30: Peanut Skin Fraction G-Red: HPLC-UV Chromatogram (bottom) versus TIC [Total Ion Chromatogram – Showing the "ms" Normal Mass Spectra Base Peaks for the Most Intense Ions in SID=1.0 Scan Range (m/z 125-600 M-H$^-$)] (top).

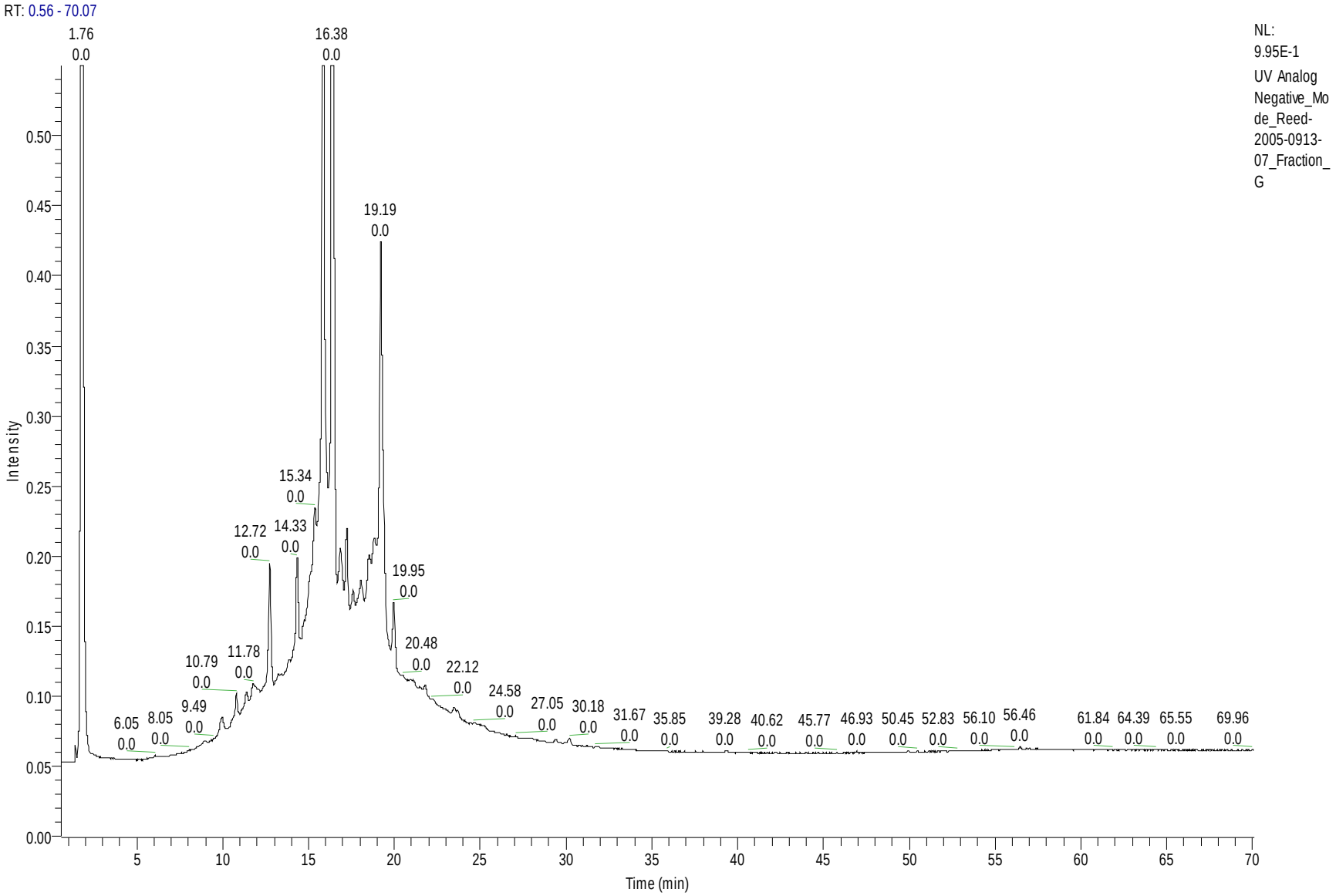

Figure A.31: HPLC-UV Chromatogram of Peanut Skin Fraction G (Obtained from Toyopearl Size Exclusion Chromatography) at 280nm.

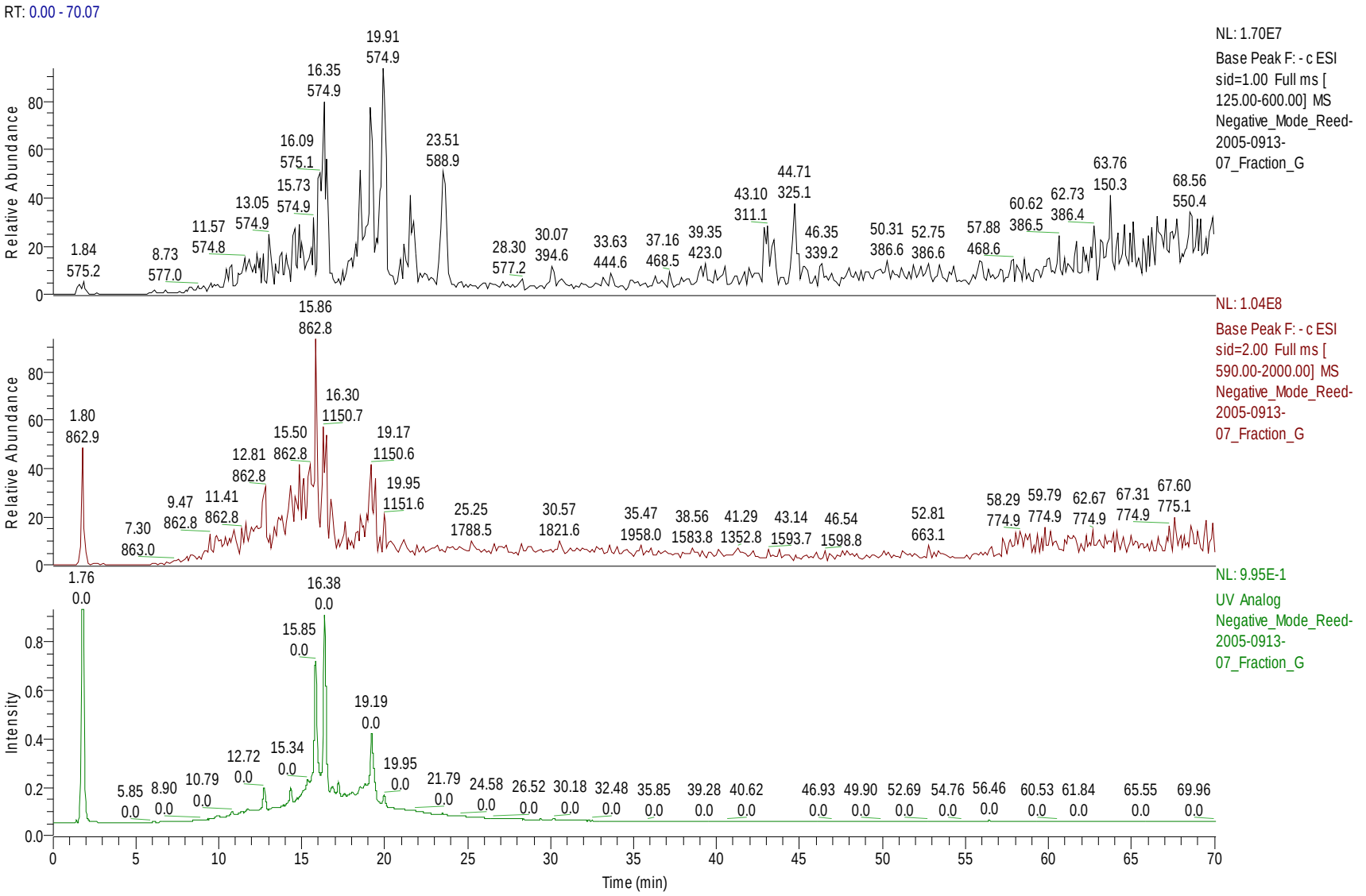

Figure A.32: Peanut Skin Fraction G: HPLC-UV Chromatogram (bottom) versus TIC's [Total Ion Chromatograms – Showing the "ms" Normal Mass Spectra Base Peaks for the Most Intense Ions in Both SID=1.0 Scan Range (m/z 125-600 M-H$^-$) (top) and SID=2.0 Scan Range (m/z 590-2000 M-H$^-$) (middle)].

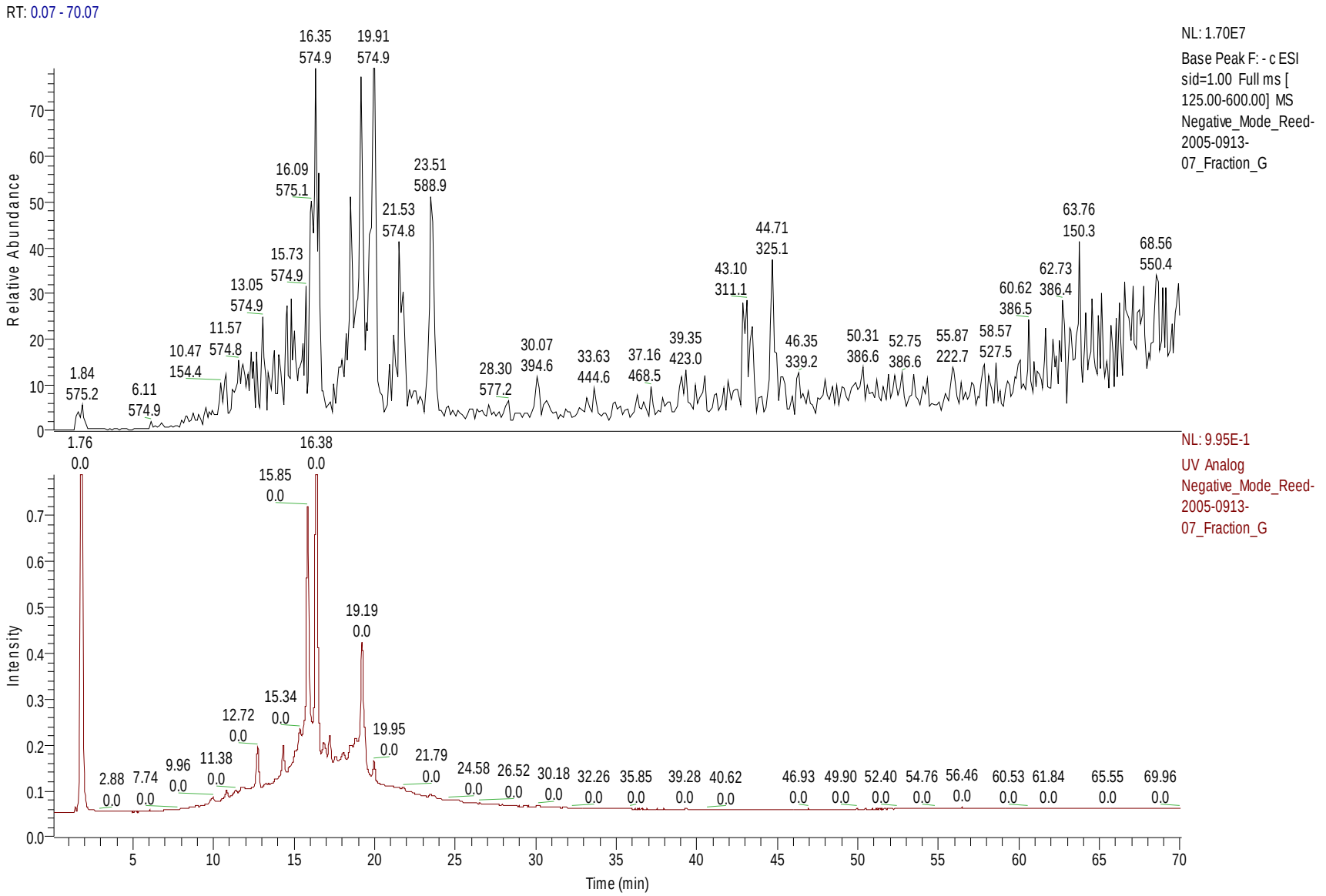

Figure A.33: Peanut Skin Fraction G: HPLC-UV Chromatogram (bottom) versus TIC [Total Ion Chromatogram – Showing the "ms" Normal Mass Spectra Base Peaks for the Most Intense Ions in SID=1.0 Scan Range (m/z 125-600 M-H$^-$)] (top).

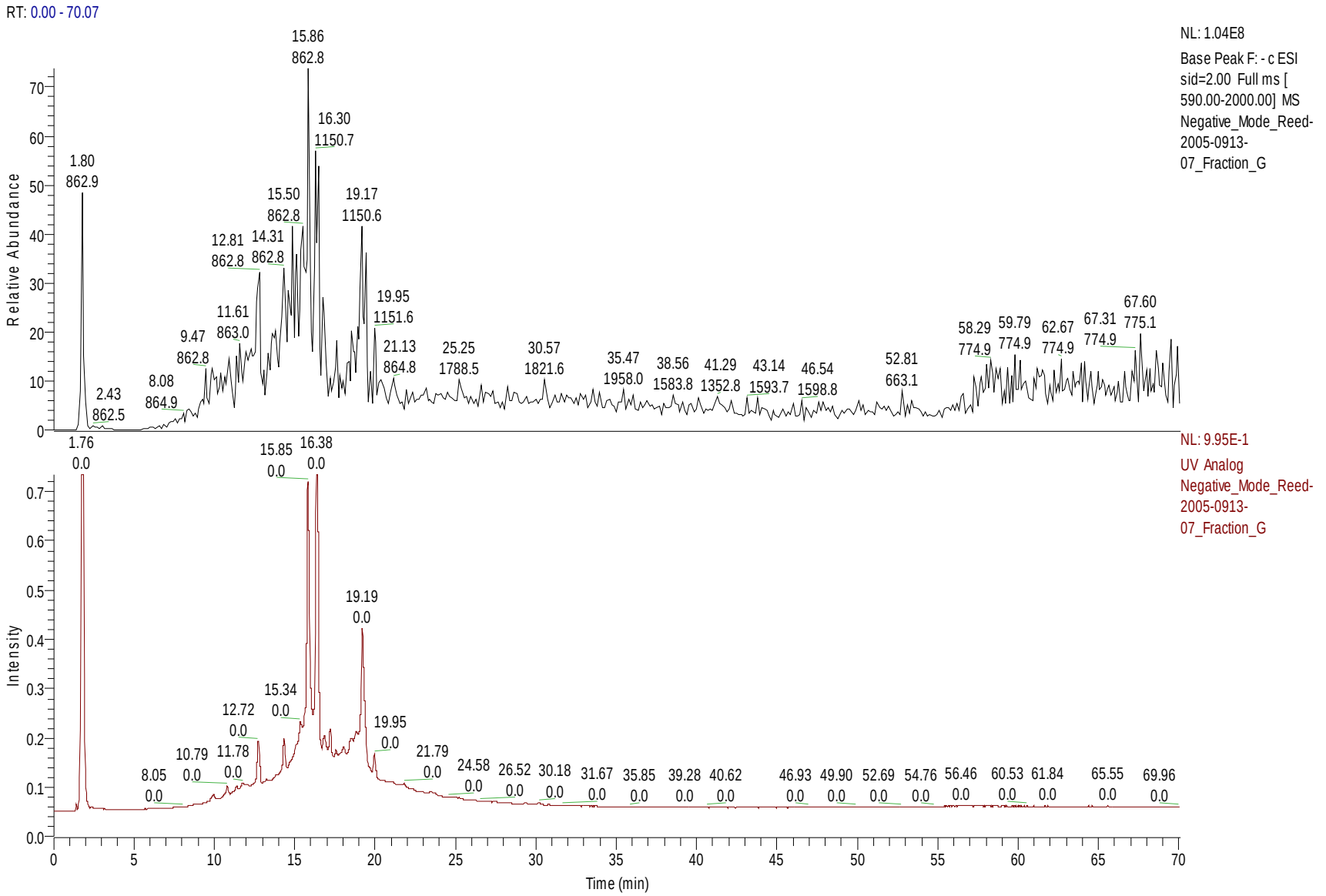

Figure A.34: Peanut Skin Fraction G: HPLC-UV Chromatogram (bottom) versus TIC [Total Ion Chromatogram – Showing the "ms" Normal Mass Spectra Base Peaks for the Most Intense Ions in SID=2.0 Scan Range (m/z 590-2000 M-H$^-$)] (top).

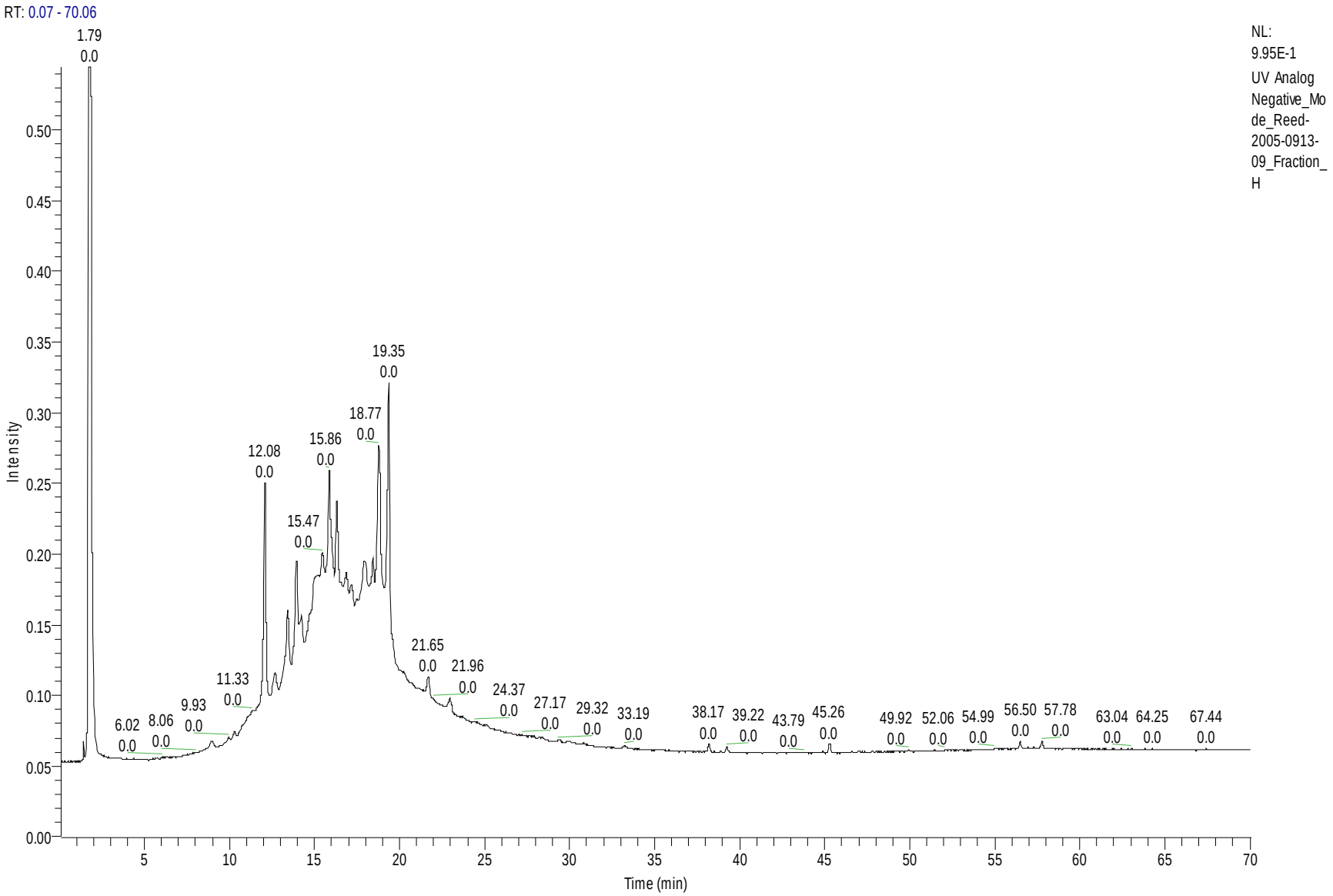

Figure A.35: HPLC-UV Chromatogram of Peanut Skin Fraction H (Obtained from Toyopearl Size Exclusion Chromatography) at 280nm.

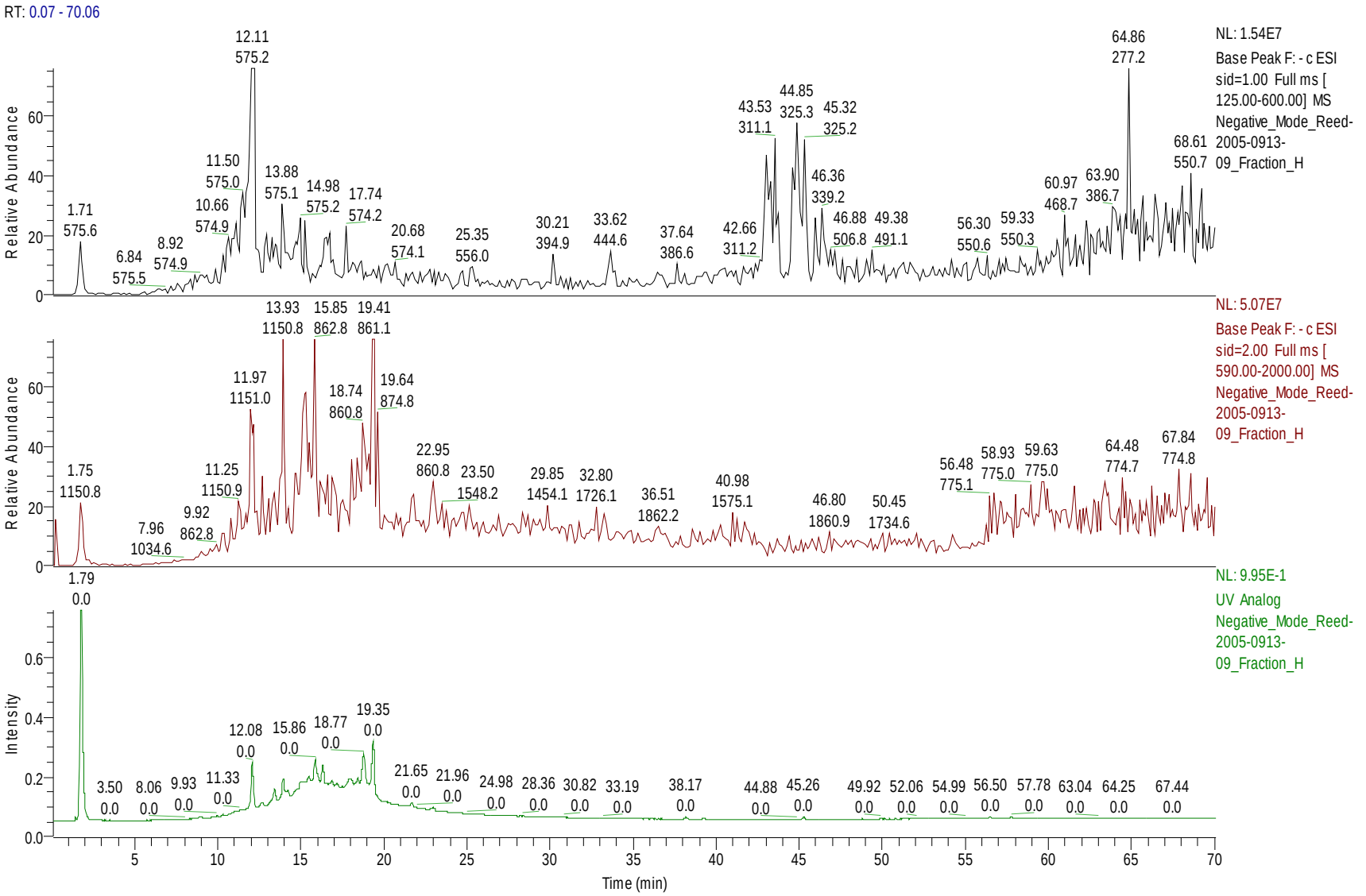

Figure A.36: Peanut Skin Fraction H: HPLC-UV Chromatogram (bottom) versus TIC's [Total Ion Chromatograms – Showing the "ms" Normal Mass Spectra Base Peaks for the Most Intense Ions in Both SID=1.0 Scan Range (m/z 125-600 M-H$^-$) (top) and SID=2.0 Scan Range (m/z 590-2000 M-H$^-$) (middle)].

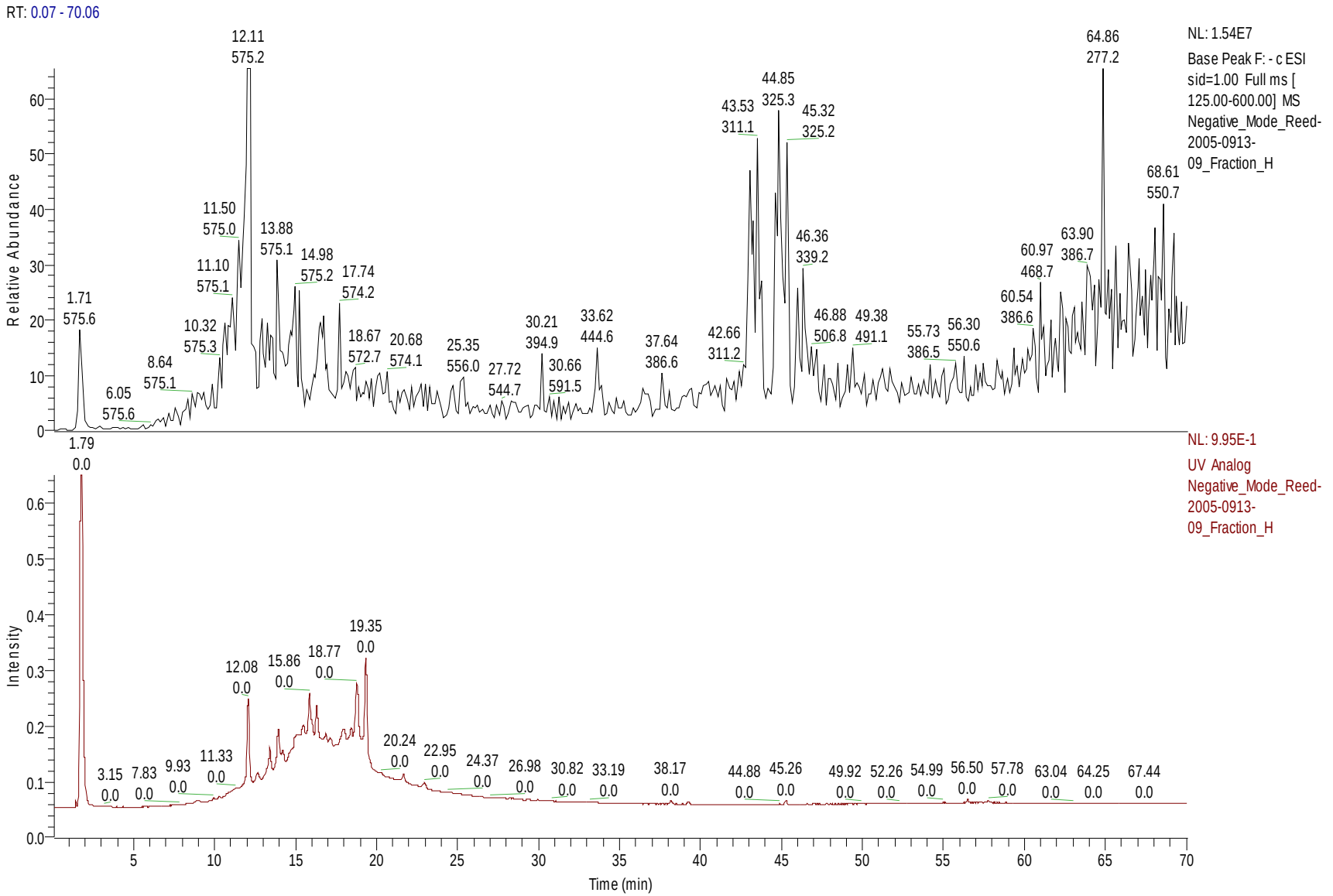

Figure A.37: Peanut Skin Fraction H: HPLC-UV Chromatogram (bottom) versus TIC [Total Ion Chromatogram – Showing the "ms" Normal Mass Spectra Base Peaks for the Most Intense Ions in SID=1.0 Scan Range (m/z 125-600 M-H$^-$)] (top).

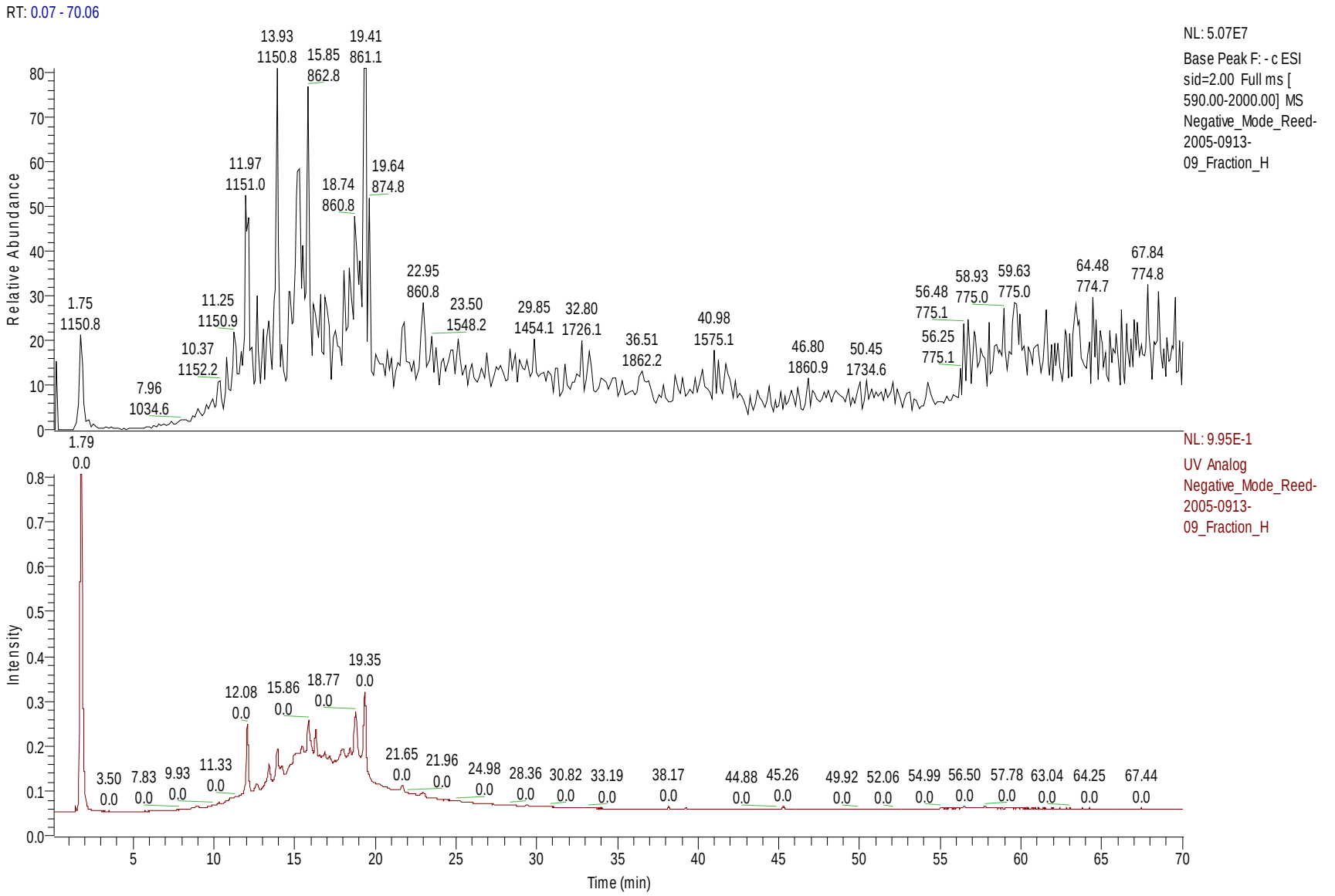

Figure A.38: Peanut Skin Fraction H: HPLC-UV Chromatogram (bottom) versus TIC [Total Ion Chromatogram – Showing the "ms" Normal Mass Spectra Base Peaks for the Most Intense Ions in SID=2.0 Scan Range (m/z 590-2000 M-H$^-$)] (top).

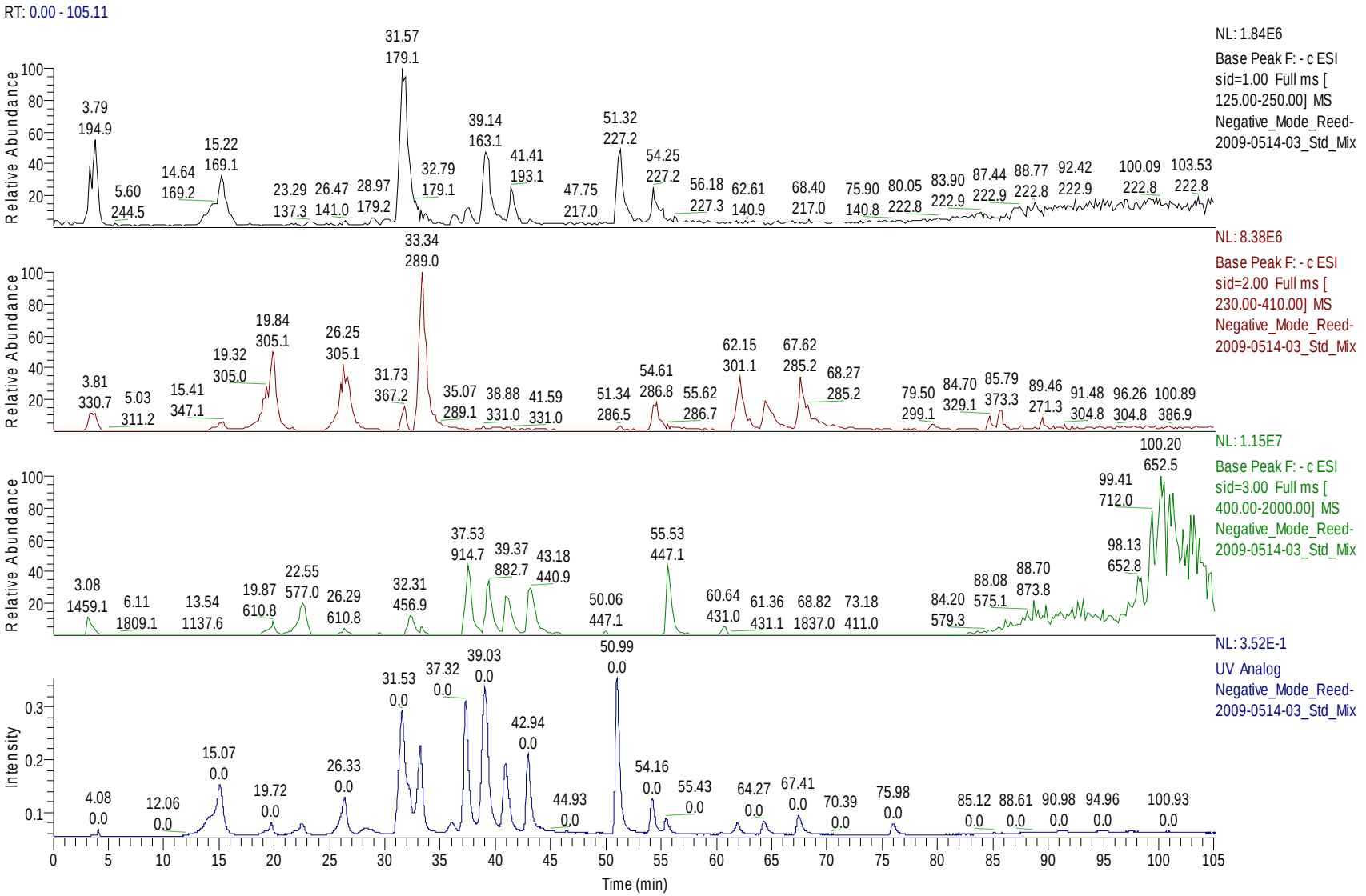

Figure A.39: Standard Mix (HPLC Method 2): HPLC-UV Chromatogram (bottom) versus TIC's [Total Ion Chromatograms – Showing the "ms" Normal Mass Spectra Base Peaks for the Most Intense Ions in SID=1.0 Scan Range (m/z 125-250 M-H$^-$) (top), SID=2.0 Scan Range (m/z 230-410 M-H$^-$) (second), and SID=3.0 Scan Range (m/z 400-2000 M-H$^-$) (third)].

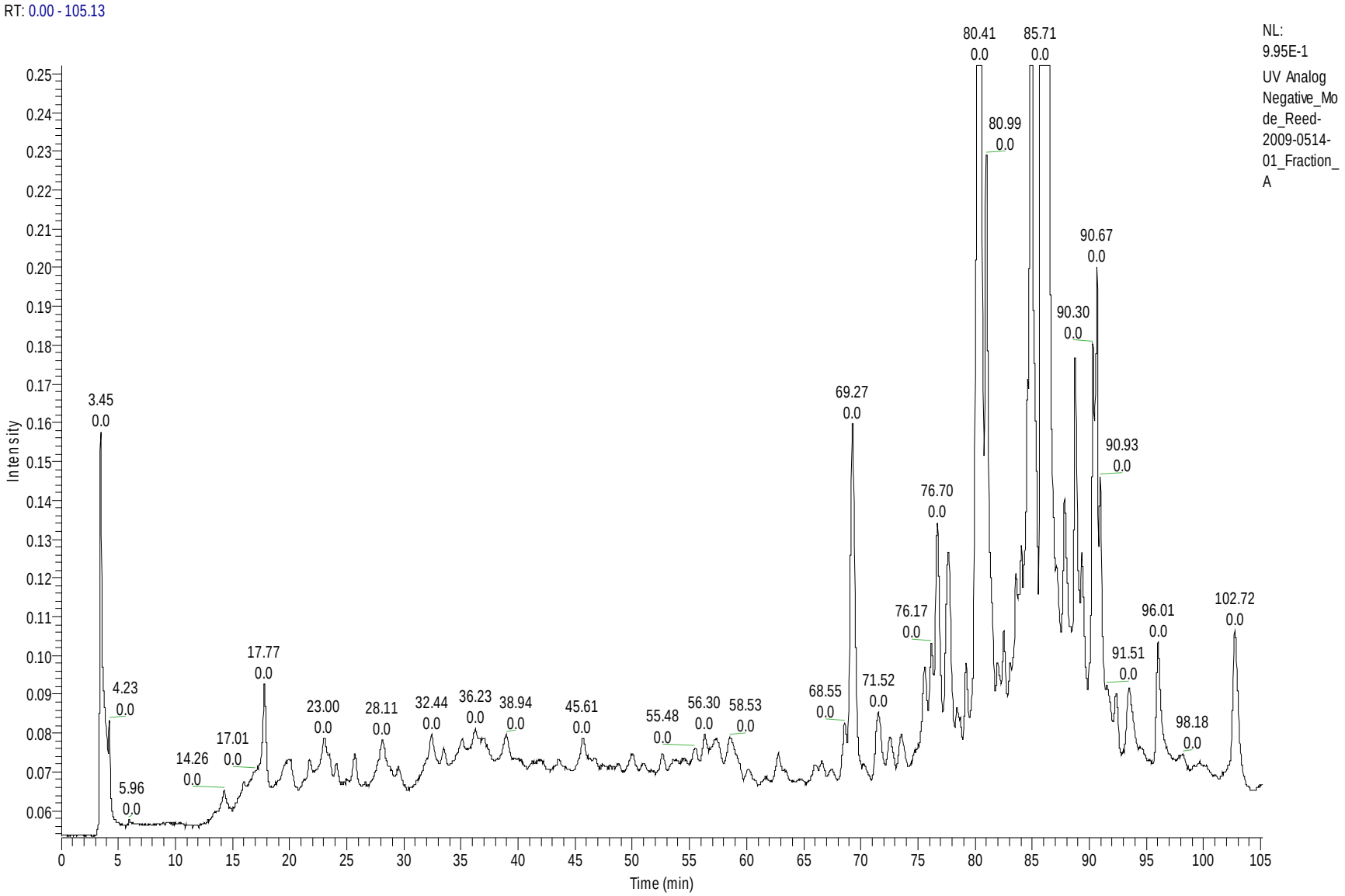

Figure A.40: HPLC-UV Chromatogram of Peanut Skin Fraction A (Obtained from Toyopearl Size Exclusion Chromatography) at 280nm using HPLC Method 2.

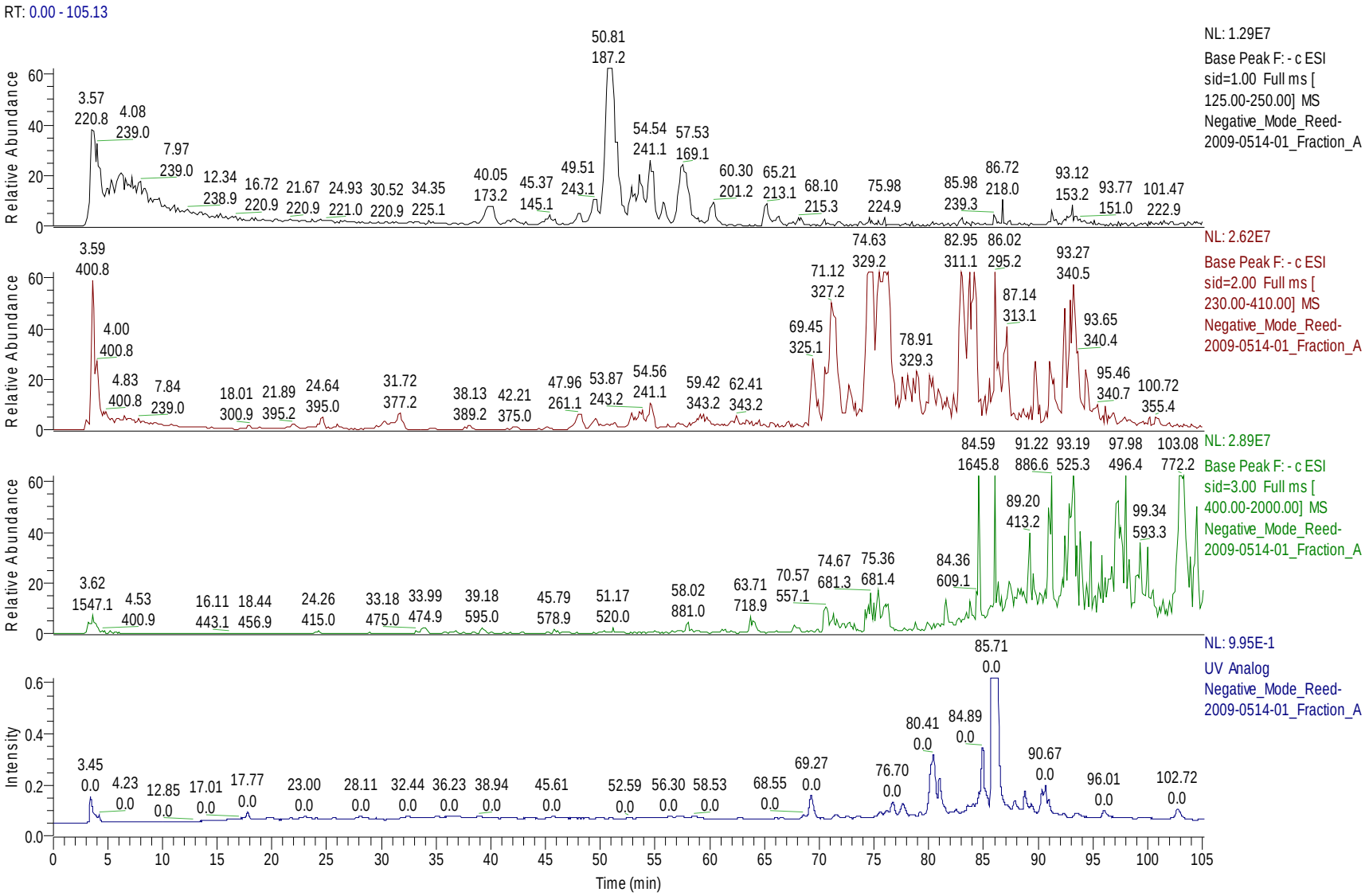

Figure A.41: Peanut Skin Fraction A (HPLC Method 2): HPLC-UV Chromatogram (bottom) versus TIC's [Total Ion Chromatograms – Showing the "ms" Normal Mass Spectra Base Peaks for the Most Intense Ions in SID=1.0 Scan Range (m/z 125-250 M-H$^-$) (top), SID=2.0 Scan Range (m/z 230-410 M-H$^-$) (second), and SID=3.0 Scan Range (m/z 400-2000 M-H$^-$) (third)].

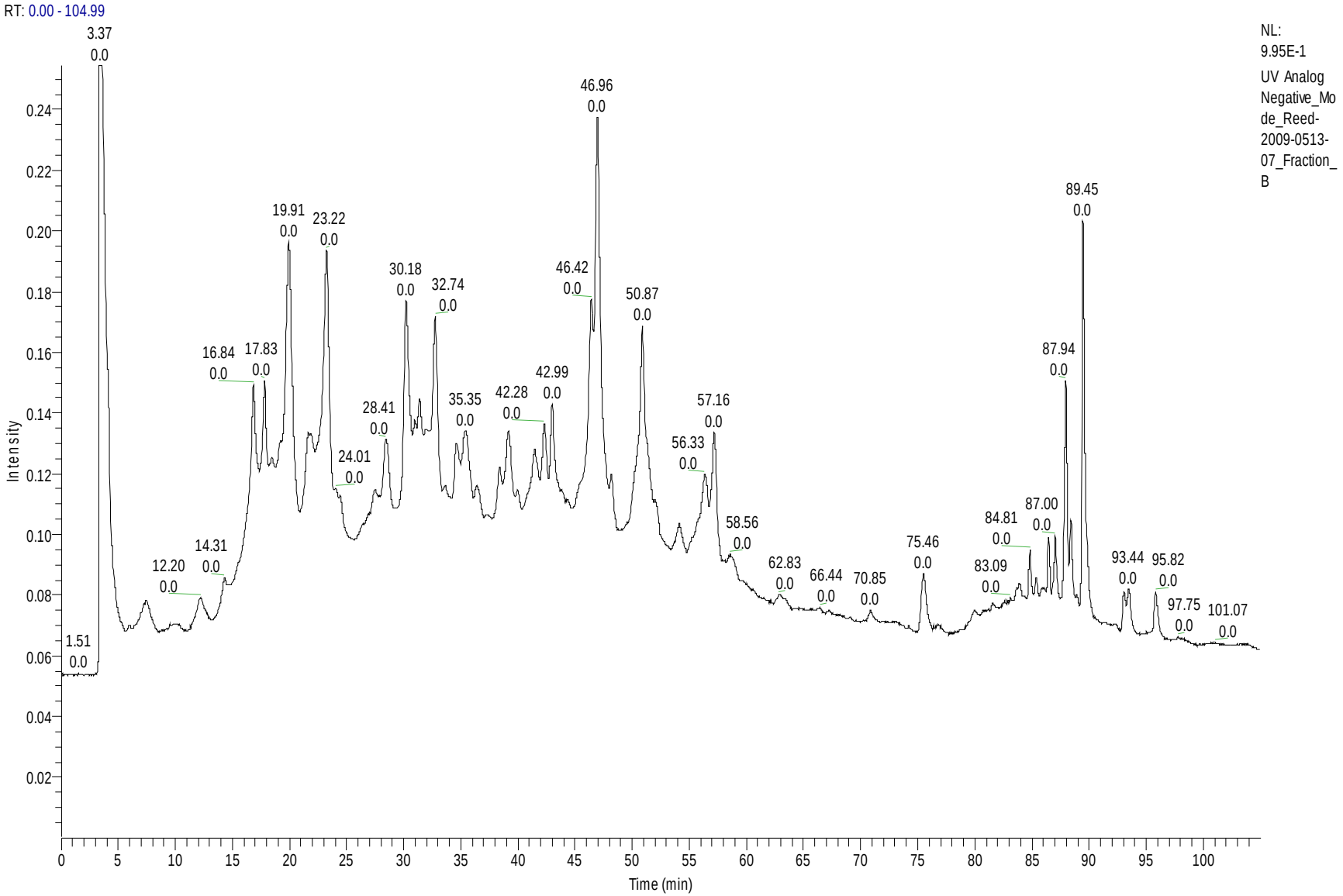

Figure A.42: HPLC-UV Chromatogram of Peanut Skin Fraction B (Obtained from Toyopearl Size Exclusion Chromatography) at 280nm using HPLC Method 2.

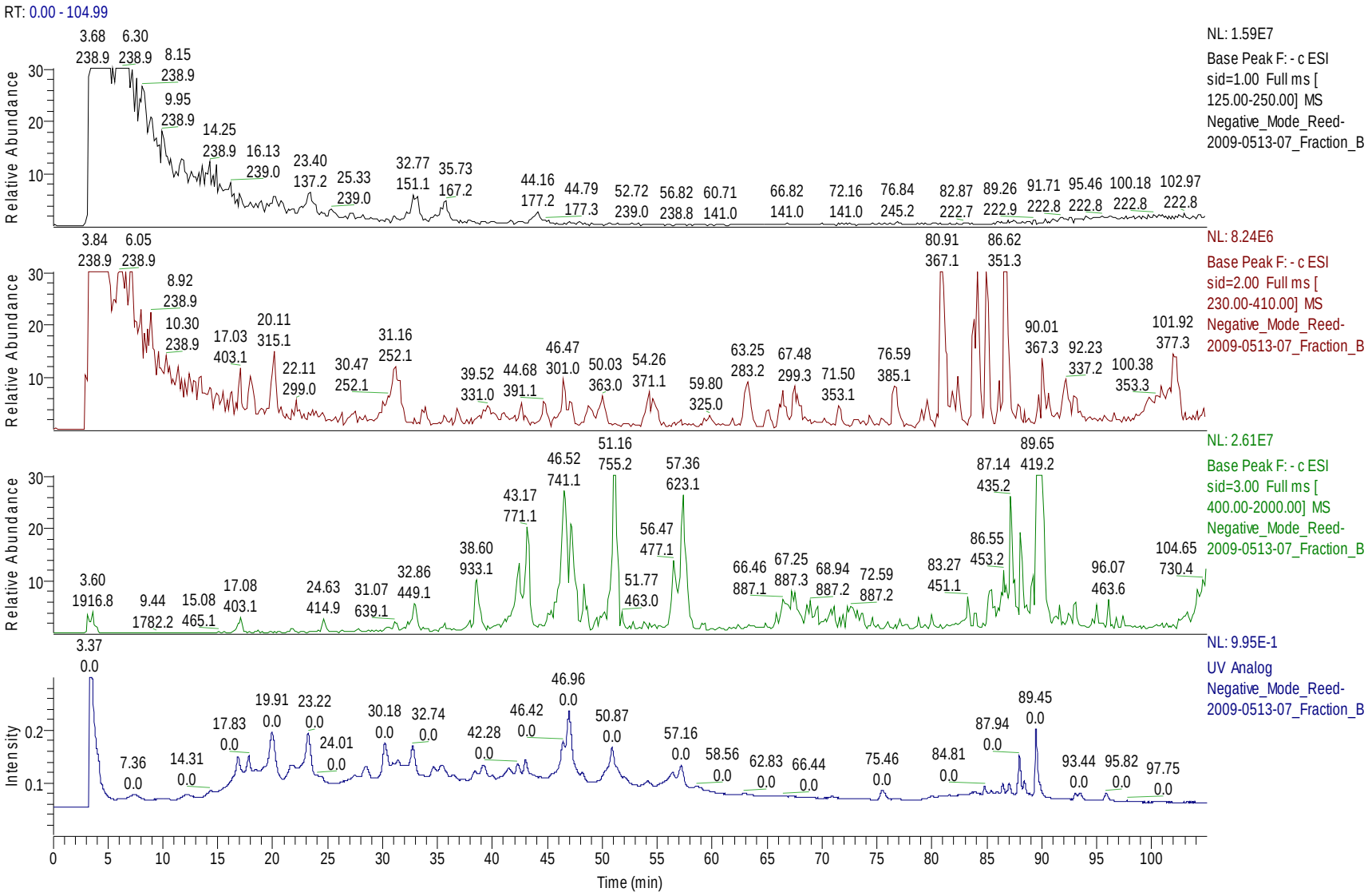

Figure A.43: Peanut Skin Fraction B (HPLC Method 2): HPLC-UV Chromatogram (bottom) versus TIC's [Total Ion Chromatograms – Showing the "ms" Normal Mass Spectra Base Peaks for the Most Intense Ions in SID=1.0 Scan Range (m/z 125-250 M-H$^-$) (top), SID=2.0 Scan Range (m/z 230-410 M-H$^-$) (second), and SID=3.0 Scan Range (m/z 400-2000 M-H$^-$) (third)].

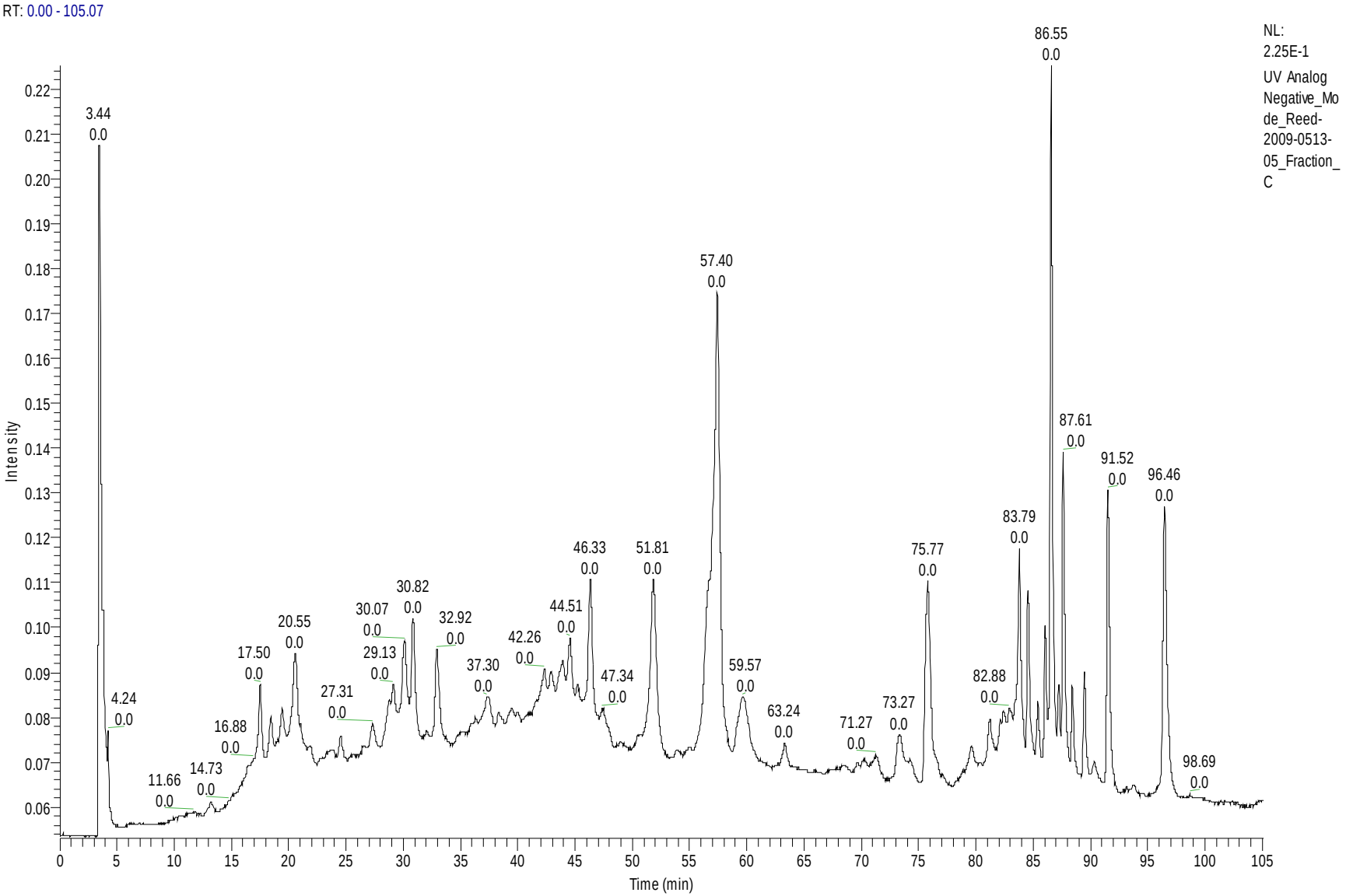

Figure A.44: HPLC-UV Chromatogram of Peanut Skin Fraction C (Obtained from Toyopearl Size Exclusion Chromatography) at 280nm using HPLC Method 2.

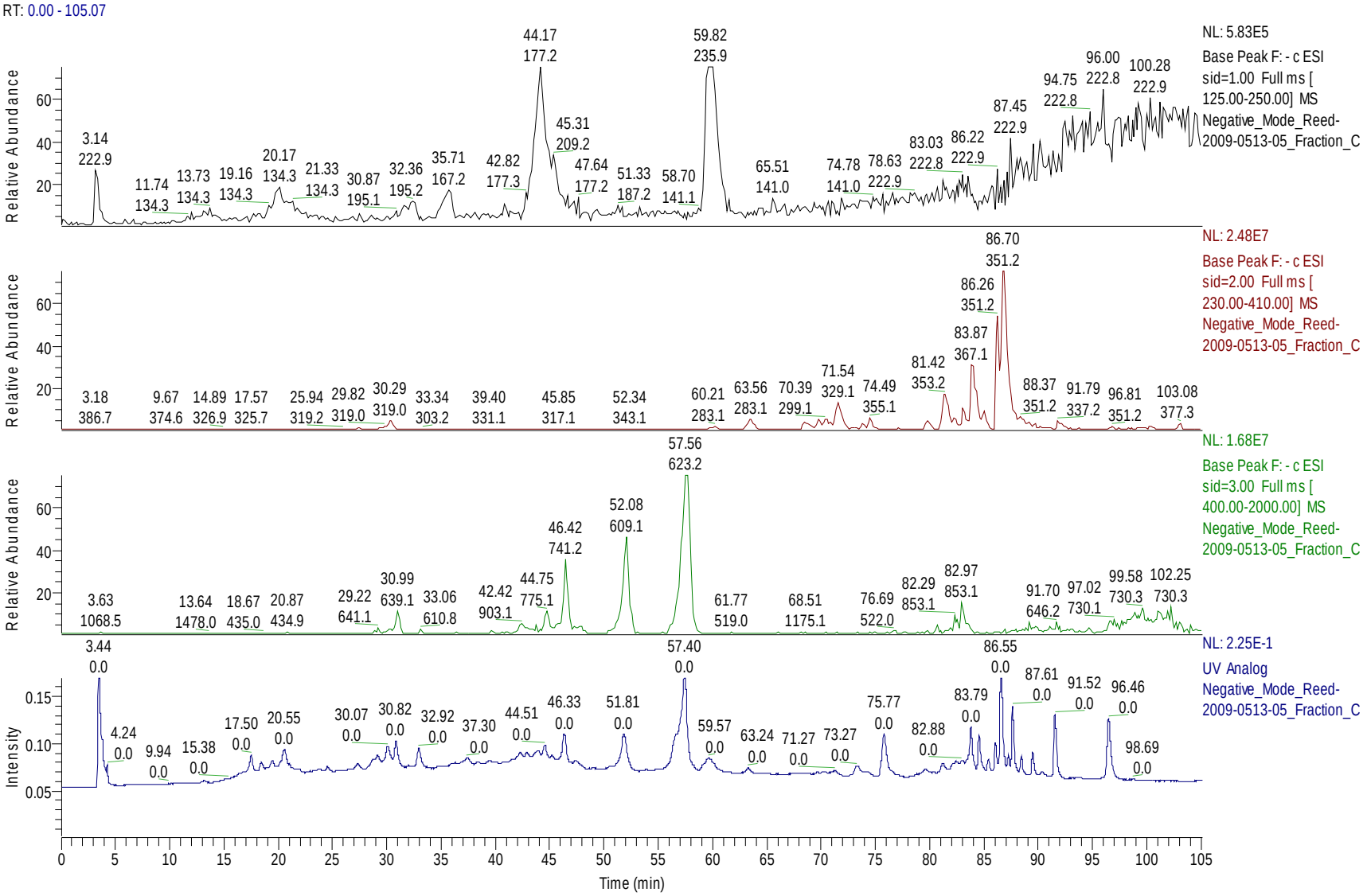

Figure A.45: Peanut Skin Fraction C (HPLC Method 2): HPLC-UV Chromatogram (bottom) versus TIC's [Total Ion Chromatograms – Showing the "ms" Normal Mass Spectra Base Peaks for the Most Intense Ions in SID=1.0 Scan Range (m/z 125-250 M-H$^-$) (top), SID=2.0 Scan Range (m/z 230-410 M-H$^-$) (second), and SID=3.0 Scan Range (m/z 400-2000 M-H$^-$) (third)].

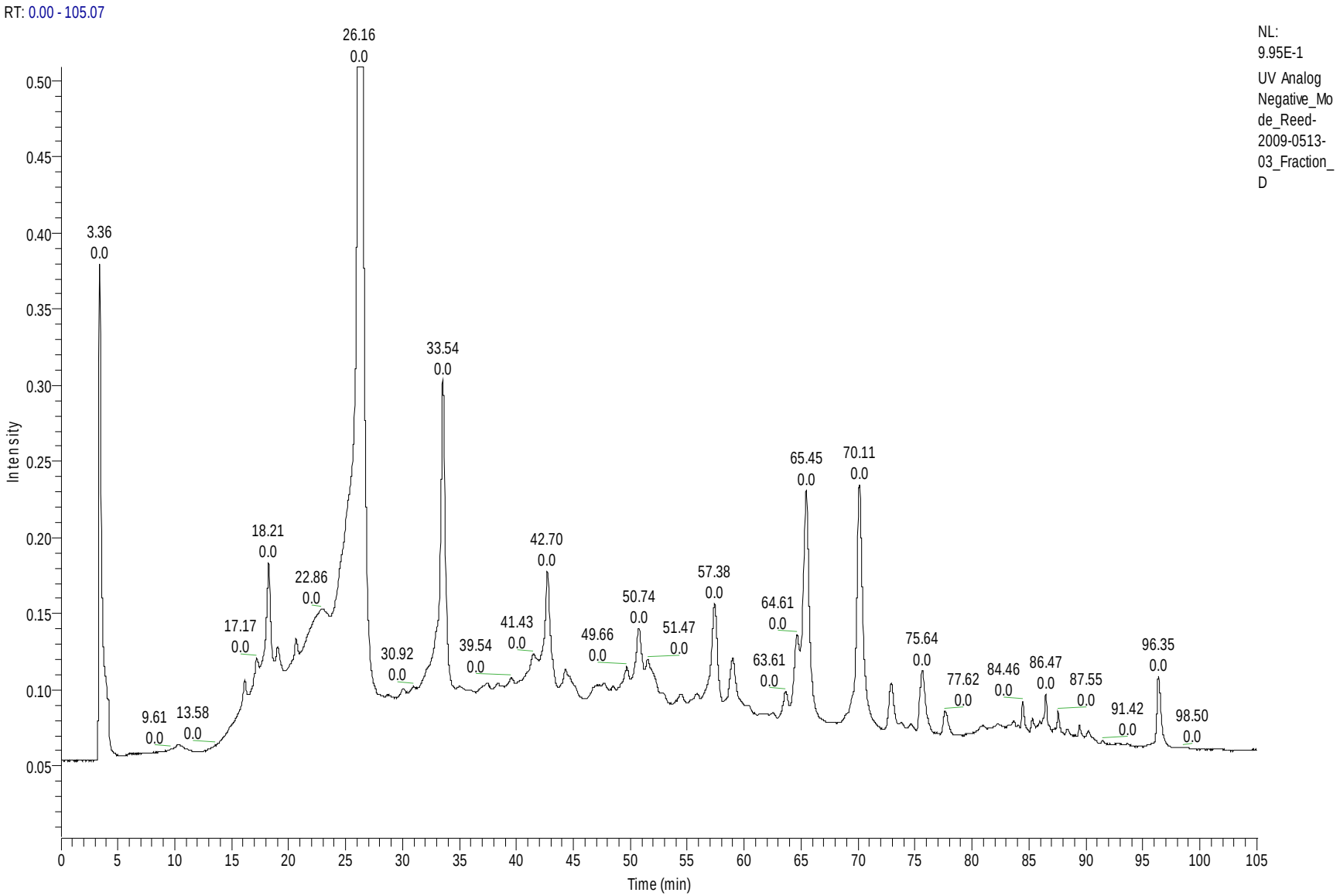

Figure A.46: HPLC-UV Chromatogram of Peanut Skin Fraction D (Obtained from Toyopearl Size Exclusion Chromatography) at 280nm using HPLC Method 2.

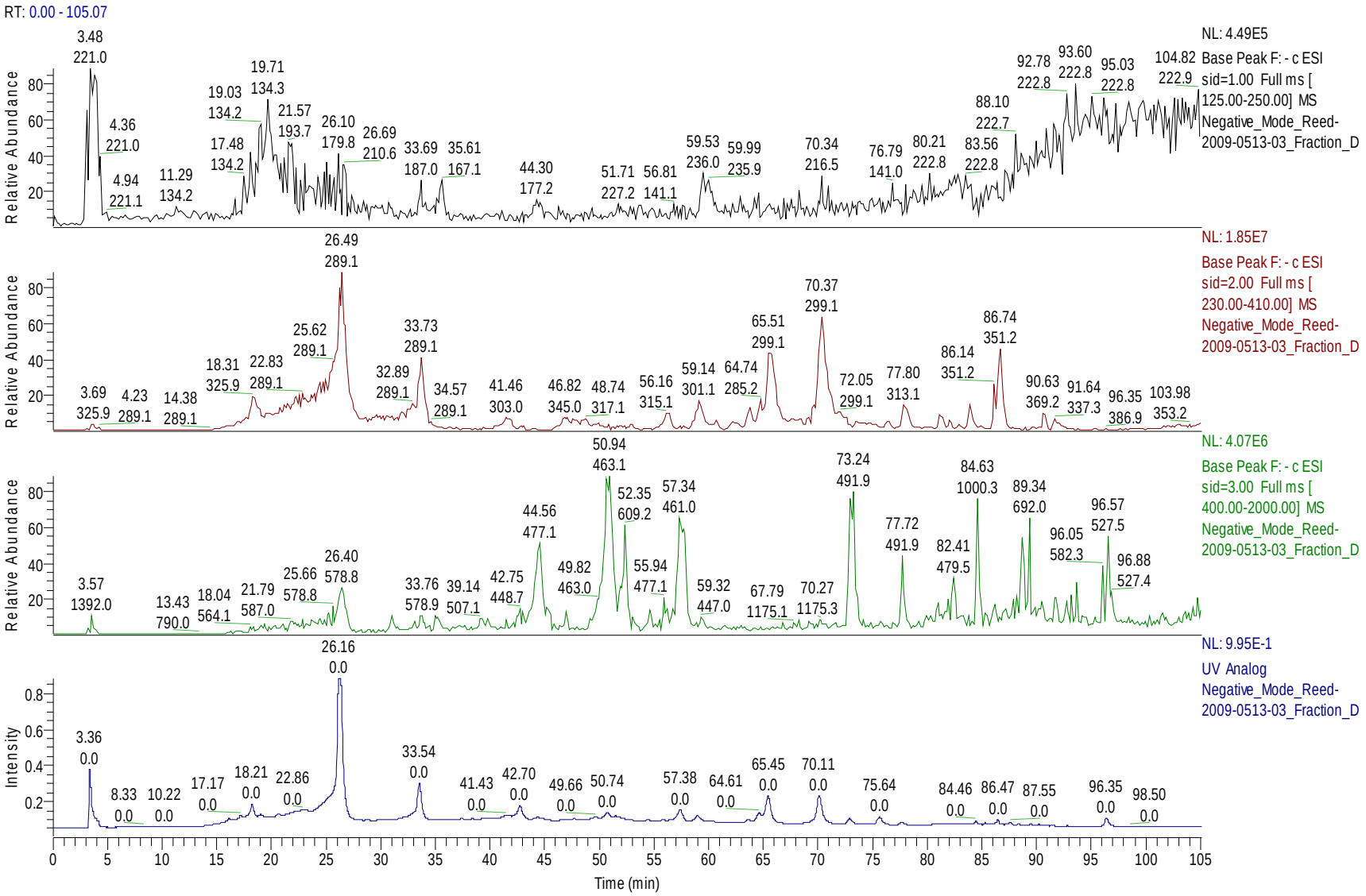

Figure A.47: Peanut Skin Fraction D (HPLC Method 2): HPLC-UV Chromatogram (bottom) versus TIC's [Total Ion Chromatograms – Showing the "ms" Normal Mass Spectra Base Peaks for the Most Intense Ions in SID=1.0 Scan Range (m/z 125-250 M-H$^-$) (top), SID=2.0 Scan Range (m/z 230-410 M-H$^-$) (second), and SID=3.0 Scan Range (m/z 400-2000 M-H$^-$) (third)].

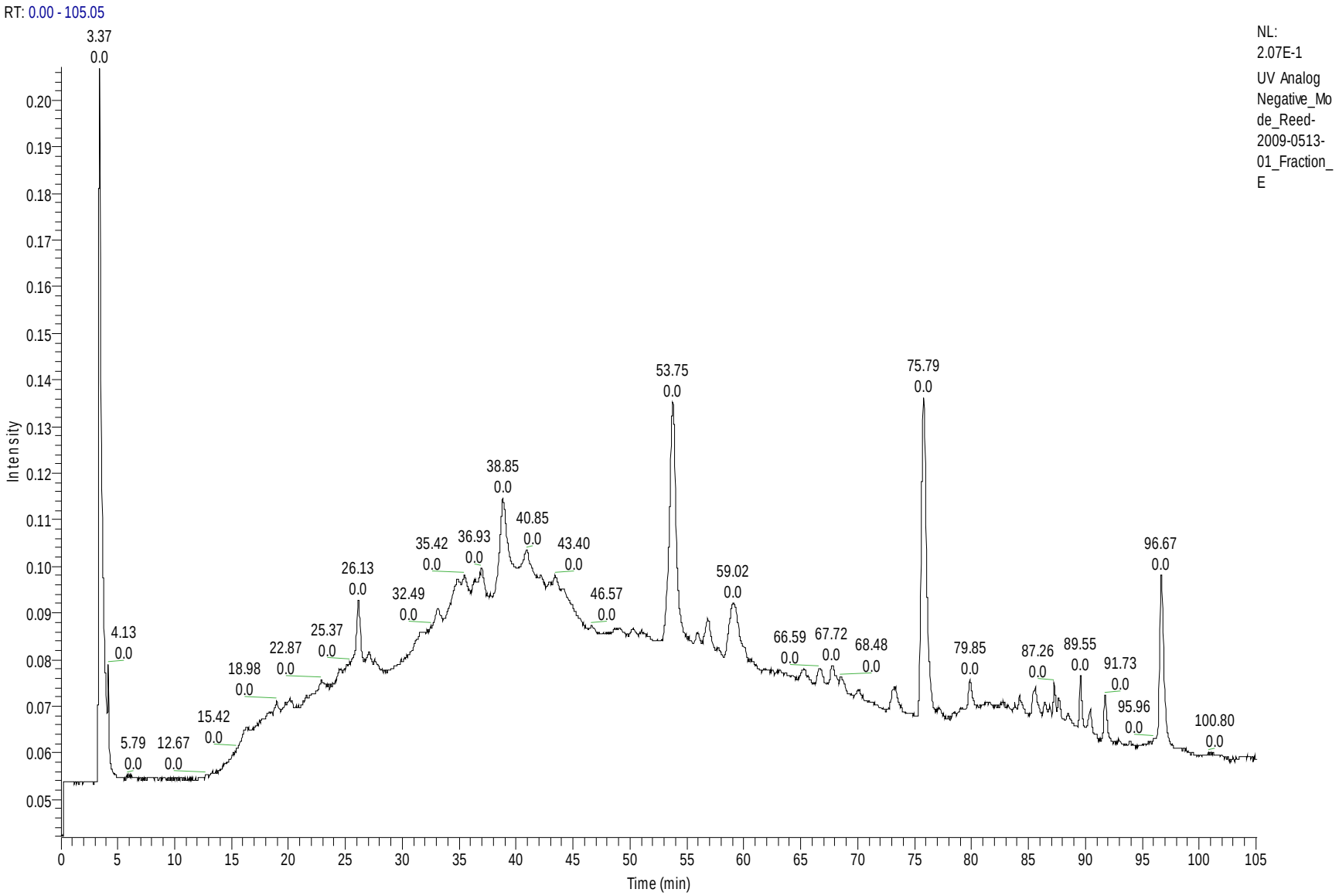

Figure A.48: HPLC-UV Chromatogram of Peanut Skin Fraction E (Obtained from Toyopearl Size Exclusion Chromatography) at 280nm using HPLC Method 2.

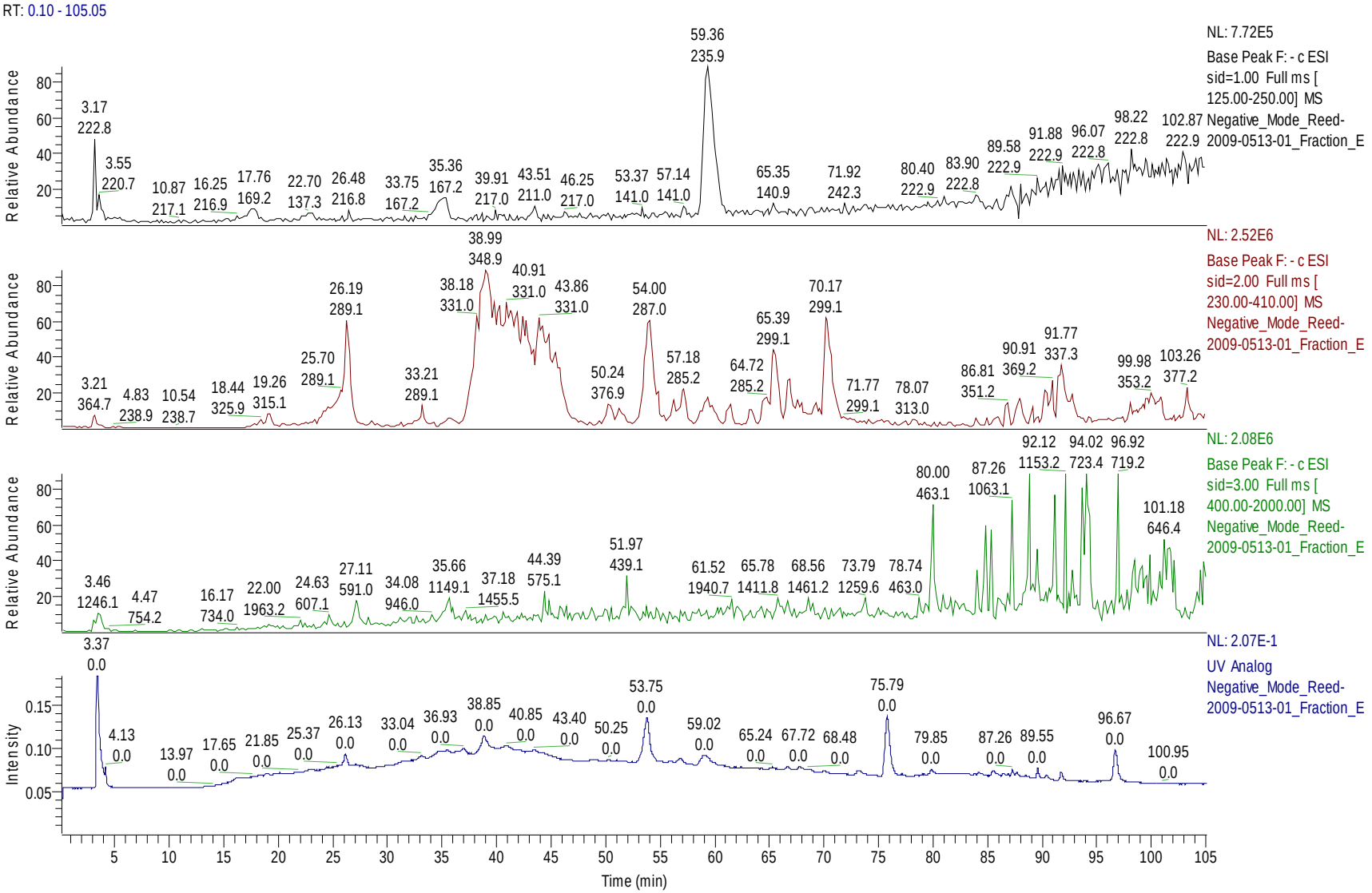

Figure A.49: Peanut Skin Fraction E (HPLC Method 2): HPLC-UV Chromatogram (bottom) versus TIC's [Total Ion Chromatograms – Showing the "ms" Normal Mass Spectra Base Peaks for the Most Intense Ions in SID=1.0 Scan Range (m/z 125-250 M-H$^-$) (top), SID=2.0 Scan Range (m/z 230-410 M-H$^-$) (second), and SID=3.0 Scan Range (m/z 400-2000 M-H$^-$) (third)].

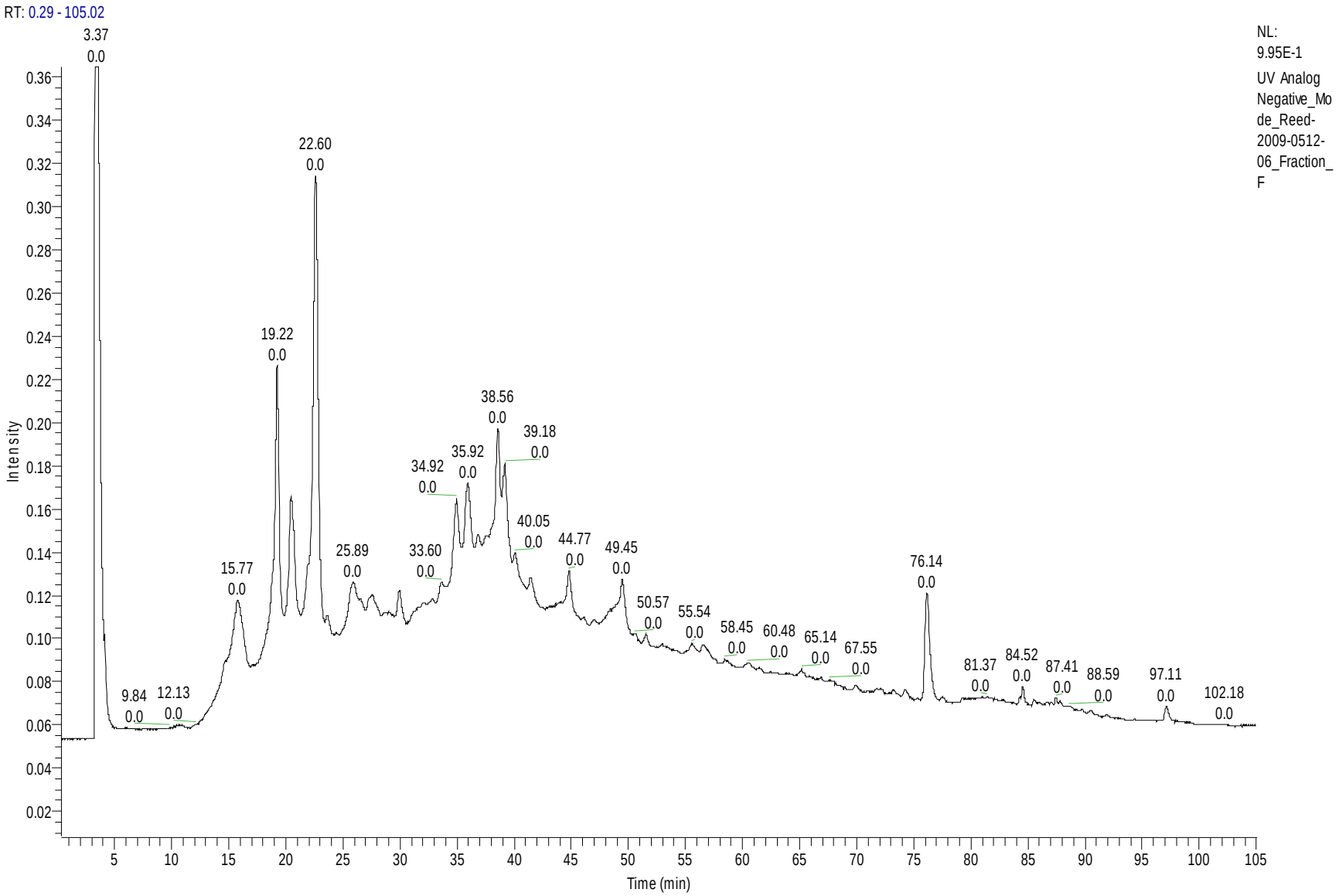

Figure A.50: HPLC-UV Chromatogram of Peanut Skin Fraction F (Obtained from Toyopearl Size Exclusion Chromatography) at 280nm using HPLC Method 2.

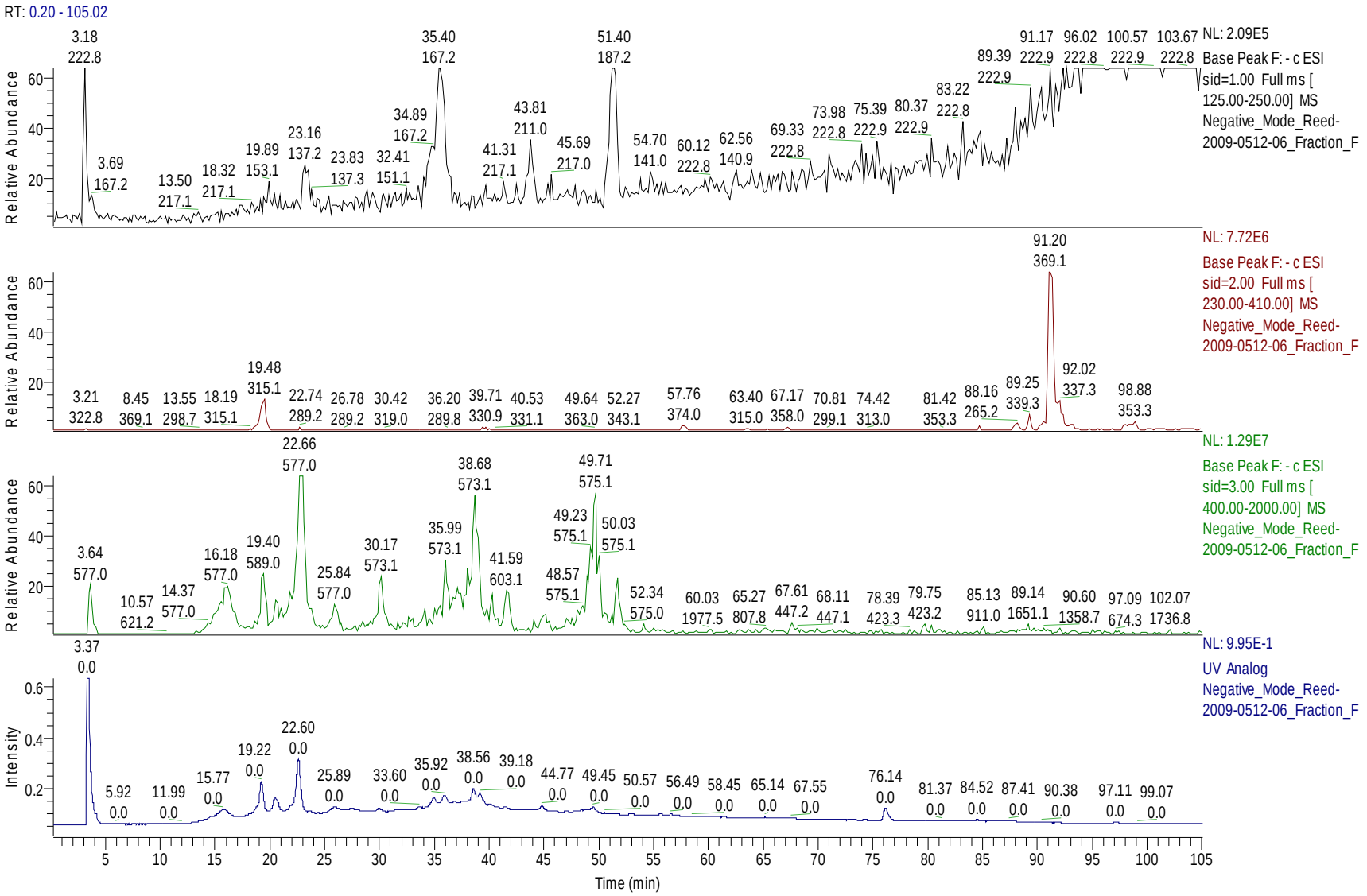

Figure A.51: Peanut Skin Fraction F (HPLC Method 2): HPLC-UV Chromatogram (bottom) versus TIC's [Total Ion Chromatograms – Showing the "ms" Normal Mass Spectra Base Peaks for the Most Intense Ions in SID=1.0 Scan Range (m/z 125-250 M-H$^-$) (top), SID=2.0 Scan Range (m/z 230-410 M-H$^-$) (second), and SID=3.0 Scan Range (m/z 400-2000 M-H$^-$) (third)].

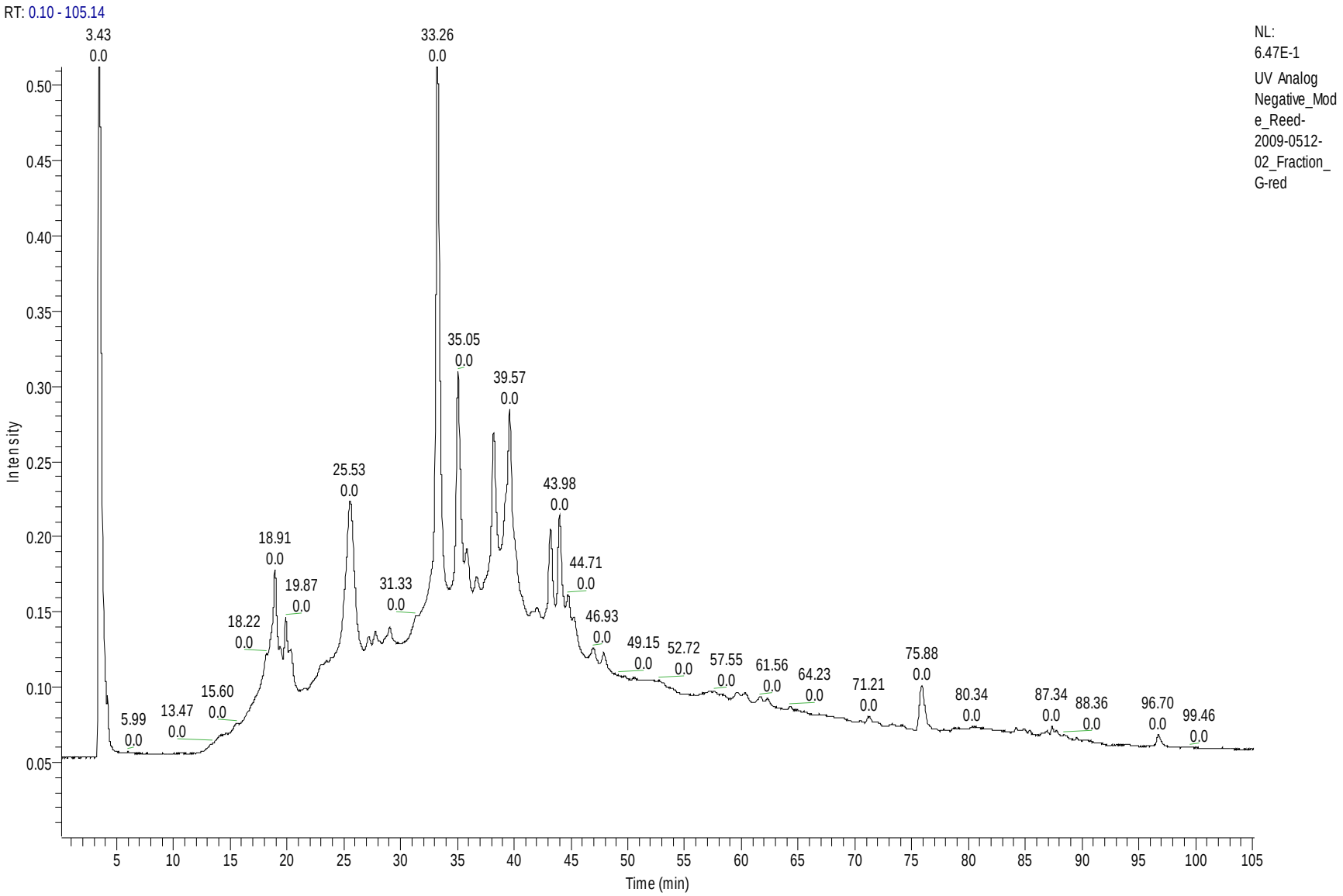

Figure A.52: HPLC-UV Chromatogram of Peanut Skin Fraction G-Red (Obtained from Toyopearl Size Exclusion Chromatography) at 280nm using HPLC Method 2.

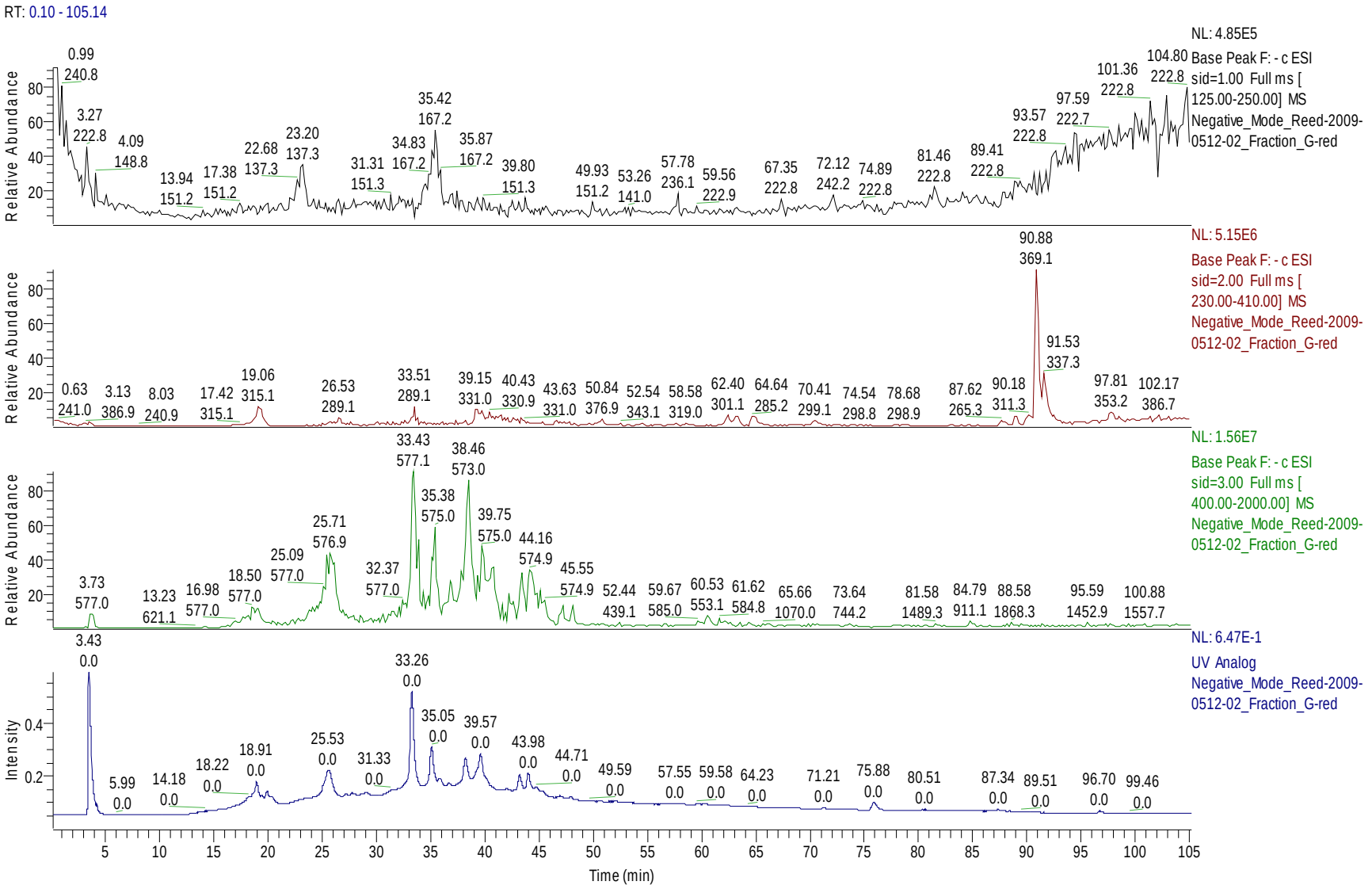

Figure A.53: Peanut Skin Fraction G-Red (HPLC Method 2): HPLC-UV Chromatogram (bottom) -vs- TIC's [Total Ion Chromatograms – Showing the "ms" Normal Mass Spectra Base Peaks for the Most Intense Ions in SID=1.0 Scan Range (m/z 125-250 M-H$^-$) (top), SID=2.0 Scan Range (m/z 230-410 M-H$^-$) (second), and SID=3.0 Scan Range (m/z 400-2000 M-H$^-$) (third)].

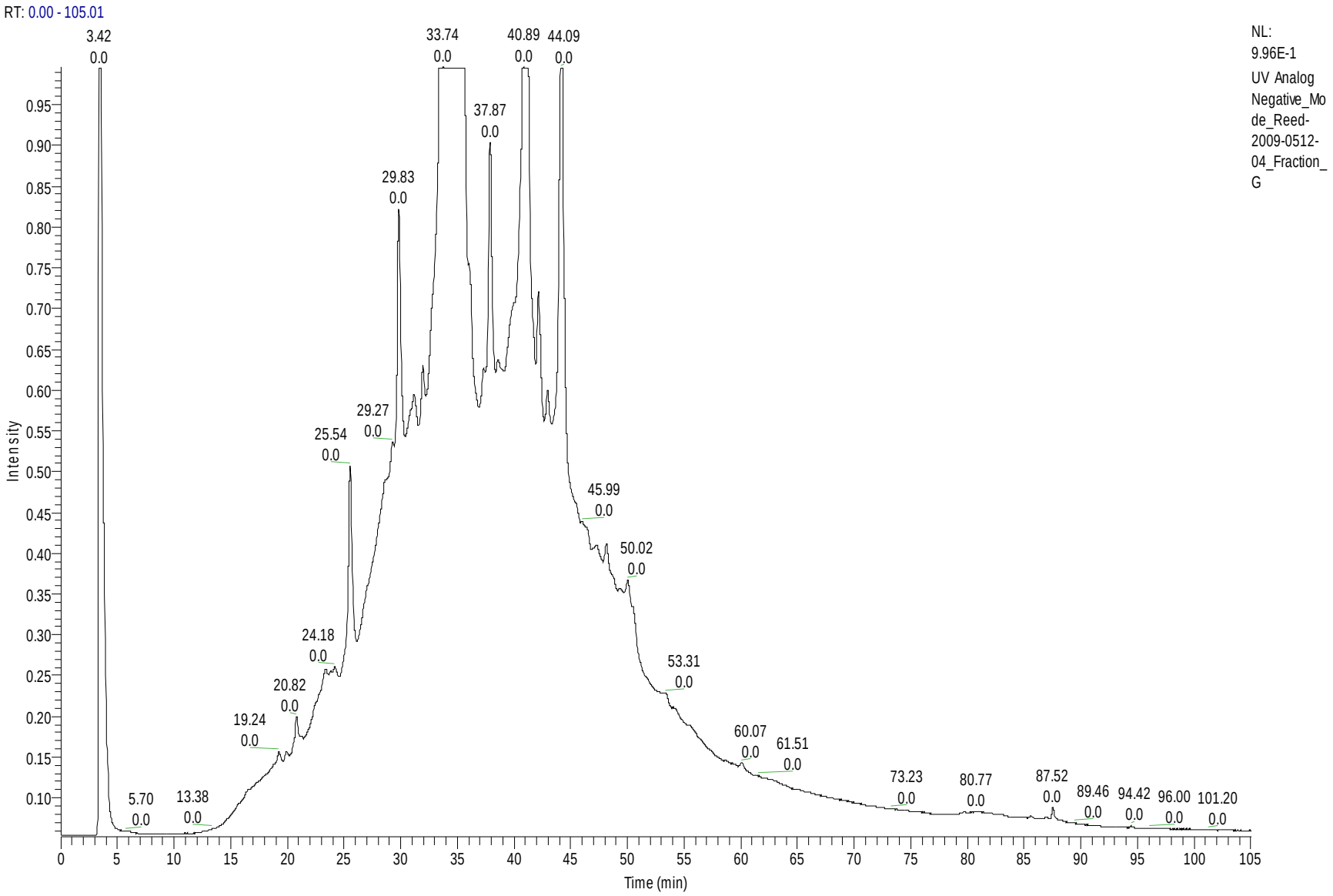

Figure A.54: HPLC-UV Chromatogram of Peanut Skin Fraction G (Obtained from Toyopearl Size Exclusion Chromatography) at 280nm using HPLC Method 2.

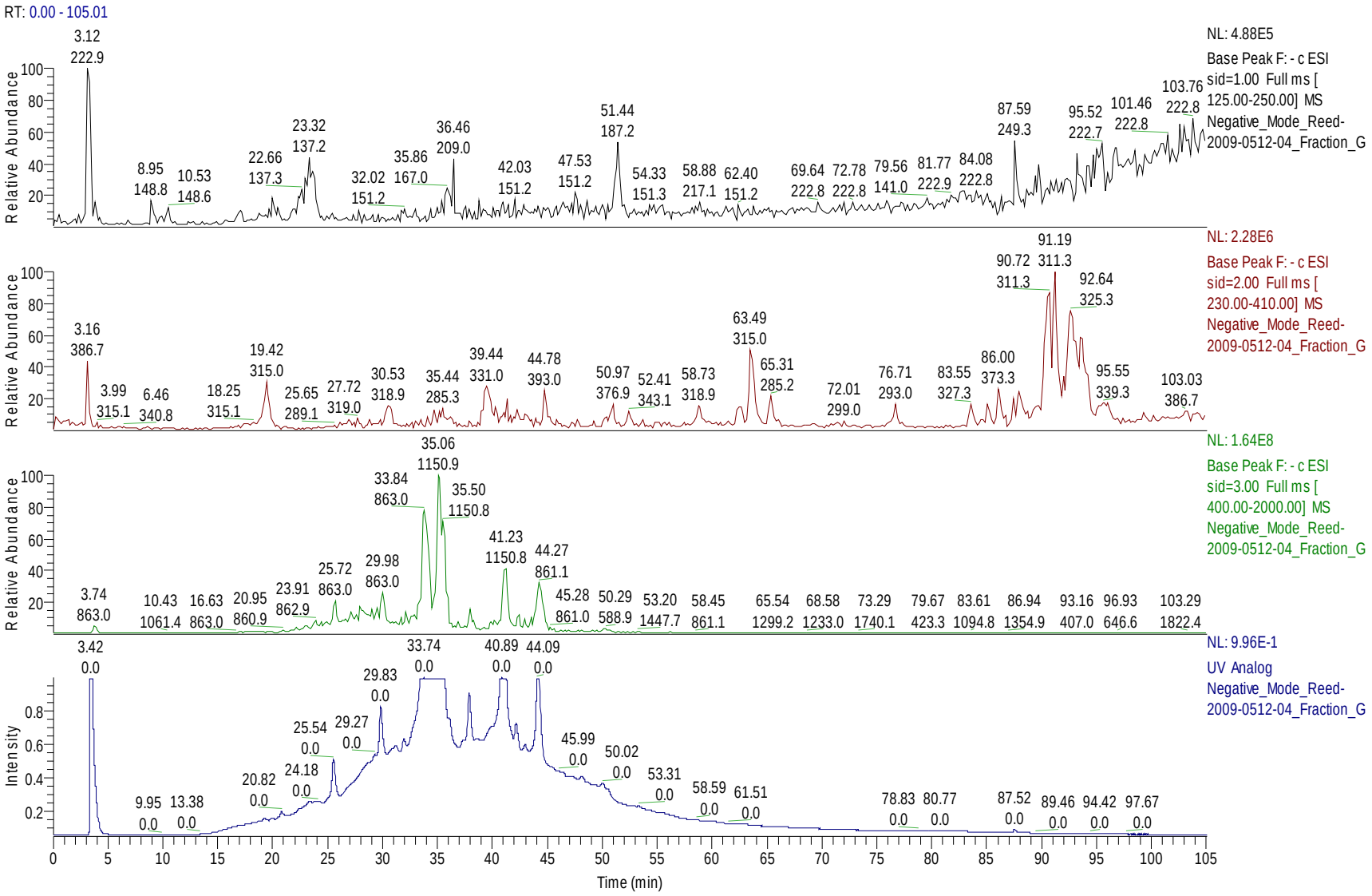

Figure A.55: Peanut Skin Fraction G (HPLC Method 2): HPLC-UV Chromatogram (bottom) versus TIC's [Total Ion Chromatograms – Showing the "ms" Normal Mass Spectra Base Peaks for the Most Intense Ions in SID=1.0 Scan Range (m/z 125-250 M-H$^-$) (top), SID=2.0 Scan Range (m/z 230-410 M-H$^-$) (second), and SID=3.0 Scan Range (m/z 400-2000 M-H$^-$) (third)].

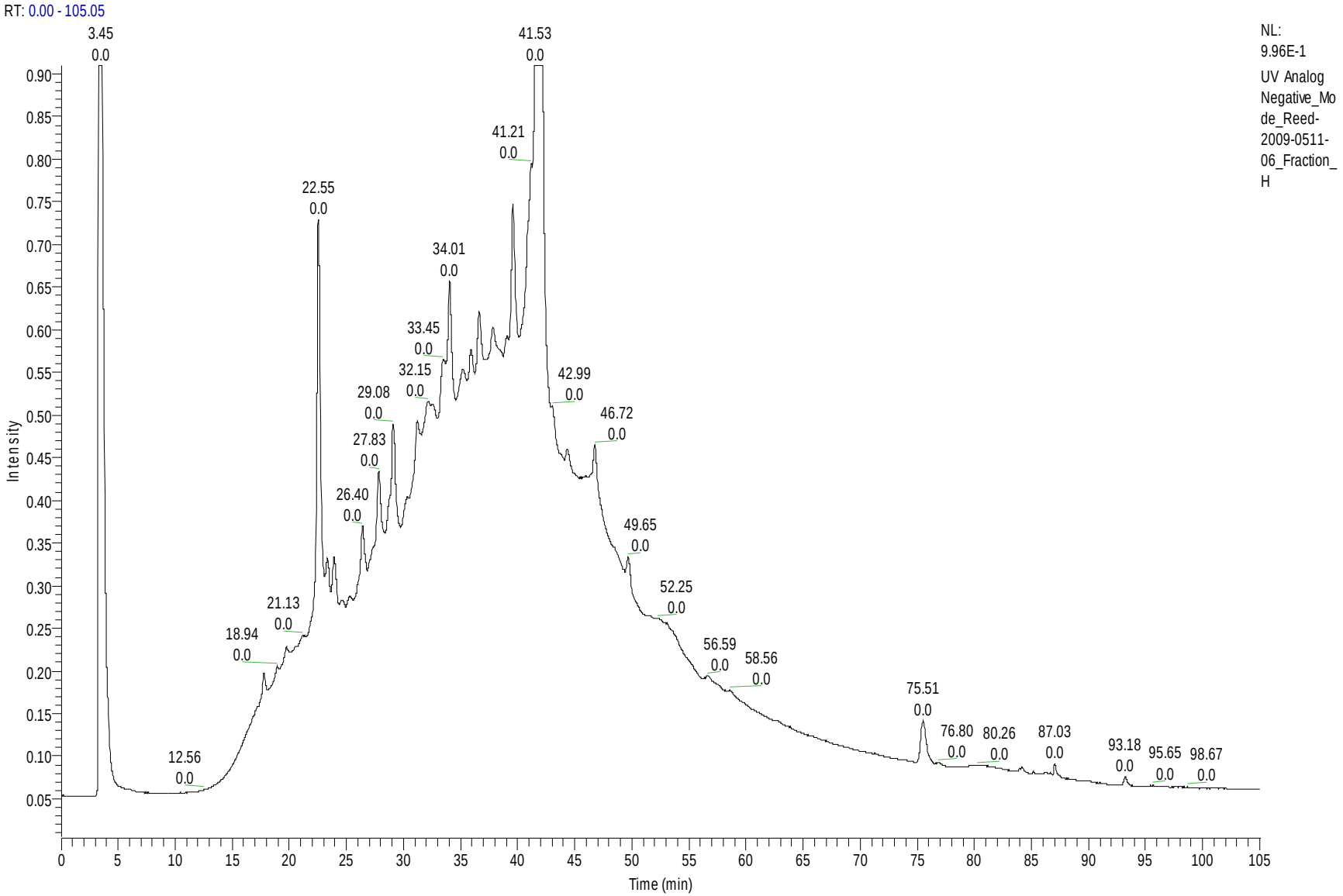

Figure A.56: HPLC-UV Chromatogram of Peanut Skin Fraction H (Obtained from Toyopearl Size Exclusion Chromatography) at 280nm using HPLC Method 2.

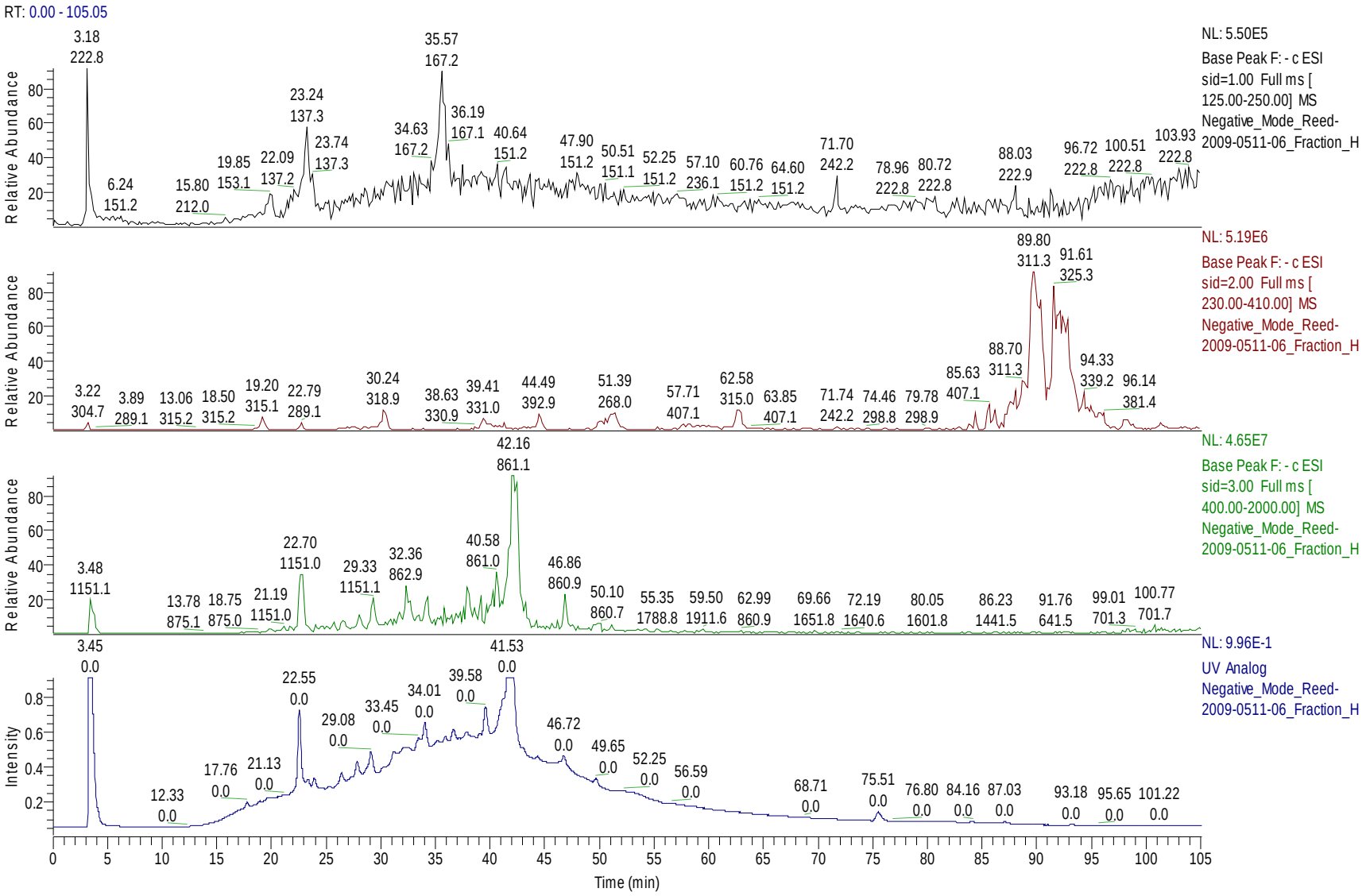

Figure A.57: Peanut Skin Fraction H (HPLC Method 2): HPLC-UV Chromatogram (bottom) versus TIC's [Total Ion Chromatograms – Showing the "ms" Normal Mass Spectra Base Peaks for the Most Intense Ions in SID=1.0 Scan Range (m/z 125-250 M-H$^-$) (top), SID=2.0 Scan Range (m/z 230-410 M-H$^-$) (second), and SID=3.0 Scan Range (m/z 400-2000 M-H$^-$) (third)].